



applied sciences

New Trends in Environmental Engineering, Agriculture, Food Production, and Analysis

Edited by

Wojciech Janczukowicz, Joanna Rodziewicz and Anna Iwaniak

Printed Edition of the Special Issue Published in *Applied Sciences*

New Trends in Environmental Engineering, Agriculture, Food Production, and Analysis

New Trends in Environmental Engineering, Agriculture, Food Production, and Analysis

Editors

Wojciech Janczukowicz

Joanna Rodziewicz

Anna Iwaniak

MDPI • Basel • Beijing • Wuhan • Barcelona • Belgrade • Manchester • Tokyo • Cluj • Tianjin



Editors

Wojciech Janczukowicz
University of Warmia and Mazury in Olsztyn
Poland

Joanna Rodziewicz
University of Warmia and Mazury in Olsztyn
Poland

Anna Iwaniak
University of Warmia and Mazury in Olsztyn
Poland

Editorial Office

MDPI
St. Alban-Anlage 66
4052 Basel, Switzerland

This is a reprint of articles from the Special Issue published online in the open access journal *Applied Sciences* (ISSN 2076-3417) (available at: https://www.mdpi.com/journal/applsci/special_issues/EEAFPA).

For citation purposes, cite each article independently as indicated on the article page online and as indicated below:

LastName, A.A.; LastName, B.B.; LastName, C.C. Article Title. <i>Journal Name</i> Year , <i>Volume Number</i> , Page Range.
--

ISBN 978-3-0365-1124-5 (Hbk)

ISBN 978-3-0365-1125-2 (PDF)

© 2021 by the authors. Articles in this book are Open Access and distributed under the Creative Commons Attribution (CC BY) license, which allows users to download, copy and build upon published articles, as long as the author and publisher are properly credited, which ensures maximum dissemination and a wider impact of our publications.

The book as a whole is distributed by MDPI under the terms and conditions of the Creative Commons license CC BY-NC-ND.

Contents

About the Editors	ix
Anna Iwaniak, Wojciech Janczukowicz and Joanna Rodziewicz New Trends in Environmental Engineering, Agriculture, Food Production, and Analysis Reprinted from: <i>Appl. Sci.</i> 2021 , <i>11</i> , 2745, doi:10.3390/app11062745	1
Agnieszka Micek, Krzysztof Józwiakowski, Michał Marzec, Agnieszka Listosz and Tadeusz Grabowski Efficiency and Technological Reliability of Contaminant Removal in Household WWTPs with Activated Sludge Reprinted from: <i>Appl. Sci.</i> 2021 , <i>11</i> , 1889, doi:10.3390/app11041889	3
Artur Mielcarek, Joanna Rodziewicz, Wojciech Janczukowicz and Kamila Ostrowska The Kinetics of Pollutant Removal through Biofiltration from Stormwater Containing Airport De-Icing Agents Reprinted from: <i>Appl. Sci.</i> 2021 , <i>11</i> , 1724, doi:10.3390/app11041724	19
Mateusz Sikora, Joanna Nowosad and Dariusz Kucharczyk Comparison of Different Biofilter Media During Biological Bed Maturation Using Common Carp as a Biogen Donor Reprinted from: <i>Appl. Sci.</i> 2020 , <i>10</i> , 626, doi:10.3390/app10020626	31
Jolanta Grochowska, Renata Augustyniak, Michał Łopata and Renata Tandyrak Is It Possible to Restore a Heavily Polluted, Shallow, Urban Lake? Reprinted from: <i>Appl. Sci.</i> 2020 , <i>10</i> , 3698, doi:10.3390/app10113698	51
Fidel Toldrá-Reig, Leticia Mora and Fidel Toldrá Developments in the Use of Lipase Transesterification for Biodiesel Production from Animal Fat Waste Reprinted from: <i>Appl. Sci.</i> 2020 , <i>10</i> , 5085, doi:10.3390/app10155085	73
Cevat Yaman Application of Sterilization Process for Inactivation of <i>Bacillus Stearothermophilus</i> in Biomedical Waste and Associated Greenhouse Gas Emissions Reprinted from: <i>Appl. Sci.</i> 2020 , <i>10</i> , 5056, doi:10.3390/app10155056	89
Fidel Toldrá-Reig, Leticia Mora and Fidel Toldrá Trends in Biodiesel Production from Animal Fat Waste Reprinted from: <i>Appl. Sci.</i> 2020 , <i>10</i> , 3644, doi:10.3390/app10103644	103
Sławomir Kasinski Mesophilic and Thermophilic Anaerobic Digestion of Organic Fraction Separated during Mechanical Heat Treatment of Municipal Waste Reprinted from: <i>Appl. Sci.</i> 2020 , <i>10</i> , 2412, doi:10.3390/app10072412	121
Songchao Zhang, Baijing Qiu, Xinyu Xue, Tao Sun, Wei Gu, Fuliang Zhou and Xiangdong Sun Effects of Crop Protection Unmanned Aerial System Flight Speed, Height on Effective Spraying Width, Droplet Deposition and Penetration Rate, and Control Effect Analysis on Wheat Aphids, Powdery Mildew, and Head Blight Reprinted from: <i>Appl. Sci.</i> 2021 , <i>11</i> , 712, doi:10.3390/app11020712	133

Petra Jiroutová and Jiří Sedlák Cryobiotechnology of Plants: A Hot Topic Not Only for Gene Banks Reprinted from: <i>Appl. Sci.</i> 2020 , <i>10</i> , 4677, doi:10.3390/app10134677	147
Marcos-Jesús Villaseñor-Aguilar, Micael-Gerardo Bravo-Sánchez, José-Alfredo Padilla-Medina, Jorge Luis Vázquez-Vera, Ramón-Gerardo Guevara-González, Francisco-Javier García-Rodríguez and Alejandro-Israel Barranco-Gutiérrez A Maturity Estimation of Bell Pepper (<i>Capsicum annuum</i> L.) by Artificial Vision System for Quality Control Reprinted from: <i>Appl. Sci.</i> 2020 , <i>10</i> , 5097, doi:10.3390/app10155097	161
Aleksandra Bykowska-Derda, Ezgi Kolay, Malgorzata Kaluzna and Magdalena Czlapka-Matyasik Emerging Trends in Research on Food Compounds and Women’s Fertility: A Systematic Review Reprinted from: <i>Appl. Sci.</i> 2020 , <i>10</i> , 4518, doi:10.3390/app10134518	179
Beata Nalepa, Sławomir Ciesielski and Marek Aljewicz The Microbiota of Edam Cheeses Determined by Cultivation and High-Throughput Sequencing of the 16S rRNA Amplicon Reprinted from: <i>Appl. Sci.</i> 2020 , <i>10</i> , 4063, doi:10.3390/app10124063	193
Anna Iwaniak and Damir Mogut Metabolic Syndrome-Preventive Peptides Derived from Milk Proteins and Their Presence in Cheeses: A Review Reprinted from: <i>Appl. Sci.</i> 2020 , <i>10</i> , 2772, doi:10.3390/app10082772	205
Anna Iwaniak, Monika Hryniewicz, Piotr Minkiewicz, Justyna Bucholska and Małgorzata Darewicz Soybean (<i>Glycine max</i>) Protein Hydrolysates as Sources of Peptide Bitter-Tasting Indicators: An Analysis Based on Hybrid and Fragmentomic Approaches Reprinted from: <i>Appl. Sci.</i> 2020 , <i>10</i> , 2514, doi:10.3390/app10072514	241
Vítor João Pereira Domingues Martinho Agricultural Entrepreneurship in the European Union: Contributions for a Sustainable Development Reprinted from: <i>Appl. Sci.</i> 2020 , <i>10</i> , 2080, doi:10.3390/app10062080	267
Miriam del Rocío Medina-Herrera, María de la Luz Xochilt Negrete-Rodríguez, José Luis Álvarez-Trejo, Midory Samaniego-Hernández, Leopoldo González-Cruz, Aurea Bernardino-Nicanor and Eloy Conde-Barajas Evaluation of Non-Conventional Biological and Molecular Parameters as Potential Indicators of Quality and Functionality of Urban Biosolids Used as Organic Amendments of Agricultural Soils Reprinted from: <i>Appl. Sci.</i> 2020 , <i>10</i> , 517, doi:10.3390/app10020517	289
Iwona Gołaś, Jacek Potorski, Małgorzata Woźniak, Piotr Niewiadomski, Ma Guadalupe Aguilera-Arreola, Araceli Contreras-Rodríguez and Anna Gotkowska-Płachta Amaranth Meal and Environmental <i>Carnobacterium maltaromaticum</i> Probiotic Bacteria as Novel Stabilizers of the Microbiological Quality of Compound Fish Feeds for Aquaculture Reprinted from: <i>Appl. Sci.</i> 2020 , <i>10</i> , 5114, doi:10.3390/app10155114	321

Daniela Lopez-Betancur, Ivan Moreno, Carlos Guerrero-Mendez, Domingo Gómez-Meléndez, Manuel de J. Macías P. and Carlos Olvera-Olvera Effects of Colored Light on Growth and Nutritional Composition of Tilapia, and Biofloc as a Food Source Reprinted from: <i>Appl. Sci.</i> 2020 , <i>10</i> , 362, doi:10.3390/app10010362	337
Zhaoquan He, Xue Shang and Tonghui Zhang Study on Water Saving Potential and Net Profit of <i>Zea mays</i> L.: The Role of Surface Mulching with Micro-Spray Irrigation Reprinted from: <i>Appl. Sci.</i> 2020 , <i>10</i> , 402, doi:10.3390/app10010402	351
Tomasz Dulski, Roman Kujawa, Martyna Godzieba and Slawomir Ciesielski Effect of Salinity on the Gut Microbiome of Pike Fry (<i>Esox lucius</i>) Reprinted from: <i>Appl. Sci.</i> 2020 , <i>10</i> , 2506, doi:10.3390/app10072506	367

About the Editors

Wojciech Janczukowicz (Professor) Wojciech Janczukowicz is a Professor at the Chair of Environment Engineering, the Faculty of Geoengineering of the University of Warmia and Mazury in Olsztyn, Poland. His scientific interests are focused on wastewater treatment using reactors with attached biomass, treatment of wastewater from agriculture and the agri-food industry, the use of an external carbon source in the processes of dephosphatization and denitrification in reactors with suspended and fixed biomass, the impact of projects on the environment, environmental management systems. During his scientific career, Wojciech Janczukowicz was a Fulbright Academic Exchange Program participant. He completed a 3-month Preacademic Course at the Texas University in Austin, USA and a 9-month study of Advanced Technologies in Biological Wastewater Treatment at the New Jersey Institute of Technology in Newark, N.J., USA (1988/1989). Prof. Wojciech Janczukowicz was also a visiting scientist at University of Sunderland, Great Britain (1-month scholarship at Ecology Centre. 1993; 3-week scholarship at Ecology Centre. 1994). He is a member of the Polish Association of Sanitary Engineers and Technicians.

Joanna Rodziewicz (University Professor) Joanna Rodziewicz is a University Professor at the Chair of Environment Engineering, the Faculty of Geoengineering of the University of Warmia and Mazury in Olsztyn, Poland. Her scientific interests are focused on wastewater treatment technologies based on attached and suspended biomass application. Her investigations are about biological, electrochemical and electrobiochemical wastewater treatment in aerobic and anaerobic biofilm reactors (rotating disc contactors (RBC), bio-electrical reactors (BER and REBC) and aerobic and anaerobic reactors with biofilm and suspended biomass (sequencing batch biofilm reactor (SBBR), anaerobic rotating disc batch reactor (ARDBR), bio-electrochemical SBBR (BSBBR). These studies concern reactors' applications for phosphorus and nitrogen removal from specific wastewater including dairy, aquaculture, soilless plant cultivation. and de-icing airport pavements. The other area of her research relates to quantitative and qualitative characteristics of sludges formed during specific wastewater treatment in biofilm reactors. Prof. Joanna Rodziewicz works also on biofilters with innovative filling for low-temperature treatment of sewage from de-icing airport runways. Joanna Rodziewicz was a participant in the training program PHARE Partnership in AMU Center Aalborg, Denmark, 2000. She is a member of the Polish Association of Environmental and Resource Economists.

Anna Iwaniak (Professor) Anna Iwaniak is a Professor at the Chair of Food Biochemistry, the Faculty of Food Science of the University of Warmia and Mazury in Olsztyn. Her scientific interests are focused on the analysis of peptides derived from food proteins, mainly searching and co-developing new tools for bioinformatic analysis useful in the studies on bioactive and functional peptides. This area is related to developing BIOPEP-UWM database of protein and bioactive peptide sequences. During her scientific career, Anna Iwaniak was awarded Marie Curie scholarship for a 3-month scientific visit at the European Bioinformatics Institute in Hinxton, Cambridgeshire (Great Britain; 01 December 2001 – 01 March 2002). In 2005, she was a post-doc at the University of British Columbia, Faculty of Food and Land Systems, Vancouver (Canada). In 2009, she was a visiting scientist at the Institute of Chemistry, Faculty of Science and Technology, University of Tartu (Estonia). Prof. Anna Iwaniak was also a visiting scientist at University of Porto (Portugal) as well as Agricultural University of Athens in Greece. She is a member of: the European Peptide Society (EPS),

the International Society for Nutraceuticals and Functional Foods (ISNFF), and the Polish Society of Food Technologists (in Polish: PTTŻ).

Editorial

New Trends in Environmental Engineering, Agriculture, Food Production, and Analysis

Anna Iwaniak ¹, Wojciech Janczukowicz ² and Joanna Rodziewicz ^{2,*}

¹ Faculty of Food Science, University of Warmia and Mazury in Olsztyn, Pl. Cieszyński 1, 10-726 Olsztyn, Poland; ami@uwm.edu.pl

² Faculty of Geoengineering, University of Warmia and Mazury in Olsztyn, Warszawska 117a, 10-719 Olsztyn, Poland; jawoj@uwm.edu.pl

* Correspondence: joanna.rodziewicz@uwm.edu.pl

Modern agriculture and aquaculture, as well as related food processing, are associated with a significant use of environmental resources and a growing impact on the natural environment. Research is being carried out on the use of modern technologies of plant breeding, animal husbandry, sustainable water, energy, sewage and waste management in food production and processing, as well as new technologies for wastewater treatment and waste disposal, in order to protect the natural environment.

This Special Issue presents the latest advances in agriculture, aquaculture, food technology, and environmental engineering, discussing, among others, the following issues: New technologies in water and wastewater treatment; new sludge and waste management systems; the role of technological processes to improve food quality and safety; new trends in the analysis of food and food components including *in vitro*, *in vivo*, and *in silico* methods; and functional and structural aspects of bioactivities of food molecules.

This book includes a series of twenty one research studies that reveal new knowledge about environmental engineering, agriculture, and food protection. The topics covered span many diverse areas including: Environmental engineering [1–8], agriculture, food properties and protection [9–17], and aquaculture [18–21].

Author Contributions: All authors contributed equally to the preparation of this manuscript. All authors have read and agreed to the published version of the manuscript.

Funding: Project financially supported by Minister of Science and Higher Education in the range of the program entitled “Regional Initiative of Excellence” for the years 2019–2022, project No. 010/RID/2018/19, amount funding 12.000.000 PLN.

Institutional Review Board Statement: Not applicable.

Informed Consent Statement: Not applicable.

Data Availability Statement: Not applicable.

Acknowledgments: This publication was only possible with the invaluable contributions from the authors, reviewers, and the editorial team of *Applied Sciences*.

Conflicts of Interest: The authors declare no conflict of interest.



Citation: Iwaniak, A.; Janczukowicz, W.; Rodziewicz, J. New Trends in Environmental Engineering, Agriculture, Food Production, and Analysis. *Appl. Sci.* **2021**, *11*, 2745. <https://doi.org/10.3390/app11062745>

Received: 8 March 2021

Accepted: 15 March 2021

Published: 18 March 2021

Publisher’s Note: MDPI stays neutral with regard to jurisdictional claims in published maps and institutional affiliations.



Copyright: © 2021 by the authors. Licensee MDPI, Basel, Switzerland. This article is an open access article distributed under the terms and conditions of the Creative Commons Attribution (CC BY) license (<https://creativecommons.org/licenses/by/4.0/>).

References

- Micek, A.; Józwiakowski, K.; Marzec, M.; Listosz, A.; Grabowski, T. Efficiency and Technological Reliability of Contaminant Removal in Household WWTPs with Activated Sludge. *Appl. Sci.* **2021**, *11*, 1889. [[CrossRef](#)]
- Mielcarek, A.; Rodziejewicz, J.; Janczukowicz, W.; Ostrowska, K. The Kinetics of Pollutant Removal through Biofiltration from Stormwater Containing Airport De-Icing Agents. *Appl. Sci.* **2021**, *11*, 1724. [[CrossRef](#)]
- Sikora, M.; Nowosad, J.; Kucharczyk, D. Comparison of Different Biofilter Media During Biological Bed Maturation Using Common Carp as a Biogen Donor. *Appl. Sci.* **2020**, *10*, 626. [[CrossRef](#)]
- Grochowska, J.; Augustyniak, R.; Łopata, M.; Tandyrak, R. Is It Possible to Restore a Heavily Polluted, Shallow, Urban Lake? *Appl. Sci.* **2020**, *10*, 3698. [[CrossRef](#)]
- Toldrá-Reig, F.; Mora, L.; Toldrá, F. Developments in the Use of Lipase Transesterification for Biodiesel Production from Animal Fat Waste. *Appl. Sci.* **2020**, *10*, 5085. [[CrossRef](#)]
- Yaman, C. Application of Sterilization Process for Inactivation of *Bacillus Stearothermophilus* in Biomedical Waste and Associated Greenhouse Gas Emissions. *Appl. Sci.* **2020**, *10*, 5056. [[CrossRef](#)]
- Toldrá-Reig, F.; Mora, L.; Toldrá, F. Trends in Biodiesel Production from Animal Fat Waste. *Appl. Sci.* **2020**, *10*, 3644. [[CrossRef](#)]
- Kasinski, S. Mesophilic and Thermophilic Anaerobic Digestion of Organic Fraction Separated during Mechanical Heat Treatment of Municipal Waste. *Appl. Sci.* **2020**, *10*, 2412. [[CrossRef](#)]
- Zhang, S.; Qiu, B.; Xue, X.; Sun, T.; Gu, W.; Zhou, F.; Sun, X. Effects of Crop Protection Unmanned Aerial System Flight Speed, Height on Effective Spraying Width, Droplet Deposition and Penetration Rate, and Control Effect Analysis on Wheat Aphids, Powdery Mildew, and Head Blight. *Appl. Sci.* **2021**, *11*, 712. [[CrossRef](#)]
- Jiroutová, P.; Sedlák, J. Cryobiotechnology of Plants: A Hot Topic not Only for Gene Banks. *Appl. Sci.* **2020**, *10*, 4677. [[CrossRef](#)]
- Villaseñor-Aguilar, M.-J.; Sánchez-Bravo, M.-G.; Padilla-Medina, J.-A.; Vázquez-Vera, J.L.; Guevara-González, R.-G.; García-Rodríguez, F.-J.; Barranco-Gutiérrez, A.-I. A Maturity Estimation of Bell Pepper (*Capsicum annum* L.) by Artificial Vision System for Quality Control. *Appl. Sci.* **2020**, *10*, 5097. [[CrossRef](#)]
- Bykowska-Derda, A.; Kolay, E.; Kaluzna, M.; Czapka-Matyasik, M. Emerging Trends in Research on Food Compounds and Women's Fertility: A Systematic Review. *Appl. Sci.* **2020**, *10*, 4518. [[CrossRef](#)]
- Nalepa, B.; Ciesielski, S.; Aljewicz, M. The Microbiota of Edam Cheeses Determined by Cultivation and High-Throughput Sequencing of the 16S rRNA Amplicon. *Appl. Sci.* **2020**, *10*, 4063. [[CrossRef](#)]
- Iwaniak, A.; Mogut, D. Metabolic Syndrome-Preventive Peptides Derived from Milk Proteins and Their Presence in Cheeses: A Review. *Appl. Sci.* **2020**, *10*, 2772. [[CrossRef](#)]
- Iwaniak, A.; Hryniewicz, M.; Minkiewicz, P.; Bucholska, J.; Darewicz, M. Soybean (*Glycine max*) Protein Hydrolysates as Sources of Peptide Bitter-Tasting Indicators: An Analysis Based on Hybrid and Fragmentomic Approaches. *Appl. Sci.* **2020**, *10*, 2514. [[CrossRef](#)]
- Martinho, V.J.P.D. Agricultural Entrepreneurship in the European Union: Contributions for a Sustainable Development. *Appl. Sci.* **2020**, *10*, 2080. [[CrossRef](#)]
- Medina-Herrera, M.D.R.; Negrete-Rodríguez, M.D.L.L.X.; Álvarez-Trejo, J.L.; Samaniego-Hernández, M.; González-Cruz, L.; Bernardino-Nicanor, A.; Conde-Barajas, E. Evaluation of Non-Conventional Biological and Molecular Parameters as Potential Indicators of Quality and Functionality of Urban Biosolids Used as Organic Amendments of Agricultural Soils. *Appl. Sci.* **2020**, *10*, 517. [[CrossRef](#)]
- Gołaś, I.; Potorski, J.; Woźniak, M.; Niewiadomski, P.; Aguilera-Arreola, M.G.; Contreras-Rodríguez, A.; Gotkowska-Płachta, A. Amaranth Meal and Environmental *Carnobacterium maltaromaticum* Probiotic Bacteria as Novel Stabilizers of the Microbiological Quality of Compound Fish Feeds for Aquaculture. *Appl. Sci.* **2020**, *10*, 5114. [[CrossRef](#)]
- Lopez-Betancur, D.; Moreno, I.; Guerrero-Mendez, C.; Gómez-Meléndez, D.; P., M.D.J.M.; Olvera-Olvera, C. Effects of Colored Light on Growth and Nutritional Composition of Tilapia, and Biofloc as a Food Source. *Appl. Sci.* **2020**, *10*, 362. [[CrossRef](#)]
- He, Z.; Shang, X.; Zhang, T. Study on Water Saving Potential and Net Profit of *Zea mays* L.: The Role of Surface Mulching with Micro-Spray Irrigation. *Appl. Sci.* **2020**, *10*, 402. [[CrossRef](#)]
- Dulski, T.; Kujawa, R.; Godzieba, M.; Ciesielski, S. Effect of Salinity on the Gut Microbiome of Pike Fry (*Esox lucius*). *Appl. Sci.* **2020**, *10*, 2506. [[CrossRef](#)]

Article

Efficiency and Technological Reliability of Contaminant Removal in Household WWTPs with Activated Sludge

Agnieszka Micek ¹, Krzysztof Józwiakowski ^{1,*}, Michał Marzec ¹, Agnieszka Listosz ¹ and Tadeusz Grabowski ^{1,2}

¹ Department of Environmental Engineering and Geodesy, University of Life Sciences in Lublin, Leszczyńskiego 7, 20-069 Lublin, Poland; agnieszka.micek@up.lublin.pl (A.M.); michal.marzec@up.lublin.pl (M.M.); agnieszka.listosz@up.lublin.pl (A.L.); tadeusz.grabowski@up.lublin.pl (T.G.)

² Roztocze National Park, Plażowa 2, 22-470 Zwierzyniec, Poland

* Correspondence: krzysztof.jozwiakowski@up.lublin.pl

Abstract: The results of research on the efficiency and technological reliability of domestic wastewater purification in two household wastewater treatment plants (WWTPs) with activated sludge are presented in this paper. The studied facilities were located in the territory of the Roztocze National Park (Poland). The mean wastewater flow rate in the WWTPs was 1.0 and 1.6 m³/day. In 2017–2019, 20 series of analyses were done, and 40 wastewater samples were taken. On the basis of the received results, the efficiency of basic pollutant removal was determined. The technological reliability of the tested facilities was specified using the Weibull method. The average removal efficiencies for the biochemical oxygen demand in 5 days (BOD₅) and chemical oxygen demand (COD) were 66–83% and 62–65%, respectively. Much lower effects were obtained for total suspended solids (TSS) and amounted to 17–48%, while the efficiency of total phosphorus (TP) and total nitrogen (TN) removal did not exceed 34%. The analyzed systems were characterized by the reliability of TSS, BOD₅, and COD removal at the level of 76–96%. However, the reliability of TN and TP elimination was less than 5%. Thus, in the case of biogenic compounds, the analyzed systems did not guarantee that the quality of treated wastewater would meet the requirements of the Polish law during any period of operation. This disqualifies the discussed technological solution in terms of its wide application in protected areas and near lakes, where the requirements for nitrogen and phosphorus removal are high.

Keywords: efficiency of contaminant removal; technological reliability; wastewater purification; activated sludge; national park



Citation: Micek, A.; Józwiakowski, K.; Marzec, M.; Listosz, A.; Grabowski, T. Efficiency and Technological Reliability of Contaminant Removal in Household WWTPs with Activated Sludge. *Appl. Sci.* **2021**, *11*, 1889. <https://doi.org/10.3390/app11041889>

Received: 29 January 2021

Accepted: 17 February 2021

Published: 21 February 2021

Publisher's Note: MDPI stays neutral with regard to jurisdictional claims in published maps and institutional affiliations.



Copyright: © 2021 by the authors. Licensee MDPI, Basel, Switzerland. This article is an open access article distributed under the terms and conditions of the Creative Commons Attribution (CC BY) license (<https://creativecommons.org/licenses/by/4.0/>).

1. Introduction

In national parks and protected areas, there are usually museums, forester's lodges, hostels, or tourist trails with resting places for visitors, which should be equipped with sanitary infrastructure that ensures their proper functioning. According to the Law on Nature Protection [1] in Poland and the Council Directive 92/43/EEC [2], in the area of national parks and nature reserves, it is forbidden to build or reconstruct any buildings or technical facilities with the exception of facilities and devices that serve to achieve the goals of the given national park or nature reserve. For this reason, it is essential in protected areas to use water supply systems and wastewater treatment plants (WWTPs) that do not interfere with the environment [3,4] and meet the criteria of sustainable development and nature protection [5–7].

Domestic wastewater generated by various tourist facilities in national parks or protected areas, just as in rural areas, is most often discharged to non-return tanks (septic tanks) and is then taken to collective WWTPs or disposed of in individual wastewater treatment systems, i.e., in so-called small household WWTPs [8,9]. A similar way of dealing with domestic sewage in protected and rural areas, where sewerage systems and collective treatment plants are lacking, is also in force in other countries around the world [10–19].

In recent years, household WWTPs have increasingly become one of the basic elements of technical infrastructure in protected areas where, due to natural and landscape values and large dispersion of tourist buildings, the installation of a sewerage network and a collective WWTP is not justified [9,13,14,17,19]. In accordance with Polish Standard PN-EN 12,566 [20], household WWTPs are defined as facilities for 50 inhabitants. However, on the basis to the Water Law [21], the maximum capacity of such systems in Poland should not exceed 5 m³/day.

Various technological solutions are currently used to treat small amounts of wastewater, such as systems with drainage pipes, systems with a sand filter, WWTPs with activated sludge, systems with a biological bed, hybrid systems (activated sludge + biological bed), and constructed wetland systems (CWs) [7,22].

A review of the literature on the evolution of wastewater management and its development over the centuries was presented by Lofrano and Brown [23]. Currently, the activated sludge method is the most commonly used for wastewater purification in the world. Activated sludge is most often used for urban wastewater treatment [24–27], as well as for industrial wastewater [28,29]. The popularity of the activated sludge method used in large WWTPs around the world has led to the development of “miniature” facilities of this type, whereby for over 30 years, attempts have been made to replicate the technological processes [24,30–35]. However, it is important for household WWTPs with activated sludge, which are used to treat small sewage amounts, to meet the appropriate criteria.

The most important aspects that should be considered during the selection of a technological solution involving small WWTPs are the efficiency of pollutant removal and the reliability of operation [4]. These criteria should be taken into account especially for WWTPs installed in protected areas [36]. In the case of WWTPs, efficiency refers to the degree of removal of particular types of pollutants, which is determined by the amount of pollutants retained in the system in relation to the amount of pollutants entering the system. Reliability, on the other hand, is defined as the ability to treat wastewater to the degree required by the wastewater receiver over the assumed operating time, including changes in the quantity and the composition of the inflow [32,33]. The reliability level corresponds to the probability of reaching a value of the indicator in the outflow from the WWTPs that is lower than the acceptable value; thus, reliability can be understood as the percentage of time during which the expected concentrations of pollutants in the treated wastewater are in accordance with the accepted standards or purification objectives [37,38].

The reliability and operational efficiency of activated sludge WWTPs have been previously studied by different authors [32,33,35,37,39–41]. However, there is still a lack of research results on the technological reliability of household WWTPs with activated sludge, which are analyzed over a longer period of time, especially in facilities operating in protected areas. A comprehensive analysis of the efficiency of operation of different types of WWTPs based on statistical inference and taking into account elements of reliability theory makes it possible to identify technological solutions which are characterized by the highest efficiency and stability of operation under changing conditions during many years of operation. This is important from the administrative, legal, and ecological point of view. It allows estimating the chances of passing possible control procedures, as well as establishing a hierarchy of particular technological solutions in terms of their influence on the environment. The results regarding the efficiency and reliability of household WWTP technologies should be an important element in planning the development of technical infrastructure, enabling the selection of optimal solutions under given conditions [32].

The purpose of this paper is to present the results of research on the technological reliability and the efficiency of domestic wastewater purification in two household WWTPs with activated sludge located in the area of the Roztocze National Park (RNP) in Poland. The paper contributes new content to science, because, in the world, there remain few studies related to the technological reliability of household WWTPs operating on a real scale.

2. Materials and Methods

2.1. Presentation of the Studied Facilities

The RNP is located in southeastern Poland in a temperate, transitional climate zone. Groundwater, as well as surface water, in the RNP is of a very good quality; thus, it is crucial to protect it from degradation [42]. In order to protect the quality of surface water and groundwater, in recent years, within the area of the RNP, some steps have been taken to build household WWTPs to treat wastewater outflowing from foresters' lodges.

For the analysis, two household WWTPs located in the area of the RNP were selected. The studied facilities consist of a four-chamber preliminary settling tank and a special reactor with activated sludge. They are located in Obrocz for the office building (facility no. 1) and Rybakówka for the forester's lodge (facility no. 2). The exact location of these facilities in the RNP was presented by Micek et al. [9]. The mean wastewater flow rate in the studied WWTPs was 1.0 and 1.6 m³/day, respectively. In Table 1, chosen technological parameters of the studied facilities are presented, and Figure 1 shows their technological scheme. The efficiency of pollutant removal in preliminary settling tanks, which are the first components of the selected household WWTPs in the RNP, was presented by Micek et al. [9].

Table 1. Technological parameters of the household WWTPs in the area of the RNP.

Technological Parameters	Facility No. 1—Obrocz	Facility No. 2—Rybakówka
Year of construction	2014	2014
Mean wastewater capacity Q (m ³ /day)	1.0	1.6
Volume of a septic tank (m ³)	5.7	5.7
Volume of an activated sludge chamber (m ³)	1.42	1.83
Wastewater receiver	soil	soil

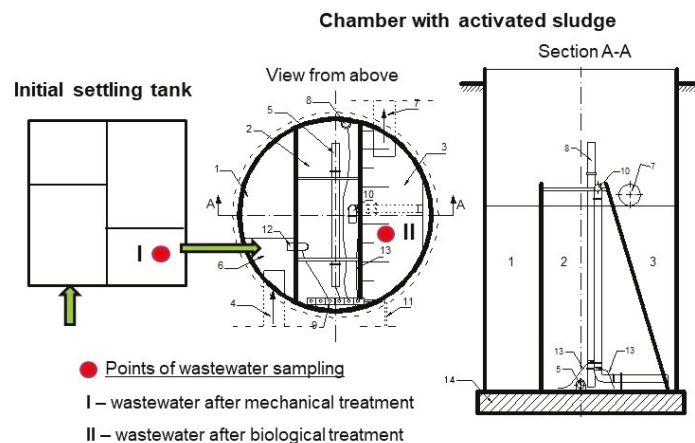


Figure 1. Technological scheme of the household wastewater treatment plants (WWTPs) in the area of the Roztocze National Park (RNP) (prepared on the basis of [43]). Scheme: 1—denitrification chamber; 2—nitrification chamber; 3—separation chamber; 4—wastewater inlet; 5—tube diffuser; 6—basket grate; 7—wastewater outlet; 8—sludge outlet; 9—air distributor; 10—sludge recirculation; 11—air supply; 12—sludge recirculation; 13—air for sludge recirculation; 14—concrete foundation.

2.2. Analytical and Statistical Methods

Studies on the technological reliability and the efficiency of pollutant removal in the two chosen facilities were performed in 2017–2019. Wastewater samples for analyses were taken in different seasons (spring, summer, autumn, and winter) from (I) the four-chamber of the preliminary settling tank—after mechanical treatment, and (II) the outflow from an activated sludge chamber—after biological treatment (Figure 1).

During the study, 20 series of analyses were done and 40 wastewater samples were taken, in which parameters such as total suspended solids (TSS), biochemical oxygen demand in 5 days (BOD₅), chemical oxygen demand (COD), total nitrogen (TN), total phosphorus (TP), pH, dissolved oxygen (DO), nitrate nitrogen, nitrite nitrogen, and ammonium nitrogen were determined. Sampling, sample transportation, processing, and analyses were completed on the basis of Polish Standards of Wastewater Examination, which are compatible with the American Public Health Association—APHA [44,45]. The laboratory apparatus used to carry out the analyses was presented in another paper published by Micek et al. [9].

The obtained measurement data enabled calculating the mean, minimum, and maximum concentration of pollutant values and their standard deviation. The mean concentrations of the analyzed pollutant parameters in the influent and effluent from the WWTPs were used to determine the efficiency of pollutant removal (Figure 2).

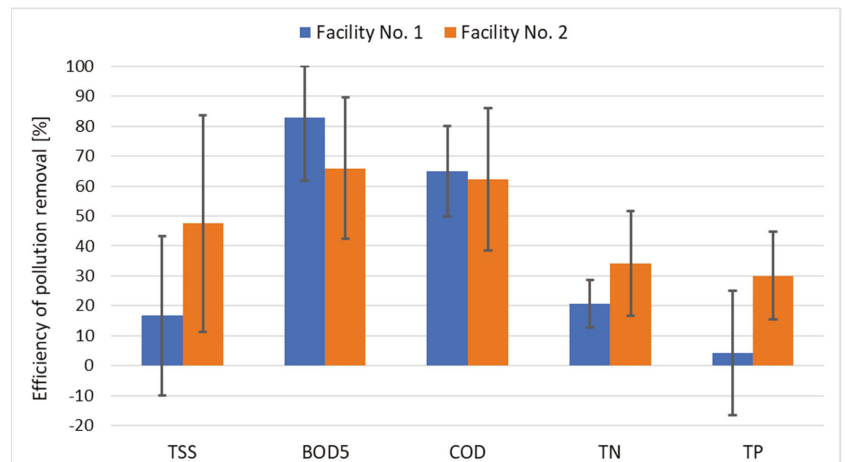


Figure 2. Average efficiency of pollutant removal in two studied household WWTPs.

The evaluation of the technological reliability of the WWTPs was carried out using elements of Weibull’s reliability theory, which is a useful tool in assessing the risk of exceeding the normative values in wastewater discharged to the receiver [46].

The Weibull distribution is characterized by the following probability density function [46]:

$$f(x) = \frac{c}{b} \cdot \frac{x - \theta}{b}^{(c-1)} \cdot e^{-\left(\frac{x-\theta}{b}\right)^c}, \quad (1)$$

where x is a variable describing the concentration of a pollution parameter in the treated effluent, b is a scale parameter, c is a shape parameter, θ is a position parameter, and e is a constant, assuming $\theta < x$, $b > 0$, $c > 0$, and $e = 2.71828$.

A variable specifying the values of basic pollution indicators (TSS, BOD₅, COD, TN, and TP) in treated wastewater ($n = 20$) was analyzed. The analysis consisted of the estimation of the Weibull distribution parameters using the maximum-likelihood method and the verification of the null hypothesis that the analyzed variable could be

described by the Weibull distribution. The null hypothesis was verified with the Hollander-Proschan test at the significance level of 0.05 [36]. Reliability was determined from the cumulative distribution function plotted in the graphs, taking into account the normative values of the indicators specified in the Polish regulations [47] for wastewater discharged from treatment plants of up to 2000 PE (population equivalent): BOD₅—40 mg O₂·dm⁻³, COD—150 mg O₂·dm⁻³, TSS—50 mg·dm⁻³, TN—30 mg·dm⁻³, and TP—5 mg·dm⁻³. In the case of TN and TP, the values defined for wastewater discharged into lakes and their tributaries, as well as directly into artificial water reservoirs located in flowing waters, were adopted as standard values [47]. The analysis was carried out using Statistica 13.

3. Results and Discussion

3.1. The Efficiency of Pollutant Removal

The chosen statistical values of pollutants in wastewater from the studied household WWTPs are presented in Tables 2 and 3. The concentrations of pollutants in wastewater inflowing to the chambers with activated sludge (after mechanical treatment) were relevantly lower in comparison to raw wastewater flowing into the preliminary settling tanks (the first element of the system), as described in an earlier paper [9]. The values of pollutant concentrations in wastewater inflowing to the activated sludge chambers in the studied WWTPs were close to those described in the literature for wastewater treated mechanically in the preliminary settling tanks [34,35,46,48–50].

Table 2. Pollutant concentrations in the inflow and outflow of facility no. 1. TSS, total suspended solids; BOD₅, biochemical oxygen demand in 5 days; COD, chemical oxygen demand; TN, total nitrogen; TP, total phosphorus.

Parameters		Statistical Indicators							
		Mean		Min		Max		Standard Deviation	
		in	out	in	out	in	out	in	out
pH	-	-	-	7.90	6.29	8.22	7.72	-	-
Dissolved oxygen	mg O ₂ /dm ³	1.62	8.02	0.23	3.15	7.02	10.56	1.63	1.97
TSS	mg/dm ³	28.7	23.9	5.3	1.3	69.0	73.0	20.9	18.6
BOD ₅	mgO ₂ /dm ³	53.0	9.0	12.3	1.0	80.0	53.0	22.1	12.9
COD	mgO ₂ /dm ³	180	63	111	20.7	236	130	34.3	27.43
Ammonium nitrogen	mg/dm ³	136.0	39.9	111.0	15.0	172.0	80.5	17.2	18.1
Nitrate nitrogen	mg/dm ³	1.97	61.17	0.09	25.5	5.70	87.7	1.89	17.88
Nitrite nitrogen	mg/dm ³	0.31	1.36	0.03	0.59	1.17	3.97	0.43	0.81
TN	mg/dm ³	160	127	121	94	207	159	24.4	15.3
TP	mg/dm ³	12.0	11.5	8.2	9.5	17.2	19.0	3.0	2.2

TSS is a measure of the floating solid content in wastewater, which indicates its clarity [51,52]. At the researched facilities no. 1 and 2, the removal efficiency of TSS was low and amounted to 17% and 48%, respectively (Figure 2). The low efficiency of TSS removal in the analyzed systems is due to the fact that a significant proportion (>60%) is removed in the preliminary settling tanks, which constitutes the first elements of the studied WWTPs [9]. Better results for TSS removal (58–94%) were found by Marzec and Józwiakowski [31] in three facilities with activated sludge but without preliminary settling tanks. Quite high TSS removal effects (90–96%) were also obtained by Jakubaszek and Stadnik [53] in household WWTPs operating with low activated sludge technology in a sequential batch reactor (SBR) system. A study conducted on two household hybrid CW WWTPs of VF/HF type (with vertical and horizontal flow) with common reed and willow, operating in the RNP, showed that they also provide quite high efficiency (80–87%) of TSS

removal [36]. Furthermore, Marzec et al. [49], in a CW with common reed, manna grass, and Virginia mallow, obtained an efficiency of TSS removal of more than 86%.

Table 3. Pollutants concentrations in the inflow and outflow of the facility no. 2.

Parameters		Statistical Indicators							
		Mean		Min		Max		Standard Deviation	
		in	out	in	out	in	out	in	out
pH	-	-	-	7.04	6.14	11.9	7.86	-	-
Dissolved oxygen	mg O ₂ /dm ³	1.29	3.03	0.21	0.60	3.75	9.48	1.09	2.37
TSS	mg/dm ³	34.5	18.1	3.8	2.7	116	48.8	31.0	14.1
BOD ₅	mgO ₂ /dm ³	85.6	29.1	16	1.6	250	63.4	58.2	24
COD	mgO ₂ /dm ³	251	95	109	18	400	179	88	52.3
Ammonium nitrogen	mg/dm ³	97.6	53.4	58	1.1	134	102	19.7	33.0
Nitrate nitrogen	mg/dm ³	0.62	11.5	0.18	0.5	1.2	54.2	0.32	17.70
Nitrite nitrogen	mg/dm ³	0.14	0.31	0.05	0.02	0.76	1.68	0.20	0.49
TN	mg/dm ³	117	77.0	60.0	35.0	182	104	25.1	18.7
TP	mg/dm ³	17.3	12.1	11.4	9.6	30.9	15.8	5.7	2.1

The conducted study shows that the average concentrations of TSS in outflow from the analyzed WWTPs were 23.9 mg/dm³ for facility no. 1 and 18.1 mg/dm³ for facility no. 2 (Tables 2 and 3). These values are lower than the permissible value (50 mg/dm³) determined in Polish regulations [47]. However, Marzec and Józwiakowski [31] found significantly higher concentrations of TSS (55–122 mg/dm³) in the outflow from three other facilities with activated sludge but without preliminary settling tanks.

BOD₅. The efficiency of BOD₅ removal in the studied facilities no. 1 and 2 was diverse and amounted to 83% and 66%, respectively (Figure 2). Similar effects of BOD₅ removal (61–95%) were found by Marzec and Józwiakowski [31] in three other facilities with activated sludge but without preliminary settling tanks. Quite high BOD₅ removal effects (92–97%) were also obtained by Jakubaszek and Stadnik [53] in household WWTPs operating with an SBR system. Very high (98–99%) BOD₅ removal efficiency was also obtained in two hybrid household CWs of VF/HF type operating in the RNP [36]. Moreover, Marzec et al. [49] in a household CW WWTP obtained an efficiency of BOD₅ removal greater than 95%.

The average BOD₅ in outflow from the studied facilities no. 1 and 2 was 9.0 and 29.1 mg/dm³, respectively (Tables 2 and 3). These results are lower than the permissible value (40 mg/dm³) specified in Polish regulations [47]. Significantly higher BOD₅ values (24.9 to 267 mg/dm³) were found by Marzec and Józwiakowski [31] in three WWTPs with activated sludge operating without a classical mechanical stage.

COD. At the studied facilities no. 1 and 2, the COD removal efficiency was similar and amounted to 65% and 62%, respectively (Figure 2). Higher effects of COD removal (59–90%) were found by Marzec and Józwiakowski [31] in three other facilities with activated sludge without preliminary settling tanks. Similarly high COD removal effects (83–90%) were also obtained by Jakubaszek and Stadnik [53] in individual SBR systems. A study of two hybrid household CW WWTPs in the RNP showed that they also provide very high (96%) COD removal efficiency [36]. In a household hybrid CW, Marzec et al. [49] also obtained more than 95% COD removal efficiency.

The average COD values in the outflow from the analyzed facilities no. 1 and 2 were 63.0 and 95.0 mg/dm³, respectively (Tables 2 and 3). These results are lower than the permissible value (150 mg/dm³) specified in Polish regulations [47]. Marzec and Józwiakowski [31] studied some household WWTPs of similar construction to the analyzed

facilities but lacking classical preliminary settling tanks, and they found higher COD values which amounted to 128–490 mg/dm³.

Total Nitrogen. In the analyzed facilities no. 1 and 2, the efficiency of TN removal was low and amounted to 21% and 34%, respectively (Figure 2). Much lower effects of TN removal (<7%) were found by Marzec and Józwiakowski [31] in three other facilities with activated sludge without preliminary settling tanks. Significantly higher effects of TN removal (51–83%) were obtained by Jakubaszek and Stadnik [53] in household WWTPs operating with SBR systems. High TN removal effects (73–86%) were also obtained by Micek et al. [36] in hybrid household CW WWTPs of VF/HF type in the RNP. Furthermore, Marzec et al. [49], in a household hybrid CW, obtained more than 86% efficiency of TN removal.

The average values of TN concentration in the outflow from the analyzed facilities no. 1 and 2 were high and amounted to 127 and 77 mg/dm³, respectively (Tables 2 and 3). These values are several times higher than the permissible limit (30 mg/dm³) required in Poland for wastewater discharged into lakes and their tributaries [47]. Even higher concentrations of TN (124–320 mg/dm³) were previously found by Marzec and Józwiakowski [31] in the outflow from three other facilities with activated sludge but without classical preliminary settling tanks.

The efficiency of TN removal in activated sludge systems depends primarily on the course of processes such as nitrification or denitrification, among others [54,55]. From the data presented in Tables 2 and 3, it can be seen that the nitrification process in the studied facilities proceeded properly, which is evidenced by a significant decrease in the concentration of ammonium nitrogen and an increase in the content of nitrate and nitrite nitrogen, as well as the concentration of oxygen in the treated wastewater. However, high concentrations of aerobic forms of nitrogen and TN in the outflow from the analyzed systems indicate that the household WWTPs with activated sludge are not able to create appropriate conditions for the denitrification process.

Total Phosphorus. In the studied facilities no. 1 and 2, the efficiency of TP removal was low and amounted to 4% and 30%, respectively (Figure 2). Marzec and Józwiakowski [31] found higher TP removal efficiencies (3–63%) in three other activated sludge facilities without preliminary settling tanks. Higher efficiencies of TP removal (46–74%) were obtained by Jakubaszek and Stadnik [53] in household WWTPs with SBR systems. A study of two household hybrid CWs of VF/HF type operating in the RNP showed that they provide significantly higher efficiency of TP removal (90–94%) than activated sludge systems [36]. Moreover, Marzec et al. [49] achieved high TP removal efficiency (over 95%) in a household hybrid CW.

The average values of TP in the outflow from the analyzed facilities no. 1 and 2 were very high and amounted to 11.5 and 12.1 mg/dm³, respectively (Tables 2 and 3). These values are more than two times higher than the permissible value (5 mg/dm³) required in Poland for wastewater discharged into lakes and their tributaries [47]. In the outflow from three other facilities with activated sludge but without preliminary settling tanks, Marzec and Józwiakowski [31] found even higher of TP concentrations in the outflow (23.2–50.6 mg/dm³).

In the process occurring in activated sludge, phosphorus is mainly removed from wastewater via assimilation, sorption, and chemical precipitation [55]. During wastewater treatment, phosphorus is assimilated by the growing biomass and should be removed with the excess sludge. Effective biological phosphorus removal requires alternating aerobic and anaerobic conditions to allow the selection and growth of specific microorganisms that exhibit the ability to store phosphorus compounds within cells [56,57]. However, the conducted studies and observations show that the analyzed activated sludge WWTPs lack an anaerobic zone and the sludge from the secondary settling tank is not regularly removed, which probably has a negative impact on the effective removal of phosphorus from wastewater and causes its high concentrations in the outflow.

On the basis of the obtained research results and the literature review, it is concluded that household WWTPs with activated sludge provide significantly lower effects of pollutant removal than hybrid CWs, especially in terms of nutrient removal. Therefore, the authors of this paper do not recommend the widespread use of household WWTPs with activated sludge in protected areas.

3.2. Technological Reliability of the Studied Systems

The reliability of the analyzed WWTPs was determined using the Weibull method. In the first step, the distribution parameters were estimated, and the null hypothesis that empirical data can be described by a Weibull distribution was verified. The datasets were the values of the main pollutant indicators (BOD₅, COD, TSS, TN, and TP) in treated wastewater.

The determined values of the distribution parameters (θ , b , c) were consistent with the assumptions made. The null hypothesis was positively verified. The goodness of fit of the obtained distributions at the significance level of $\alpha = 0.05$ was high and was 68–98% for facility no. 1 and 51–99% for facility no. 2 (Table 4).

Table 4. Parameters of the Weibull distribution and the Hollander–Proschan goodness-of-fit test ($n = 20$).

Parameter	Parameters of Weibull Distribution			Hollander–Proschan Goodness-of-Fit Test	
	θ	c	b	Stat	p
Facility no. 1—Obroc					
TSS	−0.2000	1.2122	28.9624	0.0217	0.9826
BOD ₅	0.9636	0.7691	10.0911	0.4015	0.6880
COD	14.6970	1.3850	80.1201	0.2532	0.8000
TN	58.8890	8.6765	132.4568	0.1400	0.8886
TP	9.4444	4.8527	12.5016	0.3000	0.7641
Facility no. 2—Rybakówka					
TSS	2.2929	1.3035	21.5361	0.1127	0.9102
BOD ₅	1.4000	1.0681	28.9343	−0.0998	0.9204
COD	−2.0000	1.8159	102.2153	−0.1191	0.9051
TN	−2.0000	3.1554	78.7167	−0.6526	0.5139
TP	−0.5000	5.5212	12.6970	−0.0081	0.9934

Symbols: stat—value of the test statistic, p —significance level of the test; when $p \leq 0.05$, the distribution of data does not obey a Weibull distribution.

The technological reliability of the studied WWTPs was determined on the basis of the distribution function (Figures 3–7), taking into account the limit values of the indicators, specified in the Regulation of the Minister of Maritime Economy and Inland Navigation [47] for WWTPs below 2000 PE.

Total suspended solids. The reliability of TSS removal in facility no. 1 was 86% (Figure 3A). On this basis, it can be concluded that, for a period of 51 days per year, the treatment plant malfunctioned. During this period, the concentration of TSS in treated wastewater exceeded the limit value (50 mg/dm³). According to Andraka and Dzieńis [58], for WWTPs below 2000 PE, the minimum reliability level should be 97.3%. This means that a treatment plant of this size can malfunction for 9 days per year without adversely affecting the rating of the facility. Taking these assumptions into account, it can be concluded that, in facility no. 1, the concentration of TSS in the outflow from the analyzed WWTP was excessive for 42 days per year.

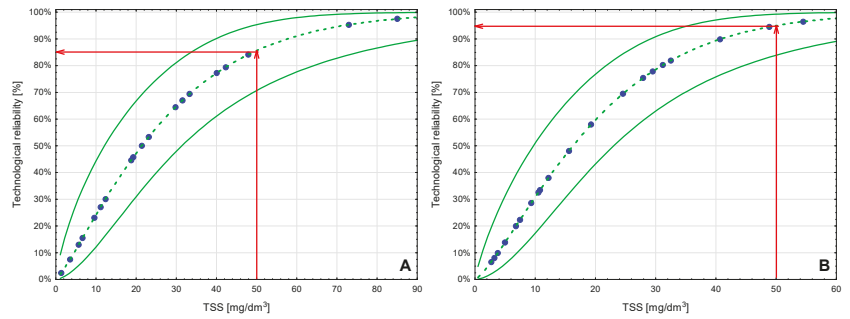


Figure 3. Weibull cumulative distribution functions and the technological reliabilities determined for TSS ((A)—facility no. 1; (B)—facility no. 2). Notation: dashed green line—reliability function, continuous green line—confidence intervals, red arrows—probability of achieving the indicators limit in the effluent.

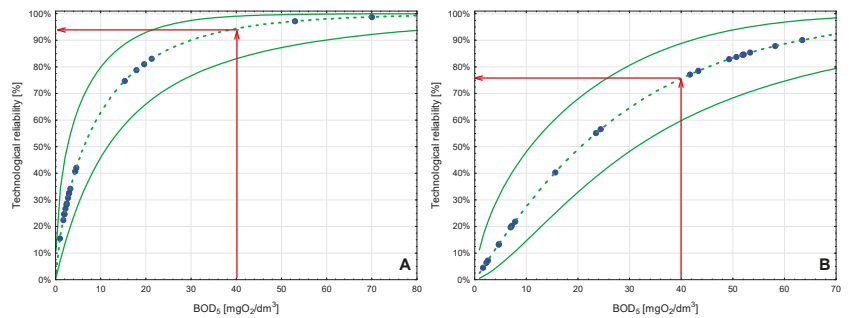


Figure 4. Weibull cumulative distribution functions and the technological reliabilities determined for BOD₅ ((A)—facility no. 1; (B)—facility no. 2). Notation: dashed green line—reliability function, continuous green line—confidence intervals, red arrows—probability of achieving the indicators limit in the effluent.

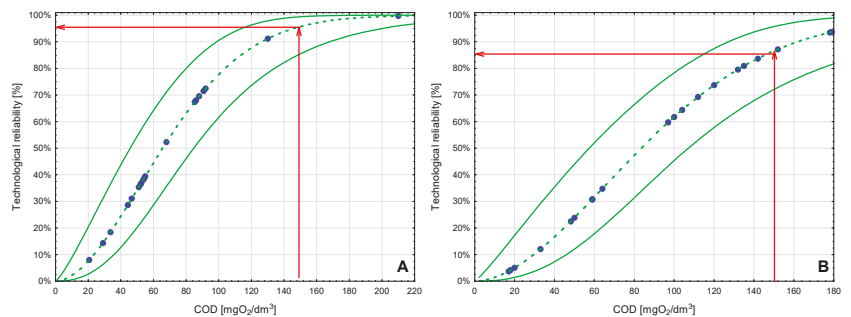


Figure 5. Weibull cumulative distribution functions and the technological reliabilities determined for COD ((A)—facility no. 1; (B)—facility no. 2). Notation: dashed green line—reliability function, continuous green line—confidence intervals, red arrows—probability of achieving the indicators limit in the effluent.

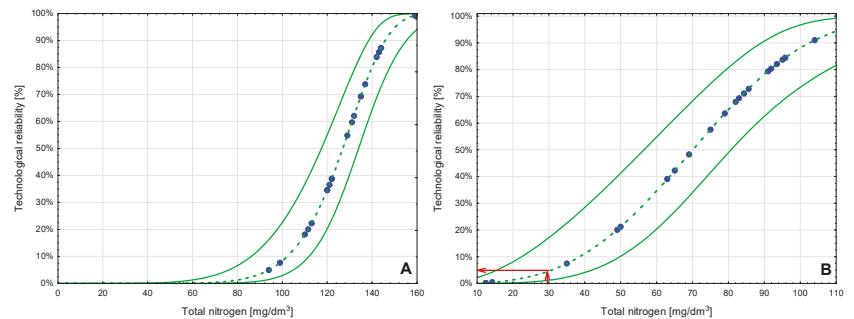


Figure 6. Weibull cumulative distribution functions and the technological reliabilities determined for TN ((A)—facility no. 1; (B)—facility no. 2). Notation: dashed green line—reliability function, continuous green line—confidence intervals, red arrows—probability of achieving the indicators limit in the effluent.

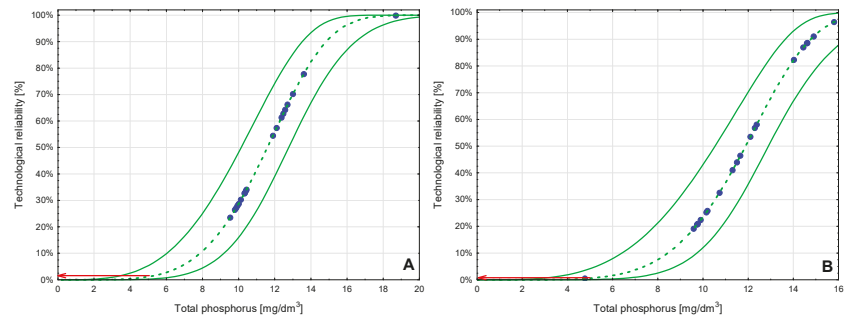


Figure 7. Weibull cumulative distribution functions and the technological reliabilities determined for TP ((A)—facility no. 1; (B)—facility no. 2). Notation: dashed green line—reliability function, continuous green line—confidence intervals, red arrows—probability of achieving the indicators limit in the effluent.

In facility no. 2, the reliability of TSS removal was 95% (Figure 3B), indicating faulty operation of the WWTP for 19 days per year. Taking into account the previously mentioned guidelines [58], it may be concluded that the level of TSS negatively influenced the facility assessment for 10 days per year. Lower reliability levels for the analyzed indicator (about 65%) were found in some studies concerning household WWTP with activated sludge conducted by Bugajski et al. [59] and Marzec [32]. However, 100% technological reliability of TSS removal in a small sequencing batch biofilm reactor (SBBR) with activated sludge was obtained by Jucherski et al. [35]. Research on two other household hybrid CW WWTPs of VF/HF type (with vertical and horizontal flow) operating in the RNP indicated that they also provide quite high (92–100%) reliability of TSS removal [36]. Additionally, Marzec et al. [33] obtained 100% reliability of TSS removal in a household CW. On the basis of the data obtained and the literature review, it appears that activated sludge systems have lower reliability of TSS removal than CW WWTPs.

BOD₅. The technological reliability of BOD₅ removal in facility no. 1 was 95% and that in facility no. 2 was 76% (Figure 4). In facility no. 1, the level of this indicator was higher than the permissible value for 10 days a year. Similarly, in facility no. 2, the level of BOD₅ was elevated for 78 days a year.

In comparison, in a WWTP of identical design but without a preliminary settling tank, the reliability of BOD₅ reduction was 70% [32]. On the other hand, Bugajski et al. [59] in a household system Biocompact BCT S-12 determined the reliability of reducing this

indicator at the level of 88%. The BOD₅ removal reliability in a small SBBR was 77% [35]. On the other hand, maximum (100%) reliability of BOD₅ removal was reported in two other household hybrid CW WWTPs in the RNP [36]. Moreover, Marzec et al. [33] achieved 100% reliability of BOD₅ removal in a household hybrid CW.

COD. The reliability of COD removal was 96% in facility no. 1 and 87% in facility no. 2 (Figure 5). The obtained reliability levels are lower than the minimum required values given by Andraka and Dzienis [58]. In relation to the annual reference period, WWTP no. 1 provided the required level of organic pollutant removal expressed by COD for 359 days, while this value for WWTP no. 2 was 326 days.

The reliability indicators obtained in the analyzed activated sludge facilities in the RPN for COD are comparable to those obtained by Bugajski et al. [59] in a household WWTP working in activated sludge technology. At the same time, in the facilities in the RPN, the reliability of COD removal was higher than that found in a treatment plant based on an identical tank design but without a preliminary settling tank (60%) [32]. The reliability of COD removal in a small SBBR was 97.8% [35]. However, similarly to the case of BOD₅, maximum (100%) COD removal reliability was reported in two other household hybrid CWs WWTPs operating in the RNP [36]. Moreover, Marzec et al. [33] achieved 100% COD removal reliability in a household hybrid CW. The presented results indicate that the reliability of COD removal in household WWTPs with activated sludge is lower than that in CWs.

Total nitrogen. Both analyzed activated sludge WWTPs were characterized by extremely low reliability of TN removal. The probability that the concentration of TN in treated wastewater will not exceed the standard value (30 mg/dm³) was 0% for facility no. 1 and 5% for facility no. 2 (Figure 6).

In the case of TN removal, facility no. 1 operated deficiently throughout the whole year and provided no assurance of passing inspection procedures. On the other hand, in WWTP no. 2, above-normative values of TN in treated wastewater occurred for a period of 338 days per year. Marzec [33], while analyzing a solution identical in terms of construction, but without a classical preliminary settling tank, obtained a reliability of TN removal at the level of 24%. The reliability of TN removal in a small SBBR was only 12.2% [35]. In contrast, TN removal reliability in two other household hybrid CW WWTPs operating in the RNP was much higher and amounted to 35% and 89% [36]. On the other hand, Marzec et al. [33] obtained 94% reliability of TN removal in a household hybrid CW. The analysis of the results of the conducted study through the prism of the results reported in the literature shows that the reliability of TN removal is lower in household WWTPs with activated sludge than in CWs.

Total phosphorus. The reliability of TP removal in the tested household WWTPs with activated sludge was even lower. The probability that the content of TP in the effluent from facility no. 1 will meet the permissible value at the operator risk of $\alpha = 0.05$ was 1%. For facility no. 2, this value was determined to be 0% (Figure 7).

During the research concerning the effluent from the analyzed facilities, no cases were observed when the values were below the permissible level 5 mg/dm³ [47]. The obtained indicators allow concluding that household WWTPs with activated sludge are faulty in terms of TP removal throughout the year. The obtained results do not give a chance for a positive assessment of the facilities regarding the content of TP in treated sewage. In a similar facility, deprived of a classical mechanical treatment stage, a low technological reliability at the level of 5% was found [33]. On the other hand, the reliability of TN removal in a small SBBR was only 21.7% [35]. In contrast, a study conducted by Micek et al. [36] showed that TP removal reliability in two other household hybrid CW WWTPs operating in the RNP was much higher and amounted to 87% and 100%. Moreover, Marzec et al. [33] in a hybrid household CW achieved 100% reliability of TP removal. Similarly to other indicators, the reliability of TP removal in household WWTPs with activated sludge was lower than in CWs.

4. Conclusions

The analyzed household WWTPs with activated sludge demonstrated relatively high levels of technological reliability and efficiency regarding the removal of pollutants in terms of TSS, BOD₅, and COD. It is worth noting that the technological reliability of the analyzed systems was higher in comparison to corresponding systems with activated sludge but without a classical preliminary settling tank [32]. On this basis, it can be concluded that the modernization of the researched facilities, which included equipping them with preliminary settling tanks, brought positive effects. The use of an additional element in the form of a preliminary settling tank as the provision of a mechanical treatment stage and the extension of the retention time of wastewater in the system have improved the process of sedimentation of solids, as well as their initial biological decomposition. Unfortunately, no positive effects on the removal of biogenic compounds were observed in the studied facilities. The efficiency of nitrogen and phosphorus removal did not exceed 34%, while the levels of technological reliability oscillated below 5%. The obtained results indicate that, in the case of biogenic compounds, the researched facilities could not guarantee a quality of treated wastewater which would be consistent with the requirements specified in the Polish law during any period of their operation. This disqualifies the analyzed technological solution in terms of its wide application in protected areas and near lakes, where the requirements for nitrogen and phosphorus removal are high. On the other hand, previous research results presented in the literature indicate that hybrid constructed wetland systems are the most effective and reliable in terms of pollutant removal from domestic wastewater [36,49,50,60,61] and, therefore, should be recommended for use in protected areas.

Author Contributions: Conceptualization, K.J.; data curation, K.J. and M.M.; formal analysis, M.M. and K.J.; investigation, A.M. and A.L.; methodology, K.J.; resources, A.M. and K.J.; supervision, M.M. and A.L.; validation, K.J.; writing—original draft, A.M. and K.J.; writing—review and editing, K.J., M.M. and T.G. All authors read and agreed to the published version of the manuscript.

Funding: This paper was co-funded by the “Excellent Science” program of the Ministry of Science and Higher Education as a part of the contract no. DNK/SP/465641/2020: “The role of agricultural engineering and environmental engineering in sustainable agriculture development”.

Institutional Review Board Statement: Not applicable.

Informed Consent Statement: Not applicable.

Data Availability Statement: Not applicable.

Acknowledgments: This paper was written on the basis of research projects funded by the Polish Ministry of Science and Higher Education—project entitled “Water, wastewater, and energy management” (contracts No. TKD/DS/1, TKD/S/1, 2017–2019), the Provincial Fund for Environmental Protection and Water Management in Lublin, Poland—project entitled “Research on the optimization of the operation of household wastewater treatment plants at forest settlements in the area of Roztoczański and Poleski National Park” (contract No. TKD/OŚ/37/2018), and the Roztoczański National Park, Poland—project entitled “Performing research on the operation of six household wastewater treatment plants located at forest settlements in the Roztoczański National Park” (contract No. TKD/U-1/IŚGiE, 2019).

Conflicts of Interest: The authors declare no conflict of interest.

References

1. *The Nature Conservation Act from 16 April 2004*; Dz. U. Nr 92, Poz. 880; SEJM: Warsaw, Poland, 2004. (In Polish)
2. Philippe, S.; Paolo, G. (Eds.) *Council Directive 92/43/EEC of 21 May 1992 on the Conservation of Natural Habitats and of Wild Fauna and Flora*; Cambridge University Press: London, UK, 1992.
3. Józwiakowski, K.; Podbrożna, D.; Kopczačka, K.; Marzec, M.; Kowalczyk-Juśko, A.; Pochwatka, P.; Listosz, A.; Malik, A. The state of water and wastewater management in the municipalities of the Polesie National Park. *J. Ecol. Eng.* **2017**, *18*, 192–199. [[CrossRef](#)]

4. Józwiakowski, K.; Podbrożna, D.; Kopczacka, K.; Jaguś, M.; Marzec, M.; Listosz, A.; Pochwatka, P.; Kowalczyk-Juško, A.; Malik, A. The state of water and wastewater management in the municipalities of the Roztocze National Park. *J. Ecol. Eng.* **2018**, *19*, 255–262. [\[CrossRef\]](#)
5. Mucha, Z.; Mikosz, J. Rational application of small wastewater treatment plants according to sustainability criteria. *Czas. Tech. Sr.* **2009**, *106*, 91–100. (In Polish)
6. Strande, L.; Weiyang, X.; Scanlon, A.; Hinckley, T.M. Evaluation criteria for implementation of a sustainable sanitation and wastewater treatment system at Jiuzhaigou National Park, Sichuan Province, China. *Environ. Manag.* **2009**, *45*, 93–104.
7. Józwiakowski, K.; Mucha, Z.; Generowicz, A.; Baran, S.; Bielińska, J.; Wójcik, W. The use of multi-criteria analysis for selection of technology for a household WWTP compatible with sustainable development. *Arch. Environ. Prot.* **2015**, *3*, 76–82. [\[CrossRef\]](#)
8. Józwiakowski, K.; Marzec, M.; Kowalczyk-Juško, A.; Gizińska-Górna, M.; Pytka-Woszczyło, A.; Malik, A.; Listosz, A.; Gajewska, M. 25 years of research and experiences about the application of constructed wetlands in southeastern Poland. *Ecol. Eng.* **2019**, *127*, 440–453. [\[CrossRef\]](#)
9. Micek, A.; Józwiakowski, K.; Marzec, M.; Listosz, A.; Malik, A. Efficiency of pollution removal in preliminary settling tanks of household wastewater treatment plants in the Roztocze National Park. *J. Ecol. Eng.* **2020**, *21*, 9–18. [\[CrossRef\]](#)
10. Steer, D.; Fraser, L.; Boddy, J.; Seibert, B. Efficiency of small constructed wetlands for subsurface treatment of single-family domestic effluent. *Ecol. Eng.* **2002**, *18*, 429–440. [\[CrossRef\]](#)
11. Brix, H.; Arias, C. The use of vertical flow constructed wetlands for on-site treatment of do-mestic wastewater: New Danish guidelines. *Ecol. Eng.* **2005**, *25*, 491–500. [\[CrossRef\]](#)
12. Puigagut, J.; Villaseñor, J.; Salas, J.J.; Becares, E.; Garcia, J. Subsurface-flow constructed wet-lands in Spain for the sanitation of small communi-ties: A comparative study. *Ecol. Eng.* **2007**, *30*, 312–319. [\[CrossRef\]](#)
13. Maunoir, S.; Philip, H.; Rambaud, A. Small wastewater treatment plants in mountain areas: Combination of septic tank and biological filter. *Water Sci. Technol.* **2007**, *56*, 65–71. [\[CrossRef\]](#) [\[PubMed\]](#)
14. Weissenbacher, N.; Mayr, E.; Niederberger, T.; Aschauer, C.; Lebersorger, S.; Steinbacher, G.; Haberl, R. Alpine infrastructure in Central Europe: Integral evaluation of wastewater treatment systems at mountain refuges. *Water Sci. Technol.* **2008**, *57*, 2017–2022. [\[CrossRef\]](#) [\[PubMed\]](#)
15. Seo, D.C.; DeLaune, R.D.; Park, W.Y.; Lim, J.S.; Seo, J.Y.; Do Lee, J.; Cho, J.S.; Heo, J.S. Evaluation of a hybrid constructed wetland for treating domestic sewage from individual housing units surrounding agricultural villages in South Korea. *J. Environ. Monit.* **2009**, *11*, 134–144. [\[CrossRef\]](#) [\[PubMed\]](#)
16. Ye, F.; Li, Y. Enhancement of nitrogen removal in towery hybrid constructed wetland to treat domestic wastewater for small rural communities. *Ecol. Eng.* **2009**, *35*, 1043–1050. [\[CrossRef\]](#)
17. Kaczor, G.; Bergel, T.; Bugajski, P.; Pijanowski, J. Aspects of sewage disposal from tourist facilities in national parks and other protected areas. *Pol. J. Environ. Stud.* **2015**, *24*, 107–114. [\[CrossRef\]](#)
18. Ghawi, A.H. Study on the Development of Household Wastewater Treatment Unit. *J. Ecol. Eng.* **2018**, *19*, 63–71. [\[CrossRef\]](#)
19. Wilk, B.; Cimocho-wicz-Rybicka, M. BIOVAC® wastewater treatment plants in the mountain national parks. *Tech. Trans.* **2018**, *1*, 113–123.
20. PN-EN 12566–3:2016–10. *Small Wastewater Treatment Plants for a Population Calculation (OLM) up to 50—Part 3: Container and/or Home Sewage Treatment Plants on Site*; Polski Komitet Normalizacyjny: Warszawa, Poland, 2016. (In Polish)
21. *Water Law. Ustawa Prawo Wodne z dnia 20 lipca 2017 r., Dz.U. 2017 poz. 1566*; SEJM: Warsaw, Poland, 2017. (In Polish)
22. Pawelek, J.; Bugajski, P. The development of household wastewater treatment plants in Poland—Advantages and disadvantages. *Acta Sci. Pol. Form. Circumictus* **2017**, *16*, 3–14. (In Polish) [\[CrossRef\]](#)
23. Lofrano, G.; Brown, J. Wastewater management through the ages: A history of mankind. *Sci. Total Environ.* **2010**, *408*, 5254–5264. [\[CrossRef\]](#)
24. Bernardes, R.S.; Klapwijk, A. Biological nutrient removal in a sequencing batch reactor treating domestic wastewater. *Water Sci. Technol.* **1996**, *33*, 29–38. [\[CrossRef\]](#)
25. Bodik, I.; Kratochvíl, K.; Herdová, B.; Tapia, G.; Gašpariková, E. Municipal wastewater treatment in the anaerobic-aerobic baffled filter at ambient temperature. *Water Sci. Technol.* **2002**, *46*, 127–135. [\[CrossRef\]](#)
26. Di Trapani, D.; Christenso, M.; Odegaard, H. Hybrid activated sludge/biofilm process for the treatment of municipal wastewater in a cold climate region: A case study. *Water Sci. Technol.* **2011**, *63*, 1121–1129. [\[CrossRef\]](#)
27. Józwiakowska, K.; Marzec, M. Efficiency and reliability of sewage purification in long-term exploitation of the municipal wastewater treatment plant with activated sludge and hydroponic system. *Arch. Environ. Prot.* **2020**, *46*, 30–41.
28. Brucculeri, M.; Bolzonella, D.; Battistoni, P.; Cecchi, F. Treatment of mixed municipal and winery wastewaters in a conventional activated sludge process: A case study. *Water Sci. Technol.* **2005**, *51*, 89–98. [\[CrossRef\]](#) [\[PubMed\]](#)
29. Orhon, D.; Babuna, F.G.; Karahan, O. Industrial wastewater treatment by activated sludge. *IWA Publ.* **2009**, *8*. [\[CrossRef\]](#)
30. Hanna, K.M.; Kellan, J.L.; Boardman, G.D. Onsite aerobic package treatment systems. *Water Res.* **1995**, *29*, 2530–2540. [\[CrossRef\]](#)
31. Marzec, M.; Józwiakowski, K. Operational and environmental problems of the functioning of mini-sewage treatment plants with activated sludge. *Pol. J. Environ. Stud.* **2007**, *16 Pt III*, 525–529.
32. Marzec, M. Reliability of removal of selected pollutants in different technological solutions of household wastewater treatment plants. *J. Water Land Dev.* **2017**, *35*, 141–148. [\[CrossRef\]](#)

33. Marzec, M. Technological reliability of utilization of biogenic pollutants in selected technologies used in small wastewater treatment plants. *Przemysł Chem.* **2018**, *97*, 753–757. (In Polish)
34. Bugajski, P.; Kurek, K.; Józwiakowski, K. Effect of wastewater temperature and concentration of organic compounds on the efficiency of ammonium nitrogen removal in a household treatment plant servicing a school building. *Arch. Environ. Prot.* **2019**, *45*, 31–37.
35. Jucherski, A.; Walczowski, A.; Bugajski, P.; Józwiakowski, K. Technological reliability of domestic wastewater purification in a small Sequencing Batch Biofilm Reactor (SBBR). *Sep. Purif. Technol.* **2019**, *224*, 340–347. [[CrossRef](#)]
36. Micek, A.; Józwiakowski, K.; Marzec, M.; Listosz, A. Technological reliability and efficiency of wastewater treatment in two hybrid constructed wetlands in the Roztocze National Park (Poland). *Water* **2020**, *12*, 3435. [[CrossRef](#)]
37. Oliveira, S.C.; Sperling, M.V. Reliability analysis of wastewater treatment plants. *Water Res.* **2008**, *42*, 1182–1194. [[CrossRef](#)] [[PubMed](#)]
38. Alderson, M.P.; dos Santos, A.B.; Mota Filho, C.R. Reliability analysis of low-cost, full-scale domestic wastewater treatment plants for reuse in aquaculture and agriculture. *Ecol. Eng.* **2015**, *82*, 6–14. [[CrossRef](#)]
39. Eisenberg, D.; Soller, J.; Sakaji, R.; Olivieri, A. A methodology to evaluate water and wastewater treatment plant reliability. *Water Sci. Technol.* **2001**, *43*, 91–99. [[CrossRef](#)]
40. Taheriyoun, M.; Moradinejad, S. Reliability analysis of a wastewater treatment plant using fault tree analysis and Monte Carlo simulation. *Environ. Monit. Assess.* **2015**, *187*, 4186. [[CrossRef](#)]
41. Bugajski, P.; Chmielowski, K.; Kaczor, G. Reliability of a collective wastewater treatment plant. *J. Ecol. Eng.* **2016**, *17*, 143–147. [[CrossRef](#)]
42. Michalczyk, Z.; Kovalchuk, I.; Chmiel, S.; Głowacki, S.; Chabudziński, Ł.; Kharkevych, V.; Voloschyn, P. Waters. In *Roztocze. Nature and Human*; Grabowski, T., Harasimuk, M., Kaszewski, B.M., Kravchuk, Y., Eds.; Roztoczański Park Narodowy: Zwierzyniec, Poland, 2015; pp. 103–122. (In Polish)
43. Czerwieńiec, D.; Trych, P. Technical Projects. Household Wastewater Treatment Plants for the Roztocze National Park. MILAGROS. Przedsiębiorstwo Realizacji Inwestycji. *Typescript*, 2004. (In Polish)
44. American Public Health Association (APHA). *Standard Methods for Examination of Water and Wastewater*, 18th ed.; American Public Health Association: Washington, DC, USA, 1992.
45. American Public Health Association (APHA). *Standard Methods for Examination of Water and Wastewater*, 21st ed.; American Public Health Association: Washington, DC, USA, 2005.
46. Józwiakowski, K.; Bugajski, P.; Mucha, Z.; Wójcik, W.; Jucherski, A.; Natawny, M.; Siwiec, T.; Mazur, A.; Obroślak, R.; Gajewska, M. Reliability of pollutants removal processes during long-term operation of one-stage constructed wetland with horizontal flow. *Sep. Purif. Technol.* **2017**, *187*, 60–66. [[CrossRef](#)]
47. *Regulation of the Minister of Maritime Economy and Inland Navigation of 12 July 2019 on Substances Which Are Particularly Harmful to the Aquatic Environment and the Conditions to Be Met When Discharging Wastewater into Water or Soil and When Discharging Rainwater or Snowmelt into Water or Water Installations*, Pos. 1311; Minister of Maritime Economy and Inland Navigation: Warsaw, Poland, 2019.
48. Bugajski, P.; Pawelek, J.; Kurek, K. Concentrations of organic and biogenic pollutants in domestic wastewater after mechanical treatment in the aspect of biological reactor design. *Infrastruct. Ecol. Rural Areas* **2017**, 1811–1822. [[CrossRef](#)]
49. Marzec, M.; Józwiakowski, K.; Debska, A.; Gizińska-Górna, M.; Pytka-Woszczyło, A.; Kowalczyk-Juško, A.; Listosz, A. The efficiency and reliability of pollutant removal in a hybrid constructed wetland with common reed, manna grass, and Virginia Mallow. *Water* **2018**, *10*, 1445. [[CrossRef](#)]
50. Marzec, M.; Gizińska-Górna, M.; Józwiakowski, K.; Pytka-Woszczyło, A.; Kowalczyk-Juško, A.; Gajewska, M. The efficiency and reliability of pollutant removal in a hybrid constructed wetland with giant miscanthus and Jerusalem artichoke in Poland. *Ecol. Eng.* **2019**, *127*, 23–35. [[CrossRef](#)]
51. Johal, E.; Walia, B.S.; Saini, M.S.; Jha, M.K. Efficiency assessment and mathematical correlation development between BOD₅ and other parameters in Jalandhar Sewage Treatment. *Int. J. Innov. Sci. Eng. Technol.* **2014**, *3*, 13088–13096.
52. Showkat, U.; Najjar, I.A. Study of efficiency of sequential batch reactor (SBR)-based sewage treatment plant. *Appl. Water Sci.* **2019**, *9*, 1–10. [[CrossRef](#)]
53. Jakubaszek, A.; Stadnik, A. Efficiency of sewage treatment plants in the sequential batch reactor. *Civ. Environ. Eng. Rep.* **2018**, *28*, 121–131. [[CrossRef](#)]
54. Ding, S.; Bao, P.; Wang, B.; Zhang, Q.; Peng, Y. Long-term stable simultaneous partial nitrification, anammox and denitrification (SNAD) process treating real domestic sewage using suspended activated sludge. *Chem. Eng. J.* **2018**, *339*, 180–188. [[CrossRef](#)]
55. Myszograj, S. Mechanisms of biological processes in domestic wastewater treatment plants. *Civ. Environ. Eng. Rep.* **2018**, *28*, 177–192. [[CrossRef](#)]
56. Quansheng, D.; Qixing, C.; Zehui, L.; Shouwei, Z. Application of microbial technology in wastewater treatment. *Prog. Appl. Microbiol.* **2017**, 23–28.
57. Bunce, J.T.; Ndam, E.; Ofiteru, I.D.; Moore, A.; Graham, D.W. A review of phosphorus removal technologies and their applicability to small-scale domestic wastewater treatment systems. *Front. Environ. Sci.* **2018**, *6*, 1–15. [[CrossRef](#)]
58. Andracka, D.; Dzienis, L. Required reliability level of wastewater treatment plants according to European and Polish regulations. *Zesz. Nauk. Politech. Białostockiej Ser. Inżynieria Sr.* **2003**, *16*, 24–28. (In Polish)

59. Bugajski, P.; Wałęga, A.; Kaczor, G. Application of the Weibull reliability analysis of household sewage treatment plant. *Gaz Woda I Tech. Sanit.* **2012**, *2*, 56–58. (In Polish)
60. Jucherski, A.; Nastawny, M.; Walczowski, A.; Józwiakowski, K.; Gajewska, M. Assessment of the technological reliability of a hybrid constructed wetland for wastewater treatment in a mountain eco-tourist farm in Poland. *Water Sci. Technol.* **2017**, *75*, 2649–2658. [[CrossRef](#)] [[PubMed](#)]
61. Wojciechowska, E.; Gajewska, M.; Ostojski, A. Reliability of nitrogen removal processes in multistage treatment wetlands receiving high-strength wastewater. *Ecol. Eng.* **2017**, *98*, 365–371. [[CrossRef](#)]

Article

The Kinetics of Pollutant Removal through Biofiltration from Stormwater Containing Airport De-Icing Agents

Artur Mielcarek ¹, Joanna Rodziewicz ^{1,*}, Wojciech Janczukowicz ¹ and Kamila Ostrowska ²

¹ Department of Environment Engineering, University of Warmia and Mazury in Olsztyn, Warszawska 117a, 10-719 Olsztyn, Poland; artur.mielcarek@uwm.edu.pl (A.M.); jawoj@uwm.edu.pl (W.J.)

² Visimind Ltd. Sp. z o.o., Trylinskiego St. 10, 10-683 Olsztyn, Poland; kamila_c@o2.pl

* Correspondence: joanna.rodziewicz@uwm.edu.pl; Tel.: +48-89-524-56-09

Abstract: The present study aimed to determine the kinetics of pollutant removal in biofilters with LECA filling (used as a buffer to prevent de-icing agents from being released into the environment with stormwater runoff). It demonstrated a significant effect of temperature and a C/N ratio on the rate of nitrification, denitrification, and organic compound removal. The nitrification rate was the highest (0.32 mg N/L·h) at 25 °C and C/N = 0.5, whereas the lowest (0.18 mg N/L·h) at 0 °C and C/N = 2.5 and 5.0. Though denitrification rate is mainly affected by the available quantity of organic substrate, it actually decreased as the C/N increased and was positively correlated with the temperature levels. Its value was found to be the highest (0.31 mg N/L·h) at 25 °C and C/N = 0.5, and the lowest (0.18 mg N/L·h) at 0 °C and C/N = 5.0. As the C/N increased, so did the content of organic compounds in the treated effluent. The lowest organic removal rates were noted for C/N = 0.5, ranging between 11.20 and 18.42 mg COD/L·h at 0 and 25 °C, respectively. The highest rates, ranging between 27.83 and 59.43 mg COD/L·h, were recorded for C/N = 0.5 at 0 and 25 °C, respectively.

Keywords: kinetics; organic compound removal; nitrification and denitrification; low temperature; wintertime airport maintenance



Citation: Mielcarek, A.; Rodziewicz, J.; Janczukowicz, W.; Ostrowska, K. The Kinetics of Pollutant Removal through Biofiltration from Stormwater Containing Airport De-Icing Agents. *Appl. Sci.* **2021**, *11*, 1724. <https://doi.org/10.3390/app11041724>

Academic Editor: Faisal I. Hai
Received: 26 January 2021
Accepted: 11 February 2021
Published: 15 February 2021

Publisher's Note: MDPI stays neutral with regard to jurisdictional claims in published maps and institutional affiliations.



Copyright: © 2021 by the authors. Licensee MDPI, Basel, Switzerland. This article is an open access article distributed under the terms and conditions of the Creative Commons Attribution (CC BY) license (<https://creativecommons.org/licenses/by/4.0/>).

1. Introduction

Air travel is considered to be one of the safest and fastest means of transport. The aviation industry stimulates the economic/cultural growth and creates many jobs. However, the day-to-day airport operations generate air, water, and soil pollution [1]. One of the main issues is the water runoff containing pollutants from runways, taxiways, washing and de-/anti-icing pads, trans-shipment points, fuel storage stations and hangars. These wastewater types contain petroleum-derived substances, surfactants, pavement de-icers, aircraft de-icing/anti-icing agents, and other organic and inorganic pollutants. In climate zones at risk of icing, the pollution caused by pavement de-icing poses a severe environmental problem. Urea, acetate, and sodium formate in the solid form, and acetate and potassium formate in the liquid form are the agents most commonly used for winter maintenance of airport pavements [2]. They release organic compounds and nitrogen into the environment while also increasing the salinity of water solutions and, thereby the salinity of areas adjacent to airports. Both the temperature [3] and the C/N ratio [4] are factors that significantly influence nitrogen conversion and contaminant removal in biofilters. Consequently, they have a major impact on the capacity to treat airport de-icing wastewater and protect the environment.

The issue of the treatment of wastewater containing de-icing agents remains unresolved. Most airports are not equipped with a wastewater treatment system. Only a few airports in the world have wetlands, which effectively remove pollutants. Unfortunately wetlands create favorable environmental conditions for birds, which may endanger airport operations. Other rarely used solutions include filters with zeolite and perlite, media made of crushed clay and granular activated carbon, a mixture of granular activated alumina

and porous concrete, granular activated lignite, half-burnt dolomite, and granular ferric hydroxides. Considering sustainable development principles, the best solution would be to use the filling made of waste materials, e.g., light weight aggregates prepared from fly ash from sewage sludge thermal treatment. It is characterized by a large specific surface, resistance to physicochemical factors, low heat conductivity, good phosphorus-sorption properties, and facilitates the deammonification process. These attributes provide good conditions for biofilm growth even at low temperatures [5,6].

The breakdown of urea into ammonium (NH_4^+) or ammonia (NH_3) is a well-known process that occurs in both aerobic and anaerobic conditions at a wide range of pH, temperature, and C/N values [7]. The resultant processes of nitrogen reduction and oxidation affect the natural environment.

The biological oxidation of NH_4^+ or ammonia NH_3 to nitrate is known as nitrification. The nitrification of ammonium in a biofilter is a two-step process in which ammonium or ammonia is first converted to nitrite (NO_2^-) and then to nitrate (NO_3^-). Its conversion to nitrite is mainly conducted by a group of obligatory autotrophic bacteria. Also, a few heterotrophs have been reported to carry out nitrification in the environment, but usually at much lower rates than autotrophic bacteria [8]. Nitrification allows converting a relatively immobile ammonium-nitrogen to highly mobile nitrate, affecting environmental quality [9]. The most effective pathway for N removal from wastewater is nitrification followed by denitrification [4]. The biological denitrification is conducted by denitrifying microbes which use nitrate as a terminal electron acceptor, and organic and inorganic substances as electron donors and energy sources for sustaining the microbial growth [10]. In the course of autotrophic denitrification, microorganisms use sulfur compounds, hydrogen, and/or iron as energy sources, and carbon dioxide and hydrocarbons as carbon sources. Microorganisms that use organic carbon compounds are the most common denitrifiers in nature [11]. The heterotrophic biological denitrification is considered more economical, implementable on a large scale, and allowing for the ultimate reduction of nitrate to nitrogen gas with high selectivity [12]. The presence of organic compounds in wastewater significantly affects nitrification and denitrification, with a low organic content promoting effective nitrification [13] and a low C/N ratio significantly reducing denitrification [4]. The denitrification rate is also determined by the availability of nitrification products (nitrites and nitrates). Furthermore, the rate of biochemical conversion and the microbial activity are directly affected by the temperature of the wastewater treatment.

Some of these parameters may be regulated easily, but due to the high specific heat capacity of water, it is nearly impossible to influence temperature. Nitrification and denitrification are elements of the N-cycle critical to the removal of nitrogen from the treatment system. While the removal of organic compounds and nitrogen from municipal wastewater has been the subject of much research and is relatively well explored, there is limited knowledge on how to eliminate such pollution from airport wastewater. The previous authors' research has shown that biofilters LECA filling could be an effective method for removing nitrogen and organic compounds from wastewater containing airfield deicing fluids. The nitrogen compounds were removed as a result of the simultaneous process of nitrification and denitrification, where the organic compounds present in the treated wastewater served as a carbon source [5,14]. To that end, the present paper provides the findings of a study aimed to determine the transformation kinetics of pollutants generated from airport maintenance, providing a means to estimate the retention time for de-icing wastewater in filters located near airports or in individual, local systems for removing such pollutants. The study was conducted under four different temperature profiles (0 °C, 4 °C, 8 °C, and 25 °C) and at 3 loading rates of de-icing agents used for winter maintenance of airport pavements, with C/N ratios of 0.5, 2.5, and 5.0.

2. Materials and Methods

2.1. Experimental Model

The experiment was performed in laboratory-scale models of biofilters operated at the Department of Environmental Engineering at the University of Warmia and Mazury in Olsztyn (Katedra Inżynierii Środowiska UWM w Olsztynie). The biofilters were loaded with a granulate having the structure of expanded-clay aggregate (with a diameter $d_{60} = 8.2$ mm, $d_{60}/d_{10} = 2.27$, bulk density of 0.88 g/cm³, hydraulic conductivity of $K_h 0.52$ cm/s and resistance to crushing of 12.6 N/mm²) prepared from fly ash from sewage sludge thermal treatment in the “Dębogórze” Wastewater Treatment Plant in Gdynia (Poland). The granulate was prepared according to the method of mechanical plasticization and fragmentation of the raw material, followed by sintering of small balls in a rotary kiln at 1200 °C [15]. Biofilters consisted of a cylindrical polyethylene pipe and a cone-shaped bottom. In the bottom of the biofilter, which was outflow part, was a drain valve used to collect samples of wastewater. The technical parameters of the biofilter were: surface area 95 cm², volume 2500 cm³, active volume 1552 cm³, total height 0.24 m and biofilter filling height 0.19 m [6]. Four temperature variants were adopted: 0 °C, 4 °C, 8 °C, and 25 °C (control biofilter). The experiment was conducted at C/N levels of 0.5 , 2.5 , and 5.0 . C/N ratio affects the efficiency of the biofilters (in relation to C and N removal). The C/N ratio applied in the study, was aimed to determine the kinetics under conditions favoring nitrification (C/N = 0.5), denitrification (C/N = 5.0) and intermediate conditions (C/N = 2.5). Stable operating temperatures were maintained by a thermostatic chamber that regulated the temperature with an accuracy of ± 0.1 °C. Synthetic wastewater, prepared from a weighted sample including commonly used agents for de-icing airport pavements and tap water, was the substrate for the experiments. The composition and physicochemical parameters of the wastewater used in the study are given in Table 1.

Table 1. Composition and parameters of the wastewater tested.

	C/N Ratio		
	0.5	2.5	5.0
CH ₄ N ₂ O (urea) [mg/L]	150.00 ± 0.10	150.00 ± 0.10	150.00 ± 0.10
HCOONa (sodium formate) [mg/L]	136.00 ± 0.10	657.00 ± 0.10	1326.00 ± 0.10
CH ₃ COOK (potassium acetate) [mg/L]	49.00 ± 0.10	237.00 ± 0.10	478.00 ± 0.10
	Parameter		
Nog. [mgN/L]	71.56 ± 2.20	71.56 ± 2.20	71.56 ± 2.20
N Kjeldhal [mgN/L]	70.80 ± 3.02	70.80 ± 3.02	70.80 ± 3.02
COD [mg/L]	100.66 ± 1.34	386.80 ± 1.94	765.50 ± 2.90
pH	7.47–8.03	7.47–8.03	7.47–8.03

To promote nitrification, a low hydraulic load of 5 dm³/m²·d and hydraulic retention time (HRT) of 4 d were adopted, equivalent to the cycle of de-icing agent application in airports. The study on the kinetics of pollutant removal started at the end of technological research lasting four months. This four month research was preceded by three months adaptive period [6]. Samples were collected after 0.5 , 6 , and 12 h of operation; then, at 12 h intervals for 84 h, with the final sample taken after 96 h of operation (Figure 1). The size of the final sample was 5 cm³.

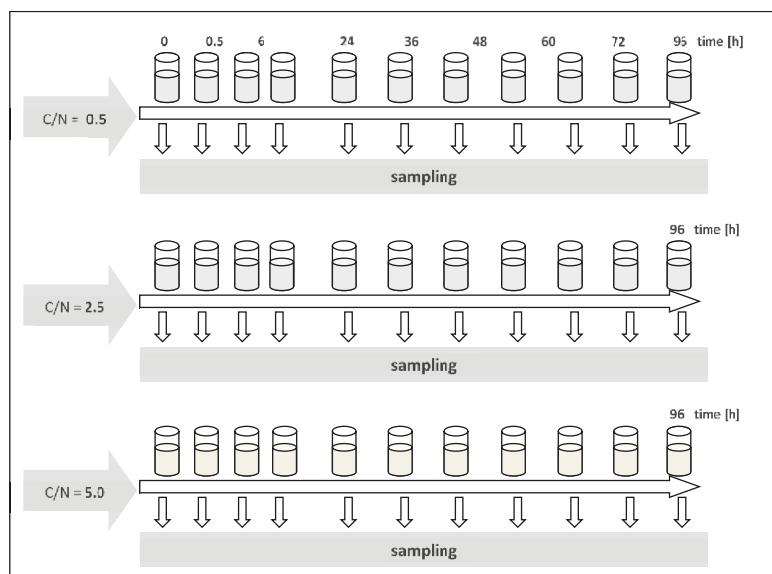


Figure 1. Schedule of sampling for the kinetics assay during the experiment.

2.2. Analytical Procedures

Determinations of nitrate concentration, nitrite concentration, ammonium nitrogen concentration, Kjeldahl total nitrogen, and organic compound concentration (COD) were carried out according to the APHA [16]. The concentration of total nitrogen (TN) was analyzed using a TNM-L analyzer (Shimadzu Corporation, Kyoto, Japan) with the “oxidative combustion-chemiluminescence” method.

2.3. Kinetics

The results of the physicochemical testing were used to determine the order of reaction and rates of organic compound removal, ammonia nitrogen oxidation and oxidized nitrogen (nitrites and nitrates) reduction. The reaction rate constant was determined using the Statistica 13.1 PL package (TIBCO Software Inc., Palo Alto, CA, USA).

The ammonia nitrogen oxidation rate was described with the formula:

$$C_{t.NoX} = C_{i.NoX} + k_{NoX} \cdot t, \tag{1}$$

where $C_{t.NoX}$ —concentration of oxidized nitrogen after time t [mgN/L]; $C_{i.NoX}$ —initial concentration of oxidized nitrogen [mgN/L]; k_{NoX} —ammonia nitrogen oxidation rate constant [h^{-1}].

The rate of nitrogen removal through denitrification was described with the formula:

$$C_{t.Nre} = C_{i.Nre} + k_{Nre} \cdot t, \tag{2}$$

where $C_{t.Nre}$ —concentration of nitrogen removed through denitrification after time t [mgN/L]; $C_{i.Nre}$ —initial concentration of nitrogen removed through denitrification [mgN/L]; k_{Nre} —oxidized nitrogen removal rate constant [h^{-1}].

The organic compound removal rate (expressed as COD) was calculated with the formula:

$$C_{t.COD} = C_{i.COD} \cdot e^{-k_{COD} \cdot t}, \tag{3}$$

where $C_{t,COD}$ —concentration of organic compounds after time t [mg/L]; $C_{i,COD}$ —initial concentration of organic compounds [mg/L]; k_{COD} —organic compound removal rate constant [h^{-1}].

3. Results and Discussion

The present study identified the kinetics of nitrification, denitrification, and organic pollutant removal from wastewater generated by wintertime airport maintenance. The experiment was conducted in four temperature variants and at different doses of the de-icing agents (sodium formate and potassium diacetate) characterized by C/N ratios, with the urea dose being constant. The use of biofilter filling promotes the formation of complex biofilms, providing favorable conditions for the development of both aerobic and anaerobic microorganisms [15]. A diverse range of parameters (which ensures the presence of various bacterial groups with different needs) creates favorable conditions for wastewater bio-treatment [17]. This, in the context of the present study, enabled the removal of organic pollutants and nitrogen species from airport de-icing wastewater. The reaction rates for the experimental variants and the goodness of fit for the model (R^2) are given in Supplementary Table S1. Changes in nitrogen concentration due to nitrification and denitrification conformed to the zero-order reaction formula, whereas the organic removal rate followed the first-order reaction formula. A comparison between the reaction rates by temperature and the biofilter's organic load was used to identify the impact of these parameters on the biofilter performance (Figure 2).

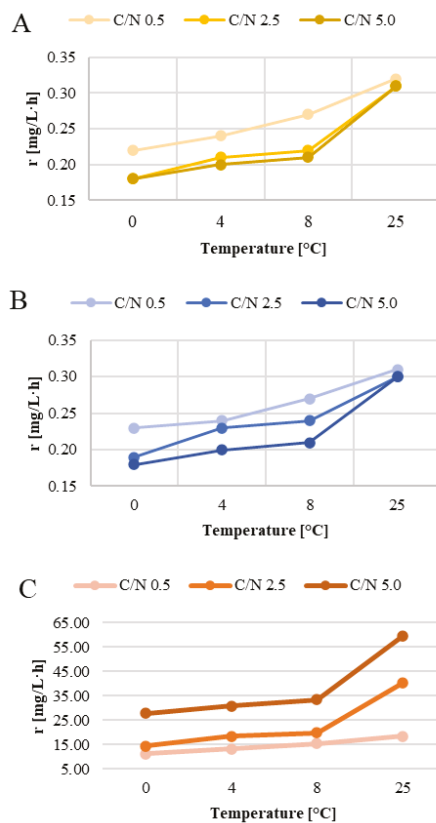


Figure 2. Effect of temperature and C/N on the rates of nitrification (A), denitrification (B), and organic pollutant removal (C).

3.1. Nitrification

The nitrifier's activity is very temperature-sensitive [3]. However, exposure to low temperatures did not impact it to the point of halting ammonia nitrogen oxidation, which followed the zero-order reaction, meaning that changes in activity levels over time were linear. Similar findings have been reported in the literature, indicating that longer HRTs may be used to improve removal performance at low temperatures [18]. The rate and efficiency of nitrification of airport de-icing wastewater increased at higher biofilter operating temperatures. In contrast, the higher organic matter content in series 2 and 3 caused a slight reduction in the ammonia nitrogen oxidation rate at lower biofilter operating temperatures (Figures 2 and 3; Supplementary Figures S1–S3). At C/N = 0.5 group, the highest nitrification rate in the entire series, i.e., 0.32 mgN/L·h, was determined in the biofilter operating at 25 °C. Lowering biofilter operating temperatures, with the other technical parameters being equal, reduced the process rate by 31.3% (to 0.22 mgN/L·h) at 0 °C. In the two remaining reactors (T = 4 and 8 °C), the nitrification rates were 25.0 and 15.6% lower, respectively. It is noteworthy that the effect of temperature on reaction kinetics is much harder to determine in biofilm reactors than in suspended-growth biomass, and not as drastic as predicted by the van't Hoff-Arrhenius equation [19]. Other factors, such as the reactor operating parameters, HRT or wastewater composition, may lessen the impact of temperature [20]. While lower temperatures do reduce nitrification rates, they also increase dissolved oxygen concentration in the water, meaning that the effect of temperature is mitigated by the higher oxygen availability. Thus, the resultant reduction in the biofilm nitrification rate was ultimately negligible (1.108% per 1 °C) [19]. The decreases in nitrification rates produced in the present experiment were similar. Autotrophic nitrification rates are, in large part, driven by high levels of readily digestible organic compounds, which promote heterotrophic bacterial growth [21]. According to De Pra et al. [22], fast-growing heterotrophic microorganisms compete for oxygen and ammonia nitrogen with nitrifying bacteria, and their metabolic intermediates may inhibit the activity of the latter. To achieve optimal nitrification conditions, the influent organic carbon must be kept under 2 kg COD/m³·d [22]. In an experiment by Zafarzadeh et al. [23], the highest nitrification rates were produced at C/N ratios under 6. Another study, by Mosquera-Corral et al. [24], showed that C/N values as low as 0.3 led to the competition between heterotrophs and autotrophs, impairing nitrification. In turn, Young et al. [25] reported that the inhibiting effect of high C/N ratios on ammoniacal nitrogen removal from treated wastewater was more pronounced at lower temperatures. This finding is corroborated by the present study, which showed that the reductions in nitrification rate and efficiency were higher at the lowest of the test temperatures (T = 0 °C), but minor at 25 °C and increased organic compound load. In series 2 (C/N = 2.5), the nitrification rate was similar to that of series 1 (0.31 mgN/L·h at 25 °C). As in series 1, the lowest nitrification rate, reaching 0.18 mgN/L·h (41.94% lower), was observed at the lowest treatment temperature (0 °C). The nitrification rates were similar in the 8 °C and 4 °C variants, reaching 0.22 and 0.21 mgN/L·h, respectively. With the higher organic carbon levels (C/N = 5) in series 3, the nitrification rate remained stable at 0.31 mgN/L·h in the control reactor (T = 25 °C). In the other reactors analyzed in this series, it was approx. one-third lower than in the control one and ranged from 0.18 mgN/L·h at 0 °C to 0.21 mg N/L·h at 8 °C.

The high nitrification efficiency obtained for wastewater samples with the higher organic compound levels may be explained by heterotrophic nitrification. Guo et al. [26] reported that numerous heterotrophic microorganisms (which are not limited to bacteria but extend to fungi and plants as well) were capable of nitrifying organic and inorganic nitrogen compounds. Such microorganisms grow faster, require lower oxygen concentrations, and tolerate higher C/N ratios than autotrophic nitrifying bacteria.

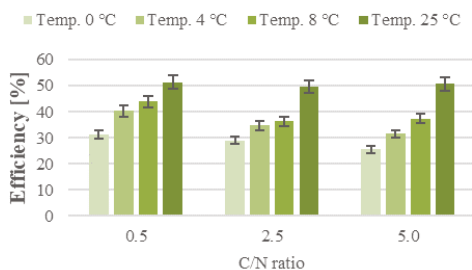


Figure 3. Nitrification efficiency in the experiment depending on temperature and C/N ratio in storm-water containing airport de-icing agents.

3.2. Nitrogen Removal

The activity of heterotrophic denitrifying bacteria is less dependent on the temperature than that of nitrifying bacteria [27]. Kadlec and Reddy [28] reported that 20–35 °C was the optimal temperature range for denitrification, which slows down considerably at temperatures lower than 10 °C and greater than 30 °C. Champagne et al. [29] noted that providing a source of readily biodegradable organic carbon helped maintain high nitrification efficiencies even at temperatures under 10 °C. In the present study, the denitrification rate increased at higher temperatures and decreased at higher C/N ratios (Figure 2; Supplementary Figures S4–S6), even though the presence of a readily available source of organic carbon is one of the main drivers of effective denitrification [30,31]. In series 1 (C/N = 0.5), oxidized nitrogen was reduced in the control reactor (T = 25 °C) at a rate of 0.31 mgN/L·h. Nitrogen removal was impeded by lowered biofilter operating temperatures, with the other technical parameters being equal. The lowest oxidized nitrogen reduction rates, at 0.22 mgN/L·h, were recorded for the biofilter operating at 0 °C. The denitrification rate was 0.30 mgN/L·h at 25 °C in series 2 and 3 (C/N = 2.5 and 5.0). Lowering the biofilter operating temperature to 0 °C reduced the performance by 36.7% and 40.0% against the control, respectively. These findings indicate that the nitrogen removal rates recorded in the study across the different experimental series did not correlate directly with the processing temperature or the C/N ratio—instead, the nitrification rate and efficiency served as the main factors. This pattern was the most strikingly evident in series 3, where the biofilters were fed with wastewater having the highest C/N ratio and were operating at optimal temperature conditions (T = 25 °C). A decreased ammonia nitrogen concentration in the effluent is indicative of intensive nitrification in the reactors. The difference between oxidized ammonia nitrogen and the nitrate/nitrite concentration in the treated wastewater shows how much nitrogen was removed. High rates of ammonia nitrogen oxidation and a low nitrite/nitrate content in the biofilter effluent, which did not exceed 12% TN in series 1 (no available organic substrate after approx. 24 h; Supplementary Figure S7) and 8% TN in the other series, suggest that nitrification and denitrification occurred simultaneously (Figures 4 and 5). The main factor enabling simultaneous nitrification and denitrification is the gradient of dissolved oxygen levels, determined by inhibited diffusion in the film [32]. Puznava et al. [33] found that a dissolved oxygen concentration of 0.5–3.0 mgO₂/dm³ reduced oxygen penetration and enabled denitrification in the internal layers. The authors obtained a denitrification efficiency of 71%, with the simultaneous nitrification reaching 96–98%. Another study, by Zinatizadeh and Ghaytoolin [34] obtained 46–50% nitrogen removal through simultaneous nitrification and denitrification at dissolved oxygen levels between 2.5 and 3.0 mgO₂/dm³, depending on the filling used in the MBBR. The nitrogen removal rates recorded in the presented study ranged from 30.1 ± 1.5% (T = 0 °C) to 43.0 ± 2.1% (T = 25 °C) in series 1 (C/N = 0.5). In the series with the higher organic compound contents (higher C/N ratios), the biofilters operating between 0 and 8 °C exhibited lower performance. The nitrogen removal rate ranged from 26.5 ± 1.3% (T = 0 °C) to 35.9 ± 1.8% (T = 8 °C) for C/N = 2.5, and from 25.0 ± 1.3% (T = 0 °C) to 31.2 ± 1.6%

($T = 8\text{ }^{\circ}\text{C}$) for $C/N = 5.0$. In the case of the biofilter operating at $25\text{ }^{\circ}\text{C}$, it was higher and reached $45.9 \pm 2.3\%$ and $46.7 \pm 2.3\%$ at $C/N = 2.5$ and 5.0 , respectively.

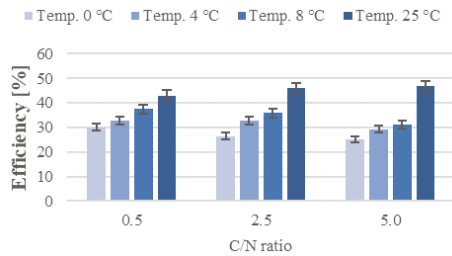


Figure 4. Effectiveness of nitrogen removal in the experiment depending on temperature and C/N ratio in storm-water containing airport de-icing agents.

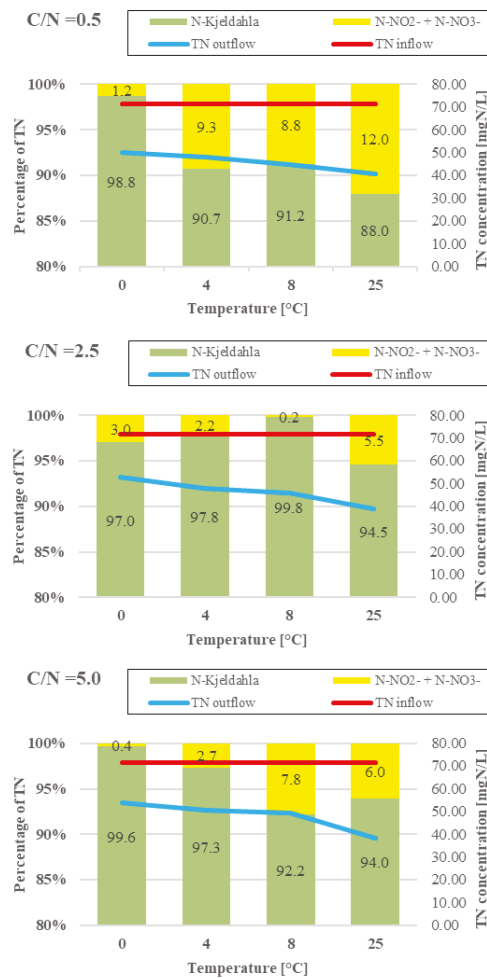


Figure 5. TN and nitrate/nitrite in the biofilter effluent (column diagram—percentage of TN; line diagram—TN concentration).

3.3. Organic Removal Rate

The temperature not only affects the rate of substrate diffusion into the cell, but also the activity of enzymes, and thus the rate of biochemical processes, which determine how quickly pollutants are biodegraded. What is more, microorganisms are able to grow and metabolize organic compounds as long as the liquid pollutant is provided, meaning that organic compounds can be efficiently removed from wastewater even at low temperatures [35]. It is believed that aerobic digestion of organic compounds proceeds at exponentially increasing rates as the temperature rises from 0 °C to 32 °C. Its rate is stable between 32 and 40 °C, then declines sharply, reaching zero at 45 °C. This correlation holds true in the systems where the process rate is not limited by substrate concentration [36]. In addition, biofilms are less susceptible to adverse variations in temperature than activated sludge systems [37]. The rates of organic compound removal obtained in the present study increased with the C/N ratios and biofilter operating temperatures (Figure 2; Supplementary Figures S7–S9). The lowest rates of organic pollutant removal were recorded for series 1 reactors (C/N = 0.5), among which the control one (T = 25 °C) produced the highest reaction rate at 21.33 mgCOD/L·h. Lowering biofilter operating temperatures to 8, 4, and 0 °C, with the other technical parameters being equal, reduced its performance by 18.4, 32.7, and 48.0%, respectively. Increasing organic carbon (C/N = 2.5) in the T = 0 °C biofilter decreased organic compound removal by 65.5%, compared with the removal rates produced at 25 °C. The reaction rates were 51.8 and 57.3% lower in the other temperature variants (8 and 4 °C, respectively). The highest reaction rates were noted in the series with the greatest initial organic pollutant levels (C/N = 5.0). The peak value of organic compound removal, reaching 58.03 mgCOD/L·h, was reached in the control bioreactor (T = 25 °C). As in the C/N = 0.5 and 2.5 series, the organic removal performance in series 3 was the poorest at 0 °C (26.76 mgCOD/L·h)—being 53.9% lower than at T = 25 °C. The biofilters operating at 8 and 4 °C produced 41.5 and 45.7% lower reaction rates, respectively. Efficiencies and reaction rates were the highest in biofilters operating at 25 °C, and the lowest values in these operating at 0 °C (Figure 6).

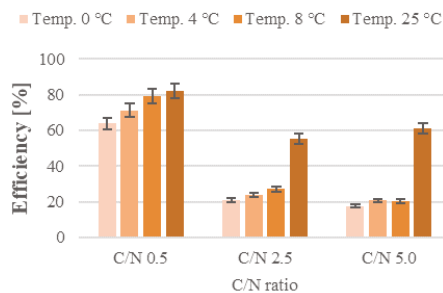


Figure 6. Efficiency of organic compound removal from stormwater containing airport de-icing agents.

However, increased C/N ratios in the subsequent series also led to higher initial levels of organic compounds in the influent, necessitating the removal of higher pollutant loads. This caused the organic compound removal rates to decrease as the C/N increased, with the sole exception of the biofilter operating at T = 25 °C and C/N = 5.0, which ensured an increase in organic pollutant removal rate from $55.4 \pm 2.8\%$ (C/N = 2.5) to $61.2 \pm 3.1\%$ (C/N = 5.0). Nevertheless, the pollutant levels (as expressed by COD) observed were the highest in series 3 (289.3–614.0 mgCOD/L), and the lowest in series 1 (17.2–35.1 mgCOD/L). These findings are in line with literature data, which indicate that as the organic pollutant load increases, so does the COD of the treated effluent. Thus, one way to improve the treatment efficiency at low temperatures is to reduce the organic load rate [37].

4. Conclusions

The study showed that the rates of nitrification, denitrification, and organic compound removal were determined not only by the reactor operating temperature, but also by the organic carbon content (C/N ratios) in treated wastewater. Reaction rates were found to decrease at progressively lower temperatures in all of the experimental series. In terms of nitrification, the reaction rates fell as the organic compound levels (sodium formate and potassium acetate) rose. The nitrification rate was the highest (0.32 mg N/L·h) at 25 °C and C/N = 0.5, whereas the lowest rate (0.18 mg N/L·h) was produced at 0 °C for C/N = 2.5 and 5.0. The impact of the higher C/N ratios was more evident at lower biofilter operating temperatures. The study did not indicate that increased organic substrate levels led to improved denitrification rates, which were instead linked to the nitrification efficiency. The denitrification rate was found to be the highest (0.31 mg N/L·h) at 25 °C and C/N = 0.5, and the lowest (0.18 mg N/L·h) at 0 °C and C/N = 5.0. The lowest organic removal rates were noted for C/N = 0.5, ranging between 11.20 and 18.42 mg COD/L·h at 0 and 25 °C, respectively. The highest rates were recorded for C/N = 0.5, ranging between 27.83 and 59.43 mg COD/L·h at 0 and 25 °C, respectively. These results indicate that a treated wastewater with C/N = 0.5 does not inhibit the activity of nitrifying bacteria and actually reduces organic pollutant levels in the effluent, while also creating optimal conditions for simultaneous nitrification and denitrification, as long as suitable biofilter filling is provided.

Supplementary Materials: The following are available online at <https://www.mdpi.com/2076-3417/11/4/1724/s1>, Figure S1: Effect of temperature on the nitrification rate—series 1 (C/N = 0.5), Figure S2: Effect of temperature on the nitrification rate—series 2 (C/N = 2.5), Figure S3: Effect of temperature on the nitrification rate—series 3 (C/N = 5.0), Figure S4: Effect of temperature on the denitrification rate—series 1 (C/N = 0.5), Figure S5: Effect of temperature on the denitrification rate—series 2 (C/N = 2.5), Figure S6: Effect of temperature on the denitrification rate—series 3 (C/N = 5.0), Figure S7: Effect of temperature on the organic removal rate—series 1 (C/N = 0.5), Figure S8: Effect of temperature on the organic removal rate—series 2 (C/N = 2.5), Figure S9: Effect of temperature on the organic removal rate—series 3 (C/N = 5.0), Table S1: Goodness of fit and the rates of nitrification, denitrification, and organic compound removal depending on the adopted operating parameters of the biofilters.

Author Contributions: Conceptualization, W.J. and J.R.; Methodology, J.R.; Software, A.M.; Validation, K.O., J.R. and A.M.; Formal Analysis, J.R.; Investigation, K.O.; Resources, K.O. and W.J.; Data Curation, K.O. and A.M.; Writing—Original Draft Preparation, A.M. and W.J.; Writing—Review & Editing, J.R.; Visualization, A.M.; Supervision, W.J.; Project Administration, K.O.; Funding Acquisition, K.O. All authors have read and agreed to the published version of the manuscript.

Funding: This research was funded by Project No. 29.610.023 of the University of Warmia and Mazury in Olsztyn, Poland.

Institutional Review Board Statement: Not applicable.

Informed Consent Statement: Not applicable.

Data Availability Statement: The data presented in this study are available on request from the corresponding author.

Conflicts of Interest: The authors declare no conflict of interest. The funders had no role in the design of the study; in the collection, analyses, or interpretation of data; in the writing of the manuscript, or in the decision to publish the results.

References

1. Sulej, A.; Polkowska, Z.; Namieśnik, J. Contaminants in airport runoff water in the vicinities of two international airports in Poland. *Polish J. Environ. Stud.* **2012**, *21*, 725–739.
2. Switzenbaum, M.S.; Veltman, S.; Mericas, D.; Wagoner, B.; Schoenberg, T. Best management practices for airport deicing stormwater. *Chemosphere* **2001**, *43*, 1051–1062. [[CrossRef](#)]
3. Kinyage, J.P.H.; Pedersen, L.F. Impact of temperature on ammonium and nitrite removal rates in RAS moving bed biofilters. *Aquac. Eng.* **2016**, *75*, 51–55. [[CrossRef](#)]

4. Yu, G.; Peng, H.; Fu, Y.; Yan, X.; Du, C.; Chen, H. Enhanced nitrogen removal of low C/N wastewater in constructed wetlands with co-immobilizing solid carbon source and denitrifying bacteria. *Bioresour. Technol.* **2019**, *280*, 337–344. [[CrossRef](#)] [[PubMed](#)]
5. Rodziewicz, J.; Mielcarek, A.; Janczukowicz, W.; Bryszewski, K.; Ostrowska, K. Treatment of wastewater containing runway de-icing agents in biofilters as a part of airport environment management system. *Sustainability* **2020**, *12*, 3608. [[CrossRef](#)]
6. Rodziewicz, J.; Mielcarek, A.; Janczukowicz, W.; Ostrowska, K.; Jóźwiakowski, K.; Bugajski, P.; Jucherski, A. Biofilter with innovative filling for low-temperature treatment of sewage from de-icing airport runways. *Sep. Purif. Technol.* **2020**, *242*, 116761. [[CrossRef](#)]
7. Katipoglu-Yazan, T.; Ubay Cokgor, E.; Insel, G.; Orhon, D. Is ammonification the rate limiting step for nitrification kinetics? *Bioresour. Technol.* **2012**, *114*, 117–125. [[CrossRef](#)]
8. Subbarao, G.V.; Sahrawat, K.L.; Nakahara, K.; Ishikawa, T.; Kishii, M.; Rao, I.M.; Hash, C.T.; George, T.S.; Srinivasa Rao, P.; Nardi, P.; et al. Biological nitrification inhibition—a novel strategy to regulate nitrification in agricultural systems. In *Advances in Agronomy*; Elsevier Inc.: Amsterdam, The Netherlands, 2012; Volume 114, pp. 249–302.
9. Sahrawat, K.L. Factors affecting nitrification in soils. *Commun. Soil Sci. Plant Anal.* **2008**, *39*, 1436–1446. [[CrossRef](#)]
10. Ghafari, S.; Hasan, M.; Aroua, M.K. Bio-electrochemical removal of nitrate from water and wastewater—A review. *Bioresour. Technol.* **2008**, *99*, 3965–3974. [[CrossRef](#)] [[PubMed](#)]
11. Van Rijn, J.; Tal, Y.; Schreier, H.J. Denitrification in recirculating systems: Theory and applications. *Aquac. Eng.* **2006**, *34*, 364–376. [[CrossRef](#)]
12. Wang, J.; Chu, L. Biological nitrate removal from water and wastewater by solid-phase denitrification process. *Biotechnol. Adv.* **2016**, *34*, 1103–1112. [[CrossRef](#)] [[PubMed](#)]
13. Zhu, S.; Chen, S. Effects of organic carbon on nitrification rate in fixed film biofilters. *Aquac. Eng.* **2001**, *25*, 1–11. [[CrossRef](#)]
14. Rodziewicz, J.; Ostrowska, K.; Janczukowicz, W.; Mielcarek, A. Effectiveness of nitrification and denitrification processes in biofilters treating waste water from de-icing airport runways. *Water* **2019**, *11*, 630. [[CrossRef](#)]
15. Rodziewicz, J.; Mielcarek, A.; Janczukowicz, W.; Białowiec, A.; Gotkowska-Płachta, A.; Proniewicz, M. Ammonia Nitrogen Transformations in a Reactor with Aggregate made of Sewage Sludge Combustion Fly Ash. *Water Environ. Res.* **2016**, *88*, 715–723. [[CrossRef](#)]
16. Federation, W.E.; APHA Association. *Standard Methods for Examination of Water and Wastewater (Standard Methods for the Examination of Water and Wastewater)*; American Public Health Association (APHA): Washington, DC, USA, 2012; ISBN 9780875532356.
17. Mielcarek, A.; Rodziewicz, J.; Janczukowicz, W.; Struk-Sokołowska, J. The impact of biodegradable carbon sources on nutrients removal in post-denitrification biofilm reactors. *Sci. Total Environ.* **2020**, *720*, 137377. [[CrossRef](#)]
18. Daija, L.; Selberg, A.; Rikmann, E.; Zekker, I.; Tenno, T.; Tenno, T. The influence of lower temperature, influent fluctuations and long retention time on the performance of an upflow mode laboratory-scale septic tank. *Desalin. Water Treat.* **2016**, *57*, 18679–18687. [[CrossRef](#)]
19. Zhu, S.; Chen, S. The impact of temperature on nitrification rate in fixed film biofilters. *Aquac. Eng.* **2002**, *26*, 221–237. [[CrossRef](#)]
20. Zhou, H.; Li, X.; Xu, G.; Yu, H. Overview of strategies for enhanced treatment of municipal/domestic wastewater at low temperature. *Sci. Total Environ.* **2018**, *643*, 225–237. [[CrossRef](#)]
21. Ge, S.; Wang, S.; Yang, X.; Qiu, S.; Li, B.; Peng, Y. Detection of nitrifiers and evaluation of partial nitrification for wastewater treatment: A review. *Chemosphere* **2015**, *140*, 85–98. [[CrossRef](#)] [[PubMed](#)]
22. De Prá, M.C.; Kunz, A.; Bortoli, M.; Perondi, T.; Chini, A. Simultaneous removal of TOC and TSS in swine wastewater using the partial nitrification process. *J. Chem. Technol. Biotechnol.* **2012**, *87*, 1641–1647. [[CrossRef](#)]
23. Zafarzadeh, A.; Bina, B.; Nikaen, M.; Attar, H.M.; Khiadani, M.H. Effect of dissolved oxygen and chemical oxygen demand to nitrogen ratios on the partial nitrification/denitrification process in moving bed biofilm reactors. *Iran. J. Biotechnol.* **2011**, *9*, 197–205.
24. Mosquera-Corral, A.; González, F.; Campos, J.L.; Méndez, R. Partial nitrification in a SHARON reactor in the presence of salts and organic carbon compounds. *Process Biochem.* **2005**, *40*, 3109–3118. [[CrossRef](#)]
25. Young, B.; Delatolla, R.; Kennedy, K.; Laflamme, E.; Stintzi, A. Low temperature MBBR nitrification: Microbiome analysis. *Water Res.* **2017**, *111*, 224–233. [[CrossRef](#)] [[PubMed](#)]
26. Guo, J.; Peng, Y.; Huang, H.; Wang, S.; Ge, S.; Zhang, J.; Wang, Z. Short- and long-term effects of temperature on partial nitrification in a sequencing batch reactor treating domestic wastewater. *J. Hazard. Mater.* **2010**, *179*, 471–479. [[CrossRef](#)] [[PubMed](#)]
27. Elgood, Z.; Robertson, W.D.; Schiff, S.L.; Elgood, R. Nitrate removal and greenhouse gas production in a stream-bed denitrifying bioreactor. *Ecol. Eng.* **2010**, *36*, 1575–1580. [[CrossRef](#)]
28. Kadlec, R.H.; Reddy, K.R. Temperature Effects in Treatment Wetlands. *Water Environ. Res.* **2001**, *73*, 543–557. [[CrossRef](#)]
29. Champagne, P.; Liu, L.; Howell, M. Aerobic Treatment in Cold-Climate Countries. In *Current Developments in Biotechnology and Bioengineering: Biological Treatment of Industrial Effluents*; Elsevier Inc.: Amsterdam, The Netherlands, 2017; pp. 161–201. ISBN 9780444636768.
30. Mielcarek, A.; Rodziewicz, J.; Janczukowicz, W.; Dabrowska, D.; Ciesielski, S.; Thornton, A.; Struk-Sokołowska, J. Citric acid application for denitrification process support in biofilm reactor. *Chemosphere* **2017**, *171*, 512–519. [[CrossRef](#)] [[PubMed](#)]
31. Rodziewicz, J.; Janczukowicz, W.; Mielcarek, A.; Filipkowska, U.; Kłodowska, I.; Ostrowska, K.; Duchniewicz, S. Anaerobic rotating disc batch reactor nutrient removal process enhanced by volatile fatty acid addition. *Environ. Technol.* **2015**, *36*, 953–958. [[CrossRef](#)]

32. Cao, Y.; Zhang, C.; Rong, H.; Zheng, G.; Zhao, L. The effect of dissolved oxygen concentration (DO) on oxygen diffusion and bacterial community structure in moving bed sequencing batch reactor (MBSBR). *Water Res.* **2017**, *108*, 86–94. [[CrossRef](#)]
33. Puznava, N.; Payraudeau, M.; Thornberg, D. Simultaneous nitrification and denitrification in biofilters with real time aeration control. *Water Sci. Technol.* **2001**, *43*, 269–276. [[CrossRef](#)]
34. Zinatizadeh, A.A.L.; Ghaytooli, E. Simultaneous nitrogen and carbon removal from wastewater at different operating conditions in a moving bed biofilm reactor (MBBR): Process modeling and optimization. *J. Taiwan Inst. Chem. Eng.* **2015**, *53*, 98–111. [[CrossRef](#)]
35. Di Trapani, D.; Christensson, M.; Torregrossa, M.; Viviani, G.; Ødegaard, H. Performance of a hybrid activated sludge/biofilm process for wastewater treatment in a cold climate region: Influence of operating conditions. *Biochem. Eng. J.* **2013**, *77*, 214–219. [[CrossRef](#)]
36. Lewandowski, Z.; Boltz, J.P. Biofilms in Water and Wastewater Treatment. In *Treatise on Water Science*; Elsevier: Amsterdam, The Netherlands, 2011; Volume 4, pp. 529–570. ISBN 9780444531933.
37. Yao, S.; Ni, J.; Ma, T.; Li, C. Heterotrophic nitrification and aerobic denitrification at low temperature by a newly isolated bacterium, *Acinetobacter* sp. HA2. *Bioresour. Technol.* **2013**, *139*, 80–86. [[CrossRef](#)] [[PubMed](#)]

Article

Comparison of Different Biofilter Media During Biological Bed Maturation Using Common Carp as a Biogen Donor

Mateusz Sikora *, Joanna Nowosad and Dariusz Kucharczyk

Department of Ichthyology and Aquaculture, University of Warmia and Mazury, Al. Warszawska 117A, PL 10-701 Olsztyn, Poland; nowosad.joanna@gmail.com (J.N.); darekk56@gmail.com (D.K.)

* Correspondence: sikora0404@gmail.com

Received: 3 December 2019; Accepted: 7 January 2020; Published: 15 January 2020

Abstract: This experiment analysed the operation of submerged and dripping biological filters with three types of filling: commercial fitting HXF12KLL (CF), two innovative polypropylene aggregates (PPA) and polyethylene screw caps for PET bottles (PSC). The experiment determined the time needed to reach full filter functionality at the maturation stage, the time needed to start successive stages of the nitrification process and the maximum concentration of each nitrogen compound in water in the recirculation systems. The filter operation characteristics after the maturation stage were also examined. These issues are crucial during the preparation and launch of new aquaculture facilities. A literature analysis indicated that the ability of biological filters to oxidise nitrogen compounds is affected by a number of factors. Studies conducted at various centres have covered selected aspects and factors affecting the effectiveness of biological filters. During this study, the model fish common carp (*Cyprinus carpio*) was used. The current experiment involved examination of biological filter maturation and operation during the carp fry rearing stage, which allowed the biofilter operation characteristics to be determined. At the third day of the experiment, the ammonium concentration reached approximately 3 mg NH₄-N/dm³. It remained at this level for 10 days and later decreased below 0.25 mg NH₄-N/dm³. The maximum nitrite concentration ranged from 11.7 mg/dm³ to 20.9 mg NO₂-N/dm³ within 9 to 20 days and later decreased with time. Nitrate concentrations were seen to increase during the experiment. The all applied biofilter media showed possibility to be used in commercial aquaculture systems.

Keywords: biofilter maturation; nitrogen compounds; recirculating aquaculture system (RAS)

1. Introduction

Annual fish and seafood consumption has been increasing steadily. The amount of fish and seafood obtained globally is limited and annual output has remained at 90 million tonnes for the past decade. For this reason, any increase in the amount of fish and seafood is associated with aquaculture and its dynamic growth. The production of aquaculture accounted for 44% of the total output in 2014 [1,2]. Installations used for animal production can be classified in regard to the degree of water recirculation: (1) open/flow-through systems, in which water is used once; (2) semi-open/semi-closed systems, in which water is used multiple times before being removed from the system, and (3) closed systems, in which only water loss is replenished. Higher degrees of water recirculation require more complex systems to purify it. RAS denotes technologies of repeated water reuse in a closed system. However, water loss in breeding systems needs to be replenished for multiple reasons, not only because of evaporation. To minimise the need for replenishing water loss, RAS systems are equipped with complex water treatment and purification systems, including mechanical and biological filters, UV sterilisation devices, water ozonation systems and others [3,4]. The most important of

these systems are biological filters, which control toxic nitrogen species and are necessary for RAS operation [3–5]. The fast increasing of aquaculture production in RAS is not possible without new developed technologies. One of the main focuses is media for biofilters, upon which the effectiveness of nitrification is dependant. This also an influence of biofilter costs, so new and cheaper biofilter media are necessary to involve in further aquaculture production growth [1–5].

The removal of toxic nitrogen from water is affected by nitrification, consisting of the biological oxidation of ammonium nitrogen to nitrite (III) nitrogen, followed by oxidation of the latter to nitrate (V) nitrogen. A crucial role in the nitrification process is played by Nitroso- (oxidation of ammonium to nitrite) and Nitro- (oxidation of nitrite to nitrate) nitrification bacteria [6,7]. Total ammonium nitrogen (TAN) is one of the major limiting factors in the design and operation of RAS systems [8] and is one of the metabolites which is formed in the digestion of proteins and the transformation of amino acids [9] given to fish with feed. It occurs as a sum of two species: dissociated (ammonium ion, NH_4^+) and undissociated (ammonia, NH_3) [8,10]. Ammonium nitrogen in its dissociated form is relatively non-toxic, whereas the undissociated form is highly toxic [8,9,11–17]. For this reason, it must be controlled [17] and removed from the system or oxidised to a less toxic nitrogen form [8,18]. Ammonia levels in RAS systems are controlled by nitrification [17]. The $\text{NH}_4^+/\text{NH}_3$ ratio depends mainly on the environment's pH. The amount of toxic NH_3 increases along with higher pH, depending on the temperature, pressure and salinity. Excessive amounts of ammonia lead to tremors in fish, coma and death [10]. The ammonia removal process is affected by a number of factors. The most important of them is the availability of oxygen (4.57 g of oxygen is needed to oxidise 1 g of ammonium nitrogen) and the rate of its diffusion into the biomembrane [8]. A decrease in water saturation with oxygen results in inhibition of ammonium nitrogen oxidation [19,20]. Important factors also include temperature, pH, salinity and organic matter burden on the biological filter [8]. Nitrite nitrogen are intermediate compounds in nitrification [6,7]. Due to their toxic effect on fish, they are an equally important factor in fish breeding as ammonium nitrogen [7,14,21,22] and are responsible for chronic diseases leading to fish death [7]. Nitrate nitrogen is the last step in the nitrification process [6,7] and has long been regarded as harmless. Recent studies have shown that it should be taken into account when optimising fish breeding. This nitrogen form is relatively harmless, but long-term exposure is suspected of having deadly toxic effects [21,23], although further studies are needed [23]. Analysis of the nitrification process gives the information if the biofilter is matured. In RAS equipped with such a biofilter, the level of ammonium and nitrite concentrations are low and stable [18]. It is especially important for finfish species, which are sensitive to toxic nitrogen compounds, like salmonids [4,6,7,11,12].

The kinetics of the reaction were not studied during the experiment, because the purpose of the study was to examine whether the applied experimental fillers for biological filters are useful in aquaculture. The reaction kinetics study is the next step after confirming the suitability of the filling used. The operation of modern aquaculture systems and their further dynamic growth requires the continuous development of new technologies [24]. It is equally important to keep in mind while developing new technologies or solutions that biological filter operation is affected by a number of factors, e.g., dissolved oxygen and the rate of its diffusion into the biomembrane, temperature, pH, salinity and organic matter burden on the biological filter, which is not always reflected in laboratory tests [7,25–27]. Considering the above, a two-step experiment was conducted on a semi-commercial scale, in which submerged and dripping biological filters with three different fillings were used, which are different from each other. CFs (commercial fitting HXF12KLL) have been designed to obtain the largest possible area in a unit of volume. In addition, their spatial structure allows the free flow of water through the centre of individual fittings, which effectively supports nitrification (nitrifiers have constant access to nitrogen compounds). PSCs (polyethylene screw caps for PET bottles) have more than three times smaller surface area per unit volume, but due to their shape, the inflow of nitrogen compounds to the biofilm is greatly facilitated. PPAs (polypropylene aggregate) have the least regular shape. A microscopic photograph reveals a lack of internal spaces on which a bacterial biofilm could develop. However, the outer structure has numerous recesses and protrusions, which are very diverse

and provide favourable conditions for the development of nitrifiers. The main donor of nitrogen compounds were common carp *Cyprinus carpio* juveniles. The study examined the dynamics of nitrogen compound transformations during biological bed maturation and matured bed operation. Moreover, increasing the daily nutrient dose allowed the bed operation to be examined with increasing loads.

A system with submerged filters with commercial fillings was used as a control. During the experiment, the hypothesis was verified that the use of polypropylene aggregate and polyethylene screw caps for PET bottles as fillers for biological filters will achieve the same effects as the use of commercial fittings HXF12KLL.

2. Materials and Methods

The experiment lasted 60 days in the submerged biological bed variant (two days of fish acclimatisation and 58 days of the water parameter measurements) using tap water. The experiment lasted 45 days in the dripping biological bed variant (two days of fish acclimatisation and 43 days of the water parameter measurements). The biological bed matured during this time, which allowed the dynamics of nitrogen compound transformations in a matured bed system to be examined. Moreover, increasing the daily nutrient dose allowed the bed operation to be examined with an increasing load. Ammonium, nitrites and nitrates' concentration in tap water at the beginning of the experiment was $0.045 \text{ mg N-NH}_4/\text{dm}^3$, $0.027 \text{ mg N-NO}_2/\text{dm}^3$ and $0.872 \text{ mg N-NO}_3/\text{dm}^3$.

2.1. Experimental Conditions

2.1.1. RAS Systems

The experiment was conducted in four identical semi-open RAS systems with 625 dm^3 volumes each (daily refill— 150 dm^3) modelled on devices used by Sikora et al. [18]. Three types of biological filter fillings were examined:

- Polypropylene aggregate (PPA) (active surface area $300\text{--}500 \text{ m}^2/\text{m}^3$ —manufacturer's data) (Figure 1A).
- Polyethylene screw caps for PET bottles (PSC) (active surface area ca. $300 \text{ m}^2/\text{m}^3$) (Figure 1B).
- Commercial fittings HXF12KLL (CF) (active surface area $859 \text{ m}^2/\text{m}^3$, Stöhr GmbH & Co. KG, Marktrodach, Germany) (Figure 1C).

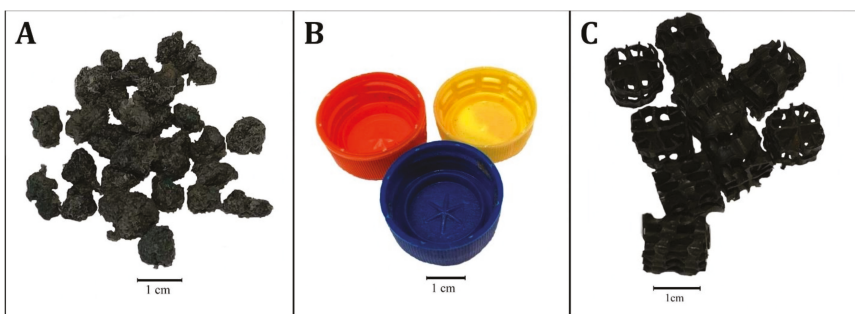


Figure 1. Polypropylene aggregate (PPA)-specific surface area—ca. 12 m^2 (A); polyethylene screw caps for PET bottles (PSC)-specific surface area—ca. 9 m^2 (B); Commercial fittings HXF12KLL (CF)-specific surface area—ca. 25.5 m^2 (C).

Each RAS system consisted of: an upper retention reservoir, a two-chamber lower retention reservoir (sedimentation chamber, pump chamber) and two rearing tanks. The systems were also fitted out with heaters, thermostats and aeration systems. The biological filter filling volume was 30 dm^3 . The specific surface area of the biological filters used was: PPA—ca. 12 m^2 , PSC—ca. 9 m^2 ,

CF—ca. 25.5 m². For submerged filters (Figure 2), the filling was placed directly in the sedimentation chamber. The filling was suspended above the sedimentation chamber in the variant with dripping filter (Figure 3), which had sprinklers mounted above them.

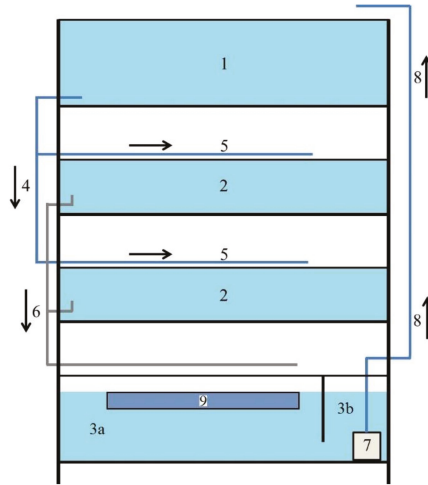


Figure 2. Recirculation aquaculture system with submerged filter scheme: 1 upper retention tank—0.251 m³, 2 rearing tank—2 × 0.096 m³, 3 lower retention tank (3a chamber with biofilter, 3b chamber with pump)—0.182 m³, 4 water inlets, 5 sprinklers, 6 water outlets, 7 pump, 8 water supply to upper retention tank, 9 submerged filter—0.030 m³.

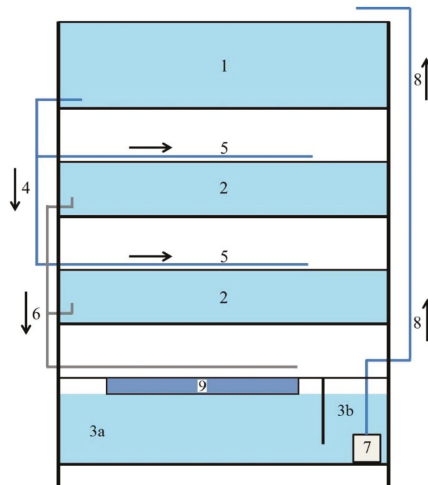


Figure 3. Recirculation aquaculture system with dripping filter scheme: 1 upper retention tank—0.251 m³, 2 rearing tank—2 × 0.096 m³, 3 lower retention tank (3a chamber with biofilter, 3b chamber with pump)—0.182 m³, 4 water inlets, 5 sprinklers, 6 water outlets, 7 pump, 8 water supply to upper retention tank, 9 dripping filter—0.030 m³.

The systems were started five days before the fish were put in them to stabilise the conditions in the recirculation systems. The circulating water temperature was 25.0 ± 0.1 °C. Before the experiment,

the systems were first thoroughly dried, disinfected with potassium permanganate at 7.5 g per run and then rinsed with water from the water supply system for 24 h.

2.1.2. Fish

Common carp juvenile (*Cyprinus carpio*), bred at the Department of Lake and River Fisheries of the University of Warmia and Mazury in Olsztyn and cultured under controlled conditions, were used in all experiment as a source of nitrogen compounds. Out-of-season carp breeding was carried out in accordance with the methodology described by Kucharczyk et al. [28], with the insemination method modified by Kucharczyk et al. [29] for burbot (*Lota lota*), ide (*Leuciscus idus*) and asp (*Aspius aspius*). The carp larvae were reared in a recirculation system at 25 ± 0.1 °C and fed brine shrimp (*Artemia salina*) nauplii for the first 25 days. Artificial feed with a granulation of 0.5–1.1 (Skretting, Norway: raw protein content 54%, fat content 18%) was introduced after that time.

In the submerged biological bed variant, 1379 ± 49 g (average \pm SD) of fry with a weight and unit length of 3.76 ± 1.55 g (average \pm SD) and 59.00 ± 8.77 mm (average \pm SD) were placed in the RAS systems. In the dripping biological bed variant, however, 1400.00 ± 0.00 g fry with a unit weight and length of 16.30 ± 4.80 g and 96.40 ± 9.65 mm were placed in the RAS systems. All fish used during the experiment are juvenile forms of common carp.

The fish (carp) were fed twice daily (at 8.30 and 15.00) during the experiment with an artificial feed with a granulation of 1.1 (Skretting, Norway: raw protein content 54%, fat content 18%) and 1.9 mm (Skretting, Norway: raw protein content 50%, fat content 20%), with a single feeding lasting 30 min. The feeding dose was set at 3% of the daily biomass (half of the daily feeding dose was provided in one feeding). Subsequently, the dose was increased daily by 3% of the initial fish biomass [30,31]. The initial daily feed dose was 20.9 ± 0.5 g (average \pm SD).

Sodium chloride was added to circulating water beginning on the day the nitrite nitrogen concentration reached $1 \text{ mg N-NO}_2/\text{dm}^3$. Nitrite shows of affinity to the $\text{Cl}^-/\text{HCO}_3^-$ ion exchange. As a result, a part of the nitrite is taken up by fish instead of chloride. Increase of chloride concentration in the water reduces nitrite uptake by fish [32].

2.2. Water Quality Measurements

Water tests started two days after the fish were placed in the systems. The water in each system was examined at 11:00 (samples were taken from the sprinkler). Hach Lange cuvette tests with a dedicated DR 5000 spectrophotometer were used for the water testing [18]:

Ammonium—cuvette test LCK 304

Nitrite—cuvette test LCK 341

Nitrate—cuvette test LCK 340

Daily ammonium assays were conducted for the initial 17 days of the experiment. The aim of this test was to check whether the compound accumulates in the water in excessive amounts. After that time, measurements were conducted every three days to monitor the total ammonium concentration in the circulating water. The nitrite concentration was checked daily throughout the experiment to determine the time needed to start stage I of nitrification (oxidation of ammonia to nitrites). The nitrate concentration in the water was tested daily for the first 28 days, after which measurements were conducted every two days to determine the time needed to start stage II of nitrification (oxidation of nitrite nitrogen to nitrate nitrogen).

Moreover, the following water parameters in the bed were measured at 11.00:

- pH—using a portable pH-meter manufactured by Oxyguard,
- Oxygen concentration ($\text{mg O}_2/\text{dm}^3$, saturation)—using an oxygen probe, a portable Polaris 2 manufactured by Oxyguard,
- Temperature—using an oxygen probe, a portable Polaris 2 manufactured by Oxyguard,

Moreover, the following water parameters were tested before the morning and afternoon feeding:

- Temperature—a probe combined with a thermostat controlling heater work,
- pH—using a portable pH-meter manufactured by Oxyguard,
- Oxygen concentration ($\text{mg O}_2/\text{dm}^3$, saturation)—using an oxygen probe, connected with the Total Commander system manufactured by Oxyguard.

2.3. Fish Measurements

The fish were measured (average weight and average total length) at the beginning and end of the experiment. Thirty fish were collected randomly and weighed with an analytical balance (KERN & Sohn GmbH, Balingen, Germany) with an accuracy of 0.1 mg. The fish body lengths were measured with a calliper MEGA 20513 (Profix, Warsaw, Poland) with an accuracy of 0.01 mm. Due to the fish size, their bodies were measured after the experiment with a ruler with an accuracy of 1 mm. Moreover, the fish biomass was determined at both the beginning and end of the experiment (analytical balance KERN & Sohn GmbH, Germany). The fish were anaesthetised during the measurements with an MS222 anaesthetic at a concentration of 50 ppm.

2.4. Statistical Analysis

The dynamics of nitrogen compound (ammonia, nitrites, nitrates) transformations were examined with a Kruskal–Wallis ANOVA test on ranks ($p > 0.05$) and subsequently by multiple comparisons of mean ranks ($p > 0.05$) for all samples. The distribution normality was verified with the Shapiro–Wilk test ($p > 0.05$) before the ANOVA test was performed. All results were analysed statistically using Statistica 13.1 software (StatSoft, Tulsa, Oklahoma, USA). In addition, in order to analyse the nature of individual stages of nitrification, regression equations were performed and the correlation coefficient (R) was calculated.

3. Results

3.1. Variant I—Use of Submerged Biological Filter

3.1.1. Ammonium Nitrogen

At the beginning of the experiment, the ammonium concentration increased rapidly in all experimental RAS and was about $3 \text{ mg N-NH}_4/\text{dm}^3$ from day 3 (Figure 4).

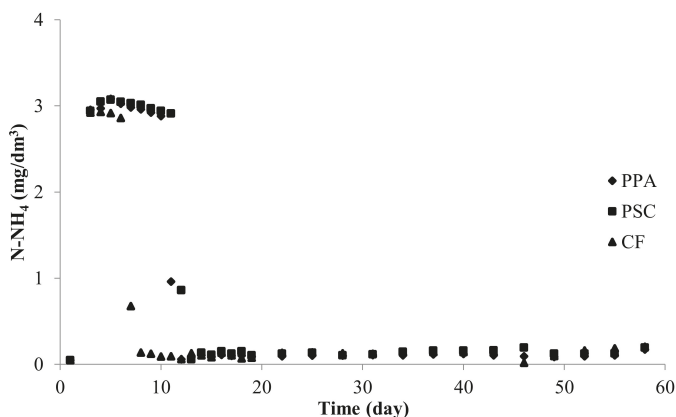


Figure 4. Ammonium nitrogen concentration in experimental systems using submerged biological filters: PPA—polypropylene aggregate, PSC—polyethylene screw caps for PET bottles, CF—commercial fittings HXF12KLL.

High ammonia levels lasted for several days and then quickly decreased. After this period, until the end of the experiment, no major increases in ammonium were recorded in RAS circuits (Table 1).

Table 1. Ammonium nitrogen concentration in RAS, in which various tested fillings (PPA—polypropylene aggregate, PSC—polyethylene screw caps for PET bottles, CF—commercial fittings HXF12KLL) were used for two separated stages, Stage I (high ammonium concentration) and Stage II (low concentrations ammonium) separated by a period of rapid drop in ammonium (break down).

Filling		Stage I	Break Down	Stage II
PPA	Average ± SD (N-NH ₄ /dm ³)	2.971 ± 0.059	0.960	0.100 ± 0.022
	Duration (d)	3–10	11	12–60
PSC	Average ± SD (N-NH ₄ /dm ³)	2.996 ± 0.056	0.860	0.133 ± 0.031
	Duration (d)	3–11	12	13–60
CF	Average ± SD (N-NH ₄ /dm ³)	2.906 ± 0.029	0,675	0.118 ± 0.040
	Duration (d)	3–6	7	8–60

3.1.2. Nitrite Nitrogen

In all RAS, nitrite levels increased for several dozen days until the maximum concentration was reached. After this time, the concentrations decreased until they reached a relatively low and stable level, which remained until the end of the experiment (Figure 5; Table 2).

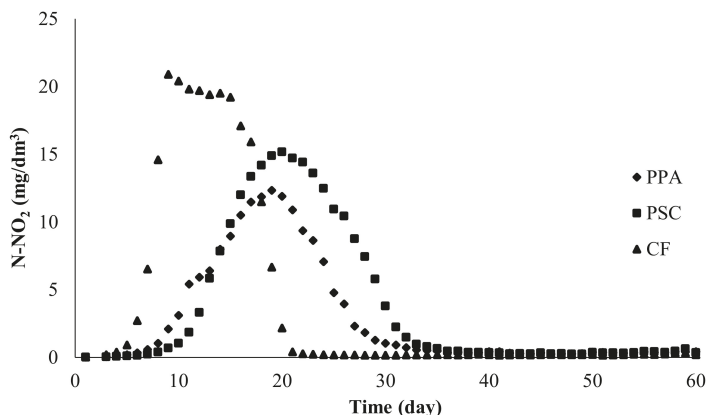


Figure 5. Nitrite nitrogen concentration in experimental systems using submerged biological filters: PPA—polypropylene aggregate, PSC—polyethylene screw caps for PET bottles, CF—commercial fittings HXF12KLL.

Table 2. Nitrite nitrogen concentration in RAS, in which various tested fillings (PPA—polypropylene aggregate, PSC—polyethylene screw caps for PET bottles, CF—commercial fittings HXF12KLL) were used for two separated stages, Stage I (high nitrite concentration) and Stage II (low nitrite concentration).

Filling	Stage I			Stage II	
	Increase (d)	Maximum Concentration (N-NO ₂ /dm ³)	Decrease (d)	Average ± SD (N-NO ₂ /dm ³)	Duration (d)
PPA	1–19	12.340	19–31	0.404 ± 0.137	14
PSC	1–20	15.180	20–33	0.412 ± 0.169	12
CF	1–9	20.900	9–21	0.211 ± 0.049	24

3.1.3. Nitrate Nitrogen

The nitrate concentration in the system with PPA as the biological filter filling increased until day 53 and reached 32.05 mg N-NO₃/dm³. It began to decrease afterwards. A similar trend was observed in the other two experiment variants. The concentration in the PSC system also rose until day 53 to reach a similar level (34.35 mg N-NO₃/dm³). The highest concentration in the system with CF filling was higher than in the other two systems (50.40 mg N-NO₃/dm³) and it was measured during a shorter time (day 44) (Figure 6).

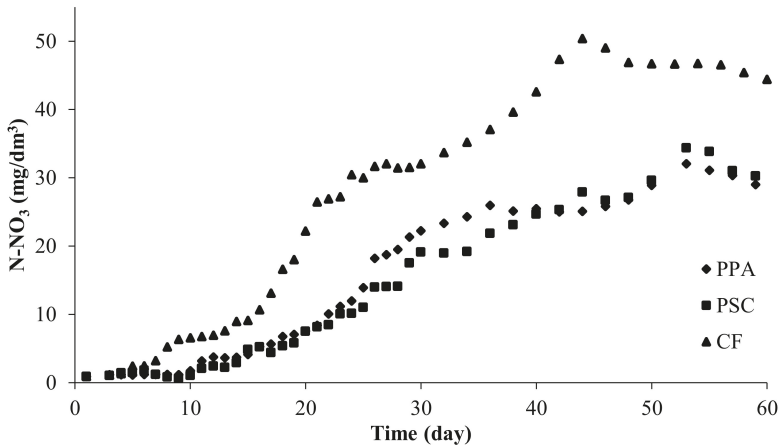


Figure 6. Nitrate nitrogen concentration in experimental systems using submerged biological filters: PPA—polypropylene aggregate, PSC—polyethylene screw caps for PET bottles, CF—commercial fittings HXF12KLL.

3.1.4. Other Water Parameters

The average water temperature in the system with PPA was 24.8 ± 0.4 °C, average pH—8.01 ± 0.15, whereas the average concentration of oxygen dissolved in water and saturation were 6.6 ± 0.7 mg O₂/dm³ and 79.8 ± 8.7%, respectively. The same parameters in the PSC system were: water temperature 24.8 ± 0.3 °C, pH 8.03 ± 0.15, dissolved oxygen concentration 6.7 ± 0.7 mg O₂/dm³, saturation 82.4 ± 8.6%. In the system with CF filling, the parameters were: water temperature 24.8 ± 0.6 °C, pH 8.06 ± 0.14, dissolved oxygen concentration 6.8 ± 0.6 mg O₂/dm³ and saturation 81.6 ± 7.2%.

3.2. Variant II—Use of Dripping Filters

The system with a submerged filter with CF filling (CFsf) was used again as the control in the second part of the experiment with dripping filters. There was a failure and leak in the system with the dripping filter filled with CF during this part of the experiment. The system was restarted in accordance with the procedure presented in the methodology.

3.2.1. Ammonium Nitrogen

As in the case of submerged filters, the concentration of ammonium in the experimental RAS systems increased rapidly and from day 3 it was about 3 mg N-NH₄/dm³ (Figure 7).

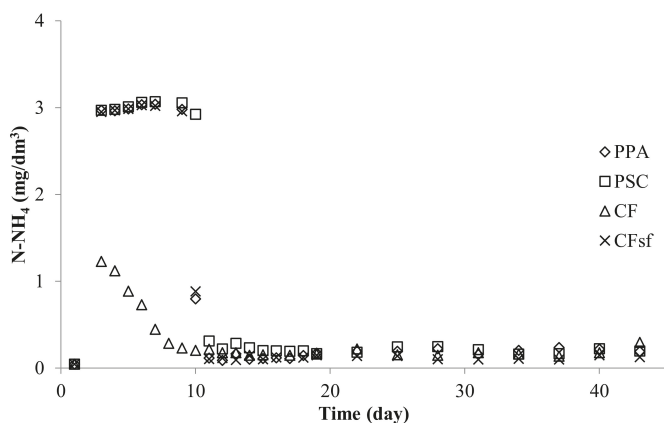


Figure 7. Ammonium nitrogen concentration in experimental systems using dripping biological filters: PPA—polypropylene aggregate, PSC—polyethylene screw caps for PET bottles, CF—commercial fittings HXF12KLL, CFsf—control submerged filter for dripping filters, commercial fittings HXF12KLL.

High ammonia levels lasted for several days and then quickly decreased. After this period, no significant increases in RAS ammonia were noted until the end of the experiment (Table 3).

Table 3. Ammonium nitrogen concentration in RAS, in which test fillings (PPA—polypropylene aggregate, PSC—polyethylene screw caps for PET bottles, CFsf—control submerged filter for dripping filters, commercial fittings HXF12KLL) were used for two separated stages: Stage I (high ammonia concentration) and Stage II (low ammonia concentrations) separated by a period of rapid drop in ammonia concentration (break down).

Filling		Stage I	Break Down	Stage II
PPA	Average ± SD (N-NH ₄ /dm ³)	2.996 ± 0.033	0.799	0.162 ± 0.048
	Duration	3–9	10	11–45
PSC	Average ± SD (N-NH ₄ /dm ³)	3.010 ± 0.055	0.313	0.209 ± 0.033
	Duration	3–10	11	12–45
CFsf	Average ± SD (N-NH ₄ /dm ³)	2.986 ± 0.033	0.884	0.120 ± 0.019
	Duration	3–9	10	11–45

Only in the system in which a failure occurred were other characteristics of ammonia concentrations noted. The highest concentration in the system with CF was recorded on day 3—1.230 mg N-NH₄/dm³—and it decreased afterwards. The ammonia concentration decreased below 0.3 mg N-NH₄/dm³ after day 8 and until the end of the experiment it fluctuated, with an average concentration of 0.188 ± 0.047 mg N-NH₄/dm³ (Figure 7).

3.2.2. Nitrite Nitrogen

In all RAS, nitrite levels increased for several dozen days, until the maximum concentration was reached. After this time, the concentrations decreased until they reached a relatively low and stable level, which remained until the end of the experiment (Figure 8; Table 4).

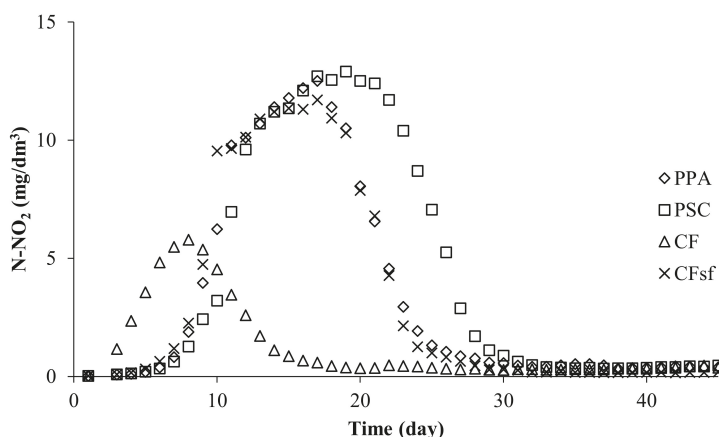


Figure 8. Nitrite nitrogen concentration in experimental systems using dripping biological filters: PPA—polypropylene aggregate, PSC—polyethylene screw caps for PET bottles, CF—commercial fittings HXF12KLL, CFsf—control submerged filter for dripping filters, commercial fittings HXF12KLL.

Table 4. Nitrite nitrogen concentration in RAS, in which test fillings (PPA—polypropylene aggregate, PSC—polyethylene screw caps for PET bottles, CF—commercial fittings HXF12KLL, CFsf—control submerged filter for dripping filters, commercial fittings HXF12KLL) were used for two separated stages: Stage I (high nitrite concentration) and Stage II (low nitrite concentration).

Filling	Stage I		Stage II		
	Increase (d)	Maximum Concentration (N-NO ₂ /dm ³)	Decrease (d)	Average ± SD (N-NO ₂ /dm ³)	Duration (d)
PPA	1–17	12.500	17–27	0.480 ± 0.139	18
PSC	1–19	12.900	19–30	0.438 ± 0.137	15
CF	1–8	5.780	8–15	0.385 ± 0.126	30
CFsf	1–17	11.700	17–26	0.261 ± 0.178	19

3.2.3. Nitrate Nitrogen

The nitrate concentration in the system with PPA as the biological filter filling increased until day 44 and reached 32.150 mg N-NO₃/dm³. It decreased slightly afterwards. A similar trend was observed in the system with PSC. The highest concentration of 30.00 mg N-NO₃/dm³ was observed on day 40 and it decreased slightly afterwards. A different situation was observed in the system with CF. The concentration of nitrate nitrogen increased to 29.800 mg N-NO₃/dm³ on day 36; afterwards it decreased until the end of the experiment, reaching 25.00 mg N-NO₃/dm³ on the last day. In the system with CFsf, the nitrate concentration increased until day 32 and reached 32.15 mg N-NO₃/dm³ and it decreased slightly afterwards (Figure 9).

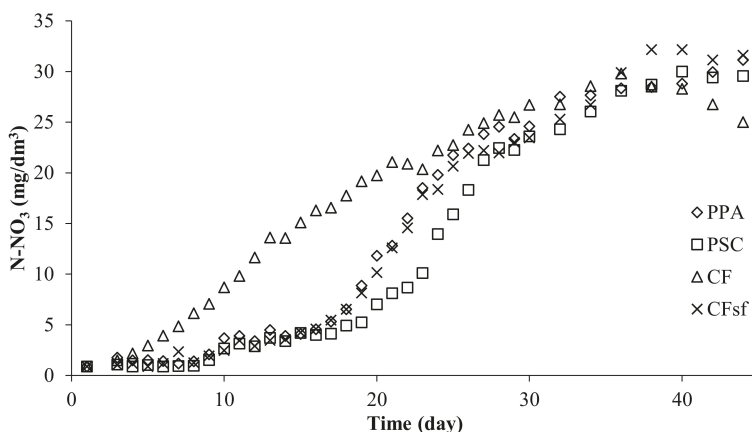


Figure 9. Nitrate nitrogen concentration in experimental systems using dripping biological filters: PPA—polypropylene aggregate, PSC—polyethylene screw caps for PET bottles, CF—commercial fittings HXF12KLL, CFsf—control submerged filter for dripping filters, commercial fittings HXF12KLL.

3.2.4. Other Water Parameters

The average water temperature in the system with PPA was 24.9 ± 0.1 °C, average pH— 8.84 ± 0.10 , whereas the average concentration of oxygen dissolved in water and saturation was 7.3 ± 0.3 mg O₂/dm³ and $88.9 \pm 3.8\%$, respectively. The same parameters in the system with PSC were: water temperature 24.9 ± 0.2 °C, pH 8.82 ± 0.10 , dissolved oxygen concentration 7.5 ± 0.4 mg O₂/dm³, saturation $92.1 \pm 3.9\%$. In the system with CF, the parameters were: water temperature 25.0 ± 0.3 °C, pH 8.83 ± 0.12 , dissolved oxygen concentration 7.0 ± 0.4 mg O₂/dm³ and saturation $85.7 \pm 4.7\%$. The parameters in the control system (CFsf) were: water temperature 24.9 ± 0.1 °C, pH 8.74 ± 0.15 , dissolved oxygen concentration 7.0 ± 0.3 mg O₂/dm³ and saturation $86.1 \pm 2.7\%$.

3.3. Statistical Analysis of Results

The results do not have a normal distribution ($p < 0.05$, Shapiro–Wilk test). A statistical analysis of the results using a Kruskal–Wallis ANOVA rank test revealed significant differences between the RAS systems ($p < 0.05$). Detailed results are provided in the table (Table 5).

Table 5. Analysis of concentrations of nitrogen compounds using Kruskal–Wallis ANOVA test on ranks ($p > 0.05$) showed differences between individual RAS systems. Results of a multiple comparison test of mean ranks for all samples: PPA—polypropylene aggregate, PSC—polyethylene screw caps for PET bottles, CF—commercial fittings HXF12KLL, CFsf—control submerged filter for dripping filters, commercial fittings HXF12KLL. Data marked with the same letter in rows did not differ statistically.

	Submerged Filter			Dripping Filter			
	PPA	PSC	CF	PPA	PSC	CF	CFsf
Ammonium	a	b	a	bc	c	bc	ab
Nitrite	bcd	bcd	a	cd	d	abc	ab
Nitrate	bc	bc	a	b	c	ab	bc

Analysis of the results of ammonium concentrations in individual RAS allowed the determination of two periods of a different character for which regression equations take a different form. After placing the fish, the concentration of ammonium in individual systems increased. High levels of ammonium were noted from day 3, followed by low ones. There was one day of intermediate values between periods. Increases and decreases of ammonium concentration occurred rapidly. In the case of a system in

which a failure occurred and it became necessary to restart it instead of a period with high concentrations, there was a period during which the concentration gradually decreased (Tables 1 and 3).

The analysis of nitrite concentration resulting in individual RAS allowed the determination of four periods with a different nature of the course. These periods for different RAS systems have a different duration but show a similar nature. In the first period, the regression equation describing the increase in concentration takes the form of an exponential function. In the second period, the concentration initially rose, reached the maximum level and began to decline and the equation takes a polynomial form. In the third period, characterized by a decrease in concentration, the equation takes on a power form. In the fourth period, nitrite concentrations remain at the same level without significant decreases or increases, and the equation again takes on a polynomial form (Table 6a,b).

Table 6. (a) Nitrite nitrogen concentration analysis in experimental RAS systems using regress equation (Reg.) and correlation coefficients (R): PPA—polypropylene aggregate, PSC—polyethylene screw caps for PET bottles, CF—commercial fittings HXF12KLL, CFsf—control submerged filter for dripping filters, commercial fittings HXF12KLL. (b) Nitrite nitrogen concentration analysis in experimental RAS systems (dripping, CF) using regress equation (Reg.) and correlation coefficient (R).

		(a)			
Type of Filter, Filling		Stage			
		I	II	III	IV
Submerged, PPA	Reg.	$y = 0.0137e^{0.5439x}$	$y = -0.1324x^2 + 4.8955x - 33.778$	$y = 6E + 10x^{-7.218}$	$y = 0.0007x^2 - 0.0651x + 1.8372$
	(R)	0.9988	0.9538	0.9916	0.6644
	Duration (d)	1–11	11–24	24–36	36–60
Submerged, PSC	Reg.	$y = 0.0117e^{0.4586x}$	$y = -0.16x^2 + 6.5599x - 52.287$	$y = 5E + 16x^{-10.96}$	$y = 0.0013x^2 - 0.1243x + 3.1995$
	(R)	0.9894	0.9909	0.9931	0.7628
	Duration (d)	1–13	13–27	27–36	36–60
Submerged, CF	Reg.	$y = 0.0115e^{0.8991x}$	$y = -0.24x^2 + 5.8161x - 14.642$	$y = 7E + 26x^{-20.47}$	$y = 0.0002x^2 - 0.0119x + 0.4015$
	(R)	0.9991	0.9031	0.9817	0.6522
	Duration (d)	1–8	8–18	18–22	22–60
Dripping, PPA	Reg.	$y = 0.0109e^{0.6266x}$	$y = -0.1126x^2 + 3.5649x - 16.232$	$y = 6E + 09x^{-6.821}$	$y = -0.0002x^2 - 0.0057 + 0.4272$
	(R)	0.9953	0.9216	0.9914	0.4423
	Duration (d)	1–11	11–19	19–31	31–45
Dripping, PSC	Reg.	$y = 0.0151e^{0.5446x}$	$y = -0.0698x^2 + 2.5974x - 11.5$	$y = 5E + 14x^{-9.983}$	$y = 0.002x^2 - 0.1489x + 3.1431$
	(R)	0.9979	0.9807	0.9913	0.9381
	Duration (d)	1–12	12–22	22–33	33–45
Submerged, CFsf	Reg.	$y = 0.0127e^{0.6536x}$	$y = -0.0698x^2 + 2.1765x - 5.6077$	$y = 2E + 12x^{-8.719}$	$y = 0.0013x^2 - 0.1001x + 2.1323$
	(R)	0.9995	0.9390	0.9914	0.9199
	Duration (d)	1–10	10–19	19–29	29–45
		(b)			
Type of Filter, Filling		Stage			
		I	II	III	
Dripping, CF	Reg.	$y = -0.0351x^3 + 0.469x^2 - 0.8346x + 0.4202$	$y = 18770x^{-3.647}$	$y = 0.001x^2 - 0.067x + 1.4065$	
	(R)	0.9998	0.9917	0.8223	
	Duration (d)	1–9	9–21	21–45	

The concentration of nitrates in RAS systems show a similar tendency. After the initial slow increase in concentration, accelerated growth followed and was then inhibited. An analysis of the obtained results showed a decrease in nitrate concentration at the end of the experiment, which is reflected in the derived regression equations (Table 7).

Table 7. Nitrate nitrogen concentration analysis in each experimental system using regress equation and correlation coefficients (R): PPA—polypropylene aggregate, PSC—polyethylene screw caps for PET bottles, CF—commercial fittings HXF12KLL, CFsf—control submerged filter for dripping filters, commercial fittings HXF12KLL.

Type of Filter, Filling	Regress Equation	Correlation Coefficients (R)
Submerged, PPA	$y = -0.0005x^3 + 0.0392x^2 - 0.1142x + 0.135$	0.9844
Submerged, PSC	$y = -0.0005x^3 + 0.0425x^2 - 0.3631x + 1.5747$	0.9946
Submerged, CF	$y = -0.0006x^3 + 0.0367x^2 + 0.5992x - 2.1153$	0.9797
Dripping, PPA	$y = -0.0017x^3 + 0.1118x^2 - 1.1623x + 3.931$	0.9884
Dripping, PSC	$y = -0.0015x^3 + 0.1082x^2 - 1.3589x + 4.808$	0.9882
Submerged, CFsf	$y = -0.0005x^3 + 0.0174x^2 + 0.9072x - 1.355$	0.9968
Dripping, CF	$y = -0.0015x^3 + 0.1052x^2 - 1.1256x + 3.7311$	0.9926

3.4. Fish

During the experiment, no mortality was observed in the reared fish.

4. Discussion

In the experiment, the dynamics of changes in nitrogen compounds in the water used for rearing fish in semi-closed RAS were analysed in detail. The dynamics of nitrogen compounds (ammonium, nitrite, nitrate) during the maturation of biological filters as well as during the operation of mature filters were examined. Furthermore, the usefulness of PPA and PSC as fillings for biological filters was demonstrated. Due to the differences in construction, all three fillings have their own advantages and disadvantages. Therefore, when comparing fillings, the analysis was based on the analysis of changes in concentrations of nitrogen compounds in water and the time needed to achieve full filter functionality. Comparing structural parameters, especially similar in terms of the size of the active surface of PSC and PPA fillings, could be subjective. The impact of structural parameters should be examined at a later stage of the study, in which the impact of individual factors (e.g., oxygen, temperature, suspense solids, diffusion rate, etc.) would be analysed on the dynamics of the nitrification process. Water exchange is necessary in aquaculture farms using a closed water cycle equipped with biological filters without denitrification due to ever increasing level of nitrate. Denitrification is the process of reducing nitrates to gaseous nitrogen. It is an anaerobic process that can sometimes occur in biological filters overloaded by biogens. The amount of water needed varies depending on several factors. The most important is the increase in nitrate concentration, which in high concentrations shows adverse effects on aquatic organisms [21,23,33]. At the start-up stage of RAS facilities, water change is required for a similar reason. High concentrations of toxic forms of nitrogen occurring during the maturation of biological filters require the use of water changes not only to supplement evaporation. In the experiment, a one-time top-up of 150 dm³ daily was used. This allowed for the dilution of nitrogen compounds and while supplementing calcium compounds in water, it also allowed better observation of the dynamics of nitrogen compound transformation processes. An important factor was also the use of common carp—a model species which is considered to be relatively resistant to adverse environmental rearing conditions [34].

Mechanical and biological filters must work together for the proper functioning of aquatic organisms [7,26,27,35,36]. The importance of the filtration process becomes significant when the breeding facility is built in RAS technology [22,37–42]. For the proper course of biological purification in the

nitrification process, the cooperation of two groups of microorganisms is required. The first group oxidizes ammonia to nitrites and the other group oxidizes the formed nitrites to nitrates [6,7,43–45]. By analysing the concentration of particular forms of nitrogen in the water used during the commissioning of breeding facilities, it is possible to observe individual stages of nitrification and thus determine whether the biological filter has gained functionality [18,45]. The unpredictability of the maturation process was shown in an experiment carried out by Pulkkinen et al. [46] illustrating the effect of the type of biological filter used (fixed and moving bed bioreactors) on nitrification in recirculating aquaculture systems. In that experiment, despite the use of filter fillings operating for six months, the faulty operation of the bed was observed, which was revealed by an initially high concentration of nitrites, whose low level was achieved only after about eleven weeks. According to these authors, such a situation was caused by disturbances in the bacterial composition produced by the shock of transportation to a laboratory. This indicates the exceptional sensibility of nitrifying bacteria to variable environmental conditions. Due to the high concentration of toxic nitrogen compounds, fish rearing in circuits with immature biological filters threatens the loss of fish being reared. This is especially true for salmonids [47]. Therefore, species resistant to elevated concentrations of nitrogen compounds should be used at the start-up stage of aquaculture facilities.

The experiment using fish as a source of compounds needed in the nitrification process allowed observation of the work of the biological filter in conditions simulating real fish breeding [18]. Research carried out in this way is very important to properly carry out the maturation process of the biological filter and obtain a filter adapted to the given conditions in RAS systems. A review of the literature has shown that this approach to the topic is rare [18,48]. Research using synthetic solutions with nitrogen compounds dominates the field [40,49,50]. In this experiment, carp was used as a model species [34] with high metabolism [31].

During the experiment, all systems noted a rapid increase in the ammonium content in water to approximately $3 \text{ mg N-NH}_4/\text{dm}^3$ (Figures 4 and 7; Tables 1 and 3). The increase in ammonium concentration resulted from placing the fish in the water cycle and starting feeding them. It should be emphasized that carp is a species with very high metabolism [31]. This level persisted from 4 days (submerged filter, CF) to 9 days (submerged filter, PSC) (Figure 4). In other filters, the duration of elevated ammonium concentration in the circuits was 7–8 days. After this period, there was a rapid, several-fold decrease in ammonium concentration in the RAS. It was assumed that the procedure involving the drying of the circuits and their disinfection through the use of potassium permanganate will eliminate nitrifying bacteria. The abrupt increase in ammonium has proved this assumption. Low concentrations persisted until the end of the experiment. In the system that was restarted, the distribution of ammonium concentrations was different (Figure 7). The first recorded results were about 60% lower than in other systems, and there was a rapid decrease in ammonium concentration. The fall curve was much milder. There is a discrepancy between the results obtained for two systems in which submerged filters filled with CF were used (Figures 4 and 7). The duration of elevated ammonium concentration for these systems was four days and eight days. The results during the experiment are divergent from the experiment carried out by Sikora et al. [18], in which no increase in ammonia concentration was observed. Kuhn et al. [45] reported similar results. In their research, they compared the effects of biological filters that were inoculated with nitrifying bacterial cultures with uninoculated filters. In unvaccinated RAS systems, ammonium nitrogen concentrations quickly rose above $2.5 \text{ mg}/\text{dm}^3$ and then decreased. The time in which the ammonium nitrogen concentration was increasing and decreasing differed for the studied filters. The curves of changes in concentration were also different. In the case of filters inoculated with bacterial cultures, the course was similar to that observed in the system, which was restarted. This example supports the suggestion that nitrifying bacterial cultures remain in this system despite disinfection with potassium permanganate. For studies based on nitrifiers immobilized in PVA (polyvinyl alcohol) and then adapted to the salty environment [51], the time needed to remove the elevated TAN concentration (initial concentration of TAN introduced into bioreactors was $10 \text{ mg}/\text{dm}^3$) to nitrite ranged from 22 days (salinity 30 ppt)

to 26 days (salinity 7.5 ppt). These are longer periods than obtained during the author's experiment. In 2015, Hu et al. [52] conducted research on the removal of nitrogen compounds from tilapia culture (*Oreochromis niloticus*) using aquaponic crops (tomato *Lycopersicon esculentum* and pak choi *Brassica campestris L. subsp. chinensis*). In these studies, they used root systems of cultured plants as growth surfaces for nitrifying bacteria. During the study, the highest TAN concentrations were reached when the TAN concentrations peaked around day 7 and were around 25 mg/dm³ (tomato) and 32.5 mg/dm³ (pak choi). These concentrations are higher than those observed in the discussed experiment; moreover, they did not decrease to a similar degree in a comparable period of time. This difference is probably due to the smaller root surface area in relation to the effective surface of the applied biological filter medias.

According to Karpinski et al. [53], the increase in nitrite concentration is delayed in relation to the increase in ammonium concentration (Figures 4, 5, 7 and 8; Tables 1, 3 and 6a). In the conducted experiment, an increase in nitrite concentrations was observed from the beginning of the experiment (Figures 5 and 8). Initially, these concentrations were relatively low compared to the observed concentrations of ammonium nitrogen, however, since the growth curve is exponential, the concentration of nitrite increased very quickly (Table 6a). Subsequently, the increase in nitrite concentration slowed down and slightly collapsed, followed by a reversal of the trend observed in the first period. Nitrite concentrations in all RAS systems dropped rapidly, reaching a relatively constant level (Figures 5 and 8, Table 6a,b). This course of concentration changes was observed in all RAS systems except the system in which the failure occurred (Table 6a). In this system, the period of deceleration and collapse of the upward trend does not occur (Table 6b). Maximum concentration values were reached much faster and they began to decrease faster. This is reflected in the equations describing the course of nitrification (Table 6a,b). The time needed to stabilize the second phase of nitrification ranged from 15 to 33 days (Figures 5 and 8). This is different from the results obtained by Kuhn et al. [45]. Despite the fact that measurements were carried out for 28 days, no downward trend was observed. This situation occurred in systems not inoculated with nitrifying bacteria. Different results were obtained in systems inoculated with nitrifiers—no increase in nitrite concentration was observed. In the research conducted by Sikora et al. [18], the time needed to stabilize the second phase of nitrification was 35 days, which is longer than the results observed in this article, although similar. Comparable times to those obtained during the experiment and to those obtained by Sikora et al. [18] were also obtained by Seo et al. [51] during an experiment with the acclimatization of nitrifiers to saltwater conditions. The acclimatization time of biological filters, and thus the time needed for nitrite oxidation to a safe level, was achieved after 33 days (salinity 7.5 and 15 ppt) and 39 days (salinity 30 ppt). Longer nitrite elimination times than observed during the experiment were also reported by Hu et al. [52]. The time needed for oxidation of nitrite to nitrate in aquaponic cultivation was about 40 and 50 days for tomato and pak choi respectively. As in the case of ammonia oxidation, the surface of the roots on which nitrifying bacteria developed was smaller than in the tested biological filter medias.

For nitrates, the recorded concentration values increased from the very beginning of the experiment. Initially, as with nitrites, this increase was slow to eventually accelerate. After a period of dynamic growth, nitrate concentrations stabilized (Figures 6 and 9; Table 7). For CF, despite the similar nature of the increase curve, the concentrations were higher during the first part of the experiment. No similar trend was observed for the same type of filter in the second part of the experiment (Figures 6 and 9). Higher values in the initial phase of growth in the second part of the experiment show the concentrations in the RAS system in which the failure occurred (Figure 9). The similar nature of the increase in nitrate concentration was reported by both Kuhn et al. [45] (circulation vaccinated with nitrifying bacteria) and Sikora et al. [18]. Kuhn et al. [45] did not observe an increase in the concentration of nitrates in the RAS system inoculated with nitrification, which was associated with the incomplete nitrification process. The nitrate concentration increase curve presented by Seo et al. [51] was comparable to the present experiment. At the end of the experiment, a decrease in nitrate concentration was observed in individual RAS systems. Probably this decrease was associated with the development of heterotrophic bacteria in the volume of water.

During this experiment, it was analysed how the concentrations of nitrogen forms in water are shaped in experimental RAS systems. On this basis, the course of the nitrification process was determined along with the time needed for the biological filter to mature. The maturation of the biological filter is largely dependent on the temperature at which the process takes place (Table 8). In systems using cool water, a mature filter can be obtained after a few months of its work, while this period is significantly shorter in systems developed for the needs of thermophilic species. Another factor that may affect the maturation of biological filters is the presence of the desired nitrifying bacteria. Biological filters inoculated with nitrifying bacteria, operating at 25 °C, show desirable properties after 53 days [54]. The use of water from tilapia culture (temperature 26.4 °C) allowed a functional biological filter to be obtained after 56 days [5]. These results do not reflect the information provided by Kolman [55], who states that at 18 °C, it takes 40 to 60 days to obtain a working biological filter. In addition, the periods given differ from those obtained by Sikora et al. [18]. Studies have shown that the time needed to mature a biological filter without inoculating the culture cycle with nitrifying bacteria cultures is 35 days at 23 °C.

Table 8. Comparison of time needed to mature biological filter in accordance with temperature on the example of literature data and conducted experiment: PPA—polypropylene aggregate, PSC—polyethylene screw caps for PET bottles, CF—commercial fittings HXF12KLL, CFsf—control submerged filter for dripping filters, commercial fittings HXF12KLL.

	Temperature (°C)	Time (d)	°D	Source of Biogens	
Sandu, et al., 2002	25.0	53	1325	No data	
Greiner and Timmons, 1998	26.4	56	1478.4	Fish	
Kolman, 2002	18.0	40–60	720–1080	No data	
Sikora et al. 2018	23.0	35	805	Fish	
Submerged, PPA	25.0	35	875	Fish	
Submerged, PSC	25.0	36	900	Fish	
Submerged, CF	25.0	21	525	Fish	
This paper	Dripping PPA	25.0	37	924	Fish
	Dripping PSC	25.0	32	800	Fish
	Submerged CFsf	25.0	18	700	Fish
	Dripping CF	25.0	18	450	Fish

The conducted tests showed that at 25 °C, without introducing nitrifying bacteria cultures into the RAS system, the time needed for the filter to mature is from 21 to 33 days. If nitrifying bacteria are present, this period may be shorter. In one of the RAS systems used for the experiment, a failure occurred. As a result of the failure, it was necessary to restart the RAS. This RAS was dried and disinfected in accordance with the adopted procedure. In this system (drip filter, CF), a functional biological filter was obtained on day 16.

5. Conclusions

The maturation of biological filters is, despite the overall repetitive pattern, a largely variable process. The time of individual stages of nitrification and their courses differ. It largely depends on the type of filter used and its filling and prevailing conditions. The obtained results showed the effectiveness of all tested biofilter media. The shortest time to biofilter maturation was when submerged CF was used. However, the maximum peak concentration of nitrite was also noted when it was used. For fish culture welfare, it is important that nitrite concentration should be as low as possible. Therefore, other tested biofilter media worked better from this point of view. New technologies are being sought, new materials are used as filter fillings and nitrification conditions are being modified. Increasingly, breeders want to increased production faster and faster. This involves the use of increasingly efficient filters that can be run faster. Research such as that described in this article is helpful, even necessary,

in learning how the nitrification process works, the conditions that shape it and what should be done to obtain fully efficient biological filters.

In addition, the article describes an unorthodox approach to new materials useful as cartridges for biological filters. Both PPA and PSC are materials that are associated as a convenient intermediate, not a useful cartridge for biological filters. However, these materials proved to be effective within the assumed parameters.

Author Contributions: The following statements should be used “Conceptualization, M.S., D.K.; Methodology, M.S., J.N.; Software, M.S.; Validation, M.S., J.N.; Formal Analysis, M.S.; Investigation, M.S.; Resources, M.S., D.K., J.N.; Data Curation, M.S.; Writing-Original Draft Preparation, M.S.; Writing-Review & Editing, M.S., J.N., D.K.; Visualization, M.S.; Supervision, D.K.; Project Administration, D.K. All authors have read and agreed to the published version of the manuscript.

Funding: This research was funded by UWM Olsztyn, project No. 18.610.005-110 and the project was financially supported by Minister of Science and Higher Education in the range of the program entitled "Regional Initiative of Excellence" for the years 2019-2022, Project No. 010/RID/2018/19, amount of funding 12.000.000 PLN.

Conflicts of Interest: The authors declare no conflict of interest.

References

1. FAO. HLEF2050 Global Agriculture. 2016. Available online: http://www.fao.org/fileadmin/templates/wsfs/docs/Issues_papers/HLEF2050_Global_Agriculture.pdf (accessed on 10 March 2016).
2. FAO. *The State of World Fisheries and Aquaculture, Contributing to Food Security and Nutrition for All*; Food and Agriculture Organization of the United Nations: Rome, Italy, 2016.
3. Timmons, N.; Timmons, M.B.; Ebeling, J.M. Recirculating Aquaculture System (RAS) Technologies. *Aquac. Mag.* **2006**, *32*, 32–39.
4. Kristensen, T.; Åtland, Å.; Rosten, T.; Urke, H.A.; Rosseland, B.O. Important influent-water quality parameters at freshwater production sites in two salmon producing countries. *Aquac. Eng.* **2009**, *41*, 53–59. [[CrossRef](#)]
5. Greiner, A.D.; Timmons, M.B. Evaluation of the nitrification rates of microbead and trickling filters in an intensive recirculating tilapia production facility. *Aquac. Eng.* **1998**, *18*, 189–200. [[CrossRef](#)]
6. Chen, S.; Ling, J.; Blancheton, J.P. Nitrification kinetics of biofilm as affected by water quality factors. *Aquac. Eng.* **2006**, *34*, 179–197. [[CrossRef](#)]
7. Empananza, E.J.M. Problems affecting nitrification in commercial RAS with fixed-bed biofilters for salmonids in Chile. *Aquac. Eng.* **2009**, *41*, 91–96. [[CrossRef](#)]
8. Eding, E.H.; Kamstra, A.; Verreth, J.A.J.; Huisman, E.A.; Klapwijk, A. Design and operation of nitrifying trickling filters in recirculating aquaculture: A review. *Aquac. Eng.* **2006**, *34*, 234–260. [[CrossRef](#)]
9. Wicks, B.J.; Joensen, R.; Tang, Q.; Randall, D.J. Swimming and ammonia toxicity in salmonids: The effect of sub lethal ammonia exposure on the swimming performance of coho salmon and the acute toxicity of ammonia in swimming and resting rainbow trout. *Aquat. Toxicol.* **2002**, *59*, 55–69. [[CrossRef](#)]
10. Randall, D.J.; Tsui, T.K.N. Ammonia toxicity in fish. *Marine Pollut. Bull.* **2002**, *45*, 17–23. [[CrossRef](#)]
11. Thurston, R.V.; Russo, R.C. Acute toxicity of ammonia to rainbow trout. *Trans. Am. Fish. Soc.* **1983**, *112*, 696–704. [[CrossRef](#)]
12. Thurston, R.V.; Russo, R.J.; Luedtke, R.J.; Smith, C.E.; Meyn, E.L.; Chakoumalos, C.; Wang, K.C.; Brown, C.J.D. Chronic toxicity of ammonia to rainbow trout. *Trans. Am. Fish. Soc.* **1984**, *113*, 56–73. [[CrossRef](#)]
13. Wood, C.M. Toxic responses of the gill. In *Target Organ Toxicity in Marine and Freshwater Teleosts*; Schlenk, D., Benson, W.H., Eds.; Taylor & Francis: London, UK, 2001; Volume 1, pp. 1–89.
14. Cheng, W.; Hsiao, I.S.; Chen, J.C. Effect of nitrite on immune response of Taiwan abalone *Haliotis diversicolor supertexta* and its susceptibility to *Vibrio parahaemolyticus*. *Dis. Aquat. Org.* **2004**, *60*, 157–164. [[CrossRef](#)] [[PubMed](#)]
15. Miron, D.S.; Moraes, B.; Becker, A.G.; Crestani, M.; Spanevello, R.; Loro, V.L.; Baldissarroto, B. Ammonia and pH effects on some metabolic parameters and gill histology of silver catfish, *Rhamdia quelen* (Heptapteridae). *Aquaculture* **2008**, *277*, 192–196. [[CrossRef](#)]
16. Benli, A.C.K.; Köksal, G.; Özkul, A. Sublethal ammonia exposure of Nile tilapia (*Oreochromis niloticus* L.): Effects on gill, liver and kidney histology. *Chemosphere* **2008**, *72*, 1355–1358. [[CrossRef](#)] [[PubMed](#)]

17. Hurtado, C.F.; Cancino-Madariaga, B. Ammonia retention capacity of nanofiltration and reverse osmosis membranes in a non-steady state system, to be use in recirculation aquaculture systems (RAS). *Aquac. Eng.* **2014**, *58*, 29–34. [[CrossRef](#)]
18. Sikora, M.; Nowosad, J.; Biegaj, M.; Kucharczyk, D.; Dębowski, M. The possibility of application of agglomerate elastomers (EPP) as media for biological bed in aquaculture. *Aquac. Res.* **2018**, *49*, 2988–2994. [[CrossRef](#)]
19. Zhu, S.; Chen, S. The impact of temperature on nitrification rate in fixed film biofilters. *Aquac. Eng.* **2002**, *26*, 221–237. [[CrossRef](#)]
20. Suhr, K.I.; Pedersen, P.B. Nitrification in moving bed and fixed bed biofilters treating effluent water from a large commercial outdoor rainbow trout RAS. *Aquac. Eng.* **2010**, *42*, 31–37. [[CrossRef](#)]
21. Hamlin, H.J. Nitrate toxicity in Siberian sturgeon (*Acipenser baeri*). *Aquaculture* **2006**, *253*, 688–693. [[CrossRef](#)]
22. Malone, R.F.; Pfeiffer, T.J. Rating fixed-film nitrifying biofilters used in recirculating aquaculture systems. *Aquac. Eng.* **2006**, *34*, 389–402. [[CrossRef](#)]
23. Camargo, J.A.; Alonso, A.; Salamanca, A. Nitrate toxicity to aquatic animals: A review with new data for freshwater invertebrates. *Chemosphere* **2005**, *58*, 1255–1267. [[CrossRef](#)]
24. Badiola, M.; Mendiola, D.; Bostock, J. Recirculating Aquaculture Systems (RAS) analysis: Main issues on management and future challenges. *Aquac. Eng.* **2012**, *51*, 26–35. [[CrossRef](#)]
25. Ling, J.; Chen, S. Impact of organic carbon on nitrification performance of different biofilters. *Aquac. Eng.* **2005**, *33*, 150–162. [[CrossRef](#)]
26. Guedart, T.C.; Losordo, T.M.; Classen, J.J.; Osborne, J.A.; DeLong, D.P. An evaluation of commercially available biological filters for recirculating aquaculture systems. *Aquac. Eng.* **2010**, *42*, 38–49. [[CrossRef](#)]
27. Guedart, T.C.; Losordo, T.M.; Classen, J.J.; Osborne, J.A.; De Long, D.P. Evaluating the effects of organic carbon on biological filtration performance in a large scale recirculating aquaculture system. *Aquac. Eng.* **2011**, *44*, 10–18. [[CrossRef](#)]
28. Kucharczyk, D.; Targońska, K.; Hliwa, P.; Gomułka, P.; Kwiatkowski, M.; Krejszef, S.; Perkowski, J. Reproductive parameters of common carp (*Cyprinus carpio* L.) spawners during natural season and out-of-season spawning. *Reprod. Biol.* **2008**, *8*, 285–289. [[CrossRef](#)]
29. Kucharczyk, D.; Nowosad, J.; Luczyński, M.J.; Targońska, K. New technique for fertilizing eggs of burbot, asp and ide under hatchery conditions. *Anim. Reprod. Sci.* **2016**, *172*, 143–147. [[CrossRef](#)]
30. Nowosad, J.; Kucharczyk, D.; Biłas, M.; Palińska-Żarska, K.; Krejszef, S. Optimization of feeding rate of juvenile common carp, (*Cyprinus carpio* L.), during short intensive rearing under controlled conditions. *Experiment* **2013**, *15*, 1056–1063.
31. Nowosad, J.; Żarski, D.; Biłas, M.; Dryl, K.; Krejszef, S.; Kucharczyk, D. Dynamics of ammonia excretion in juvenile common tench, *Tincatinca* (L.), during intensive rearing under controlled conditions. *Aquac. Int.* **2013**, *21*, 629–637. [[CrossRef](#)]
32. Svobodová, Z.; Máchová, J.; Poleszczuk, G.; Höda, J.; Hamááková, J.; Kroupová, H. Nitrite poisoning of fish in aquaculture facilities with water-recirculating systems. *Acta Vet. Brno* **2005**, *74*, 129–137. [[CrossRef](#)]
33. Kuhn, D.D.; Smith, S.A.; Boardman, G.D.; Angier, M.W.; Marsh, L.; Flick, G.J., Jr. Chronic toxicity of nitrate to Pacific white shrimp, *Litopenaeus vannamei*: Impacts on survival, growth, antennae length, and pathology. *Aquaculture* **2010**, *309*, 109–114. [[CrossRef](#)]
34. Tanikawa, D.; Nakamura, Y.; Tokuzawa, H.; Hirakata, Y.; Hatamoto, M.; Yamaguchi, T. Effluent treatment in an aquaponics-based closed aquaculture system with single-stage nitrification–denitrification using a down-flow hanging sponge reactor. *Int. Biodeterior. Biodegrad.* **2018**, *132*, 268–273. [[CrossRef](#)]
35. Losordo, T.M.; Hobbs, A.O. Using computer spreadsheets for water flow and biofilter sizing in recirculating aquaculture production systems. *Aquac. Eng.* **2000**, *23*, 95–102. [[CrossRef](#)]
36. Crab, R.; Avnimelech, Y.; Defoirdt, T.; Bossier, P.; Verstraete, W. Nitrogen removal techniques in aquaculture for sustainable production. *Aquaculture* **2007**, *270*, 1–14. [[CrossRef](#)]
37. Hargrove, L.L.; Westerman, P.W.; Losordo, T.M. Nitrification in three-stage and single-stage floating bead biofilters in a laboratory-scale recirculating aquaculture system. *Aquac. Eng.* **1996**, *15*, 67–80. [[CrossRef](#)]
38. van Rijn, J. The potential for integrated biological treatment systems in recirculating fish culture. *Rev. Aquac.* **1996**, *139*, 181–201. [[CrossRef](#)]

39. Ridha, M.T.; Cruz, E.M. Effect of biofilter media on water quality and biological performance of the Nile tilapia *Oreochromis niloticus* L. reared in a simple recirculating system. *Aquac. Eng.* **2001**, *24*, 157–166. [[CrossRef](#)]
40. Zhu, S.; Chen, S. An experimental study on nitrification biofilm performances using a series reactor system. *Aquac. Eng.* **1999**, *20*, 245–259. [[CrossRef](#)]
41. Żarski, D.; Kucharczyk, D.; Targońska, K.; Chyla, B.; Dobrotowicz, A. Dynamics of changes in nitrogen and phosphorus compounds during intensive rearing of ide, *leuciscusidus* (L.), in a recirculating system. *Arch. Pol. Fish.* **2008**, *16*, 459–467. [[CrossRef](#)]
42. Żarski, D.; Kucharczyk, D.; Targońska, K.; Krejszeff, S.; Czarkowski, T.; Babiarsz, E.; Nowosielska, D.B. Dynamics of nitrogen and phosphorus in closed and semi-closed recirculating aquaculture systems during the intensive culture of goldfish, *Carassius auratus auratus* (L.), juveniles. *Arch. Pol. Fish.* **2010**, *18*, 187–193. [[CrossRef](#)]
43. Ebeling, J. Biofiltration. In *Presentation Notebook of the Aquacultural Engineering Society Workshop; Intensive Fin-fish Systems and Technologies*: Orlando, FL, USA, 2001; pp. 47–56.
44. Itoi, S.; Ebihara, N.; Washio, S.; Sugita, H. Nitrite-oxidizing bacteria, nitrospira, distribution in the outer layer of the biofilm from filter materials of a recirculating water system for the goldfish *Carassius auratus*. *Aquaculture* **2007**, *264*, 297–308. [[CrossRef](#)]
45. Kuhn, D.D.; Drahos, D.D.; Marsh, L.; Flick, G.J., Jr. Evaluation of nitrifying bacteria product to improve nitrification efficacy in recirculating aquaculture systems. *Aquac. Eng.* **2010**, *43*, 78–82. [[CrossRef](#)]
46. Pulkkinen, J.T.; Eriksson-Kallio, A.M.; Aalto, S.L.; Tirola, M.; Koskela, J.; Kiuru, T.; Vielma, J. The effects of different combinations of fixed and moving bed bioreactors on rainbow trout (*Oncorhynchus mykiss*) growth and health, water quality and nitrification in recirculating aquaculture systems. *Aquac. Eng.* **2019**, *85*, 98–105. [[CrossRef](#)]
47. Davidson, J.; Good, C.; Williams, C.; Summerfelt, S.T. Evaluating the chronic effects of nitrate on the health and performance of post-smolt Atlantic salmon *Salmo salar* in freshwater recirculation aquaculture systems. *Aquac. Eng.* **2017**, *79*, 1–8. [[CrossRef](#)]
48. Hamlin, H.J.; Michaels, J.T.; Beaulaton, C.M.; Graham, W.F.; Dutt, W.; Steinbach, P.; Losordo, T.M.; Schrader, K.K.; Main, K.L. Comparing denitrification rates and carbon sources in commercial scale upflow denitrification biological filters in aquaculture. *Aquac. Eng.* **2008**, *38*, 79–92. [[CrossRef](#)]
49. delos Reyes, A.A., Jr.; Lawson, T.B. Combination of a bead filter and rotating biological contactor in a recirculating fish culture system. *Aquac. Eng.* **1996**, *15*, 27–39. [[CrossRef](#)]
50. Barak, Y.; van Rijn, J. Biological phosphate removal in a prototype recirculating aquaculture treatment system. *Aquac. Eng.* **2000**, *22*, 121–136. [[CrossRef](#)]
51. Seo, J.-K.; Jung, I.-H.; Kim, M.-R.; Kim, B.J.; Nam, S.-W.; Kim, S.-K. Nitrification performance of nitrifiers immobilized in PVA (polyvinyl alcohol) for a marine recirculating aquarium system. *Aquac. Eng.* **2001**, *24*, 181–194. [[CrossRef](#)]
52. Hu, Z.; Lee, J.W.; Chandran, K.; Kim, S.; Brotto, A.C.; Khanal, S.K. Effect of plant species on nitrogen recovery in aquaponics. *Bioresour. Technol.* **2015**, *188*, 92–98. [[CrossRef](#)]
53. Karpiński, A.; Szkudlarek, M.; Zakęś, Z. Nitrification in recirculation systems. Practical remarks about maturation of the biologically active filter. *Komunikaty Rybackie* **1999**, *3*, 11–14. (In Polish)
54. Sandu, S.I.; Boardman, G.D.; Watten, B.J.; Brazil, B.L. Factors influencing the nitrification efficiency of fluidized bed filter with a plastic bead medium. *Aquac. Eng.* **2002**, *26*, 41–59. [[CrossRef](#)]
55. Kolman, R. Effectiveness of a biological shelf filter used to treat water in a recirculation system during trout rearing. *Arch. Pol. Fish.* **1992**, *1* (Suppl. 1), 1–37. (In Polish)



© 2020 by the authors. Licensee MDPI, Basel, Switzerland. This article is an open access article distributed under the terms and conditions of the Creative Commons Attribution (CC BY) license (<http://creativecommons.org/licenses/by/4.0/>).

Article

Is It Possible to Restore a Heavily Polluted, Shallow, Urban Lake?

Jolanta Grochowska *, Renata Augustyniak, Michał Łopata and Renata Tandyrak

Department of Water Protection Engineering and Environmental Microbiology, Institute of Engineering and Environmental Protection, University of Warmia and Mazury, St. Prawocheńskiego 1, 10-720 Olsztyn, Poland; rbrzoza@uwm.edu.pl (R.A.); michal.lopata@uwm.edu.pl (M.Ł.); renatat@uwm.edu.pl (R.T.)

* Correspondence: jgroch@uwm.edu.pl

Received: 17 April 2020; Accepted: 25 May 2020; Published: 27 May 2020

Abstract: The research was carried out on Karczemne Lake, a water reservoir located in Kartuzi (northern Poland, Pomeranian Lake District). Monitoring of the water and bottom sediment of Karczemne Lake showed a very high level of contamination of the reservoir by a long-term inflow of untreated municipal sewage. The trophic status index of total phosphorus (TP) was unusually high at 101, and the TP content in the bottom sediments— 31 mg g^{-1} (dry weight)—was the highest value recorded worldwide in a lake. Based on the monitoring results, to achieve constant improvement of the water quality, we recommend a completely new, safe and economically justified method of bottom sediment removal and management. A very important aspect of this method is the prevention of uncontrolled sewage discharge back into the lake basin. Removed sediment with interstitial water will be pumped through a pipeline and transported to a sewage treatment plant. In the sediment mining field in which the sludge will be removed, the first phase of phosphorus inactivation will be carried out to chemically precipitate pollutants distributed in the water column as a result of sediment resuspension. After the deepening of the entire lake basin, the method of phosphorus inactivation will be carried out on the entire surface of the lake as the next stage of restoration. A supporting activity will be biomanipulation. Before the restoration is started, the municipal sewerage system will be modernized.

Keywords: urban lake; restoration; dredging; phosphorus inactivation; biomanipulation

1. Introduction

Strong anthropopressure in the catchment areas of lakes (urbanization, industrialization, deforestation and intensive livestock), which stimulates an increased supply of nutrients to waters, causes the acceleration of eutrophication [1–3]. Accelerated eutrophication is exemplified by strong cyanobacterial blooms, species depletion at all trophic levels, the disappearance of valuable fish species and the deterioration of the taste and smell of the water, which leads to the cessation of the reservoir being used for municipal and recreational purposes [4–6]. A sign of excessive eutrophy of the lake is an increase in nutrient concentrations (nitrogen and phosphorus) in the water and an uneven distribution of the amount of oxygen in the water column [7–9]. The surface layers of the reservoir are usually saturated with oxygen, while at the bottom, anaerobic conditions prevail, promoting the release of nutrients from bottom sediments. In oligotrophic and mesotrophic lakes, bottom sediments are a “trap” that bind excess nutrients, especially phosphorus. In degraded lakes, in which the bottom water layers are deoxygenated and therefore accompanied by a reduction in redox potential, the reverse process takes place. The stored substances, such as nutrients, are released into the near-bottom water layers [10–12]. This phenomenon is called internal loading. The amount of nutrients in the bottom sediment of the lake is extremely high. The sediments of degraded lakes are the main, inexhaustible source of biogenic compounds. Considering the content of the most important

nutrient—phosphorus—in the particular parts of lake ecosystems, it was found that approximately 90% of the total phosphorus was contained in the upper 10-cm layer of the bottom sediments [13]. This result clearly indicates the need to limit this “source”. The inhibition of internal loading is the main goal of all lake restoration methods, including artificial aeration, phosphorus inactivation, capping and the Rippl method [14–16].

The removal of bottom sediment is widely regarded as a radical but highly effective restoration method for shallow, heavily degraded reservoirs [17]. The complete removal of bottom sediment to the parent rock floor guarantees radical renovation of the lake and an increase in its volume, which often has previously been decreased due to the inflow of excessive pollution. Considering the thickness of sediments in postglacial lakes, often up to several meters or more, this method should be considered unrealistic.

Innovative lake restoration projects using the dredge method should be preceded by detailed monitoring of water and bottom sediment. Therefore, lake monitoring should be started with an examination of the spatial composition of bottom sediments to precisely determine the thickness of the most contaminated layer that is supposed to be removed. In addition, uncovered deposits that remain in the lake should be poor in nutrients, while phosphorus, as the main element responsible for eutrophication, must be stored in a biologically inactive form, i.e., as residual phosphorus or calcium-bound phosphorus [18–20]. This method of removing bottom deposits is very rarely used due to its complexity, cost and implementation difficulties. However, although the name of the method refers to bottom sediment removal, such a project must also take into account the output development and processing/utilization of the solid and liquid fractions [15,16,21]. The processing, management and utilization of deposits is often the greatest logistical and economic challenge.

An example of a very inept attempt at lake restoration by the bottom sediment removal method was the case of Mogileńskie Lake in Poland. The sediment and interstitial water removed from the lake were not properly managed, and before they were processed, the effluents returned to the lake water, destroying the initial effects and causing an ecological catastrophe [22].

In the case of the restoration of the Swedish Lake Trummen, the sediment was pumped to simple settling ponds constructed in an abandoned farming area from which the topsoil had first been removed. The runoff water from the settling ponds—a mixture of lake and interstitial water—was treated with aluminum sulfate in a simple plant for the precipitation of phosphate and suspended matter. Before restoration, the total phosphorus content of the lake water was approximately $600 \mu\text{g L}^{-1}$. The phosphorus concentration of the water from the settling ponds was on the order of milligrams per liter before the treatment. After precipitation, the total phosphorus content of the runoff water was approximately $30 \mu\text{g/L}$ [23]. The area designated for the infrastructure to process the liquid and solid output was approximately 30 ha. It should be noted that it is rare to find so much space in the vicinity of a lake that can be used to safely convert the removed deposit.

According to a study of the Vajgar artificial reservoir by Björk et al. [24], the top of the sediment that had accumulated in the pond served as an uncontrolled source of nutrients and was removed. The sediment pumping started in August 1991, and by the end of 1992, approximately $330,000 \text{ m}^3$ of sediment had been pumped out of the pond and transported in pipes to seven settling lagoons approximately 2.5 km away, each of which was approximately 1 ha in area and 3–5 m deep. The sediment transported from the fish pond had a dry mass content of 10–15%. The whole cost was approximately US \$850,000.

The above examples indicate that the removal of bottom sediments from reservoirs is logistically very difficult, and in the case of ill-considered solutions, it can cause the opposite effect—an ecological disaster. Another disadvantage of this method is the very high cost; therefore, before developing a project to extract sediments, the spatial distribution of the phosphorus in the sediment should be determined to accurately indicate the thickness of the sediment, the extraction of which will guarantee the improvement of the state of the lake as a result of stopping the emission of pollutants from the sediments back into the water column.

The aim of the study was to determine the spatial distribution of pollutants in bottom sediment and interstitial water of Karczemne Lake and on their basis to determine the thickness and volume of sediment necessary for extraction to improve the quality of water in the reservoir. This research has allowed the development of the concept of a completely new, safe and economically justified method of mining and managing the bottom sediments. The proposed method will prevent uncontrolled effluent drainage back into the lake basin. In addition, it does not require the construction of a completely new bottom sediment treatment system consisting of presses, centrifuges, polymer-dosing stations, water-conditioning equipment and reaction pools. After sediment is removed from the lake bowl, phosphorus inactivation and biomanipulation is also recommended.

2. Material and Methods

2.1. Study Site

Karczemne Lake (54°19'42" N, 18°11'27" E) is a strongly degraded urban lake located in the Kaszubian Lake District and belongs to the macroregion of the Eastern Pomeranian District in Kartuzy town [25]. Karczemne Lake is a shallow, polymictic, flow-through lake. Its area is 40.4 ha, and its maximum depth is 2.3 m (Figure 1). More detailed morphometric parameters of the lake are given in Table 1.



Figure 1. Location of the Karczemne Lake.

Table 1. Morphometric parameters of Karczemne Lake.

Parameter	Value
Elevation of normal water table (m AMSL)	203.7
Lake surface (ha)	40.4
Maximum depth (m)	3.2
Average depth (m)	1.98
Relative depth	0.0050
Depth indicator	0.62
Volume (in thousand m ³)	798.3
Maximum length (m)	1282
Maximum width (m)	445
Elongation indicator	2.9
Average width (m)	315
Shoreline length (m)	3163
Indicator of shoreline development	1.4

From the early 1950s, Karczemne Lake was transformed into a receiver for domestic sewage, as well as sewage from dairies, slaughterhouses, breweries, furniture factories and municipal hospitals. Over 30 years, 60% of the raw municipal sewage went to Karczemne Lake through six sanitary sewers. With the expansion of the urban area, the amount of municipal sewage increased. Impurities from emerging single-family housing were collected in leaking cesspits, which caused some of the pollution to seep into the ground and migrate toward the lake. Some cesspits had overflows to the combined sewerage network, and municipal sewage flowed directly to the lake in this way. It was also possible to illegally connect sanitary sewers from individual domestic properties to the stormwater drainage system and directly discharge sewage to the lake from homes located along the shore. The improvement of water and sewage management in Kartuzy City began in the mid-1970s. In 1982, a mechanical-biological sewage treatment plant was opened. In the 1990s, almost the entire city was connected to a sanitary sewerage system, and it was only in 2010 that the management of stormwater began to be organized through the construction of settling tanks and stormwater separators. Until 2018, the stormwater drainage network in Kartuzy covered only part of the city—17%. This situation meant that during heavy rainfall, local flooding occurred, and the excess rainwater and snowmelt from streets that did not have a rainwater drainage system penetrated the sanitary sewer system, overloading it. The connection of the existing stormwater drainage system to the sanitary sewer system caused raw sewage to load into the lake.

The total catchment basin of Karczemne Lake covers 5.15 km². This area is covered by two entirely different (in their ability to activate the load of nutrients in a surface flow) forms of land use: forests (57%) and urbanized areas (43%). The direct catchment of Karczemne Lake, excluding the area covered by the drainage system collecting rainwater, covers 0.45 km²: wasteland constitutes 20.7% of its total surface area, and forests grow over the other 79.3%. The calculations of the amount of nutrients that are annually brought to the lake with a watercourse or from outfalls were performed based on their actual concentration in water (total phosphorus—TP and total nitrogen—TN) and flows measured at the individual stations during yearly field studies. The partial load for a given day was the product of the volume of water (momentary flow) and the concentration of given nutrients in the water. Nutrient loads were calculated with a generally accepted method of time periods. The magnitude of a lake load with nutrients originating from surface flows from the direct catchment was calculated with a method that is recommended and applied by the OECD (Organisation for Economic Cooperation and Development) that involves the use of flow coefficients. The load of nutrients introduced to a lake with precipitation was determined based on the coefficients of pollution deposition per surface unit. It was assumed that angling baits are the main sources of pollution resulting from the recreational use of lakes. Based on the data obtained from Group No 57 of the Polish Angling Association from Kartuzy and conversion factors described by Wołos and Mioduszczyńska [26], the average number of anglers who used baits was calculated for each of the lakes. It was also assumed that the average content of biogenic compounds in fish feed was 3.0 g P and 12.0 g N per kg of bait.

Until the end of 2018, Karczemne Lake was a receiver of nutrient loads from both the catchment and atmosphere, which involved the following basic components: areal sources; inflow of waters via a watercourse that links Karczemne Lake with Mielenko Lake (this watercourse flows into the reservoir in the central part of the west bank); point sources (6 stormwater outfalls and sometimes the illegal discharge of municipal sewage); atmospheric sources and recreation, such as angling. The total loads of phosphorus and nitrogen introduced into Karczemne Lake were 134.7 kg P year⁻¹ (0.330 g P m⁻² year⁻¹) and 1133.8 kg N year⁻¹ (2.80 g N m⁻² year⁻¹), respectively. The permissible and dangerous (critical) loads calculated for this lake from Vollenweider's hydrological model [27] were 0.030 g P m⁻² year (12.1 kg year⁻¹) and 0.060 g P m⁻² year (24.2 kg year⁻¹), respectively. The analysis revealed that the total phosphorus load introduced from external sources to the lake exceeded the dangerous load and was responsible for accelerated eutrophication. The phosphorus load introduced to Karczemne Lake was 550% higher than the critical load.

2.2. Water Sample Collection and Analysis

The physicochemical properties of water samples from Karczemne Lake were determined over an annual cycle (April 2018, June 2018, August 2018 and November 2018). Samples were taken at the point of the maximum depth (Figure 2). The scope of the water analysis included the total phosphorus (TP; standard methods 2012), total nitrogen (TN; Shimadzu TOC 5000 analyzer, Kyoto, Japan), chlorophyll a by the colorimetric method (after concentration on a glass fiber filter Whatman GF/B and extraction with acetone—Nanocolor UV/vis, Macherey-Nagel (GmbH & Co., KG, Frankfurt, Germany); 750/664 nm before and 750/665 nm after acidification) and visibility (Secchi disc).

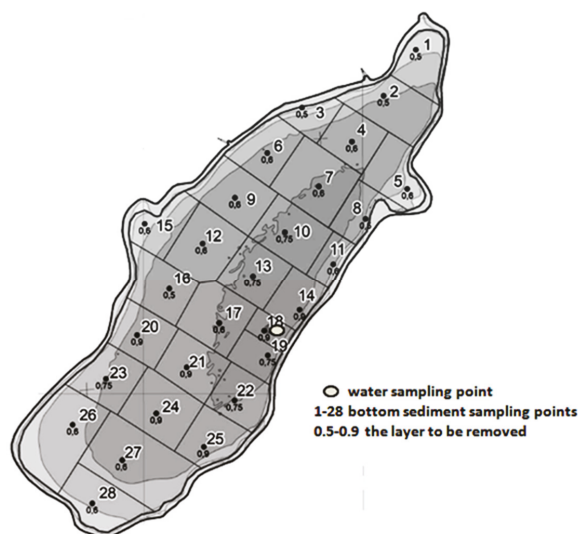


Figure 2. The spatial distribution of research points with the thickness of the sediment layer meant to mining.

The trophic state index (TSI) was calculated based on the concentrations of total phosphorus, total nitrogen and chlorophyll a, as well as Secchi disc visibility [28,29].

The coefficient of variation (CV) for the repeated analysis was 2% [30].

2.3. Bottom Sediment Collection

The bottom sediment sampling was carried out on 7, 8, 9 and 11 March 2018. Samples for analysis were taken at 28 research stations (Figure 2), for which geographical coordinates were determined (Table 2).

The sediment cores were obtained using a Kajak tube sampler (KC Company, Silkeborg, Denmark). Every core length included the sediment layer down to the parent rock (floor). In this way, the thickness of the retrieved sediments was determined precisely at individual sites, and their organoleptic properties were assessed. During the collection, individual cores were divided into layers with a thickness of 30 cm (a—0–30 cm, b—31–60 cm, c—61–90 cm, d—91–120 cm, e—121–150 cm and f—151–180 cm) and prepared as separate samples. A total of 112 material samples were collected from the bottom of the lake.

Table 2. Geographical coordinates of sediment sampling points from Karczemne Lake.

Point Number	Latitude	Longitude
1	N:54°33'27.5"	E: 18°19'61.4"
2	N:54°33'19.0"	E:18°19'51.1"
3	N:54°33'16.9"	E:18°19'25.3"
4	N:54°33'10.6"	E:18°19'41.0"
5	N:54°33'01.8"	E:18°19'58.5"
6	N:54°33'08.5"	E:18°19'14.3"
7	N:54°33'02.3"	E:18°19'30.5"
8	N:54°32'96.3"	E:18°19'45.3"
9	N:54°33'00.3"	E:18°19'04.0"
10	N:54°32'93.9"	E:18°19'19.7"
11	N:54°32'87.9"	E:18°19'35.0"
12	N:54°32'91.8"	E:18°18'93.8"
13	N:54°32'85.7"	E:18°19'09.6"
14	N:54°32'79.4"	E:18°19'24.3"
15	N:54°32'95.5"	E:18°18'75.4"
16	N:54°32'83.4"	E:18°18'83.2"
17	N:54°32'77.0"	E:18°18'98.9"
18	N:54°32'75.5"	E:18°19'13.1"
19	N:54°32'71.0"	E:18°19'14.3"
20	N:54°32'74.8"	E:18°18'72.9"
21	N:54°32'68.8"	E:18°18'88.6"
22	N:54°32'62.6"	E:18°19'03.7"
23	N:54°32'66.7"	E:18°18'63.1"
24	N:54°32'60.3"	E:18°18'78.9"
25	N:54°32'54.1"	E:18°18'94.0"
26	N:54°32'58.2"	E:18°18'52.5"
27	N:54°32'51.7"	E:18°18'68.2"
28	N:54°32'43.7"	E:18°18'58.6"

2.4. Bottom Sediment and Interstitial Water Sample Analysis

The output, after being transported to the laboratory, was weighed to determine the volumes and densities of the fresh samples. The samples were then dried to constant weight, and the volume and density were redetermined. The interstitial water was obtained from the sediment by centrifugation at 3000 rpm for 20 min according to Brzozowska and Gawrońska [31].

In the interstitial water samples, ammonia was examined by ionic chromatography using an ICS-5000 DIONEX DC, TKN by IL 550 TOC-TN analyzer, Hach Inc. (Larimer Country, CO, USA), phosphates and total P were measured by a Nano color spectrophotometer, and organic P was calculated as the difference between the TP and phosphate amounts. In the investigated sediments, organic matter was measured by LOI (the percent weight loss during the ignition) using weight analysis [31], total nitrogen was measured by the Kjeldahl method and silica was measured using weight analysis after preliminary digestion of the sediment sample in a mixture of strong mineral acids (H₂SO₄, HClO₄ and HNO₃ 1:2:3) and filtering through a No. 390 filter. The phosphorus fractions were analyzed by sequential extraction according to the Rydin and Welch method [32] modified by van Hullebush et al. [33]. In the analyzed sediments, samples were examined for the following:

- Labile phosphorus (NH₄Cl-P; after 2 × 2 h extraction in 1 M NH₄Cl),
- Phosphorus sensitive for redox potential changes (BD-P; after 2 h extraction in 0.11 M buffered dithionite solution),
- Phosphorus bound with aluminum and organic matter (NaOH-TP; after 16 h extraction in 0.1 M NaOH and mineralization of extract using the 10 N mixture of H₂SO₄ and HClO₄),
- Phosphorus bound with aluminum and iron oxides and hydroxides (NaOH-rP; directly in the NaOH extract),

- Phosphorus bound with organic matter (NaOH-nrP; was calculated as the difference between NaOH-TP and NaOH-rP),
- Calcium bound phosphorus (HCl-P; after 16 h extraction in 0.5 M HCl),
- Residual phosphorus (res-P; was calculated as the difference between TP after mineralization using a mixture of H₂SO₄ and HClO₄ and the sum of the fractions of NH₄Cl-P, BD-P, NaOH-TP and HCl-P).

Extracted phosphorus was determined using the molybdate blue method according to Hermanowicz et al. [34]. The results were statistically analyzed (basic statistics—mean values, standard deviation) using a Statistica 13.0 software package [35].

2.5. Studies of the Spatial Variability of Phosphorus and Nitrogen Concentrations in the Bottom Sediment

Lake restoration using the dredge method must be planned very precisely. The most important element of the project is to precisely define the thickness of the deposits that should be removed from the ecosystem. The thickness needed to remove the deposits is determined on the basis of the changes in phosphorus content in the sediment and the fractions in which phosphorus is present. The analysis of the Karczemne Lake bottom was planned in such a way to obtain the most complete information about the structure of its bottom. Due to the lack of data regarding the thickness and properties of the bottom sediments, probes were planned at points evenly distributed over the whole bottom surface of the lake. This methodical approach is recommended by the EPA [36] in situations with limited preliminary data. The results of the soundings referred to the partial surfaces of the lake bottom for which the given probing point was the geometric center (Voronoi diagrams; Wolfram Math Worlds [37]).

2.6. Studies of Heavy Metals and Persistent Organic Pollutant Contents

In accordance with the guidelines included in the Ordinance of Ministry of the Environment (OME) [38] on waste recovery outside installations and equipment, six aggregate samples were prepared for analyzing the content of stable organic pollutants (POPs), polycyclic aromatic hydrocarbons (PAHs) and heavy metals in the sediments.

- No. 1—mixed sediment sample taken from stations 1–15, layers a (0–30 cm) and b (31–60 cm);
- No. 2—mixed sediment sample taken from stations 1–15, layers c (61–90 cm) and d (91–120 cm);
- No. 3—mixed sediment sample taken from stations 16–28, layers a (0–30 cm) and b (31–60 cm);
- No. 4—mixed sediment sample taken from stations 16–28, layers c (61–90 cm) and d (91–120 cm);
- No. 5—mixed sediment sample taken from station 5, layers a (0–30 cm) and b (31–60 cm);
- No. 6—mixed sediment sample taken from station 5, layers c (61–90 cm) and d (91–120 cm).

Limitations on the further use of bottom sediments or other types for development can result from higher than normal heavy metal content according to Hermanowicz et al. [34] or the presence of extremely hazardous persistent organic pollutants (POPs), such as hexachlorobenzene (HCB), polychlorinated biphenyls (PCBs) and polycyclic aromatic hydrocarbons (PAHs). Analyses of heavy metals, polycyclic aromatic hydrocarbons and polychlorinated biphenyls were performed by the AAS (Atomic Absorption Spectrometer), ICP-AES (Inductively Coupled Plasma-Atomic Emission Spectrometer) and GC MS (Gas Chromatography Mass Spectrometry) methods. The coefficient of variation (CV) for the repeated analysis was 2% [30].

The usefulness of deposits for development was verified based on The Act on Waste [39] and concentrations of toxic substances caused by pollution [39]. The waste catalog classifies bottom sediments as waste with code 17 05 05 (dredging spoil containing or contaminated with dangerous substances), with the note that the sediments are hazardous waste or 17 05 06 (dredging spoil other than those mentioned in 17 05 05).

3. Results

3.1. Trophic Status

The value of every index calculated from the concentrations of total phosphorus, total nitrogen, visibility and chlorophyll a exceeded TSI 70 (Figure 3). This demonstrated strong pollution of the analyzed lake.

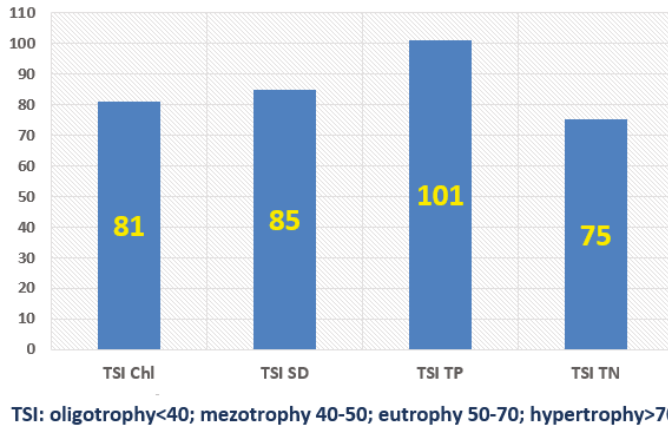


Figure 3. The trophic status index (TSI) calculated on the basis of visibility (SD) chlorophyll concentrations (Chl), total phosphorus (TP) and total nitrogen (TN).

3.2. Phosphorus and Nitrogen Content in the Interstitial Water of Karczemne Lake

The interstitial water of Karczemne Lake was rich in biogenic compounds. The mean content of total phosphorus varied between 0.61 and 10.0 mg P L⁻¹ (Figure 4).

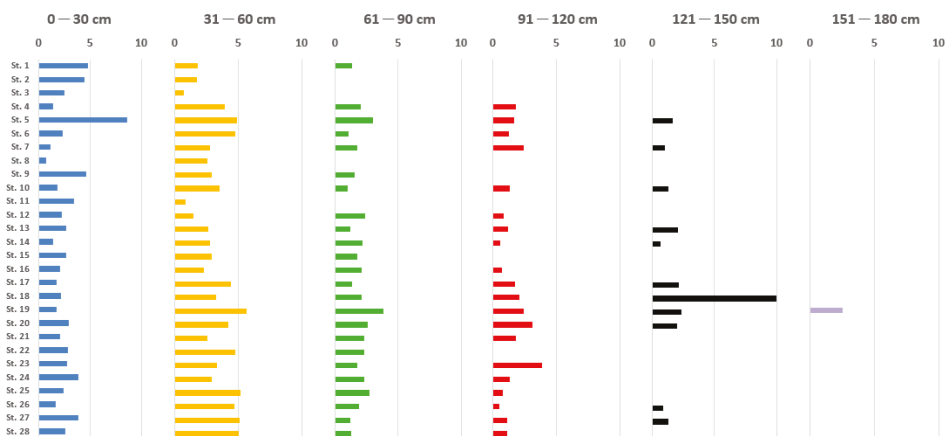


Figure 4. Mean content of total phosphorus in the interstitial water of Karczemne Lake (mg P L⁻¹).

In the composition of total phosphorus in the interstitial water of the deeper sediment layers, organic phosphorus predominated, while in the layer with a thickness of 30 cm, phosphates prevailed. The highest concentration of phosphorus was recorded in the interstitial water separated from the bottom sediment that was under the influence of anthropopression, i.e., near the outlet of stormwater

collectors that previously experienced the inflow of domestic and industrial sewage. Sewage discharge points were located along the eastern shore of the lake. There, the maximum concentration of total phosphorus usually occurred in the interstitial water of the b layer: 31–60 cm.

The mean total nitrogen content in the interstitial water of Karczemne Lake varied from 9.60 to 71.40 mg N L⁻¹ (Figure 5). The concentrations of TN in the interstitial water clearly increased with depth in the sediment. In the nitrogen structure, the organic form was predominant. In the analyzed water, mineral nitrogen was in the form of ammonium nitrogen, the amount of which varied between 4.00 (St. 2 a) and 37.80 mg N L⁻¹ (St. 27 e). The values of ammonium nitrogen increased in the interstitial water in the sediment. The highest ammonia contents were found in the interstitial water of the bottom sediment located in the area bounded by 2 m and 3 m isobaths and at probing point No. 5.

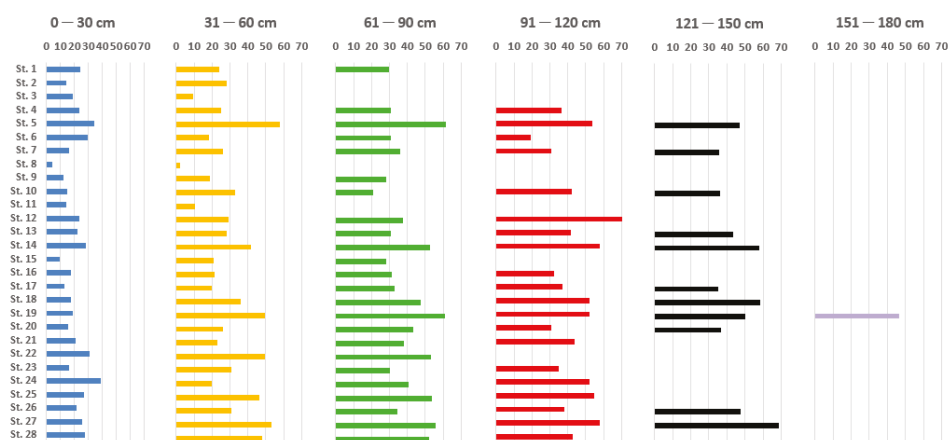


Figure 5. Mean content of total nitrogen in the interstitial water of Karczemne Lake (mg N L⁻¹).

3.3. Density and Hydration of the Analyzed Bottom Sediment

Spatially, the bottom sediments of Karczemne Lake were characterized by a heterogeneous structure and variations in thickness and degree of consolidation.

The maximum thickness of modern sediments was 1.8 m. The thickness of the deposit is related to the long-term supply of sewage, which results in clear shallowing of the lake bed. Littoral deposits were characterized by the smallest thicknesses, with an average of 60 cm.

The deposits with the largest thickness occurred in the region of the maximum depth of the lake and in the places of inflow of municipal and industrial sewage.

The bottom sediments of Karczemne Lake had a loose structure that was susceptible to resuspension (agitation). The sediment mean hydration in the 30 cm thick layer fluctuated from approximately 94–95% (Figure 6).

More dense and compact structures were observed only in the lower layers of the cores, especially in the littoral zone (Figure 7). The boundaries of structures within the cores were not clearly marked. The floor layer, constituting the native soil, was gytja, i.e., organic and mineral sediment comprised mainly of the remains of allochthonous organisms with an admixture of sands. The mean density of the deposits of Karczemne Lake ranged from 0.99 to 1.45 g cm⁻³, and on average, it was 1.05 g cm⁻³ (Figure 7).

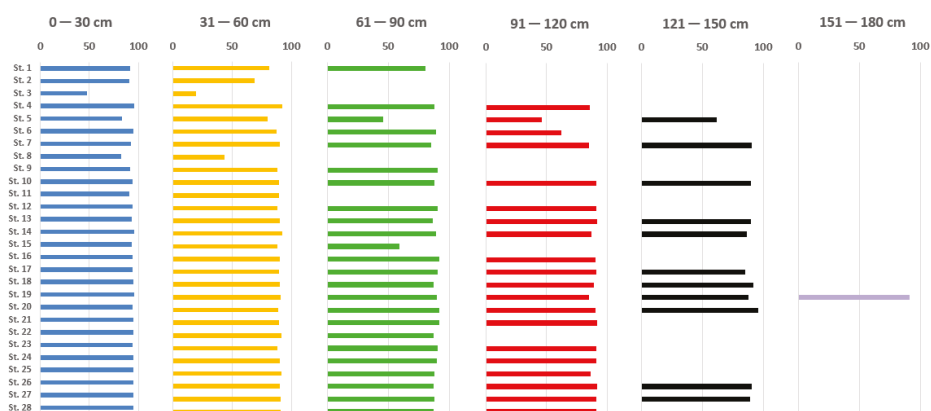


Figure 6. Mean hydration of the bottom sediment of Karczemne Lake (%).

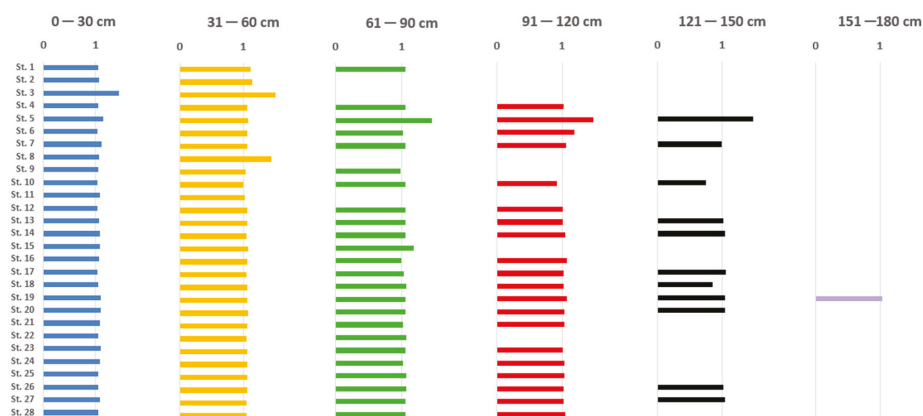


Figure 7. Mean density of the bottom sediment of Karczemne Lake (g cm^{-3}).

3.4. Chemical Composition of Bottom Sediment of Karczemne Lake

The average chemical composition of the bottom sediments of Karczemne Lake was quite variable. The sediments that accumulated in the central part of the basin, up to a depth of 60 cm, can be considered mixed according to the Stangenberg nomenclature [40] because none of the components was present in amounts exceeding 50% of the dry mass. The organic matter in these sediments ranged from 15.8% to 43.5% of the dry mass. In the coastal regions of the lake and in deeper levels of sediment from the central part of the reservoir, the dominant component was silica, accounting for up to 92% of the dry mass. These bottom deposits can be described as silicate. The amounts of nitrogen in the analyzed sediments varied from 0.20% to 2.50% N dry weight (Figure 8a–d). Lower concentrations of nitrogen were found in the northern part of the lake along the axis determined by the inflow of the Klasztorna Struga (sounding stations 1–8). In the rest of the reservoir, the bottom deposits were richer in nitrogen, especially in the areas of the maximum depth of the basin.

The main components of the sorption complex of the bottom sediments of Karczemne Lake were iron (approximately 3.5% d.w.) and aluminum (approximately 3.0% d.w.). The combination of phosphorus and iron is unstable due to the variable valence of iron. Under anaerobic conditions, iron turns into a reduced form, releasing phosphates into the water. The bottom sediment of Karczemne Lake contained very high amounts of phosphorus, ranging from 0.1% to 7.3% of the dry mass (Figure 8a–d).

Maximum amounts were found in the layer of deposits with a thickness of 60 cm and, at some points, up to 90 cm. Below 90 cm, much lower values were observed (Figure 8a–d).

The mean concentrations of total phosphorus in the bottom sediments of Karczemne Lake were very high. To date, no other lake in Poland has recorded such high values of phosphorus. The maximum amount of total phosphorus was found at research point number 5: 31.856 mg P g⁻¹ d.w. in the surface sediments of layer a (0–30 cm). Phosphorus amounts exceeding 10 mg P g⁻¹ d.w. were found at the following research points: 1 a (14.1 mg P g⁻¹ d.w.), 10 a (11.2 mg P g⁻¹ d.w.), 14 a (10.4 mg P g⁻¹ d.w.), 14 b (14.4 mg P g⁻¹ d.w.), 15 a (22.9 mg P g⁻¹ d.w.), 16 a (16.9 mg P g⁻¹ d.w.), 24 b (12.9 mg P g⁻¹ d.w.), 26 a, b (12.0 mg P g⁻¹ d.w.), 28 a (13.6 mg P g⁻¹ d.w.) and 28 b (16.6 mg P g⁻¹ d.w.; Figure 8a–d).

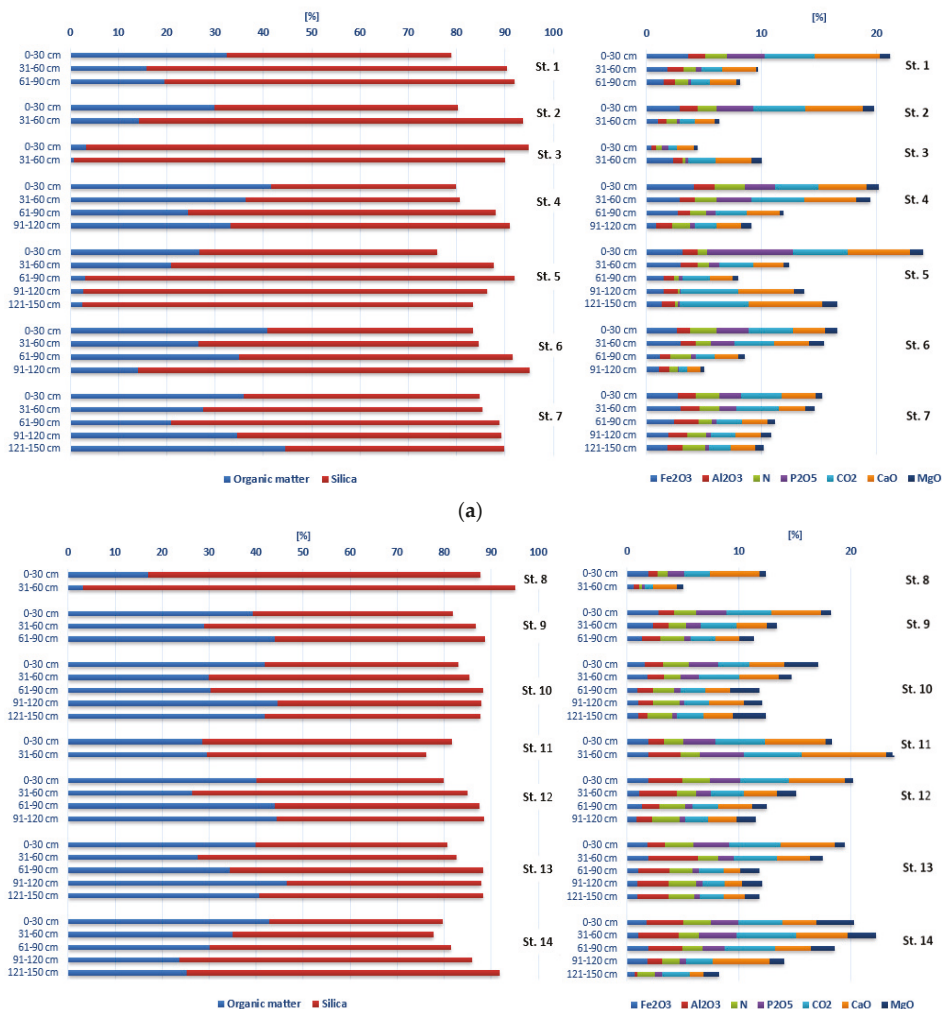


Figure 8. Cont.

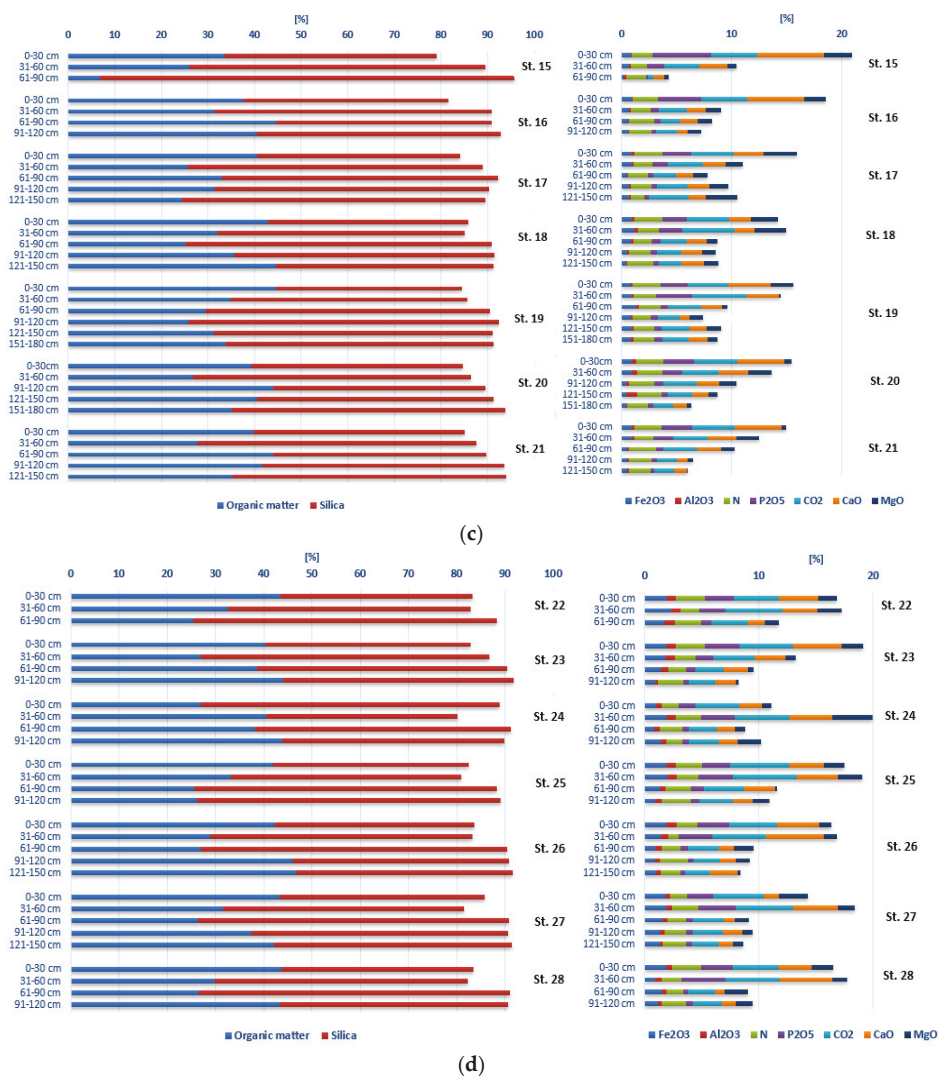


Figure 8. (a) The mean chemical composition of bottom sediment of Karczemne Lake—Stations 1–7; (b) the mean chemical composition of bottom sediment of Karczemne Lake—Stations 8–14; (c) the mean chemical composition of bottom sediment of Karczemne Lake—Stations 15–21 and (d) the mean chemical composition of bottom sediment of Karczemne Lake—Stations 22–28.

3.5. Phosphorus Fractions in the Bottom Sediments

The analysis of particular phosphorus percentages of the total phosphorus showed that the dominant types were NaOH-rP (phosphorus associated with organic matter), which made up over 82% of TP at research point number 5, and calcium-related phosphorus (HCl-P), whose presence at points 24, 26 and 28 exceeded 45% of the TP. Residual phosphorus (res-P) made up 25% of the TP at some research points, and at point 14, it exceeded 35% in the 30–60 cm layer.

Additionally, the NaOH-rP fraction (phosphorus bound mainly with aluminum) at some sites occurred in higher amounts, exceeding 20% of the TP. These fractions are moderately biologically

available (NaOH-rP and NaOH-nrP), poorly available (HCl-P) or biologically inaccessible (res-P; Figure 9).

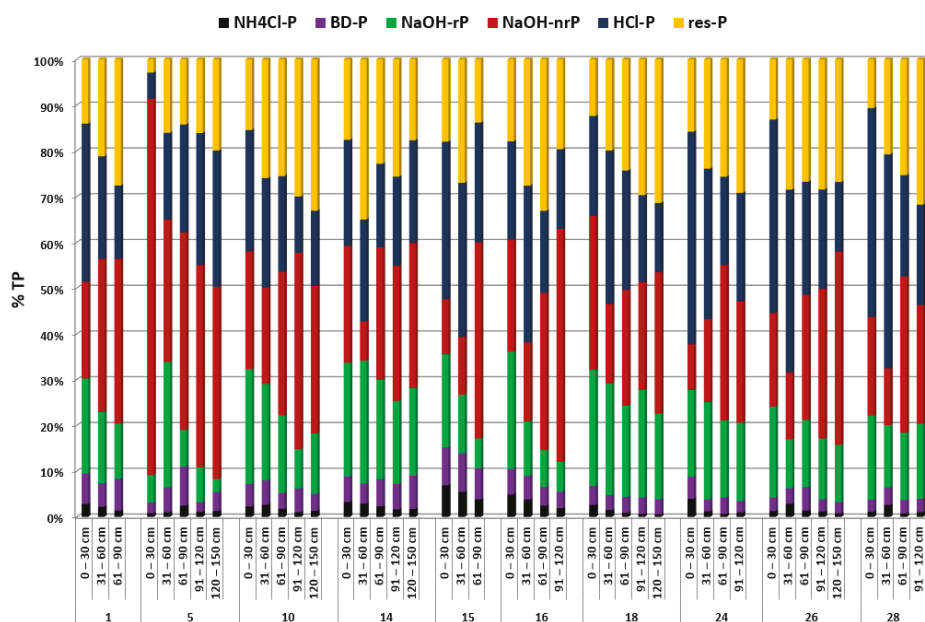


Figure 9. Share of phosphorus fractions (as %TP) at selected bottom sediment research stations.

The most mobile fractions of phosphorus— $\text{NH}_4\text{Cl-P}$ (phosphorus loosely bound to sediment) and BD-P (phosphorus sensitive to redox potential changes)—made up a small percentage of the total phosphorus (typically only a few percent). However, due to the extremely high content of total phosphorus in the surface layer of sediments, a few percent of the TP translates into very high mobile phosphorus content, especially in the case of the BD-P fraction; at several research points, the content of this fraction was higher than $2.5 \text{ mg P g}^{-1} \text{ d.w.}$ (Figure 9). These values indicate a serious threat to the quality of Karczemne Lake water. In addition, NaOH-rP and NaOH-nrP were present in very high proportions in the studied sediments. These fractions are mobilized by the increased reaction in the interphase water. In a polluted reservoir such as Karczemne Lake, with its low depth and polymictic water dynamics, intense photosynthesis may affect the increase in pH in the sediment waters (interphase) and thus stimulate an internal supply of phosphorus from the NaOH-rP and NaOH-nrP fractions (Figure 9).

3.6. Stable Organic Pollutants (POPs), Polycyclic Aromatic Hydrocarbons (PAHs) and Heavy Metal Contents in the Sediments

In sample No. 1, taken from research points 1–15 from layers a (0–30 cm) and b (31–60 cm), exceedances were found in the content of benzo (a) pyrene— $1.21 \text{ mg kg}^{-1} \text{ d.w.}$ in the ratio to the standard of $1.0 \text{ mg kg}^{-1} \text{ d.w.}$; benzo (b) fluoranthene— $1.88 \text{ mg kg}^{-1} \text{ d.w.}$, compared to the norm of $1.5 \text{ mg kg}^{-1} \text{ d.w.}$; benzo (g, h, i) perylene— $1.44 \text{ mg kg}^{-1} \text{ d.w.}$, compared to the norm of $1.0 \text{ mg kg}^{-1} \text{ d.w.}$ and indeno (1, 2, 3-cd) pyrene— $1.75 \text{ mg kg}^{-1} \text{ d.w.}$, compared to the norm of $1.0 \text{ mg kg}^{-1} \text{ d.w.}$ (Table 3).

In sample No. 3, taken from research points 16–28 from layers a (0–30 cm) and b (31–60 cm), exceedances were found in the content of benzo (a) pyrene— $2.10 \text{ mg kg}^{-1} \text{ d.w.}$ in the ratio to the standard of $1.0 \text{ mg kg}^{-1} \text{ d.w.}$; benzo (a) anthracene— $1.69 \text{ mg kg}^{-1} \text{ d.w.}$, compared to the norm of $1.5 \text{ mg kg}^{-1} \text{ d.w.}$; benzo (b) fluoranthene— $3.57 \text{ mg kg}^{-1} \text{ d.w.}$ in ratio to the standard— 1.5 mg kg^{-1}

d.w.; benzo (g, h, i) perylene—2.65 mg kg⁻¹ d.w., compared to the norm of 1.0 mg kg⁻¹ d.w. and indeno (1,2,3-cd) pyrene—1.86 mg kg⁻¹ d.w., compared to the standard of 1.0 mg kg⁻¹ d.w.

Table 3. Organic pollutants and heavy metal contents in bottom sediment of Karczemne Lake.

Parameter	Norm	SampleNo. 1	SampleNo. 2	SampleNo. 3	SampleNo. 4	SampleNo. 5
As	<30 mg/kg d.w.	9.77	5.0	13.3	6.05	12.7
Cr	<200 mg/kg d.w.	29.1	18.8	40.1	33.2	44.1
Zn	<1000 mg/kg d.w.	406.0	104.0	503.0	152.0	843.0
Cd	<7.5 mg/kg d.w.	0.543	0.050	0.794	0.050	0.846
Cu	<150 mg/kg d.w.	93.5	25.9	123.0	38.4	247.0
Ni	<75 mg/kg d.w.	19.9	13.8	25.8	21.9	22.5
Pb	<200 mg/kg d.w.	97.2	31.6	126.0	49.4	317.0
Hg	<1.0 mg/kg d.w.	0.60	0.22	0.68	0.26	0.30
Benzo(a) anthracene	<1.5 mg/kg d.w.	1.13	0.361	1.69	0.240	13.0
Benzo(b) fluoranthene	<1.5 mg/kg d.w.	1.88	0.69	3.57	0.55	14.40
Benzo(k) fluoranthene	<1.5 mg/kg d.w.	0.803	0.270	1.380	0.246	5.770
Benzo(g, h, i) perylene	<1.0 mg/kg d.w.	1.44	0.548	2.65	0.72	7.34
Benzo(a) pyrene	<1.0 mg/kg d.w.	1.21	0.410	2.10	0.39	9.75
Dibenzo(a, h) anthracene	<1.0 mg/kg d.w.	0.297	0.020	0.482	0.020	3.24
Indeno(1, 2, 3-c,d) pyrene	<1.0 mg/kg d.w.	1.75	0.976	1.86	0.916	8.03

In sample No. 5, taken from research point 5 from layers a (0–30 cm) and b (31–60 cm), exceedances were found in the range of benzo (a) pyrene—9.75 mg kg⁻¹ d.w., compared to the norm of 1.0 mg kg⁻¹ d.w.; benzo (a) anthracene—13.0 mg kg⁻¹ d.w., compared to the norm of 1.5 mg kg⁻¹ d.w.; benzo (b) fluoranthene—14.4 mg kg⁻¹ d.w., compared to the norm of 1.5 mg kg⁻¹ d.w.; benzo (g, h, i) perylene—7.34 mg kg⁻¹ d.w., compared to the norm of 1.0 mg kg⁻¹ d.w.; benzo (k) fluoranthene—5.77 mg kg⁻¹ d.w., compared to the norm of 1.5 mg kg⁻¹ d.w.; dibenzo (a, h) anthracene—3.24 mg kg⁻¹ d.w., compared to the norm of 1.0 mg kg⁻¹ d.w.; indeno (1, 2, 3-cd) pyrene—8.03 mg kg⁻¹ d.w., compared to the norm of 1.0 mg kg⁻¹ d.w.; Cu—247 mg kg⁻¹ d.w., compared to the standard of 150 mg kg⁻¹ d.w. and Pb—317 mg kg⁻¹ d.w., compared to the standard of 200 mg kg⁻¹ d.w.

In samples No. 2, 4 and 6, exceedances beyond the limit values were not found (Table 3).

With reference to the regulation, 40% of the bottom sediment of Karczemne Lake did not meet the requirements of uncontaminated spoil (code in the waste catalog 17 05 06) and constituted a dangerous sediment, i.e., catalog code 17 05 05, and should be disposed by incineration. Sixty percent of the output could be transferred for further use after prior dilution, i.e., mixing with sediments formed during the wastewater treatment process. In the case of introducing it to the ground (leveling, reclamation and fertilization), the provisions of the OME [38] on the method of conducting the assessment of the ground surface pollution indicate that dredged spoil on the surface of the earth cannot make the original classification of the soil or soil quality change as a result of its deposit.

3.7. Mass Calculation

The results of the research on the spatial variability of phosphorus content and its fractions in the Karczemne Lake sediments enabled the precise determination of sediment layers that need to be removed from particular sectors of the ecosystem bottom. The deposit thicknesses indicated for removal in each of the separated bottom sediment sectors are presented in Table 4. Considering the sector areas and the thickness of the layer to be removed, the volume of deposits to be dredged from Karczemne Lake was 240 013 m³ (Table 4). Based on the density of the sediment and the degree of hydration, it was estimated that the fresh mass of the output will be 2,588,054.7 Mg and that the dry weight of the output will be 2691.35 Mg (Table 4). The amount of nutrients that will be removed from the ecosystem along with the sediments and interstitial waters will be 212.86 Mg of phosphorus and 405.67 Mg of nitrogen (Table 5).

Table 4. Characteristics of physical parameters of bottom sediments with respect to the spatial volume balance and the mass of potential output to be removed.

Number of Sampling Point	Sector Area (m ²)	The Thickness of Layer to Be Removed (m)	Volume of the Layer to Be Removed (m ³)	Wet Sludge Mass to Be Removed (kg m ⁻²)	Dry Sludge Mass to Be Removed (kg m ⁻²)
1	10,273	0.5	5136.5	5,575,868.5	710,711.3
2	15,100	0.5	7550	828,312.1	1,516,022.2
3	6000	0.5	3000	4,413,593.9	2,830,379.8
4	11,345	0.6	6807	722,245.9	437,108.8
5	11,495	0.6	6897	7,727,772.4	1,394,499.5
6	12,500	0.6	7500	7,980,278.1	703,813.3
7	18,600	0.6	11,160	1,216,534.6	962,287.8
8	8200	0.5	4100	5,010,261.5	1,811,746.2
9	15,900	0.6	9540	9,947,672.0	1,012,203.0
10	14,770	0.75	11,077.5	1,136,233.6	1,022,676.0
11	6080	0.6	3648	385,594.4	379,970.6
12	16,100	0.6	9660	1,014,576.2	886,400.8
13	12,800	0.75	9600	10,225,571.2	923,673.7
14	9280	0.9	8352	8,857,878.2	672,286.9
15	10,650	0.6	6390	6,914,467.2	634,595.0
16	13,600	0.5	6800	8,700,205.6	682,288.6
17	15,950	0.6	9570	10,052,152.6	817,790.2
18	5020	0.9	4518	4,794,241.8	445,579.2
19	6900	0.75	5175	5,566,142.9	402,880.1
20	11,900	0.9	10,710	11,550,996.8	952,646.0
21	12,880	0.9	11,592	12,182,956.9	979,039.5
22	11,540	0.75	8655	9,116,970.7	719,112.3
23	12,670	0.75	9502.5	10,270,607.7	912,577.6
24	16,100	0.9	14,490	15,329,075.7	1,277,107.1
25	11,600	0.9	10,440	11,070,268.6	945,021.8
26	23,750	0.6	14,250	15,094,698.4	1,111,633.9
27	26,320	0.6	15,792	16,859,229.9	1,158,047.5
28	13,500	0.6	8100	8,529,586.9	615,247.2
Total	360,823	-	240,013	2,588,054.7 Mg	269,173.5 Mg

Table 5. The load of phosphorus and nitrogen can be withdrawn from the Karczemne Lake with bottom sediments and interstitial water.

Number of Sampling Point	Sector Area (m ²)	The Content of TP in Bottom Sediment		The Content of TN in Bottom Sediment		The Content of TP in Interstitial Water		The Content of TN in Interstitial Water	
		kg P m ⁻²	kg P sector ⁻¹	kg N m ⁻²	kg N sector ⁻¹	g P m ⁻²	kg P sector ⁻¹	g N m ⁻²	kg N sector ⁻¹
1	10,273	0.46	4691.2	0.94	9697.7	1.62	16.66	10.60	109.28
2	15,100	0.49	7468.5	1.12	16,966.2	1.45	21.86	7.68	116.02
3	6000	0.6	3769.7	1.47	8830.2	0.68	4.06	5.11	30.67
4	11,345	0.48	5439.5	0.83	9365.5	1.52	17.25	13.70	155.35
5	11,495	2.09	24,007.2	1.15	13,180.0	3.34	38.44	23.60	259.46
6	12,500	0.55	6874.1	0.89	11,157.5	1.92	24.06	14.10	176.74
7	18,600	0.36	6636.8	0.90	16,760.7	1.07	19.94	11.80	219.26
8	8200	0.45	3657.5	0.49	4050.8	0	0	0	0
9	15,900	0.52	8290.4	1.10	17,477.6	2.03	32.25	8.33	132.49
10	14,770	0.46	6825.0	1.24	18,387.5	1.61	23.82	11.90	176.41
11	6080	0.92	5622.0	1.02	6223.1	0.95	5.77	3.81	23.15
12	16,100	0.40	6495.5	1.05	16,854.2	1.03	16.55	14.40	232.24
13	12,800	0.49	6276.8	1.44	18,369.0	1.62	20.75	17.90	229.39
14	9280	0.79	7361.0	1.48	13,706.1	1.75	16.24	33.70	312.44
15	10,650	0.77	8215.0	1.00	10,636.5	1.53	16.26	8.28	88.22
16	13,600	0.43	5860.4	0.97	13,139.7	1.21	16.45	10.70	146.09
17	15,950	0.39	6199.2	0.96	15,312.6	0.68	26.87	9.01	143.67
18	5020	0.57	2870.8	1.61	8087.3	2.04	10.22	27.20	136.37
19	6900	0.59	4052.4	1.20	8280.0	2.57	17.71	27.20	187.60
20	11,900	0.58	6852.3	1.62	19,283.5	2.68	31.88	23.40	277.93
21	12,880	0.52	6693.0	1.58	20,405.3	1.91	24.61	22.60	291.16
22	11,540	0.52	5952.7	1.31	15,134.8	2.44	28.18	29.50	339.86
23	12,670	0.55	6926.7	1.32	16,781.5	1.90	24.07	16.80	213.24
24	16,100	0.59	9531.7	1.57	25,236.6	2.52	40.64	27.40	441.00
25	11,600	0.73	8413.8	1.75	20,258.9	2.84	32.94	36.50	423.60
26	23,750	0.57	13,646.0	0.55	12,975.1	1.75	41.62	14.60	347.12
27	26,320	0.54	14,224.2	0.82	21,536.3	2.51	66.03	21.90	576.67
28	13,500	0.68	9168.3	0.85	11,464.8	2.13	28.72	20.80	281.20
Total	360,823	-	212.2 Mg	-	399.6 Mg	-	0.66 Mg	-	6.07 Mg
				TOTAL P	212.86 Mg				
				TOTAL N	405.70 Mg				

4. Discussion

The results of monitoring have shown that the water and bottom sediment of Karczemne Lake should be classified at the “below good” level. The lake does not meet the requirements of the Water Framework Directive of the European Union [41]. With such high nutrient concentrations and excess organic matter, the natural inhibition of the severe degradation of the lake is impossible. In addition to the very poor water quality, the bottom sediments of the analyzed lake also contain extremely high concentrations of pollutants. The concentrations of total phosphorus in the bottom sediments of Karczemne Lake were very high compared to those of other lakes [42–44]. To date, no other lake in Poland has recorded such high values of phosphorus. The maximum amount of total phosphorus was found at research point number 5: 31.8 mg P g⁻¹ d.w. in the surface sediments of layer a (0–30 cm). Bojakowska [45] reported that in Karczemne Lake sediments, a maximum of 1.9% TP in dry matter was found, which corresponds to 19 mg P g⁻¹ d.w., while previous studies carried out by Grochowska et al. [46] showed a maximum of just over 12 mg P g⁻¹ d.w. in the surface layer of sediments (10 cm thick) taken from the deepest research point. For comparison, the maximum phosphorus content found by Kentzer [47] in the bottom sediment of dystrophic Zmarle Lake was slightly above 10 mg P g⁻¹ d.w. In the sediments of Długie Lake in Olsztyn, which was polluted for many years by domestic sewage, the level of phosphorus in the bottom sediments ranged from 4 to 6 mg P g⁻¹ d.w. [48]. According to Sahin et al. [49], the amount of phosphorus in the sediments ranged from approximately 0.5 to 20.2 mg P g⁻¹ d.w. However, Augustyniak [50] suggested that in the sediments of shallow lakes were not contaminated by sewage, the phosphorus content is usually low and does not exceed 2–3 mg P g⁻¹ d.w. Karczemne Lake was a domestic sewage receiver for over 60 years. The pollution loads introduced with the sewage inflow deposited on the bottom of the reservoir forming a layer of so-called “modern sediments”. In oligotrophic lakes, the thickness of the sediment increases by 1 mm each year, and in hypertrophic lakes, it increases by approximately 1 cm [50]. Such high phosphorus content in the bottom sediments, especially in the surface layer, is certainly the result of massive sewage pollution taking place over the last several decades. Station 5, with the highest level of phosphorus, is located in the immediate vicinity of the collector discharging sewage into the lake, which for many years was the main source of pollution. It has been reported that in the deepest layers of the sediment (from 60 cm and in some positions from 90 to 150 cm deep into the sediment), the recorded amounts of total phosphorus are from approximately 0.5 (St. 5) to approximately 3 mg P g⁻¹ d.w. (St. 18), which gives an overview of the concentration of total phosphorus before the pollution of the lake. Due to the low depth and polymictic nature of the reservoir bottom, sediment certainly undergoes resuspension, which in some sites could cause higher phosphorus contents in the deeper layer of sediment (30–60 cm), e.g., stations 24, 26 and 28. The vertical profiles of the phosphorus and total phosphorus fractions in the sediments at selected research stations show very rich concentrations of phosphorus in more detail as the deposit depth increases in Karczemne Lake. Theoretically, this phosphorus can easily be mobilized, providing a serious load of pollutants to the water of the analyzed reservoir.

4.1. Reduction in Pollution Loads by Protective Methods

Currently, the sewage network of the city of Kartuzy is being modified, which is necessary to decrease the high nutrient loads from wastewater. In addition, renovation work is being carried out in the tributary to Karczemne Lake (Klasztorna Struga) and involves the regulation of the riverbed and the fascine. In-stream and riparian vegetation will be restored in the channel. The aboveground parts of hydrophilic plants assimilate biogenic elements and increase aesthetic value [51]. In turn, the underground parts of plants (rhizomes and roots) release oxygen into the rhizosphere, which supports the processes of biodegradation of organic matter and nitrification, as well as biogenic substances. *Glyceria maxima*, *Phalaris arundinacea* and *Phragmites australis* will be planted in the channel of the Klasztorna Struga. The last protective action is the prohibition of angling baits.

Applying all of the aforementioned solutions will result in a reduction in the external load of the lake by approximately 80%.

4.2. Conception of Restoration Treatments

In the past, Karczemne Lake was overloaded by pollution from the catchment, which was a result of the long-term input of raw wastewater, including domestic, sanitary, storm and industrial waste. Under these conditions, it is necessary to use the optimal method of lake restoration after protection techniques are implemented in the catchment. The optimal restoration method for Karczemne Lake will be the removal of deposits due to their unusually high concentration of phosphorus. Additionally, for the stabilization of environmental conditions in the reservoir, the phosphorus inactivation method and biomanipulation will be applied.

For the purpose of restoration treatments in Karczemne Lake, there are separate extraction fields (10) in which the outputs of the liquid and solid fractions will be successively carried out for removal. The field currently undergoing the deposit removal process will be separated from the rest of the lake by a plastic curtain to prevent the movement of the deposit. The removal of the deposits will be carried out by a method with the use of an innovative device, the only type of equipment in Europe (suction dredge with wormwheel), precisely designed for lake dredging. Extracted output will be pumped to a pipeline on the northern shore of the lake and later by hydrotransport to a sewage treatment plant.

This technical solution guarantees prevention of the uncontrolled runoff of leachate back into the lake basin. The pipeline will be made of plastic (Figure 10).

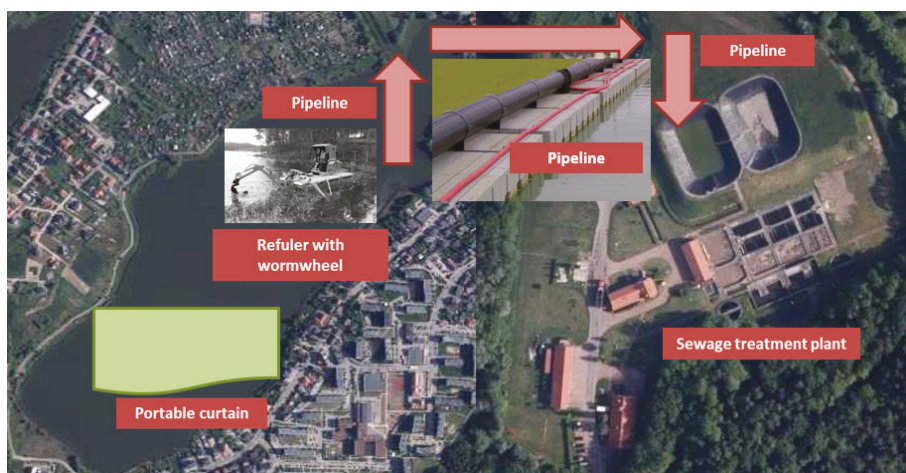


Figure 10. The scheme of planned restoration.

The proposed method does not require the construction of a completely new deposit treatment system consisting of presses, centrifuges, polymer-dosing stations, water-conditioning equipment and reaction pools (Figure 10).

In the sewage treatment plant, the sediment will be dehydrated in centrifuges and then subjected to hygienization. The part of the sediment that is contaminated with heavy metals will be transported for utilization.

Unpolluted sediments extracted from the lake and processed at the sewage treatment plant can also be valuable material for improving the soil structure, as they may contain premineralized organic compounds and easily digestible fertilizers, including macro- and microelements such as nitrogen, 1.5% N; phosphorus 3, 5% P₂O₅; calcium, 4.22% CaO; magnesium, 1.6% MgO and iron, 1.8% Fe₂O₃

(average contents of elements in dry mass of the Karczemne Lake sediments). Another form of deposit utilization can be the reclamation of degraded areas, for example, landfills [52–54].

In relation to the current level of external loads, the quantities of phosphorus and nitrogen that will be extracted from the lake during reclamation (loads coming with surface inflow, outlets of rainwater collectors, recreation and atmospheric precipitation) correspond to the amount of pollution that reaches the lake in 1300 years for phosphorus and 300 years for nitrogen. This confirms the validity of the assumptions behind the reclamation methods adopted, for which the priority was to remove the bottom sediments outside the ecosystem.

The removal of the bottom sediments from Karczemne Lake will be carried out within two years, from spring to the moment of the lake ice cover.

In the extraction field in which the sediment will be removed, the first phase of phosphorus inactivation to chemically precipitate pollutants distributed in the water column as a result of the dredging will be carried out. After the entire lake basin has been dredged, the next four stages of phosphorus inactivation (spring, autumn, spring and autumn) will be carried out. Based on the experience and research results obtained by the Department of Water Protection Engineering in the field of lake reclamation by phosphorus inactivation [2,7,55,56], two types of coagulants will be dosed: PAX 18 and PIX 111. The doses of PIX and PAX coagulants were determined on the basis of the phosphorus fractions in the water and bottom sediments and the amount of natural components in the sediments having sorption capacity in relation to phosphorus, such as Al, Fe and Ca [57,58].

The calculated doses of aluminum coagulant for Karczemne Lake were as follows: the area of the central zone of the lake was 20.0 ha, the volume of the central zone was 660,000 m³, the demand of the profundal sediment for aluminum was 23.6 g m⁻², the demand for aluminum with which to bind the phosphorus in the water column in the central zone was 1650 kg and the total amount of reactive aluminum was 6370.8 kg. The total dose of PAX 18 was 70,787.0 kg.

Next, the dose of the iron coagulant for Karczemne Lake was calculated as follows: the area of the coastal zone was 20.4 ha, the volume of the coastal zone was 378,000 m³, the demand of the littoral deposits for iron was 44.26 g m⁻², the demand for iron for binding the phosphorus in the water depth in the coastal zone was 945 kg and the total amount of reactive iron was 9974.0 kg. The total dose of PIX 111 was 74,433.0 kg.

To maintain the positive effects of restoration in Karczemne Lake, rational fish farming should be utilized. This method can be implemented through the use of biomanipulation, which involves the conscious shaping of the biocenosis of aquatic organisms by changing the species composition of ichthyofauna. The main goal of biomanipulation is to increase the number of large forms of zooplankton, mainly Cladocera, and through their control, feed the amount of phytoplankton, which are the first link in the trophic pyramid, thus reducing water blooms.

To achieve this effect, the number of sedentary fish, such as bleak, sunflower, small perch, juvenile roach, silverfish, bream and crucian, which feed on zooplankton or seek food in bottom sediments, should be limited. The reduction in these fish assemblies can be achieved, inter alia, through selective harvesting (without the use of towed tools). According to Goldyn [59], at least 75% of the initial fish should be harvested. This treatment should be intense and short term and should optimally occur within one year but no later than two years. The best effects result from the use of a large amount of pike fry. The recommended amount of recessed fry is at least 1000 pcs/ha [59], and the restocking material should have a size exceeding 10 cm because at this stage of development, the pike is going to feed on fish.

5. Conclusions

After detailed monitoring of the water and bottom sediment of Karczemne Lake, the methods proposed for protection and restoration of the lake discussed above enable us to realistically assess the potential opportunities for the renewal of severely degraded shallow, urban lakes. Considering the chemical composition of the water and bottom sediments of Karczemne Lake, external conditions,

long-term economic and environmental aspects and the development of new technologies, it appears that an optimal variant of the approach taken to achieve permanent water quality improvement might consist of modernization of the urban sewerage system and restorative actions, including the removal of the bottom sediments from Karczemne Lake by a completely new, safe and economically justified method of mining and managing bottom sediments and phosphorus inactivation along with supportive actions in the form of biomanipulation. The technology of bottom sediment removal along with the construction of a hydrotransport pipeline, the phosphorus inactivation method and biomanipulation will have a total cost of US \$2,100,000.

Author Contributions: Conceptualization J.G. and M.L., investigation J.G., M.L., R.T., R.A., verification R.A. and R.T., writing-original draft preparation J.G. and R.A., writing-reviewing and editing J.G., R.A., M.L., R.T. All authors have read and agreed to the published version of the manuscript.

Funding: “Project financially supported by Minister of Science and Higher Education in the range of the program entitled “Regional Initiative of Excellence” for the years 2019–2022, project No. 010/RID/2018/19, amount funding 12.000.000 PLN”.

Acknowledgments: Authors thank the Community of Kartuzy.

Conflicts of Interest: Authors declare no conflict of interest.

References

1. Grochowska, J.; Tandyrak, R.; Wiśniewski, G. Long-term hydrochemical changes in a lake after the application of several protection measures in the catchment. *Pol. J. Nat. Sci.* **2014**, *29*, 251–263.
2. Grochowska, J.; Augustyniak, R.; Łopata, M. How durable is the improvement of environmental conditions in a lake after the termination of restoration treatments. *Ecol. Eng.* **2017**, *104*, 23–29. [[CrossRef](#)]
3. Huser, B.J.; Futter, M.N.; Wang, R.; Fölster, J. Persistent and widespread long-term phosphorus declines in Boreal lakes in Sweden. *Sci. Total Environ.* **2018**, *613–614*, 240–249. [[CrossRef](#)] [[PubMed](#)]
4. Dodds, W.K.; Bouska, W.W.; Eitzmann, J.L.; Pilger, T.J.; Pitts, K.I.; Riley, A.J.; Schloesser, J.A.; Thornbrugh, D.J. Eutrophication of U.S. freshwaters: Analysis of potential economic damages. *Environ. Sci. Technol.* **2009**, *43*, 12–19. [[CrossRef](#)]
5. Liu, D.; Wang, P.; Wei, G.; Dong, W.; Hui, F. Removal of algal blooms from freshwater by the coagulation-magnetic separation method. *Environ. Sci. Pollut. Res.* **2013**, *20*, 60–65. [[CrossRef](#)]
6. Huser, B.J.; Futter, M.; Lee, J.T.; Perniel, M. In-lake measures for phosphorus control: The most feasible and cost-effective solution for long-term management of water quality in urban lakes. *Water Res.* **2016**, *97*, 142–152. [[CrossRef](#)]
7. Grochowska, J.; Brzozowska, R.; Łopata, M. Durability of changes in phosphorus compounds in water of an urban lake after application of two reclamation methods. *Water Sci. Technol.* **2013**, *68*, 234–239. [[CrossRef](#)]
8. Grochowska, J.; Brzozowska, R. Influence of different recultivation methods on durability of nitrogen compounds changes in the waters of an urban lake. *Water Environ. J.* **2015**, *29*, 228–235. [[CrossRef](#)]
9. Dunalska, J.A.; Grochowska, J.; Wiśniewski, G.; Napiórkowska-Krzebietke, A. Can we restore badly degraded urban lakes? *Ecol. Eng.* **2015**, *82*, 432–441. [[CrossRef](#)]
10. Perkins, R.G.; Underwood, G.J.C. The potential for phosphorus release across the sediment-water interface in an eutrophic reservoir dosed with ferric sulphate. *Water Res.* **2001**, *35*, 1399–1406. [[CrossRef](#)]
11. Younha, W.; Yajun, W.; Jianxin, Z.; Yunying, W. Phosphorus release from lake sediments: Effects of pH, temperature and dissolved oxygen. *KSCE J. Civ. Eng.* **2014**, *18*, 323–329.
12. Dunalska, J.A.; Wiśniewski, G. Can we stop the degradation of lakes? Innovative approaches in lake restoration. *Ecol. Eng.* **2016**, *95*, 714–722. [[CrossRef](#)]
13. Kajak, Z. Hydrobiology–Limnology. In *Inland Water Ecosystems*; PWN: Warsaw, Poland, 2002; pp. 1–212.
14. Lee, J.T. Minneapolis Chain of Lakes phosphorus reduction strategy. In *Proceedings of the National Conference of Retrofit Opportunities for Water Resource Protection in Urban Environments*, Chicago, IL, USA, 9–12 February 1998; USEPA, Office of Research Development: Washington, DC, USA, 1999. EPA/625/R-99/002.
15. Cooke, G.D.; Welch, E.B.; Peterson, S.A.; Newroth, P.R. *Restoration and Management of Lakes and Reservoirs*; Taylor & Francis: Abingdon, UK; CRC Press: Boca Raton, FL, USA, 2005.

16. Zamparas, M.; Zacharias, I. Restoration of eutrophic freshwater by managing internal nutrient loads. *Sci. Total Environ.* **2014**, *496*, 551–562. [[CrossRef](#)] [[PubMed](#)]
17. Rosińska, J.; Kozak, A.; Dondajewska, R.; Kowalczyńska-Madura, K. Water quality response to sustainable restoration measures Case study of urban Swarzędzkie Lake. *Ecol. Indic.* **2018**, *84*, 437–449. [[CrossRef](#)]
18. Sheng-rui, W.; Xiangcan, J.; Haichao, Z.; Fengchang, W. Phosphorus fractions and its release in the sediments from the shallow lakes in the Middle and Lower Reaches of Yangtze River Area. *Colloids Surf. A Physicochem. Eng. Asp.* **2006**, *273*, 109–116.
19. Siwek, H. Speciation analysis of phosphorus in bottom sediments—comparison of two methods. *J. Elem.* **2010**, *15*, 161–170.
20. Xiaoli, W. Phosphorus fractionation and bio-availability in surface sediments from the Middle and Lower Reaches of the Yellow River. *Procedia Environ. Sci.* **2012**, *12*, 379–386.
21. Klapper, H. Technologies for lake restoration. *J. Limnol.* **2003**, *62*, 73–90. [[CrossRef](#)]
22. Environmental Monitoring Library. *Report of the Voivodship Inspectorate for Environmental Protection*; Environmental Monitoring Library: Bydgoszcz, Poland, 2003; pp. 1–182, ISBN 83-7217-204-8.
23. Björk, S. Lake restoration techniques—Proceedings of the International Congress on Lake Pollution and Recovery. In Proceedings of the European Water Pollution Control Association, Rome, Italy, 15–18 April 1985; pp. 202–212.
24. Björk, S.; Pokorný, J.; Hauser, V. Restoration of lakes through sediment removal, with case studies from lakes Trummen, Sweden and Vajgar, Czech Republic. In *Restoration of Lakes, Streams, Floodplains, and Bogs in Europe. Principles and Case Studies*; Eiseltová, M., Ed.; Springer: Berlin/Heidelberg, Germany, 2010.
25. Kondracki, J. *Physical Geography of Poland*; PWN: Warsaw, Poland, 2011; pp. 1–463.
26. Wolos, A.; Mioduszewska, H. Impact of anglers using groundbaits on fishing effects and nutrient balance of aquatic ecosystems. *Fish. Announc.* **2003**, *1*, 23–27.
27. Vollenweider, R.A. Advances In defining critical loading level for phosphorus in lake eutrophication. *Mem. INST. Ital. Hydrobiol.* **1976**, *33*, 53–83.
28. Carlson, R.E. A trophic state index for lakes. *Limnol. Oceanogr.* **1977**, *22*, 361–369. [[CrossRef](#)]
29. Kratzer, C.R.; Brezonik, P.L. A Carlson—Type trophic state index for nitrogen in Florida lakes. *Water Res. Bull.* **1981**, *17*, 713–715. [[CrossRef](#)]
30. Kaca, E. Measurements of water flow volume and mass of substance contained in it, and its uncertainty on the example of fish ponds. *Water Environ. Rural Areas* **2003**, *13*, 31–57.
31. Brzozowska, R.; Gawrońska, H. The influence of a long-term artificial aeration on th nitrogen compounds exchange between bottom sediments and water in Lake Długie. *Oceanol. Hydrobiol. Stud.* **2009**, *38*, 113–119. [[CrossRef](#)]
32. Rydin, E.; Welch, E.B. Aluminum dose required to inactivate phosphate in lake sediments. *Water Res.* **1998**, *32*, 2969–2976. [[CrossRef](#)]
33. Van Hullebush, E.; Auvray, F.; Deluchat, V.; Chazal, P.M.; Baudu, M. Phosphorus fractionation and short-term mobility in the surface sediment of a polymictic shallow lake treated with a low dose of alum (Courtille Lake, France). *Water Air Soil Pollut.* **2003**, *146*, 75–91. [[CrossRef](#)]
34. Hermanowicz, W.; Dożańska, W.; Dojlido, J.; Kozirowski, B.; Zerbe, J. *Physico-Chemical Study of Water and Wastewater*; Arkady: Warsaw, Poland, 1999.
35. Tibco Software Inc. STATISTICA Version 13.0. 2018. Available online: <https://www.tibco.com/resources/product-download/tibco-statistica-trial-download-windows> (accessed on 5 June 2018).
36. EPA. *Parameters of Water Quality. Interpretation and Standards*; Environmental Protection Agency: Wexford, Ireland, 2001.
37. Wolfram MathWorld-web’s most extensive mathematic. Available online: <https://mathworld.wolfram.com/VoronoiDiagram.html> resources (accessed on 5 April 2020).
38. Ordinance of the Ministry of the Environment of 11 May 2015 on the recovery of waste outside installations and equipment. *J. Laws* 2015 (Set log 2015, item 796); 2015. Available online: <http://prawo.sejm.gov.pl/isap.nsf/download.xsp/WDU20150000796/O/D20150796.pdf> resources (accessed on 5 April 2020).
39. Ordinance of the Ministry of the Environment of 1 September 2016 on the method of conducting an assessment of the soil surface pollution. *J. Laws* 2016 (Set log 2016, item 1395); 2016. Available online: <http://prawo.sejm.gov.pl/isap.nsf/download.xsp/WDU20160001395/O/D20161395.pdf> (accessed on 5 April 2020).

40. Augustyniak, R.; Neugebauer, M.; Kowalska, J.; Szymański, D.; Wiśniewski, G.; Filipkowska, Z.; Grochowska, J.; Łopata, M.; Parszuto, K.; Tandyrak, R. Bottom deposits of stratified, seepage, urban lake (on the example of Tyrsko Lake, Poland) as a factor potentially shaping lake water quality. *J. Ecol. Eng.* **2015**, *18*, 55–62. [[CrossRef](#)]
41. Directive, W.F. Directive 2000/60/EC of the European Parliament and of the Council of 23 October 2000 establishing a framework for Community action in the field of water policy. *Off. J. Eur. Communities* **2000**, *22*, 1–73.
42. Kowalczyńska-Madura, K.; Dondajewska, R.; Gołdyn, R.; Kozak, A.; Messyasz, B. Internal phosphorus loading from the bottom sediments of a dimictic lake during its sustainable restoration. *Water Air Soil Pollut.* **2018**, *229*. [[CrossRef](#)]
43. Smal, H.; Ligeza, S.; Baran, S.; Wójcikowska-Kapusta, A.; Obroślak, R. Nitrogen and phosphorus in bottom sediments of two small dam reservoir. *Pol. J. Environ. Stud.* **2013**, *22*, 1479–1489.
44. Ishii, Y.; Yabe, T.; Nakamura, M.; Amano, Y.; Komatsu, N.; Watanabe, K. Effect of nitrate mobilization from bottom sediment in shallow eutrophic lakes. *J. Water Environ. Technol.* **2009**, *7*, 75–83. [[CrossRef](#)]
45. Bojakowska, I. Phosphorus in lake sediments of Poland—Results of monitoring research. *Limnol. Rev.* **2016**, *16*, 15–25. [[CrossRef](#)]
46. Grochowska, J.; Brzozowska, R.; Grzybowski, M.; Napiórkowska-Krzebietke, A.; Bigaj, I.; Szymański, D.; Zieliński, R. *Physicochemical Tests of Water and Bottom Sediments as well as Hydrological Measurements of 4 Lakes: Mielenka, Tavern, Large and Small Monastery and Their Catchments in Terms of the Possibility of Reservoir Protection against Degradation*; Commune Office in Kartuzy: Kartuzy, Poland, 2013; Typescript, not published data.
47. Kentzer, A. *Phosphorus and Its Biologically Available Fractions in Lake Sediments of Various Trophies*; UMC: Toruń, Poland, 2001; pp. 1–111.
48. Brzozowska, R.; Gawrońska, H. Influence of a multi-year artificial aeration of a lake using destratification method on the sediment-water phosphorus exchange. *Arch. Environ. Prot.* **2005**, *31*, 71–88.
49. Şahin, Y.; Demirak, A.; Keskin, F. Phosphorus fractions and its potential release in the sediments of Koycegiz Lake, Turkey. *Lakes Reserv. Ponds* **2012**, *6*, 139–153.
50. Augustyniak, R. *The Influence of Physico-Chemical and Microbiological Factors on Internal Supply of Phosphorus in Selected Urban Lakes*; Committee of Environmental Engineering of the Polish Academy of Sciences: Lublin, Poland, 2018; Volume 140, pp. 1–230.
51. Jucherski, A.; Walczowski, A. Influence of selected macrophytes on sewage treatment effectiveness in the slope soil-vegetation filtration beds. *Probl. Agric. Eng.* **2012**, *20*, 115–124.
52. Gałka, B.; Witkowski, M. Characteristics of bottom sediments of the Młyny dam reservoir and the possibility of its agricultural use. *Water Environ. Rural Areas* **2010**, *10*, 53–63.
53. Maj, K.; Koszelnik, P. Methods of the management of bottom sediment. *J. Civ. Eng. Environ. Archit.* **2016**, *63*, 157–169.
54. Eymontt, A.; Wierzbicki, K. Hydromechanical technology of bottom sediment mining. *Probl. Agric. Eng.* **2017**, *4*, 19–27.
55. Gawrońska, H.; Łopata, M.; Jaworska, B. The effectiveness of the phosphorus inactivation method in reducing the trophy of lakes of different morphometrical and hydrological features. *Limnol. Rev.* **2007**, *7*, 27–34.
56. Grochowska, J.; Augustyniak, R.; Łopata, M.; Parszuto, K.; Tandyrak, R.; Płachta, A. From saprotrophic to clear water status: The restoration path of a degraded urban lake. *Water Air Soil Pollut.* **2019**. [[CrossRef](#)]
57. Rydin, E.; Welch, E.B. Dosing alum to Wisconsin lake sediments based on in vitro formation of aluminum bound phosphate. *Lake Reserv. Manag.* **1999**, *15*, 324–331. [[CrossRef](#)]
58. Gawrońska, H.; Brzozowska, R.; Grochowska, J.; Lossow, K. Effectiveness of PAX and PIX coagulants in phosphorus reduction in a lake—Laboratory experiments. *Limnol. Rev.* **2001**, *1*, 73–82.
59. Gołdyn, R. Biomanipulation in water reservoirs as a method of reclamation. *Munic. Rev.* **2007**, *6*, 70–72.



Review

Developments in the Use of Lipase Transesterification for Biodiesel Production from Animal Fat Waste

Fidel Toldrá-Reig ^{1,†}, Leticia Mora ² and Fidel Toldrá ^{2,*}

¹ Instituto de Tecnología Química (CSIC-UPV), Universitat Politècnica de València, Camino de Vera s/n, 46022 Valencia, Spain; reigtold@gmail.com

² Instituto de Agroquímica y Tecnología de Alimentos (CSIC), Avenue Agustín Escardino 7, Paterna, 46980 Valencia, Spain; lemoso@iata.csic.es

* Correspondence: ftoldra@iata.csic.es; Tel.: +34-9639-000-22

† Current address: CNRS, 25 rue des Martyrs, B.P. 166, 38042 Grenoble CEDEX 9, France.

Received: 30 June 2020; Accepted: 21 July 2020; Published: 23 July 2020

Abstract: Biodiesel constitutes an attractive source of energy because it is renewable, biodegradable, and non-polluting. Up to 20% biodiesel can be blended with fossil diesel and is being produced and used in many countries. Animal fat waste represents nearly 6% of total feedstock used to produce biodiesel through alkaline catalysis transesterification after its pretreatment. Lipase transesterification has some advantages such as the need of mild conditions, absence of pretreatment, no soap formation, simple downstream purification process and generation of high quality biodiesel. A few companies are using liquid lipase formulations and, in some cases, immobilized lipases for industrial biodiesel production, but the efficiency of the process can be further improved. Recent developments on immobilization support materials such as nanoparticles and magnetic nanomaterials have demonstrated high efficiency and potential for industrial applications. This manuscript reviews the latest advances on lipase transesterification and key operational variables for an efficient biodiesel production from animal fat waste.

Keywords: biodiesel; fuel; energy generation; lipase; immobilized lipase; animal waste; lard; tallow; animal fat; transesterification

1. Introduction

Animal byproducts generated in the European Union slaughterhouses represent nearly 17 million tons per year and, from them, 5 million tons inedible byproducts result from rendering and are mostly used for energy generation like biofuels and biodiesel [1–3]. After rendering byproducts, fat is obtained from beef tallow, mutton tallow, pork lard and chicken fat [4,5]. Such fat is majorly composed of triacylglycerols with fatty acids of 16 to 18 carbons. The most abundant saturated fatty acids are palmitic (16:0) and stearic (18:0) acids; the major monounsaturated fatty acid is oleic acid (18:1) and the most abundant polyunsaturated fatty acids are linoleic (18:2) and arachidonic (20:4) acids [6,7]. Animal fat waste is also obtained from the meat processing industry and from recycled waste from the cooking business [8,9] that are classified as yellow grease if the content of free fatty acids is lower than 15% by weight and brown grease when it is higher than 15% [10]. In 2019, more than 800 thousand tons of animal fats, equivalent to 6% of total feedstock, were used to produce biodiesel in the European Union [11,12], while 8.4% of total feedstock was used in the case of the US, consisting of mainly 74 tons of poultry fat, 132 tons of tallow and 243 thousand tons of white grease [13].

Biodiesel produced from animal fats is cheaper than when made from vegetable oils. An additional advantage is that fossil CO₂ reduction is higher when using animal fat for biodiesel generation; nearly 80% CO₂ reduction may be reached for animal fat in comparison to 30% reduction when using vegetable oil [14,15]. The bioenergy demand is continuously increasing and in 2050 it is expected

to reach 30% of the fuel consumed in the world for road transport [15,16]. Research on biodiesel production is trying to maximize the yield and minimize the costs by using better catalysts that can be reused and improve the transesterification efficiency [17,18]. Furthermore, the feedstock used as raw material for biodiesel production represents up to 80% of the total cost [19] and it explains its variability in different geographic areas depending on the climate and agriculture [20].

Total biodiesel world production has been increasing progressively year by year, reaching nearly 45 million tons in 2019 [12]. The European Union has the largest biodiesel production through its 202 plants producing more than 14 million tons of biodiesel in 2019 [11,21]. More than 5.6 million tons of biodiesel were produced in the US in 2019 through its 91 plants [13,22]. Nearly 80% of new diesel vehicles are prepared for B20 use that consists of fossil diesel blended with 20% biodiesel [13].

Transesterification through alkaline catalysis is the preferred process at industrial biodiesel production plants [23]. However, raw materials like animal fat that contain moisture and free fatty acids are troublesome for alkaline transesterification due to soap formation. Acid catalysis does not have such troubles, but the reaction is much slower than alkaline catalysis, needs a larger size reactor and requires a higher alcohol to fat molar ratio [24]. Heterogeneous catalysts are not sensitive to the presence of free fatty acids and moisture, can catalyze esterification and transesterification simultaneously, and can be separated from the reaction media. However, such solid catalysts tend to form three phases resulting in a reduced reaction rate and high energy consumption [25]. The simultaneous esterification and transesterification also occur with supercritical technology where high temperature and pressure conditions (i.e., >250 °C and 10 MPa) increase the solubility and reduce the mass transfer limitation resulting in good efficiency but with high energy consumption [26–28]. Pseudo catalytic transesterification using biochar as the porous material for the pseudo-catalytic reaction at more than 300 °C has the same advantages as supercritical transesterification, but also has high energy consumption [29,30]. Therefore, animal fats may be processed for biodiesel production through enzymatically catalyzed transesterification even though some issues, like the cost of lipase and its poor stability, can be improved through immobilization [31]. Lipases have the advantage to generate biodiesel under mild reaction conditions through the conversion of free fatty acids and triacylglycerols in the presence of an acyl acceptor [32]. This manuscript reviews and discusses the latest advances in the use of free and immobilized lipases for an efficient transesterification of animal fat waste.

2. Mechanisms of Action of Lipases

Lipases, triacylglycerol ester hydrolases (EC 3.1.1.3), are serine hydrolases with an active site containing an amino-acid triad of serine, histidine and aspartate [32]. Lipases are obtained from a variety of sources such as animal and plant tissues and microorganisms. Lipases show a wide range of pH and temperature for activity and vary from strain to strain regarding specificity and hydrolysis rate [33] Lipases exhibit good stability in non-aqueous mediums and exhibit neutral pH range; such stability is increased when the enzyme is immobilized.

Lipases can catalyze esterification, inter-esterification, and trans-esterification reactions in non-aqueous environments. Lipases catalyze the hydrolysis of triacylglycerols at the aqueous-non aqueous interface but these enzymes can also catalyze the synthesis of esters from alcohols and long chain fatty acids in low moisture environment [33]. Lipases follow a two-step mechanism for the generation of fatty acid methyl esters in transesterification reactions, usually through the Ping-Pong Bi Bi mechanism [34].

Most triacylglycerol lipases are regiospecific because they can only hydrolyze primary ester bonds at the sn-1 and sn-3 positions, external positions within the triacylglycerol, and can generate either one free fatty acid and diacylglycerol, or two free fatty acids and 2-monoacylglycerol that remain unhydrolyzed. The full process from triacylglycerols into biodiesel and glycerol as end products is shown in Figure 1. Regiospecificity is characteristic of extracellular bacterial lipases from *Bacillus* sp. [35,36].

Monoacylglycerol lipases (EC 3.1.1.23) catalyze the hydrolysis at the specific sn-2 position of 2-monoacylglycerol into free fatty acid and glycerol. Such lipases may be present in the enzyme extract and masked when measuring activity with standard activity methods like those based on triolein hydrolysis measurement. Monoacylglycerol lipases have been the object of few studies [37], although they might be present in some microbial enzyme preparations [38]. Other lipases are nonspecific and can act on any of the ester bonds of the triacylglycerol and therefore break down the triacylglycerol to release free fatty acids and glycerol as the final products. This is the case of lipases from *Staphylococcus aureus* and *hyicus* [39], *Geotrichum candidum*, *Corynebacterium acnes*, *Penicillium cyclopium* [24] and *Chromobacterium viscosu* [40]. Another alternative for the hydrolysis of monoacylglycerols is the acyl migration in the glycerol backbone from the sn-2 position to sn-1 or sn-3 positions [41].

The specificity of lipases depends on the length of fatty acids, presence of double bonds, branched groups and, consequently, reaction rates may have important variations depending on the composition of triacylglycerols present in the fat waste. Lipases are especially active against medium to long chain fatty acids, which are those more usual in animal fat waste [17].

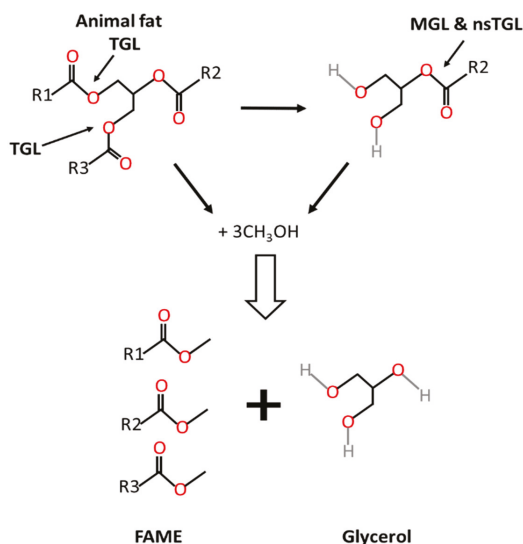


Figure 1. Transesterification of animal fat to biodiesel. TGL: triacylglycerol lipase; nsTGL: non specific triacylglycerol lipase; MGL: monoacylglycerol lipase.

3. Sources of Lipases

Most lipases originated from microorganisms and are produced in fermenters under controlled conditions (see Table 1). Lipases are produced by a variety of gram-positive and gram-negative bacterial strains, especially from the genera of *Pseudomonas* [42,43], also by filamentous fungus that are commercially important such as those belonging to the genera of *Rhizopus* sp. [44], *Aspergillus* sp. [45], *Penicillium* sp. [46], *Geotrichum* sp. [33], *Mucor* sp. [47] and *Thermomyces* sp. [48]. Lipases produced from yeasts are also relevant such as those from *Candida* sp. [49,50].

Extracellular lipases are secreted into the production medium and recovered from the microorganism broth. Then, lipases are further separated and purified but downstream processing is costly. Intracellular lipases imply the use of whole cell microorganisms and this fact reduces the costs of enzyme extraction and purification but the efficiency and biodiesel yield is low when catalyzing an oily substrate due to mass transfer limitations for substrate penetration and product release [28,51].

Some whole cell biocatalysts used to produce biodiesel are filamentous fungi like *Aspergillus* and *Rhizopus* [49].

Table 1. Bacteria, yeasts and filamentous fungi producing lipase and sources of isolation.

Lipase Origin	Reference
<i>Pseudomonas fluorescens</i>	[52]
<i>Burkholderia cepacia</i>	[42,50,53,54]
<i>Staphylococcus haemolyticus</i>	[55]
<i>Chromobacterium viscosum</i>	[56]
<i>Phichia pastoris</i>	[57]
<i>Mucor miehei</i>	[58]
<i>Thermomyces lanuginosus</i>	[59,60]
<i>Aspergillus oryzae</i>	[61]
<i>Aspergillus niger</i>	[62,63]
<i>Aspergillus terreus</i>	[64]
<i>Rhizopus oryzae</i>	[41,65,66]
<i>Rhizomucor miehei</i>	[60,67]
<i>Geotrichum candidum</i>	[68]
<i>Candida antarctica</i>	[66,69–71]
<i>Candida cylindracea</i>	[72]
<i>Candida rugosa</i>	[50,73,74]

4. Free Lipase

Lipases constitute an attractive catalyst for transesterification in those wastes containing large amounts of moisture and free fatty acids, which is the case of animal fat and is what makes it troublesome for alkaline transesterification. Table 2 shows some examples of the use of free lipases for biodiesel production from animal fat waste. The use of lipases has relevant advantages over conventional alkali catalysts. The most relevant are the absence of soap formation in the reactor, insensitivity to water content and acidity value, moderate reaction conditions, broad substrate range, good purity of biodiesel after transesterification and absence of pollutants, especially when treating cooking oil waste containing large amounts of free fatty acids [75]. On the contrary, there are also important disadvantages such as the high enzyme costs, poor enzyme stability, and the enzyme deactivation by alcohol [76] and partly by the generated glycerol [66].

As said, lipases are sensitive to the alcohol, in most cases methanol, used for biodiesel production and this fact increases the operational costs. There are some alternatives to avoid enzyme damage by methanol: stepwise addition of methanol to reaction mixtures avoiding a high concentration [65], the use of co-solvents like hydrophilic tert-butanol that dissolve glycerol and methanol and therefore allow high transesterification yields and rates [77], also the addition of longer-chain alcohols [78], or methyl or ethyl acetate as acyl acceptors [79,80]. Another solution is the use of novel lipases that can support one-step addition of high methanol concentration [81]. In this sense, another solution is the use of tools like protein engineering, recombinant methods and metabolic engineering that are used to improve thermostability as well as stability in organic solvents [80]. Glycerol may be extracted with organic solvents although the enzyme activity may be affected [81].

Lipase transesterification requires an extended time of reaction, and has a slow conversion rate as shown in Table 2. The recovery of the enzyme is rather difficult and the enzyme stability is poorer at high temperature and pH [81–84]. All these troubles have hindered its adoption at an industrial scale and therefore, transesterification with alkaline catalysis is still preferred at biodiesel-producing industrial plants [23]. However, such troubles experienced with enzymes can be partly overcome through its immobilization on a solid material that acts as enzyme carrier and increases its stability and efficiency [81,85,86]. Immobilization also allows an easy downstream separation from the product and decreases cost [82]. However, recyclability is an issue because lipases tend to lose activity after continuous operation [86]. In any case, it was reported that the use of soluble lipases might be more

competitive if the commercial enzymes would have a price 50 times lower than the immobilized lipase [25,87]

Table 2. Biodiesel production with various free soluble lipases.

Lipase Source	Feedstock	Conditions (T, alcohol:oil, t)	Yield (%)	References
<i>A. niger</i>	Waste cooking oil	45 °C, 4.2:1, 30 h	90 ^a	[63]
<i>T. lanuginosus</i>	Beef tallow	35 °C, 4.5:1, 6 h	84.6 ^a	[88]
<i>C. antarctica</i>	Lard	30 °C, 1:1, 72 h	74 ^a	[89]
<i>C. antarctica</i>	Lard	50 °C, 5:1, 20 h	97.2 ^b	[90]
<i>Candida</i> sp	Lard	40 °C, 3:1, 30 h	87.4 ^b	[91]
<i>T. lanuginosus</i>	Chicken fat	-	89.04 ^b	[92]
<i>C. antarctica</i>	Chicken fat	32 °C, 3:1, 24 h	96 ^a	[71]

^a Biodiesel yield (wt/wt.%) was determined as the methyl esters amount produced by the lipases in the reaction process divided by the initial amount of esters; or ^b by the amount of oil.

5. Immobilized Lipase

5.1. Types of Supports and Immobilization Procedures

The immobilization of lipases consists of the retention of the enzyme at the surface of the support material. In this way, immobilized lipases show an improved efficiency and reduced costs, with longer enzyme stability and better resistance to denaturation by alcohol. There are many available supports of organic, synthetic and inorganic nature for lipase immobilization. Such materials may vary in characteristics such as particle dimensions, shape, pore volume, hydrophobicity, and density and must be stable to physical, chemical, and microbial degradation [93]. Porous supports with controlled pore distribution are very interesting for lipase immobilization because they offer an extensive surface area and therefore, higher enzyme loading. However, caution must be observed if pores are too small because they could get blocked by the enzyme, reducing its efficiency.

There is a large variety of immobilization procedures (see Figure 2) such as adsorption, covalent binding, cross-linking, entrapment, or encapsulation that have been developed to enhance the catalytic activity, and its stability, and make possible the reutilization of the enzyme in relation to the soluble lipase [94]. Some methods like cross-linking enzyme aggregates are not considered in this review because even though they are inexpensive, highly efficient, and do not need support for immobilization, they have rather poor mechanical stability [95].

Immobilization by adsorption on materials such as water-absorbing polymer, hydrophobic macroporous polypropylene particles or silica gel is simple, but can result in an undesirable leakage making it necessary to assure the retention of the enzyme by additional ionic or covalent bonds. This can be an ion exchange resin or cross-linking with glutaraldehyde [68]; performance was improved by crosslinking with glutaraldehyde. The stability in acid pH was improved as well as thermostability at 45–50 °C. It retained 80% of relative biodiesel production after 5 consecutive batches [96]. Adsorption of lipase from *Burkholderia cepacia* was compared to covalent immobilization on epoxy acrylic resin. The adsorbed enzyme gave a higher conversion than the covalent one after a three-step addition of ethanol, 68% vs 47% [97]. The covalently immobilized enzyme showed lower affinity towards diglycerides and monoglycerides; this was attributed to blockage of the active groups by the covalent bonds to the support material, which resulted in enzyme rigidity [98]. Mesoporous materials are attractive because they have high surface area, larger pore volume, absence of toxicity, and good stability [99]. Examples of reported immobilized lipases used in recent studies are shown in Table 3.

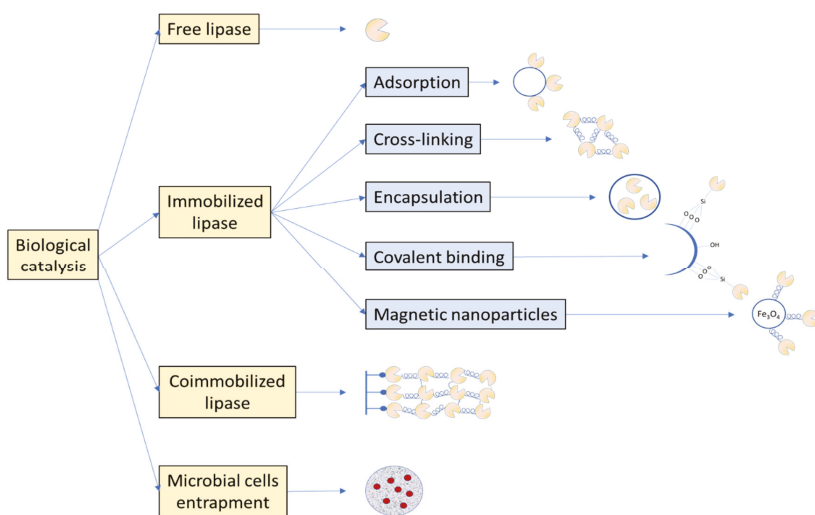


Figure 2. Major types of biological catalysis for biodiesel generation.

Table 3. Biodiesel production with various immobilized lipases.

Lipase Source	Feedstock	Immobilization	Yield ^a (%)	No. Cycles	References
<i>A. niger</i>	Sardine oil	Activated carbon	94.5 ^a	5	[62]
<i>T. lanuginosus</i>	Lard	Silica gel	97.6 ^a	20	[90]
<i>C. antarctica</i>	Waste cooking oil	Silica nanoflower pickering emulsion	98.5 ^a	15	[70]
<i>B. cepacia</i>	Castor oil	Polyvinylalcohol alginate	75 ^b	6	[85]
<i>R. miehei</i> and <i>C. antarctica</i>	Waste cooking oil	Epoxy functionalized silica	91.5 ^a	14	[100]
<i>Streptomyces</i> sp	Waste cooking oil	XAD 1180 resin	95.45 ^a	4	[79]
<i>B. cepacia</i>	Beef tallow	Polysiloxane–polyvinyl alcohol (SiO ₂ –PVA) hybrid composite	89 ^a	-	[101]
<i>C. antarctica</i>	Waste fish oil	Acrylic resin	95 ^a	4	[102]
<i>C. antarctica</i>	Waste fish oil	Acrylic resin	75 ^a	10	[103]

^a Biodiesel yield (wt/wt.%) was determined as the methyl esters amount produced by the lipases in the reaction process divided by the initial amount of esters, or ^b by the amount of oil.

There is a good affinity for immobilization of lipases on hydrophobic supports [104], giving a fast and good attachment by hydrophobic adsorption [105]. Transesterification of waste lard was tested with immobilized lipase B from *Candida antarctica* with the assistance of ultrasound for improving the dispersion and collision of the reagent molecules. Ultrasonic wave amplitude, ultrasonic cycles, and reaction parameters were optimized and a kinetic model was developed [69]. Pulsed ultrasound irradiation increased by about 3 times the synthesis rate of fatty acid ethyl ester by lipases immobilized on hydrophobic carriers like octadecyl-sepabeads [106].

Porous silica nanoflowers have center-radial pore structure that allows the load of lipase inside the structure to have good mass transfer for substrates and products [107]. Dichlorodimethylsilane was used to modify the silica nanoflowers for the adsorption of *Candida antarctica* lipase B and the biocatalytic pickering emulsion was constructed [94]. Pickering emulsion stabilized by hybrid nanoparticles [108], solid particles [109], or carbon nanotubes crosslinked with lipase [110], have been constructed and successfully used [111,112]. In this way, this emulsion facilitates biphasic reactions and simplifies the recovery of lipase that remains in its microenvironment [113].

Metal-organic frameworks provide advantages for immobilization: they can be easily separated, they offer an extended surface area that can be tuned, they have adequate pore size, have structural and functional diversity and good stability. Immobilization may be through adsorption, encapsulation,

and coprecipitation [114]. Lipase is strongly adsorbed by metal-chelating affinity immobilization that is a simple technique with the advantage that support may be reused [54]. Desorption agents may cause the desorption of the enzyme that can be also achieved by changing the pH value [115]. The compound n-hexane could reduce the deactivation of AGMNP-CO₂⁺-PFL from methanol. It was reported that biodiesel production from oil transesterification was higher with n-hexane than using tert-butanol [70,94].

Encapsulation immobilization entraps lipase by a co-precipitation method and crosslinking agents like glutaraldehyde are used to interconnect the enzymes. However, there is a high mass transfer resistance that reduces its efficiency.

The entrapment of cells having lipase activity appears to be a simple and attractive technique. Lipase immobilized in silicon granules or calcium alginate beads, with glucose supplementation for cells maintenance, achieved an increased number of cycles, 28 instead of 23, while keeping 90% activity [33]. Whole cell, recombinant methods and protein and metabolic engineering are promising options to increase lipase applications [82].

5.2. Magnetic Nanocarriers

Materials like magnetite (Fe₃O₄) are used as support for immobilization because they allow a rapid separation from the reaction medium when an external magnetic field is applied [116]. The development of magnetic nanoparticles (MNPs) as a support for enzymes immobilization has been recently reviewed [117]. Typical magnetic nanomaterials include iron oxide (Fe₃O₄ and γ -Fe₂O₃), alloy-based (CoPt₃ and FePt), pure metal (Fe and Co), and spinel-type ferromagnet (MgFe₂O₄, MnFe₂O₄, and CoFe₂O₄) [117]. Examples of lipase immobilized in various types of magnetic nanoparticles are shown in Table 4.

Table 4. Biodiesel production with various immobilized lipases using magnetic nanoparticles as carriers.

Lipase Source	Carrier	Immobilization	Yield ^a (%)	No. Cycles	References
<i>B. cepacia</i>	Silica coated hydroxyapatite and glutaraldehyde	Encapsulation	98	4	[118]
<i>A. terreus</i>	Iron oxide polydopamine	Covalent bonding	92	7	[64]
<i>T. lanuginosis</i> & <i>C. antarctica</i>	Core-shell structured iron oxide	Covalent bonding	99	11	[119]
<i>P. fluorescens</i>	Co ²⁺ chelated, with 3-glycidoxypropyltrimethoxysilane	Adsorption	95	10	[70]
<i>R. miehei</i> and <i>T. lanuginosa</i>	Silica core shell iron oxide with tryethylamine	Covalent bonding	93.1	5	[60]
<i>C. antarctica</i>	Poly(urea-urethane) encapsulated magnetite	Encapsulation	95	8	[120]
<i>C. antarctica</i>	Magnetic iron oxide with 1-Butyl-3-methylimidazolium tetrafluoroborate & 3-aminopropyltriethoxysilane	Covalent bonding	89.4	5	[121]
<i>B. cepacia</i>	Polysiloxane-polyvinyl alcohol hybrid magnetic-polymer composite	Covalent bonding	96.5	-	[122]

^a Biodiesel yield (wt/wt.%) was determined as the methyl esters amount produced by the lipases in the reaction process divided by the initial amount of esters.

Magnetic nanoparticles (MNPs) have good biocompatibility and non-toxicity but tend to aggregate and oxidize, so they need to be functionalized on the surface and use a cross-linking agent to bind the enzyme. One way is by using silica coating where a silica shell is formed on the surface by using amino-functional reagents like 3-aminopropyl triethoxysilane (APTES). Fe₃O₄ particles were encapsulated with mesoporous silicon and modified with APTES or 3-mercaptopropyl trimethoxysilane (MPTMS) followed by binding of the lipase with glutaraldehyde. APTES-modified Fe₃O₄ particles were reported to give better yield of biodiesel (90%) than MPTMS particles [75]. *Burkholderia* sp. lipase on Fe₃O₄ MNPs also achieved 90% conversion [123].

Another way to protect MNPs is with organic polymers, including synthetic polymers and biopolymers. The polymer can be either incorporated into the precursor solution to form Fe₃O₄ MNPs

or externally to create the core shell [117]. The polymer surface provides numerous functional groups that facilitate the enzyme binding. Magnetic chitosan binds the lipase by covalent attachment [124].

Separation of nanobiocatalysts is difficult in an oily system [119] but the magnetic properties of MNPs can facilitate the separation of enzyme from reaction media. In this way, the reaction may be immediately finished as well as using the enzyme for further uses [117].

5.3. Coimmobilization

Some works have proposed to use coimmobilization of enzymes. The advantage is that the first enzyme releases the product that is transferred to the next coimmobilized enzyme with a short diffusional distance. This is especially relevant for lipases due to their specificity for triacylglycerols ester bonds. The mixture of 1,3-specific lipase and a non-specific lipase enhances the global activity because it removes the limiting acyl-migration step. Several coimmobilized systems have been studied for biodiesel production like *Candida rugosa* lipase and *Rhizopus oryzae* lipase simultaneously on silica gel [74], *Candida antarctica* lipase B and *Thermomyces lanuginosus* lipase, on the surface of the *Phichia pastoris* cell [57], and *Rhizomucor miehei* and *Candida antarctica* lipases on epoxy-functionalized silica [67,100].

Lipases are coimmobilized on the same material surface in order to get better global activity and improved enzyme specificity and selectivity for hydrolysis of triacylglycerols as well as those generated diacylglycerols and monoacylglycerols that must be further hydrolyzed [96]. However, the most active enzyme may get some loss of activity through this procedure [125]. A different coimmobilization strategy was proposed by immobilizing several lipases layer-by-layer using abcoating with polyethylenimine [126]. Other authors have used coating with PEI/glutaraldehyde to form 5 enzyme layers of lipases A and B from *Candida antarctica*, lipases from *Rhizomucor miehei*, and *Thermomyces lanuginosus* and phospholipase Lecitase Ultra [125]. Although it gives an innovative way for fats hydrolysis some problems might arise either from inhibition by coating agents used, high costs of different lipases used or steric hindrance for accessibility of triacylglycerols to the active site of lipases immobilized in the inner layers.

6. Industrial Applications of Lipase-Catalyzed Biodiesel

Even though transesterification through alkaline catalysis is the preferred process in the majority of industrial biodiesel production plants [23], a few lipase-based processes have already been implemented to plant-scale operation. The collaboration of Novozymes (Bagsvaerd, Denmark) with Piedmont Biofuels (Pittsboro, NC, USA) resulted in a patent application to produce fatty acid alkyl esters, by a lipolytic enzyme in a solution containing triacylglycerol, alcohol, water, and glycerol [93,127]. Viesel Fuel (Terrac Stuart, FL, USA) upgraded in 2013 its facility through an enzymatic process developed by Novozymes (Denmark) to use brown grease and waste cooking oil to produce up to 11 million gallons biodiesel per year using Eversa Transform[®] lipase from Novozymes, a soluble lipase produced by a genetically modified strain of *Aspergillus oryzae* [128], and an ion exchange resin system for removal of remaining free fatty acids during crude biodiesel refining [129,130]. Viesel Fuel, Novozymes and Tactical Fabrication also collaborated with Buster Biofuels to upgrade its facility in San Diego (CA, USA) to produce up to 5 million gallons per year [131]. Lvming and Environmental Protection Technology Co. Ltd. (Shanghai, China) used lipase of *Candida* sp. to produce 10,000 tons per year from waste frying oil [95]. A plant in Sumaré (Sao Paulo, Brazil) produces biodiesel from mixed beef tallow and soybean oil using Callera[®] Trans L lipase in a batch reactor [132]. These companies are using liquid lipase formulations but the efficiency of the process can be improved further by using recent developments in immobilized lipases. So, Hunan Rivers Bioengineering Co. Ltd. (Hunan, China) was reported to use Novozym 435[®] lipase in a stirred tank reactor to produce 20,000 tons of biodiesel per year. The enzyme is a lipase B from *Candida antarctica* immobilized on a resin consisting of macroporous support formed by poly(methyl methacrylate) crosslinked with divinylbenzene [133]. New technology protected with patents [134] has been provided by EnzymoCore, a leading global

producer company founded in 2007 in Israel and with several active biodiesel plants around the world. This company has developed modified-immobilized enzymes, supported on solid organic resins, with high resistance to methanol and able to produce biodiesel from any type of oil or fat, even those cheap and with very large content of free fatty acids and polar lipids [135].

7. Conclusions

Animal fat waste, usually resulting from slaughterhouses, the meat processing industry, and cooking facilities, is being increasingly used for biodiesel production. Transesterification through alkaline catalysis is the preferred process at industrial biodiesel production plants. Transesterification with lipases has not been attractive for industry yet because of the higher operative costs in comparison to alkaline catalysis; transesterification with lipases has problems including poor enzyme stability, difficulties in reusability, and denaturation by alcohol although they are not affected by water and free fatty acids typically found in animal fats. However, a few companies could solve such troubles since they are running liquid lipase formulations for producing biodiesel from cooking oil waste at industrial scale. However, the efficiency of the process can be further improved. Recent developments in immobilized lipases and availability of different types of supports such as mesoporous materials, silica nanoflowers, pickering emulsion, and metal-organic frameworks demonstrate improved efficiency and reduced costs. Immobilization of the enzyme in such materials increases its stability and makes it more resistant to denaturation by alcohol. Magnetic nanomaterials constitute an even better support for enzyme immobilization because they can be recovered when an external magnetic field is applied. These nanoparticles are functionalized on the surface by coating with silica or organic polymers that enhance the efficiency of the process. The entrapment of whole cells with lipase activity, appears to be simple and efficient although more research is needed. Coimmobilization of lipases is an innovative process, but not so attractive for industrial application. It needs further research because of the need for different lipases that increases the costs and the efficiency affected by steric difficulties for enzymes to hydrolyze triacylglycerols.

Author Contributions: Conceptualization, F.T.; resources, F.T.-R. and L.M.; writing—original draft preparation, F.T.-R.; writing—review and editing, F.T.-R., L.M. and F.T.; supervision, F.T. All authors have read and agreed to the published version of the manuscript.

Funding: This research was funded by European Marie Curie project, grant number 614281 (HIGHVALFOOD) and European Regional Development Fund.

Conflicts of Interest: The authors declare no conflict of interest. The funders had no role in the design of the study; they had no role in the collection, analyses, or interpretation of data; and they had no role in the writing of the manuscript, or in the decision to publish the results.

References

1. Rosson, E.; Sgarbossa, P.; Pedrielli, F.; Mozzon, M.; Bertani, R. Bioliquids from raw waste animal fats: An alternative renewable energy source. *Biomass Convers. Biorefin.* **2020**, 1–16. [CrossRef]
2. EFPRA. Rendering in Numbers. 2016. Available online: <https://efpra.eu/wp-content/uploads/2016/11/Rendering-in-numbers-Infographic.pdf> (accessed on 20 March 2020).
3. Toldrá, F.; Mora, L.; Reig, M.; Mora, L. New insights into meat by-product utilization. *Meat Sci.* **2016**, *120*, 54–59. [CrossRef] [PubMed]
4. Akhil, U.S.; Alagumalai, A. A Short Review on Valorization of Slaughterhouse Wastes for Biodiesel Production. *ChemistrySelect* **2019**, *4*, 13356–13362. [CrossRef]
5. Barik, D.; Vijayaraghavan, R. Effects of waste chicken fat derived biodiesel on the performance and emission characteristics of a compression ignition engine. *Int. J. Ambient Energy* **2018**, *41*, 88–97. [CrossRef]
6. Prates, J.; Alfaia, C.; Alves, S.; Bessa, R. Fatty acids. In *Handbook of Analysis of Edible Animal by-Products*; Nollet, L.M.L., Toldrá, F., Eds.; CRC Press: Boca Raton, FL, USA, 2011; pp. 137–159.
7. Mora, L.; Toldrá-Reig, F.; Prates, J.A.M.; Toldrá, F. Cattle by-products. In *Byproducts from Agriculture and Fisheries: Adding Value for Food, Feed, Pharma and Fuels*; Simpson, B.K., Aryee, A.N., Toldrá, F., Eds.; Wiley: Chichester, UK, 2020; pp. 43–55.

8. Baladincz, P.; Hancsók, J. Fuel from waste animal fats. *Chem. Eng. J.* **2015**, *282*, 152–160. [CrossRef]
9. Mora, L.; Toldrá-Reig, F.; Reig, M.; Toldrá, F. Possible uses of processed slaughter by-products. In *Sustainable Meat Production and Processing*; Galanakis, C.M., Ed.; Academic Press/Elsevier: London, UK, 2019; pp. 145–160.
10. Banković-Ilić, I.B.; Stojković, I.J.; Stamenković, O.S.; Veljković, V.B.; Hung, Y.-T. Waste animal fats as feed stocks for biodiesel production. *Renew. Sustain. Energy Rev.* **2014**, *32*, 238–254. [CrossRef]
11. Ramos, M.; Dias, A.P.S.; Puna, J.F.; Gomes, J.; Bordado, J.C. Biodiesel Production Processes and Sustainable Raw Materials. *Energies* **2019**, *12*, 4408. [CrossRef]
12. Flach, B.; Lieberz, S.; Bolla, S. EU Biofuels Annual 2019, Gain Report NL9022, USDA Foreign Agricultural Service. 2019. Available online: <http://gain.fas.usda.gov/Pages/Default.aspx> (accessed on 6 May 2020).
13. US Energy Information Administration. *Monthly Biodiesel Production Report*; US Department of Energy: Washington, DC, USA, 2020. Available online: <https://www.eia.gov/biofuels/biodiesel/production/biodiesel.pdf> (accessed on 5 May 2020).
14. IPPR. Time for Change: A New Vision for the British Economy—The Interim Report of the IPPR Commission on Economic Justice. 2017. Available online: <http://www.ippr.org/cej-time-for-change> (accessed on 25 March 2020).
15. IRENA. Global Energy Transformation: A Roadmap to 2050. 2018. Available online: https://www.irena.org/-/media/Files/IRENA/Agency/Publication/2018/Apr/IRENA_Report_GET_2018.pdf (accessed on 14 April 2020).
16. Cernat, A.; Pana, C.; Negurescu, N.; Lazaroiu, G.; Nutu, C.; Fuiiorescu, D.; Toma, M.; Nicolici, A. Combustion of preheated raw animal fats-diesel fuel blends at diesel engine. *J. Therm. Anal. Calorim.* **2019**, *140*, 2369–2375. [CrossRef]
17. Toldrá-Reig, F.; Mora, L.; Toldrá, F. Trends in biodiesel production from animal fat waste. *Appl. Sci.* **2020**, *10*, 3644.
18. Lawan, I.; Garba, Z.N.; Zhou, W.; Zhang, M.; Yuan, Z. Synergies between the microwave reactor and CaO/zeolite catalyst in waste lard biodiesel production. *Renew. Energy* **2020**, *145*, 2550–2560. [CrossRef]
19. Bušić, A.; Kundas, S.; Morzak, G.; Belskaya, H.; Mardetko, N.; Santek, M.I.; Komes, D.; Novak, S.; Šantek, B. Recent Trends in Biodiesel and Biogas Production. *Food Technol. Biotechnol.* **2018**, *56*, 152–173. [CrossRef] [PubMed]
20. Mahlia, T.; Syazmi, Z.; Mofijur, M.; Abas, A.P.; Bilad, M.; Ong, H.C.; Silitonga, A. Patent landscape review on biodiesel production: Technology updates. *Renew. Sustain. Energy Rev.* **2020**, *118*, 109526. [CrossRef]
21. Bockey, D. The significance and perspective of biodiesel production—A European and global view. *OCL* **2019**, *26*, 40. [CrossRef]
22. Biodiesel. Available online: <https://www.biodiesel.org/what-is-biodiesel/biodiesel-basics> (accessed on 21 March 2020).
23. Kristi, M.; Milbrandt, A.; Lewis, J.; Schwab, A. *Bioenergy Industry Status 2017 Report*; National Renewable Energy Laboratory: Golden, CO, USA, 2018. Available online: <https://www.nrel.gov/docs/fy20osti/75776.pdf> (accessed on 5 May 2020).
24. Canakci, M.; Sanli, H. Biodiesel production from various feedstocks and their effects on the fuel properties. *J. Ind. Microbiol. Biotechnol.* **2008**, *35*, 431–441. [CrossRef] [PubMed]
25. Wancura, J.H.C.; Tres, M.V.; Jahn, S.L.; de Oliveira, J.V. Lipases in liquid formulation for biodiesel production: Current status and challenges. *Biotechnol. Appl. Biochem.* **2019**. [CrossRef] [PubMed]
26. Shin, H.-Y.; Lee, S.-H.; Ryu, J.-H.; Bae, S.-Y. Biodiesel production from waste lard using supercritical methanol. *J. Supercrit. Fluids* **2012**, *61*, 134–138. [CrossRef]
27. Marulanda, V.F.; Anitescu, G.; Tavlarides, L.L. Investigations on supercritical transesterification of chicken fat for biodiesel production from low-cost lipid feedstocks. *J. Supercrit. Fluids* **2010**, *54*, 53–60. [CrossRef]
28. Thangaraj, B.; Solomon, P.-R.; Muniyandi, B.; Ranganathan, S.; Lin, L. Catalysis in biodiesel production—A review. *Clean Energy* **2019**, *3*, 2–23. [CrossRef]
29. Vakros, J. Biochars and Their Use as Transesterification Catalysts for Biodiesel Production: A Short Review. *Catalysts* **2018**, *8*, 562. [CrossRef]
30. Lee, J.; Jung, J.-M.; Oh, J.-I.; Ok, Y.S.; Lee, S.-R.; Kwon, E.E. Evaluating the effectiveness of various biochars as porous media for biodiesel synthesis via pseudo-catalytic transesterification. *Bioresour. Technol.* **2017**, *231*, 59–64. [CrossRef]
31. Issariyakul, T.; Kulkarni, M.G.; Dalai, A.K.; Bakhshi, N.N. Production of biodiesel from waste fryer grease using mixed methanol/ethanol system. *Fuel Process Technol.* **2007**, *88*, 429–436. [CrossRef]

32. Melani, N.B.; Tambourgi, E.B.; Silveira, E. Lipases: From Production to Applications. *Sep. Purif. Rev.* **2019**, *49*, 143–158. [[CrossRef](#)]
33. Maldonado, R.R.; Lopes, D.B.; Aguiar-Oliveira, E.; Kamimura, E.S.; Macedo, G.A. A review on geotrichum lipases: Production, purification, immobilization and applications. *Chem. Biochem. Eng.* **2016**, *30*, 439–454. [[CrossRef](#)]
34. Alzuhair, S.; Ling, F.W.; Limsong, J. Proposed kinetic mechanism of the production of biodiesel from palm oil using lipase. *Process Biochem.* **2007**, *42*, 951–960. [[CrossRef](#)]
35. Sugihara, A.; Tani, T.; Tominaga, Y. Purification and characterization of a novel thermostable lipase from *Bacillus* sp. *J. Biochem.* **1991**, *109*, 211–216.
36. Lanser, A.C.; Manthey, L.K.; Hou, C.T. Regioselectivity of new bacterial lipases determined by hydrolysis of triolein. *Curr. Microbiol.* **2002**, *44*, 336–340. [[CrossRef](#)]
37. Tsurumura, T.; Tsuge, H. Substrate selectivity of bacterial monoacylglycerol lipase based on crystal structure. *J. Struct. Funct. Genom.* **2014**, *15*, 83–89. [[CrossRef](#)]
38. Li, P.-Y.; Zhang, Y.-Q.; Zhang, Y.; Jiang, W.-X.; Wang, Y.-J.; Zhang, Y.-S.; Sun, Z.-Z.; Li, C.-Y.; Zhang, Y.-Z.; Shi, M.; et al. Study on a Novel Cold-Active and Halotolerant Monoacylglycerol Lipase Widespread in Marine Bacteria Reveals a New Group of Bacterial Monoacylglycerol Lipases Containing Unusual C(A/S)HSMG Catalytic Motifs. *Front. Microbiol.* **2020**, *11*, 9. [[CrossRef](#)]
39. Davranov, K. Microbial lipases in biotechnology (review). *Appl. Biochem. Microbiol.* **1994**, *30*, 527–534.
40. Jaeger, K.-E.; Ransac, S.; Dijkstra, B.W.; Colson, C.; Heuvel, M.; van Misset, O. Bacterial lipases. *FEMS Microbiol. Rev.* **1994**, *15*, 29–63. [[CrossRef](#)]
41. Wei, L.; Li, R.W.; Qiang, L.; Wei, D.; Liu, D.H. Acyl migration and kinetics study of 1(3)-positional specific lipase of *Rhizopus oryzae*-catalyzed methanolysis of triglyceride for biodiesel production. *Process Biochem.* **2010**, *45*, 1888–1893.
42. Sánchez, D.A.; Tonetto, G.M.; Ferreira, M.L. *Burkholderia cepacia* lipase: A versatile catalyst in synthesis reactions. *Biotechnol. Bioeng.* **2018**, *115*, 6–24. [[CrossRef](#)] [[PubMed](#)]
43. Encinar, J.M.; González, J.F.; Sánchez, N.; Nogales-Delgado, S. Sunflower oil transesterification with methanol using immobilized lipase enzymes. *Bioproc. Biosyst. Eng.* **2019**, *42*, 157–166. [[CrossRef](#)] [[PubMed](#)]
44. Riyadi, F.A.; Alam, M.Z.; Salleh, M.N.; Salleh, H.M. Optimization of thermostable organic solvent-tolerant lipase production by thermotolerant *Rhizopus* sp. Using solid-state fermentation of palm kernel cake. *3 Biotech* **2017**, *7*, 300. [[CrossRef](#)]
45. Oliveira, F.; Moreira, C.; Salgado, J.M.; Abrunhosa, L.; Venancio, A.; Belo, I. Olive pomace valorization by *Aspergillus* species: Lipase production using solid-state fermentation. *J. Sci. Food Agric.* **2016**, *96*, 3583–3589. [[CrossRef](#)]
46. Pandey, N.; Dhakar, K.; Jain, R.; Pandey, A. Temperature dependent lipase production from cold and pH tolerant species of *Penicillium*. *Mycosphere* **2016**, *7*, 1533–1545. [[CrossRef](#)]
47. Calabrò, V.; Ricca, E.; De Paola, M.G.; Curcio, S.; Iorio, G. Kinetics of enzymatic trans-esterification of glycerides for biodiesel production. *Bioproc. Biosyst. Eng.* **2010**, *33*, 701–710. [[CrossRef](#)] [[PubMed](#)]
48. Dizge, N.; Aydiner, C.; Imer, D.Y.; Bayramoglu, M.; Tanriseven, A.; Keskinler, B. Biodiesel production from sunflower, soybean, and waste cooking oils by transesterification using lipase immobilized onto a novel microporous polymer. *Bioresour. Technol.* **2009**, *100*, 1983–1991. [[CrossRef](#)] [[PubMed](#)]
49. Gog, A.; Roman, M.; Tos, M.; Paizs, C.; Dan Irimie, F. Biodiesel production using enzymatic transesterification e Current state and Perspectives. *Renew. Energy* **2012**, *39*, 10–16. [[CrossRef](#)]
50. Shah, S.; Gupta, M.N. Lipase catalyzed preparation of biodiesel from Jatropha oil in a solvent free system. *Process Biochem.* **2007**, *42*, 409–414. [[CrossRef](#)]
51. Cubides-Roman, D.C.; Perez, V.H.; de Castro, H.F.; Orrego, C.E.; Giraldo, O.H.; Silveira, E.G.; David, G.F. Ethyl esters (biodiesel) production by *Pseudomonas fluorescens* lipase immobilized on chitosan with magnetic properties in a bioreactor assisted by electromagnetic field. *Fuel* **2017**, *196*, 481–487. [[CrossRef](#)]
52. Li, W.; Du, W.; Liu, D. *Rhizopus oryzae* IFO 4697 whole cell catalyzed methanolysis of crude and acidified rapeseed oils for biodiesel production in tert-butanol system. *Process Biochem.* **2007**, *42*, 1481–1485. [[CrossRef](#)]
53. Kaieda, M.; Samukawa, T.; Kondo, A.; Fukuda, H. Effect of methanol and water contents on production of biodiesel fuel from plant oil catalyzed by various lipases in a solvent-free system. *J. Biosci. Bioeng.* **2001**, *91*, 12–15. [[CrossRef](#)]

54. Li, K.; Wang, J.; He, Y.; Cui, G.; Abdulrazaq, M.A.; Yan, Y. Enhancing enzyme activity and enantioselectivity of *Burkholderia cepacia* lipase via immobilization on melamine glutaraldehyde dendrimer modified magnetic nanoparticles. *Chem. Eng. J.* **2018**, *351*, 258–268. [[CrossRef](#)]
55. Kim, S.H.; Kim, S.; Park, S.; Kim, H.K. Biodiesel production using cross-linked *Staphylococcus haemolyticus* lipase immobilized on solid polymeric carriers. *J. Mol. Catal. B Enzym.* **2013**, *85–86*, 10–16. [[CrossRef](#)]
56. Shah, S.; Sharma, S.; Gupta, M.N. Biodiesel preparation by lipase-catalyzed transesterification of Jatropha oil. *Energy Fuels* **2004**, *18*, 154–159. [[CrossRef](#)]
57. Ji, Q.; Wang, B.; Tan, J.; Zhu, L.; Li, L. Immobilized multienzymatic systems for catalysis of cascade reactions. *Process Biochem.* **2016**, *51*, 1193–1203. [[CrossRef](#)]
58. Handayani, R.; Wahyuningrum, D.; Zulfikar, M.A.; Nurbaiti, S.; Radiman, C.L.; Buchari, R. The synthesis of biodiesel catalyzed by *Mucor miehei* lipase immobilized onto aminated polyethersulfone membranes. *Bioresour. Bioproc.* **2016**, *3*, 22. [[CrossRef](#)]
59. Costa Rodrigues, R.; Volpato, G.; Ayub, M.A.Z.; Wada, K. Lipase-catalysed ethanolysis of soybean oil in a solvent-free system using central composite design and response surface methodology. *J. Chem. Technol. Biotechnol.* **2008**, *83*, 849–854. [[CrossRef](#)]
60. Ashjari, M.; Garmroodi, M.; Asl, F.A.; Emampour, M.; Yousefi, M.; Lish, M.P.; Habibi, Z.; Mohammadi, M. Application of multi-component reaction for covalent immobilization of two lipases on aldehyde-functionalized magnetic nanoparticles; production of biodiesel from waste cooking oil. *Process Biochem.* **2020**, *90*, 156–167. [[CrossRef](#)]
61. Chen, G.; Ying, M.; Li, W. Enzymatic conversion of waste-cooking oils into alternative fuel biodiesel. *Appl. Biochem. Biotechnol.* **2006**, *132*, 911–921. [[CrossRef](#)]
62. Arumugam, A.; Ponnusami, V. Production of biodiesel by enzymatic transesterification of waste sardine oil and evaluation of its engine performance. *Helvion* **2017**, *3*, 00486. [[CrossRef](#)] [[PubMed](#)]
63. Lv, L.; Dai, L.; Du, W.; Liu, D. Effect of water on lipase NS81006-catalyzed alcoholysis for biodiesel production. *Process Biochem.* **2017**, *58*, 239–244. [[CrossRef](#)]
64. Touqeer, T.; Mumtaz, M.W.; Mukhtar, H.; Irfan, A.; Akram, S.; Shabbir, A.; Rashid, U.; Nehdi, I.A.; Choong, T.S.Y. Fe₃O₄-PDA-Lipase as Surface Functionalized NanoBiocatalyst for the Production of Biodiesel Using Waste Cooking Oil as Feedstock: Characterization and Process Optimization. *Energies* **2020**, *13*, 177. [[CrossRef](#)]
65. Kaieda, M.; Samukawa, T.; Matsumoto, T.; Ban, K.; Kondo, A.; Shimada, Y.; Noda, H.; Nomoto, F.; Ohtsuka, K.; Izumoto, E.; et al. Biodiesel fuel production from plant oil catalyzed by *Rhizopus oryzae* lipase in a water-containing system without an organic solvent. *J. Biosci. Bioeng.* **1999**, *88*, 627–631. [[CrossRef](#)]
66. Duarte, S.H.; Hernández, G.L.P.; Canet, A.; Benaiges, M.D.; Maugeria, F.; Valero, F. Enzymatic biodiesel synthesis from yeast oil using immobilized recombinant *Rhizopus oryzae* lipase. *Bioresour. Technol.* **2015**, *183*, 175–180. [[CrossRef](#)]
67. Shahedi, M.; Yousefi, M.; Habibi, Z.; Mohammadi, M.; As'habi, M.A. Co-immobilization of *Rhizomucor miehei* lipase and *Candida antarctica* lipase B and optimization of biocatalytic biodiesel production from palm oil using response surface methodology. *Renew. Energy* **2019**, *141*, 847–857. [[CrossRef](#)]
68. Matsuda, T.; Marukado, R.; Mukoyama, M.; Harada, T.; Nakamura, K. Asymmetric reduction of ketones by *Geotrichum candidum*: Immobilization and application to reactions using supercritical carbon dioxide. *Tetrahedron Asymmetry* **2008**, *19*, 2272–2275. [[CrossRef](#)]
69. Adewale, P.; Dumont, J.-M.; Ngadi, M. Enzyme-catalyzed synthesis and kinetics of ultrasonic assisted methanolysis of waste lard for biodiesel production. *Chem. Eng. J.* **2016**, *284*, 158–165. [[CrossRef](#)]
70. Wang, L.; Liu, X.; Jiang, Y.; Liu, P.; Zhou, L.; Ma, L.; He, Y.; Li, H.; Gao, J. Silica Nanoflowers-Stabilized Pickering Emulsion as a Robust Biocatalysis Platform for Enzymatic Production of Biodiesel. *Catalysts* **2019**, *9*, 1026. [[CrossRef](#)]
71. Antonio, D.C.; Amancio, L.P.; Rosset, I.G. Biocatalytic Ethanolysis of Waste Chicken Fat for Biodiesel Production. *Catal. Lett.* **2018**, *148*, 3214–3222. [[CrossRef](#)]
72. Lara, P.V.; Park, E.Y. Potential application of waste activated bleaching earth on the production of fatty acid alkyl esters using *Candida cylindracea* lipase in organic solvent system. *Enzym. Microb. Technol.* **2004**, *34*, 270–277. [[CrossRef](#)]

73. Matinja, A.I.; Zain, N.A.M.; Suhaimi, M.S.; Alhassan, A.J. Optimization of biodiesel production from palm oil mill effluent using lipase immobilized in PVA alginate- sulfate beads. *Renew. Energy* **2019**, *135*, 1178–1185. [[CrossRef](#)]
74. Lee, J.H.; Kim, S.B.; Yoo, H.Y.; Lee, J.H.; Han, S.O.; Park, C.; Kim, S.W. Co-immobilization of *Candida rugosa* and *Rhizopus oryzae* lipases and biodiesel production. *Korean J. Chem. Eng.* **2013**, *30*, 1335–1338. [[CrossRef](#)]
75. Christopher, L.P.; Kumar, H.; Zambare, V.P. Enzymatic biodiesel: Challenges and opportunities. *Appl. Energy* **2014**, *119*, 497–520. [[CrossRef](#)]
76. Bandikari, R.; Qian, J.; Baskaran, R.; Liu, Z.; Wu, G. Bio-affinity mediated immobilization of lipase onto magnetic cellulose nanospheres for high yield biodiesel in one time addition of methanol. *Bioresour. Technol.* **2018**, *249*, 354–360. [[CrossRef](#)]
77. López, E.N.; Medina, A.R.; Moreno, P.A.G.; Cerdán, L.E.; Valverde, L.M.; Grima, E.M. Biodiesel production from *Nannochloropsis gaditana* lipids through transesterification catalyzed by *Rhizopus oryzae* lipase. *Bioresour. Technol.* **2016**, *203*, 236–244. [[CrossRef](#)]
78. Iso, M.; Chen, B.; Eguchi, M.; Kudo, T.; Shrestha, S. Production of biodiesel fuel from triglycerides and alcohol using immobilized lipase. *J. Mol. Catal. B Enzym.* **2001**, *16*, 53–58. [[CrossRef](#)]
79. Goembira, F.; Saka, S. Optimization of biodiesel production by supercritical methyl acetate. *Bioresour. Technol.* **2013**, *131*, 47–52. [[CrossRef](#)]
80. Razack, S.A.; Durairasan, S. Response surface methodology assisted biodiesel production from waste cooking oil using encapsulated mixed enzyme. *Waste Manage.* **2016**, *47*, 98–104. [[CrossRef](#)]
81. Wang, X.; Qin, X.; Li, D.; Yang, B.; Wang, Y. One-step synthesis of high-yield biodiesel from waste cooking oils by a novel and highly methanol-tolerant immobilized lipase. *Bioresour. Technol.* **2017**, *235*, 18–24. [[CrossRef](#)] [[PubMed](#)]
82. Hwang, H.T.; Qi, F.; Yuan, C.; Zhao, X.; Ramkrishna, D.; Liu, D.; Varma, A. Lipase-Catalyzed Process for Biodiesel Production: Protein Engineering and Lipase Production. *Biotechnol. Bioeng.* **2014**, *111*, 639. [[CrossRef](#)] [[PubMed](#)]
83. Pollardo, A.A.; Lee, H.; Lee, D.; Kim, S.; Kim, J. Solvent effect on the enzymatic production of biodiesel from waste animal fat. *J. Clean. Prod.* **2018**, *185*, 382–388. [[CrossRef](#)]
84. Kumar, D.; Das, T.; Giri, B.S.; Verma, B. Preparation and characterization of novel hybrid bio-support material immobilized from *Pseudomonas cepacia* lipase and its application to enhance biodiesel production. *Renew. Energy* **2020**, *147*, 11–24. [[CrossRef](#)]
85. Al-Zuhair, S.; Hasan, M.; Ramachandran, K. Kinetics of the enzymatic hydrolysis of palm oil by lipase. *Process Biochem.* **2003**, *38*, 1155–1163. [[CrossRef](#)]
86. Chesterfield, D.M.; Rogers, P.L.; Al-Zaini, E.O.; Adesina, A.A. Production of biodiesel via ethanolysis of waste cooking oil using immobilised lipase. *Chem. Eng. J.* **2012**, *207*, 701–710. [[CrossRef](#)]
87. Remonato, D.; Santin, C.M.T.; Oliveira, D.; Di Luccio, M.; Oliveira, J.V. FAME Production from Waste Oils Through Commercial Soluble Lipase Eversa® Catalysis. *Ind. Biotechnol.* **2016**, *12*, 254–262. [[CrossRef](#)]
88. Wancura, J.H.C.; Rosset, D.V.; Tres, M.V.; Oliveira, J.V.; Mazutti, M.A.; Jahn, S.L. Production of biodiesel catalyzed by lipase from *Thermomyces lanuginosus* in its soluble form. *Can. J. Chem. Eng.* **2018**, *96*, 2361–2368. [[CrossRef](#)]
89. Lee, K.T.; Foglia, T.A.; Chang, K.S. Production of alkyl ester as biodiesel from fractionated lard and restaurant grease. *J. Am. Oil Chem. Soc.* **2002**, *79*, 191–195. [[CrossRef](#)]
90. Huang, Y.; Zheng, H.; Yan, Y. Optimization of Lipase-Catalyzed Transesterification of lard for Biodiesel Production Using Response Surface Methodology. *Appl. Microbiol. Biotechnol.* **2010**, *160*, 504–515. [[CrossRef](#)]
91. Lu, J.; Nie, K.; Xie, F.; Wang, F.; Tan, T. Enzymatic synthesis of fatty acid methyl esters from lard with immobilized *Candida* sp. 99–125. *Process Biochem.* **2007**, *42*, 1367–1370. [[CrossRef](#)]
92. Da Silva, J.R.P.; da Costa, F.P.; Lerin, L.A.; Ninow, J.L.; Oliveira, V.; de Oliveira, D. Application of Different Methodologies to Produce Fatty Acid Esters Using the Waste Chicken Fat Catalyzed by Free NS 40116 Lipase. *Ind. Biotechnol.* **2019**, *5*, 293–302. [[CrossRef](#)]
93. Poppe, J.K.; Fernandez-Lafuente, R.; Rodrigues, R.C.; Záchia Ayub, M.A. Enzymatic reactors for biodiesel synthesis: Present status and future prospects. *Biotechnol. Adv.* **2015**, *33*, 511–525. [[CrossRef](#)] [[PubMed](#)]

94. Wang, J.; Li, K.; He, Y.; Wang, Y.; Han, X.; Yan, Y. Enhanced performance of lipase immobilized onto Co²⁺-chelated magnetic nanoparticles and its application in biodiesel production. *Fuel* **2019**, *255*, 115794. [[CrossRef](#)]
95. Cui, J.D.; Jia, S.R. Optimization protocols and improved strategies of cross-linked enzyme aggregates technology: Current development and future challenges. *Crit. Rev. Biotechnol.* **2015**, *35*, 15–28. [[CrossRef](#)]
96. Yan, J.; Yan, Y.; Liu, S.; Hu, J.; Wang, G. Preparation of cross-linked lipase-coated micro-crystals for biodiesel production from waste cooking oil. *Bioresour. Technol.* **2011**, *102*, 4755–4758. [[CrossRef](#)]
97. Lopresto, C.G.; De Paola, M.G.; Albo, L.; Policicchio, M.F.; Chakraborty, S.; Calabro, V. Comparative analysis of immobilized biocatalyst: Study of process variables in trans-esterification reaction. *3 Biotech* **2019**, *9*, 443. [[CrossRef](#)]
98. Mateo, C.; Palomo, J.M.; Fernandez-Lorente, G.; Guisan, J.M.; Fernandez-Lafuente, R. Improvement of enzyme activity, stability and selectivity via immobilization techniques. *Enzym. Microb. Technol.* **2007**, *40*, 1451–1463. [[CrossRef](#)]
99. Zhou, Z.; Hartmann, M. Progress in enzyme immobilization in ordered mesoporous materials and related applications. *Chem. Soc. Rev.* **2013**, *42*, 3894–3912. [[CrossRef](#)]
100. Babaki, M.; Yousefi, M.; Habibi, Z.; Mohammadi, M. Process optimization for biodiesel production from waste cooking oil using multi-enzyme systems through response surface methodology. *Renew. Energy* **2017**, *105*, 465–472. [[CrossRef](#)]
101. Da Rós, P.C.M.; Silva, G.A.M.; Mendes, A.A.; Santos, J.C.; de Castro, H.F. Evaluation of the catalytic properties of *Burkholderia cepacia* lipase immobilized on non-commercial matrices to be used in biodiesel synthesis from different feedstocks. *Bioresour. Technol.* **2010**, *101*, 5508–5516. [[CrossRef](#)] [[PubMed](#)]
102. Angulo, B.; Fraile, J.M.; Gil, L.; Herrerias, C.I. Comparison of Chemical and Enzymatic Methods for the Transesterification of Waste Fish Oil Fatty Ethyl Esters with Different Alcohols. *ACS Omega* **2020**, *5*, 1479–1487. [[CrossRef](#)] [[PubMed](#)]
103. Marin-Suarez, M.; Mendez-Mateos, D.; Guadix, A.; Guadix, E.M. Reuse of immobilized lipases in the transesterification of waste fish oil for the production of biodiesel. *Renew. Energy* **2019**, *140*, 1–8. [[CrossRef](#)]
104. Rodrigues, R.C.; Virgen-Ortiz, J.J.; dos Santos, J.C.; Berenguer-Murcia, Á.; Alcantara, A.R.; Barbosa, O.; Ortiz, C.; Fernandez-Lafuente, R. Immobilization of lipases on hydrophobic supports: Immobilization mechanism, advantages, problems, and solutions. *Biotechnol. Adv.* **2019**, *37*, 746–770. [[CrossRef](#)] [[PubMed](#)]
105. Manoel, E.A.; dos Santos, J.C.; Freire, D.M.; Rueda, N. Fernandez-Lafuente, R. Immobilization of lipases on hydrophobic supports involves the open form of the enzyme. *Enzym. Microb. Technol.* **2015**, *71*, 53–57. [[CrossRef](#)] [[PubMed](#)]
106. Quilles, J.C., Jr.; Ferrarezi, A.L.; Borges, J.P.; Rossi, J.S.; Bocchini, D.A.; Gomes, E.; da Silva, R.; Boscolo, M. Ultrasound affects the selectivity and activity of immobilized lipases applied to fatty acid ethyl ester synthesis. *Acta Sci-Technol.* **2020**, *42*, 46582. [[CrossRef](#)]
107. Zhou, W.J.; Fang, L.; Fan, Z.; Albela, B.; Bonneviot, L.; De Campo, F.; Pera Titus, M.; Clacens, J.M. Tunable catalysts for solvent-free biphasic systems: Pickering interfacial catalysts over amphiphilic silica nanoparticles. *J. Am. Chem. Soc.* **2014**, *136*, 4869–4872. [[CrossRef](#)]
108. Jiang, Y.; Liu, X.; Chen, Y.; Zhou, L.; He, Y.; Ma, L.; Gao, J. Pickering emulsion stabilized by lipase-containing periodic mesoporous organosilica particles: A robust biocatalyst system for biodiesel production. *Bioresour. Technol.* **2014**, *153*, 278–283. [[CrossRef](#)]
109. Zhang, W.; Fu, L.; Yang, H. Micrometer-Scale Mixing with Pickering Emulsions: Biphasic Reactions without Stirring. *ChemSusChem* **2014**, *7*, 391–396. [[CrossRef](#)]
110. Wang, L.; Liu, X.; Jiang, Y.; Zhou, L.; Ma, L.; He, Y.; Gao, J. Biocatalytic Pickering Emulsions Stabilized by Lipase-Immobilized Carbon Nanotubes for Biodiesel Production. *Catalysts* **2018**, *8*, 587. [[CrossRef](#)]
111. Shi, J.; Wang, X.; Zhang, S.; Tang, L.; Jiang, Z. Enzyme-conjugated ZIF-8 particles as efficient and stable Pickering interfacial biocatalysts for biphasic biocatalysis. *J. Mater. Chem. B* **2016**, *4*, 2654–2661. [[CrossRef](#)] [[PubMed](#)]
112. Chen, Z.; Zhao, C.; Ju, E.; Ji, H.; Ren, J.; Binks, B.P.; Qu, X. Design of Surface-Active Artificial Enzyme Particles to Stabilize Pickering Emulsions for High-Performance Biphasic Biocatalysis. *Adv. Mater.* **2016**, *28*, 1682–1688. [[CrossRef](#)] [[PubMed](#)]
113. Yang, B.; Leclercq, L.; Clacens, J.M.; Rataj, V.N. Acidic/amphiphilic silica nanoparticles: New eco-friendly Pickering interfacial catalysis for biodiesel production. *Green Chem.* **2017**, *19*, 4552–4562. [[CrossRef](#)]

114. Talin, A.A.; Centrone, A.; Ford, A.C.; Foster, M.E.; Stavila, V.; Haney, P.; Kinney, R.A.; Szalai, V.; El Gabaly, F.; Yoon, H.P.; et al. Tunable electrical conductivity in metal-organic framework thin-film devices. *Science* **2014**, *343*, 66–69. [CrossRef] [PubMed]
115. Lin, J.; Liu, Y.; Chen, S.; Le, X.; Zhou, X.; Zhao, Z.; Ou, Y.; Yang, J. Reversible immobilization of laccase onto metal-ion-chelated magnetic microspheres for bisphenol A removal. *Int. J. Biol. Macromol.* **2016**, *84*, 189–199. [CrossRef]
116. Netto, C.G.; Toma, H.E.; Andrade, L.H. Superparamagnetic nanoparticles as versatile carriers and supporting materials for enzymes. *J. Mol. Catal. B Enzym.* **2013**, *85*, 71–92. [CrossRef]
117. Bilal, M.; Zhao, Y.; Rasheed, T.; Iqbal, H.M.N. Magnetic nanoparticles as versatile carriers for enzymes immobilization: A review. *Int. J. Biol. Macromol.* **2018**, *120*, 2530–2544. [CrossRef]
118. Yang, H.; Zhang, W. Surfactant Imprinting Hyperactivated Immobilized Lipase as Efficient Biocatalyst for Biodiesel Production from Waste Cooking Oil. *Catalysts* **2019**, *9*, 914. [CrossRef]
119. Ngo, T.P.N.; Li, A.; Tiew, K.-W.; Li, Z. Efficient transformation of grease to biodiesel using highly active and easily recyclable magnetic nanobiocatalyst aggregates. *Bioresour. Technol.* **2013**, *145*, 233–239. [CrossRef]
120. Chiaradia, V.; Soares, N.S.; Valério, A.; de Oliveira, D.; Araújo, P.H.H.; Sayer, C. Immobilization of *Candida antarctica* Lipase B on Magnetic Poly(Urea-Urethane) Nanoparticles. *Appl. Biochem. Biotechnol.* **2016**, *180*, 558–575. [CrossRef]
121. Miao, C.; Yang, L.; Wang, Z.; Luo, W.; Li, H.; Lv, P.; Yuan, Z. Lipase immobilization on amino-silane modified superparamagnetic Fe₃O₄ nanoparticles as biocatalyst for biodiesel production. *Fuel* **2018**, *224*, 774–782. [CrossRef]
122. Mijone, P.D.; Vilas-Boas, R.N.; Bento, H.B.S.; Rodrigues, B.S.B.; de Castro, R.H.F. Coating and incorporation of iron oxides into a magnetic-polymer composite to be used as lipase support for ester syntheses. *Renew. Energy* **2020**, *149*, 1167–1173. [CrossRef]
123. Tran, D.-T.; Chen, C.-L.; Chang, J.-S. Immobilization of *Burkholderia* sp. Lipase on a ferric silica nanocomposite for biodiesel production. *J. Biotechnol.* **2012**, *158*, 112–119. [CrossRef] [PubMed]
124. Xie, W.; Wang, J. Immobilized lipase on magnetic chitosan microspheres for transesterification of soybean oil. *Biomass. Bioenergy* **2012**, *36*, 373–380. [CrossRef]
125. Arana-Peña, S.; Rios, N.S.; Mendez-Sanchez, C.; Lokha, Y.; Carballares, D.; Gonçalves, L.R.B.; Fernandez-Lafuente, R. Coimmobilization of different lipases: Simple layer by layer enzyme spatial ordering. *Int. J. Biol. Macromol.* **2020**, *145*, 856–864. [CrossRef]
126. Virgen-Ortíz, J.J.; dos Santos, J.C.S.; Berenguer-Murcia, Á.; Barbosa, O.; Rodrigues, R.C.; Fernandez-Lafuente, R. Polyethylenimine: A very useful ionic polymer in the design of immobilized enzyme biocatalysts. *J. Mater. Chem. B* **2017**, *5*, 7461–7490. [CrossRef]
127. Nielsen, P.M. Production of Fatty Acid Alkyl Esters. World Patent WO/2012/098114, 26 July 2012.
128. Fraga, F.C.; Valério, A.; de Oliveira, V.A.; Di Luccio, M.; de Oliveira, D. Effect of magnetic field on the Eversa[®] Transform 2.0 enzyme: Enzymatic activity and structural conformation. *Int. J. Biol. Macromol.* **2019**, *122*, 653–658. [CrossRef]
129. Viesel. Available online: <https://gstarbio.com/es/> (accessed on 25 June 2020).
130. Chen, X.; Li, L.; Deng, L.; Pedersen, J.N.; Li, L.; Guo, Z.; Cong, F.; Xu, X. Biodiesel Production Using Lipases. In *Lipid Modification by Enzymes and Engineered Microbes*; Bornscheuer, U.T., Ed.; Academic Press/AOCS Press: London, UK, 2018; pp. 343–373.
131. Kotrba, R. Realizing the Vision to Reclaim, Recycle, Refuel. *Biodiesel Magazine*. 2015. Available online: <http://www.biodieselmagazine.com/articles/265452/realizing-the-vision-to-reclaim-recycle-refuel> (accessed on 22 June 2020).
132. Wancura, J.H.C.; Rosset, D.V.; Brondani, M.; Mazutti, M.A.; de Oliveira, J.V.; Tres, M.V.; Jahn, S.L. Soluble lipase-catalyzed synthesis of methyl esters using a blend of edible and nonedible raw materials. *Bioproc. Biosyst. Eng.* **2018**, *41*, 1185–1193. [CrossRef]
133. Ortiz, C.; Ferreira, M.L.; Barbosa, O.; dos Santos, J.C.S.; Rodrigues, R.C.; Berenguer-Murcia, A.; Briand, L.E.; Fernandez-Lafuente, R. Novozym 435: The “perfect” lipase immobilized biocatalyst? *Catal. Sci. Technol.* **2019**, *9*, 2380. [CrossRef]

134. Sobhi, B. Modified-Immobilized Enzymes of High Tolerance to Hydrophilic Substrates in Organic Media. US Patent US9,068,175 B2, 30 June 2015.
135. Enzymocore. Available online: <https://enzymocore.com/about-us/our-enzymatic-technology/> (accessed on 22 June 2020).



© 2020 by the authors. Licensee MDPI, Basel, Switzerland. This article is an open access article distributed under the terms and conditions of the Creative Commons Attribution (CC BY) license (<http://creativecommons.org/licenses/by/4.0/>).

Article

Application of Sterilization Process for Inactivation of *Bacillus Stearotherophilus* in Biomedical Waste and Associated Greenhouse Gas Emissions

Cevat Yaman

Environmental Engineering, College of Engineering, Imam Abdulrahman Bin Faisal University, Dammam 34212, Saudi Arabia; cyaman@iau.edu.sa

Received: 26 June 2020; Accepted: 21 July 2020; Published: 23 July 2020

Abstract: This study investigated the biomedical waste collection, transportation, and treatment activities in the city of Kocaeli, Turkey. As an alternative to incineration technology, a steam autoclave was used to sterilize the biomedical waste. Information regarding the collection, transportation, treatment and associated greenhouse gas emissions (GHG) were also investigated. Prior to sterilization, biological indicator vials containing *Bacillus stearotherophilus* were placed in the center of the load to ensure that the pathogens were destroyed. GHG emissions were calculated based on the fuel consumed by the biomedical waste collection vehicles and the electricity/natural gas used at the sterilization plant. Results of this work revealed that the total biomedical waste generated per year increased from 1362 tons in 2009 to 2375 tons in 2019. The amount of biomedical waste generated per hospital bed was determined as $1.19 \text{ kg} \cdot \text{bed}^{-1} \cdot \text{day}^{-1}$. Results show that for efficient sterilization of biomedical wastes, the steam treatment system process should be operated at a contact time of 45 min, a temperature of $150 \text{ }^\circ\text{C}$, and at a steam pressure of 5 bar. Biological indicator tests showed that the number of living *Bacillus stearotherophilus* decreased significantly, with removal rates greater than $6\log_{10}$. Finally, it was determined that the biomedical waste management activities generated a total of GHG emissions of 5573 ton CO_2 equivalency ($\text{tCO}_2\text{-e}$) from 2009 to 2019. Furthermore, the average global warming factor (GWF) was calculated to be 0.269 $\text{tCO}_2\text{-e}$ per ton of biomedical waste generated. This study showed that the sterilization process is very effective in destroying the pathogens and the management of biomedical waste generates considerable amounts of GHG emissions.

Keywords: infectious waste; sterilization; biomedical waste; greenhouse gas; *Bacillus stearotherophilus*

1. Introduction

The appropriate management of biomedical waste is extremely important due to its significant environmental and health hazards. Recently, many attempts have been made to better manage the biomedical waste problem. Authorities define biomedical waste as the waste generated during the diagnosis and treatment of people and animals. If not properly handled, biomedical waste poses a great risk of infection through the spread of pathogens from health institutions into the environment [1]. Medical devices are now being manufactured for single use only, thus further increasing the amount of biomedical waste especially in developing countries. This will result in a rapid increase in biomedical waste amounts that should be disposed in a safe manner [2]. In the literature, there are different names for biomedical wastes such as hospital waste, regulated biomedical waste and infectious waste [3,4]. The terms infectious waste and biomedical waste are usually used for wastes that cannot be disposed of in a municipal solid waste landfill due to their pathogenic content. The safe disposal of biomedical wastes is of a great concern for the generators and the public. Different treatment methods can be applied in the treatment of biomedical waste. The main purpose in the treatment of biomedical wastes is to make it safe for human and environmental health. The methods used

to make biomedical waste harmless can be grouped as incineration, sterilization, plasma pyrolysis, and microwaving. In the US, about 60% of biomedical waste is incinerated, 37% is sterilized, and the rest is treated by different methods [4]. Within the scope of medical waste statistics, it was reported that 89,545 tons of medical waste was collected from 1550 health institutions operating as of the end of 2018 in Turkey. The amount of medical waste collected in 2018 increased by 4% compared to the previous year. Of this amount, 92.3% of the medical waste collected was sterilized and 7.7% was sent to incineration facilities [5]. Alternative treatment methods to incineration have always been the focus of biomedical waste generators. For example, sterilization or autoclave methods use shredders to reduce the waste volume. Sterilization inactivates microorganisms by using the saturated steam and is commonly used to treat infectious biomedical waste [6,7]. Thermal processes are applied as low, medium and high temperature depending on the process temperature applied. As a method, the thermal process is applied as the wet (steam) and dry heat treatment. In dry heat treatment, heat is applied to biomedical waste without adding water or steam. Heat is delivered to the waste by conduction, convection or thermal radiation. The processing time and the temperature to be applied depend on the characterization and quantity of the biomedical waste treated. The process temperature to be applied should not be too high to prevent the volatile organic compounds that can be released from the plastic wastes but should be sufficient for the sterilization of waste [6]. The process of sterilization is the treatment of biomedical wastes with steam at high temperature and pressure. If the temperature and contact time are sufficient, this process inactivates many types of microorganisms. Biomedical waste containers are placed in a closed chamber and sterilized with steam for a certain time at the required pressure and temperature. As a general practice, biomedical waste is steamed at 121 °C for 30 min at 2 bar and approximately 99.99 percent of microorganisms are inactivated by this process [8–10]. Biomedical wastes can be landfilled together with municipal solid wastes after steam treatment and size reduction.

Sterilization is the process of completely destroying all kinds of microbial life, including bacterial spores in biomedical wastes, by physical, chemical, and mechanical methods, or reducing the level of these microorganisms by 99.9999% (6 log₁₀ reduction). Whether the biomedical wastes treated by sterilization are rendered harmless is tested using chemical and biological indicators. Chemical indicators are used in the autoclave sterilization of biomedical waste. When the sterilization is completed, color change must be detected in the chemical indicator carrier that has been autoclaved together with the waste. In the biological indicator test, the viability of the biological indicator is used to detect whether all potential infectious microorganisms have been destroyed in the sterilized waste. It is a tubular test indicator with *Bacillus stearothermophilus*, which is known to be the most resistant microorganism to heat. If the test result is negative, the sterilized biomedical waste is sent to the landfill, but if the test result is positive, the sterilization process should be repeated. Ananta, Heinz [11] reported that *Bacillus stearothermophilus* spores can be inactivated by high-pressure treatment, but only if it is applied at an elevated temperatures. Rajan, Pandrangi [12] also reported that, while the thermal inactivation of spores followed first-order kinetics, the Weibull model best described the inactivation of *Bacillus stearothermophilus* spores. Iciek, Papiewska [13] conducted a study to investigate the combined effect of temperature, pH and NaCl concentration on the thermal inactivation of *Bacillus stearothermophilus* and observed that the sterilization temperature and pH of the sterilized medium as well as the concentration of NaCl, had a significant effect on spore activation and destruction.

Greenhouse Gas Emissions

Global greenhouse gas (GHG) emissions have grown since pre-industrial periods, with a 70% increase between 1970 and 2004 [14]. Since pre-industrial times, increased greenhouse gas emissions from human activities have caused a significant increase in the atmospheric greenhouse gas concentrations. Between 1970 and 2004, global emissions of CO₂, CH₄, N₂O, hydrofluorocarbons (HFCs), perfluorocarbons (PFCs) and sulphur hexafluoride (SF₆), described by their global warming potential (GWP), have increased by 70% from 28.7 to 49 Giga ton (Gt) CO₂-eq. CO₂ emissions grew by approximately 80% between

1970 and 2004, representing 77% of the total greenhouse gas emissions in 2004. Between 1970 and 2004, the greatest growth in global greenhouse gas emissions came from the energy supply sector, with an increase of 145%. The Intergovernmental Panel on Climate Change (IPCC) predicts that global greenhouse gas emissions will continue to increase over the next few decades [14]. However, IPCC also estimates that studies have demonstrated a significant economic potential for reducing global greenhouse gas emissions over the next decades that could balance the projected growth of global emissions or reduce emissions below current levels. GHG emissions will then need to peak and decline to stabilize greenhouse gas concentrations in the atmosphere. The lower the level of stabilization, the faster this peak and drop will have to occur. Reduction efforts over the next two to thirty years will have a major impact on opportunities to reach lower levels of stability.

The generation, transportation and disposal practices of wastes potentially generate greenhouse gas emissions [15]. Total GHG emissions resulting from waste management activities in the world are about 1.3 GtCO₂-e, corresponding to about 2.8 percent of total GHG emissions [14]. Approximately, 3.3% of total greenhouse gas emissions originate from waste management activities in Turkey [16]. The total greenhouse gas emissions of Kocaeli city for 2016 were calculated as 25.1 million tons of CO₂-e. Of the total greenhouse gas emission, 65.3% of total emissions were from fixed sources, 17.4% from industrial processes, 15.0% from transportation, 1.4% from land use and 0.9% from waste management [17]. The collection, transportation and transfer of waste is not included in waste management activities, but in the estimation of mobile greenhouse gas resources (cars, trucks) [17]. The units of GHG emissions are converted into CO₂ equivalency (CO₂-e) in order to better identify and evaluate GHG emissions. Another term commonly used to describe GHG emissions is called global warming factor (GWF). The GWF identifies the amount of GHG emissions generated per ton of biomedical waste collected, transported and sterilized. GWF used in this study is based on a 100-year time period as reported in the recent IPCC assessment report [18]. In the literature, there is no study that investigated the GHG emissions from biomedical waste collection and treatment systems in the city of Kocaeli, Turkey. This study had two main objectives. The first objective was to verify if efficient biomedical waste treatment can occur under standard operating parameters in steam treatment systems in the city of Kocaeli, Turkey. The second objective was to investigate the greenhouse gas (GHG) emissions generated during the transportation and treatment of biomedical waste.

2. Materials and Methods

2.1. Description of the Study Area

This study was conducted in the city of Kocaeli, which has a population of 1,875,493 and is located in the northwest of Turkey (Figure 1). According to the Turkish Statistical Institute, 81,024 tons of biomedical waste were collected and treated by sterilization, incineration and other methods in 2016 in Turkey [5]. Based on this biomedical waste amount, about 450 million healthcare facility visits were recorded in 2016. Generally, biomedical wastes are segregated and placed in 10-L durable red plastic bags in the study area. Sharps and needles are first collected in yellow rigid plastic boxes and then placed in red plastic bags. As a safety rule, 1/3 of the capacity of the bags is always left empty. After tying the bags securely, they are temporarily stored in designated rooms and collected daily by licensed collection vehicles. Kocaeli Metropolitan Municipality has 9 biomedical waste collection vehicles operating for the 27 healthcare institutions and other small clinics. The collected biomedical waste is transported to an 8 ton.day⁻¹ capacity sterilization plant located at the Kocaeli landfill site.



Figure 1. Location map of the study region [19].

2.2. Collection and Transportation of Biomedical Waste

The biomedical waste management system implemented in Kocaeli city includes the disposal of all biomedical wastes originating from all public hospitals, private hospitals, dialysis centers, family health centers, laboratories and district municipalities within the borders of the municipality. Biomedical wastes, excluding pathological and hazardous wastes, generated in the boundaries of Kocaeli city and district municipalities are collected and sterilized at the biomedical waste sterilization facility within the scope of national biomedical waste regulation and then disposed in the solid waste landfill. Biomedical waste amounts from the public hospitals, private hospitals, dialysis centers, family health centers and laboratories in the study area are given in Table 1.

Table 1. Amounts of biomedical waste generated in Kocaeli city in 2019.

Health Centers	Number of Beds	Biomedical Waste Amount (kg)	Biomedical Waste Per Bed (kg/bed.year)
Gebze Fatih	326	112,777	1.033
Danca Farabi	350	130,433	1.039
Kocaeli Public	335	137,765	1.119
Izmit Seka	305	99,950	1.235
Golcuk Necati Celik	175	60,835	0.984
Kandira M. Kazim Dinc	52	19,131	1.044
Korfez	52	17,973	1.105
Karamursel	45	20,942	1.038
Dilovasi	25	12,586	1.398
Anadolu Sağlık Merkezi	201	134,297	1.994
VM Biomedicalpark	121	75,681	2.006
Cihan	120	41,534	1.878
Gebze Biomedicalpark	118	69,980	1.039
Yuzyl	112	57,551	1.781
Akademi	110	34,321	1.543
Konak	107	30,329	0.937
Medar Golcuk	101	15,870	0.851
Korfez Marmara	79	30,264	0.472
Kocaeli Private	75	27,906	1.150
Acibadem	61	32,700	1.117
Gebze Merkez	56	34,487	1.610
Gebze Medar	75	39,507	1.849
Romatem Physical Therapy and Rehabilitation (FTR) Hospital	27	1937	1.582
Hospital Park Darica	20	898	0.215
Cagin Goz	25	1972	1.336
Dunya Goz	11	2062	0.237
Kocaeli University	727	358,451	1.481
Total	3811	1,610,139	Average = 1.19

In the study region, biomedical wastes are accumulated separately, where they occur, without being mixed with other wastes. Sharps, needles, infectious wastes, hazardous wastes and pathological wastes are collected in appropriate containers, which are compatible with the waste. The collected biomedical waste is first taken to the temporary biomedical waste storage of the health institution and then delivered to the biomedical waste collection vehicle. Once the biomedical waste is brought to the disposal site, the sharps, needles and infectious wastes are subjected to sterilization, while the pathological wastes and hazardous wastes are incinerated at the hazardous waste incineration plant located near the sterilization plant. The biomedical waste management system used in this study is given in Figure 2.

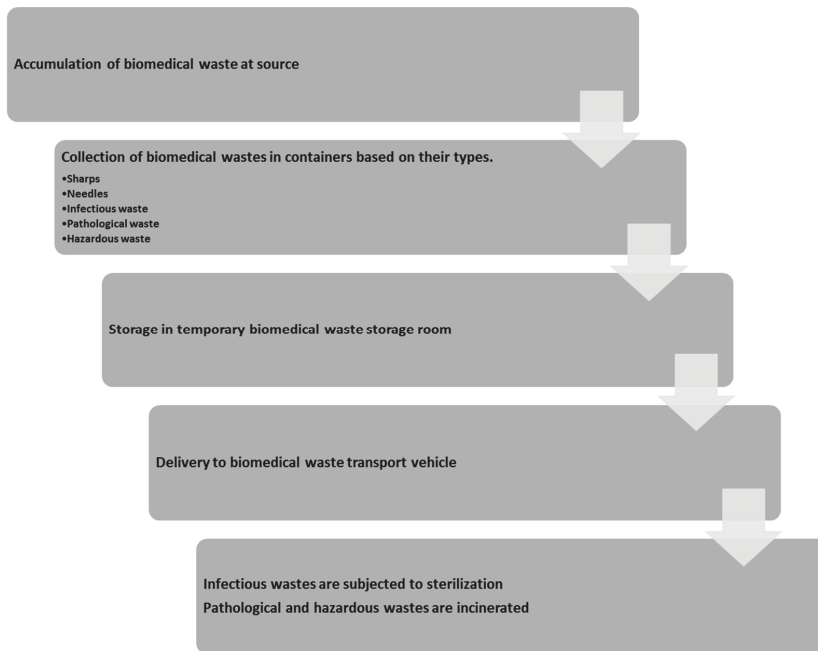


Figure 2. The biomedical waste management system, displaying the relevant steps.

2.3. Sterilization of Biomedical Waste

In this study, a steam autoclave was used to sterilize the pathogens. Autoclaving is an efficient wet heat treatment and disinfection process. The steam autoclave was operated during this study at a contact time of 45 min, a temperature of 150 °C, and at a steam pressure of 5 bar. The minimum time required for contact depends on factors such as the temperature applied, the moisture content of the waste and the penetration of steam into the waste [9]. The following steps were applied during the biomedical waste treatment in this study. 1—Pre-heating: hot steam was injected into the jacket of the autoclave to pre-heat the autoclave; 2—Waste loading: waste containers were loaded into the autoclave. During the loading, the chemical and biological indicators were placed in the middle of the waste load to monitor the sterilization effectiveness. The autoclave door was closed and sealed; 3—Air discharge: air was discharged through pre-vacuuming; 4—Steam treatment: steam was injected into the autoclave chamber until reaching the required temperature; 5—Steam discharge: steam was discharged from the autoclave, by using a condenser; 6—Waste unloading: the treated waste was removed together with the chemical and biological indicator strips; and 7—Mechanical treatment: the treated waste was introduced into a shredder before the final disposal in the Kocaeli landfill.

2.4. Biological and Chemical Testing

The chemical indicator used at every charge was in the form of a strip and was removed from the autoclave tank together with the biomedical waste at the end of each treatment period. The chemical indicator was used if the tank had reached a sufficient temperature by changing the color on the strip. The biological indicator used in the control of the sterilization process was applied for one charge a day as stated in the Turkish biomedical waste regulation. According to the Turkish biomedical waste regulation, sportive bacteria *Bacillus stearothermophilus* or *Bacillus subtilis* standard origins should be used as biological indicators, because these microorganisms are more resistant to high humidity and high temperatures than other disease-causing microorganisms. A minimum reduction of $4 \log_{10}$ – $6 \log_{10}$ is required in *Bacillus stearothermophilus* or *Bacillus subtilis* bacteria spores for the sterilization process to be considered valid. To control this, a certain number of *Bacillus stearothermophilus* spore-inoculated test strips were placed in the middle of the waste in a heat-resistant and vapor permeable container and the system was operated under normal conditions. At the end of the process, the test strips were removed from the waste. At the same time, at least one untreated biological indicator strip was also cultured in parallel as the positive control and incubated for 48 h at 30 °C for *Bacillus stearothermophilus*.

Since it is difficult to determine whether all microbial activities were completely destroyed, a probability function was defined at the end of sterilization based on the number of microorganisms that have survived. This function is often referred to as the reduction of the microorganisms that are most resistant to the sterilization process. Inactivation used today is defined as \log_{10} reduction. This is defined as the difference between the logarithmic numbers of test organisms that can survive before and after the sterilization process and can be expressed by the formula as follows:

$$\log_{10} (\text{cfu/g}) \text{ R} = \log_{10} (\text{cfu/g}) \text{ TO} - \log_{10} (\text{cfu/g}) \text{ OS} \quad (1)$$

where \log_{10} (colony forming unit (cfu).g⁻¹) R is the logarithmic number of reduction (R) of test organisms, \log_{10} (cfu.g⁻¹) TO is the number of test organisms (TO) tested in the sterilization unit, \log_{10} (cfu.g⁻¹) OS is the number of test organisms that survived (OS) after sterilization, and cfu.g⁻¹ is the microorganism colony formation in 1 g of waste. At the end of the sterilization period, the tank was discharged and the sterilized wastes were loaded into the shredder. Then, the shredded wastes were disposed of in a municipal soil waste landfill located near the sterilization plant.

2.5. Greenhouse Gas Emissions

In order to determine the total diesel fuel used by the collection vehicles, an average fuel consumption of 0.5 L per km traveled was selected [20]. Fruergaard, Astrup [21] reported that for each 1 L of diesel fuel, 0.5 kg CO₂-e was generated for provision and 2.7 kg CO₂-e for combustion, which gives a total of 3.2 kg CO₂-e.L⁻¹. These values were selected to calculate the total GHG emissions in this study. Upon determining the total amount of GHG emissions, a GWF for each year was estimated by dividing the total amount GHG emissions by the yearly total collected and treated biomedical waste. The amounts of GHG emissions resulting from electricity consumption at the sterilization plant was determined by using the emission factor of 0.480 kg CO₂-e.kWh⁻¹ provided for Turkey by the International Energy Agency (IEA) [22]. The amount of GHG emissions from natural gas consumption at the sterilization plant was determined by using the conversion factor of 10.34 kWh.m⁻³ natural gas (1000 Btu.ft⁻³) for electricity/natural gas energy equivalence [23].

3. Results

3.1. Quantification of Biomedical Waste

Results of this study showed that the total biomedical waste generated per year increased from 1362 tons in 2009 to 2375 tons in 2019 (Table 2). The amount of biomedical waste generated per hospital bed varied between 0.21 and 2.00 kg.bed⁻¹.day⁻¹ with an average value of 1.19 kg.bed⁻¹.day⁻¹ as of

December 2019. This range seems to be similar compared to a study conducted in Istanbul, in which the daily averages of biomedical waste amount per hospital varied from 0.43 to 1.68 kg.bed⁻¹.day⁻¹ [20]. The average diesel fuel consumed per kg of medical waste collected and transported was calculated as 0.041667 L kg⁻¹. In addition, the average electricity and natural gas consumed at the sterilization plant was calculated as 0.00944 kWh kg⁻¹ and 0.02687 m³ kg⁻¹, respectively.

Table 2. Amounts of biomedical waste collected and treated from 2009 to 2019 and the associated fuel usages.

Year	Biomedical Waste Generated (kg.year ⁻¹)	Trip Number to Sterilization Plant	Consumed Diesel (L.year ⁻¹)	Electric Consumed at the Sterilization Plant (kW.year ⁻¹)	Natural Gas Consumed at the Sterilization Plant (m ³ .year ⁻¹)
2009	1,361,545	1362	56,731	12,855	37,205
2010	1,350,605	1351	56,275	12,751	36,904
2011	1,572,606	1573	65,525	14,846	42,968
2012	1,755,567	1756	73,149	16,572	44,789
2013	1,758,089	1758	73,254	16,596	47,670
2014	1,850,428	1850	77,101	17,467	50,552
2015	1,946,386	1946	81,099	18,373	53,433
2016	2,164,089	2164	90,170	20,427	56,315
2017	2,231,941	2232	92,998	21,067	59,196
2018	2,356,404	2356	98,184	22,241	62,078
2019	2,375,297	2375	98,971	22,420	64,959
Total	20,722,957	20,723	863,457	195,616	556,068

3.2. Inactivation of *Bacillus Stearothermophilus*

In order to determine whether all the potentially infectious microorganisms were destroyed in the waste from the sterilization process, it needed to be checked whether the biological indicator microorganisms treated with the waste remained alive or dead. According to the Turkish biomedical waste regulation, a minimum reduction of between 4 log₁₀ and 6 log₁₀ is required in *Bacillus stearothermophilus* bacteria spores for the sterilization process to be considered valid. This was done by placing a certain number of *Bacillus stearothermophilus* spores containing an inoculated test indicator in the middle of the waste in a heat-resistant and vapor-permeable tube. At the end of the charge, the tube containing *Bacillus stearothermophilus* was taken from the waste, and the appropriate medium described by the producer of the biological indicator was plated on an agar medium. Meanwhile, at least one biological indicator that had not been subjected to sterilization was cultured as a positive control and incubated for 48 h at 55 °C for *Bacillus stearothermophilus*. In the chemical indicator test, when the result of the examination was negative, these biomedical wastes were re-sterilized by adding a biological indicator. These wastes were kept in biomedical waste temporary storage area until the biological indicator tests were completed. Even if there was no microbial reproduction as a result of the biological indicator, these wastes were re-sterilized. In this study, biological indicator tests showed that, with a contact time of 45 min, a temperature of 150 °C, and at a steam pressure of 5 bar, the number of living *Bacillus stearothermophilus* decreased significantly. Daily bioindicator tests showed that the removal rates for *Bacillus stearothermophilus* were always greater than 6 log₁₀.

3.3. Greenhouse Gas Emissions

A total of 20,722,957 kg (≈20,723 tons) biomedical waste was generated in the study area between 2009 and 2019. It was confirmed by the authorities that each biomedical waste collection and transport vehicle carried approximately 1 ton of waste in each trip to the sterilization plant. Thus, the total trip numbers between 2009 and 2019 were 20,723, which included a round-trip drive from the first collection point to the sterilization plant and back to the same collection point. It was calculated, based on the information provided by the authorities, that approximately 863,457 L of gasoline was consumed by the biomedical waste collection vehicles between 2009 and 2019. For the calculation of fuel usage, an

average diesel consumption of 0.5 L per 1 km traveled was selected, which was also recommended by Korkut [20]. Yearly average electricity and natural gas consumptions at the sterilization plant were provided by the plant operator as shown in Table 2. The total amounts of electricity and natural gas consumed between 2009 and 2019 were 195,616 kWh and 556,068 m³, respectively. Table 3 summarizes the basic data and parameters used in the GHG calculation [21–23].

Table 3. The basic data and parameters used in the global greenhouse gas (GHG) calculation.

Fuel	Unit GHG Equivalency	Consumed between 2009 and 2019	Total GHG Generated in the Study
Diesel	3.2 kg CO ₂ -e L ⁻¹	863,457 L	2763 tCO ₂ -e
Electricity	0.480 kg CO ₂ -e kWh ⁻¹	195,616 kWh	93.9 tCO ₂ -e
Natural gas	4.96 kg CO ₂ -e m ⁻³	556,068 m ³	2758 tCO ₂ -e

Figure 3 shows the amount of GHG emissions and global warming factors (GWFs) generated during the transportation and treatment of biomedical waste from 2009 to 2019. The amounts of yearly GHG emissions from the consumption of diesel fuel were calculated based on the emission factor of 3.2 kg CO₂-e.L⁻¹ [21]. The total amount of GHG emissions generated from the biomedical waste collection and transportation vehicles between 2009 and 2019 was calculated as 2763 tCO₂-e.year⁻¹. The International Energy Agency (IEA) reported that 1 kWh of electricity consumption in Turkey can generate 0.480 kg CO₂-e [22]. Thus, by using the emission factor of 0.480 kg CO₂-e.kWh⁻¹, yearly GHG emissions from electricity consumption varied between 6.12 and 10.76 tCO₂-e.year⁻¹. The total amount of GHG emissions generated from the electricity usage at the sterilization plant between 2009 and 2019 was calculated as 93.9 tCO₂-e.year⁻¹. The conversion factor for the electricity/natural gas energy equivalence was taken as 10.34 kWh.m⁻³ natural gas (1000 Btu.ft⁻³) [23]. Thus, by using the emission factor of 0.480 kg CO₂-e.kWh⁻¹ in this study, yearly GHG emissions from natural gas usage varied between 183.16 and 322.41 tCO₂-e.year⁻¹. The total amount of GHG emissions generated from the natural gas usage at the sterilization plant between 2009 and 2019 was 2758 tCO₂-e.year⁻¹. Finally, the total amount of GHG emissions resulting from the use of diesel fuel for waste collection and transportation vehicles, and electricity and natural gas uses at the sterilization plant, was calculated as 5573 tCO₂-e.year⁻¹ from 2009 to 2019 (Figure 3). The GWF values varied between 0.265 and 0.272 tCO₂-e.ton⁻¹, with an average value of 0.269 tCO₂-e.ton⁻¹ of biomedical waste collected, transported and sterilized. It can be concluded from Figure 3 that the greater the amount of biomedical waste collected and sterilized, the more GHG emissions generated. As the amount of biomedical waste has increased over time, the amounts of GWF decreased from 0.272 to 0.265 tCO₂-e.ton⁻¹.

Figure 4 shows the amount of GHG emissions resulting from different fuels for biomedical waste collection, transport and treatment between 2009 and 2019. The amount of diesel fuel used by the biomedical waste collection and transport vehicles was used to calculate the GHG emissions from these activities. On the other hand, natural gas and electricity were only consumed at the sterilization plant for different purposes such as lighting, heating and running the autoclaves. The highest GHG emissions were observed from the natural gas use at the sterilization plant. Yearly GHG emissions from diesel combustion varied from 177 tCO₂-e to 312 tCO₂-e during the study period. However, GHG emissions from electricity consumption at the sterilization plant was much lower compared to that of diesel fuel combustion and natural gas use.

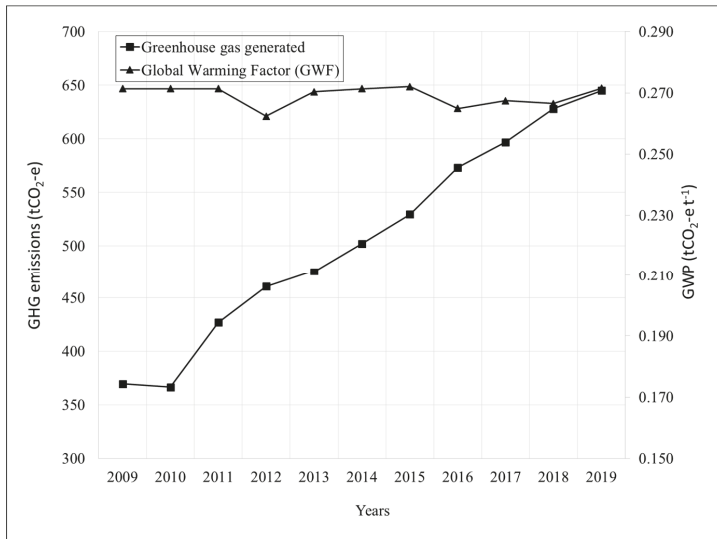


Figure 3. The amounts of greenhouse gases (GHG) versus the global warming factor (GWF) generated during the transportation and treatment of biomedical waste from 2009 to 2019.

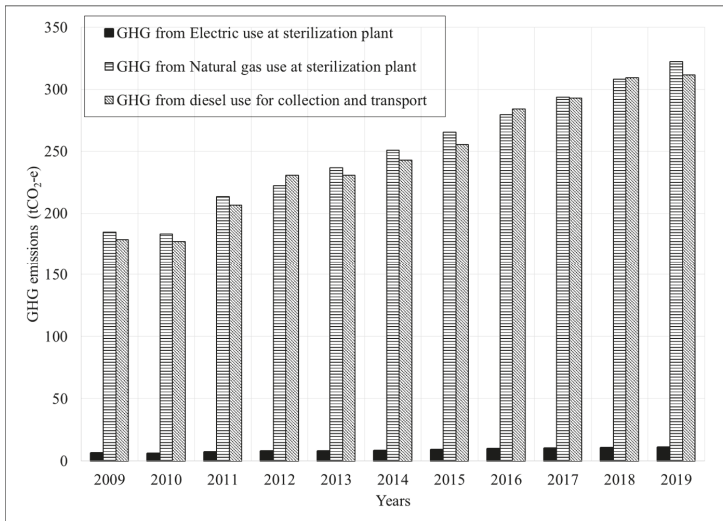


Figure 4. Amounts of GHG emissions from different fuels for biomedical waste collection, transport and treatment between 2009 and 2019.

4. Discussion

In this study, the average amount of biomedical waste generated per hospital bed was calculated as 1.19 kg.bed⁻¹.day⁻¹. In one study, Mato and Kassenga [24] reported biomedical waste amounts varying between 0.84 and 5.8 kg.bed⁻¹.day⁻¹. Abu-Qudais [25] found at five Jordanian hospitals that the average daily biomedical waste generation rates varied between 0.29 and 1.36 kg.bed⁻¹.day⁻¹. In a similar study conducted at Italian hospitals, the biomedical waste generation rates varied between 0.2 and 3.5 kg.bed⁻¹.day⁻¹ [26].

Daily routine bioindicator tests have shown that the removal rates for *Bacillus stearothermophilus* were always higher than $6 \log_{10}$ in this study. Sterilization effectiveness varies with many parameters that affect the heat transfer and vapor penetration, such as waste contents, waste density, moisture content, and container types [27,28]. In order to prevent any damage on the shredder, it was ensured in this study that the incoming waste was always free of metal objects. Sterilization efficiency is usually observed by giving a level of assurance at 10^{-3} or 10^{-6} , which indicates that there is a chance in thousands and millions, respectively. Essentially, this means that at least 3 or $6 \log_{10}$ pathogen reductions should be maintained. This level of reduction is usually possible because steam sterilization autoclaves are generally operated at minimum standards (121 °C for 30 min or 134 °C for 5 min) [8,10]. The steam autoclave in this study performed at a contact time of 45 min, a temperature of 150 °C, and at a steam pressure of 5 bar. However, some studies claim that these parameters are not sufficient for the complete sterilization of all biomedical waste types [28,29]. For instance, the inclusion of a grinding system before sterilization allows better sterilization due to a larger waste surface area for steam. Shredding transforms waste into an unrecognizable form and provides a volume reduction of up to 80% [7]. The shredder system achieved approximately 70 to 80% volume reduction throughout this study. It should be noted, however, that the use of integrated shredders and autoclaves can cause repeated failures and high maintenance costs [30–32]. As stated by the World Health Organization (WHO), in order to select the best biomedical waste treatment technology, they must pose minimal human health impact, minimal environmental impact, and must be cost-effective and easily implemented [33].

The advantages and disadvantages of five biomedical treatment technologies are summarized as follows [34]: 1—Landfilling: it is one of the oldest methods for biomedical waste disposal in undeveloped countries. However, biomedical waste landfilling includes some serious disadvantages such as the contamination of soil and water, the spreading of pathogens, and high GHG emissions. The only advantage of the landfilling of biomedical waste is the low cost and easy operation; 2—Sterilization: this process is preferred in several applications because it offers many advantages such as excellent efficiency, short treatment times, lower cost, minimum GHG emissions and air pollutants, environment-friendly technology, and the availability of wide range of autoclave sizes. However, sterilization has some disadvantages, such as the odor problem, unsuitability for hazardous and pathological wastes, and shredder requirement; 3—Incineration: the incineration of biomedical waste is suitable for all waste types, provides a high volume reduction, has a potential for energy recovery, and provides complete sterilization. The disadvantages of incineration include the following: a—the equipment is more costly to operate than the other alternatives, b—the process must meet the stringent regulatory requirements of air pollution control, c—heavy metals are usually found in the ash, d—it produces high GHG emissions, and e—dioxins and furans can be generated; 4—Microwaving: microwaving is another technology that can be used for biomedical waste treatment. The advantages of microwaving technology include the following, a—it is an environment-friendly technology, b—it offers high volume reduction, c—it produces no liquid waste, and d—it generates minimum air pollutants. The disadvantages of microwaving include; high cost, not suitable for all waste types, odor problems, and high GHG emissions; and 5—Plasma pyrolysis: this process has the following advantages, a—it is suitable for all types of wastes, b—it occupies less space, c—it is environmentally sound, d—it does not require a chimney, e—toxic residuals are minimum, f—it does not require segregation, g—energy recovery is possible, and h—it can reduce the waste volume by over 90%.

The collection and transport of biomedical waste would likely result in GHG emissions similar to the GHG emissions from municipal solid waste (MSW) collection and transport activities. However, treatment systems for MSW and biomedical waste are completely different, except for incineration. Therefore, GHG emissions from these different treatment systems for MSW and biomedical waste would also be different compared to each other. For instance, a net GWF of $-0.274 \text{ tCO}_2\text{-e.ton}^{-1}$ was reported in the literature in a landfill gas (LFG) combustion unit, which indicated that 1 ton of MSW landfilled in order to generate electricity by burning LFG eliminated 0.274 tCO_2 of GHG emission [19]. In a similar LFG to energy study, Malakahmad, Abualqumboz [35] reported an average GHG emission

of 0.291 tCO₂-e.ton⁻¹. Yaman [19] reported GWF of −0.94 tCO₂-e.ton⁻¹ from the combustion of MSW (waste to energy), which indicated that the incineration process eliminates more GHG emissions than it generates. This of course takes into account the energy generated from the incineration process that would offset the additional GHG emissions arising from different energy generation systems. Similar to four different studies, GWFs of −0.01, −0.12, −0.2385, and −1.019 tCO₂-e.ton⁻¹ were also reported, respectively [36–39]. Khan, Khan [40] and Ali, Wang [41] conducted case studies and reported that the treatment and disposal of biomedical wastes can also be assessed according to their greenhouse gas emission rates.

The current waste management practices of countries can effectively reduce greenhouse gas emissions from the waste sector. For example, a wide variety of mature, environmentally friendly technologies are available to reduce emissions and provide common benefits for public health, environmental protection and sustainable development. Collectively, these technologies can directly reduce greenhouse gas emissions or prevent significant greenhouse gas generation. It also represents an important and growing potential for the indirect reduction of greenhouse gas emissions by minimizing, recycling and reusing waste, the conservation of raw materials, improved energy and resource efficiency, and the prevention of fossil fuel use. It should also be emphasized that there are high uncertainties regarding global waste greenhouse gas emissions resulting from national and regional differences in definitions, data collection and statistical analysis. Reducing greenhouse gas emissions from waste should be addressed in the context of integrated waste management. For instance, life cycle assessment (LCA) is an important tool to consider both the direct and indirect effects of waste management technologies and policies [42–44].

5. Conclusions

In this study, the collection, transport and steam sterilization of biomedical waste and the associated GHG emissions from these processes were investigated. The results of the steam sterilization system performed effective treatment for biomedical wastes containing needles, syringes and other non-hazardous and non-pathological infectious wastes. *Bacillus stearothermophilus* bacteria were investigated for the effectiveness of steam on bacteria during the sterilization process. It was observed during this study that the steam autoclave performed most effectively at a contact time of 45 min, a temperature of 150 °C, and at a steam pressure of 5 bar, to inactivate *Bacillus stearothermophilus*. Under these operational conditions, daily bioindicator tests showed that the removal rates for *Bacillus stearothermophilus* were always greater than 6log₁₀.

It was shown in this study that the biomedical waste collection, transport and sterilization processes generated a total of GHG emissions of 5573 tCO₂-e from 2009 to 2019. A large part of the GHG emissions generated in this study was from the combustion of diesel fuel by biomedical waste collection and transportation vehicles and the natural gas consumed at the sterilization plant. On the other hand, the use of electricity at the sterilization plant produced less GHG emissions than that of diesel and electricity use. Furthermore, the average GWF was calculated as 0.269 tCO₂-e per ton of biomedical waste collected, transported and sterilized. The biomedical waste treatment by steam sterilization seems to be a safe and cost-effective treatment method compared to incineration, which can release hazardous air pollutants and GHGs. However, precautions should be taken to reduce the amount of GHG emissions by, for example, using electricity-powered biomedical waste collection vehicles, using solar energy panels on the roofs of sterilization plants, and also using biodegradable biomedical waste collection bags.

Life cycle assessment (LCA) can provide decision-support tools. There are many combined mitigation strategies that can be implemented cost effectively by the public or private sector, using LCA and other decision-support tools. Therefore, as a future work, a complete and comprehensive study of LCA should be conducted to determine the complete GHG emissions from medical waste collection, transport and sterilization process.

Funding: This research received no external funding.

Acknowledgments: The author would like to thank Kocaeli Metropolitan Municipality (Turkey), IZMIT Waste and Residue Treatment Incineration and Utilization Corporation (IZAYDAS) for providing the data, and Imam Abdulrahman Bin Faisal University for academic support.

Conflicts of Interest: The author declares no conflict of interest.

References

1. Mohee, R. Medical Wastes Characterization in Healthcare Institutions in Mauritius. *Waste Manag. (New York, NY)* **2005**, *25*, 575–581. [CrossRef] [PubMed]
2. Mbongwe, B.; Mmereki, B.T.; Magashula, A. Healthcare waste management: Current practices in selected healthcare facilities, Botswana. *Waste Manag.* **2008**, *28*, 226–233. [CrossRef] [PubMed]
3. Rutala, W.A.; Mayhall, C.G. Medical Waste. *Infect. Control Hosp. Epidemiol.* **1992**, *13*, 38–48. [CrossRef] [PubMed]
4. USEPA. Medical Waste. Available online: <http://www.epa.gov/osw/nonhaz/industrial/medical/> (accessed on 2 February 2020).
5. TÜİK. Turkish Statistical Institute. Available online: www.tuik.gov.tr/ (accessed on 3 February 2020).
6. Toktobaev, N.; Emmanuel, J.; Djumalieva, G.; Kravtsov, A.; Schuth, T. An innovative national health care waste management system in Kyrgyzstan. *Waste Manag. Res. J. Int. Solid Wastes Public Clean. Assoc. ISWA* **2015**, *33*, 130–138. [CrossRef]
7. Voudrias, E.; Graikos, A. Infectious Medical Waste Management System at the Regional Level. *J. Hazard. Toxic Radioact. Waste* **2014**, *18*, 04014020. [CrossRef]
8. Karagiannidis, A.; Papageorgiou, A.; Perkoulidis, G.; Sanida, G.; Samaras, P. A multi-criteria assessment of scenarios on thermal processing of infectious hospital wastes: A case study for Central Macedonia. *Waste Manag.* **2010**, *30*, 251–262. [CrossRef]
9. HCWH. *Non-Incineration Medical Waste Treatment Technologies in Europe*; Health Care without Harm Europe: Prague, Czech Republic, 2004.
10. WHO. *Safe Management of Waste from Health-Care Activities*; World Health Organization: Geneva, Switzerland, 1999.
11. Ananta, E.; Heinz, V.; Schlüter, O.; Knorr, D. Kinetic studies on high-pressure inactivation of *Bacillus stearothermophilus* spores suspended in food matrices. *Innov. Food Sci. Emerg. Technol.* **2001**, *2*, 261–272. [CrossRef]
12. Rajan, S.; Pandrangi, S.; Balasubramaniam, V.M.; Yousef, A.E. Inactivation of *Bacillus stearothermophilus* spores in egg patties by pressure-assisted thermal processing. *LWT—Food Sci. Technol.* **2006**, *39*, 844–851. [CrossRef]
13. Iciek, J.; Papiewska, A.; Molska, M. Inactivation of *Bacillus stearothermophilus* spores during thermal processing. *J. Food Eng.* **2006**, *77*, 406–410. [CrossRef]
14. IPCC. AR4 Climate Change 2007: Mitigation of Climate Change. Available online: <https://www.ipcc.ch/report/ar4/wg3/> (accessed on 4 February 2020).
15. Yang, D.; Xu, L.; Gao, X.; Guo, Q.; Huang, N. Inventories and reduction scenarios of urban waste-related greenhouse gas emissions for management potential. *Sci. Total Environ.* **2018**, *626*, 727–736. [CrossRef]
16. UNFCCC. National Greenhouse Gas Factors 2016. Available online: <https://unfccc.int/process/transparency-and-reporting/reporting-and-review-under-the-convention/greenhouse-gas-inventoriesannex-i-parties/national-inventory-submissions-2018> (accessed on 15 March 2020).
17. REC. *Kocaeli Greenhouse Gas Inventory and Climate Change Action Plan*; REC: Kocaeli, Turkey, 2018.
18. IPCC. IPCC 6th Assessment Report. Available online: <https://www.ipcc.ch/assessment-report/ar6/> (accessed on 5 February 2020).
19. Yaman, C. Investigation of greenhouse gas emissions and energy recovery potential from municipal solid waste management practices. *Environ. Dev.* **2020**, *33*, 100484. [CrossRef]
20. Korkut, E.N. Estimations and analysis of medical waste amounts in the city of Istanbul and proposing a new approach for the estimation of future medical waste amounts. *Waste Manag.* **2018**, *81*, 168–176. [CrossRef] [PubMed]

21. Fruergaard, T.; Astrup, T.; Ekvall, T. Energy use and recovery in waste management and implications for accounting of greenhouse gases and global warming contributions. *Waste Manag. Res. J. Int. Solid Wastes Public Clean. Assoc. ISWA* **2009**, *27*, 724–737. [[CrossRef](#)] [[PubMed](#)]
22. IEA. *Energy Policies of International Energy Agency Countries 2016 Review Turkey*; IEA: Paris, France, 2016.
23. DOE. *Energy Consumption of Die Casting Operations*; US Department of Energy: Washington, DC, USA, 2003.
24. Mato, R.R.A.M.; Kassenga, G.R. A study on problems of management of medical solid wastes in Dar es Salaam and their remedial measures. *Resour. Conserv. Recycl.* **1997**, *21*, 1–16. [[CrossRef](#)]
25. Abu-Qudais, H. Techno-economic assessment of municipal solid waste management in Jordan. *Waste Manag.* **2007**, *27*, 1666–1672. [[CrossRef](#)] [[PubMed](#)]
26. Liberti, L. Optimization of Infectious Hospital Waste Management in Italy: Part II. Waste Characterization by Origin. *Waste Manag. Res. J. Int. Solid Wastes Public Clean. Assoc. ISWA* **1996**, *14*, 417–431. [[CrossRef](#)]
27. Maamari, O.; Mouaffak, L.; Kamel, R.; Brandam, C.; Lteif, R.; Salameh, D. Comparison of steam sterilization conditions efficiency in the treatment of Infectious Health Care Waste. *Waste Manag.* **2016**, *49*, 462–468. [[CrossRef](#)]
28. Lemieux, P.; Sieber, R.; Osborne, A.; Woodard, A. Destruction of spores on building decontamination residue in a commercial autoclave. *Appl. Environ. Microbiol.* **2006**, *72*, 7687–7693. [[CrossRef](#)]
29. Tiller, T.; Linscott, A. Evaluation of a Steam Autoclave for Sterilizing Medical Waste at a University Health Center. *Am. J. Infect. Control* **2004**, *32*, E9. [[CrossRef](#)]
30. Tsakona, M.; Anagnostopoulou, E.; Gidarakos, E. Hospital waste management and toxicity evaluation: A case study. *Waste Manag.* **2007**, *27*, 912–920. [[CrossRef](#)]
31. Ferreira, V.; Teixeira, M.R. Healthcare waste management practices and risk perceptions: Findings from hospitals in the Algarve region, Portugal. *Waste Manag.* **2010**, *30*, 2657–2663. [[CrossRef](#)] [[PubMed](#)]
32. Graikos, A.; Voudrias, E.; Papazachariou, A.; Iosifidis, N.; Kalpakidou, M. Composition and production rate of medical waste from a small producer in Greece. *Waste Manag.* **2010**, *30*, 1683–1689. [[CrossRef](#)] [[PubMed](#)]
33. Hossain, M.S.; Santhanam, A.; Nik Norulaini, N.A.; Omar, A.K. Clinical solid waste management practices and its impact on human health and environment—A review. *Waste Manag.* **2011**, *31*, 754–766. [[CrossRef](#)] [[PubMed](#)]
34. Khadem Ghasemi, M.; Mohd Yusuff, R. Advantages and Disadvantages of Healthcare Waste Treatment and Disposal Alternatives: Malaysian Scenario. *Pol. J. Environ. Stud.* **2016**, *25*, 17–25. [[CrossRef](#)]
35. Malakahmad, A.; Abualqumboz, M.S.; Kutty, S.R.M.; Abunama, T.J. Assessment of carbon footprint emissions and environmental concerns of solid waste treatment and disposal techniques; case study of Malaysia. *Waste Manag.* **2017**, *70*, 282–292. [[CrossRef](#)] [[PubMed](#)]
36. Smith, A.; Brown, K.; Ogilvie, S.; Rushton, K.; Bates, J. *Waste Management Options and Climate Change. Final Report to the European Commission DG Environment*; European Commission: Luxembourg, Luxembourg 2001.
37. USEPA. A Life-Cycle Assessment of Emission and Sinks. In *Solid Waste Management and Greenhouse Gas*; USEPA: Washington DC, USA, 2010.
38. Chen, T.-C.; Lin, C.-F. Greenhouse gases emissions from waste management practices using Life Cycle Inventory model. *J. Hazard. Mater.* **2008**, *155*, 23–31. [[CrossRef](#)]
39. Christensen, T.H.; Gentil, E.; Boldrin, A.; Larsen, A.W.; Weidema, B.P.; Hauschild, M. C balance, carbon dioxide emissions and global warming potentials in LCA-modelling of waste management systems. *Waste Manag. Res.* **2009**, *27*, 707–715. [[CrossRef](#)]
40. Khan, B.A.; Khan, A.A.; Ali, M.; Cheng, L. Greenhouse gas emission from small clinics solid waste management scenarios in an urban area of an underdeveloping country: A life cycle perspective. *J. Air Waste Manag. Assoc.* **2019**, *69*, 823–833. [[CrossRef](#)]
41. Ali, M.; Wang, W.; Chaudhry, N. Application of life cycle assessment for hospital solid waste management: A case study. *J. Air Waste Manag. Assoc.* **2016**, *66*, 1012–1018. [[CrossRef](#)]
42. Thorneloe, S.; Weitz, K.; Jambeck, J. Moving from Solid Waste Disposal to Materials Management in the United States. In *Proceedings of the Tenth International Waste Management and Landfill Symposium, Cagliari, Italy, 3–7 October 2005*.

43. Weitz, K.; Thorneloe, S.; Nishtala, S.; Yarkosky, S.; Zannes, M. The Impact of Municipal Solid Waste Management on Greenhouse Gas Emissions in the United States. *J. Air Waste Manag. Assoc. (1995)* **2002**, *52*, 1000–1011. [[CrossRef](#)]
44. WRAP. *Environmental Benefits of Recycling, an International Review of Life Cycle Comparisons for Key Materials in the UK Recycling Sector*; WRAP: Banbury, UK, 2006.



© 2020 by the author. Licensee MDPI, Basel, Switzerland. This article is an open access article distributed under the terms and conditions of the Creative Commons Attribution (CC BY) license (<http://creativecommons.org/licenses/by/4.0/>).

Review

Trends in Biodiesel Production from Animal Fat Waste

Fidel Toldrá-Reig ^{1,†}, Leticia Mora ² and Fidel Toldrá ^{2,*}

¹ Instituto de Tecnología Química (CSIC-UPV), Universitat Politècnica de València, Camino de Vera s/n, 46022 Valencia, Spain; reigtold@gmail.com

² Instituto de Agroquímica y Tecnología de Alimentos (CSIC), Avenue Agustín Escardino 7, 46980 Paterna, Valencia, Spain; lemoso@iata.csic.es

* Correspondence: ftoldra@iata.csic.es; Tel.: +34-96-3900022

† Current Address: CNRS, 25 rue des Martyrs, B.P. 166, 38042 Grenoble CEDEX 9, France.

Received: 20 April 2020; Accepted: 21 May 2020; Published: 25 May 2020

Abstract: The agro-food industry generates large amounts of waste that contribute to environmental contamination. Animal fat waste constitutes some of the most relevant waste and the treatment of such waste is quite costly because environmental regulations are quite strict. Part of such costs might be reduced through the generation of bioenergy. Biodiesel constitutes a valid renewable source of energy because it is biodegradable, non-toxic and has a good combustion emission profile and can be blended up to 20% with fossil diesel for its use in many countries. Furthermore, up to 70% of the total cost of biodiesel majorly depends on the cost of the raw materials used, which can be reduced using animal fat waste because they are cheaper than vegetable oil waste. In fact, 6% of total feedstock corresponded to animal fat in 2019. Transesterification with alkaline catalysis is still preferred at industrial plants producing biodiesel. Recent developments in heterogeneous catalysts that can be easily recovered, regenerated and reused, as well as immobilized lipases with increased stability and resistance to alcohol denaturation, are promising for future industrial use. This manuscript reviews the available processes and recent advances for biodiesel generation from animal fat waste.

Keywords: biodiesel; fuel; energy generation; agricultural waste; food waste; animal waste; lard; tallow; animal fat; transesterification

1. Introduction

Animal byproduct production, as part of the meat and poultry processing chain, is huge. For instance, it represents nearly 17 million tons per year only in the European Union [1]. Most of the waste results from over 328 million pigs, sheep, beef, goats and dairy cattle and 6 billion chickens, turkeys and other poultry that are slaughtered every year in Europe [2]. After rendering, materials classified as edible which amount up to 12 million tons, are processed in a variety of food and feed related sectors [3]. The remaining byproducts that are considered inedible have other applications for disposal such as biofuels and biodiesel for energy generation [4,5]. It is energy generation, especially biodiesel production, that is one of the most attractive and expanding applications [6]. In this sense, the production of biodiesel guarantees a better profitability of inedible animal byproducts. Animal waste also consists of the organic matter resulting from the meat processing industry as well as from human consumption. Biodiesel consists of mono-alkyl esters of long chain fatty acids produced from oil or fat, but the use of vegetable oil adds a high price to biodiesel, and this has prompted the use of animal fats as an interesting alternative. In addition to its renewability, biodiesel also constitutes an attractive alternative because it offers better lubricating properties than fossil diesel fuel and it is biodegradable and non-toxic. It also has an improved cetane number and high flash point [7]. Biodiesel also contributes to sustainability by reducing the carbon footprint due to lower CO₂ emission compared to fossil diesel fuel [8]. CO₂ is one of the most relevant gases because it contributes up

to 72% of greenhouse gases [9]. Biodiesel from animal fat achieves nearly 80% fossil CO₂ reduction in comparison to 30% for soya [5]. In addition, the emission of polycyclic aromatic hydrocarbons is 75–90% lower than in conventional diesel, whereas total unburned hydrocarbon is 90% lower [10,11]. The emissions of sulfur and CO are also reduced [12].

The International Energy Agency reported that bioenergy must increase up to 25% until 2025 and continue to grow, and is estimated to reach 30% of the world's road transport fuel mix by 2050 [13,14]. Biodiesel is mostly produced from vegetable oils and animal fats and has been the object of research and development in recent decades. Research is directed towards the use of low grade feedstock, with the possibility of reusing catalysts and improving efficiency of reactors for transesterification [15]. In fact, oil and fat materials used as raw materials are of high relevance because they are estimated to represent 60–80% of the total cost of biodiesel production [16]. Therefore, it is important to select the best materials in each case because they are affected by the geographic location, climate and agriculture [11]. Several countries such as Malaysia, Indonesia, Argentina, USA, Brazil, and the Philippines, as well as countries in the EU, are using biodiesel as a good source of renewable and biodegradable energy [17]. A consumption of 17.4 million liters of biodiesel was reported in 2019 with 63% of this consumption by France, Germany, Spain, Sweden and Italy [18]. The total biodiesel world production in 2019 was approximately 35 to 45 million tons and is steadily increasing year by year [19]. The European Union is the world's largest biodiesel producer and, on an energy basis, represents nearly 75% of the total transport biofuels market. In fact, the European biodiesel industry has more than 202 plants and production in 2019 exceeded 14 million tons of biodiesel [18,20]. US production of biodiesel was more than 5.6 million tons in 2019 and came from 91 plants with a capacity of 8.3 million tons per year [21,22]. Biodiesel is usually blended up to 20% with fossil diesel fuels in most countries due to its complete miscibility and the unnecessary need for engine modification at such percentage. For instance, a 20% blend is used in the United States while at least a 10% blend is used in China [23]. Blends receive the name B5, B10 or B20 when the biodiesel volume content is 5%, 10% and 20%, respectively. Today, more than 78% of diesel vehicles coming off production lines are approved for up to B20 use [21]. For biodiesel to be blended with normal fossil diesel, it must comply in Europe with EN14214 from the European Committee of Standardization (ISO) and in the US with ASTM6751 from the American Society for Testing and Materials [5].

Biodiesel can be used in existing diesel engines without the need for substantial modification. Biodiesel has a higher oxygen content than conventional diesel and the carbon to hydrogen ratio is also lower. This explains the major advantages of biodiesel such as lower emission of particulate matter, but also a lesser content of sulfur, hydrocarbon and carbon monoxide [24,25]. The major challenge nowadays is the production of environmentally and economically viable biodiesel [23] and the use of animal fat waste could contribute towards achieving this goal. This review is highlighting the latest advances in the available processes for biodiesel production from animal fat waste.

To elaborate on the present review, the literature search was performed in Web of Science (WoS) database from 1 January 2010 to 28 February 2020. The terms "biodiesel production," "animal fat" and "transesterification" were used for the survey of published papers. In total, 1602 publications were found, 1594 of them in English, with most found over the last three years. Of these, 1541 manuscripts were research articles, 141 were reviews, 210 corresponded to meetings, 27 corresponded to books, and the rest fell under another category. Eligibility criteria were established as: (a) full-text with English language article; (b) articles selected were published in scientific journals that apply a peer review system; (c) books, workshops, conference reports, theses and case reports were excluded due to lack of peer review; (d) articles with other feedstocks like vegetable oils; and (e) articles that only analyzed the overall performance of the process and did not provide specific parameters for comparison or evaluation were not included. Titles and abstracts of manuscripts were further evaluated for selection of manuscripts and those selected were used for the current review. Some relevant publications published before 2010 were also considered as well as websites of producers and international

agencies with current data and updated information on industrial use of feedstocks, animal fats and biodiesel production.

2. Animal Fats as Feedstock

About 328 million animals (cattle, sheep, pigs and goats) and 6 billion poultry (mainly chickens and turkeys) were slaughtered in 2014 in the European Union [2]. Such a high number of slaughtered animals produces enormous amounts of waste animal residue including fats that need to be treated to reduce pollution or recycled to give them some added value [26,27]. Such fats include beef tallow extracted from rendering fatty tissue of cattle, mutton tallow from rendering sheep, pork lard from rendering pigs and chicken fat from rendering feathers, blood, skin, offal and trims [28,29]. The wet rendering process includes the presence of water and fats heated below 49 °C. The goal is separation of the fat from the protein fraction. Other fats are those resulting from meat and the meat processing industry and those from recycling of the industrial cooking business. Such recycled greases that are produced from heated animal fats collected from commercial and industrial cooking can be classified as yellow grease and brown grease depending on the content of free fatty acids (FFA). Yellow grease is considered if FFA < 15% by weight and brown grease when FFA > 15% [30].

Typical fatty acid composition of pork lard, beef tallow, mutton tallow and poultry fats are shown in Table 1. There is a wide variety depending on the animal species [31] but in general, they contain common types of fatty acids, most of them having 16 to 18 carbons. Most relevant fatty acids are palmitic (16:0) and stearic (18:0) acids as saturated fatty acids (SFA); oleic acid (18:1) as monounsaturated fatty acids (MUFA); and linoleic (18:2) and arachidonic (20:4) acids as polyunsaturated fatty acids (PUFA) [32]. Due to their high content of saturated fatty acids (near 40% SFA), ruminant and pig fats are predominantly solid while those from chicken fat (nearly 30–33% of saturated fatty acids) are almost liquid or in semi-solid form [33]. Therefore, it must be taken into account that raw animal fats are mostly in a solid state at ambient temperature and therefore, preheating at 45 °C is required for their use as fuel for diesel engine [14]. Further, such high content in saturated fatty acids generally results in more stable biodiesel with high cetane numbers (more than 50 for lard and tallow).

One of the main applications of inedible animal fat byproducts is the production of biodiesel [6,34]. Inedible animal byproducts are structured into three categories within the EU that are defined according to their risk to human or animal health. Category 1 has the highest risk, Category 2 still offers a high risk, while Category 3 offers the lowest risk and is fit for human consumption although generally not used for human food because of its non-edible content or for commercial reasons. Major uses for Category 3 byproducts are as feed and pet food. In any case, fats from all three categories can be destined to biodiesel production and some stakeholders have reported that Category 3 provides better quality for biodiesel production [35]. Nearly 81% of caul and lung fat and 26% of cod and kidney, knob and channel fat from cattle are destined for biodiesel production. In the case of sheep fats, 88% of caul fat, 43.3% of lung fat and 67.1% of knob and channel fat are destined for biodiesel production [36]. In 2019, the total amount of vegetable oil and animal fat used as feedstock for biodiesel exceeded 13 million tons in the EU. From them, 800 thousand tons (6% of total feedstock) corresponded to animal fats, and such amount has remained fairly constant since 2014 [18,19]. In the case of the US, animal fats represented 8.4% of total feedstock and were poultry fat, tallow and white grease with amounts of 74, 132 and 243 thousand tons, respectively [21].

Table 1. Typical composition in major fatty acids (as % of total fatty acids) of pork, beef, mutton and chicken fats.

Fatty Acid		Pork Lard	Beef Tallow	Mutton Tallow	Poultry Fat
		[37]	[38]	[39]	[40]
Myristic	C14:0	1.6	1.6	2.2	0.4
Palmitic	C16:0	25.1	21.6	21.1	21.6
Stearic	C18:0	12.6	17.7	11.6	6.3
Palmitoleic	C16:1	2.8	2.5	2.1	3.2
Oleic	C18:1	36.5	31.5	38.7	30.0
Linoleic	C18:2	16.5	3.3	10.2	28.4
Linolenic	C18:3	1.1	1.3	0.6	2.4
Arachidonic	C20:4	0.3	-	-	3.4
Docosapentaenoic	C22:5	0.2	-	-	0.3
Docosahexaenoic	C22:6	-	-	-	0.8
Total saturated	SFA	39.4	49.1	40.4	29.1
Total monounsaturated	MUFA	39.7	41.0	47.1	33.2
Total polyunsaturated	PUFA	20.9	10.0	12.5	37.6

3. Transesterification for Producing Biodiesel from Animal Fats

The major steps in the production of biodiesel from animal fat waste are shown in Figure 1. A pretreatment is needed because feedstocks like animal fats usually contain a high amount of free fatty acids (FFA) and water which reduces the yield of biodiesel [41] and increases production costs because of the difficulty of separation and purification [42,43]. Biodiesel is produced through the transesterification reaction of a fat with a short-chain alcohol in the presence of a catalyst. Different catalysts are available to be used for biodiesel production. Those most typically used in transesterification reactions are alkalis (sodium hydroxide, sodium methoxide, potassium hydroxide, potassium methoxide, sodium amide, sodium hydride, potassium amide and potassium hydride), acids (sulfuric acid, phosphoric acid, hydrochloric acid or organic sulfonic acid), heterogeneous catalysts like enzymes (lipases) and complex catalysts like silicates, zirconias, nanocatalysts, etc. [44]. A faster reaction rate of animal fats transesterification is obtained using alkali catalysts in comparison to acid catalysts [45,46] which are 4000 times faster [47] as well as less expensive and readily available [48]. Sodium and potassium hydroxides run quite well, and methoxides perform better but are more expensive [47]. Polyol-derived alkoxide base catalysts were prepared by heating aqueous sodium hydroxide solution and polyols under vacuum pressure [49] and potassium glyceroxide catalysts were produced from potassium hydroxide and non-volatile, non-toxic polyols like byproduct glycerol by heating and drying, making it cheap to produce. Furthermore, the rate of transesterification reactions in methanol was reported to be comparable to those observed for the conventional potassium methoxide catalyst under the same reaction conditions [50]. On the other hand, the use of acid catalysts for a transesterification reaction results in slower reaction rates and requires a higher alcohol to fat molar ratio and a larger reactor that may be subject to corrosion [51]. Acid catalysts are mainly used for reducing the free fatty acids content before its transesterification with alkaline catalysts [47].

The most commercially used short-chain alcohol for the transesterification reaction is methanol because of its cheap price, but other alcohols such as ethanol, propanol and butanol may also be used [52]. Transesterification consists of the conversion of triacylglycerols to diacylglycerols, releasing one fatty acid. Then, diacylglycerols are converted to monoacylglycerols, releasing a second fatty acid and, finally, monoacylglycerols are converted to glycerol, releasing a third fatty acid. In general, transesterification has a high conversion efficiency and low cost [53]. However, once a pretreatment has been performed [54], the efficiency of the transesterification reaction depends on many variables like the time and temperature of the reaction, type and molar ratio of alcohol, type and amount of catalyst used, the amount of water present in the reaction media, the composition of fatty acids and the release of free fatty acids to the reaction media. In industrial processing plants, approximately 100 kg of fat react with 10 kg of a short-chain alcohol (usually methanol) in the presence of an alkaline

catalyst, either sodium hydroxide or potassium hydroxide, to generate 100 kg of biodiesel and 10 kg of glycerin [55].

Examples of operating conditions during the transesterification step for production of biodiesel from animal fats are shown in Table 2. The optimum alcohol to oil molar ratio to get a biodiesel yield higher than 90% in alkaline catalyzed transesterification is reported to be around 6:1 which gives enough alcohol the capability to break the fatty acid–glycerol linkages. The use of a ratio greater than 6:1 gives a better yield in some cases but could hinder the glycerol separation process [56].

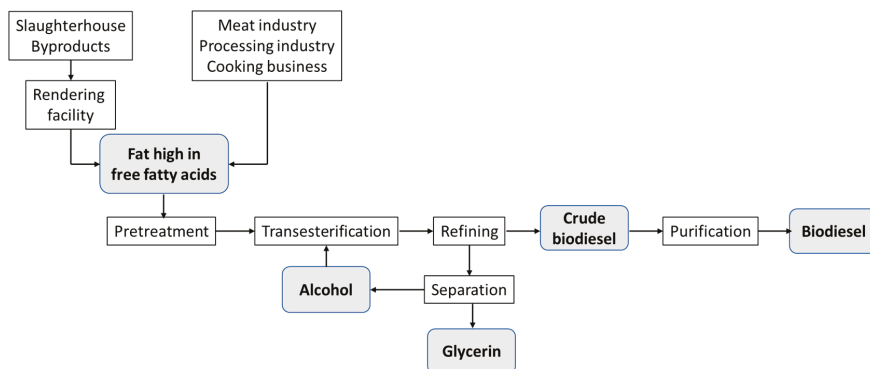


Figure 1. Major steps in the production of biodiesel from animal fat waste. Adapted from [46,47,53].

Table 2. Examples of operating conditions during the transesterification step for the production of biodiesel from animal fat waste.

Animal Fat	Catalyst	Weight	Reaction	Alcohol:Oil	Operating	References
		(% to Fat)	Yield (%)	Ratio	Conditions	
Beef tallow	KOH	0.8	90.8	6:1	60 °C, 2 h	[57,58]
Pork Lard	KOH	0.8	91.4	6:1	60 °C, 2 h	[57,58]
Poultry fat	KOH	0.8	76.8	6:1	60 °C, 2 h	[57,58]
Chicken waste	KOH	1	-	6:1	60 °C, 2 h	[59]
Duck tallow	KOH	1	97.1	3:1	65 °C, 3 h	[60]
Pork fat	KOH	0.5	97.3	6:1	65 °C, 2 h	[61]
Catfish fat	KOH	0.8	92.7	6:1	50 °C, 0.75 h	[62]
Chicken fat	KOH	0.8	82.0	8:1	60 °C, 1 h	[63]
Swine lard	KOH	1.1	98.0	7.4:1	65 °C, 3 h	[64]
Mutton fat	MgO-KOH	20	98.0	22:1	65 °C, 20 min	[65]
Chicken fat	H ₂ SO ₄	1.25	99.0	1:30	50 °C, 24 h,	[24]
Mutton tallow	H ₂ SO ₄	1.25	93.2	1:30	60 °C, 24 h	[24]
Chicken fat	NaOMe	1	88.5	6:1	60 °C, 4 h	[66]
Chicken fat	Nano CaO	1	88.5	9:1	60 °C, 5 h	[67]
Chicken fat	Composite membrane & NaOMe	1	98.1	1:1	70 °C, 3 h	[68]
Chicken fat	CaO/CuFe ₂ O ₄	3	94.5	15:1	70 °C, 4 h	[69]
Lard	35%CaO/zeolite	8	90.9	30:1	65 °C, 1.25 h	[15]
Chicken fat	AC/CuFe ₂ O ₄ encapsulated with CaO	3	95.6	12:1	65 °C, 4 h	[70]
Brown grease	Mesoporous silica diphenylammonium triflate	15	98.0	15:1	95 °C, 2 h	[71]
Brown grease	ZnO/ZrO ₂	0.8	78.0	1:1.5	200 °C, 2 h	[72]
Lard	Supercritical methanol	-	89.9	45:1	335 °C, 20 MPa, 15 min Agitation 500 rpm	[73]
Waste lard	Immobilized lipase from <i>Candida antarctica</i>	6	96.8	6:1	50 °C, 30 min Ultrasound assisted	[74]

Table 2. Cont.

Animal Fat	Catalyst	Weight	Reaction	Alcohol:Oil	Operating	References
		(% to Fat)	Yield (%)	Ratio	Conditions	
Beef tallow	Immobilized lipase from <i>Burkholderia cepacia</i>	20	89.7	12:1	50 °C, 48 h	[75]
Animal fat	Immobilized lipase from <i>Candida antarctica</i>	10	79	50:6	40 °C, 6 h	[76]
Lard	Lipase from <i>Candida</i> sp	20	87.4	3:1	40 °C, 30 h	[77]
Lard	Lipase from <i>Candida antarctica</i>	10	74	1:1	30 °C, 72 h	[78]
Lard	Lipase from <i>Candida antarctica</i>	2–6	97.2	5:1	50 °C, 20 h	[79]

As previously mentioned, if an alkaline catalyst is used for transesterification and there is a high content of free fatty acids, the reaction efficiency is drastically reduced because of the reaction of such free fatty acids with the catalyst resulting in soap formation [80,81]. This causes a loss of catalyst and ester product [82] and reduces the biodiesel yield to low levels, and therefore, the production costs increase [83]. The soap formation also makes glycerol separation and biodiesel purification difficult, which increases the cost of the resulting alkaline wastewater treatment [84]. The quality can also be affected due to side reactions producing unwanted products [85]. The free fatty acid content in animal fats is within the range of 5–30%, making a pretreatment necessary [26]. For an effective transesterification reaction, it is recommended that a limit in free fatty acids be equivalent to 1.0–1.5% [86], or an acid value below 2 mg KOH/g of oil [87]. There are different strategies in order to get such reduction in free fatty acids. For instance, waste pork fats containing free fatty acids within the range 4.9–13.5% were esterified for 4 h at 65 °C with 0.5 wt.% H₂SO₄ or 1.0 wt.% p-toluene sulfonic acid, keeping a 6:1 methanol to fat molar ratio, and the acid value was reduced below 2 mg KOH/g [61]. Furthermore, the waste fat of rendered pork was reported to have a high acid value of 4.3 mg KOH/g, but it could be reduced down to 0.75 mg KOH/g through a standard titration pretreatment method using sulfuric acid, even though it can be corrosive [23]. A continuous esterification process that reduced the reactor cost and reaction time, was designed for pretreatment deacidification using an ion exchange resin reaching an acid value reduced to 0.89 mg KOH/g and a conversion rate as high as 99.26% [80].

Thus, pretreatments are necessary to remove the excess of water, free fatty acids and suspended solids of animal fats before transesterification. Some of such pretreatments for moisture reduction are heat drying, silica gel, calcium chloride or anhydrous sodium sulfate [88–90]. The excess of free fatty acids may be removed by neutralization and separation [78]. Finally, the suspended matter may be removed by filtration under vacuum or through cellulose filters [88,90]. However, although the quality and yield of biodiesel are better, pretreatment steps result in additional costs [91].

An alternative process would be a two-step transesterification being the first step—an acid-catalyzed pretreatment to esterify the free fatty acids and thus, reducing their content—and the second step, where triacylglycerols undergo transesterification with the alkaline catalyst [52]. Other alternatives to consider are heterogeneous acid and base catalysts that have better tolerance to high water content and free fatty acids and can be re-used [82].

Heterogeneous catalysts offer the possibility of recycling and reducing the biodiesel production steps. Basic zeolites, alkaline earth metal oxides and hydrotalcites constitute some of the most used in recent literature. CaO is one of the most used catalysts and it has been loaded onto zeolite that offers a large surface area [15]. However, CaO can be poisoned when contacting water and carbon dioxide, making it not so attractive for industrial operation [92]. This catalyst could be recycled but the biodiesel yield is rapidly decreased down to 37.5% after its third use. Several nanocatalysts like nano CaO [48], activated carbon/CuFe₂O₄ encapsulated with CaO [69] and KF/CaO nanocatalysts [93] have been reported at the laboratory scale. Such nanocatalysts show a higher catalytic efficiency, better rigidity, larger specific surface area and better resistance to saponification [69].

Heterogeneous solid acid catalysts are reported to give lower yields. However, they have some advantages in the case of animal fats because they are insensitive to the problem of

contents in free fatty acids and can perform esterification and transesterification simultaneously. Furthermore, the purification of biodiesel is avoided, and another advantage is the easier separation of the catalyst from the reaction products [94].

In cases where there is a high content of moisture and free fatty acids (e.g., animal fats), the enzymatically catalyzed transesterification is more attractive. Lipase converts both free fatty acids and triglycerides into biodiesel in the presence of an acyl acceptor. The main advantages are the mild reaction conditions, high selectivity and specificity of transesterification, broader substrate range, no soap formation, lower alcohol to oil ratio, lower requirements for purification and higher yields [95]. However, the major cost is due to the enzyme itself and its poor stability and longer reaction time, and the slow conversion rate because of the diffusion caused by its byproduct [96]. These troubles can be partly overcome through enzyme immobilization on an inert support that increases the enzyme stability, avoids the need for enzyme separation and improves process efficiency [97,98]. Other costs are derived from the deactivation of the enzyme at high molar ratios of alcohol to fat [96]. Three solutions have been proposed, which are using methanol stepwise addition, replacing methanol with an acyl acceptor like methyl acetate or ethyl acetate or using a solvent like t-butanol to get an improved solubility of methanol [99]. A variety of lipases from diverse microorganisms such as *Candida antarctica*, *Candida rugosa*, *Pseudomonas cepacia*, *Pseudomonas* spp. and *Rhizomucor miehei*, and immobilized lipases (i.e., Lipozyme[®] RMIM from *Rhizomucor miehei* or Novozym[®] 435 from *Candida antarctica*), have been reported in the literature [100]. It must be pointed out that transesterification with alkaline catalysis is still preferred at industrial plants producing biodiesel. In spite of much research on heterogeneous and enzyme catalysts, biodiesel producers have not yet adopted these technologies [101].

4. Quality of Biodiesel Produced from Animal Fat Waste

Biodiesel has to comply with regulations EN14214 from the European Committee of Standardization (ISO) and the ASTM6751-3 from the American Society for Testing and Materials (ASTM). There are relevant benefits in the use of biodiesel produced from animal fats, such as the emission of polycyclic aromatic hydrocarbons being reduced by 75–90% and total unburned hydrocarbon by 90% when using biodiesel produced from animal fats when compared to conventional diesel [10,11]. The emissions of sulfur dioxide and CO are also reduced [12] as well as the particulate matter and nitrous oxides at part loads [18,66]. The properties of biodiesel produced from animal fats are compiled in Table 3. The cetane number reflects the ignition characteristics of the fuel. A high number is associated with better ignition quality [47]. The cetane number of biodiesels produced from animal fats is >50 and higher than that produced from vegetable oils due to their content of saturated fats (higher than 40%) and lower content of carbon and higher content of oxygen in comparison to conventional diesel [14]. The acid value is associated with the content in free fatty acids which, at high concentrations, can cause corrosion of the fuel supply system of the engine [66]. The cold filter plugging point (CFPP) represents the lowest temperature that a volume of liquid fuel will still flow through a given filter in a determined period of time when the fuel components start to gel or crystallize [102]. It is especially important for cold weather conditions. CFPP of biodiesel from animal fats is higher than 2 °C due to a higher content of saturated fatty acids. Flash point is the temperature at which the biodiesel exposed to a flame will ignite. Biodiesel from animal fats has a flash point higher than 150 °C and this provides better safety during transport and storage [47]. Biodiesel provides good lubricity that helps for a longer engine life [103]. However, the viscosity is higher than 3.5 mm²/s due to the saturated fats that give higher amounts of CH₂ in the fatty acid methyl esters [104] which might create problems in pumping and combustion [11]. Finally, the percentage of free glycerin reflects the amount of glycerol remaining in the final biodiesel and, if the content is high, it could result in coking of the injector and damage to the fuel injection [47].

The cost of the obtained biodiesel from animal fat waste depends on several parameters such as the cost of the feedstock, the amount of free fatty acids and the type of necessary pretreatment, the type of catalyst, the operational maintenance and the type of purification for the biodiesel [105]. The refining of

crude biodiesel obtained from animal waste is more costly than that from vegetable oils. Large amounts of glycerine (glycerol) are produced during transesterification which need to be removed because they influence the quality of the fuel and reduce the engine durability. The purification process (see Figure 1) usually consists of either wet washing based on water, dry washing based on adsorption and ion exchange, or novel methods based on liquid–liquid extraction, deep eutectic solvents or membranes. The purification step will thus remove glycerol as well as other impurities like residual catalyst, unconverted fats, and soap, and provides a better quality of biodiesel fuel [106]. About 1 kg of glycerol is produced for each 10 kg of biodiesel [107]. The recovered glycerol may be used for pharmaceutical, food, personal care biopolymers, or fuel additive applications although the value is low due to the large worldwide production of glycerol [92,105].

Table 3. Properties of biodiesel produced from animal fat waste.

Properties	EN14214 Limits	Poultry Fat [47]	Poultry Fat [58]	Chicken Fat [29]	Chicken Fat [108]	Chicken Fat [66]	Pork Lard [58]	Pork Lard [61]	Mutton Tallow [24]	Beef Tallow [47]	Beef Tallow [58]
Density at 15 °C (kg/m ³)	860–900	-	877	830	870	883	873	870	856	-	870
Viscosity at 40 °C (mm ² /s)	3.50–5.00	4.50	6.86	3.5	5.4	4.94	5.08	4.74	-	4.82	5.35
Cetane number	>51.0	-	-	50	58.4	-	-	56.9	59.0	-	-
Acid value (mg KOH/g)	<0.50	0.044	0.55	-	0.8	0.22	0.22	0.23	0.65	0.147	0.20
Iodine value (g/100 g)	<120	-	78.8	-	-	-	75.6	66.7	126	-	44.4
Water content (mg/kg)	-	-	1201	-	-	-	184	500	200	-	374
Flash point (°C)	>120	>160	172	50	174	171.8	147	175	-	>160	171
Pour point (°C)	-	-	-	-6	-	-6	-	-	-5	-	10
Cloud point (°C)	-	6.1	-	-	-	-5	-	-	-4	16	-
Free glycerin (%)	-	0.002	-	-	-	0.19	-	-	-	0.008	-
Cold filter plugging point (°C)	8	2	3	-	-	-	5	-20 to 5	-	14	10

5. Developments in Improving Biodiesel Production from Animal Fats

China has been the most active country in publishing patents in the period 1999–2018 with 647 patents on biodiesel. The US had 266 patents, with more than 50% of them focused on reactors technology and processing methods [11]. There has also been patenting activity on pretreatment methods as well as on catalysts for improving the transesterification process. Specific examples of patents for biodiesel production from animal fat waste are shown in Table 4.

Table 4. Selected patents for biodiesel production from animal fat waste.

Animal Feedstock	Particular Conditions	Catalyst	Biodiesel Characteristics	References
Lard oil, tallow oil, fish oil,	Hydrodeoxygenation and hydroisomerization of the oil in a single step	Pt and Pd and an acidic component	Mixture of C14 to C18 paraffins having a ratio of iso to normal paraffins of 2 to 8; less than 5 ppm sulfur; and acceptable lubricity	[100,109,110]
Animal oil, fish oil, lard, rendered fats, tallow	Unwanted water removed by cross-flow filtration	Immobilized lipase	Separation of formed crude biodiesel and crude glycerol from the second reaction medium by using a fourth cross-flow filtration cassette	[111]
Animal fats	Degumming; physical refining (heating and vacuum pulling); and glycerolysis	H ₂ SO ₄ , ZnO	Possibility of using various starting feed stocks with heat integration to minimize operating costs	[112]
Animal fats incl. 10–20% free fatty acids	Esterification in two steps	96% H ₂ SO ₄	The amount of FFA in the mixture is reduced to <3% by weight	[113,114]
Animal fats	Esterification reaction of free fatty acids if higher than a set value	Alkali catalyst KOH	Distillation to remove byproducts like glycerol and alcohol	[115]
Beef oil, pork oil, animal fats such as fish oil	Transesterification with lower alcohol content	Alkali catalyst KOH	Reducing costs by producing glycerin and glycerin derivatives in high yield and purity	[116]

Technologies for process intensification like ultrasonic and microwave have been developed to be applied in transesterification and improve biodiesel production. The goal is to improve the miscibility of oils and methanol and thus increase the yield of the transesterification [73,117]. Immiscible liquids can be emulsified at an industrial scale through the use of low frequency ultrasonic irradiation. In the case of microwave irradiation, reactants can be efficiently and rapidly heated to the target temperature [118]. Other process intensification technologies like static mixers [119], capillary reactors [120,121], microreactors [122,123] or oscillatory flow reactors [124] are also intended to accelerate the reaction rate and enhance biodiesel production.

The use of microwave heating for animal fats containing up to 20% free fatty acids allowed for a decrease in the required time for free fatty acid reduction and increased the final yield [66]. Another alternative was the use of supercritical methanol with temperatures of 300 °C–400 °C, pressures up to 41.1 MPa, alcohol to fat ratios of 3:1 and 6:1, and short time (between 2–6 min) that gave 88% conversion for chicken fat [125]. The yield of biodiesel obtained with refined lard could also be obtained with waste lard containing fatty acids and water with no need for pretreatment [72]. Supercritical processes give faster reaction rates with no catalyst and avoid the need for pretreatment even in the presence of free fatty acids and water associated with the use of animal fats [30]. Other authors have assayed the transesterification with immobilized lipase in supercritical CO₂ and reported its contribution in reducing the interaction between methanol and enzyme, reducing its toxicity [75] and immediately separating CO₂ from the product.

New heterogeneous catalysts that can be easily recovered, regenerated and reused have been developed for biodiesel production. Such catalysts include alkaline earth metal oxides such as CaO and MgO, hydrotalcite, acid zirconia and alumina-based catalysts and immobilized lipase [20]. The use of a new nano catalyst consisting of CaO/CuFe₂O₄ during the transesterification process was successfully assayed for biodiesel production from chicken fat [69]. A sodium silicate catalyst that does not saponify with free fatty acids during transesterification was recently assayed to produce biodiesel that could be blended up to 30% with diesel, giving good performance. The brake specific fuel was 26% higher than diesel and the brake thermal efficiency was 4% lower while CO was reduced by 24.4% and hydrocarbons by 22.9%. However, no emission was increased by 11% at full load [25]. Shells of *Mytilus galloprovincialis*—waste from fish industry—containing CaO that can be used as a catalyst, were used for transesterification of jojoba oil. As CaO could be contaminated with CO₂ and H₂O, it was calcined immediately before use [126]. Calcined scallop shell was also reported as a very active catalyst for transesterification of rapeseed oil [127].

Recently, a cheap and safe catalyst consisting of metal hydrated salts was proposed for the pretreatment of animal fats with a high content of free fatty acids that could be esterified up to 99% with alcohol under mild conditions [128]. The methyl esters remained in the oily phase and could be used for transesterification directly with alkaline catalysts. On the other hand, a biorefining strategy for animal fat waste was proposed for the conversion of free fatty acids into triglycerides that could be blended with fossil diesel and be used in engine combustion systems [129]. Recently, adsorbents like magnesium aluminum hydroxycarbonate and 1,3,5-trimethyl-2,4,6-tris(3,5-ditert-butyl-4-hydroxybenzyl) benzene were proposed to enhance the oxidative stability of biodiesel and its blends and therefore retard their degradation. The acid value could be reduced up to 9%. In this way, the adsorbents can remove the precursors of the aging of biodiesel by stabilizing the generated free radicals and preventing them from starting new oxidation chains [130]. Precipitates of steryl glucosides are found in biodiesel produced from vegetable oils and may produce filter blockage. Their removal is achieved through adsorption with 3% silica at 112 °C for 72 min [131]. Finally, it is important to mention that Neste renewable diesel is produced through the hydrogen catalyzed conversion of triglycerides into the corresponding alkanes and propane. Nearly 3 million tons are produced in five plants and mixed with fossil diesel for its use in aviation, turbines, generators and ships [132].

6. Conclusions

Biodiesel produced from agricultural waste has been rapidly expanded around the world due to its relevant advantages such as being biodegradable, renewable and sulphur-free. The cost of biodiesel majorly depends on the cost of the raw materials being used, with animal fat waste being cheaper than vegetable oil waste. Animal fats, usually found as waste from slaughterhouses, the meat processing industry, and cooking facilities, can be used as feedstock for biodiesel production. As reported in this manuscript, there are numerous processes already available for the production of biodiesel from animal fats and operating conditions during transesterification. There are also alternative solutions for pretreatment which mainly depend on the moisture and FFA content of such residues. Alkaline catalysis is still preferred at industrial plants producing biodiesel because it is faster than acid catalysis and cheaper than most alternative catalysts including acid catalysts and lipases. Although much research has been published on heterogeneous and acid and enzyme catalysts which avoid the challenges of water and FFA in animal fats, biodiesel producers have not yet adopted these technologies. However, there are recent developments that are promising for future industrial use. This is the case with heterogeneous catalysts that can be easily recovered, regenerated and reused, and immobilized lipases that improve efficiency and reduce costs by increasing enzyme stability and making the enzyme more resistant to denaturation by alcohol.

Author Contributions: Conceptualization, F.T.; resources, F.T.-R. and L.M.; writing—original draft preparation, F.T.-R.; writing—review and editing, F.T.-R., L.M. and F.T.; supervision, F.T. All authors have read and agreed to the published version of the manuscript.

Funding: This research was funded by European Marie Curie project, grant number 614281 (HIGHVALFOOD) and European Regional Development Fund.

Conflicts of Interest: The authors declare no conflict of interest. The funders had no role in the design of the study; in the collection, analyses, or interpretation of data; in the writing of the manuscript, or in the decision to publish the results.

References

- Zalouk, S.; Barbati, S.; Sergent, M.; Ambrosio, M. Disposal of animal by-products by wet air oxidation: Performance optimization and kinetics. *Chemosphere* **2009**, *74*, 193–199. [CrossRef]
- EFPPA. Rendering in Numbers. 2016. Available online: <https://efpra.eu/wp-content/uploads/2016/11/Rendering-in-numbers-Infographic.pdf> (accessed on 20 March 2020).
- Toldrá, F.; Mora, L.; Reig, M.; Mora, L. New insights into meat by-product utilization. *Meat Sci.* **2016**, *120*, 54–59. [CrossRef]
- Rosson, E.; Sgarbossa, P.; Pedrielli, F.; Mozzon, M.; Bertani, R. Bioliquids from raw waste animal fats: An alternative renewable energy source. *Biomass Convers. Biorefinery* **2020**, 1–16. [CrossRef]
- EFPPA. The Facts about Biofuels and Bioliquids. 2016. Available online: <https://efpra.eu/wp-content/uploads/2016/11/The-facts-about-biofuels-and-bioliquids.pdf> (accessed on 3 April 2020).
- Baladincz, P.; Hancsók, J. Fuel from waste animal fats. *Chem. Eng. J.* **2015**, *282*, 152–160. [CrossRef]
- Nigam, P.S.; Singh, A. Production of liquid biofuels from renewable resources. *Prog. Energy Combust. Sci.* **2011**, *37*, 52–68. [CrossRef]
- Mansir, N.; Teo, S.H.; Rashid, U.; Saiman, M.I.; Tan, Y.P.; Abdulkareem-Alsultan, G.; Taufiq-Yap, Y. Modified waste egg shell derived bifunctional catalyst for biodiesel production from high FFA waste cooking oil. A review. *Renew. Sustain. Energy Rev.* **2018**, *82*, 3645–3655. [CrossRef]
- IPPR. Time for Change: A New Vision for the British Economy—The Interim Report of the IPPR Commission on Economic Justice. 2017. Available online: <http://www.ippr.org/cej-time-for-change> (accessed on 25 March 2020).
- Carraretto, C. Biodiesel as alternative fuel: Experimental analysis and energetic evaluations. *Energy* **2004**, *29*, 2195–2211. [CrossRef]
- Mahlia, T.; Syazmi, Z.; Mofijur, M.; Abas, A.P.; Bilal, M.; Ong, H.C.; Silitonga, A. Patent landscape review on biodiesel production: Technology updates. *Renew. Sustain. Energy Rev.* **2020**, *118*, 109526. [CrossRef]

12. Shaghghi, S.; Ghahderijani, M.; Dehrouyeh, M.H. Optimization of Indicators Pollutant Emission Following Blending Diesel Fuel with Waste Oil-Derived Biodiesel. *J. Oleo Sci.* **2020**, *69*, 337–346. [CrossRef]
13. IRENA. Global Energy Transformation: A Roadmap to 2050. 2018. Available online: https://www.irena.org/-/media/Files/IRENA/Agency/Publication/2018/Apr/IRENA_Report_GET_2018.pdf (accessed on 14 April 2020).
14. Cernat, A.; Pana, C.; Negurescu, N.; Lazaroiu, G.; Nutu, C.; Fuioreescu, D.; Toma, M.; Nicolici, A. Combustion of preheated raw animal fats-diesel fuel blends at diesel engine. *J. Therm. Anal. Calorim.* **2019**, *140*, 2369–2375. [CrossRef]
15. Lawan, I.; Garba, Z.N.; Zhou, W.; Zhang, M.; Yuan, Z. Synergies between the microwave reactor and CaO/zeolite catalyst in waste lard biodiesel production. *Renew. Energy* **2020**, *145*, 2550–2560. [CrossRef]
16. Bušić, A.; Kundas, S.; Morzak, G.; Belskaya, H.; Mardetko, N.; Santek, M.I.; Komes, D.; Novak, S.; Šantek, B. Recent Trends in Biodiesel and Biogas Production. *Food Technol. Biotechnol.* **2018**, *56*, 152–173. [CrossRef] [PubMed]
17. Balat, M.; Balat, H. Progress in biodiesel processing. *Appl. Energy* **2010**, *87*, 1815–1835. [CrossRef]
18. Ramos, M.; Dias; Puna; Gomes, J.F.; Bordado, J.; Dias, A.P.S.; Puna, J. Biodiesel Production Processes and Sustainable Raw Materials. *Energies* **2019**, *12*, 4408. [CrossRef]
19. Flach, B.; Lieberz, S.; Bolla, S. EU Biofuels Annual 2019, Gain Report NL9022, USDA Foreign Agricultural Service. 2019. Available online: <http://gain.fas.usda.gov/Pages/Default.aspx> (accessed on 6 May 2020).
20. Bockey, D. The significance and perspective of biodiesel production—A European and global view. *OCL* **2019**, *26*, 40. [CrossRef]
21. US Energy Information Administration. *Monthly Biodiesel Production Report*; US Department of Energy: Washington, DC, USA, 2020. Available online: <https://www.eia.gov/biofuels/biodiesel/production/biodiesel.pdf> (accessed on 5 May 2020).
22. Biodiesel. Available online: <https://www.biodiesel.org/what-is-biodiesel/biodiesel-basics> (accessed on 21 March 2020).
23. Gumahin, A.C.; Galamiton, J.M.; Allerite, M.J.; Valmorida, R.S.; Laranang, J.-R.L.; Mabayo, V.I.; Arazo, R.O.; Ido, A.L. Response surface optimization of biodiesel yield from pre-treated waste oil of rendered pork from a food processing industry. *Bioresour. Bioprocess.* **2019**, *6*, 1–13. [CrossRef]
24. Bhatti, H.N.; Hanif, M.A.; Qasim, M.; Rehman, A. Biodiesel production from waste tallow. *Fuel* **2008**, *87*, 2961–2966. [CrossRef]
25. Xue, J.; Grift, T.E.; Hansen, A.C. Effect of biodiesel on engine performances and emissions. *Renew. Sustain. Energy Rev.* **2011**, *15*, 1098–1116. [CrossRef]
26. Mora, L.; Toldrá-Reig, F.; Prates, J.A.M.; Toldrá, F. Cattle by-products. In *Byproducts from Agriculture and Fisheries: Adding Value for Food, Feed, Pharma and Fuels*; Simpson, B.K., Aryee, A.N., Toldrá, F., Eds.; Wiley: Chichester, West Sussex, UK, 2020; pp. 43–55.
27. Mora, L.; Toldrá-Reig, F.; Reig, M.; Toldrá, F. Possible uses of processed slaughter by-products. In *Sustainable Meat Production and Processing*; Galanakis, C.M., Ed.; Academic Press/Elsevier: London, UK, 2019; pp. 145–160.
28. Akhil, U.S.; Alagumalai, A. A Short Review on Valorization of Slaughterhouse Wastes for Biodiesel Production. *Chem. Sel.* **2019**, *4*, 13356–13362. [CrossRef]
29. Barik, D.; Vijayaraghavan, R. Effects of waste chicken fat derived biodiesel on the performance and emission characteristics of a compression ignition engine. *Int. J. Ambient Energy* **2018**, *41*, 88–97. [CrossRef]
30. Banković-Ilić, I.B.; Stojković, I.J.; Stamenković, O.S.; Veljkovic, V.B.; Hung, Y.-T. Waste animal fats as feed stocks for biodiesel production. *Renew. Sustain. Energy Rev.* **2014**, *32*, 238–254.
31. Karmakar, A.; Karmakar, S.; Mukherjee, S. Properties of various plants and animals feedstocks for biodiesel production. *Bioresour. Technol.* **2010**, *101*, 7201–7210. [CrossRef] [PubMed]
32. Prates, J.; Alfaia, C.; Alves, S.; Bessa, R. Fatty acids. In *Handbook of Analysis of Edible Animal by-Products*; Nollet, L.M.L., Toldrá, F., Eds.; CRC Press: Boca Raton, FL, USA, 2011; pp. 137–159.
33. Oner, C.; Altun, Ş. Biodiesel production from inedible animal tallow and an experimental investigation of its use as alternative fuel in a direct injection diesel engine. *Appl. Energy* **2009**, *86*, 2114–2120. [CrossRef]
34. Jayathilakan, K.; Sultana, K.; Radhakrishna, K.; Bawa, A.S. Utilization of byproducts and waste materials from meat, poultry and fish processing industries: A review. *J. Food Sci. Technol.* **2011**, *49*, 278–293. [CrossRef]
35. Ecofys. Indirect Emissions from Rendered Animal Fats Used for Biodiesel. 2016. Available online: <https://ec.europa.eu/energy/sites/ener/files/documents/Annex%20II%20Case%20study%202.pdf> (accessed on 7 May 2020).

36. Walsh, C. *The Use of Animal by-Products*; EBLEX: Stoneleigh Park, UK, 2014; pp. 1–73.
37. Toldrá, F.; Rubio, M.A.; Navarro, J.L.; Cabrerizo, L. Quality aspects of pork and its nutritional impact. In *Quality of Fresh and Processed Foods. Advances in Experimental Medicine and Biology*; Shahidi, F., Spanier, A.M., Ho, C.-T., Braggins, T., Eds.; Kluwer Academic/Plenum Publishers: New York, NY, USA, 2004; Volume 542, pp. 25–32.
38. Realini, C.; Duckett, S.; Brito, G.; Rizza, M.D.; De Mattos, D. Effect of pasture vs. concentrate feeding with or without antioxidants on carcass characteristics, fatty acid composition, and quality of Uruguayan beef. *Meat Sci.* **2004**, *66*, 567–577. [[CrossRef](#)]
39. Castro, T.; Manso, T.; Mantecon, A.R.; Guirao, J.; Jimeno, V. Fatty acid composition and carcass characteristics of growing lambs fed diets containing palm oil supplements. *Meat Sci.* **2005**, *69*, 757–764. [[CrossRef](#)]
40. Zduńczyk, Z.; Gruzauskas, R.; Semaskaite, A.; Juskievicz, J.; Raceviciute-Stupeliene, A.; Wroblewska, M. Fatty acid profile of breast muscle of broiler chickens fed diets with different levels of selenium and vitamin. *Eur. Poult. Sci.* **2011**, *75*, 264–267.
41. Gebremariam, S.; Marchetti, J.M. Economics of biodiesel production: Review. *Energy Convers. Manag.* **2018**, *168*, 74–84. [[CrossRef](#)]
42. Pinnarat, T.; Savage, P.E. Assessment of noncatalytic biodiesel synthesis using supercritical reaction conditions. *Ind. Eng. Chem. Res.* **2008**, *47*, 6801–6808. [[CrossRef](#)]
43. van Kasteren, J.; Nisworo, A. A process model to estimate the cost of industrial scale biodiesel production from waste cooking oil by supercritical transesterification. *Resour. Conserv. Recycl.* **2007**, *50*, 442–458. [[CrossRef](#)]
44. Ma, F.; Hanna, M.A. Biodiesel production: A review. *Bioresour. Technol.* **1999**, *70*, 1–15. [[CrossRef](#)]
45. Dias, J.M.; Alvim-Ferraz, M.C.; Almeida, M.F.; Alvim-Ferraz, M.D.C. Production of biodiesel from acid waste lard. *Bioresour. Technol.* **2009**, *100*, 6355–6361. [[CrossRef](#)]
46. Kirubakaran, M.; Selvan, V.A.M. A comprehensive review of low cost biodiesel production from waste chicken fat. *Renew. Sustain. Energy Rev.* **2018**, *82*, 390–401. [[CrossRef](#)]
47. Atabani, A.; Silitonga, A.S.; Badruddin, I.A.; Mahlia, T.M.I.; Masjuki, H.; Mekhilef, S. A comprehensive review on biodiesel as an alternative energy resource and its characteristics. *Renew. Sustain. Energy Rev.* **2012**, *16*, 2070–2093. [[CrossRef](#)]
48. Thangaraj, B.; Solomon, P.-R.; Muniyandi, B.; Ranganathan, S.; Lin, L. Catalysis in biodiesel production—a review. *Clean Energy* **2019**, *3*, 2–23. [[CrossRef](#)]
49. Gok, H.Y.F.; Shen, J.; Emami, S.; Reaney, M.J.T. Polyol-Derived Alkoxide/Hydroxide Base Catalysts I. Production. *J. Am. Oil Chem. Soc.* **2012**, *90*, 291–298. [[CrossRef](#)]
50. Pradhan, S.; Shen, J.; Emami, S.; Naik, S.N.; Reaney, M.J.T. Fatty acid methyl esters production with glycerol metal alkoxide catalyst. *Eur. J. Lipid Sci. Technol.* **2014**, *116*, 1590–1597. [[CrossRef](#)]
51. Canakci, M.; Sanli, H. Biodiesel production from various feedstocks and their effects on the fuel properties. *J. Ind. Microbiol. Biotechnol.* **2008**, *35*, 431–441. [[CrossRef](#)] [[PubMed](#)]
52. Ramadhas, A.S.; Jayaraj, S.; Muraleedharan, C. Biodiesel production from high FFA rubber seed oil. *Fuel* **2005**, *84*, 335–340. [[CrossRef](#)]
53. Van Gerpen, J. Biodiesel processing and production. *Fuel Process. Technol.* **2005**, *86*, 1097–1107. [[CrossRef](#)]
54. Alptekin, E.; Canakci, M. Optimization of pretreatment reaction for methylester production from chicken fat. *Fuel* **2010**, *89*, 4035–4039. [[CrossRef](#)]
55. US Department of Energy. Biodiesel Production and Distribution. Alternative Fuels Data Center. 2020. Available online: https://afdc.energy.gov/fuels/biodiesel_production.html (accessed on 6 May 2020).
56. Atadashi, I.M. The effects of alcohol to oil molar ratios and the type of alcohol on biodiesel production using transesterification process. *Egypt. J. Pet.* **2016**, *25*, 21–31.
57. Mata, T.M.; Mendes, A.M.; Caetano, N.S.; Martins, A.A. Properties and Sustainability of Biodiesel from Animal Fats and Fish Oil. *Chem. Eng. Trans.* **2014**, *38*, 175–180.
58. Mata, T.M.; Cardoso, N.; Ornelas, M.; Caetano, N.S. Sustainable production of biodiesel from tallow, lard and poultry fat and its quality evaluation. *Energy Fuel* **2010**, *25*, 4756–4762. [[CrossRef](#)]
59. Lin, C.-W.; Tsai, S.-W. Production of biodiesel from chicken wastes by various alcohol-catalyst combinations. *J. Energy S. Afr.* **2017**, *26*, 36–45. [[CrossRef](#)]
60. Chung, K.-H.; Kim, J.; Lee, K.-Y. Biodiesel production by transesterification of duck tallow with methanol on alkali catalysts. *Biomass Bioenergy* **2009**, *33*, 155–158. [[CrossRef](#)]

61. Encinar, J.M.; Sánchez, N.; Martínez, G.; García, L. Study of biodiesel production from animal fats with high free fatty acid content. *Bioresour. Technol.* **2011**, *102*, 10907–10914. [[CrossRef](#)]
62. Huong, L.T.T.; Tan, P.M.; Hoa, T.T.V. Biodiesel Production from Fat of Tra Catfish via Heterogeneous Basic-Catalyzed Transesterification Using Ultrasonic Mixing. *e-J. Surf. Sci. Nanotechnol.* **2011**, *9*, 477–481. [[CrossRef](#)]
63. Chavan, S.B.; Yadav, M.; Singh, R.; Kumbhar, R.R.; Sharma, Y.C. Production of biodiesel from three indigenous feedstock: Optimization of process parameters and assessment of various fuel properties. *Environ. Prog. Sustain. Energy* **2017**, *36*, 788–795. [[CrossRef](#)]
64. He, C.; Mei, Y.; Zhang, Y.; Liu, L.; Li, P.; Zhang, Z.; Jing, Y.; Li, G.; Jiao, Y. Enhanced biodiesel production from diseased swine fat by ultrasound-assisted two-step catalyzed process. *Bioresour. Technol.* **2020**, *304*, 123017. [[CrossRef](#)]
65. Mutreja, V.; Singh, S.; Ali, A. Biodiesel from mutton fat using KOH impregnated MgO as heterogeneous catalysts. *Renew. Energy* **2011**, *36*, 2253–2258. [[CrossRef](#)]
66. Alptekin, E.; Canakci, M. Optimization of transesterification for methyl ester production from chicken fat. *Fuel* **2011**, *90*, 2630–2638. [[CrossRef](#)]
67. Keihani, M.; Esmaili, H.; Rouhi, P. Biodiesel production from chicken fat using nano-calcium oxide catalyst and improving the fuel properties via blending with diesel. *Phys. Chem. Res.* **2018**, *6*, 521–529.
68. Shi, W.; Li, J.; He, B.; Yan, F.; Cui, Z.; Wu, K.; Lin, L.; Qian, X.; Cheng, Y. Biodiesel production from waste chicken fat with low free fatty acids by an integrated catalytic process of composite membrane and sodium methoxide. *Bioresour. Technol.* **2013**, *139*, 316–322. [[CrossRef](#)]
69. Seffati, K.; Honarvar, B.; Esmaili, H.; Esfandiari, N. Enhanced biodiesel production from chicken fat using CaO/CuFe₂O₄ nanocatalyst and its combination with diesel to improve fuel properties. *Fuel* **2019**, *235*, 1238–1244. [[CrossRef](#)]
70. Seffati, K.; Esmaili, H.; Honarvar, B.; Esfandiari, N. AC/CuFe₂O₄@CaO as a novel nanocatalyst to produce biodiesel from chicken fat. *Renew. Energy* **2020**, *147*, 25–34. [[CrossRef](#)]
71. Ngo, H.L.; Zafiroopoulos, N.A.; Foglia, T.A.; Samulski, E.T.; Lin, W. Mesoporous Silica-Supported Diarylammonium Catalysts for Esterification of Free Fatty Acids in Greases. *J. Am. Oil Chem. Soc.* **2009**, *87*, 445–452. [[CrossRef](#)]
72. Kim, M.; DiMaggio, C.; Yan, S.; Wang, H.; Salley, S.O.; Ng, K.Y.S. Performance of heterogeneous ZrO₂ supported metaloxide catalysts for brown grease esterification and sulfur removal. *Bioresour. Technol.* **2011**, *102*, 2380–2386. [[CrossRef](#)]
73. Shin, H.-Y.; Lee, S.-H.; Ryu, J.-H.; Bae, S.-Y. Biodiesel production from waste lard using supercritical methanol. *J. Supercrit. Fluids* **2011**, *61*, 134–138. [[CrossRef](#)]
74. Adewale, P.; Dumont, M.-J.; Ngadi, M. Enzyme-catalyzed synthesis and kinetics of ultrasonic assisted methanolysis of waste lard for biodiesel production. *Chem. Eng. J.* **2016**, *284*, 158–165. [[CrossRef](#)]
75. Da Rós, P.C.; Silva, G.A.; Mendes, A.A.; Santos, J.C.; De Castro, H.F. Evaluation of the catalytic properties of Burkholderia cepacia lipase immobilized on non-commercial matrices to be used in biodiesel synthesis from different feedstocks. *Bioresour. Technol.* **2010**, *101*, 5508–5516. [[CrossRef](#)] [[PubMed](#)]
76. Pollardo, A.A.; Lee, H.-S.; Lee, D.; Kim, S.; Kim, J. Solvent effect on the enzymatic production of biodiesel from waste animal fat. *J. Clean. Prod.* **2018**, *185*, 382–388. [[CrossRef](#)]
77. Lu, J.; Nie, K.; Xie, F.; Wang, F.; Tan, T. Enzymatic synthesis of fatty acid methyl esters from lard with immobilized Candida sp. 99-125. *Process. Biochem.* **2007**, *42*, 1367–1370. [[CrossRef](#)]
78. Lee, K.-T.; Foglia, T.A.; Chang, K.-S. Production of alkyl ester as biodiesel from fractionated lard and restaurant grease. *J. Am. Oil Chem. Soc.* **2002**, *79*, 191–195. [[CrossRef](#)]
79. Huang, Y.; Zheng, H.; Yan, Y. Optimization of Lipase-Catalyzed Transesterification of Lard for Biodiesel Production Using Response Surface Methodology. *Appl. Biochem. Biotechnol.* **2008**, *160*, 504–515. [[CrossRef](#)]
80. Li, H.; Lv, P.; Wang, Z.; Miao, C.; Yuan, Z. Biodiesel continuous esterification process experimental study and equipment design. *Biomass Conv. Bioref.* **2020**, in press. [[CrossRef](#)]
81. Talebian-Kiakalaieh, A.; Amin, N.A.S.; Mazaheri, H. A review on novel processes of biodiesel production from waste cooking oil. *Appl. Energy* **2013**, *104*, 683–710. [[CrossRef](#)]
82. Lotero, E.; Liu, Y.; Lopez, D.E.; Suwannakarn, K.; Bruce, D.A.; Goodwin, J.G. Synthesis of Biodiesel via Acid Catalysis. *Ind. Eng. Chem. Res.* **2005**, *44*, 5353–5363. [[CrossRef](#)]

83. Vicente, G.; Martínez, M.; Aracil, J. Integrated biodiesel production: A comparison of different homogeneous catalysts systems. *Bioresour. Technol.* **2004**, *92*, 297–305. [CrossRef]
84. Anitha, A.; Dawn, S.S. Performance Characteristics of Biodiesel Produced from Waste Groundnut Oil using Supported Heteropolyacids. *Int. J. Chem. Eng. Appl.* **2010**, *1*, 261–265. [CrossRef]
85. Balat, M. Potential alternatives to edible oils for biodiesel production—A review of current work. *Energy Convers. Manag.* **2011**, *52*, 1479–1492. [CrossRef]
86. Mashad, H.M.; Zhang, R.; Avena-Bustillos, R.J. A two-step process for biodiesel production from salmon oil. *Biosyst. Eng.* **2008**, *99*, 220–227. [CrossRef]
87. Idowu, I.; Pedrola, M.O.; Wylie, S.; Teng, K.; Kot, P.; Phipps, D.; Shaw, A. Improving biodiesel yield of animal waste fats by combination of a pre-treatment technique and microwave technology. *Renew. Energy* **2019**, *142*, 535–542. [CrossRef]
88. Felizardo, P.; Correia, M.J.N.; Raposo, I.; Mendes, J.F.; Berkemeier, R.; Bordado, J. Production of biodiesel from waste frying oils. *Waste Manag.* **2006**, *26*, 487–494. [CrossRef]
89. Kumar, G.N.; Selvan, V.A.M. Effects of alumina nanoparticles in waste chicken fat biodiesel on the operating characteristics of a compression ignition engine. *Clean Technol. Environ. Policy* **2015**, *17*, 681–692. [CrossRef]
90. Predojević, Z.J. The production of biodiesel from waste frying oils: A comparison of different purification steps. *Fuel* **2008**, *87*, 3522–3528. [CrossRef]
91. Patil, P.; Deng, S. Optimization of biodiesel production from edible and non-edible vegetable oils. *Fuel* **2009**, *88*, 1302–1306. [CrossRef]
92. Faba, L.; Díaz, E.; Ordóñez, S. Recent developments on the catalytic technologies for the transformation of biomass into biofuels: A patent survey. *Renew. Sustain. Energy Rev.* **2015**, *51*, 273–287. [CrossRef]
93. Wen, L.; Wang, Y.; Lu, D.; Hu, S.; Han, H. Preparation of KF/CaO nanocatalyst and its application in biodiesel production from Chinese tallow seed oil. *Fuel* **2010**, *89*, 2267–2271. [CrossRef]
94. Abbaszaadeh, A.; Ghobadian, B.; Omidkhah, M.R.; Najafi, G. Current biodiesel production technologies: A comparative review. *Energy Convers. Manag.* **2012**, *63*, 138–148. [CrossRef]
95. Christopher, L.P.; Kumar, H.; Zambare, V.P. Enzymatic biodiesel: Challenges and opportunities. *Appl. Energy* **2014**, *119*, 497–520. [CrossRef]
96. Issariyakul, T.; Kulkarni, M.G.; Dalai, A.K.; Bakhshi, N.N. Production of biodiesel from waste fryer grease using mixed methanol/ethanol system. *Fuel Process. Technol.* **2007**, *88*, 429–436. [CrossRef]
97. Al-Zuhair, S.; Hasan, M.; Ramachandran, K. Kinetics of the enzymatic hydrolysis of palm oil by lipase. *Process. Biochem.* **2003**, *38*, 1155–1163. [CrossRef]
98. Wang, X.; Qin, X.; Li, D.; Yang, B.; Wang, Y. One-step synthesis of high-yield biodiesel from waste cooking oils by a novel and highly methanol-tolerant immobilized lipase. *Bioresour. Technol.* **2017**, *235*, 18–24. [CrossRef]
99. Tan, T.; Lu, J.; Nie, K.; Deng, L.; Wang, F. Biodiesel production with immobilized lipase: A review. *Biotechnol. Adv.* **2010**, *28*, 628–634. [CrossRef] [PubMed]
100. Helwani, Z.; Othman, M.; Aziz, N.; Kim, J.; Fernando, W. Solid heterogeneous catalysts for transesterification of triglycerides with methanol: A review. *Appl. Catal. A Gen.* **2009**, *363*, 1–10. [CrossRef]
101. Kristi, M.; Milbrandt, A.; Lewis, J.; Schwab, A. *Bioenergy Industry Status 2017 Report*; National Renewable Energy Laboratory: Golden, CO, USA, 2018. Available online: <https://www.nrel.gov/docs/fy20osti/75776.pdf> (accessed on 5 May 2020).
102. Kumar, M.; Sharma, M.P. Selection of potential oils for biodiesel production. *Renew. Sustain. Energy Rev.* **2016**, *56*, 1129–1138. [CrossRef]
103. Basha, S.A.; Gopal, K.R.; Jebaraj, S. A review on biodiesel production, combustion, emissions and performance. *Renew. Sustain. Energy Rev.* **2009**, *13*, 1628–1634. [CrossRef]
104. Canoira, L.; Rodríguez-Gamero, M.; Querol, E.; Alcántara, R.; Lapuerta, M.; Oliva, F. Biodiesel from Low-Grade Animal Fat: Production Process Assessment and Biodiesel Properties Characterization. *Ind. Eng. Chem. Res.* **2008**, *47*, 7997–8004. [CrossRef]
105. Rezania, S.; Oryani, B.; Park, J.; Hashemi, B.; Yadav, K.K.; Kwon, E.E.; Hur, J.; Cho, J. Review on transesterification of non-edible sources for biodiesel production with a focus on economic aspects, fuel properties and by-product applications. *Energy Convers. Manag.* **2019**, *201*, 112155. [CrossRef]

106. Sander, A.; Koščak, M.A.; Kosir, D.; Milosavljević, N.; Vuković, J.P.; Magić, L. The influence of animal fat type and purification conditions on biodiesel quality. *Renew. Energy* **2018**, *118*, 752–760. [[CrossRef](#)]
107. Atadashi, I.; Aroua, M.K.; Aziz, A.A. High quality biodiesel and its diesel engine application: A review. *Renew. Sustain. Energy Rev.* **2010**, *14*, 1999–2008. [[CrossRef](#)]
108. Jagadale, S.S.; Jugulkar, L.M. Production and analysis of chemical properties of chicken fat based biodiesels and its various blends. *Int. J. Eng. Res. Dev.* **2012**, *1*, 34–37.
109. Herskowitz, M.; Landau, M.; Reizner, I.; Kaliya, M. Production of Diesel Fuel from Vegetable and Animal Oils. U.S. Patent Application US2006207166, 28 September 2006.
110. Herskowitz, M. Reaction System for Production of Diesel Fuel from Vegetable and Animal Oils. World Patent WO2008035155, 20 March 2008.
111. Hoff, M.V.; Benson, T.; Bell, J.; Pugh, M. Biodiesel Fuel Production, Separation Methods and Systems. U.S. Patent 13765782, 16 February 2012.
112. Lavella, P.S.R.; Pullo, P.; Pullo, G.V. Method and System for Integrated Biodiesel Production. U.S. Patent US20140020282A1, 23 January 2014.
113. Scott, M. Process for Producing Biodiesel and Related Products. World Patent WO2014202980A3, 19 June 2014.
114. Scott, M. Process for Producing Biodiesel and Related Products. China Patent CN106753812A, 31 May 2017.
115. Matsumura, M. Method for Producing Biodiesel Fuel. Japanese Patent JP2005350632A, 22 December 2015.
116. Matsumura, M. Technique for Producing Low-Exhaust Type Biodiesel Fuel. Japanese Patent JP2005350630A, 22 December 2015.
117. Stavarache, C.; Vinatoru, M.; Maeda, Y. Aspects of ultrasonically assisted transesterification of various vegetable oils with methanol. *Ultrason. Sonochem.* **2007**, *14*, 380–386. [[CrossRef](#)] [[PubMed](#)]
118. Breccia, A.; Esposito, B.; Fratadocchi, G.B.; Fini, A. Reaction Between Methanol and Commercial Seed Oils Under Microwave Irradiation. *J. Microw. Power Electromagn. Energy* **1999**, *34*, 3–8. [[CrossRef](#)]
119. Thompson, J.C.; He, B.B. Biodiesel Production Using Static Mixers. *Trans. ASABE* **2007**, *50*, 161–165. [[CrossRef](#)]
120. Canter, N. Making biodiesel in a microreactor. *Tribol. Lubr. Technol.* **2006**, *62*, 15–17.
121. Sun, J.; Ju, J.; Ji, L.; Zhang, L.; Xu, N. Synthesis of Biodiesel in Capillary Microreactors. *Ind. Eng. Chem. Res.* **2008**, *47*, 1398–1403. [[CrossRef](#)]
122. Madhawan, A.; Arora, A.; Das, J.; Kuila, A.; Sharma, S. Microreactor technology for biodiesel production: A review. *Biomass Convers. Biorefinery* **2017**, *8*, 485–496. [[CrossRef](#)]
123. Junior, J.M.C.; Naveira-Cotta, C.P.; De Moraes, D.B.; Neto, P.I.; Maia, I.A.; Da Silva, J.V.L.; Alves, H.; Tiwari, M.K.; Souza, C.G. Innovative Metallic Microfluidic Device for Intensified Biodiesel Production. *Ind. Eng. Chem. Res.* **2019**, *59*, 389–398. [[CrossRef](#)]
124. Harvey, A.P.; Mackley, M.R.; Seliger, T. Process intensification of biodiesel production using a continuous oscillatory flow reactor. *J. Chem. Technol. Biotechnol.* **2003**, *78*, 338–341. [[CrossRef](#)]
125. Marulanda, V.F.; Anitescu, G.; Tavlarides, L.L. Investigations on supercritical transesterification of chicken fat for biodiesel production from low cost lipid feedstocks. *J. Supercrit. Fluids* **2010**, *54*, 53–60. [[CrossRef](#)]
126. Sánchez, M.; Marchetti, J.M.; Boulifi, N.E.; Aracil, J.; Martínez, M. Kinetics of Jojoba oil methanolysis using a waste from fish industry as catalyst. *Chem. Eng. J.* **2015**, *262*, 640–647. [[CrossRef](#)]
127. Kouzu, M.; Kajita, A.; Fujimori, A. Catalytic activity of calcined scallop shell for rapeseed oil transesterification to produce biodiesel. *Fuel* **2016**, *182*, 220–226. [[CrossRef](#)]
128. Di Bitonto, L.; Pastore, C. Metal hydrated-salts as efficient and reusable catalysts for pre-treating waste cooking oils and animal fats for an effective production of biodiesel. *Renew. Energy* **2019**, *143*, 1193–1200. [[CrossRef](#)]
129. Ndiaye, M.; Arhaliass, A.; Legrand, J.; Roelens, G.; Kerihuel, A. Reuse of waste animal fat in biodiesel: Biorefining heavily-degraded contaminant-rich waste animal fat and formulation as diesel fuel additive. *Renew. Energy* **2020**, *145*, 1073–1079. [[CrossRef](#)]
130. Kpan, J.; Krahl, J. Sustaining the Oxidation Stability of Biodiesel and Its Blends in Plug-in Hybrid Vehicles Using Adsorbents. *Energy Fuels* **2019**, *33*, 11181–11186. [[CrossRef](#)]

131. Saeong, P.; Saisriyoot, M.; Thanapimmetha, A.; Srinophakun, P. The response surface optimization of steryl glucosides removal in palm biodiesel using silica adsorption. *Fuel* **2017**, *191*, 1–9. [CrossRef]
132. Neste Renewable Synthetic Diesel. 2020. Available online: https://web.archive.org/web/20100418133813/http://www.climatechange.ca.gov/events/2006-06-27+28_symposium/presentations/CalHodge_handout_NESTE_OIL.PDF (accessed on 5 May 2020).



© 2020 by the authors. Licensee MDPI, Basel, Switzerland. This article is an open access article distributed under the terms and conditions of the Creative Commons Attribution (CC BY) license (<http://creativecommons.org/licenses/by/4.0/>).

Article

Mesophilic and Thermophilic Anaerobic Digestion of Organic Fraction Separated during Mechanical Heat Treatment of Municipal Waste

Slawomir Kasinski

Department of Environmental Biotechnology, University of Warmia and Mazury in Olsztyn, Sloneczna St. 45G, 10-709 Olsztyn, Poland; slawek@kasinski.pl; Tel.: +48-604-580-234

Received: 18 February 2020; Accepted: 28 March 2020; Published: 1 April 2020

Abstract: The objective of this study was to investigate the effect of process temperature on semi-continuous anaerobic digestion of the organic fraction separated during autoclaving of municipal waste. Tests were carried out in reactors with full mixing. Biogas production was higher in thermophilic conditions than in mesophilic conditions (0.92 L/g volatile solids at 55 °C vs. 0.42 L/g volatile solids at 37 °C, respectively). The resulting methane yields were 0.25–0.32 L CH₄/g VS and 0.56–0.70 L CH₄/g VS in mesophilic and thermophilic conditions, respectively. In both variants, the methane share was over 70% *v/v*. This work also discusses the potential impact of Maillard compounds on the efficiency of the fermentation process, which were probably produced during the process of autoclaving of municipal waste. These results indicate that, after autoclaving, the organic fraction of municipal waste can be an effective substrate for anaerobic digestion in thermophilic conditions.

Keywords: Mechanical Heat Treatment; autoclaving; autoclaving of municipal waste; mesophilic fermentation; thermophilic fermentation; anaerobic digestion

1. Introduction

Mechanical Heat Treatment (MHT) is a relatively new and poorly investigated technology for processing municipal solid waste. MHT uses a combination of mechanical and thermal-based technologies to separate a waste stream into several component parts and enable further options for recycling and biological treatment. MHT sterilizes pathogens, deodorizes the waste stream, reduces waste mass (mainly by dehydration), compacts plastics and disintegrates labels on glass bottles, food packaging and cans. The separated utility fractions produced by MHT, including pre-residual derived fuel (pre-RDF), account for up to 80% of the initial waste mass [1].

The most common method of thermally treating municipal waste is autoclaving. This technology is used by the majority of existing European MHT plants operating on a technical scale [2]. Technologically, the MHT process consists of a grinding stage (I), autoclaving (II) and mechanical separation of material fractions (III). The largest fraction obtained during MHT is the organic remaining fraction (ORF), mechanically separated after full-scale autoclaving of unsorted municipal solid waste (Figure 1). Depending on the technological process and the composition of the waste, this fraction constitutes up to 61.5% of the initial weight of waste [3]. This fraction consists mainly of thermally processed organic waste, such as paper, kitchen and garden waste and other organics, which are turned into a very homogenous fibrous material under the influence of temperature [4]. According to Papadimitriou [1], a properly conducted MHT process enables approximately 80% of the initial waste stream to be recycled/recovered. However, this level of effectiveness can only be obtained if the entire organic fraction remaining after the process of autoclaving is managed.

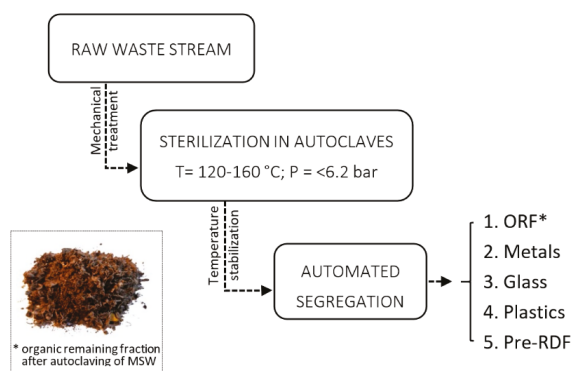


Figure 1. Flow-chart illustrating a process for Mechanical Heat Treatment of Municipal Solid Waste.

Although autoclaving dissolves paints on cans and other packages and thus could contribute to heavy metal pollution of organic fiber [4,5], contamination resulting from autoclaving is similar to that from the most effective mechanical–biological treatment systems [4]. The process of autoclaving disrupts the lignocellulosic structure in organic waste [6], which theoretically facilitates the decomposition of organic matter, both in aerobic and anaerobic conditions. A test performed by Wojnowska-Baryla et al. [7] showed that the effect of waste sterilization during autoclaving is not permanent, and the organic remaining fraction converts to biologically unstable material that could not be landfilled without posttreatment (ca. $AT_4 = 25 \text{ g O}_2 \text{ kg}^{-1} \text{ TS}$). The separated ORF can be also contaminated with glass and other foreign matter, which limits the production of high-quality compost [8]. For this reason, research on the aerobic treatment of the autoclaved organic fraction is being conducted with the goal of achieving aerobic stabilization, i.e., in passive aeration conditions [7]. Another test, performed by Kulikowska et al. [9], showed that stabilize from autoclaved municipal solid waste might be a source of valuable humic substances (HS). The maximum HS production of 82–120 mg/g OM was similar to that in composts from different kinds of organic waste, which partly justifies the practical use of the autoclave process in a waste circular economy.

Due to the above-mentioned problems with compost management after autoclaving, there is interest in anaerobic digestion of autoclaved organic wastes. However, research done so far has usually been carried out in batch conditions, with the use of agricultural waste or synthetically prepared organic waste. Menardo et al. [10] investigated the impact of the autoclaving process on anaerobic digestion of swine slurry and obtained 115% higher production of methane when the slurry was autoclaved at 120 °C. Similarly, when waste activated sludge was digested in a CSTR reactor, methane production was 12% and 25% higher after autoclaving at 135 °C and 190 °C, respectively, than without autoclaving [11]. In contrast, some data indicates decreased biogas production and biodegradability of autoclaved organic mass. Tampio et al. [12] compared the efficiency of anaerobic digestion of autoclaved (160 °C, 6.2 bar) and untreated food waste in semi-continuously fed mesophilic reactors. The authors observed lower specific methane yield during digestion of autoclaved substrate even after a long period of microbial acclimatization (473 days of the process). Similar results were obtained by García et al. [5], who compared the efficiency of the process of anaerobic digestion of autoclaved (145 °C, 600 kPa) and untreated source-separated OFMSW (organic fraction of municipal solid waste). Both Tampio et al. [12], as well as García et al. [5], indicate that reduced biogas production can be caused by Maillard compounds produced during the autoclaving process.

It should be clearly stated that there is a lack of research using autoclaved organic municipal waste, especially that obtained from installations operating under technical conditions. Due to the fact that MHT is a technology in the developmental phase, there is a need to expand knowledge in this field. The uniqueness of the organic remaining fraction obtained during MHT of municipal waste, including

its homogeneity and fibrous structure, makes it impossible to determine the impact of the autoclaving process on anaerobic digestion of ORF. However, anaerobic digestion of ORF obtained during the autoclaving process still is an interesting and noteworthy topic. Therefore, the objective of this study was to investigate the effect of process temperature on anaerobic digestion of the organic remaining fraction mechanically separated after full-scale autoclaving of unsorted municipal solid waste. The tests were carried out in mesophilic and thermophilic conditions in reactors with full mixing.

2. Materials and Methods

2.1. Methods of Sampling and Characteristics of Test Material

Substrates for anaerobic digestion were obtained from the organic fraction of municipal waste separated in the MHT plant in Różanki (Poland). Autoclaving was preceded by the separation of large waste items from the mixed waste stream and mechanical homogenization (pre-preparation) to achieve grain sizes of <350 mm. The pre-prepared waste was treated in autoclaves under saturated steam conditions, at 120 °C–150 °C and 2–5 bar. The production and condensation of steam took place in a closed system. Mechanical treatment took place after the autoclaving process to separate recyclable materials. After autoclaving, the separated ORF had a particle size of <10 mm and comprised ca. 30% of the waste.

A sample of ORF for anaerobic digestion was collected from a randomly formed heap of about 5 m³, from which the laboratory sample was separated by the trapezoidal diverging method [13]. In accordance with the methodology, the sample was divided into three laboratory parts with a total volume of 45 L, which were then transported in sterile containers to the testing site. One part was subjected to basic physico-chemical and respirometric tests. The remaining two parts were ground to a grain size of <1 mm and then used as the research substrate. The grinding was necessary to facilitate feeding of the waste into the reactor through the narrow hole of the shutoff valve. Additionally, according to Izumi et al. [14], grinding enhances the solubilization of organic matter, which was important during the preparation of the feeding mixture (described in Section 2.3). Grinding also affects the process of methanization of organic matter [14].

The physico-chemical properties of ORF are presented in Table 1. The ORF sample for anaerobic digestion had a neutral pH and an organic substance content of 58% DM. Morphological analysis indicated that this fraction was homogenous and had a glass share of 1–2% by mass, which limits its use as soil conditioner. The fraction showed high hygroscopicity—opening a container with a sample caused the dry matter content to decrease from 84% to 69% within 7 days. At 31% humidity, the AT4 value was 26.09 g O₂/kg DM, which indicated the need to stabilize the fraction prior to storage. The analytical methods used for physico-chemical characterization of ORF are described below in Section 2.4.

Table 1. Characteristics of organic remaining fraction (ORF) after autoclaving, fraction <10 mm.

Characteristic	Unit	Value
pH	-	7.5
COD (soluble)	mg/L	4140
Total Nitrogen (N)	% w/w	1.07
Ammonia Nitrogen	% w/w	0.08
Phosphorus	% w/w	0.50
Total solids	% w/w	84
Volatile solids	% DM	58
AT4	mg O ₂ /g DM	26.09

2.2. Test Stand

Anaerobic digestion experiment was carried out in accordance with VDI [15] and DIN [16] standards. The tests were carried out in two stainless steel fermenters with full mixing and an active

volume of 6 L. The fermenters were equipped with an agitator with adjustable rotation speed and a heating mantle. Properly located valves enabled substrate feeding and collection of post-fermentation residues. The produced gas was collected with a separate valve in Tedlar bags. The reactors worked in a semi-continuous system and were fed with the sterile waste substrate once a day after the collection of post-fermentation waste. A scheme of the reactors is presented in Figure 2.

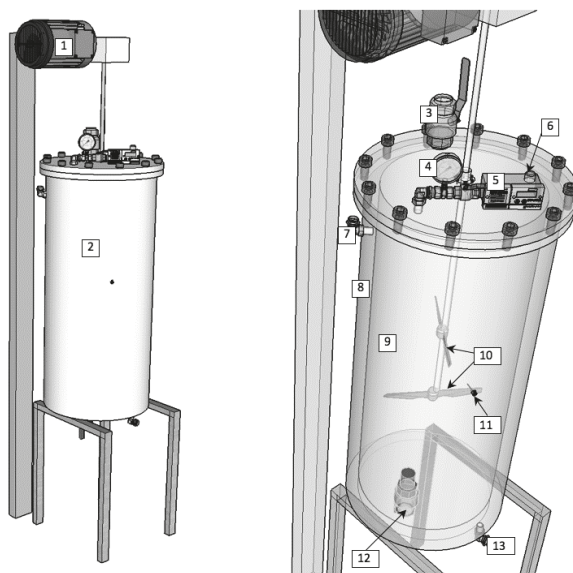


Figure 2. Experimental stand. (1) Electric engine, (2) fermenter with tooling, (3) shutoff valve/substrate feeder, (4) manometer, (5) biogas flow meter, (6) biogas outlet, (7) water jacket feed valve, (8) watercoat, (9) reactor chamber, (10) stirrers, (11) PT-100 temperature sensor, (12) shutoff valve/post-fermentation outlet, (13) water jacket drain valve.

2.3. Digestion Set-up

Technological studies were carried out for 90 days in two technological variants differing in process temperature. Variant 1 was conducted at 37 °C; variant 2, at 55 °C. In both variants, the organic loading rate (OLR) and the hydraulic retention time (HRT) were 2 g VS/L-d and 30 d, respectively.

The feed was the ground ORF separated by MHT of municipal waste and mixed with tap water at a ratio of 1:7. The reactor was inoculated with anaerobic sludge originating from the municipal wastewater treatment plant in Olsztyn (north of Poland, population 175,000). The characteristics of the inoculum were as follows: pH, 7.31; COD, 1520 mg/L; ammonium, 88 mg NNH₄/L; alkalinity, 77 mval/L; concentration of total solids, 76.2 g/L; phosphate, 409 mg P-PO₄/L. For acclimatization to the temperature in the reactor, the inoculum was left in the reactor for 20 days, after which, dosing of the substrate to the reactor began.

2.4. Analytical Monitoring of the Process

The separated ORF after autoclaving was analyzed in terms of pH, COD, total nitrogen, ammonium nitrogen, phosphorus, total solids and volatile solids. The analyses were performed by the Institute of Soil Science and Plant Cultivation (IUNG), State Research Institute in Puławy, Poland. As presented above, at the start of the experiment, the inoculum was analyzed to measure the pH, COD, ammonium, alkalinity, total solids concentration and phosphates.

The post-fermentation residues were analyzed in terms of total solids and volatile solids concentration. The liquid phase of the post-fermentation residues (obtained by centrifuging the digestate samples for 10 min at 9000 rpm) was analyzed with regard to pH, COD, ammonium nitrogen, phosphates and volatile fatty acids (VFAs). The analyses of post-fermentation residues were performed at one-day intervals during the first 20 days and then at two-day intervals.

Analyses of total solids, volatile solids, COD, alkalinity, ammonium nitrogen and phosphates conducted by IUNG and in our laboratories were all performed according to standard methods for examination of water and wastewater, APHA [17]. According to the methodology of the IUNG, total nitrogen was analyzed by elemental analysis using a FLASH 2000 elemental analyzer (Thermo Scientific, USA), phosphorus content was analyzed by the spectrophotometric method based on an ammonium molybdate reaction.

VFAs (acetate, propionate, isobutyrate, butyrate, isovalerate, valerate, isocaproate and caproate) were analyzed using a gas chromatograph (GC, Varian 3800, Australia) equipped with a capillary column (Factor-Four VF-1 ms, 30 m × 0.25 mm i.d., 1.0 μm film; Varian). A volatile acid standard mix (Supelco, USA) was used as the standard. The flame ionization detector (FID) was operated at 280 °C with an injection port temperature of 250 °C. The split ratio was 1:100. The initial column temperature was set to 100 °C, then raised at a rate of 20 °C/min to 200 °C and finally held at 200 °C for 1 min. Helium was used as the carrier gas at a flow rate of 1.0 mL/min. Samples were prepared for VFA analysis according to Gilroyed et al. (2010).

To determine the biological stability of the ORF, the AT4 analysis was performed. The AT4 analysis (performed in triplicate) is a respiration test employing a manometric method, which was performed with the Oxitop Control measuring system. Waste samples were incubated at 20 °C in the presence of a 1M sodium hydroxide solution (for CO₂ absorption) for four days.

The volume and composition of the biogas produced during fermentation were monitored. This analysis was carried out daily on averaged samples collected in Tedlar bags. The gas composition, including oxygen, carbon dioxide and methane content, was measured using a GA 2000 PLUS gas analyzer (Geotech).

3. Results and Discussion

During the first 50 days of fermentation, the biogas productivity was similar in both mesophilic (37 °C) and thermophilic conditions (55 °C): 3154–7803 mL/d and 3365–6874 mL/d, respectively, corresponding to yields of 0.26–0.65 L/g VS and 0.28–0.57 L/g VS, respectively. After 50 days, biogas productivity was higher in thermophilic conditions than in mesophilic conditions. In thermophilic conditions, the productivity first increased to about 12,000 mL/d (2000 mL/L), then stabilized at about 11,000 mL/d (0.92 L/g VS). In mesophilic conditions, the biogas productivity was about 5000 L/d (0.42 L/g VS). After initial fluctuations, in both variants, the production of biogas stabilized on about the 70th day of the process. The resulting methane yields were 0.25–0.32 L CH₄/g VS and 0.56–0.70 L CH₄/g VS in mesophilic and thermophilic conditions, respectively (Figure 3).

This difference in biogas productivity between mesophilic and thermophilic conditions is consistent with what has been reported in the literature [18]. Interestingly, however, the biogas productivity in the present study is higher than that in other studies. For example, Cavinato et al. [19] reported that, during co-fermentation of waste activated sludge with biowaste, the specific biogas production increased from 0.34 to 0.49 L/g TVS when the reactor temperature was changed from mesophilic (37 °C) to thermophilic (55 °C). The final values of methane yield, however, seem to be higher than those reported in the literature. Forster-Carneiro et al. [20] examined anaerobic digestion under thermophilic conditions (55 °C) of three source-separated organic fractions of waste: food waste, OFMSW and shredded OFMSW. The authors obtained methane yields of 0.18 L CH₄/g VS, 0.05 L CH₄/g VS and 0.08 L CH₄/g VS, respectively. Zhang et al. [21], during batch anaerobic digestion of source-separated food wastes, obtained 0.43 L CH₄/g VS. Interestingly, the authors used grinding and freezing as a

method of pre-treatment and noted that the average methane content of biogas was 73%, similar to the present results.

In the initial phase of fermentation, the methane content in the biogas increased to around 70% and 60% *v/v* at 37 °C and 55 °C, respectively. Then, regardless of the process temperature, methane synthesis slowed. At 37 °C, the slowdown took place between the 12th and 44th day; and at 55 °C, between the 12th and 50th day. In the stabilization phase, the methane content was about 75% *v/v* in both variants (Figure 4).

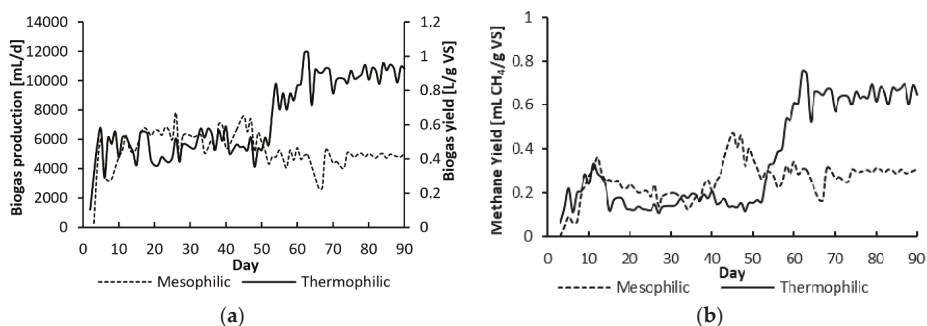


Figure 3. Biogas production (a) and methane yield properties (b) obtained during the anaerobic digestion of ORF.

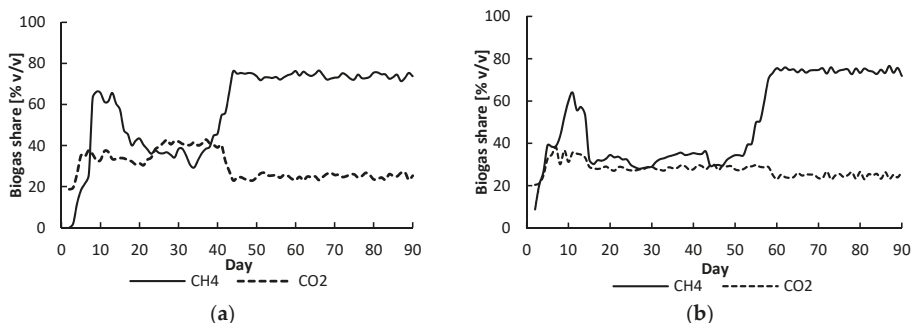


Figure 4. Changes in the biogas composition during the anaerobic digestion of ORF; (a) mesophilic—temperature 37 °C, (b) thermophilic—temperature 55 °C.

In the present study, the short burst of intense methanogenic activity at the start of the process can be explained by the fact that anaerobic digester sludge was used as the inoculum. This type of sludge has been reported to be the best inoculum for a rapid start-up, as it has much higher numbers of acetoclastic methanogens than other start-up materials, such as cattle manure [22]. The subsequent slowdown in methane synthesis in both research variants may be related to the need for the microorganisms to adapt to the new substrate, as the methane share did not correlate with the other process parameters that were monitored. It is interesting to note, however, that not only was the proportion of methane high in comparison to other literature reports [23,24], but the methane content was high in both variants despite substantial differences in the process parameters (pH, VFA concentration).

The VFA concentrations differed in the two variants. At 37 °C, the VFA concentration first increased, then decreased and stabilized at about 600 mg VFA/L. At 55 °C, the VFA concentration increased from day 20 of the process, after which it ranged from 1500 to 2500 mg/L until it stabilized at 2400–2600 mg/L. In both reactors, the concentration of propionic acid was higher than that of acetic acid. From day 20 of the process, the acetic acid concentration was around 5.5-times higher at 55 °C

than at 37 °C. At 55 °C, the concentrations of caproic and isobutyric acids were 147–184 mg/L and 84–101 mg/L, respectively. At 37 °C, in contrast, these acids were present only during the earlier stages of the process and their concentrations were relatively low (Figure 5).

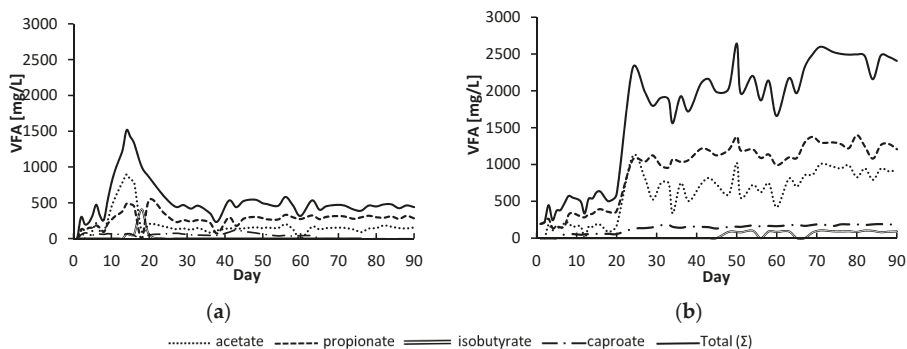


Figure 5. Qualitative and quantitative changes of volatile fatty acids (VFA) during the anaerobic digestion of ORF after autoclaving; (a) mesophilic—temperature 37 °C, (b) thermophilic—temperature 55 °C.

At both operational temperatures, propionate constituted the majority of the VFAs. Similar results were obtained by Kim et al. [25] during co-digestion of anaerobic sludge and dog food in a CSTR reactor and by Labatut et al. [26] during co-digestion of cow manure and dog food in a CSADs reactor. Labatut et al. [26] attributed propionate accumulation to free energy limitations imposed by molecular hydrogen. According to the authors, thermophilic bacteria that oxidize LCFA have a higher PH₂ threshold than their mesophilic counterparts (10–2.4 atm vs. 10–3 atm, respectively). Thus, LCFAs can be degraded to a greater extent at thermophilic temperatures, potentially producing additional H₂ and further inhibiting propionate oxidation. This, compounded by faster hydrolysis rates, can make thermophilic digesters more susceptible to propionate accumulation, and consequently process upsets. However, this is only speculation in the case of the present study, as the partial hydrogen pressure was not measured during the tests.

Another interesting hypothesis concerns the effect of compounds formed during Maillard's reaction on the efficiency of methanogenesis. These compounds are produced by reactions between amino acids and carbohydrates at temperatures above 100 °C [27,28], and they inhibit microbial activity [29,30]. It can, therefore, be assumed that such compounds were formed during autoclaving of the municipal waste used in the present study. This may well have lowered the efficiency of anaerobic digestion in mesophilic conditions, as reported by Tampio et al. [12] and García et al. [5]. In addition, the efficiency of anaerobic digestion under mesophilic conditions was not reduced in the present study, as also reported by Nakajima-Kambe et al. [31]. This suggests that, under thermophilic conditions, the microorganisms adapted to the presence of Maillard compounds. Considering that the methanogens' activity was not lowered, an explanation would be the inhibitory effect of Maillard compounds on the acetogenesis process at 37 °C, which would result in less biogas production with a higher methane content. However, it should be remembered that other inhibitors, such as furfural, hydroxymethylfurfural (HMF) or phenols could also be formed during the autoclaving process. Thus, further investigations would be necessary to indicate which inhibitors were present.

During fermentation at 37 °C, the pH remained between 7.84 and 8.33. At 55 °C, it was higher and ranged from 8.03 to 8.51. Similar results were obtained by Song et al. [32] during single-stage mesophilic and thermophilic digestion of sewage sludge. Normally, increased gas production accompanies increasing pH because methanogenesis reduces VFA and produces alkalinity. In the presented studies, the changes in VFA did not affect the pH changes during fermentation. Song et al. [32] indicate that the increase in pH was caused by the degradation of nitrogenous compounds; nevertheless,

in the present studies, such an association was not found (Figure 6). In both research variants, an increase in the concentration of dissolved organic compounds in the reactors was observed. At 37 °C, the increase occurred in the first 15 days and was on average 218 mg COD/L·d. After this time, the COD concentration stabilized at a level between 3200 and 3680 mg COD/L. At 55 °C, the concentration of organic compounds dissolved on day 70 of the process increased by an average of 52 mg/L·d. After this time, the concentration stabilized within the range of 4840–5000 mg/L. From day 70 of the process, COD concentration was about 1.4 times higher at 55 °C than at 37 °C (Figure 6). The course of changes in the concentration of ammonium nitrogen in both reactors was similar. After an initial increase, the ammonium nitrogen concentration dropped, then increased starting on day 30 and, finally, stabilized from the 70th day at 169–207 mg/L and 262–304 mg/L at 37 °C and 55 °C, respectively. The initial concentration of orthophosphate was two-fold lower at 37 °C than at 55 °C, and it decreased at a rate two-times slower (0.63 mg/L·d). The final concentrations of orthophosphate were 19.96 mg/L and 28.43 mg/L at 37 °C and 55 °C, respectively (Figure 6). The initial increase in nitrogen concentration was related to the rapid biodegradation of the organic matter contained in the autoclaved municipal waste. The slowdown of the biodegradation process from the 30th day of the process may have been due to the inhibitory effect of ammonium nitrogen on the fermentation process [33,34], the effect of Maillard compounds, or the effect of other inhibitory compounds formed during the autoclaving process. From the 70th day of the process, ammonium nitrogen and other process indicators (COD, phosphate, VS) stabilized, which confirms that the microorganisms had adapted to the process conditions, which is similar to the findings of Hashimoto [35].

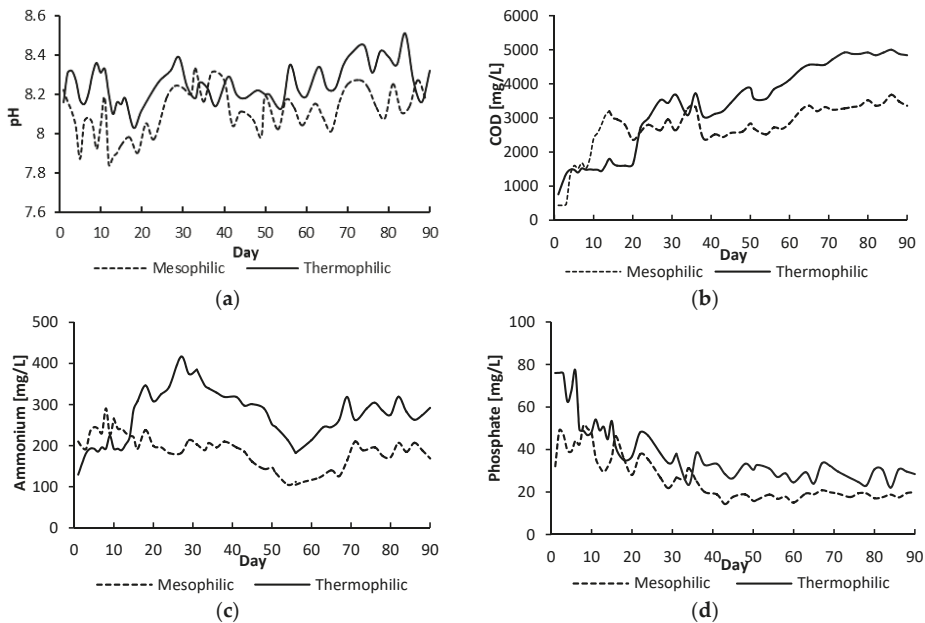


Figure 6. Changes of pH (a), dissolved organic matter (COD) (b), ammonium nitrogen (c) and orthophosphates (d) during the anaerobic digestion of ORF after autoclaving.

The results of Fisher’s exact test ($p = 0.29609$) did not show a significant effect of temperature on the efficiency of organic compounds removal. The efficiency of organic compounds removal in the initial stage was above 90%. After 70 days of anaerobic digestion, it dropped to 67–69% at 37 °C and 68–71% at 55 °C. Until the first complete replacement of the reactor volume (day 30), the average reduction in organic compound removal at 37 °C was 0.53%/d, after which it was 0.08%/d, although the technological conditions

remained the same. In the second variant, the changes were slower: 0.37%/d and 0.1%/d, respectively. The reduction in the use of organic compounds by microorganisms resulted in an increase in dry matter in the reactors. During the first 30 days, the changes took place more dynamically: at 37 °C, the organic dry matter content increased from 6.02 to 12.77 g/L; and at 55 °C, from 3.67 to 12.54 g/L. From the 70th day of the fermentation process, stabilization of the organic dry matter content was observed in both reactors at 18.39–20.14 g/L and 17.67–19.34 g/L, respectively (Figure 7).

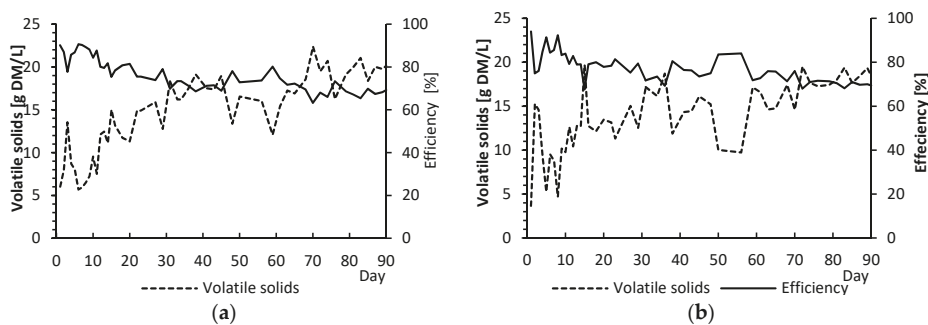


Figure 7. Efficiency of removal of organic compounds during the anaerobic digestion of ORF after autoclaving; (a) mesophilic—temperature 37 °C, (b) thermophilic—temperature 55 °C.

The lack of a significant influence of temperature on the intensity of the transformation of organic compounds seems to be consistent with other reports. Similar results were obtained by Song et al. [26] during a single stage of mesophilic and thermophilic fermentation of sewage sludge. In the present study, ammonium nitrogen accumulated along with an increase in VS. This is particularly evident under thermophilic conditions, in which accumulation of VS and ammonium nitrogen occurred on the 30th day of the process (correlation coefficient = 0.71). In mesophilic conditions, no correlation between these parameters was found.

4. Conclusions

The obtained results indicate that temperature influences the efficiency of the fermentation process. The process carried out under thermophilic conditions (55 °C) was characterized by higher biogas productivity, higher production of fatty acids, higher pH, higher concentration of chemical compounds and higher efficiency of organic compounds removal. In the present study, the biogas productivity at 55 °C at the time of process stabilization was 0.92 L/g VS, which was double the productivity at 37 °C (0.42 L/g VS). This is not surprising, considering that overall digestion rates can be up to 2.25 times faster at thermophilic temperatures than at mesophilic ones [18]. It should be assumed that the adaptation of microorganisms to the substrate took place around the 70th day of the process. Taking into account the characteristics of the substrate given in Table 1, biogas productivity was 0.20 m³/Mg FM and 0.45 m³/Mg FM, which is particularly interesting for application purposes on a technical scale.

This study has shown that the organic fraction of municipal waste separated during MHT of municipal waste can be an effective substrate for anaerobic digestion in thermophilic conditions.

Funding: Project financially supported by Minister of Science and Higher Education the range of the program entitled “Regional Initiative of Excellence” for years 2019–2020, project No. 010/RID/2018/19, amount funding 12.000.000 PLN.

Conflicts of Interest: The authors declare no conflicts of interest.

References

1. Papadimitriou, E.K. *Evaluating the Effect of Autoclaving on the Rate of Bioprocessing of Waste—Characteristics of Autoclaving Condensate and Autoclaved Biodegradables from Non-Segregated MSW; Report to Defra*; University of Leeds: Leeds, UK, 2007.
2. Bien, J.D. Mechanical Heat Treatment (MHT) of Municipal Waste in the Context of Circular Economy (Polish). *Eng. Prot. Environ.* **2017**, *2*, 221–236. [[CrossRef](#)]
3. Papageorgiou, A.; Barton, J.R.; Karagiannidis, A. Assessment of the greenhouse effect impact of technologies used for energy recovery from municipal waste: A case for England. *J. Environ. Manag.* **2009**, *90*, 2999–3012. [[CrossRef](#)] [[PubMed](#)]
4. Papadimitriou, E.K.; Barton, J.R.; Stentiford, E.I. Sources and levels of potentially toxic elements in the biodegradable fraction of autoclaved non-segregated household waste and its compost/digestate. *Waste Manag. Res.* **2008**, *26*, 419–430. [[CrossRef](#)] [[PubMed](#)]
5. García, A.; Maulini, C.; Torrente, J.M.; Sánchez, A.; Barrena, R.; Font, X. Biological treatment of the organic fibre from the autoclaving of municipal solid wastes; preliminary results. *Biosyst. Eng.* **2012**, *112*, 335–343. [[CrossRef](#)]
6. Papadimitriou, E.K. Hydrolysis of organic matter during autoclaving of commingled household waste. *Waste Manag.* **2010**, *30*, 572–582. [[CrossRef](#)]
7. Wojnowska-Baryła, I.; Kulikowska, D.; Bernat, K.; Kasiński, S.; Zaborowska, M.; Kielak, T. Stabilisation of municipal solid waste after autoclaving in a passively aerated bioreactor. *Waste Manag. Res.* **2019**, *37*, 542–550. [[CrossRef](#)]
8. Eley, M.H.; Guinn, G.R.; Bagghi, J. Cellulosic materials recovered from steam classified municipal solid wastes as feedstocks for conversion to fuels and chemicals. *App. Biochem. Biotechnol.* **1995**, *51/52*, 387–397. [[CrossRef](#)]
9. Kulikowska, D.; Bernat, K.; Wojnowska-Baryła, I.; Klik, B.; Michałowska, S.; Kasiński, S. Stabilizate from Autoclaved Municipal Solid Waste as a Source of Valuable Humic Substances in a Waste Circular Economy. *Waste Biomass Valoriz.* **2019**, 1–11. [[CrossRef](#)]
10. Menardo, S.; Balsari, P.; Dinuccio, E.; Gioelli, F. Thermal pre-treatment of solid fraction from mechanically-separated raw and digested slurry to increase methane yield. *Bioresour. Technol.* **2011**, *102*, 2026–2032. [[CrossRef](#)]
11. Bougrier, C.; Delgenès, J.P.; Carrère, H. Effects of thermal treatments on five different waste activated sludge samples solubilisation, physical properties and anaerobic digestion. *Chem. Eng. J.* **2008**, *139*, 236–244. [[CrossRef](#)]
12. Tampio, E.; Ervasti, S.; Paavola, T.; Heaven, S.; Banks, C.; Rintala, J. Anaerobic digestion of autoclaved and untreated food waste. *Waste Manag.* **2014**, *34*, 370–377. [[CrossRef](#)] [[PubMed](#)]
13. Kasinski, S.; Slota, M.; Markowski, M.; Kaminska, A. Municipal waste stabilization in a reactor with an integrated active and passive aeration system. *Waste Manag.* **2016**, *50*, 31–38. [[CrossRef](#)]
14. Izumi, K.; Okishio, Y.K.; Nagao, N.; Niwa, C.; Yamamoto, S.; Toda, T. Effects of particle size on anaerobic digestion of food waste. *Int. Biodeterior. Biodegrad.* **2010**, *64*, 601–608. [[CrossRef](#)]
15. VDI 4630. *Fermentation of organic materials: Characterisation of Substrate, Sampling, Collection of Material Data, Fermentation Tests [1872]*; VDI Gesellschaft Energietechnik: Düsseldorf, Germany, 2006.
16. DIN 38 414-8: *German Standard Methods for the Examination of Water, Waste Water and Sludge; Sludge and Sediments (group S). Determination of the Amenability to Anaerobic Digestion (S 8)*; Deutsches Institut für Normung e.V.: Berlin, Germany, 1985.
17. American Public Health Association (APHA). *Standard Methods for the Examination of Water and Wastewater*, 18th ed.; American Public Health Association: Washington, DC, USA, 1992.
18. O'Rourke, J.T. *Kinetics of Anaerobic Waste Treatment at Reduced Temperatures*; Stanford University: Stanford, CA, USA, 1968.
19. Cavinato, C.; Bolzonella, D.; Pavan, P.; Fatone, F.; Cecchi, F. Mesophilic and thermophilic anaerobic co-digestion of waste activated sludge and source sorted biowaste in pilot-and full-scale reactors. *Renew. Energy* **2013**, *55*, 260–265. [[CrossRef](#)]
20. Forster-Carneiro, T.; Pérez, M.; Romero, L.I. Thermophilic anaerobic digestion of source-sorted organic fraction of municipal solid waste. *Bioresour. Technol.* **2008**, *99*, 6763–6770. [[CrossRef](#)] [[PubMed](#)]

21. Zhang, R.; El-Mashad, H.M.; Hartman, K.; Wang, F.; Liu, G.; Choate, C.; Gamble, P. Characterization of food waste as feedstock for anaerobic digestion. *Bioresour. Technol.* **2007**, *98*, 929–935. [[CrossRef](#)] [[PubMed](#)]
22. Tyagi, V.K.; Fdez-Güelfo, L.A.; Zhou, Y.; Álvarez-Gallego, C.J.; Garcia, L.R.; Ng, W.J. Anaerobic co-digestion of organic fraction of municipal solid waste (OFMSW): Progress and challenges. *Renew. Sustain. Energy Rev.* **2018**, *93*, 380–399. [[CrossRef](#)]
23. Liu, D.; Liu, D.; Zeng, R.J.; Angelidaki, I. Hydrogen and methane production from household solid waste in the two-stage fermentation process. *Water Res.* **2006**, *40*, 2230–2236. [[CrossRef](#)]
24. Vindis, P.; Mursec, B.; Janzekovic, M.; Cus, F. The impact of mesophilic and thermophilic anaerobic digestion on biogas production. *J. Achiev. Mater. Manuf. Eng.* **2009**, *36*, 192–198.
25. Kim, M.; Ahn, Y.H.; Speece, R.E. Comparative process stability and efficiency of anaerobic digestion; mesophilic vs. thermophilic. *Water Res.* **2002**, *36*, 4369–4385. [[CrossRef](#)]
26. Labatut, R.A.; Angenent, L.T.; Scott, N.R. Conventional mesophilic vs. thermophilic anaerobic digestion: A trade-off between performance and stability? *Water Res.* **2014**, *53*, 249–258. [[CrossRef](#)] [[PubMed](#)]
27. Müller, J.A. Prospects and problems of sludge pre-treatment process. *Water Sci. Technol.* **2001**, *44*, 121–128. [[CrossRef](#)] [[PubMed](#)]
28. Nursten, H.E. *The Maillard Reaction: Chemistry, Biochemistry and Implications*; Royal Society of Chemistry: London, UK, 2005.
29. Chandra, R.; Bharagava, R.N.; Rai, V. Melanoidins as major colourant in sugarcane molasses based distillery effluent and its degradation. *Bioresour. Technol.* **2008**, *99*, 4648–4660. [[CrossRef](#)] [[PubMed](#)]
30. Kim, K.W.; Lee, S.B. Inhibitory effect of Maillard reaction products on growth of the aerobic marine hyperthermophilic archaeon *Aeropyrum pernix*. *Appl. Environ. Microbiol.* **2003**, *69*, 4325–4328. [[CrossRef](#)] [[PubMed](#)]
31. Nakajima-Kambe, T.; Shimomura, M.; Nomura, N.; Chanpornpong, T.; Nakahara, T. Decolorization of molasses wastewater by *Bacillus* sp. under thermophilic and anaerobic conditions. *J. Biosci. Bioeng.* **1999**, *87*, 119–121. [[CrossRef](#)]
32. Song, Y.C.; Kwon, S.J.; Woo, J.H. Mesophilic and thermophilic temperature co-phase anaerobic digestion compared with single-stage mesophilic and thermophilic digestion of sewage sludge. *Water Res.* **2004**, *38*, 1653–1662. [[CrossRef](#)]
33. Gallert, C.; Winter, J. Mesophilic and thermophilic anaerobic digestion of source-sorted organic wastes: Effect of ammonia on glucose degradation and methane production. *Appl. Microbiol. Biotechnol.* **1997**, *48*, 405–410. [[CrossRef](#)]
34. Poggi-Varaldo, H.M.; Rodriguez-Vazquez, R.; Fernandez-Villagomez, G.; Esparza-Garcia, F. Inhibition of mesophilic solid-substrate anaerobic digestion by ammonia nitrogen. *Appl. Microbiol. Biotechnol.* **1997**, *47*, 284–291. [[CrossRef](#)]
35. Hashimoto, A.G. Thermophilic and mesophilic anaerobic fermentation of swine manure. *Agric. Wastes* **1983**, *6*, 175–191. [[CrossRef](#)]



© 2020 by the author. Licensee MDPI, Basel, Switzerland. This article is an open access article distributed under the terms and conditions of the Creative Commons Attribution (CC BY) license (<http://creativecommons.org/licenses/by/4.0/>).

Article

Effects of Crop Protection Unmanned Aerial System Flight Speed, Height on Effective Spraying Width, Droplet Deposition and Penetration Rate, and Control Effect Analysis on Wheat Aphids, Powdery Mildew, and Head Blight

Songchao Zhang ^{1,2,3}, Baijing Qiu ^{1,2,*}, Xinyu Xue ^{3,*}, Tao Sun ³, Wei Gu ³, Fuliang Zhou ⁴ and Xiangdong Sun ⁵

¹ Key Laboratory of Modern Agricultural Equipment and Technology, Ministry of Education, Jiangsu University, Zhenjiang 212013, China; zhangsongchao@caas.cn

² Key Laboratory of Plant Protection Engineering, Ministry of Agriculture and Rural Affairs, Zhenjiang 212013, China

³ Nanjing Institutes of Agricultural Mechanization, Ministry of Agriculture and Rural Affairs, Nanjing 210014, China; sun13951662796@sina.com (T.S.); guwei01@caas.cn (W.G.)

⁴ Nanjing University of Aeronautics and Astronautics, Nanjing 210016, China; zhoufuliang_uav@sina.com

⁵ Wuxi Hanhe Aviation Technology Co., Ltd., Wuxi 214135, China; tongxm@hanhe-aviation.com

* Correspondence: qbj@ujs.edu.cn (B.Q.); xuexinyu@caas.cn (X.X.); Tel.: +86-511-8879-7338 (B.Q.); +86-25-8434-6243 (X.X.)

Abstract: As a new type of crop protection machinery, the Crop Protection Unmanned Aerial System (CPUAS) has developed rapidly and been widely used in China; currently, how to use the CPUAS scientifically has become a top priority. However, the relationships between the operating parameters of the CPUAS and the effective spraying width (ESW), droplet distribution characteristics, and control effects of insect pests and diseases are not clear yet. Therefore, three levels of flight speed (FS) as 3, 4, and 5 m/s, three levels of flight height (FH) as 1.5, 2.0, and 2.5 m, and spraying volume 2.0 L/min experiments were carried out to investigate the effects of FS and FH on the ESW, droplet deposition uniformity (DDU), and droplet penetration rate (DPR) by using an electric single-rotor CPUAS CE20. Based on the obtained results, combined with the insect pests and diseases occurrence agronomic laws, the optimal operation parameters of the CPUAS were selected to control the wheat aphids, powdery mildew, and head blight. The results showed that the ESW of CE20 was not consistent, the maximum value was 5.78 m, and the minimum one was 2.51 m. The FS had a highly significant impact on ESW ($p = 0.0033 < 0.01$), while the FH and the interaction between FS and FH had no significant impact on ESW. The coefficients of variation (CV) of the droplet deposition were between 23.3% and 34.4%, which meant good deposition uniformity. The FH ($p = 0.0019$) and the interaction between FS and FH ($p = 0.02$) had significant impacts on the DDU. The control effects on aphids were 78.71% (1 day), 84.88% (3 days), and 90.42% (7 days), the control effects on powdery mildew were 77.17% (7 days) and 82.83% (14 days), and the control effect on head blight was 88.32% (20 days). This study proved that by the optimization of parameters and the combination of agronomy, good control effects for insect pests and diseases could be achieved by the CPUAS. The research results would provide some technical supports for CPUAS application.

Keywords: crop protection UAS; operation parameters; wheat agronomy; droplet distribution; aphid; powdery mildew; head blight; control effect



Citation: Zhang, S.; Qiu, B.; Xue, X.; Sun, T.; Gu, W.; Zhou, F.; Sun, X. Effects of Crop Protection Unmanned Aerial System Flight Speed, Height on Effective Spraying Width, Droplet Deposition and Penetration Rate, and Control Effect Analysis on Wheat Aphids, Powdery Mildew, and Head Blight. *Appl. Sci.* **2021**, *11*, 712. <https://doi.org/10.3390/app11020712>

Received: 20 December 2020

Accepted: 10 January 2021

Published: 13 January 2021

Publisher's Note: MDPI stays neutral with regard to jurisdictional claims in published maps and institutional affiliations.



Copyright: © 2021 by the authors. Licensee MDPI, Basel, Switzerland. This article is an open access article distributed under the terms and conditions of the Creative Commons Attribution (CC BY) license (<https://creativecommons.org/licenses/by/4.0/>).

1. Introduction

Wheat (*Triticum aestivum*) is one of the four major food crops in China, which is also one of the most important food crops around the world. The high yield of wheat is of great significance for solving the problems of poverty and hunger. The aphid (*Aphidoidea*) [1,2], powdery mildew (*Blumeria graminis*) [3,4], and head blight (*Fusarium graminearum* Schw.) [5]

are the major insect pest and diseases threatening the high quality and yield of wheat, which could occur from the turning green stage to the flowering stage. According to the forecast report from the National Agro-Tech Extension and Service Center of China on 13 November 2020, only the head blight would occur in an area of 6 million hectares in China in 2021, and 133.33 million hectares need to be prevented and controlled totally. How to effectively and quickly control insect pests and diseases of wheat, especially aphids, powdery mildew, and head blight is an urgent problem that farmers need to address.

In recent years, the Crop Protection Unmanned Aerial System (CPUAS) has developed rapidly in China [6–8], not only the technical level but also the application area have been already the first around the world [9,10]. With the real-time kinematic high-precision positioning technology and flight control technology, almost all the CPUASs have achieved fixed altitude and speed. Furthermore, the application of obstacle avoidance technology and terrain-following technology has improved the safety and accuracy of the CPUASs [7,11–13]. The high single pesticide application efficiency of CPUASs with an average of about 0.8–2.8 hectares is its obvious advantage [14]. In addition, the operators could be separated from the pesticide tanks on the CPUASs, which would prevent the pesticide poisonings to the operators.

Researchers have carried out many studies on how to make good use of the CPUASs for improving the pesticide utilization rate and achieving effective control of the crop diseases and insect pests. Al-Heidary et al. [15] studied the influences on the aerial spraying drift from the perspective of the droplets (size, velocity, evaporation, diameter distribution), which provided certain reference significance for this research. Qiu et al. [16] studied the effects of flight height (FH) and flight speed (FS) on the droplet deposition uniformity, and the results showed that the two factors and the interaction between them all affected the deposition and uniformity; the relationship model between deposition uniformity and FH/FS has been established for guiding the actual production application. For a multi-rotor CPUAS, Zhang et al. [17] investigated the effects of FS and FH on the effective spraying width (ESW) and droplet penetration rate (DPR) and reported that the FS had significant impacts on the ESWs, and the impacts of both FS and FH on the DPRs were highly significant. This research involved the effects of operating parameters on the droplet deposition of aerial spraying, which had great reference value for the studies of this article. For different crops, insect pests, and diseases, some scholars had also studied the effects of the aerial application parameters on the droplet deposition characters and control effects. Qin et al. [18] explored the effects of CPUAS spraying height and speed on droplet penetration and deposition uniformity on the rice. Xiao et al. [19] reported that the CPUAS had a poor droplet coverage rate, droplet density, and deposition uniformity, leading to a slightly lower control effect on pepper comparing with the electric air-pressure knapsack sprayers. Lou et al. [20] reported the good control effects of aphids and spider mites of 63.7% and 61.3% when the FH were 1.5 and 2 m above cotton. Chen et al. [21] and Wang et al. [22] reported that when the FS was 5 m/s and the FH was 1.5 m, the maximum deposition volume could be obtained in the lower layer of rice canopy. Wang et al. [23] suggested coarse droplet size and higher spray volume on wheat pests and diseases for better control effects with CPUAS. Chen et al. [24] suggested small particle sizes droplets to improve the control effect of rice plant hoppers for CPUAS.

The above studies focus on the selection of CPUAS application parameters, and the results have proved the feasibility of CPUAS for insect pests and diseases control of crops and promoted the popularization and application of CPUAS [7,16,25]. However, one factor is easy to be overlooked during the CPUAS application. As a kind of agricultural crop protection machinery with the inevitable trend for the intelligent development of green agriculture [26,27], its application should fully combine with the agronomy, so it is critical to analyze and evaluate the application with agronomies for achieving ideal and expected control effects. The occurrence time and the position on the plant of the insect pests and diseases as well as the plant height and density should be considered into the actual pesticide application. As a result of different insect pests and diseases occurrence laws,

the pesticide liquid droplet deposition should be targeted to achieve better control effects. Meanwhile, the operation parameters should be changed with different plant physiological characteristics in the field, correspondingly affecting the droplet deposition characteristics. This study aims to investigate the effects of the CPUAS operation parameters on the ESW and droplet deposition characteristics on the wheat canopy. Based on the investigations, the optimized parameters have been chosen to control the aphids, powdery mildew, and head blight combined with the occurrence laws and the wheat plant characteristics. The control effects have been evaluated. The studies would provide some references for the scientific application of the CPUAS.

2. Materials and Methods

2.1. Experimental Site, Wheat Characteristics, and Weather Conditions

The experiment site was located in the wheat field of Sihong agricultural demonstration base (33.3636° N, 118.2599° E) in Suqian City, Jiangsu Province, China. The trials were out carried on 11 March, 14 April, and 16 May 2019, with the crop at the Turning green, Heading, and Blooming stages, respectively, and in correspondence with the local timings for controlling wheat aphids, powdery mildew, and head blight

The wheat variety is Qianmai 33, and it was sowed in the field (60 m × 120 m) with 225 kg/ha seed density. The leaf area index was measured by the canopy analyzer LAI-2200C (LI-COR company, Lincoln, NE, USA). The main characters of the wheat and the weather conditions are shown in Table 1.

Table 1. The wheat characteristics and weather conditions.

Test Time	Growth Period	Mean Height	Mean Leaf Area Index	Mean Wind Speed	Mean Temperature	Mean Relative Humidity
11 March 2019	Turning green stage	13.5 cm	1.05	1.2 ± 0.20 m/s	12.6 ± 0.30 °C	65.2 ± 1.55%
14 April 2019	Heading stage	51.4 cm	4.35	0.8 ± 0.15 m/s	22.3 ± 0.40 °C	45.6 ± 0.15%
16 May 2019	Blooming stage	68.7 cm	5.47	1.4 ± 0.25 m/s	28.6 ± 0.20 °C	52.8 ± 0.76%

2.2. CPUAS and Experimental Materials

The tested CPUAS of CE20 (Wuxi Hanhe Aviation Technology Co., Ltd. Wuxi, China, as shown in Figure 1) is an electric single-rotor CPUAS with real-time kinematic Global Positioning System (RTK-GPS). It is fully autonomous flying with the routes planned by the mobile app, and the FS, FH, and the spraying volume can be also set on the mobile app with the accuracy controlled within 0.30 m, 0.30 m/s, and 0.05 L/min, respectively. The main technical parameters are shown in Table 2.



Figure 1. The Crop Protection Unmanned Aerial System (CPUAS) CE20.

Table 2. The main technical parameters of CE20.

Items	Parameters
UAAS size	1880 mm × 618 mm × 758 mm
Rotor diameter	2388 mm
Battery capacity	28,000 mAh × 2
Boom length	1442 mm
Maximum load	20 L
Number of nozzles	2
Type of nozzles	Hydraulic
Arrangement of nozzles	800 mm on both sides of the fuselage
Spraying volume	2.0 L/min
Spraying width	3–5 m

Water-sensitive paper (WSP) was used to collect the droplets during the experiments. High-concentration insecticide and fungicide were used for aerial spraying to control aphids, powdery mildew, and head blight.

2.3. Experimental Treatments

2.3.1. Experiment Design

According to the actual applications, the FS was set three levels as 3, 4, and 5 m/s, the FH was set three levels as 1.5, 2.0, and 2.5 m, and the spraying volume was set as 2.0 L/min during the experiments. The CE20 flew from the acceleration area to the stop spraying area along the center line of the sampling area with autonomous mode [28]. A total of nine treatments are shown in Table 3 with the treatment parameters.

Table 3. The experiment treatment designs.

Treatments	FS	FH	Spraying Volume
T1	3.0 m/s	1.5 m	2.0 L/min
T2	3.0 m/s	2.0 m	2.0 L/min
T3	3.0 m/s	2.5 m	2.0 L/min
T4	4.0 m/s	1.5 m	2.0 L/min
T5	4.0 m/s	2.0 m	2.0 L/min
T6	4.0 m/s	2.5 m	2.0 L/min
T7	5.0 m/s	1.5 m	2.0 L/min
T8	5.0 m/s	2.0 m	2.0 L/min
T9	5.0 m/s	2.5 m	2.0 L/min

2.3.2. Sampling Point Arrangements

The whole experimental area was divided into flight acceleration area, sampling area, and stop spraying area. The flight acceleration area and the stop spraying area were both 50 m long in order to ensure that the CPUAS could accelerate to a predetermined speed and stop in a timely manner. The sampling points were arranged along the vertical direction of the CPUAS flight route symmetrically with three repetitions with a 10 m interval. Twenty-one sampling points were arranged symmetrically on both sides of the flight route for each repetition line. The sampling points were labeled S1 to S21 from left to right; the central one was S11. The interval distance between sampling points S10 and S11 was 1.0 m, while that between sampling points S9 and S10 was 0.50 m, and that between sampling points S9 and S1 was 0.25 m. The right and left sampling points are distributed symmetrically. The layout of sampling is shown in Figure 2.

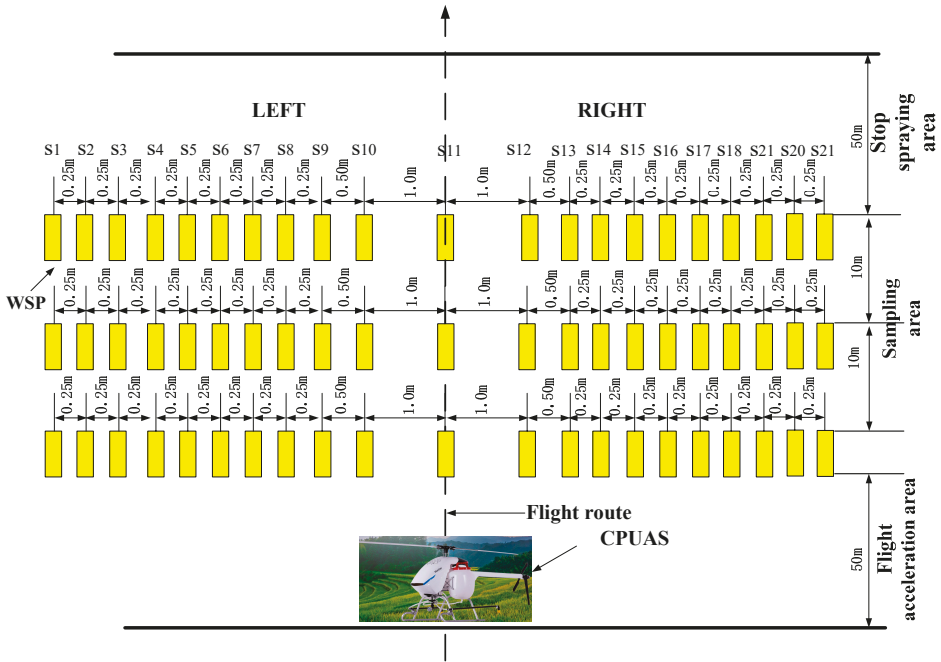


Figure 2. The field sampling layout (top view).

The WSPs were fixed horizontally on the upper (the Turning green stage) or on the upper and lower layers (Heading and Blooming stages) at each sampling point without overlapping as Figure 3 shows, and there was a 15 cm vertical distance both to the top canopy of the wheat and to the ground. The bandwidths were measured by collecting droplets from the upper layer WSPs during the Turning stage, and the penetration rates were calculated by the collecting droplets from both the upper and layer WSPs during the Blooming stage.

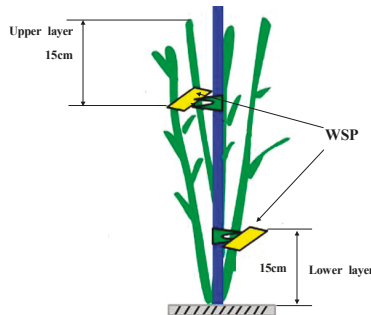


Figure 3. Upper and lower layers of water-sensitive papers (WSPs) on the sampling point.

The control check (CK) area was reserved for checking the control effect of insect pests and diseases.

2.4. Evaluation Method of ESW and Droplet Deposition

The WSPs were scanned to 600 dpi digital JPG images after each test in the lab and analyzed by the DepositScan (DS) [29]. The droplet deposition density, uniformity, and the DPR were analyzed further based on the droplet deposition JPG images.

According to the standard ‘Technical specification of quality evaluation for crop protection UAS’ (NY/T3213-2018) [30], the first sampling point of droplet quantity not less than 15 droplets per square centimeters (cm²) was judged as the boundary of the ESW each line. In this paper, the average bandwidth value analyzed of the three lines was the ESW of each flight for accuracy.

The droplet deposition uniformity was evaluated with the coefficient of variation (CV, %) of coverage rates [31] on the WSPs calculated from the DS within the ESW. The CV calculation Equation [18] is as follows.

$$CV = \frac{S}{\bar{X}} \times 100\% \tag{1}$$

$$S = \sqrt{\frac{\sum_{i=1}^n (X_i - \bar{X})^2}{(n - 1)}} \tag{2}$$

where *S* is the standard deviation, *X_i* is the number of droplets per unit zone in the sampling card, \bar{X} is the average number of droplets per unit zone in the sampling card, and *n* is the total number of sampling cards in reach repetition.

The droplet penetrability into the canopies was expressed by (DPR, %) and calculated by the follow formula.

$$DPR = \frac{y_l}{y_u} \times 100\% \tag{3}$$

where *y_l*, *y_u* are the coverage rates of the lower layer and the upper WSP of each sampling point within the ESW range, respectively.

Analysis of variance (ANOVA) was conducted for investigating the significances of FS and FH on the ESW, DPR, and droplet deposition uniformity (DDU), taking the FS and FH as independent variables, and the ESW, DPR, and DDU as dependent variables [8,20].

2.5. Control Effect Survey of Aphids, Powdery Mildew, and Head Blight

The pesticides recommended by the local crop protection station were used to control wheat diseases and insect pests. The information of aerial spraying date, major pest and disease, pesticides, and dosage, is shown in Table 4.

Table 4. The major wheat pests, diseases, and pesticide applications.

Spraying Date	Pest and Disease	Pesticides and Dosage
12 March 2019	Aphids	Abamectin cypermethrin, Emulsion, 4.50 g a.i./ha
15 April 2019	Powdery mildew	Phenamacril, Suspension concentrate, 375 g a.i./ha
		Epoxiconazole, Suspension concentrate (SC), 15.75 g a.i./ha
17 May 2019	Head blight	Tebuconazole and Prochloraz, Emulsion in Water (EW), 202.5 g a.i./ha
		Phenamacril, Suspension concentrate (SC), 375 g a.i./ha

The control effect survey of aphids was evaluated by the live aphid quantity before and after application according to the standard ‘Rules for the investigation and forecast of wheat aphids’ [32]. The assessment was made by sampling five locations for wheat aphids. The aphid quantity of 10 plots of wheat per location was investigated before spraying, and

the wheat plants were labeled. One day, 3 days, and 7 days after application, the quantity of live aphids in the same location and plant was investigated again [33,34]. The control effect of aphids was calculated according to Equations (4) and (5). The control effect of powdery mildew was evaluated by the disease index (*DI*) changing according to the standard ‘Rules for the investigation and forecast of wheat powdery mildew’ [35]. The wheat plant *DIs* of 9 plots were investigated randomly, and the wheat plants were labeled. Seven days and 14 days after application, the *DIs* of the same plants were investigated again [36]. The control effect of powdery mildew was calculated according to Equations (6) and (7). The control effect of head blight was evaluated by the *DI* changing according to the standard ‘Rules for monitoring and forecast of the wheat head blight’ [37]. The same as the powdery mildew *DIs* investigations, the plant *DIs* of head blight were investigated again [38]. The control effect of head blight was calculated according to Equations (8) and (9). The wheat plants of the CK area were used as the reference during the evaluations.

$$\eta_d = \frac{n_b - n_a}{n_b} \times 100\% \tag{4}$$

$$CE_y = \frac{\eta_{dT} - \eta_{dCK}}{1 - \eta_{dCK}} \times 100\% \tag{5}$$

$$DI_w = F \times \frac{\sum(d_i \times l_i)}{L} \times 100 \tag{6}$$

$$CE_w = \frac{DI_{wCK} - DI_{wT}}{DI_{wCK}} \times 100\% \tag{7}$$

$$DI_c = \frac{\sum(h_i \times i)}{H \times 4} \times 100 \tag{8}$$

$$CE_c = \frac{DI_{cCK} - DI_{cT}}{DI_{cCK}} \times 100\% \tag{9}$$

where η_d is the aphid dropping rate, n_b is the quantity of live aphids per hundred plants of wheat before spraying application, n_a is the quantity of live aphids per hundred plants of wheat after spraying application, CE_y is the aphid control effect, η_{dT} is the aphid dropping rate in the treatment area, η_{dCK} is the aphid dropping rate in the CK area; DI_w is the disease index of powdery mildew, F is the diseased leaf rate of powdery mildew, d_i is the powdery mildew severity levels, l_i is the number of each diseased leaves of powdery mildew, L is the total number of diseased leaves in the powdery mildew survey, CE_w is the powdery mildew control effect, DI_{wCK} is the disease index of the powdery mildew in the CK area, DI_{wT} is the disease index of powdery mildew in the treated area; DI_c is the disease index of head blight, h_i is the number of each diseased ear of head blight, i is the head blight severity levels, H is the total number of diseased ears in the head blight survey, CE_c is the head blight control effect, DI_{cCK} is the disease index of the head blight in the CK area, DI_{cT} is the disease index of the head blight in the treated area.

3. Results

3.1. Test Data Statistics

The average bandwidth of each treatment was as the ESW. The DDU (coefficient of variation (CV), %) were calculated according to Equation (1). The test result data are shown in the Table 5.

From Table 5, it could be seen that the ESW of CE20 was not consistent and decreased as the FS increased overall, the ESW were among 2.51 to 5.78 m, and the maximum value was 5.78 m (T2). The CV represents the DDU, which means the smaller the CV, the more uniform the distribution of the droplet deposition. The CVs were all not exceeding 35%, of which the minimum one was 23.30% (T1 and T4) and the maximum one was 34.40% (T6), which meant good deposition uniformity within the ESWs.

Table 5. Test result data of bandwidths, droplet deposition uniformities, and penetration rates.

Treatment Number	ESW	CV
T1	5.42 m	23.30%
T2	5.78 m	24.80%
T3	4.58 m	26.20%
T4	3.51 m	23.30%
T5	5.75 m	26.20%
T6	4.17 m	34.40%
T7	2.58 m	27.20%
T8	2.77 m	28.15%
T9	2.51 m	32.65%

3.2. The ESW Analyses

The ESW increased first and then decreased with the same FS under the FH of 3, 4, and 5 m, respectively (Figure 4). This change trend was most significant at the FS of 4.0 m/s, the ESW increase rate was 63.82% comparing T4 (ESW = 3.51 m) with T5 (ESW = 5.75 m), and the ESW decrease rate was 27.48% comparing T5 (ESW = 5.75 m) with T6 (ESW = 4.17 m). From Figure 4, the ESWs under an FS of 3.0 m/s were larger than those of same FH at 4.0 or 5.0 m/s. The ESW showed a monotonous downward trend with the same FH (Figure 5) obviously under the FS of 1.5, 2.0, and 2.5 m/s, respectively. This trend was obvious at the FH of 1.5 and 2.5 m, and the ESW maximum decrease rate was 52.40% comparing T1 (ESW = 5.42 m) with T7 (ESW = 2.58 m). From Figure 5, the ESWs under an FH of 2.0 m were larger than those of the same FS at 1.5 or 2.5 m. Therefore, it could be considered that the FS and the FH affected the ESWs. Comparing Figure 4 with Figure 5, it could be seen that FS had a larger effect on EWS than FH.

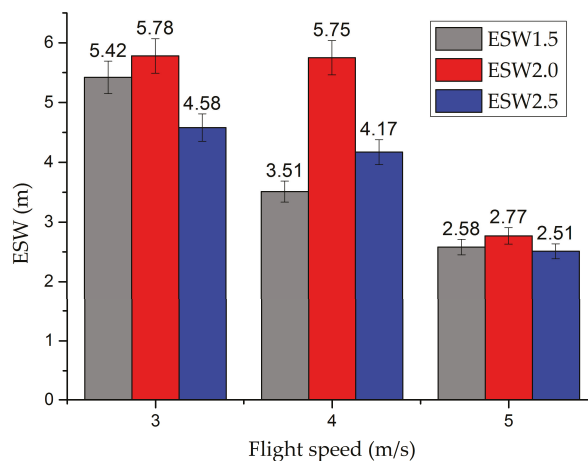


Figure 4. Effective spraying width (ESW) changes under different speeds. Note: ESW1.5, ESW2.0, ESW2.5 represent the ESW when the flight height (FH) was 1.5, 2.0, and 2.5 m, respectively.

The two-way ANOVA was conducted to verify the significance effect of FS and FH on ESW at the p -value = 0.05 level, and the results are shown in Table 6. The FS has a highly significant impact on ESW ($p = 0.0033 < 0.01$), the FH has no significant impact on the ESW ($p = 0.136 > 0.05$), and the interaction between FS and FH also has no significant impact on ESW ($p = 0.906 > 0.05$).

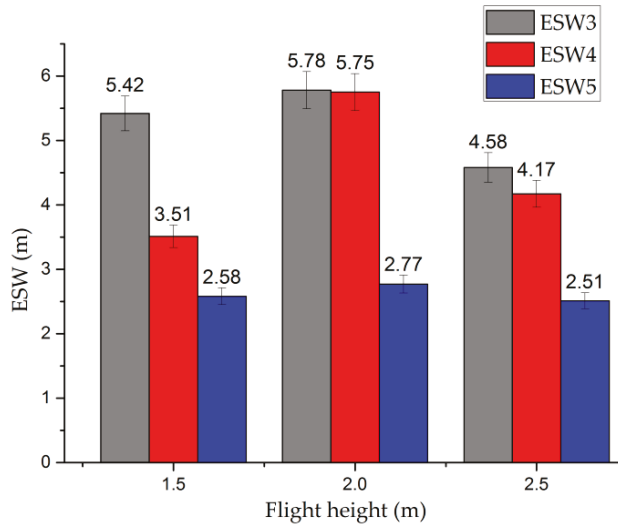


Figure 5. ESW changes under different heights. Note: ESW3, ESW4, and ESW5 represent the ESW when the flight speeds (FS) were 3.0, 4.0 m/s, and 5.0 m/s, respectively.

Table 6. Two-way analysis of variance for ESWs.

Source of Variance	df	F	p-Value	Significance
FS	2	2.23	0.0033	** 1
FH	2	12.93	0.136	NS 2
FS × FH	4	0.91	0.906	NS

^{1,2}: p means the significance level of the factor affecting the result, $p < 0.01$ (** represents factors that are highly significant on the test result), $p < 0.05$ (* represents factors that have a significant impact on the test result), NS (NS represents factors that have no significant impact on the test result).

3.3. The Deposition Uniformity Analyses

The two-way ANOVA results (Table 7) indicated that the FH as well as the interaction between FS and FH have significant impacts on the DDU. This law is also shown in Figure 6. The CV of droplet deposition tended to become larger with the increase of FH, which meant that the DDU becomes worse.

Table 7. Two-way analysis of variance for droplet deposition uniformity (DDUs).

Source of Variance	df	F	p-Value	Significance
FS	2	2.23	0.827	NS 1
FH	2	12.93	0.019	* 2
FS × FH	4	0.91	0.032	*

^{1,2}: p means the significance level of the factor affecting the result, $p < 0.01$ (** represents factors that have a highly significant impact on the test result), $p < 0.05$ (* represents factors that have a significant impact on the test result), NS (NS represents factors that have no significant impact on the test result).

The droplet deposition uniformity was an important indicator to evaluate the aerial spraying quality. The average CV of the droplet deposition was 27.35% for the nine treatments, the maximum one was 34.4% (T6), and the minimum one was 23.3% (T1, T4). Figure 6 showed the droplet deposition uniformity of each treatment by CVs.

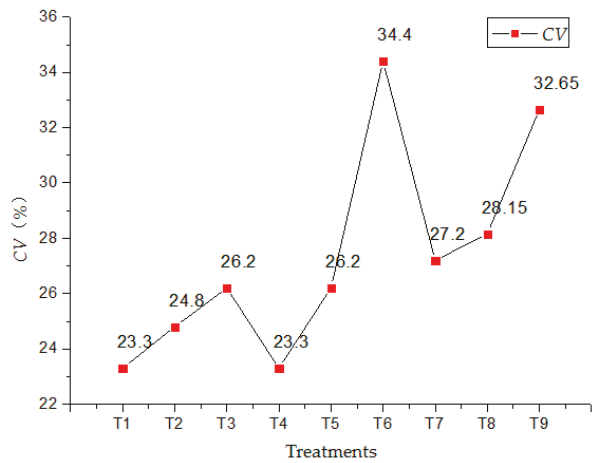


Figure 6. Droplet deposition uniformity of each treatment by coefficients of variation (CVs).

3.4. The DPR Analyses

The results showed that the DPRs of the nine treatments had no obvious correlation with the changes of the FS or FH. The larger the ESW, the higher the spraying efficiency, so in this study, the DPRs under several treatments (T1, T2, T5) with larger ESW were calculated according to Equation (3), which were 60.1%, 54.6%, and 52.7%, respectively.

3.5. The Control Effect Analysis

The aerial spraying efficiency was given priority with T5 operation parameters to control the aphids, the T1 operation parameters were selected to control the powdery mildew and head blight with larger ESW and good DPR. The wheat plants infected aphids, powdery mildew and head blight were shown in Figure 7.



Figure 7. Wheat aphids, powdery mildew, and head blight occurrence in the test field.

The control effect of aphids is shown in Figure 8. The quantity of aphids per hundred plants of wheat declined to 172 on the first day, 128 on the third day, and 97 on the seventh day in the treated area after application; the decline rate was obvious, while the quantity

rose to 645, 678, and 803 from 587 on the corresponding dates in the CK area. The aphid control effect was 78.71% on the first day, 84.88% on the third day, and 90.41% on the seventh day, respectively.

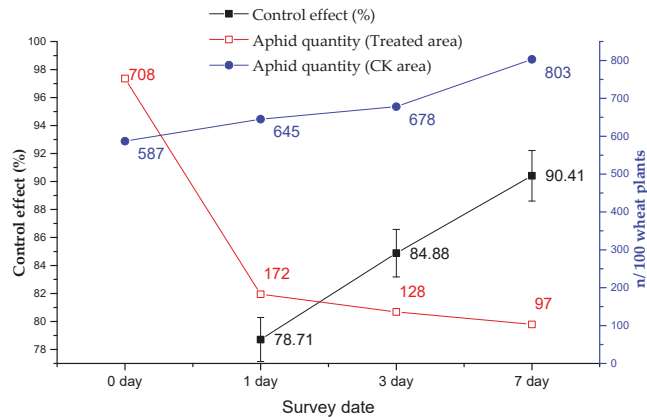


Figure 8. Wheat aphids control effect.

The control effects of powdery mildew and head blight are shown in Table 8. For the powdery mildew, the control effect was $77.17 \pm 1.15\%$ on the seventh day and $82.83 \pm 2.98\%$ on the fourteenth day after application, and for the head blight, the control effect was $88.32 \pm 1.50\%$ on the twentieth day after application.

Table 8. Control effects of powdery mildew and head blight.

Disease	Period	Date	Control Effect
Powdery mildew	Heading stage	7 d	$77.17 \pm 1.15\%$
		14 d	$82.83 \pm 2.98\%$
Head blight	Blooming stage	20 d	$88.32 \pm 1.50\%$

4. Discussion

As a new type of crop protection machinery, some details of the CPUAS application need to be clarified. The ESW, DDU, and DPR are the most important indicators for evaluating qualities of the spraying by CPUAS, and the operation parameters FH and FS, which can be controlled manually, affected ESW, DDU, and DPR. In this article, the results showed that the ESW of CE20 was not consistent and changed as the FS and FH changed, which were consistent with the existing findings [16,17]. The FS had a highly significant impact ($p = 0.0033 < 0.01$) on the ESW, while the FH had no significant impact ($p = 0.136 > 0.05$) on it, and the ESW value was negatively correlated as the FS varies, which is consistent with the conclusions of Zhang et al. [17]. Through comparison from the treatments, it could be seen that the spraying DDU of CE20 was very good with CVs among 23.3% to 34.4%. The two-way ANOVA results showed that the FH ($p = 0.019 < 0.05$) and the interaction between FS and FH ($p = 0.032 < 0.05$) both had significant impacts on the DDU, and the DDU could be improved by appropriately reducing FH and FS. This conclusion was slightly different with some existing conclusions. According to Qiu et al. [16], both the FS and FH had highly significant impacts on the DDU, and the interaction between FS and FH had significant impacts on the DDU. The reason may be the different type of CPUAS and the spraying volume, which needed further research. For the DPR, although results showed that it had no obvious correlation with the changes of the FS or FH, the slower the FS, the lower the FH, and the larger the spraying volume, the more droplets deposited in

the lower layer of the crop canopy according to Chen et al. [21] and Wang et al. [22], so a larger spraying volume was suggested if permitted. Based on the test results, optimized parameters of T5 and T1 were selected for aerial spraying operations to control wheat aphids, powdery mildew, and head blight. The control effects could satisfy the actual application. The existing research [23] showed that better control of wheat diseases and insect pests was achieved when using a coarse droplet size and higher spray volume. The control effect of powdery mildew was lower than that of head blight, although the height and canopy density of the wheat during the Heading stage were both lower than those during the Blooming stage (see Table 1); the reason may be related to disease characteristics. The powdery mildew mainly occurs in the middle and lower layers of the wheat plants, while the head blight occurs mainly in the upper layers (ears), so the pesticide droplets would be more likely to contact the leaves infected with head blight.

5. Conclusions

The research results in this study show that the ESW, DDU, DPR, and even the spraying efficiency are closely related to the operation parameters. The above results reflected that with the aerial spraying parameters optimized, the obtained control effects of aphids, powdery mildew, and head blight could meet the actual requirements in general. Therefore, it is considered that the combined operation parameters used in actual application is inappropriate. It should be combined with the agronomic requirements to select the appropriate parameters based on the crop types, the growth period, the pests and diseases characteristics, and even the environmental conditions to achieve good prevention and control effects.

For wheat, stripe rust, powdery mildew, and head blight are the major diseases that are harmful to the wheat yield [3–5,39,40], and different requirements are required in chemical crop protection applications, respectively. The stripe rust would occur from the wheat Tillering stage to the Filling stage [40], the powdery mildew mainly occurs between the Heading stage and the Milky stage of wheat [40], and the head blight mainly occurs from the Heading stage to the Filling stage [41]. For the disease occurrence parts, the stripe rust occurs in the middle and lower parts of the wheat, the powdery mildew occurs and develops from the bottom to the top layer, and the head blight is concentrated on the upper layer (ears) of wheat. According to the results of this study, when controlling the head blight, priority should be given to increase the ESW, and the FS is appropriately reduced, taking into account the aerial spraying efficiency. When controlling the powdery mildew, the penetration of droplets is an effective consideration, and the FH should be reduced possibly. When controlling the stripe rust, the ESW and the penetration should be both considered for the parameter optimization combined with the growth period of wheat.

In this study, the CPUAS of CE20 was tested, and the conclusions above were only applicable to it. Different type CPUASs may have different spraying and droplet deposition characteristics, such as single-rotor and multi-rotor CPUAS; thus, systematic experiments should be carried out to determine the optimal parameter combinations before application. Future research should be focused on the relationship among the parameters [8,16,17], the canopy structure [42], and the wind field [43,44] on the droplet deposition effect, and establish the correlation of them to achieve the best management practice and control effect.

Author Contributions: S.Z., B.Q., and X.X. conceived the idea of the experiments. S.Z., T.S., W.G., F.Z., and X.S. performed the experiments and analyzed the data. S.Z., B.Q., and X.X. wrote and revised the paper. All authors have read and agreed to the published version of the manuscript.

Funding: This research was funded by the National Key Research and Development Program of China (Grant No. 2017YFD0701000), the National Natural Science Foundation of China (Grant No.31701327), the earmarked fund for China Agriculture Research System (CARS-12), the Agricultural Science and Technology Innovation Project of the Chinese Academy of Agricultural Sciences, Crop Protection Machinery Team (Grant No. CAAS-ASTIP-CPMT), the Science and Technology Development Plan of Suzhou, Jiangsu Province (Grant No. SNG2020042), the Jiangsu Science and Technology Development Plan (BE2019305).

Institutional Review Board Statement: Not applicable.

Informed Consent Statement: Not applicable.

Data Availability Statement: The data used to support the findings of this study are available from the first author or the corresponding author upon request.

Acknowledgments: The authors are very grateful to Sihong agricultural demonstration base for proving the test field and the pesticides, and to the help of Sijun Yang and Jilin Du during the tests.

Conflicts of Interest: The authors declare no conflict of interest.

References

- Li, Q.; Fan, J.; Sun, J.; Zhang, Y.; Chen, J. Anti-plant defense response strategies mediated by the secondary symbiont hamiltonella defensa in the wheat aphid sitobion miscanthi. *Front. Microbiol.* **2019**, *10*, 2419. [CrossRef]
- Li, Y.; Li, Z.; Zhao, L.; Hu, Z.; Zhao, H. Development of a wheat aphid population dynamics model based on cusp catastrophe theory. *Int. J. Biomath.* **2020**, 2050078. [CrossRef]
- Li, T. Research progress of wheat powdery mildew forecasting method. *Meteor. Environ. Sci.* **2013**, *36*, 44–48. (In Chinese)
- Zou, Y.; Qiao, H.; Cao, X.; Liu, W.; Fan, J.; Song, Y. Regionalization of wheat powdery mildew overwintering in China based on digital elevation. *J. Integr. Agric.* **2018**, *17*, 901–910. [CrossRef]
- Huang, C.; Jiang, Y.; Wu, J.; Qiu, K.; Yang, J. Occurrence and characteristics and reason analysis of wheat head blight in 2018 in China. *Plant Prot.* **2019**, *4*, 160–163. (In Chinese)
- Lan, Y.; Wang, G. Development situation and prospects of China's crop protection UAV industry. *Agric. Eng. Technol.* **2018**, *38*, 17–27. (In Chinese)
- Lan, Y.; Chen, S. Current status and trends of plant protection UAV and its spraying technology in China. *Int. J. Precis. Agric. Aviat.* **2018**, *1*, 1–9. [CrossRef]
- Zhang, S.; Xue, X.; Sun, T.; Gu, W.; Zhang, C.; Peng, B.; Sun, X. Evaluation and comparison of two typical kinds UAAS based on the first industry standard of China. *Int. Agric. Eng. J.* **2020**, *29*, 331–340.
- He, X.; Bonds, J.; Herbst, A.; Langenakens, J. Recent development of unmanned aerial vehicle for plant protection in East Asia. *Int. J. Agric. Biol. Eng.* **2017**, *10*, 18–30.
- Yang, F.; Xue, X.; Cai, C.; Sun, Z.; Zhou, Q. Numerical simulation and analysis on spray drift movement of multirotor plant protection unmanned aerial vehicle. *Energies* **2018**, *11*, 2399. [CrossRef]
- Wang, L.; Lan, Y.; Zhang, Y.; Zhang, H.; Tahir, M.; Ou, S.; Liu, X.; Chen, P. Applications and prospects of agricultural Unmanned aerial vehicle obstacle avoidance technology in China. *Sensors* **2019**, *19*, 642. [CrossRef] [PubMed]
- Lan, Y.; Chen, S.; Fritz, B.K. Current status and future trends of precision agricultural aviation technologies. *Int. J. Agric. Biol. Eng.* **2017**, *10*, 1–17.
- Cao, G.; Li, Y.; Nan, F.; Liu, D.; Chen, C.; Zhang, J. Development and analysis of plant protection control system and route planning research. *Chin. Soc. Agric. Mach.* **2020**, *8*, 1–16. (In Chinese)
- Wang, G.; Han, Y.; Li, X.; Andaloro, J.; Chen, P.; Hoffmann, W.; Han, X.; Chen, S.; Lan, Y. Field evaluation of spray drift and environmental impact using an agricultural unmanned aerial vehicle (UAV) sprayer. *Sci. Total Environ.* **2020**, *737*, 139793. [CrossRef]
- Al-Heidary, M.; Douzals, J.; Sinfort, C.; Vallet, A. Influence of spray characteristics on potential spray drift of field crop sprayers: A literature review. *Crop Prot.* **2014**, *63*, 120–130. [CrossRef]
- Qiu, B.; Wang, L.; Cai, D.; Wu, J.; Ding, G.; Guan, X. Effects of flight altitude and speed of unmanned helicopter on spray deposition uniform. *Chin. Soc. Agric. Eng.* **2013**, *29*, 25–32. (In Chinese)
- Zhang, S.; Qiu, B.; Xue, X.; Sun, T.; Peng, B. Parameters optimization of crop protection UAS based on the first industry standard of China. *Int. J. Agric. Biol. Eng.* **2020**, *13*, 29–35. [CrossRef]
- Qin, W.; Qiu, B.; Xue, X.; Chen, C.; Xu, Z.; Zhou, Q. Droplet deposition and control effect of insecticides sprayed with an unmanned aerial vehicle against plant hoppers. *Crop Prot.* **2016**, *85*, 79–88. [CrossRef]
- Xiao, Q.; Du, R.; Yang, L.; Han, X.; Lan, Y. Comparison of droplet deposition control efficacy on phytophthora capsica and aphids in the processing pepper field of the unmanned aerial vehicle and knapsack sprayer. *Agronomy* **2020**, *10*, 215. [CrossRef]
- Lou, Z.; Xin, F.; Han, X.; Lan, Y.; Fu, W. Effect of unmanned aerial vehicle flight height on droplet distribution, drift and control of cotton aphids and spider mites. *Agronomy* **2018**, *8*, 187. [CrossRef]
- Chen, S.; Lan, Y.; Li, J.; Zhou, Z.; Jin, J.; Liu, A. Effect of spray parameters of small unmanned helicopter on distribution regularity of droplet deposition in hybrid rice canopy. *Trans. Chin. Soc. Agric. Eng.* **2016**, *32*, 40–46. (In Chinese)
- Wang, C.; Song, J.; He, X.; Wang, Z.; Wang, S.; Meng, Y. Effect of flight parameters on distribution characteristics of pesticide spraying droplets deposition of plant-protection unmanned aerial vehicle. *Trans. Chin. Soc. Agric. Eng.* **2017**, *33*, 109–116. (In Chinese)
- Wang, G.; Lan, Y.; Qi, H.; Chen, P.; Hewitt, A.; Han, Y. Field evaluation of an unmanned aerial vehicle (UAV) sprayer: Effect of spray volume on deposition and the control of pests and disease in wheat. *Pest Manag. Sci.* **2019**, *75*, 1546–1555. [CrossRef] [PubMed]

24. Chen, P.; Lan, Y.; Huang, X.; Qi, H.; Wang, G.; Wang, J.; Wang, L.; Xiao, H. Droplet deposition and control of planthoppers of different nozzles in two-stage rice with a quadrotor unmanned aerial vehicle. *Agronomy* **2020**, *10*, 303. [\[CrossRef\]](#)
25. Zhu, H.; Li, H.; Zhang, C.; Li, J.; Zhang, H. Performance Characterization of the UAV Chemical Application Based on CFD Simulation. *Agronomy* **2019**, *9*, 308. [\[CrossRef\]](#)
26. Meng, Y.; Zhou, G.; Wu, C. Discussion on application and promotion of agricultural plant protection unmanned aerial vehicle in China. *China Plant Prot.* **2014**, *34*, 33–39.
27. Shang, C.Y.; Cai, J.F.; Huang, S.J.; Pan, H.L.; Zhong, F.L. Applications status and prospect analysis of agricultural UAVs in China. *J. Anhui Agric. Sci.* **2017**, *45*, 193–195.
28. Xue, X.; Lan, Y.; Sun, Z.; Chang, C.; Hoffmann, W. Develop an unmanned aerial vehicle based automatic aerial spraying system. *Comput. Electron. Agric.* **2016**, *128*, 58–66. [\[CrossRef\]](#)
29. Zhu, H.; Salyani, M.; Fox, R. A portable scanning system for evaluation of spray deposit distribution. *Comput. Electron. Agric.* **2011**, *76*, 38–43. [\[CrossRef\]](#)
30. NY/T 3213-2018. *Chinese Standard: Technical Specification of Quality Evaluation for Crop Protection UAS*; The Ministry of Agriculture and Rural Affairs of the People's Republic of China: Beijing, China, 2018. (In Chinese)
31. Smith, D. Uniformity and recovery of broadcast spray using fan nozzles. *Trans. ASAE* **1992**, *35*, 39–44. [\[CrossRef\]](#)
32. NY/T 612-2002. *Rules for Investigation and Forecast of Wheat Aphides*; The Ministry of Agriculture and Rural Affairs of the People's Republic of China: Beijing, China, 2002. (In Chinese)
33. Yuan, W.; Xu, B.; Ran, G.C.; Chen, H.P.; Zhao, P.Y.; Huang, Q.L. Application of imidacloprid controlled-release granules to enhance the utilization rate and control wheat aphid on winter wheat. *J. Integr. Agric.* **2020**, *19*, 3045–3053. [\[CrossRef\]](#)
34. Wang, G.; Lan, Y.; Yuan, H.; Qi, H.; Chen, P.; Ouyang, F.; Han, Y. Comparison of spray deposition, control efficacy on wheat aphids and working efficiency in the wheat field of the unmanned aerial vehicle with boom sprayer and two conventional knapsack sprayers. *Appl. Sci.* **2019**, *9*, 218. [\[CrossRef\]](#)
35. NY/T 613-2002. *Rules for Investigation and Forecast of Wheat Powdery Mildew [Blumeria Graminis (DC.) Speer]*; The Ministry of Agriculture and Rural Affairs of the People's Republic of China: Beijing, China, 2002. (In Chinese)
36. Qin, W.; Xue, X.; Zhang, S.; Gu, W.; Wang, B. Droplet deposition and efficiency of fungicides sprayed with small uav against wheat powdery mildew. *Int. J. Agric. Biol. Eng.* **2018**, *11*, 27–32. [\[CrossRef\]](#)
37. GB/T 15796-2011. *Rules for Monitoring and Forecast of the Wheat Head Blight (Fusarium Graminearum Schw./Gibberella Zeae(Schw.) Petch)*; General Administration of Quality Supervision, Inspection and Quarantine of the People's Republic of China, National Standardization Administration of China: Beijing, China, 2011. (In Chinese)
38. Yobo, K.; Mngadi, Z.; Laing, M. Efficacy of two potassium silicate formulations and two trichoderma strains on fusarium head blight of wheat. *Proc. Natl. Acad. Sci. India. B* **2019**, *89*, 185–190. [\[CrossRef\]](#)
39. Ma, Z. Researches and control of wheat stripe rust in China. *J. Plant. Protect.* **2018**, *45*, 1–6. (In Chinese)
40. Cao, S.; Luo, H.; Jin, M.; Jin, S.; Duan, X.; Zhou, Y. Intercropping influenced the occurrence of stripe rust and powdery mildew in wheat. *Crop Prot.* **2015**, *70*, 40–46. [\[CrossRef\]](#)
41. Dweba, C.; Figlan, S.; Shimelis, H.; Motaung, T.; Sydenham, S.; Mwadzingeni, L. Fusarium head blight of wheat: Pathogenesis and control strategies. *Crop Prot.* **2017**, *91*, 114–122. [\[CrossRef\]](#)
42. Meng, Y.; Su, J.; Song, J.; Chen, W.; Lan, Y. Experimental evaluation of uav spraying for peach trees of different shapes: Effects of operational parameters on droplet distribution. *Comput. Electron. Agric.* **2020**, *170*, 105282. [\[CrossRef\]](#)
43. Chen, S.; Lan, Y.; Li, J.; Zhou, Z.; Liu, A.; Mao, Y. Effect of wind field below unmanned helicopter on droplet deposition distribution of aerial spraying. *Int. J. Agric. Biol. Eng.* **2017**, *10*, 67–77.
44. Li, J.; Shi, Y.; Lan, Y.; Guo, S. Vertical distribution and vortex structure of rotor wind field under the influence of rice canopy. *Comput. Electron. Agric.* **2019**, *159*, 140–146. [\[CrossRef\]](#)

Review

Cryobiotechnology of Plants: A Hot Topic Not Only for Gene Banks

Petra Jiroutová * and Jiří Sedlák

Research and Breeding Institute of Pomology Holovousy Ltd., Holovousy 129, 508 01 Hořice, Czech Republic; jiri.sedlak@vsuo.cz

* Correspondence: petra.jiroutova@vsuo.cz

Received: 8 June 2020; Accepted: 6 July 2020; Published: 7 July 2020

Abstract: Agriculture has always been an important part of human evolution. Traditionally, farming is changing and developing with regard to challenges it faces. The major challenges of modern agriculture are food and nutrition safety for the growing world population. Promoting species and genetic diversity in agriculture appears to be an important approach to dealing with those challenges. Gene banks all around the world play a crucial role in preserving plant genetic resources for future crop improvements. The plant germplasm can be preserved in different ways, depending on the species or form of stored plant tissue. This review focuses on a special preservation method—cryopreservation. Cryopreservation is an effective technique for storing living systems at ultra-low temperatures, usually in liquid nitrogen or its vapor phase. This conservation method is crucial for plants that do not produce seeds or that produce non-germinating seeds, as well as for plants that propagate vegetatively. Moreover, based on the cryopreservation method, a novel plant biotechnology tool for pathogen eradication called cryotherapy has been developed. The use of liquid nitrogen eliminates plant pathogens such as viruses, phytoplasmas, and bacteria. Our article reviews recent advances in cryo-biotechnologies such as cryopreservation and cryotherapy, with special focus on studies concerning fruit plants.

Keywords: cryopreservation; cryotherapy; food safety; liquid nitrogen; biotechnology; fruit plants

1. Introduction

Plant genetic resources are highly important for the maintenance of agro-biodiversity and for food safety. These genetic resources, as donors of valuable traits, can be used to breed new, more productive crops with better resistance to biotic or abiotic stresses [1]. Seed storage is one of the most convenient methods for long-term conservation of plant genetic resources. However, a large number of plant species are not suitable for seed banking because they are highly heterozygous or have recalcitrant seeds that cannot be desiccated. These species are usually conserved in field collections. This type of collection is beneficial because it provides immediate access to plant material during all phenophases. However, plants in field collections are exposed to many environmental threats such as pests, diseases, and adverse weather conditions. Maintenance of this type of collection is also labor-intensive and expensive [2].

In vitro gene banks, where plants are vegetatively propagated and grown on a medium under sterile conditions, are an alternative to seed or field banking. In vitro-grown plants are stored in growing chambers that significantly save storage space and protect plants against harmful environmental factors. However, because the plantlets require periodical subcultivation on fresh medium, this method is not ideal for long-term storage [3].

Cryopreservation is the most valuable method for long-term conservation of plant germplasm. It is based on the storage of biological material at ultra-low temperatures in liquid nitrogen (−196 °C)

or in its vapor phase ($-150\text{ }^{\circ}\text{C}$). This temperature suspends cell division and metabolic and biochemical activities, thus preventing genetic alteration during long-term storage [4].

More than 60 years ago, the first work on plant cryopreservation was published. In 1956, Akira Sakai reported the successful survival of cold hardened and prefrozen mulberry twigs after exposure to liquid nitrogen [5]. The next challenging step in the field of cryopreservation was to freeze fully hydrated tissues such as callus and suspension cells, where there is a high risk of the formation of lethal intracellular ice-crystals. For this purpose, slow freezing protocols were developed. However, this method was not sufficient for cryopreservation of organized tissues (e.g., meristems), which led to the development of fast freezing protocols (encapsulation-dehydration, droplet vitrification, etc.) [6]. To date, several methods and techniques of cryopreservation have been reported. Nevertheless, the nub is always the same. Plant tissue is first physically or osmotically dehydrated to remove all freezable water, and to avoid water crystallization and lethal injuries during the following freezing in liquid nitrogen [7].

Ultra-low temperatures can also be successfully used for pathogen annihilation. This novel progressive technique is called cryotherapy and is based on protocols that have been originally established for cryopreservation. In the process of cryotherapy, infected plant cells are eliminated using the fatal efficacy of the liquid nitrogen (the ultra-low temperature) in combination with subsequent warming [8]. One of the major advantages of using ultra-low temperature treatment for pathogen eradication is that there is no need for special equipment other than that which is used in a basic plant tissue culture laboratory. This means that cryotherapy can be efficiently incorporated into the cryopreservation methods already used in gene banks [9].

In this review article, we present updated and comprehensive information concerning the development and progress of plant cryopreservation and cryotherapy, with a focus on horticultural crops and a special focus on apples, which belong to one of the most extensively studied species in this field.

2. Cryopreservation of Plants

Originally, plant cryopreservation was based on studies of the basic biology of freezing [10]. Gradual improvements in the technology and intensive research work over the past decades have resulted in great progress in the field of ultra-low temperature preservation of plant germplasm [11]. The development and improvement of cryopreservation techniques and their application to new plant species remains the center of attention of many cryogenic labs and gene banks around the world.

2.1. Plant Cryopreservation Methods

Nowadays, several methods of cryopreservation exist, including both classical and new techniques (Figure 1). Advantages and disadvantages of each method, as well as other factors such as available facilities, plant species, and the type of stored germplasm, have to be considered during the process of method selection (Table 1). Often more than a single cryoprotocol is suitable for successful plant cryopreservation, considering some modifications of established methods [12]. The first step in cryopreservation is removing freezable water from tissues by dehydration. A water content of less than $0.25\text{ g H}_2\text{O g/dm}$ (dm; dry mass) is often termed ‘unfreezable’ water, and plant cells containing $0.25\text{--}0.4\text{ g H}_2\text{O g/dm}$ usually survive the liquid nitrogen exposure [13]. Proper dehydration can be achieved osmotically by treatment with highly concentrated solutions, in which case the driving force for dehydration is the concentration gradient between the solution and the intracellular liquid. The second widely used method of dehydration is air-drying, where the water is removed by the air flow [14]. In any case, the process of dehydration is essential for successful cryopreservation to avoid intracellular freezing and irreversible injury of cells caused by the formation of ice crystals [1].

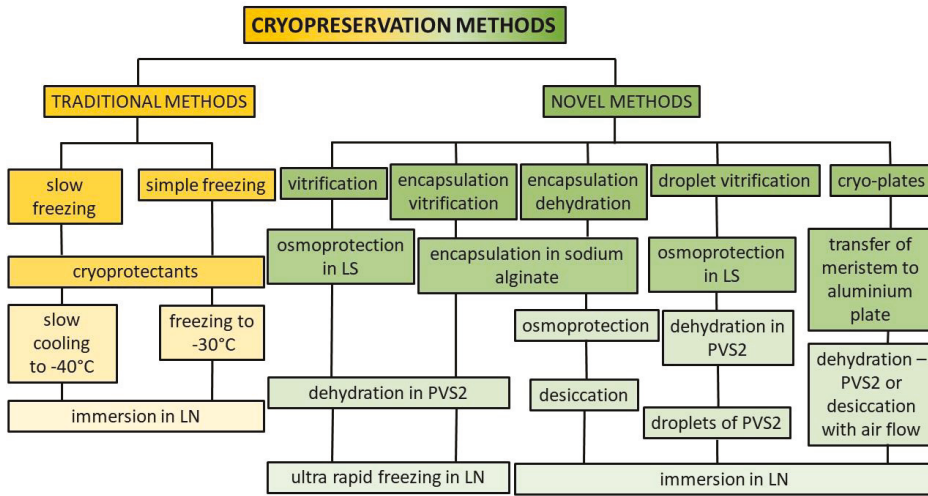


Figure 1. Schematic diagram of major methods and steps of cryopreservation of shoot tips.

2.1.1. Classical Cryopreservation Methods

Classical cryopreservation methods were developed more than 40 years ago, and two main techniques are traditionally used: (i) slow freezing, and (ii) simple one-step freezing [7]. Slow freezing (also known as the two-step freezing method) includes pretreatment of samples with cryoprotectants such as dimethylsulfoxide (DMSO), glycerol, ethylene glycol, and sucrose. The samples are then slowly cooled at a controlled rate of 0.3–0.5 °C/min to –40 °C, and then rapidly immersed in liquid nitrogen. This method requires a programmable freezer [15]. On the other hand, no special equipment is required for simple one-step freezing. Samples pretreated with cryoprotectants are simply frozen at –30 °C for dehydration, and then immersed directly in liquid nitrogen [16]. Although these classical methods have been successfully applied to a range of plant materials, new and gentler cryogenic methods such as vitrification, encapsulation, and cryo-plates have been developed recently.

2.1.2. Vitrification

This approach is one of the most widely applied plant cryopreservation methods because it is relatively easy to carry out, no special equipment is needed, and it usually displays a high percentage of recovery. Vitrification is based on the formation of an amorphous glassy structure from intracellular solutes [1]. The plant material is treated with a highly concentrated vitrification solution that removes most or all freezable water from cells. The dehydrated material is then ultra-rapidly frozen by immersion in liquid nitrogen. The combination of dehydration and rapid freezing of cells causes residual water to solidify without crystallization, which could injure the living cells [17].

Three main glycerol-based vitrification solutions (PVS1, PVS2, and PVS3) with different compositions have been reported. PVS1 consists of 19% (w/v) glycerol, 13% (w/v) ethylene glycol, 13% (w/v) propylene glycol, and 6% (w/v) DMSO dissolved in 0.5 M sorbitol. PVS2 consists of 30% (w/v) glycerol, 15% (w/v) ethylene glycol, and 15% (w/v) DMSO dissolved in 0.4 M sucrose. PVS3 consists of 50% (w/v) glycerol and 50% (w/v) sucrose dissolved in water [18]. In addition, two glycerol-free vitrification solutions were published in the past—the Towill cocktail (containing 35% ethylene glycol, 1 M DMSO, and 10% polyethylene glycol) and the Watanabe cocktail (containing 44.5% DMSO and 18.7% sorbitol) [19,20].

Among them, PVS2 is the most widespread, because of its less toxic effect on plant cells. Nevertheless, it cannot be used without any osmoprotection, because direct dehydration by PVS2

causes damages to the cells and tissues of many plants. For successful cryopreservation, it is necessary to implement osmoprotection pretreatment with a loading solution (LS) containing 2 M glycerol and 0.4 M sucrose that induces osmo-tolerance and enables plants to achieve higher rates of recovery after cryopreservation [21,22].

Two main vitrification-based methods, namely encapsulation-vitrification and droplet vitrification, have been developed via the modification and optimization of vitrification techniques. The encapsulation-vitrification method was first reported by Matsumoto et al. (1995) [23] and combines encapsulation of plant germplasm within alginate beads and dehydration using a highly concentrated vitrification solution. The major merits of this mixed technique are better protection of encapsulated plant samples during vitrification and reduction of time needed for dehydration, compared to that of the classical encapsulation-dehydration method [22]. Using the method called droplet vitrification, shoot tips pretreated with LS and subsequently treated with vitrification solution are inserted individually into droplets of PVS2 that are placed on a strip of aluminum foil. The whole aluminum foil is then directly immersed in liquid nitrogen. The main benefit of this technique is the achievement of very high cooling/warming rates [24,25].

Table 1. List of various cryopreservation methods.

Method	Plant Species	Main Advantage	Main Disadvantage	Survival Rate	References
slow freezing	<i>Asparagus officinalis</i>	high survival rate	need of a programmable freezer	100%	Kumu et al. 1983 [15]
simple one-step freezing	<i>Solanum goniocalyx</i>	no special equipment required	low survival rate	20%	Grout and Heneshaw 1978 [16]
vitrification	<i>Citrus sinensis</i> Osb. (nucellar cells)	relatively easy to carry out	not suitable for all plant species (without additional osmoprotection)	80%	Sakai et al. 1990 [21]
encapsulation-vitrification	<i>Wasabia japonica</i>	better protection of encapsulated shoot tips	more laborious method	95%	Matsumoto et al. 1995 [23]
encapsulation-dehydration	<i>Solanum phureja</i>	no need of toxic cryoprotectants	time-consuming method	40%	Fabre and Dereuddre 1990 [26]
cryo-plate methods	<i>Tanacetum cinerariifolium</i>	easy method to carry out with more shoot tips	not suitable for all plant species (toxic cryoprotectants)	77%	Yamamoto et al. 2011 [27]

2.1.3. Encapsulation-Dehydration

This method was first reported by Fabre and Dereuddre (1990) [26] and combines the encapsulation of plant samples with alginate beads and physical dehydration carried out with silica gel or in the air flow in a laminar flow cabinet [1]. Applying this method, plant material is precultured with 0.3–0.6 M sucrose medium for one to three days and then incubated in a liquid medium supplemented with sucrose and sodium alginate. Finally, this mixture is released drop by drop into liquid medium containing calcium chloride. Alginate beads with explants encapsulated inside them are formed during this process. The bead formation is followed by culturing in highly concentrated sucrose solution to achieve the osmoprotection, subsequent physical dehydration to a water content of 20%–30%, and direct immersion in liquid nitrogen (Figure 2) [26]. The encapsulation-dehydration method is relatively simple; however, it requires more time-consuming handling of encapsulated samples. The main advantage of this method is elimination of the need for other cryoprotectants such as DMSO and ethylene glycol that could be toxic for plants and could cause genetic changes after regrowth [22].

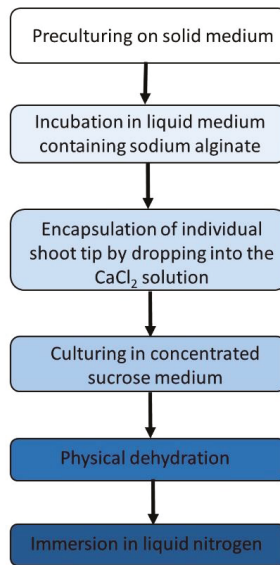


Figure 2. Schematic diagram of the encapsulation-dehydration cryopreservation method.

2.1.4. Cryo-Plate Methods

The newest cryogenic procedures use cryo-plates. Two main cryo-plate methods, known as the V and D cryo-plate methods, can be distinguished [22] based on the dehydration process. Using the former method, explants are dehydrated on cryo-plates using PVS2 vitrification [27], whereas the latter method uses air dehydration of explants [28]. In both methods, shoot tips are placed in small wells of an aluminum cryo-plate with alginate beads and dehydrated there with PVS2 solution or with air flow in a laminar flow cabinet, depending on the particular method. Afterwards, the cryo-plate is directly immersed into liquid nitrogen. The main advantage of cryo-plate techniques is their user-friendliness, mainly due to the easy handling of samples on the aluminum plates [27,28]. Successful cryopreservation using cryo-plates methods has been reported for many plant species including strawberry [29], sugarcane [30], date palm [31], mat rush [32], and potato [33].

3. Pathogen-Free Plant Material

Phytoplasmas, bacteria, viruses, and other plant pathogens cause harmful plant diseases that negatively affect crop yield, crop industry, and food safety every year [8,34]. Vegetatively propagated plants tend to accumulate pathogens that are transmitted to new plants in infected cuttings, tubers, roots, and other vegetative propagules [35]. Pathogen-free plant material is essential not only for higher productivity of agricultural and horticultural crops, but is also pivotal for long-term preservation of plant germplasm [36].

3.1. Conventional Methods for Pathogen Eradication

Conventional methods for pathogen eradication are based on *in vitro* meristem culture, as well as heat treatment (thermotherapy) and chemical treatment (chemotherapy), both of which are followed by meristem culture [37–41]. Although these traditional methods have been widely used for acquiring virus-free plants, all of them have some drawbacks.

The meristem culture method is based on the assumption that the youngest meristematic cells are free of viruses and other plant pathogens. Therefore, the extension and regeneration of small shoot

tips containing the meristem (0.2–0.4 mm) and two to four leaf primordia should lead to pathogen-free plants [36,39]. The major limitations of meristem culture techniques are difficulties in excising tiny meristems and a low regeneration rate of shoot tips.

The use of heat treatment is another well-known conventional method for pathogen eradication in plants. Generally, thermotherapy is based on keeping the target in vitro cultivated plants at a temperature of 35 °C–42 °C for four to six weeks. Both temperature range and duration of thermotherapy are virus-type- and plant-species-dependent [42,43]. The need for specific and expensive laboratory equipment such as a growth chamber with precise temperature control is the major limitation of thermotherapy [44]. Moreover, this method cannot be used for infected plants that are not resistant to higher temperatures and it does not work for all viruses [45].

Another method used for plant pathogen elimination is chemotherapy. In this technique, in vitro-grown plants are treated with antiviral chemicals like ribavirin, whose positive effect on virus eradication has been reported [46,47]. In this method, optimization of the dose and duration of the treatment is crucial because a high concentration of antiviral compounds in the culture medium can negatively affect the growth of in vitro plants through their phytotoxic activity. The sensitivity of in vitro plants to antivirotics is species- and genotype-specific [45,47]. Because of the abovementioned limitations linked to traditional methods for pathogen eradication, it would be beneficial to develop some more efficient and simpler methods for obtaining pathogen-free plants. In this respect, cryotherapy, i.e., treatment with ultra-low temperatures, could be a useful biotechnological tool with great potential.

3.2. Cryotherapy

Cryotherapy of shoot tips as a method for pathogen elimination from infected plants was first reported in 1997 by Brison et al. [48], who successfully eradicated Plum pox virus (PPV) from in vitro-grown infected shoot tips of interspecific *Prunus* rootstock [48]. The crux of this technique consists in the treatment of infected materials in liquid nitrogen for a short period of time [49,50]. Cryotherapy relies on plant cryopreservation protocols that are available for a wide range of vegetatively propagated and economically important plant species. Thus, cryotherapy has been successfully applied to many plant species such as potato (*Solanum tuberosum* L.) [51], sweet potato (*Ipomea batatas* L.) [52], banana (*Musa* spp.) [53], raspberry (*Rubus idaeus* L.) [54], grapevine (*Vitis vinifera* L.) [55,56], and apple (*Malus* spp.) [57–59].

To date, large numbers of pathogens (mostly viruses) have been eradicated via cryotherapy. These include, for example, two common viruses infecting sweet potatoes—sweet potato feathery mottle virus (SPFMV) and sweet potato chlorotic stunt virus (SPCVS)—that interact synergistically and cause the sweet potato virus disease (SPVD). Both these viruses can be eliminated with 100% efficiency using cryotherapy [60,61]. Cryotherapy was also successfully applied to the eradication of two viruses infecting potato plants: potato leafroll virus (PLRV) and potato virus Y (PVY), which were among the most important viruses limiting sustainable and profitable potato production [51]. Cucumber mosaic virus (CMV) and banana streak virus (BSV) viruses, which infect bananas and cause diseases that are linked to a reduction in fruit yield or obstruction of breeding and germplasm dissemination, were effectively eradicated by cryotherapy [53]. Successful applications of cryotherapy was also reported for viruses infecting grapes, such as grape virus A (GVA) and grapevine leafroll-associated viruses (GLRaV), that cause economic losses in viticulture [55,56,62]. In addition, viruses infecting less common crops such as garlic and artichoke were recently eradicated using ultra-low temperature treatment [63,64]. Other pathogens such as phytoplasmas and bacteria can also be eradicated from plants via cryotherapy. For example, the sweet potato little leaf phytoplasma (SPLL), which causes heavy yield losses in infected plants, was efficiently eliminated from all sweet potato shoot tips via treatment with liquid nitrogen [60]. Another, more recent example of eradication of phytoplasma by using cryotherapy was reported in 2015. Jujube witches' broom phytoplasma (*Candidatus Phytoplasma ziziphi*) was fully eliminated from infected Chinese jujube (*Ziziphus jujuba*) plants [65]. So far, only one successful elimination of bacteria—a Gram-negative bacteria attacking *Citrus*, *Fortunella*, and *Poncirus*

species and causing citrus Huanglongbing disease (HLB) disease, also called “citrus greening”—from infected plants by cryotherapy was reported [66]. Ding et al. demonstrated that cryotherapy is a powerful tool for elimination of this bacteria from infected sweet orange (*Citrus sinensis* L.) and other citrus species such as mandarin, pomelo, and Beijing lemon.

3.2.1. Mechanism

Cryotherapy is mostly applied to shoot tips, because they contain a unique meristematic zone consisting of small cells with small vacuoles and a higher nucleo-cytoplasmic ratio [67]. Those cells are more resistant to dehydration, which prevents the formation of ice crystals in cells during freezing [68]. Simply, cryo-treatment with liquid nitrogen destroys the differentiated cells, while meristematic cells survive and are able to self-renew, divide, differentiate, and regenerate to new virus-free plants (Figure 3). Because of this phenomena, cryotherapy is most effective for the elimination of pathogens infecting differentiated cells such as banana streak virus (BSV), cucumber mosaic virus (CMV), grape virus A (GVA), potato leafroll virus (PLRV), and potato virus Y (PVY) [51,53,62]. On the other hand, the eradication of pathogens that are able to infect meristematic cells, such as raspberry bushy dwarf virus (RBDV), pelargonium flower break virus (PFBV), and pelargonium line pattern virus (PLPV), is significantly more complicated [67,69]. It has been reported that a combination of cryotherapy and thermotherapy led to virus-free plants. Thermotherapy first inhibits movement of the virus toward the meristematic cells of the shoot tips and at the same time causes subcellular alterations, for example, enlargement of vacuoles, which results in much fewer surviving cells after subsequent cryotherapy. The combination of these two techniques enables an enhancement in the eradication of viruses localized in the meristem [67].

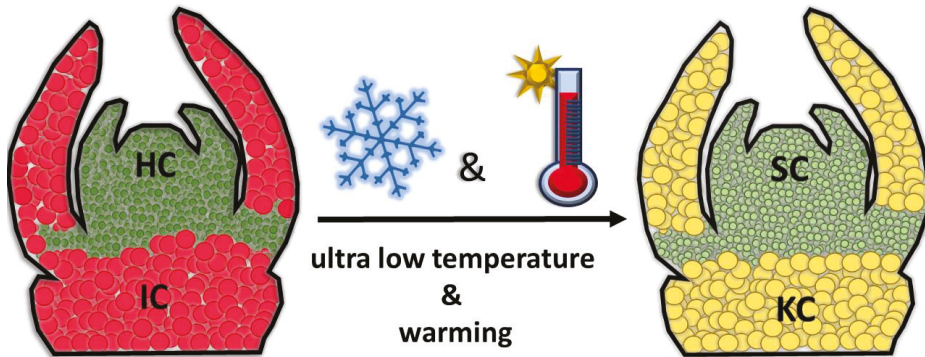


Figure 3. Schematic diagram of shoot tip cryotherapy. HC = healthy cells, IC = infected cells, SC = survived cells, KC = killed cells.

3.2.2. Merits and Demerits

Compared to other methods for pathogen eradication in plants, cryotherapy of shoot tips has the following advantages: (i) easier handling with meristems due to the lack of correlation between the size of the shoot tip and pathogen eradication rate [49,70]; (ii) high efficiency of pathogen eradication [49,71]; (iii) no need for special and expensive equipment, and (iv) it is easy to handle a large number of samples [36,49]. The major limitation of the wider application of the cryotherapy to produce pathogen-free plant material is the genotype- or often also cultivar-dependent response of plants to cryo-treatment. This means that each cryoprotocol needs to be developed and optimized for every single plant species or cultivar [68,72]. Although the risk of somaclonal variation during short-term cryotherapy is minimal, it is important to verify the genetic stability of regenerated plants [72].

4. Cryobiotechnology of *Malus* (Apple)

Many protocols used for cryopreservation of fruit plants have been reported. However, long-term germplasm storage of economically important horticultural woody plants in cryopreserved collections remains well-established, mainly for apple and pear plants [73,74]. Furthermore, among all plant species, *Malus* (apple) is one of the most extensively studied with respect to cryopreservation of the plant germplasm over the last decades. Interestingly, many protocols applied to other species originated from cryopreservation procedures that were first demonstrated with apples [73].

Traditionally, field collections and in vitro culture are used for preservation of *Malus* germplasm. Seed banking can be applicable only for the preservation of wild *Malus* species germplasm, since apple is genetically highly heterozygous [75,76]. Cryopreservation of apple seeds is possible after their drying to achieve 6%–19% moisture content [77]. It is valuable to cryopreserve pollen for immediate availability for breeding programs. Successful cryopreservation of *Malus* pollen has been reported many times. According to the published data, this pollen stored in liquid nitrogen can retain viability for at least 15 years [78–80].

The cryopreservation of shoot tips of in vitro-grown plants and cryopreservation of dormant buds are the most commonly used techniques for ultra-low temperature long-term storage of vegetatively propagated species (cultivars) [81]. Up to date, all known techniques for cryopreservation of shoot tips were used for *Malus*. The very first experiments concerning *Malus* in vitro shoot tip cryopreservation used classical two-step freezing [82,83]. The first experiments failed to enable regrowth of frozen shoot tips, suggesting that excessive cryo-injury occurred in the treated cells during the cryoprotocol. Wu et al. [84] overcame this problem in 1999 via optimization of the cryoprotocol by inserting the pretreatment of shoot tips with a cryoprotectant mixture and achieved a 66% shoot regrowth. Other early experiments were accomplished by using the PVS2 vitrification technique, with an average regrowth level of about 66% in different examined apple cultivars, rootstocks, and wild apple species [85]. Studies on the cryopreservation of in vitro shoot tips by encapsulation, linked with either dehydration or vitrification, have been reported. The first encapsulation-dehydration protocol was described in 1992 by Niino and Sakai [86] and subsequently more cryoprotocols using this or encapsulation-vitrification method were developed or optimized for a wide spectrum of *Malus* cultivars [84,87–89]. Finally, in 2010 Halmagyi et al. tested [90] the efficiency of two droplet cryopreservation techniques, droplet-vitrification and droplet-freezing, that included in vitro-grown shoot tips as materials for long-term storage. This study showed that the droplet-vitrification method allowed a high regrowth level of cryopreserved shoot tips, and consequent study [91] pointed out the effects of preculture conditions on the level of regenerated shoot tips after cryopreservation using this method.

Sakai and Nishiyama (1978) [92] were the first to mention the cryopreservation of in vivo apple dormant buds. In general, dormant bud cryopreservation procedures consist of desiccation and slow cooling to $-35\text{ }^{\circ}\text{C}$ prior to liquid nitrogen exposure [73]. Based on data from the National Laboratory for Genetic Resources Preservation (NLGRP), the lack of a need for aseptic cultures, high processing throughput, and approximately ten-times-lower cost of cryoprocessing compared to shoot tip cryopreservation are the major advantages of this method [74]. Most protocols used for ultra-low temperature storage of dormant apple buds are based on the original outlines by Forsline [93,94], involving: cutting of winter hardened twigs in segments containing the dormant bud, desiccation at a temperature from $-4\text{ }^{\circ}\text{C}$ to $-5\text{ }^{\circ}\text{C}$ of the segments until moisture content is reduced to about 30%, cooling in a programmable slow cooler to a final temperature of $-30\text{ }^{\circ}\text{C}$, and placing the cooled segments in liquid nitrogen vapor or liquid nitrogen for long-term storage. For plant regeneration, recovered scions with dormant buds are grafted directly on pot-grown rootstocks, or it is also possible to excise shoot tips from cryopreserved buds and place them on culture medium [95]. Successful regeneration of cryopreserved buds is tightly linked with the cold hardening of these buds before cryopreservation, rather than with the phase of endodormancy [96].

Several papers in recent years focused on pathogen eradication in apples by using cryotherapy. For example, the vitrification cryotherapy technique was reported by Romadanova et al. (2016) [97]. They infected apple cultivars and rootstocks and treated them with ultra-low temperatures to eliminate four different viruses (apple chlorotic leaf spot closterovirus (ACLSV), apple stem pitting virus (ASPV), apple stem grooving virus (ASGV), apple mosaic virus (ApMV)). Their therapy resulted in the production of virus-free plants for seven out of nine tested cultivars. In another study, the encapsulation-dehydration method was applied to in vitro-grown apple rootstocks M9 and M26 to eliminate ASPV and ASGV viruses. Cryotherapy was successful for ASPV but failed for ASGV. A probable explanation of this result was the different distribution of viruses in shoot tips. Although ASPV was not detected in the upper part of the apical dome and leaf primordia, ASGV was [89]. Results obtained two years later also showed that elimination of ASGV by cryotherapy had some limitations due to its localization in the shoot tip [58]. Finally, a recent study from the same research group examined the effect of another cryotherapy technique, i.e., droplet-vitrification, on the eradication of three latent apple viruses (ACLSV, ASGV, ASPV) from an infected 'Monalisa' apple cultivar. Cryotherapy was successful for the elimination of ASPV and ACLSV with 100% and 95% efficiencies, respectively. However, only 35% of regenerated plants were free of ASGV [59].

5. Conclusions

Cryopreservation is a progressive method for long-term storage of plant germplasm that uses the ultra-low temperature of liquid nitrogen to minimize the metabolism of living cells. This technique has great application potential in biotechnology, agriculture, horticulture, and breeding programs. Several methods and protocols for cryopreservation of plant germplasm were reviewed in this manuscript, and each of them has its merits and demerits, which should be considered before cryopreservation (Table 1). Cryopreservation can serve as an alternative storage solution to the traditional field collections. It also has possible applications in the conservation of endangered plant species germplasm. Ultra-low temperatures can be used not only for the storage of germplasm, but also for the eradication of plant pathogens, for which the term "cryotherapy" was coined. Cryotherapy of shoot tips is a promising method for plant pathogen eradication that can be easily used for different plant species and cultivars with available cryopreservation protocols. It can be carried out in a basically-equipped tissue culture laboratory, shows promising results in production of pathogen-free regenerants, and minimizes the risk of genetic changes during treatment compared to the classical methods. To date, more than 10,000 accessions of in vitro propagated crop plants are safely cryopreserved for the long term, and over 80% of these belong to five main crops (potato, cassava, bananas, mulberry, and garlic). In this review, we show that much of the work has already been done in the field of plant cryobiotechnology. However, some important challenges still remain and limit a more scaled applications of cryopreservation. For example, post-thaw regeneration of some important crop species (cassava, sweet potato) is still extremely low. Some plant species survive cryopreservation, but they are not able to root and stop the growth and development [6]. Altogether, for the future, the optimization and modification of the existing protocols will be required for more plant species and cultivars.

Author Contributions: Conceptualization, P.J. and J.S.; investigation, P.J.; writing—original draft preparation, P.J.; writing—review and editing, P.J. and J.S.; project administration, P.J.; funding acquisition, J.S. All authors have read and agreed to the published version of the manuscript.

Funding: This research was funded by Ministry of Education, Youth and Sport of the Czech Republic; grant number LO1608 "Research Pomological Centre".

Conflicts of Interest: The authors declare no conflict of interest.

References

1. Kaviani, B. Conservation of Plant Genetic Resources by Cryopreservation. *Aust. J. Crop Sci.* **2011**, *5*, 778–800.
2. Engelmann, F.; Engels, J.M.M. Technologies and strategies for ex situ conservation. In *Managing Plant Genetic Diversity*; Engels, J.M.M., Ramanatha Rao, V., Brown, A.H.D., Jackson, M.T., Eds.; CABI: Wallingford, UK, 2002; pp. 89–103.
3. Höfer, M.; Hanke, M.-V. Cryopreservation of fruit germplasm. *Vitr. Cell. Dev. Biol.-Plant* **2017**, *53*, 372–381. [[CrossRef](#)]
4. Walters, C.; Volk, G.M.; Stanwood, P.C.; Towill, L.E.; Koster, K.L.; Forsline, P.L. Long-term survival of cryopreserved germplasm: Contributing factors and assessments from thirty year old experiments. *Acta Hortic.* **2011**, *1*, 113–120. [[CrossRef](#)]
5. Sakai, A. Survival of plant tissue of super-low temperatures. *Plant Physiol.* **1956**, *14*, 17.
6. Panis, B. Sixty years of plant cryopreservation: From freezing hardy mulberry twigs to establishing reference crop collections for future generations. *Acta Hortic.* **2019**, *1*, 1–8. [[CrossRef](#)]
7. Kalaiselvi, R.; Rajasekar, M.; Gomathi, S. Cryopreservation of plant materials—A review. *IJCS* **2017**, *5*, 560–564.
8. Kaya, E.; Galatali, S.; Guldag, S.; Celik, O. A New Perspective on Cryotherapy: Pathogen Elimination Using Plant Shoot Apical Meristem via Cryogenic Techniques. In *Plant Stem Cells Methods and Protocols*; Naseem, M., Dandekar, T., Eds.; Humana: New York, NY, USA, 2020; pp. 137–148.
9. Panis, B.; Helliot, B.; Strosse, H.; Remy, S.; Lepoivre, P.; Swennen, R. Germplasm conservation, virus eradication and safe storage of transformation competent cultures in banana: The importance of cryopreservation. *Acta Hortic.* **2005**, *1*, 51–60. [[CrossRef](#)]
10. Sakai, A. Survival of Plant Tissue at Super-Low Temperature III. Relation between Effective Prefreezing Temperatures and the Degree of Front Hardiness. *Plant Physiol.* **1965**, *40*, 882–887. [[CrossRef](#)]
11. Reed, B.M. Plant cryopreservation: A continuing requirement for food and ecosystem security. *Vitr. Cell. Dev. Biol.-Plant* **2017**, *53*, 285–288. [[CrossRef](#)]
12. Reed, B.M. Implementing cryogenic storage of clonally propagated plants. *Cryo Lett.* **2001**, *22*, 97–104.
13. Volk, G.M.; Walters, C. Plant vitrification solution 2 lowers water content and alters freezing behavior in shoot tips during cryoprotection. *Cryobiology* **2006**, *52*, 48–61. [[CrossRef](#)] [[PubMed](#)]
14. Rahman, S.; Lamb, J. Air drying behavior of fresh and osmotically dehydrated pineapple. *J. Food Process. Eng.* **1991**, *14*, 163–171. [[CrossRef](#)]
15. Kumu, Y.; Harada, T.; Yakuwa, T. Development of a whole plant from a shoot tip of *Asparagus officinalis* L. frozen down to –196 degrees centigrade. *J. Fac. Agric. Hokkaido Univ.* **1983**, *61*, 285–294.
16. Grout, B.W.W.; Henshaw, G.G. Freeze Preservation of Potato Shoot-tip Cultures. *Ann. Bot.* **1978**, *42*, 1227–1229. [[CrossRef](#)]
17. Taylor, M.J.; Song, Y.C.; Brockbank, K.G.M. Vitrification in Tissue Preservation: New Developments. In *Life in the Frozen State*; Fuller, B.J., Lane, N., Benson, E.E., Eds.; CRC Press: London, UK, 2004; pp. 603–644, ISBN 978-0-203-64707-3.
18. Teixeira, A.S.; Faltus, M.; Zámečník, J.; González-Benito, M.E.; Molina-García, A.D. Glass transition and heat capacity behaviors of plant vitrification solutions. *Thermochim. Acta* **2014**, *593*, 43–49. [[CrossRef](#)]
19. Towill, L. Cryopreservation of isolated mint shoot tips by vitrification. *Plant Cell Rep.* **1990**, *9*, 9. [[CrossRef](#)]
20. Watanabe, K.; Steponkus, P.L. Vitrification of *Oryza sativa* L. cell suspensions. *Cryo Lett.* **1995**, *16*, 255–262.
21. Sakai, A.; Kobayashi, S.; Oiyama, I. Cryopreservation of nucellar cells of navel orange (*Citrus sinensis* Osb. var. *brasiliensis* Tanaka) by vitrification. *Plant Cell Rep.* **1990**, *9*, 9. [[CrossRef](#)]
22. Matsumoto, T. Cryopreservation of plant genetic resources: Conventional and new methods. *Rev. Agric. Sci.* **2017**, *5*, 13–20. [[CrossRef](#)]
23. Matsumoto, T.; Sakai, A.; Takahashi, C.; Yamada, K. Cryopreservation of in vitro-grown apical meristems of wasabi (*Wasabia japonica*) by encapsulation-vitrification method. *Cryo Lett.* **1995**, *16*, 189–196.
24. Kartha, K.K.; Leung, N.L.; Mroginski, L.A. In vitro Growth Responses and Plant Regeneration from Cryopreserved Meristems of Cassava (*Manihot esculenta* Crantz). *Z. Pflanzenphysiol.* **1982**, *107*, 133–140. [[CrossRef](#)]
25. Leunufna, S.; Keller, E.R.J. Investigating a new cryopreservation protocol for yams (*Dioscorea* spp.). *Plant Cell Rep.* **2003**, *21*, 1159–1166. [[CrossRef](#)] [[PubMed](#)]

26. Fabre, J.; Dereuddre, J. Encapsulation Dehydration—A New Approach to Cryopreservation of Solanum Shoot-Tips. *Cryo Lett.* **1990**, *11*, 413–426.
27. Yamamoto, S.; Rafique, T.; Priyantha, W.S.; Fukui, K.; Matsumoto, T.; Niino, T. Development of a Cryopreservation Procedure Using Aluminium Cryo-plates. *Cryo Lett.* **2011**, *32*, 256–265.
28. Niino, T.; Yamamoto, S.I.; Fukui, K.; Castillo Martinez, C.R.; Arizaga, M.V.; Matsumoto, T.; Engelmann, F. Dehydration improves cryopreservation of mat rush (*Juncus decipiens Nakai*) basal stem buds on cryo-plates. *Cryo Lett.* **2013**, *34*, 549–560.
29. Yamamoto, S.; Fukui, K.; Rafique, T.; Khan, N.I.; Castillo Martinez, C.R.; Sekizawa, K.; Matsumoto, T.; Niino, T. Cryopreservation of in vitro-grown shoot tips of strawberry by the vitrification method using aluminium cryo-plates. *Plant Genet. Res.* **2012**, *10*, 14–19. [[CrossRef](#)]
30. Rafique, T.; Yamamoto, S.; Fukui, K.; Mahmood, Z.; Niino, T. Cryopreservation of sugarcane using the V cryo-plate technique. *Cryo Lett.* **2015**, *36*, 51–59.
31. Salma, M.; Fki, L.; Engelmann-Sylvestre, I.; Niino, T.; Engelmann, F. Comparison of droplet-vitrification and D-cryoplate for cryopreservation of date palm (*Phoenix dactylifera* L.) polyembryonic masses. *Sci. Hortic.* **2014**, *179*, 91–97. [[CrossRef](#)]
32. Niino, T.; Wunna; Watanabe, K.; Nohara, N.; Rafique, T.; Yamamoto, S.; Fukui, K.; Arizaga, M.V.; Martinez, C.R.C.; Matsumoto, T.; et al. Cryopreservation of mat rush lateral buds by air dehydration using aluminum cryo-plate. *Plant Biotechnol.* **2014**, *31*, 281–287. [[CrossRef](#)]
33. Yamamoto, S.; Wunna; Rafique, T.; Arizaga, M.V.; Fukui, K.; Gutierrez, E.J.C.; Martinez, C.R.C.; Watanabe, K.; Niino, T. The Aluminum Cryo-plate Increases Efficiency of Cryopreservation Protocols for Potato Shoot Tips. *Am. J. Potato Res.* **2015**, *92*, 250–257. [[CrossRef](#)]
34. Waterworth, H.E.; Hadidi, A. Economical losses due to plant viruses. In *Plant Virus Disease Control*; Hadidi, A., Khetarpal, R.K., Koganezawa, H., Eds.; APS Press: St Paul, MN, USA, 1998; pp. 1–13.
35. Esquinas-Alcázar, J. Protecting crop genetic diversity for food security: Political, ethical and technical challenges. *Nat. Rev. Genet.* **2005**, *6*, 946–953. [[CrossRef](#)] [[PubMed](#)]
36. Wang, Q.; Valkonen, J.P.T. Cryotherapy of shoot tips: Novel pathogen eradication method. *Trends Plant Sci.* **2009**, *14*, 119–122. [[CrossRef](#)] [[PubMed](#)]
37. Kassanis, B. Heat inactivation of leaf-roll virus in potato tubers. *Ann. Appl. Biol.* **1950**, *37*, 339–341. [[CrossRef](#)]
38. Klein, R.E. Eradication of Potato Viruses X and S from Potato Shoot-Tip Cultures with Ribavirin. *Phytopathology* **1983**, *73*, 1049. [[CrossRef](#)]
39. Faccioli, V.C.; Marani, F. Virus elimination by meristem tipculture and tip micrografting. In *Plant Virus Disease Control*; Hadidi, A., Khetarpal, R.K., Koganezawa, H., Eds.; APS Press: St. Paul, MN, USA, 1998; pp. 346–380.
40. Kidulile, C.E.; Miinda Ateka, E.; Alakonya, A.E.; Ndunguru, J.C. Efficacy of chemotherapy and thermotherapy in elimination of *East African cassava mosaic virus* from Tanzanian cassava landrace. *J. Phytopathol.* **2018**, *166*, 739–745. [[CrossRef](#)]
41. Vivek, M.; Modgil, M. Elimination of viruses through thermotherapy and meristem culture in apple cultivar ‘Oregon Spur-II’. *Virus Dis.* **2018**, *29*, 75–82. [[CrossRef](#)]
42. Wang, M.-R.; Cui, Z.-H.; Li, J.-W.; Hao, X.-Y.; Zhao, L.; Wang, Q.-C. In vitro thermotherapy-based methods for plant virus eradication. *Plant Methods* **2018**, *14*, 87. [[CrossRef](#)]
43. Panattoni, A.; Luvisi, A.; Triolo, E. Review. Elimination of viruses in plants: Twenty years of progress. *Span. J. Agric. Res.* **2013**, *11*, 173. [[CrossRef](#)]
44. Mink, G.I.; Wample, R.; Howell, W.E. Heat treatment of perennial plants to eliminate phytoplasmas, viruses, and viroids while maintaining plant survival. In *Plant Virus Disease Control*; Hadidi, A., Khetarpal, R.K., Koganezawa, H., Eds.; APS Press: St. Paul, MN, USA, 1998; pp. 332–345.
45. Hu, G.; Dong, Y.; Zhang, Z.; Fan, X.; Ren, F.; Zhou, J. Virus elimination from in vitro apple by thermotherapy combined with chemotherapy. *Plant Cell Tissue Organ. Cult.* **2015**, *121*, 435–443. [[CrossRef](#)]
46. James, D.; Trytten, P.A.; Mackenzie, D.J.; Towers, G.H.N.; French, C.J. Elimination of apple stem grooving virus by chemotherapy and development of an immunocapture RT-PCR for rapid sensitive screening. *Ann. Appl. Biol.* **1997**, *131*, 459–470. [[CrossRef](#)]
47. Paprštejn, F.; Sedlák, J.; Svobodová, L.; Polák, J.; Gadiou, S. Results of in vitro chemotherapy of apple cv. Fragrance—Short communication. *Hort. Sci.* **2013**, *40*, 186–190. [[CrossRef](#)]

48. Brison, M.; De Boucaud, M.-T.; Pierronnet, A.; Dosba, F. Effect of cryopreservation on the sanitary state of a cv *Prunus rootstock* experimentally contaminated with *Plum Pox Potyvirus*. *Plant Sci.* **1997**, *123*, 189–196. [[CrossRef](#)]
49. Feng, C.; Wang, R.; Li, J.; Wang, B.; Yin, Z.; Cui, Z.; Li, B.; Bi, W.; Zhang, Z.; Li, M.; et al. Production of Pathogen-Free Horticultural Crops by Cryotherapy of In vitro-Grown Shoot Tips. In *Protocols for Micropropagation of Selected Economically-Important Horticultural Plants*; Lambardi, M., Ozudogru, E.A., Jain, S.M., Eds.; Methods in Molecular Biology; Humana Press: Totowa, NJ, USA, 2012; Volume 994, pp. 463–482.
50. Wang, Q.C.; Panis, B.; Engelmann, F.; Lambardi, M.; Valkonen, J.P.T. Cryotherapy of shoot tips: A technique for pathogen eradication to produce healthy planting materials and prepare healthy plant genetic resources for cryopreservation. *Ann. Appl. Biol.* **2009**, *154*, 351–363. [[CrossRef](#)]
51. Wang, Q.; Liu, Y.; Xie, Y.; You, M. Cryotherapy of Potato Shoot Tips for Efficient Elimination of *Potato Leafroll Virus* (PLRV) and *Potato Virus Y* (PVY). *Potato Res.* **2006**, *49*, 119–129. [[CrossRef](#)]
52. Wang, Q.C.; Valkonen, J.P.T. Efficient elimination of sweetpotato little leaf phytoplasma from sweetpotato by cryotherapy of shoot tips. *Plant Pathol.* **2008**, *57*, 338–347. [[CrossRef](#)]
53. Helliot, B.; Panis, B.; Poumay, Y.; Swennen, R.; Lepoivre, P.; Frison, E. Cryopreservation for the elimination of cucumber mosaic and banana streak viruses from banana (*Musa* spp.). *Plant Cell Rep.* **2002**, *20*, 1117–1122. [[CrossRef](#)]
54. Wang, Q.; Valkonen, J.P.T. Improved recovery of cryotherapy-treated shoot tips following thermotherapy of in vitro-grown stock shoots of raspberry (*Rubus idaeus* L.). *Cryo Lett.* **2009**, *30*, 170–182.
55. Pathirana, R.; McLachlan, A.; Hedderley, D.; Carra, A.; Carimi, F.; Panis, B. Removal of *Leafroll viruses* from infected grapevine plants by droplet vitrification. *Acta Hortic.* **2015**, *1*, 491–498. [[CrossRef](#)]
56. Bi, W.-L.; Hao, X.-Y.; Cui, Z.-H.; Pathirana, R.; Volk, G.M.; Wang, Q.-C. Shoot tip cryotherapy for efficient eradication of *Grapevine leafroll-associated virus-3* from diseased grapevine in vitro plants. *Ann. Appl. Biol.* **2018**, *173*, 261–270. [[CrossRef](#)]
57. Li, B.-Q.; Feng, C.-H.; Wang, M.-R.; Hu, L.-Y.; Volk, G.; Wang, Q.-C. Recovery patterns, histological observations and genetic integrity in *Malus* shoot tips cryopreserved using droplet-vitrification and encapsulation-dehydration procedures. *J. Biotechnol.* **2015**, *214*, 182–191. [[CrossRef](#)]
58. Bettoni, J.C.; Costa, M.D.; Souza, J.A.; Volk, G.M.; Nickel, O.; Da Silva, F.N.; Kretzschmar, A.A. Cryotherapy by encapsulation-dehydration is effective for in vitro eradication of latent viruses from ‘Marubakaido’ apple rootstock. *J. Biotechnol.* **2018**, *269*, 1–7. [[CrossRef](#)] [[PubMed](#)]
59. Bettoni, J.C.; Souza, J.A.; Volk, G.M.; Dalla Costa, M.; Da Silva, F.N.; Kretzschmar, A.A. Eradication of latent viruses from apple cultivar ‘Monalisa’ shoot tips using droplet-vitrification cryotherapy. *Sci. Hortic.* **2019**, *250*, 12–18. [[CrossRef](#)]
60. Wang, Q.C.; Valkonen, J.P.T. Elimination of two viruses which interact synergistically from sweetpotato by shoot tip culture and cryotherapy. *J. Virol. Methods* **2008**, *154*, 135–145. [[CrossRef](#)] [[PubMed](#)]
61. Feng, C.; Yin, Z.; Ma, Y.; Zhang, Z.; Chen, L.; Wang, B.; Li, B.; Huang, Y.; Wang, Q. Cryopreservation of sweetpotato (*Ipomoea batatas*) and its pathogen eradication by cryotherapy. *Biotechnol. Adv.* **2011**, *29*, 84–93. [[CrossRef](#)]
62. Wang, Q.; Mawassi, M.; Li, P.; Gafny, R.; Sela, I.; Tanne, E. Elimination of *Grapevine virus A* (GVA) by cryopreservation of in vitro-grown shoot tips of *Vitis vinifera* L. *Plant Sci.* **2003**, *165*, 321–327. [[CrossRef](#)]
63. Vieira, R.L.; Da Silva, A.L.; Zaffari, G.R.; Steinmacher, D.A.; De Freitas Fraga, H.P.; Guerra, M.P. Efficient elimination of virus complex from garlic (*Allium sativum* L.) by cryotherapy of shoot tips. *Acta Physiol. Plant.* **2015**, *37*, 1733. [[CrossRef](#)]
64. Taglienti, A.; Tiberini, A.; Barba, M. Cryotherapy: A new tool for the elimination of artichoke viruses. *J. Pathol.* **2013**, *95*. [[CrossRef](#)]
65. Wang, R.R.; Mou, H.Q.; Gao, X.X.; Chen, L.; Li, M.F.; Wang, Q.C. Cryopreservation for eradication of Jujube witches’ broom phytoplasma from Chinese jujube (*Ziziphus jujuba*): Cryopreservation for phytoplasma eradication. *Ann. Appl. Biol.* **2015**, *166*, 218–228. [[CrossRef](#)]
66. Ding, F.; Jin, S.; Hong, N.; Zhong, Y.; Cao, Q.; Yi, G.; Wang, G. Vitrification–cryopreservation, an efficient method for eliminating *Candidatus Liberobacter asiaticus*, the citrus Huanglongbing pathogen, from in vitro adult shoot tips. *Plant Cell Rep.* **2008**, *27*, 241–250. [[CrossRef](#)] [[PubMed](#)]

67. Wang, Q.; Cuellar, W.J.; Rajamäki, M.-L.; Hirata, Y.; Valkonen, J.P.T. Combined thermotherapy and cryotherapy for efficient virus eradication: Relation of virus distribution, subcellular changes, cell survival and viral RNA degradation in shoot tips. *Mol. Plant Pathol.* **2008**, *9*, 237–250. [[CrossRef](#)]
68. Benson, E.E. Cryopreservation of Phytodiversity: A Critical Appraisal of Theory & Practice. *Crit. Rev. Plant Sci.* **2008**, *27*, 141–219. [[CrossRef](#)]
69. Gallard, A.; Mallet, R.; Chevalier, M.; Grapin, A. Limited elimination of two viruses by cryotherapy of pelargonium apices related to virus distribution. *Cryo Lett.* **2011**, *32*, 111–122.
70. Wang, B.; Wang, R.-R.; Cui, Z.-H.; Bi, W.-L.; Li, J.-W.; Li, B.-Q.; Ozudogru, E.A.; Volk, G.M.; Wang, Q.-C. Potential applications of cryogenic technologies to plant genetic improvement and pathogen eradication. *Biotechnol. Adv.* **2014**, *32*, 583–595. [[CrossRef](#)] [[PubMed](#)]
71. Yin, Z.; Feng, C.; Wang, B.; Wang, Q.; Engelmann, F.; Lambardi, M.; Panis, B. Cryotherapy of shoot tips: A newly emerging technique for efficient elimination of plant pathogens. *Acta Hortic.* **2011**, *1*, 373–384. [[CrossRef](#)]
72. Engelmann, F. Plant cryopreservation: Progress and prospects. *Vitr. Cell Dev. Biol. Plant* **2004**, *40*, 427–433. [[CrossRef](#)]
73. Benelli, C.; De Carlo, A.; Engelmann, F. Recent advances in the cryopreservation of shoot-derived germplasm of economically important fruit trees of *Actinidia*, *Diospyros*, *Malus*, *Olea*, *Prunus*, *Pyrus* and *Vitis*. *Biotechnol. Adv.* **2013**, *31*, 175–185. [[CrossRef](#)]
74. Jenderek, M.M.; Tanner, J.D.; Chao, C.T.; Blackburn, H. How applicable are dormant buds in cryopreservation of horticultural woody plant crops? The *Malus* case. *Acta Hortic.* **2019**, *1*, 317–322. [[CrossRef](#)]
75. Forsline, P.; Aldwinckle, H.S.; Dickson, E.; Luby, J.J.; Hokanson, S.C. Collection, maintenance, characterization, and utilization of wild apples of Central Asia. *Hortic. Rev.* **2003**, *29*, 1–62.
76. Volk, G.M.; Richards, C.M.; Forsline, P.L. A comprehensive approach toward conserving *Malus* germplasm. *Acta Hortic.* **2010**, *1*, 177–182. [[CrossRef](#)]
77. Michalak, M.; Piitta-Michalak, B.P.; Chmielarz, P. Desiccation tolerance and cryopreservation of wild apple (*Malus sylvestris*) seeds. *Seed Sci. Technol.* **2015**, *43*, 480–491. [[CrossRef](#)]
78. Volk, G.M. Collecting pollen for genetic resources conservation. In *Collecting Plant Genetic Diversity: Technical Guidelines 2011 Update*; Guarino, L., Ramanatha Rao, V., Goldberg, E., Eds.; Bioversity International: Rome, Italy, 2011; pp. 1–10.
79. Xu, J.; Li, B.; Liu, Q.; Shi, Y.; Peng, J.; Jia, M.; Liu, Y. Wide-scale pollen banking of ornamental plants through cryopreservation. *Cryo Lett.* **2014**, *35*, 312–319.
80. Beltrán, R.; Valls, A.; Cebrián, N.; Zornoza, C.; García Breijo, F.; Reig Armiñana, J.; Garmendia, A.; Merle, H. Effect of temperature on pollen germination for several *Rosaceae* species: Influence of freezing conservation time on germination patterns. *PeerJ* **2019**, *7*, e8195. [[CrossRef](#)]
81. Wang, M.-R.; Chen, L.; Teixeira da Silva, J.A.; Volk, G.M.; Wang, Q.-C. Cryobiotechnology of apple (*Malus* spp.): Development, progress and future prospects. *Plant Cell Rep.* **2018**, *37*, 689–709. [[CrossRef](#)] [[PubMed](#)]
82. Stushnoff, C.; Seufferheld, M. Cryopreservation of Apple (*Malus* Species) Genetic Resources. In *Cryopreservation of Plant Germplasm I*; Bajaj, Y.P.S., Ed.; Biotechnology in Agriculture and Forestry; Springer: Heidelberg, Germany, 1995; Volume 32, pp. 87–101, ISBN 978-3-642-08184-2.
83. Kuo, C.C.; Lineberger, B.D. Survival of in vitro culture tissues of Jonathan apples exposed to $-196\text{ }^{\circ}\text{C}$. *Hortic. Sci.* **1985**, *20*, 764–767.
84. Wu, Y.; Engelmann, F.; Zhao, Y.; Zhou, M.; Chen, S. Cryopreservation of apple shoot tips: Importance of cryopreservation technique and of conditioning of donor plants. *Cryo Lett.* **1999**, *20*, 121–130.
85. Niino, T.; Sakai, A.; Yakuwa, H.; Nojiri, K. Cryopreservation of in vitro-grown shoot tips of apple and pear by vitrification. *Plant Cell Tissue Organ Cult.* **1992**, *28*, 261–266. [[CrossRef](#)]
86. Niino, T.; Sakai, A. Cryopreservation of alginate-coated in vitro-grown shoot tips of apple, pear and mulberry. *Plant Sci.* **1992**, *87*, 199–206. [[CrossRef](#)]
87. Paul, H.; Daigny, G.; Sangwan-Norreeel, B.S. Cryopreservation of apple (*Malus* \times *Domestica* Borkh.) shoot tips following encapsulation-dehydration or encapsulation-vitrification. *Plant Cell Rep.* **2000**, *19*, 768–774. [[CrossRef](#)]
88. Feng, C.-H.; Cui, Z.-H.; Li, B.-Q.; Chen, L.; Ma, Y.-L.; Zhao, Y.-H.; Wang, Q.-C. Duration of sucrose preculture is critical for shoot regrowth of in vitro-grown apple shoot-tips cryopreserved by encapsulation-dehydration. *Plant Cell Tissue Organ Cult.* **2013**, *112*, 369–378. [[CrossRef](#)]

89. Li, B.-Q.; Feng, C.-H.; Hu, L.-Y.; Wang, M.-R.; Wang, Q.-C. Shoot tip culture and cryopreservation for eradication of *Apple stem pitting virus* (ASPV) and *Apple stem grooving virus* (ASGV) from apple rootstocks ‘M9’ and ‘M26’: Eradication of apple virus. *Ann. Appl. Biol.* **2015**, *168*, 142–150. [[CrossRef](#)]
90. Halmagyi, A.; Deliu, C.; Isac, V. Cryopreservation of *Malus cultivars*: Comparison of two droplet protocols. *Sci. Hortic.* **2010**, *124*, 387–392. [[CrossRef](#)]
91. Halmagyi, A.; Vălimăreanu, V.; Coste, A.; Deliu, C.; Isac, V. Cryopreservation of *Malus* shoot tips and subsequent plant regeneration. *Rom. Biotechnol. Lett.* **2010**, 79–85.
92. Sakai, A.; Nishiyama, Y. Cryopreservation of winter vegetative buds of hardy fruit trees in liquid nitrogen. *Hortic. Sci.* **1978**, *13*, 223–227.
93. Forsline, P.L.; McFerson, J.R.; Lamboy, W.F.; Towill, L.E. Development of base and active collections of *malus* germplasm with cryopreserved dormant buds. *Acta Hortic.* **1998**, 75–78. [[CrossRef](#)]
94. Forsline, P.L.; Towill, L.E.; Waddell, J.W.; Stushnoff, C.; Lamboy, W.F.; McFerson, J.R. Recovery and Longevity of Cryopreserved Dormant Apple Buds. *J. Am. Soc. Hortic. Sci.* **1998**, *123*, 365–370. [[CrossRef](#)]
95. Towill, L.E.; Ellis, D.D. Cryopreservation of Dormant Buds. In *Plant Cryopreservation: A Practical Guide*; Reed, B.M., Ed.; Springer: New York, NY, USA, 2008; pp. 421–442.
96. Bilavcik, A.; Zamecnik, J.; Faltus, M. Cryotolerance of apple tree bud is independent of endodormancy. *Front. Plant Sci.* **2015**, *6*. [[CrossRef](#)]
97. Romadanova, N.V.; Mishustina, S.A.; Gritsenko, D.I.; Omasheva, M.Y.; Galiakparov, N.N.; Reed, B.M.; Kushnarenko, S.V. Cryotherapy as a method for reducing the virus infection of apples (*Malus* sp.). *Cryo Lett.* **2016**, *37*, 1–9. [[CrossRef](#)]



© 2020 by the authors. Licensee MDPI, Basel, Switzerland. This article is an open access article distributed under the terms and conditions of the Creative Commons Attribution (CC BY) license (<http://creativecommons.org/licenses/by/4.0/>).

Article

A Maturity Estimation of Bell Pepper (*Capsicum annuum* L.) by Artificial Vision System for Quality Control

Marcos-Jesús Villaseñor-Aguilar ^{1,2}, Micael-Gerardo Bravo-Sánchez ¹, José-Alfredo Padilla-Medina ¹, Jorge Luis Vázquez-Vera ¹, Ramón-Gerardo Guevara-González ³, Francisco-Javier García-Rodríguez ¹ and Alejandro-Israel Barranco-Gutiérrez ^{1,4,*}

¹ Doctorado en Ciencias de la Ingeniería, Tecnológico Nacional de México en Celaya, Celaya 38010, Mexico; mavillasenor@itess.edu.mx (M.-J.V.-A.); gerardo.bravo@itcelaya.edu.mx (M.-G.B.-S.); alfredo.padilla@itcelaya.edu.mx (J.-A.P.-M.); m1903054@itcelaya.edu.mx (J.L.V.-V.); francisco.garcia@itcelaya.edu.mx (F.-J.G.-R.)

² Departamento de Ingeniería Mecatrónica, Tecnológico Nacional de México en Salvatierra, Salvatierra 38933, Mexico

³ Grupo de Bioingeniería Básica y Aplicada, Facultad de Ingeniería, Facultad de Ingeniería, Universidad Autónoma de Querétaro, El Marques 76265, Mexico; ramon.guevara@uaq.mx

⁴ Cátedras-CONACyT, García Cubas esq. Av. Tecnológico, Celaya 38010, Mexico

* Correspondence: israel.barranco@itcelaya.edu.mx

Received: 4 June 2020; Accepted: 21 July 2020; Published: 24 July 2020

Abstract: Sweet bell peppers are a Solanaceous fruit belonging to the *Capsicum annuum* L. species whose consumption is popular in world gastronomy due to its wide variety of colors (ranging green, yellow, orange, red, and purple), shapes, and sizes and the absence of spicy flavor. In addition, these fruits have a characteristic flavor and nutritional attributes that include ascorbic acid, polyphenols, and carotenoids. A quality criterion for the harvest of this fruit is maturity; this attribute is visually determined by the consumer when verifying the color of the fruit's pericarp. The present work proposes an artificial vision system that automatically describes ripeness levels of the bell pepper and compares the Fuzzy logic (FL) and Neuronal Networks for the classification stage. In this investigation, maturity stages of bell peppers were referenced by measuring total soluble solids (TSS), ° Brix, using refractometry. The proposed method was integrated in four stages. The first one consists in the image acquisition of five views using the Raspberry Pi 5 Megapixel camera. The second one is the segmentation of acquired image samples, where background and noise are removed from each image. The third phase is the segmentation of the regions of interest (green, yellow, orange and red) using the connect components algorithm to select areas. The last phase is the classification, which outputs the maturity stage. The classificatory was designed using Matlab's Fuzzy Logic Toolbox and Deep Learning Toolbox. Its implementation was carried out onto Raspberry Pi platform. It tested the maturity classifier models using neural networks (RBF-ANN) and fuzzy logic models (ANFIS) with an accuracy of 100% and 88%, respectively. Finally, it was constructed with a content of ° Brix prediction model with small improvements regarding the state of art.

Keywords: bell pepper; maturity; fuzzy logic; computational vision

1. Introduction

Native to the Americas, sweet bell peppers are a Solanaceous fruit belonging to the *Capsicum annuum* L. species. It is a non-pungent fruit that is valued for its color, flavor, and nutritional attributes including ascorbic acid, polyphenolics, and various carotenoids. It comes in a wide variety of colors (ranging green, yellow, orange, red, and purple), shapes, and sizes, as well as because it has a

high content of ascorbic acid, polyphenols, and other antioxidants. Nowadays, bell peppers are widely consumed in various ways, dehydrated, preserved, frozen, or raw for packaged salads. Generally, the harvest of bell peppers is determined by the size, color, and texture of the fruit. Traditionally, the harvest of this fruit is done by reaching physiological maturity when the pericarp becomes thick and the fruit reaches the typical size. However, estimating pepper maturity at the green stage can be difficult even for fruit with similar physical attributes [1]. Under certain conditions, bell peppers can begin to ripen during shipping. Partially ripened fruit, classified as chocolate or suntan, have lower market values than at the solid color stage.

The bell peppers reach their optimum state of maturity for use in the kitchen when they are in solid color. Consumers prefer this fruit in its best stage of maturity more so than its physical appearance and nutritional content [2]. Dutch researchers specializing in the sensory area, reported that study groups have considered that more ripeness of bell peppers is sweeter and has a red pepper aroma, while those in the green stage were rated for bitterness and aroma of herbs and cucumber [3]. On the other hand, ripe peppers are more expensive to produce, due to the longer time required for ripening and the greater likelihood of damage from insects or disease. Furthermore, ripe peppers are more susceptible to physical damage during transport. In addition, they have a shorter shelf life due to the stage of maturity at which they are harvested. These fruits are non-climacteric regarding postharvest respiratory patterns. At the mentioned stage, bell peppers will progress through the normal ripening process to degrade chlorophyll while simultaneously synthesizing a variety of red and yellow carotenoids. The red and yellow varieties are the peppers most on demand by consumers, followed by the orange and purple varieties [4].

Bell pepper contains provitamin A, carotenoids, and xanthophylls. Many studies have focused on improving retention of these compounds during processing and storage [5–10] that increase their concentration as the fruit reaches a major state of maturity. Bell peppers also contain high concentrations of ascorbic acid ($0.15\text{--}2.0\text{ mg}\cdot\text{g}^{-1}$ fresh weight) compared to other fruits and vegetables [11–30]. The production of ascorbic acid in peppers and other fruits are related to glucose metabolism and light exposure, and concentrations of both ascorbic acid and sugar reduction typically increases with the stage of maturity [14]. Polyphenolics are also an important chemical component in bell peppers and impart functional properties to the plant such as disease resistance and potential health benefits to consumers. Some studies found that total phenolics, including the flavonoid quercetin, decrease with increased maturity for yellow bell peppers, but increased for other pepper varieties [6]. Estrada et al. [31] also demonstrated a decrease in free phenolic concentrations in peppers over five stages of maturity. Pepper growers could reduce field production costs by hastening the fruit ripening rate on the plant or by harvesting the fruit before attaining full color and completing the ripening process during storage without appreciable loss in quality or phytochemical attributes. An important criterion for consumers of sweet pepper is its sweetness, commonly estimated with the content of soluble solids (SSC) [22]. This parameter is associated with the different stages of fruit maturity [24–28]. The measurement of SSCs is traditionally a destructive test, to perform it, the most used instrument is the refractometer. This is an optical instrument that measures the refractive index of the juice from the sample [29,30].

At present, the food industry has demanded the use of non-invasive high precision measuring equipment that determines the external and internal quality parameters of the fruits [32]. In this respect, one of the disciplines that has had a great impact on fruit quality control is computational vision (VC). This has the characteristic that emulates the functionality of human vision and allows spatial and optical information from the captured image of the sample. Different investigations have been reported with VC focused on determining the degrees of ripeness of various fruits such as persimmon, strawberries, pomegranate, and tomato [33–35]. The present work aims to implement an artificial vision system that automatically describes the ripeness levels of the bell pepper.

More recently, total soluble solids (TSS) or Brix grades are a classical tool to determine the maturity of the fruits in the food industry even though it is a destructive technique. The content

of TSS consists of 80–95% sugars and the measure of TSS is associated with the dissolved sugars in cell juice [36]. These authors affirmed that the quantity of sugars in the fruit depends mainly on the variety, the assimilatory yield of the leaves, the leaf/fruit ratio, the climatic conditions during the development of the fruit, the state of development, and the maturity. The accumulation of sugars is associated with the development of optimum quality for consumption. Although the sugars can be transported to the fruit by the sap, they are also contributed by the splitting of the starch reserves of the fruits [36]. When the fruits in general have their highest sugar content, they have reached their physiological maturity, which coincides with what was investigated in relation to the bell peppers and their greater ripeness [37]. The TSS content showed a constant increase as the fruit maturity status increased, which could be seen with an increase in color fastness in the sample bell peppers. The ascending behavior of TSS content is consistent with that reported in the literature [37]. Kays [38] explained that, when the fruit is ripening in the plant, the sugars increase their concentration by the translocation of sucrose from the leaves, which occurs in most species. However, there is also the recycling of the respiratory substrate from the carbon stored in the fruit. Overall, highly significant positive correlations of soluble solids content were found with this research. The measurement of the TSS was done in triplicate with two different refractometers, an ATAGO Refractometer (MASTER-M model, Tokyo, Japan), Brix measurement scale of 0.0–33.0%, with a minimum of 0.2%, an accuracy of $\pm 0.2\%$, and repeatability of $\pm 0.1\%$; and a HANNA brand refractometer, model HI 96802 (Woonsocket, RI, USA), Brix measurement scale of 0.0–85.0%, with a temperature range of 0–80 °C, an accuracy of $\pm 0.2\%$, and repeatability of $\pm 0.1\%$.

Figure 1 shows the distribution of Brix grades of soluble solids content in the four stages of maturity of the fruit. This allowed us to establish that the grouping of the samples contemplates different stages of maturity of the bell pepper. This describes an increase in sugars from maturity Stage 1 to Stage 3 and the maximum sugar content is in State 4.

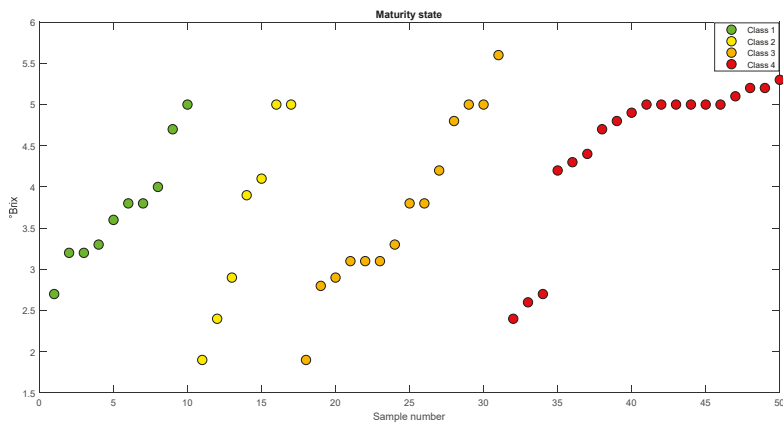


Figure 1. Distribution of Brix Grades in different stages of maturity.

2. Related Work

Currently, the high demand in the food industry has created the need for a fast and effective way to control the quality of products, which has led to the application of intelligent systems such as artificial vision that helps determine the internal and external properties of the fruits resulting in the stage of maturity. Different authors have focused on determining the maturity of various fruits such as apricot, nightshade, citrus, coffee, and mango. It is worth mentioning several studies that have focused on determining the maturity of bell peppers and estimating total soluble solids [39].

Harel et al. [40] classified their maturity using the random forest algorithm, which identified four classes: fully green, partially colored immature, mature partially colored, and colored.

Elhariri et al. [41] used an algorithm based on a support vector machine (SVM) for classification. This identified five maturity classes associated with green and red shades.

Shamili et al. [42] proposed a polynomial regression model that estimated the soluble solids content of mango. The descriptor that he proposed was the normal values of * a of the images captured from five types of mangoes; the samples he used had different percentages of skin coloration of 0%, 20%, 25%, 50%, and more than 50%.

Li et al. [43] used hyperspectral imaging in the visible and near-infrared (VNIR) and short-wave near-infrared (SWIR) regions focused on measuring maturity, firmness, and suspended sediment concentration (SSC). This research showed that there is a strong correlation between the SSC and the average spectra obtained from one or two opposite sides of the fruit in the SWIR region.

Another similar work was carried out by Teerachaichayut et al. [44], who proposed several models for limes to determine total soluble solids (TSS) and titratable acidity (TA) using partial least square regression.

3. Materials and Methods

3.1. Samples

A sample set of 50 bell peppers produced in the Laja-Bajió region, Guanajuato, Mexico was analyzed. The selected sample attributes consider different maturity degrees and homogeneous size [45]. For the training of the vision system, fruits with homogeneous and defined colors were chosen. Therefore, samples showing heterogeneous colors with various spots in the pericarp were excluded for this stage but were included for general testing. The bell peppers were classified into four classes, as shown in Figure 2. Class 1 grouped ten green samples. Class 2 was made up of seven yellow fruits. Class 3 was fourteen orange pigmented fruits. In Class 4, nineteen samples with a red hue were grouped.

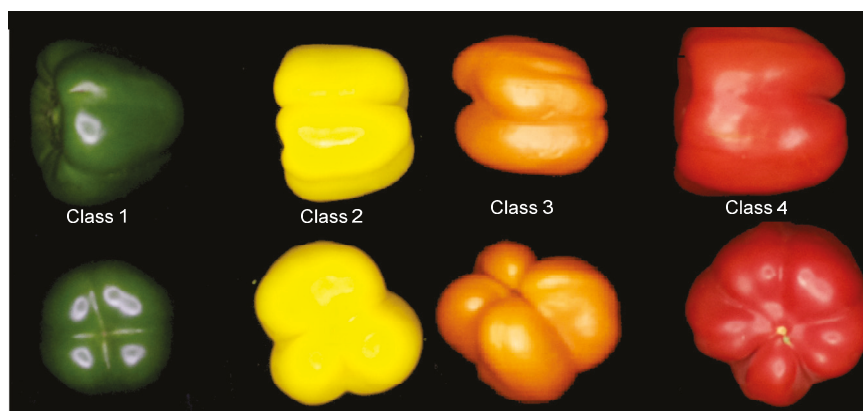


Figure 2. Samples of bell peppers in different degrees of maturity.

3.2. General Structure of Artificial Vision System

Figure 3 shows the proposed method for predicting the sugar content of bell pepper. The first step of the proposed method was the acquisition of the image samples using computer vision system (VCS). The second step was the segmentation of the fruit in the image, where the background and the supersaturated pixels were removed. The third step was the masking step to identify the regions of interest with green (GPOI), yellow (YPOI), orange (OPOI), and red (RPOI) pixels. These were obtained by means of four masks that use the red, green, blue (RGB) components of the segmented images. The fourth step was to obtain the areas of each region of interest (GAROI, YAROI, OAROI and RAROI).

The fifth step was the classification of the fruit with the areas from the filters. The last step was the prediction of ° Brix, which was done with the class and the areas determined by the masks.

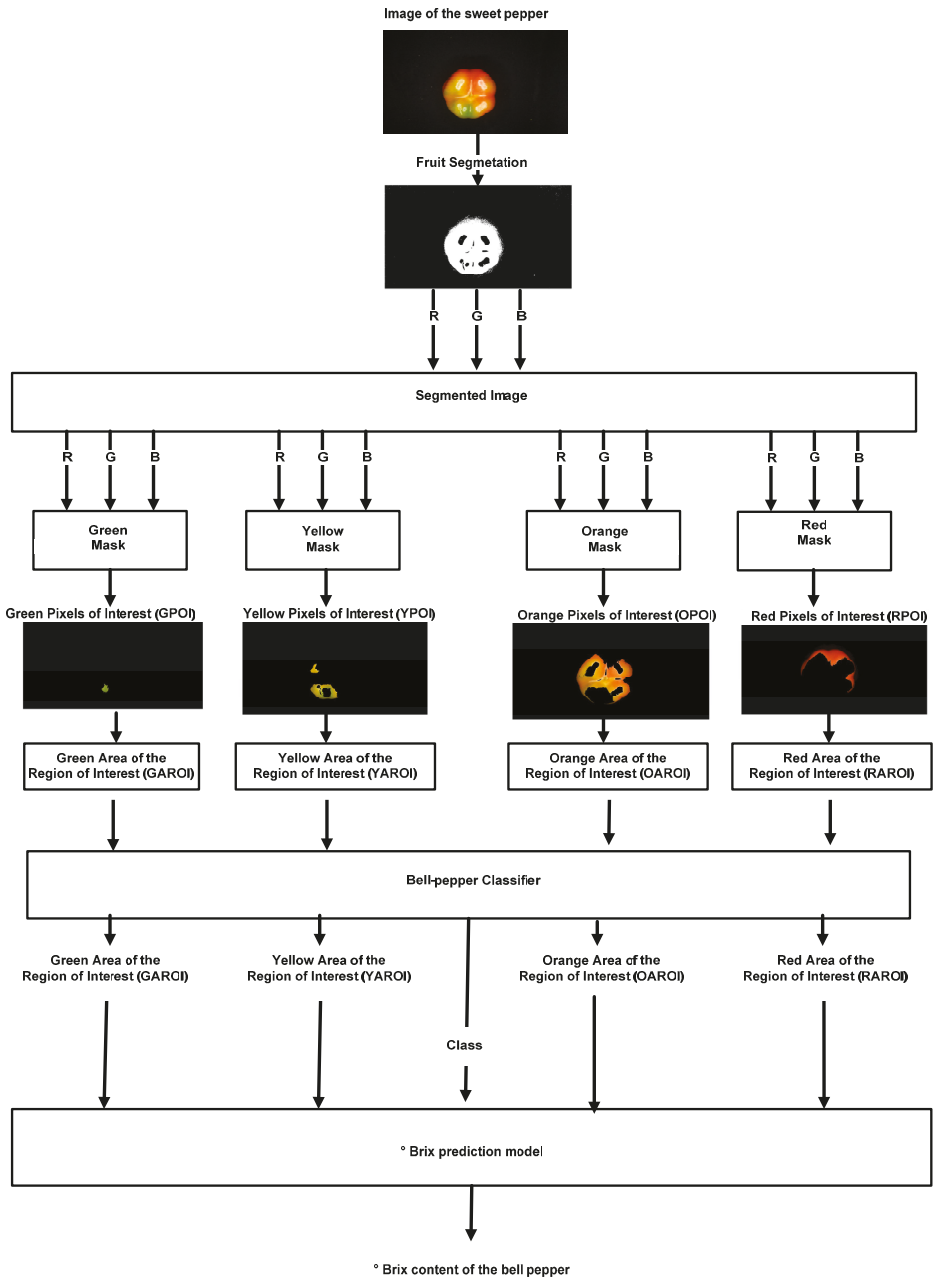


Figure 3. Proposed method to classify degrees of maturity in the bell pepper.

3.3. Image Acquisition

Five images per fruit were captured, as shown in Figure 4. The image format was JPG with a resolution of $768 \times 1366 \times 3$. The acquisition was made with a computational vision system (VSC) that operates with OpenCV-Python language. This was integrated by the isolation, lighting, image capture, and image processing subsystems. The insulation subsystem consisted of a black cabinet of dimensions $38 \text{ cm} \times 38 \text{ cm} \times 43 \text{ cm}$, which allowed the reduction of variations in lighting. The architecture used by the lighting subsystem was a 5.4 W led ring configuration placed 30 cm above sample. The image capture was performed with Raspberry camera module (8 megapixels), and the processing platform was Raspberry Pi 3 card [33].



Figure 4. Images acquired by vision system.

3.4. Automatic Sample Classification

In the second phase, the degrees and averages of the RGB channels of the segmented images of each fruit were mapped, as shown in Figure 5. G (green) corresponds to samples belonging to Class 1, Y (yellow) label to samples of Class 2, O (orange) label to the samples of Class 3, and R (red) label to the samples of Class 4. In the last phase, the regions of interest corresponding to the green, yellow, orange, and red tones were carried out.

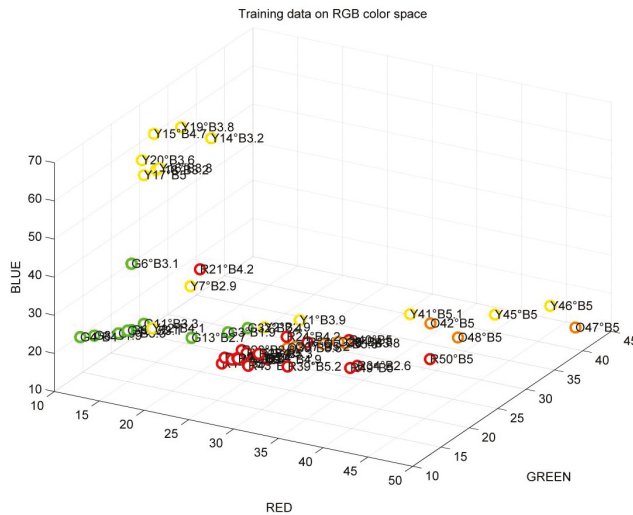


Figure 5. Mapping averages of the red, green, blue (RGB) channels for four classes of bell peppers.

3.5. Obtaining Regions of Interest

Obtaining regions of interest used the methodology proposed by Goel et al [32], as shown in Figure 6. (i) The first step required the binarization of the captured images, which was done using the Hue, Saturation, Value (HSV) color space model. This change in the color space model allowed obtaining the frequency of each color in the visible spectrum with component H, the purity of color

with component S, and the proximity of the pixel to black and white with component V. The thresholds used to segment the background of the samples were $122 \leq H \leq 255$, $127 \leq S \leq 255$, and $-0 \leq V \leq 255$ using a range from 0 to 255. (ii) The second step was segmentation of images of each view of bell pepper using a component connection algorithm, and later all the small regions smaller than 400 pixels that did not correspond to the binarized image of the sample were discriminated. (iii) The last step was to use respective masks to obtain regions of interest due to its color. Table 1 shows the four ranges of the Hue parameters to identify the pixel areas with green ($47 \leq H \leq 118$), yellow ($32 \leq H \leq 46$), orange ($15 \leq H \leq 32$), and red ($155 \leq H \leq 241$) hue of the images. Most of the masks except the red mask one used the range from 0 to 255 for the S and V components to identify the different color regions. The red mask used a smaller range of the S component that allowed the areas with orange and red pixels to be correctly identified. These thresholds were obtained using the 50 samples where each of its segmented images was analyzed. These masks identify the pixels corresponding to the green, yellow, orange, and red shades.

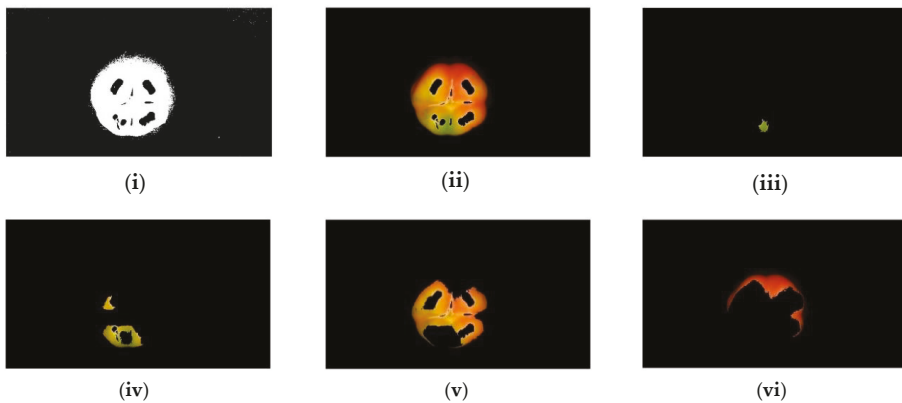


Figure 6. Pre-processing of images: (i) binarization of the image captured from the fruit; (ii) segmentation of the image and discrimination of areas; (iii) obtaining segmented sample applying the green mask of interest region; (iv) obtaining segmented sample applying the yellow mask of interest region; (v) obtaining segmented sample applying the orange mask of interest region; and (vi) obtaining segmented sample applying the red mask of interest region.

Table 1. Segmentation mask thresholds.

Green Mask					
H min	H max	S min	S max	V min	V max
47	118	0	255	0	255
Yellow Mask					
H min	H max	S min	S max	V min	V max
32	46	0	255	0	255
Orange Mask					
H min	H max	S min	S max	V min	V max
15	32	0	255	0	255
Red Mask					
L min	L min	L min	L min	L min	L min
241	155	11	247	0	255

3.6. Maturity Status Estimator

3.6.1. Artificial Neural Network (ANN)

Artificial neural networks (ANN) are mathematical models that emulate the functioning of biological neural networks. This was used in this study for its structural simplicity, learning skills, and its application for the approach, classification, and pattern recognition. Figure 7 presents the ANN architecture that was used to estimate the ° Brix content of the fifty samples presented in Figure 1. Its architecture consisted of an input layer, three hidden layers, and an output layer. The input layer is used to present the training and test patterns that correspond to the GAROI, YAROI, OAROI, and RAROI regions of interest. The hidden first layer used radial base-type activation functions, each of its neurons calculating the similarity between the input and its training set. The second hidden layer adds the values of each neuron from the first hidden layer that are multiplied by their weight associated with each neuron to obtain the class that the sample belongs to. The third layer of neurons employs neurons with sigmoidal-type firing functions where the sample classification information and the four regions of interest were weighted. The output layer is of the linear type, allowing the Brix content to be estimated using the weights associated with the neurons of the third hidden layer.

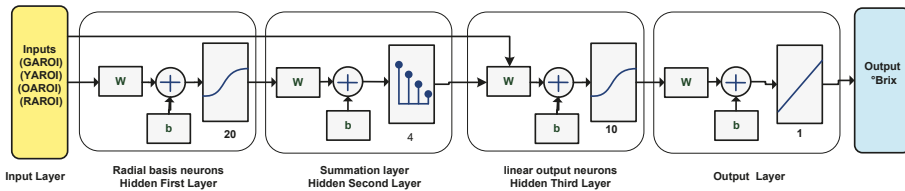


Figure 7. Brix prediction Artificial neural networks (ANN) model.

One of the ANNs most used in classification tasks is radial basis function ANN (RBF-ANN), as shown in Figure 8. Its architecture uses an input layer, hidden layers, and output layer. The input layer is used to present the training and test patterns. The hidden layer is made up of radial (Gaussian) functions that are completely interconnected between all its nodes with the input layer, which are activated by this function. The output layer is activated by the linear functions that determine the classification and is interconnected with all the nodes of the hidden layer.

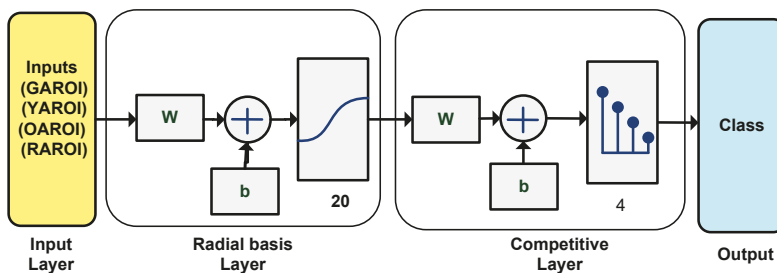


Figure 8. RBF-ANN maturity classifier.

The proposed RBFNN classification models were developed with Matlab’s Deep Learning Toolbox. The main difference between them is the number of neurons that the hidden layer contains, as shown in Table 2. The inputs used by each classifier are the interest regions with shades of green, yellow, orange, and red and the outputs are the four classes. The model design used 70% of the data for training, 20% for validation, and the rest for the testing stage.

Table 2. RBF-ANN maturity classifier.

	Inputs	Number of Neurons in the Hidden Layer	Output	Epochs	Accuracy
Model 1	4	4	4	10	92%
Model 2	4	5	4	10	98%
Model 3	4	8	4	10	100%
Model 4	4	10	4	10	100%
Model 5	4	15	4	10	100%

Together, three models of two-layer feed-forward network with sigmoid hidden neurons and linear output neurons (Fitnet) are proposed. Figure 9 presents the architecture of the implemented model to predict the ° Brix content of bell peppers. Three models were proposed where their main difference is the number of neurons in the hidden layer, as shown in Table 3; the precision of each model to predict the ° Brix was different.

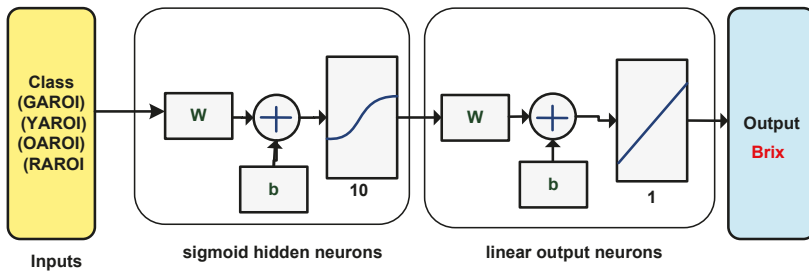


Figure 9. Architectural description of the model for ° Brix prediction using Fitnet.

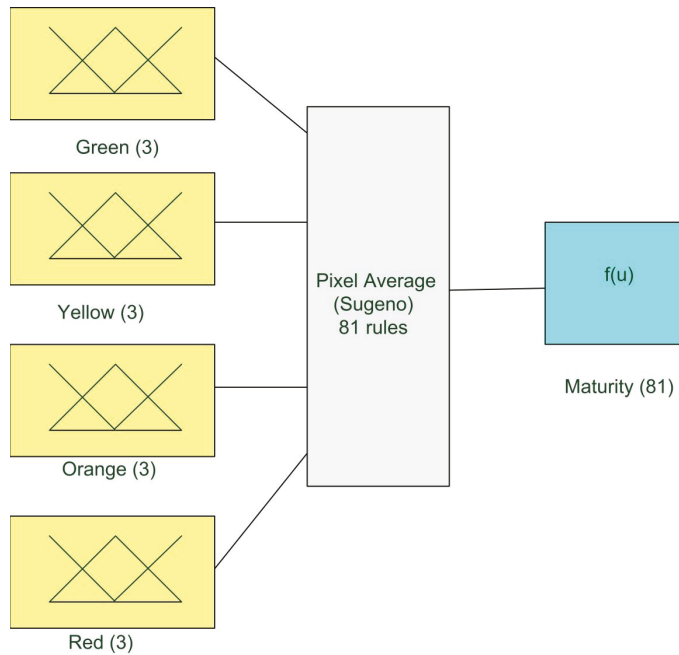
Table 3. Models using neural network Feedback prediction of Brix degrees.

	Inputs	Number of Neurons in the Hidden Layer	Output	Epochs	Mean Squared Error (MSE)	Pearson Correlation Coefficient (R)
Model 6	4	4	1	10	0.5483	0.68659
Model 7	4	5	1	10	0.5013	0.50130
Model 8	4	8	1	10	0.5016	0.73176
Model 9	4	10	1	10	0.4676	0.75910
Model 10	4	15	1	10	0.3888	0.79543

3.6.2. Fuzzy Logic

Fuzzy Logic (FL) is a discipline of Artificial Intelligence that analyzes real-world information on a scale between true and false. This is integrated by three stages: fuzzification, the inference that uses a series of linguistic rules, and defuzzification. Figure 10 shows a structure of the fuzzy classification system proposed to classify bell peppers. It has four inputs and one output.

The regions of interest of each shade correspond to the input and are used to identify the degree of maturity associated with the output fuzzy system. It is used to identify segments or regions of interest with shades of green, yellow, orange, and red. The output has different ranges for each class.



System Pixel Average: 4 inputs, 1 outputs, 81 rules

Figure 10. Fuzzy maturity classifier.

Fuzzification of the input variables was carried out with membership functions of triangular type, which are characterized by their easy implementation in hardware. The linguistic variables used were low, medium, and high, as shown in Figures 11–14. The mathematical functions of each membership function are described in Equations (1)–(12). Together, the different pixel areas were used to increase the sensitivity of the fuzzy system to infer maturity changes.

$$LowGAROI = \left\{ \frac{50 - GAROI}{50} \mid 0 < GAROI \leq 50 \right. \left. \frac{GAROI - 50}{50} \mid 50 < GAROI \leq 100 \right. \quad (1)$$

$$MediumGAROI = \left\{ \frac{GAROI}{50} \mid 0 < GAROI \leq 50 \right. \left. \frac{100 - GAROI}{50} \mid 50 < GAROI \leq 100 \right. \quad (2)$$

$$HighGAROI = \left\{ 1 \mid 100 < GAROI \leq 100 \right. \left. \frac{GAROI - 50}{50} \mid 50 < GAROI \leq 100 \right. \quad (3)$$

$$LowYAROI = \left\{ \frac{29.09 - YAROI}{29.09} \mid 0 < YAROI \leq 16.48 \right. \left. \frac{YAROI - 16.48}{16.48} \mid 16.48 < YAROI \leq 34.73 \right. \quad (4)$$

$$MediumYAROI = \left\{ \frac{YAROI}{29.09} \mid 0 < YAROI \leq 29.09 \right. \left. \frac{58.17 - YAROI}{29.08} \mid 29.09 < YAROI \leq 58.17 \right. \quad (5)$$

$$HighYAROI = \left\{ 1 \mid 0 < YAROI \leq 29.09 \right. \left. \frac{YAROI - 29.09}{29.09} \mid 29.09 < YAROI \leq 58.17 \right. \quad (6)$$

$$LowOAROI = \left\{ \frac{16.48 - OAROI}{16.48} \mid 0 < OAROI \leq 16.48 \right. \left. \frac{OAROI - 34.73}{18.25} \mid 16.48 < OAROI \leq 34.37 \right. \quad (7)$$

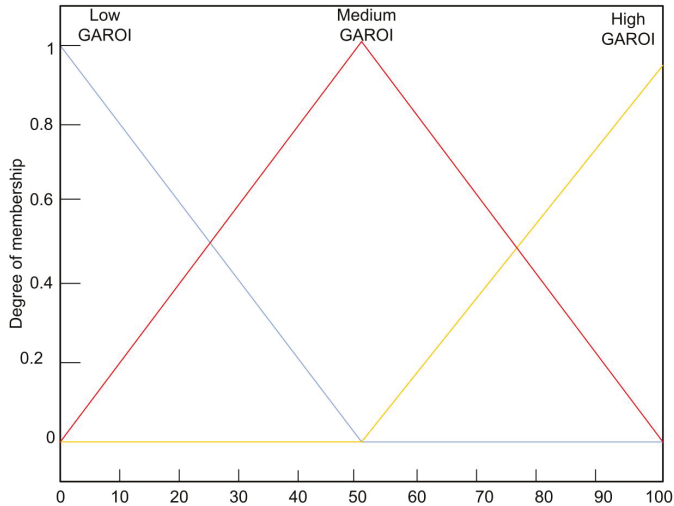
$$MediumOAROI = \left\{ \frac{16.48 - OAROI}{16.48} \mid 0 < OAROI \leq 16.48 \right. \left. \frac{OAROI - 34.73}{18.25} \mid 16.48 < OAROI \leq 34.37 \right. \quad (8)$$

$$HighOAROI = \left\{ \frac{16.48 - OAROI}{16.48} \mid 0 < OAROI \leq 16.48 \right. \left. \frac{OAROI - 34.73}{18.25} \mid 16.48 < OAROI \leq 34.37 \right. \quad (9)$$

$$\text{Low RROI} = \begin{cases} \frac{16.48 - RROI}{16.48} & 0 < RROI \leq 16.48 \\ \frac{RROI - 34.73}{18.25} & 16.48 < RROI \leq 34.37 \end{cases} \quad (10)$$

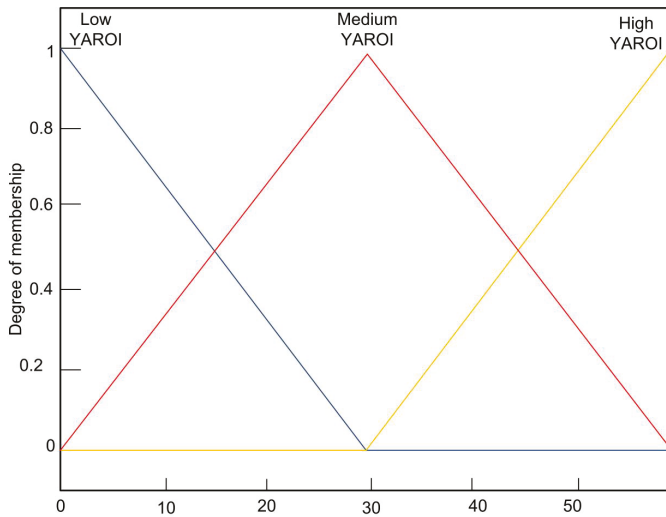
$$\text{Medium RROI} = \begin{cases} \frac{16.48 - RROI}{16.48} & 0 < RROI \leq 16.48 \\ \frac{RROI - 34.73}{18.25} & 16.48 < RROI \leq 34.37 \end{cases} \quad (11)$$

$$\text{High RROI} = \begin{cases} \frac{16.48 - RROI}{16.48} & 0 < RROI \leq 16.48 \\ \frac{RROI - 34.73}{18.25} & 16.48 < RROI \leq 34.37 \end{cases} \quad (12)$$



Green

Figure 11. Membership functions of GAROI input.



Yellow

Figure 12. Membership functions of YAROI input.

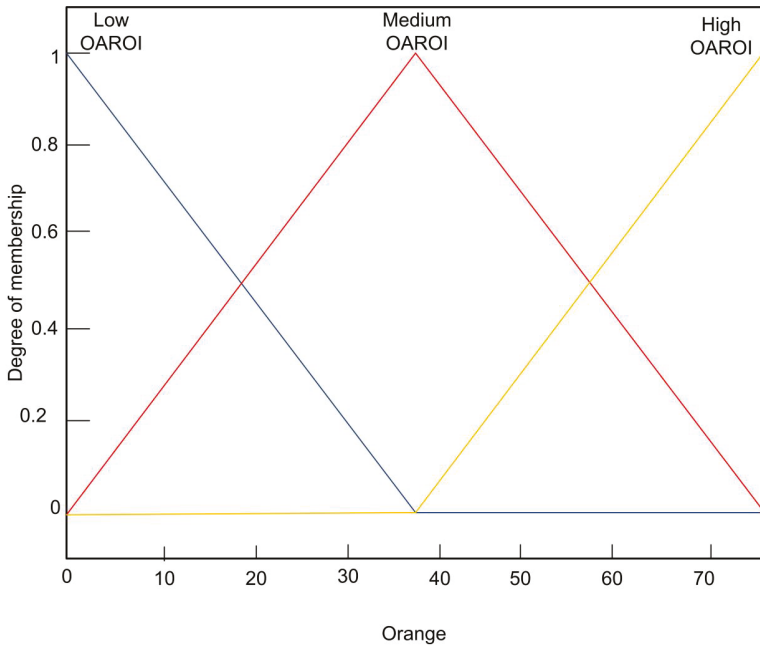


Figure 13. Membership functions of OAROI input.

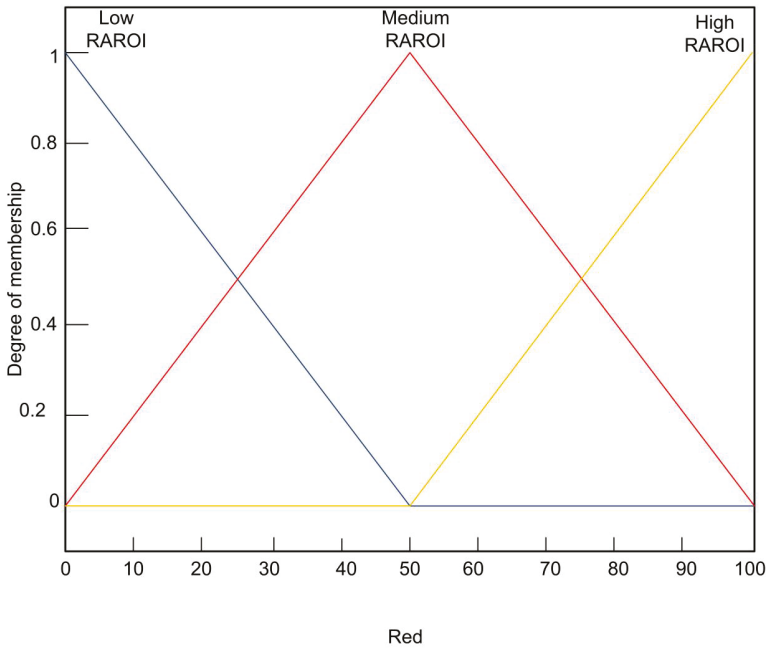


Figure 14. Membership functions of RAROI input.

Figure 15 shows the fuzzy Takagi–Sugeno model used for the development of the classifier; this was selected for its low computational cost unlike the Mandami model. It uses 81 inference rules

obtained from using fuzzy values of interest regions. The transforming fuzzy values of classification output was carried out using Equation (13). The final output is determined by rules using Z_i levels of output and weight w_i of the rule.

$$Final\ Output = \frac{\sum_{i=1}^N w_i Z_i}{\sum_{i=1}^{18} w_i} \tag{13}$$

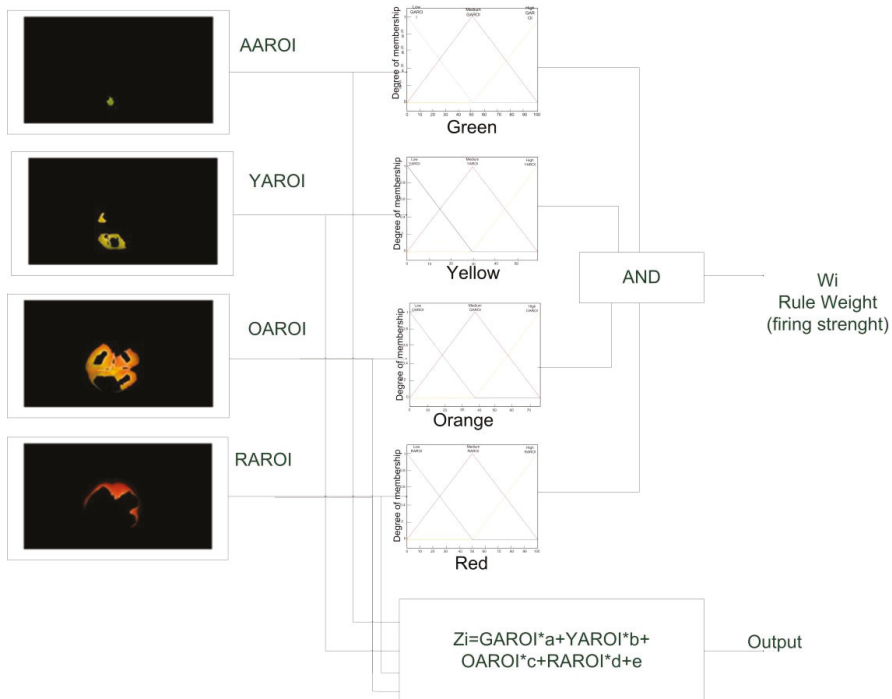


Figure 15. Operation of Takagi–Sugeno rules to classify maturity of bell peppers.

Five fuzzy classification models were designed using the Matlab R2014a Fuzzy Logic Toolbox. Its training used a set of 50 vectors consisting of areas the interest regions in shades of green, yellow, orange, and red and their label corresponding to their maturity. The training used 10 epochs. The main difference between the models is the number of membership functions. Table 4 shows the number of membership functions used by each model and their training error.

Table 4. Classification models.

	Number of GROI Membership Functions	Number of YROI Membership Functions	Number of OROI Membership Functions	Number of RROI Membership Functions	Training Error RMSE $\times 10^{-6}$
Model 11	2	2	2	2	930.46
Model 12	3	2	2	3	479.86
Model 13	2	3	3	2	19.466
Model 14	3	3	3	3	9.8679
Model 15	4	4	4	4	2.0339

Three models were proposed where their main difference is the number of neurons in the hidden layer, as shown in Table 5; the precision of each model to predict the Brix degrees was different.

Table 5. Models using FL prediction of ° Brix.

	Number of GROI Membership Functions	Number of YROI Membership Functions	Number of OROI Membership Functions	Number of RROI Membership Functions	Mean Squared Error (MSE)	Root Mean Squared Error (RMSE)	Pearson Correlation Coefficient (R)
Model 16	3	3	3	3	5.923	2.433	0.499
Model 17	4	3	3	4	0.891	0.944	0.696
Model 18	3	4	4	3	1.645	1.282	0.424

4. Results

Figure 16 shows the accuracy of the 10 maturity classifier models using ANN and FL. The first five models are type ANN (blue circles) and the next five models are type FL (red squares). It can be seen that the proposed models which used ANN achieved greater than 90% accuracy, unlike those that used FL. Together, the models that had good precision are Models 13–15. Finally, the worst models were Models 11 and 12 with an accuracy of less than 70%. In Figure 17, the prediction error of the model is presented, where it can be highlighted that the models which use ANN have lower least squared medium error. Five ANN models (blue circles) and three FL models (red squares) are shown.

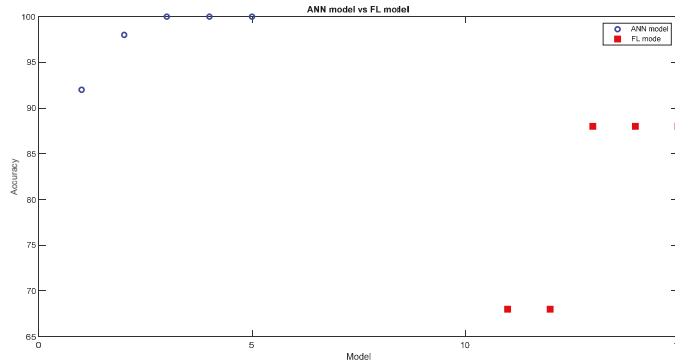


Figure 16. Comparison of maturity prediction models.

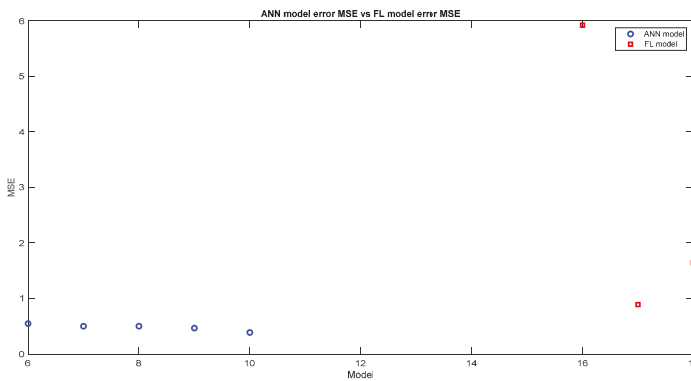


Figure 17. Comparison of ° Brix prediction models.

5. Discussion

The main contribution of this work is the development of a ° Brix content prediction system for bell pepper maturity. According to the results, the models with FL achieved a maximum precision of

88% in identifying the four stages of maturity corresponding to the shades of green, yellow, orange, and red. The models with ANN have 100% precision to identify samples of green and red color similar to the results reported by Elhariri et al. [41]. Of the results obtained, Model 8 was the one that presented a correlation of $R = 0.79543$ between the green, yellow, orange, and red regions of interest and $^{\circ}$ Brix. This result is similar to that reported by Shamili [42] and is slightly superior to those reported by Leiva-Valenzuela et al. [46] ($R = 0.788$) and Rahman et al. [47] ($R = 0.74$). The advantage is that our proposal uses a visible RGB camera and they used a high-cost multispectral camera. Figure 18 shows the estimation.

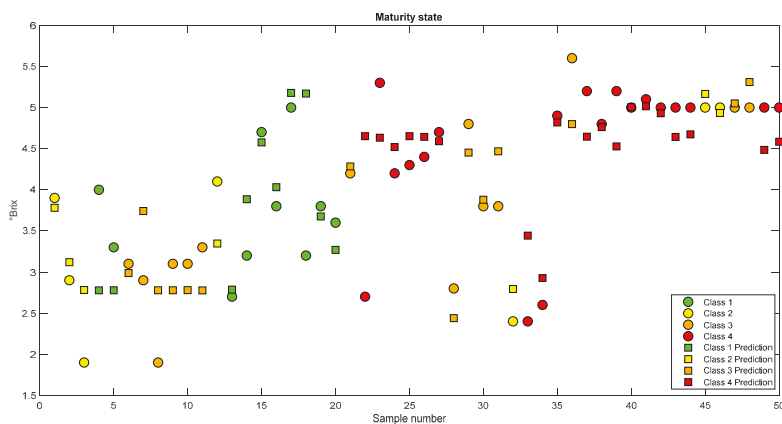


Figure 18. The samples $^{\circ}$ Brix was measured with refractometry. The measurements are presented as circles and the proposed system's estimates are indicated by squares.

6. Conclusions

In this work, a new classification system is proposed to evaluate the bell peppers maturity using an artificial vision system. According to the results obtained, it can be concluded that the proposed architecture improves the $^{\circ}$ Brix prediction using the regions of interest associated with the color of the pericarp. The correlation obtained was $R = 0.7929$ with the use of the NETFIT-ANN, surpassing the model designed with FL with a correlation of $R = 0.696$. Together, it was possible to classify 100% of the classes of the samples with the use of a model that uses the RBF-ANN architecture. This architecture presented a better result than the FL models that obtained a maximum accuracy of 88%. The present work demonstrated that it is possible to identify the degrees of maturity of the peppers using an artificial vision system that is sensitive to the total soluble solids content of the fruit. It has the advantage of using a low-cost RGB camera instead of a multispectral one, and it is a non-destructive technique to estimate $^{\circ}$ Brix. This vision system model is applicable to real scenarios in the industrial sector such as online processes. Furthermore, it is a system that can be used to predict the $^{\circ}$ Brix content in real time. As further research, the development of a prediction system for ascorbic acid, polyphenolics, and various carotenoids has been completed.

Author Contributions: Conceptualization, M.-J.V.-A., M.-G.B.-S. and A.-I.B.-G.; methodology, J.-A.P.-M.; software, M.-J.V.-A.; validation, M.-G.B.-S.; formal analysis, J.L.V.-V.; investigation, R.-G.G.-G.; data curation, F.-J.G.-R.; writing—original draft preparation, M.-G.B.-S. and M.-J.V.-A.; writing—review and editing, A.-I.B.-G.; and supervision, A.-I.B.-G. All authors have read and agreed to the published version of the manuscript.

Funding: This research was funded by CONACyT and Tecnológico Nacional de Mexico.

Conflicts of Interest: The authors declare no conflict of interest.

Link to Images Database: <https://drive.google.com/drive/u/0/folders/1gzmh1E16IPGkMnHX8yOfp2FjUbgNsW6>

References

1. Tadesse, T.; Hewett, E.W.; Nichols, M.A.; Fisher, K.J. Changes in physicochemical attributes of sweet pepper cv. Domino during fruit growth and development. *Sci. Hortic.* **2002**, *93*, 91–103. [[CrossRef](#)]
2. Frank, C.A.; Nelson, R.G.; Simonne, E.H.; Behe, B.K.; Simonne, A.H. Consumer preferences for color, price, and vitamin C content of bell peppers. *HortScience* **2001**, *36*, 795–800. [[CrossRef](#)]
3. Luning, P.A.; van der Vuurst, D.V.R.; Yuksel, D.; Ebenhorst-Seller, T.; Wichers, H.J.; Roozen, J.P. Combined instrumental and sensory evaluation of flavor of fresh bell peppers (*Capsicum annuum*) harvested at three maturation stages. *J. Agric. Food Chem.* **1994**, *42*, 2855–2861. [[CrossRef](#)]
4. Saltveit, M.E., Jr. Carbon dioxide, ethylene, and color development in ripening mature green bell peppers. *J. Am. Soc. Hortic. Sci.* **1977**, *102*, 523–525.
5. Howard, L.R.; Hernandez-Brenes, C. Antioxidant content and market quality of jalapeno pepper rings as affected by minimal processing and modified atmosphere packaging. *J. Food Qual.* **1998**, *21*, 317–327. [[CrossRef](#)]
6. Howard, L.R.; Talcott, S.T.; Brenes, C.H.; Villalon, B. Changes in phytochemical and antioxidant activity of selected pepper cultivars (*Capsicum species*) as influenced by maturity. *J. Agric. Food Chem.* **2000**, *48*, 1713–1720. [[CrossRef](#)]
7. Hornero-Mendez, D.; Minguez-Mosquera, M.I. Xanthophyll esterification accompanying carotenoid overaccumulation in chromoplast of *Capsicum annuum* ripening fruits is a constitutive process and useful for ripeness index. *J. Agric. Food Chem.* **2000**, *48*, 1617–1622. [[CrossRef](#)]
8. Hornero-Mendez, D.; Minguez-Mosquera, M.I. Rapid spectrophotometric determination of red and yellow isochromic carotenoid fractions in paprika and red pepper oleoresins. *J. Agric. Food Chem.* **2001**, *49*, 3584–3588. [[CrossRef](#)]
9. Markus, F.; Daood, H.G.; Kapitany, J.; Biacs, P.A. Change in the carotenoid and antioxidant content of spice red pepper (paprika) as a function of ripening and some technological factors. *J. Agric. Food Chem.* **1999**, *47*, 100–107. [[CrossRef](#)]
10. Minguez-Mosquera, M.; Hornero-Mendez, D. Comparative study of the effect of paprika processing on the carotenoids in peppers (*Capsicum annuum*) of the Bola and Agridulce varieties. *J. Agric. Food Chem.* **1994**, *42*, 1555–1560. [[CrossRef](#)]
11. Curl, A.L. The carotenoids of red bell peppers. *J. Agric. Food Chem.* **1962**, *10*, 504–509. [[CrossRef](#)]
12. Molinari, A.F.; De Castro, L.R.; Antoniali, S.; Pornchaloempong, P.; Fox, A.J.; Sargent, S.A.; Lamb, E.M. The potential for bell pepper harvest before full color development. *Proc. Fla. State Hort. Soc.* **2000**, *112*, 143–146.
13. Osuna-Garcia, J.A.; Wall, M.M.; Waddell, C.A. Endogenous levels of tocopherols and ascorbic acid during fruit ripening of new Mexi-can-type chile (*Capsicum nnuum* L.) cultivars. *J. Agric. Food Chem.* **1998**, *46*, 5093–5096. [[CrossRef](#)]
14. Russo, V.M.; Howard, L.R. Carotenoids in pungent and nonpungent peppers at various developmental stages grown in the field and glasshouse. *J. Sci. Food Agric.* **2002**, *82*, 615–624. [[CrossRef](#)]
15. Ryall, A.L.; Lipton, W.J. Handling transportation and storage of fruits and vegetables. In *Vegetables and Melons*, 2nd ed.; AVI Publ. Co.: Westport, CT, USA, 1979; p. 587.
16. Yahia, E.M.; Contreras-Padilla, M.; Gonzalez-Aguilar, G. Ascorbic acid content in relation to ascorbic acid oxidase activity and polyamine content in tomato and bell pepper fruits during development, maturation and senescence. *LWT* **2001**, *34*, 452–457. [[CrossRef](#)]
17. Matsufuji, H.; Nakamura, H.; Chino, M.; Takeda, M. Antioxidant activity of capsanthin and the fatty acid esters in paprika (*Capsicum annuum*). *J. Agric. Food Chem.* **1998**, *46*, 3468–3472. [[CrossRef](#)]
18. Cantliffe, D.J.; Goodwin, P. Red color enhancement of pepper fruits by multiple applications of ethephon. *J. Am. Soc. Hortic. Sci.* **1975**, *100*, 157–161.
19. Simonne, A.H.; Simonne, E.H.; Eitenmiller, R.R.; Mills, H.A.; Green, N.R. Ascorbic Acid and Provitamin A Contents in Unusually Colored Bell Peppers (*Capsicum annuum* L.). *J. Food Compos. Anal.* **1997**, *10*, 299–311. [[CrossRef](#)]
20. Garcia-Mier, L.; Jimenez-Garcia, S.N.; Guevara-González, R.G.; Feregrino-Perez, A.A.; Contreras-medina, L.M.; Torres-Pacheco, I. Elicitor Mixtures Significantly Increase Bioactive Compounds, Antioxidant Activity, and Quality Parameters in Sweet Bell Pepper. *J. Chem.* **2015**, *2015*, 269296. [[CrossRef](#)]

21. Chávez-Mendoza, C.; Sanchez, E.; Muñoz-Marquez, E.; Sida-Arreola, J.P.; Flores-Cordova, M.A. Bioactive Compounds and Antioxidant Activity in Different Grafted Varieties of Bell Pepper. *Antioxidants* **2015**, *4*, 427–446. [CrossRef]
22. Chen, H.Z.; Zhang, M.; Bhandari, B.; Guo, Z. Evaluation of the freshness of fresh-cut green bell pepper (*Capsicum annuum* var. *grossum*) using electronic nose. *LWT* **2018**, *87*, 77–84. [CrossRef]
23. Baenas, N.; Belović, M.; Ilic, N.; Moreno, D.A.; García-Viguera, C. Industrial use of pepper (*Capsicum annuum* L.) derived products: Technological benefits and biological advantages. *Food Chem.* **2019**, *274*, 872–885. [CrossRef] [PubMed]
24. Wan, P.; Toudeshki, A.; Tan, H.; Ehsani, R. A methodology for fresh tomato maturity detection using computer vision. *Comput. Electron. Agric.* **2018**, *146*, 43–50. [CrossRef]
25. Zhang, B.; Gu, B.; Tian, G.; Zhou, J.; Huang, J.; Xiong, Y. Challenges and solutions of optical-based nondestructive quality inspection for robotic fruit and vegetable grading systems: A technical review. *Trends Food Sci. Technol.* **2018**, *81*, 213–231. [CrossRef]
26. Li, C.; Cao, Q.; Guo, F. A method for color classification of fruits based on machine vision. *WSEAS Trans. Syst.* **2009**, *8*, 312–321.
27. Cavallo, D.P.; Cefola, M.; Pace, B.; Logrieco, A.F.; Attolico, G. Non-destructive automatic quality evaluation of fresh-cut iceberg lettuce through packaging material. *J. Food Eng.* **2018**, *223*, 46–52. [CrossRef]
28. Huang, Y.; Lu, L.R.; Chen, K. Prediction of firmness parameters of tomatoes by portable visible and near-infrared spectroscopy. *J. Food Eng.* **2018**, *222*, 185–1984. [CrossRef]
29. Guo, W.; Li, W.; Yang, B.; Zhu, Z.Z.; Liu, D.; Zhu, X. A novel noninvasive and cost-effective handheld detector on soluble solids content of fruits. *J. Food Eng.* **2019**, *257*, 1–9. [CrossRef]
30. Munera, S.; Besada, C.; Aleixos, N.; Talens, P.; Salvador, A.; Sun, D.W.; Cubero, S.; Blasco, J. Non-destructive assessment of the internal quality of intact persimmon using colour and VIS/NIR hyperspectral imaging. *LWT* **2017**, *77*, 241–248. [CrossRef]
31. Estrada, B.; Bernal, M.A.; Diaz, J.; Pomar, F.; Merino, F. Fruit development in *Capsicum annuum*: Changes in capsaicin, lignin, free phenolics, and peroxidase patterns. *J. Agric. Food Chem.* **2000**, *48*, 6234–6239. [CrossRef]
32. Goel, N.; Sehgal, P. Fuzzy classification of pre-harvest tomatoes for ripeness estimation—An approach based on automatic rule learning using decision tree. *Appl. Soft Comput. J.* **2015**, *36*, 45–56. [CrossRef]
33. Villaseñor-Aguilar, M.J.; Botello-Álvarez, J.E.; Pérez-Pinal, F.J.; Cano-Lara, M.; León-Galván, M.F.; Bravo-Sánchez, M.G.; Barranco-Gutierrez, A.I. Fuzzy classification of the maturity of the tomato using a vision system. *J. Sensors* **2019**, *2019*, 1–12. [CrossRef]
34. Constante, P.; Gordon, A.; Chang, O.; Pruna, E.; Acuna, F.; Escobar, I. Artificial Vision Techniques to Optimize Strawberrys Industrial Classification. *IEEE Lat. Am. Trans.* **2016**, *14*, 2576–2581. [CrossRef]
35. Fashi, M.; Naderloo, L.; Javadikia, H. The relationship between the appearance of pomegranate fruit and color and size of arils based on image processing. *Postharvest Biol. Technol.* **2019**, *154*, 52–57. [CrossRef]
36. Osterloh, A.; Ebert, G.; Held, W.-H. *Lagerung von Obst Und Südfrüchten*; Verlag Ulmer: Stuttgart, Germany, 1996; p. 253.
37. Wills, R.B.H.; McGlasson, B.; Graham, D.; Joyce, D. *Postharvest: An Introduction to the Physiology and Handling of Fruit, Vegetables and Ornamentals*; CAB International: New York, NY, USA, 1998; p. 262.
38. Kays, S. *Postharvest Biology*; Exon Press: Athens, GA, USA, 2004; p. 568.
39. El-Mesery, H.S.; Mao, H.; Abomohra, A.E.-F. Applications of Non-destructive Technologies for Agricultural and Food Products Quality Inspection. *Sensors* **2019**, *19*, 846. [CrossRef]
40. Harel, B.; Parmet, Y.; Edan, Y. Maturity classification of sweet peppers using image datasets acquired in different times. *Comput. Ind.* **2020**, *121*, 103274. [CrossRef]
41. Elhariri, E.; El-Bendary, N.; Hussein, A.M.M.; Hassanien, A.E.; Badr, A. Bell Pepper Ripeness Classification based on Support Vector Machine. In Proceedings of the 2014 International Conference on Engineering and Technology (ICET), Cairo, Egypt, 19–20 April 2014.
42. Shamili, M. The estimation of mango fruit total soluble solids using image processing technique. *Sci. Hortic.* **2019**, *249*, 383–389. [CrossRef]
43. Li, X.; Wei, Y.; Xu, J.; Feng, X.; Wu, F.; Zhou, R.; Jin, J.; Xu, K.; Yu, X.; He, Y. SSC and pH for sweet assessment and maturity classification of harvested cherry fruit based on NIR hyperspectral imaging technology. *Postharvest Biol. Technol.* **2018**, *143*, 112–118. [CrossRef]

44. Teerachaichayut, S.; Huong, T.H. Non-destructive prediction of total soluble solids, titratable acidity and maturity index of limes by near infrared hyperspectral imaging. *Postharvest Biol. Technol.* **2017**, *133*, 20–25. [[CrossRef](#)]
45. Arias, R.; Lee, T.-C.; Logendra, L.; Janes, H. Correlation of Lycopene Measured by HPLC with the L*, a*, b* Color Readings of a Hydroponic Tomato and the Relationship of Maturity with Color and Lycopene Content. *J. Agric. Food Chem.* **2000**, *48*, 1697–1702. [[CrossRef](#)]
46. Leiva-Valenzuela, G.A.; Lu, R.; Aguilera, J.M. Prediction of firmness and soluble solids content of blueberries using hyperspectral reflectance imaging. *J. Food Eng.* **2013**, *115*, 91–98. [[CrossRef](#)]
47. Rahman, A.; Kandpal, L.M.; Lohumi, S.; Kim, M.S.; Lee, H.; Mo, C.; Cho, B.-K. Nondestructive Estimation of Moisture Content, pH and Soluble Solid Contents in Intact Tomatoes Using Hyperspectral Imaging. *Appl. Sci.* **2017**, *7*, 109. [[CrossRef](#)]



© 2020 by the authors. Licensee MDPI, Basel, Switzerland. This article is an open access article distributed under the terms and conditions of the Creative Commons Attribution (CC BY) license (<http://creativecommons.org/licenses/by/4.0/>).

Review

Emerging Trends in Research on Food Compounds and Women's Fertility: A Systematic Review

Aleksandra Bykowska-Derda ¹, Ezgi Kolay ¹, Malgorzata Kaluzna ²
and Magdalena Czlapka-Matyasik ^{1,*}

¹ Institute of Human Nutrition and Dietetics, Poznan University of Life Sciences, 31 Wojska Polskiego St., 60-624 Poznań, Poland; aleksandra.derda@up.poznan.pl (A.B.-D.); ezgi.kolay@up.poznan.pl (E.K.)

² Department of Endocrinology, Metabolism and Internal Medicine, Poznan University of Medical Sciences, 49 Przybyszewskiego St., 60-355 Poznan, Poland; mkaluzna@ump.edu.pl

* Correspondence: magdalena.matyasik@up.poznan.pl; Tel.: +48-61-846-62-04

Received: 28 May 2020; Accepted: 24 June 2020; Published: 29 June 2020

Featured Application: The application of this systematic review is a comprehensive study of food compounds, nutrition, food production, health and environmental sciences in improving female fertility.

Abstract: Pro-healthy behaviours, including the diet, are significant factors in maintaining women's fertility health. However, to improve the patient's nutrition management, it is important to seek food-derived bioactive compounds to support fertility treatment. This review analysed recent studies of food compounds related to fertility, using databases including PubMed, Web of Science and Science Direct as well as PRISMA (preferred reporting items for systematic reviews) to ensure complete and transparent reporting of systematic reviews. This review lists foods associated with a higher birth rate, using original papers from the last five years (2015). The analysis included the impact of food compounds such as caffeine, fatty acids, folates and vitamin D, as well as the intake of fish, whole grains, dairy and soya. In addition, dietary patterns and total diet composition supporting women's fertility were also analysed. The results will encourage further research on the relationship between food components and fertility.

Keywords: female infertility; nutrient; vitamin D; folates; soy; antioxidants; minerals; vitamins; food research trends; environmental impact

1. Introduction

Fertility, known as the ability to establish a clinical pregnancy, is dependent on multiple factors, including female age, environmental pollution, diet, tobacco use, alcohol intake, as well as diseases affecting endocrine function and the anatomy of the reproduction system [1,2]. In turn, infertility is medically defined as a failure to establish a clinical pregnancy after 12 months of regular and unprotected sexual intercourse. It is estimated that infertility in women of child-bearing age is 1 in 7 couples in developed countries and 1 in 4 couples in developing countries, which is increasing significantly [1]. The demand for infertility services is still growing and can be improved thanks to technological advances and the development of medicine.

Factors influencing fertility may be unmodifiable, such as age and environment, or could be medically treated, such as health status—including endocrine disorders. Furthermore, some factors could be modifiable, such as health behaviours, dietary patterns and micronutrient intake.

It has been confirmed that in-vitro fertilisation success rate seems to be highest during the summer months when the pollution of particulate matter (PM) is at its lowest [3]. Phthalates, which may negatively influence the fertility health of women [4], were found to affect the occupational health

of hairdressers [5]. Some primary factors, such as excess body weight or underweight, also decrease the rate of fertility [6,7]. Body saturation with vitamin D was suggested to have a beneficial influence on fertility [8–12].

The recommendations by the Committee of the American Society for Reproductive Medicine in collaboration with the Society for Reproductive Endocrinology and Infertility American Society for Reproductive Medicine, advise females to follow a healthy diet, avoid alcohol and decrease caffeine intake to a moderate level [13]. It is also advisable for women to supplement folate (400 µg/day) to decrease the chance of neural tube defects [13]. However, there is some evidence showing that some food ingredients and specific dietary patterns in women may be positively associated with pregnancy and live birth rates [14–16].

One of the food ingredients widely discussed in the context of fertility is sugar. It was shown that its presence in the diet reduces nutritional density and worsens its nutritional quality [17]. The possible mechanism between sugar-sweetened beverages and fertility was explained by increased insulin resistance, leading to oxidative stress. This relation may deleteriously affect semen quality and ovulatory function. Such a mechanism was hypothesised by Hatz, et al. [18], who studied a group of nearly five thousand women and found that fertility and the amount of sugar consumed in sugar-sweetened beverages (particularly sodas and energy drinks) was associated with lower fecundability [18].

A large group of compounds that are still being studied are bioactive compounds in food. Their roles in oxidative stress and fertility have been presented in many studies [19–22], including several studies on female animal models and bioactive food compounds [23–25]. Their role is hypothesised to diminish the effect on the endocrine system of disruptive chemicals. For example, there is some evidence that animals treated with BPA (Bisphenol A), after maternal supplementation of folate and a high phytoestrogen diet, influence oocyte growth and foetal methylation of DNA [26,27]. Other studies have highlighted that a low dose (but not a high dose) of ginger powder, improved the follicle counts of rats [23]. Therefore, it is not clear what dose will be as effective on humans. Additionally, human fertility is affected by complex and multiple factors which could be difficult to expose animals to.

The time of preconception may motivate couples to adopt healthier behaviours and to seek information on factors improving fertility. Even though medical consultation is still the most common source for seeking advice for fertility, social media and the internet also play significant roles [28]. The choice of supplement options is vast, as the fertility supplement market is continuously growing and it has been estimated to be worth USD 1.45 billion globally in 2018 [29]. The use of supplements is not always recommended by healthcare professionals, and their misuse may even pose a threat to health.

The literature related to food compounds and fertility has not been extensively collected, and there is no consensus on what the trends are in these studies or what groups of food ingredients should be considered as supportive or detrimental to fertility. In light of this evidence, an analysis of diet ingredients, food research (e.g., ginger, BPA) and fertility could lead to new supporting therapy strategies that affect the birth rate through the modulation of eating habits. Accordingly, this review provides an analysis of new food compound research influencing fertility and revises recent studies involving the impact of food bioactive compounds on women's fertility.

2. Materials and Methods

2.1. Search Strategy

A systematic search of literature published before December 2019 was performed in PubMed (National Institute of Health, USA) (<https://www.ncbi.nlm.nih.gov/pubmed>), Web of Science (Clarivate Analytics, USA) (<https://www.webofknowledge.com>), Scopus (Elsevier, RELX Group plc), (<https://www.scopus.com>) and Science Direct (Elsevier, RELX Group plc) (<https://www.sciencedirect.com/>) to identify studies describing the association between bioactive food compound intake and

women's fertility. The search strategy was restricted to English language original articles. The following types of documents were excluded: review, book and book chapters.

The search was based upon the following index terms, titles or abstracts listed below: ((bioactive OR nutrient OR food OR ingredient OR vitamin OR mineral OR antioxidant OR phytonutrient) AND (fertility)). The protocol was registered in the "PROSPERO International prospective register of systematic reviews" PROSPERO 2020: CRD42020160223 and is available on https://www.crd.york.ac.uk/prospero/display_record.php?ID=CRD42020160223.

2.2. Inclusion and Exclusion Criteria

Studies on the influence of food compounds on infertility, signs and symptom changes in patients affected by infertility were included. Studies using different food components concerning changes in the concentration of biomarkers for the assessment of infertility and changes in symptoms were analysed. The systematic search included a population of women in the reproductive age 21–50 with diagnosed infertility or healthy women trying to conceive. All studies conducted on animals and case reports were excluded. The studies included were both qualitative and quantitative. A quality assessment of questionable articles was performed with a checklist described by Kmet et al. [30]. Articles written in a language other than English were excluded. Since the search included new trends in food research, it only included articles within the last five years (2015).

2.3. Study Extraction Process

The study selection process includes an assessment of articles based upon titles, abstracts and full text, which were performed by two independent researchers in parallel in each database. At each step of the assessment, all disagreements between the researchers were resolved after consultation with the review coordinator. Only in the case of disagreement during the title assessment process was the paper included in the next step. Full-texts of all records that were selected in the abstract review phase were searched for through the library of Poznan University of Life Sciences.

3. Results

A total of 4609 studies were screened for inclusion in this systematic review. After the elimination process (Figure 1), a total of 25 qualitative studies and 4 quantitative studies were included. The studies were performed internationally and included the following countries USA (n = 20) [15,31–45], Australia (n = 1) [46], New Zealand (n = 1) [46], Ireland (n = 1) [46], United Kingdom (n = 2) [46,47], China (n = 1) [48], Denmark (n = 4) [41,43,49,50], Greece (n = 1) [14], Iran (n = 2) [51,52], Brazil (n = 2) [53,54], Canada (n = 1) [43], Russia (n = 1) [55], Italy (n = 2) [56,57], Spain (n = 1) [58]. The articles concerned female fertility and the intake of a Mediterranean dietary pattern (n = 2) [51,57], fruit, vegetables and whole grain intake (n = 3) [38,46,53], fish (n = 1) [42], dairy (n = 3) [15,43,44], types of fatty acids (n = 4) [39–41], soy (n = 2) [32,33], caffeine (n = 3) [45,50,54], folate and B12 (n = 4) [34,35,59,60], melatonin (n = 1) [58], CoQ10 (n = 1) [48] as well as a combination of different compounds (n = 4) [37,47,52,55]. The women who participated in the studies were either planning pregnancy (n = 6) [36,40,41,45,46,55], infertile (n = 3) [49,51,55], undergoing or subjected to assistive reproductive technology (ART) therapy (n = 16) [14,15,31,34,35,39,42,44,50,52–54,57,58]. The main results of the studies have been summarized in Table 1 (qualitative studies) and Table 2 (quantitative studies).

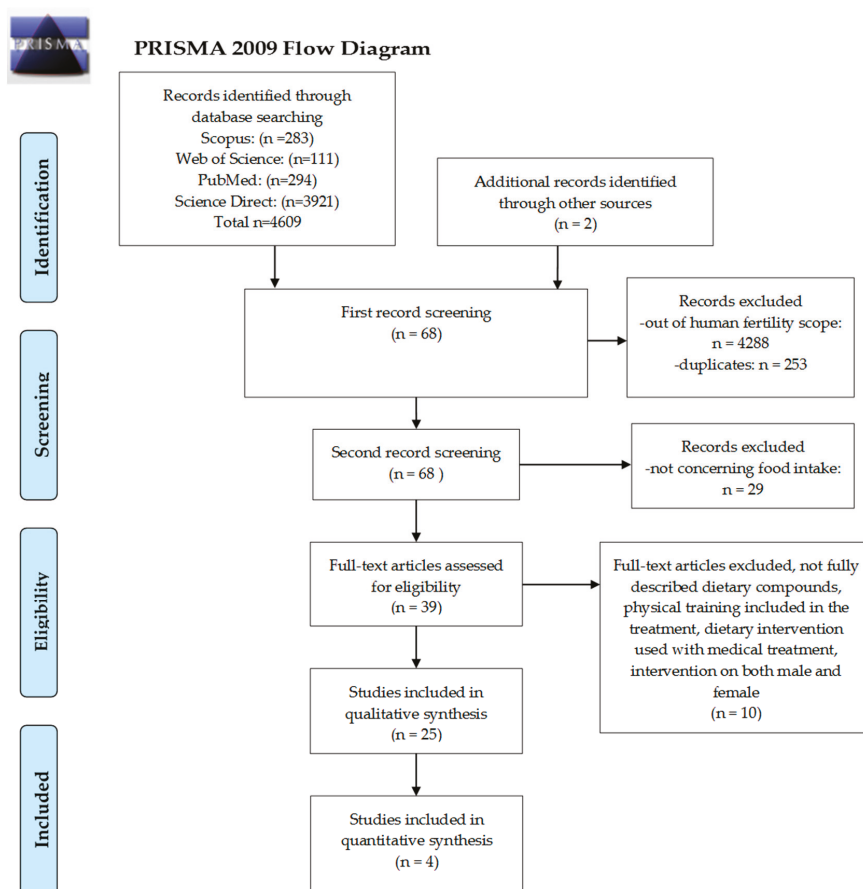


Figure 1. Preferred reporting items for systematic reviews (PRISMA) Study selection process diagram.

Table 1. Qualitative studies on bioactive food components and women’s fertility included in the review process.

Study	Sample	Assessment Tool	Results
Dietary Patterns			
Ricci et al. 2019 [57], Italy	n = 474 ART	FFQ	There were no consistent associations between adherence to a Mediterranean diet and successful obstetrics outcomes. There was an effect of the average adherence score on a Mediterranean diet on oocyte number and clinical pregnancy in women >35 years old but no effect on live birth.
Jahangirifar et al. 2019 [51], Iran	n = 140 infertile	FFQ	High adherence to the healthy dietary pattern was associated with a high average number of oocytes when compared with low adherence.
Karayiannis et al. 2018 [14], Greece	n = 244 non-obese ART	FFQ	Mediterranean diet score was positively related to clinical pregnancy and live birth among women <35 years old but not among women ≥35 years
Gaskins et al. 2019 [31], USA	n = 357 ART	FFQ	Pro-fertility dietary pattern (supplemental intake of folate, B12, low-pesticide residue produce, high intake of whole grains, seafood, dairy, soy foods) has a higher likelihood of live birth.

Table 1. Cont.

Study	Sample	Assessment Tool	Results
Fruits, Vegetables and Wholegrains			
Grieger et al. 2018 [46] Australia, New Zealand, Ireland, UK	n = 5628 nulliparous with low-risk singleton pregnancies	FFQ	Low intake of fruit and high intake of fast food was associated with an increase in time to pregnancy and infertility
Braga et al. 2015 [53], Brazil	n = 269 ART	FFQ	The intake of cereals, vegetables and fruits positively influenced the embryo quality at the cleavage stage. The intake of fruits influenced the likelihood of blastocyst formation. The intake of red meat had a negative effect on the implantation rate and the likelihood of pregnancy.
Gaskins et al. 2016 [38], USA	n = 273 ART	FFQ	High whole grain intake was related to a high probability of live birth.
Fatty Acids			
Eskew et al. 2017 [39], USA	n = 60 ART	Serum fatty acid index	Trans FA and elaidic FA had a negative correlation with IVF outcomes, other FA did not have any consistent correlations
Mumford et al. 2016 [40], USA	n = 259 regularly menstruating women	24h dietary record Serum reproductive hormones	Dietary docosapentaenoic acid (DPA) intake was associated with a reduced risk of anovulation
Wise et al. 2018 [41], USA, Denmark	n = 1290 (USA), n = 1126 (Denmark) attempting pregnancy	FFQ	High trans FA and low ω -3 FA intake was associated with reduced fecundity
Fish			
Nassan et al. 2018 [42], USA	n = 351 ART	FFQ	Fish intake was positively related to the proportion of cycles resulting in a live birth.
Dairy			
Wise et al. 2017 [43], USA, Denmark	n = 2426 attempting pregnancy	FFQ	High phosphorus and lactose intake was associated with high fecundability
Afeiche et al. 2015, [15], USA	n = 232 ART	FFQ	High dairy intake was associated with high chances of live birth
Souter et al. 2017 [44], USA	n = 265 ART	FFQ Antral follicle count (AFC)	High dairy protein intake was associated with lower AFC
Caffeine			
Setti et al. 2018 [54], Brazil	n = 524 ART	FFQ	≥ 3 servings of regular or diet soft drinks were associated with oocyte dysmorphism, lower embryo quality on 2–3 days of culture, and had a mild effect on blastocyst formation, implantation and pregnancy rate. Consumption of sweetened coffee was negatively associated with embryo quality.
Wesseling et al. 2016 [45], USA and Canada	n = 2135 pregnancy planner	FFQ	Preconception caffeine intake was not appreciably associated with pregnancy. Caffeinated coffee intake showed little association with pregnancy. Black tea, but not green tea, was associated with a slight decrease in pregnancy
Lyngsø et al. 2019 [50], Denmark	n = 1708 ART	FFQ	Intake of 1–5 cups of coffee versus none had a higher probability of achieving a pregnancy or a live birth when receiving IUI. No associations were found, between coffee consumption and achieving a pregnancy or a live birth from IVF/ICSI.
Soya			
Chavarro et al. 2016 [32], USA	n = 239 ART	FFQ Urinary BPA	BPA was inversely associated with live birth rate unless women had a high intake of soy.
Vanegas et al. 2015 [33], USA	n = 315 ART	FFQ	Dietary soy intake was positively related to the probability of live birth.

Table 1. Cont.

Study	Sample	Assessment Tool	Results
Folate			
Gaskins et al. 2019 [34], USA	n = 304 ART	FFQ residence-based daily nitrogen dioxide (NO ₂), ozone, fine particulate, and black carbon concentrations	Supplemental folate intake modified the association of NO ₂ exposure and livebirth
Mínguez-Alarcón et al. 2016 [35], USA	n = 178 ART	FFQ Urinary BPA	High BPA was associated with a lower probability of implantation among women with <400 µg/day intake of folate, but not among women with ≥400 µg/day
Vitamin D			
Fung et al. 2017 [36], USA	n = 132 healthy attempting pregnancy	Serum 25(OH)D, 24h diet recalls every 3 months	Women with vit. D intake below EAR and serum 25(OH)D at risk for inadequacy had a lower pregnancy rate
Jensen et al. 2019 [49], Denmark	n = 16212 infertile	Vitamin D fortification in margarine (mandatory in the nation since 1985)	Exposition to fortified margarine was associated with an increased chance of live birth.
Antioxidants			
Skalnaya et al. 2019 [55], Russia	n = 150 healthy n = 169 pregnant n = 75 miscarriage n = 91 primary infertility	Serum metal levels Iron, copper, manganese	Serum Cu levels in women with miscarriage and infertility were 30 and 35% lower than those in pregnant women. Serum Cu levels were significantly associated both with and reproductive health problems
Li et al. 2019 [37], USA	n = 349 ART	FFQ	There were inverse associations of β-carotene intake from foods and of lutein and zeaxanthin intake with live birth rates. Total consumption of vitamins A, C, and E before infertility treatment was not associated with live birth rates.

25(OH)D-25-hydroxyvitamin D, ART—Assistive Reproductive Technologies, AMH—Anti-Mullerian Hormone, FSH—Follicle-stimulating Hormone, FFQ—Food Frequency Questionnaire, EAR—Estimated Average Requirement, BPA—Bisphenol A, FA—fatty acid, IVF—In Vitro Fertilization, ICSI—Intracytoplasmic Sperm Injection.

Table 2. Quantitative studies concerning bioactive food components and female fertility qualified for the review.

Study	Treatment	Sample	Clinical Pregnancy Rate [%]	Embryo Quality	Fertilisation Rate [%]	Live Birth Rate [%]
Yangying et al. 2018 [48], China	Coenzyme Q10 600mg/day 60 days preceding IVF	Control group n = 93	25	0 (0,1.75)	45	22
		Study group n = 76	32	1 (0;2)	67	32
		poor ovarian response	50	2.3	51.1	50
Espino et al. 2019 [58], Spain	Melatonin 3mg/day and 6mg/day for 40 days	healthy control n = 10	20	(0.5;4.0)	47.9	20
		subjected to 2nd IVF:	30	2.0	67.4	30
		no melatonin n = 10	30	(0.4;3.6)	63.7	30
		3mg/day n = 10	30	5.1	63.7	30
Agrawal et al. 2012 [47], UK	Multiple micronutrient supplement or folic acid alone 3-6 months	6mg/day n = 10	30	(2.8;7.4)	63.7	30
		Micronutrients n = 29	66.7	4.6	63.7	30
Fatemi et al. [52], Iran	Vitamin E, 400 mg/day and vitamin D3, 50,000 IU/one in two weeks, placebo 8 weeks	Folic Acid n = 27	39.3	(2.8;6.3)	N/A	N/A
		Intervention group n = 52	62.1	71.20%	73.3	20
		Placebo n = 53	22.6	67.50%	70.9	7
		Women scheduled for ICSI				

IVF—In Vitro Fertilization, ICSI—Intracytoplasmic Sperm Injection.

4. Discussion

This systematic review aimed to identify emergent trends in food compounds studies which influence women's fertility. We qualified a total of 29 studies from the past five years among women planning to conceive either naturally or with assisted reproductive technologies.

4.1. Dietary Patterns, Intake of Fruits, Vegetables and Whole Grains

The modern diet and nutrition analysis based on dietary patterns also assessed the nutrition behaviours as a whole, rather than looking at a single nutrient. Dietary patterns are defined as the quantity, variety, or combination of different foods and beverages in a diet and the frequency in which they are habitually consumed. The frequency reflects food compounds consumed in the diet directly. The most common dietary patterns are pro-healthy, Mediterranean, western and dairy-related [61,62]. The results of this systematic review (presented in Table 1) showed that a high intake of fruits and vegetables and adherence to a pro-healthy dietary pattern is associated with a higher average number of oocytes [51] and embryo quality [53]. The Mediterranean dietary pattern has been associated with supporting fertility health in women. Karayannis et al. found that this dietary pattern is only related to the live birth rate in women under the age of 35 [14]. Another study showed that it was related only to higher oocyte number and clinical pregnancy in women over 35 [57]. The Mediterranean diet is characterised by a high intake of extra virgin olive oil, vegetables, fruits, cereals, nuts and legumes, a moderate intake of fish and other meat, dairy products and red wine and low intakes of eggs and sweets [63]. Another dietary pattern used in the studies was a fertility diet dietary pattern characterised by the intake of supplemental folate and B12, low-pesticide residue produce, high intake of whole grains, seafood, dairy and soy foods. This dietary pattern was positively related to the likelihood of live birth [31].

4.2. Fatty Acids and Fish Intake

The current review has shown that there is no conclusive evidence about the impact of polyunsaturated fatty acids, including the intake of omega-3 on human fertility [13]. The results of the review are inconclusive: two studies found an association between omega-3 fatty acids and fertility [40,41], while another study found no impact of these fatty acids on fertility [39]. However, all of the studies analysing fatty acid intake found that the amount of trans fatty acid consumed is negatively related to the live birth ratio [39,41]. These results also support Grieger et al., who found that a high consumption of fast foods (a rich source of trans fatty acids) influences fertility [46].

4.3. Dairy

For many years, the topic of high dairy intake has been controversial and linked with both a positive and negative impact on the health of women [16,64,65]. Nevertheless, to date, most of the studies concerning female reproductive health have been skewed towards a positive association. Moreover, all of the studies in this systematic search, including the period 2015–2019 concerning dairy intake and fertility, have found at least a small positive relationship between these variables [15,43,44]. It should be noted that dairy foods are generally perceived as a pro-healthy dietary attribute. We studied this group of foods previously and found that a more significant effect on dairy consumption by women was the family environment than health-related protective factors [66].

4.4. Caffeine

Decreasing the caffeine intake to moderate during the time of preconception has been recommended to couples who plan pregnancy [13]. A high intake of caffeine, especially black tea [45] and coffee with added sugar and diet soft drinks [54] has been related to a lower live birth rate. However, coffee intake of 1–5 cups daily has been associated with higher chances of a live birth than none [50]. The intake of caffeine and coffee may be associated with more favourable dietary patterns and health behaviours

which could influence fertility [67]. This could be the reason why different types of caffeinated beverages bring contrasting results.

4.5. Soy

The use of nutrients as factor diminishing adverse health effects of environmental pollutants was found in research concerning soy. Soy, as the food product containing phytosterols, could alleviate the effect of endocrine disruptor bisphenol A. This hypothesis is supported by a study concerning women undergoing ART, urinary bisphenol A and soy intake and their influence on live birth rate [32]. Intake of soya, regardless of environmental pollutants, was also related to a higher probability of live birth [33]. High soy intake has also been related to weight loss in women with polycystic ovary syndrome (PCOS), which may improve health and disease results [68]. The results of the above studies show that food ingredients may not always have a direct impact on fertility and their indirect impact is equally important. However, more studies concerning soy intake on fertility and women's health are needed. Many studies suggest that high soy intake may cause interference with ovarian function because of its high phytoestrogen content [69,70]. More studies are needed to determine the appropriate intake of soy of women trying to conceive, since an excessive intake of soy may not be safe.

4.6. Folate

The Center for Disease Control and Prevention (CDC) in the United States, recommends that healthy women with a low risk of birth defects should supplement 400 µg a day of folic acid at least 12 weeks before conception and early pregnancy to avoid neural tube defects [71]. However, it is unknown whether folate intake is related to female fertility. Recent studies have turned to methylenetetrahydrofolate reductase (MTHFR) gene mutations as the cause of recurrent miscarriages [72]. It seems that supplementation of vitamins B6, B12 and supraphysiologic methylfolate could help women with MTHFR gene mutations to conceive [73]. A high intake of folate and B12 was associated with an increased birth rate in women undergoing ART [59]. A high folate-to-homocysteine ratio was related to a lower risk of anovulation in regularly menstruating females [60]. Interesting retrospective studies were also conducted on supplemental folate intake and pollutant exposure among women undergoing ART. The subjects with high pollutant exposure had a lower rate of live birth [35] or implantation ratio [34]; however, folate supplementation positively modified these results in both studies. These results agree with the animal studies mentioned previously [26,27].

4.7. Vitamin D

During the current study, a number of studies were found which analysed the effect of vitamin D [8–11,36,49,74–78]. Nine of them showed a positive, statistically significant association with female fertility [8,9,11,36,49,74,76–78]. However, since only possible interactions with food compounds were searched for, and vitamin D is mostly formed under sun exposure, two of them concerning vitamin D dietary intake were included in the review. Summing up the issues of vitamin D and fertility, it should be emphasised that food products fortified with vitamin D could be advisable [49] for some populations, not only because of the fertility support but also overall health [79].

4.8. Antioxidants

The search also resulted in study findings involved in other single micronutrients. In a Russian study concerning serum metal concentration in the blood of women, it was found that females with infertility and miscarriage had a lower concentration of copper than pregnant women [55]. Moreover, there was no difference between the copper levels of pregnant women and a healthy control group, which supports the hypothesis that copper may play a role in female fertility.

A diet rich in antioxidants, such as the Mediterranean dietary pattern could improve fertility, although the only recent study concerning the intake of antioxidants did not support this hypothesis. Moreover, the intake of foods with a high concentration of β-carotene, lutein and zeaxanthin was

inversely associated with live birth rates [37]. The reasoning of these results may be variable, starting from the accuracy of the food frequency questionnaire used in the study to the dietary pattern which leads to these results. The most important is the fact that supplementing antioxidants as fertility support or for other health conditions could be dangerous and should not be advised to the patients.

4.9. Other Food Compounds

Most of the studies found in the systematic search were qualitative and retrospective, although four prospective randomised trials published between 2015 and 2019 were also included in the review (Table 2). The studies concerned coenzyme Q10 [48], melatonin [58] and multiple nutrient supplementation of vitamin E and D [52] as well as numerous micronutrient or only folate supplement [47]. All of the included study interventions had a positive effect on the pregnancy rate and should be further studied to support fertility treatment nutritionally.

5. Conclusions

In conclusion, it should be noted that reproductive performance is influenced by food and type of nutrition. The findings of the current study suggest that the importance of food production. In particular, the availability and intake of pro-healthy food compounds is a significant factor supporting fertility in females. Women planning pregnancy should especially ensure an intake of fruits and vegetables, folate and vitamin D. A high intake of sweetened beverages and trans-fatty acids appears to decrease the chance of pregnancy and live birth rate. Soy food intake needs to be further analysed because of its endocrine-disruptive properties. Environmental pollution influences fertility around the world, and the appropriate intake of bioactive food compounds could diminish this effect. However, the excessive intake of specific micronutrients, such as antioxidants, may decrease fertility. More randomised prospective studies are needed to analyse the impact of micronutrients on fertility, taking into consideration the patient environment and environmental pollution.

Author Contributions: Conceptualisation, M.C.-M. and A.B.-D.; methodology, M.C.-M., M.K. and A.B.-D.; investigation, A.B.-D. and E.K.; resources, M.C.-M.; data curation, A.B.-D. and E.K.; writing—original draft preparation, A.B.-D.; writing—review and editing, A.B.-D., E.K., M.K., M.C.-M.; supervision, M.C.-M.; project administration, M.C.-M.; funding acquisition, M.C.-M.; All authors have read and agreed to the published version of the manuscript.

Funding: This research received no external funding.

Conflicts of Interest: The authors declare no conflict of interest.

References

1. Vander Borgh, M.; Wyns, C. Fertility and infertility: Definition and epidemiology. *Clin. Biochem.* **2018**, *62*, 2–10. [[CrossRef](#)] [[PubMed](#)]
2. Mascarenhas, M.N.; Flaxman, S.R.; Boerma, T.; Vanderpoel, S.; Stevens, G.A. National, Regional, and Global Trends in Infertility Prevalence Since 1990: A Systematic Analysis of 277 Health Surveys. *PLoS Med.* **2012**, *9*, 1–12. [[CrossRef](#)] [[PubMed](#)]
3. Kang, J.; Lee, J.Y.; Song, H.; Shin, S.J.; Kim, J. Association between in vitro fertilization success rate and ambient air pollution: A possible explanation of within-year variation of in vitro fertilization success rate. *Obs. Gynecol. Sci.* **2020**, *63*, 72–79. [[CrossRef](#)] [[PubMed](#)]
4. Rattan, S.; Zhou, C.; Chiang, C.; Mahalingam, S.; Brehm, E.; Flaws, J.A. Exposure to endocrine disruptors during adulthood: consequences for female fertility. *J. Endocrinol.* **2017**, *233*, R109–R129. [[CrossRef](#)]
5. Kolena, B.; Petrovicova, I.; Sidlovska, M.; Hlisenikova, H.; Tomasovova, E.; Zoldakova, V.; Trajtelova, H.; Rybansky, L.; Wimmerova, S.; Trnovec, T. Phthalates exposure and occupational symptoms among Slovakian hairdressing apprentices. *Appl. Sci.* **2019**, *9*, 3321. [[CrossRef](#)]
6. Silvestris, E.; de Pergola, G.; Rosania, R.; Loverro, G. Obesity as disruptor of the female fertility. *Reprod. Biol. Endocrinol.* **2018**, *16*, 22. [[CrossRef](#)] [[PubMed](#)]

7. Kudesia, R.; Wu, H.; Hunter Cohn, K.; Tan, L.; Lee, J.A.; Copperman, A.B.; Yurttas Beim, P. The Effect of Female Body Mass Index on in Vitro Fertilization Cycle Outcomes: A Multi-Center Analysis. *J. Assist. Reprod. Genet.* **2018**, *35*, 2013–2023. [[CrossRef](#)] [[PubMed](#)]
8. Bednarska-Czerwińska, A.; Olszak-Wąsik, K.; Olejek, A.; Czerwiński, M.; Tukiendorf, A. Vitamin D and anti-müllerian hormone levels in infertility treatment: The change-point problem. *Nutrients* **2019**, *11*, 1053. [[CrossRef](#)]
9. Kokanall, D.; Karaca, M.; Ozakşit, G.; Elmas, B.; Üstün, Y.E. Serum Vitamin D Levels in Fertile and Infertile Women with Polycystic Ovary Syndrome. *Geburtshilfe Frauenheilkd.* **2019**, *79*, 510–516. [[CrossRef](#)]
10. Yilmaz, N.; Ersoy, E.; Tokmak, A.; Sargin, A.; Ozgu-Erdinc, A.S.; Erkaya, S.; Ibrahim Yakut, H. Do serum vitamin D levels have any effect on intrauterine insemination success? *Int. J. Fertil. Steril.* **2018**, *12*, 164–168. [[CrossRef](#)]
11. Krul-Poel, Y.H.M.; Koenders, P.P.; Steegers-Theunissen, R.P.; ten Boekel, E.; ter Wee, M.M.; Louwers, Y.; Lips, P.; Laven, J.S.E.; Simsek, S. Vitamin D and metabolic disturbances in polycystic ovary syndrome (PCOS): A cross-sectional study. *PLoS One* **2018**, *13*, e0204748. [[CrossRef](#)] [[PubMed](#)]
12. Jukic, A.M.Z.; Baird, D.D.; Wilcox, A.J.; Weinberg, C.R.; Steiner, A.Z. 25-Hydroxyvitamin D (25(OH)D) and biomarkers of ovarian reserve. *Menopause* **2018**, *25*, 811–816. [[CrossRef](#)] [[PubMed](#)]
13. Pfeifer, S.; Butts, S.; Fossum, G.; Gracia, C.; La Barbera, A.; Mersereau, J.; Odem, R.; Paulson, R.; Penzias, A.; Pisarska, M.; et al. Optimizing natural fertility: A committee opinion. *Fertil. Steril.* **2017**, *107*, 52–58. [[CrossRef](#)] [[PubMed](#)]
14. Karayiannis, D.; Kontogianni, M.D.; Mendorou, C.; Mastrominas, M.; Yiannakouris, N. Adherence to the Mediterranean diet and IVF success rate among non-obese women attempting fertility. *Hum. Reprod.* **2018**, *33*, 494–502. [[CrossRef](#)] [[PubMed](#)]
15. Afeiche, M.C.; Chiu, Y.H.; Gaskins, A.J.; Williams, P.L.; Souter, I.; Wright, D.L.; Hauser, R.; Chavarro, J.E. Dairy intake in relation to in vitro fertilization outcomes among women from a fertility clinic. *Hum. Reprod.* **2016**, *31*, 563–571. [[CrossRef](#)]
16. Gaskins, A.J.; Chavarro, J.E. Diet and fertility: a review. *Am. J. Obstet. Gynecol.* **2018**, *218*, 379–389. [[CrossRef](#)]
17. Czapka-Matyasik, M.; Lonnie, M.; Wadolowska, L.; Frelich, A. “Cutting down on sugar” by non-dieting young women: An impact on diet quality on weekdays and the weekend. *Nutrients* **2018**, *10*, 1463. [[CrossRef](#)]
18. Hatch, E.E.; Wesselink, A.K.; Hahn, K.A.; Michiel, J.J.; Mikkelsen, E.M.; Sorensen, H.T.; Rothman, K.J.; Wise, L.A. Intake of Sugar-sweetened Beverages and Fecundability in a North American Preconception Cohort. *Epidemiology* **2018**, *29*, 369–378. [[CrossRef](#)]
19. Ruder, E.H.; Hartman, T.J.; Blumberg, J.; Goldman, M.B. Oxidative stress and antioxidants: Exposure and impact on female fertility. *Hum. Reprod. Update* **2008**. [[CrossRef](#)]
20. Ruder, E.H.; Hartman, T.J.; Goldman, M.B. Impact of oxidative stress on female fertility. *Curr. Opin. Obstet. Gynecol.* **2009**, *21*, 219–222. [[CrossRef](#)]
21. Smits, R.M.; Mackenzie-Proctor, R.; Fleischer, K.; Showell, M.G. Antioxidants in fertility: Impact on male and female reproductive outcomes. *Fertil. Steril.* **2018**, *110*, 578–580. [[CrossRef](#)] [[PubMed](#)]
22. Agarwal, A.; Aponte-Mellado, A.; Premkumar, B.J.; Shaman, A.; Gupta, S. The effects of oxidative stress on female reproduction: A review. *Reprod. Biol. Endocrinol.* **2012**, *10*, 49. [[CrossRef](#)] [[PubMed](#)]
23. Yilmaz, N.; Seven, B.; Timur, H.; Yorganci, A.; Inal, H.A.; Kalem, M.N.; Kalem, Z.; Han, O.; Bilezikci, B. Ginger (zingiber officinale) might improve female fertility: A rat model. *J. Chin. Med. Assoc.* **2018**, *81*, 905–911. [[CrossRef](#)] [[PubMed](#)]
24. Chen, Z.-G.; Luo, L.-L.; Xu, J.-J.; Zhuang, X.-L.; Kong, X.-X.; Fu, Y.-C. Effects of plant polyphenols on ovarian follicular reserve in aging rats. *Biochem. Cell Biol.* **2010**, *88*, 737–745. [[CrossRef](#)] [[PubMed](#)]
25. Li, N.; Wang, J.; Wang, X.; Sun, J.; Li, Z. Icaritin exerts a protective effect against D-galactose induced premature ovarian failure via promoting DNA damage repair. *Biomed. Pharmacother.* **2019**, *118*, 109218. [[CrossRef](#)]
26. Muhlhauser, A.; Susiarjo, M.; Rubio, C.; Griswold, J.; Gorence, G.; Hassold, T.; Hunt, P.A. Bisphenol A effects on the growing mouse oocyte are influenced by diet. *Biol. Reprod.* **2009**, *80*, 1066–1071. [[CrossRef](#)]
27. Dolinoy, D.C.; Huang, D.; Jirtle, R.L. Maternal nutrient supplementation counteracts bisphenol A-induced DNA hypomethylation in early development. *Proc. Natl. Acad. Sci. USA* **2007**, *104*, 13056–13061. [[CrossRef](#)]
28. Walker, R.; Blumfield, M.; Truby, H. Beliefs and advice-seeking behaviours for fertility and pregnancy: A cross-sectional study of a global sample. *J. Hum. Nutr. Diet.* **2018**, *31*, 486–495. [[CrossRef](#)]

29. Grand View Research Fertility Supplements Market Size, Share & Trends Analysis Report By Ingredient (Natural, Synthetic/Blend), By Product (Capsules, Tablets, Soft gels), By End Use, By Distribution Channel, And Segment Forecasts, 2019–2025. Available online: <https://www.grandviewresearch.com/industry-analysis/fertility-supplements-market> (accessed on 19 December 2019).
30. Kmet, L.M.; Lee, R.C.; Cook, L.S. *Standard Quality Assessment Criteria for Evaluating Primary Research Papers from a Variety of Fields*. HTA Initiative # 13 Series; 2004; ISBN 1-896956-71-XX. Available online: <https://era.library.ualberta.ca/items/48b9b989-c221-4df6-9e35-af782082280e> (accessed on 28 June 2020).
31. Gaskins, A.J.; Nassan, F.L.; Chiu, Y.H.; Arvizu, M.; Williams, P.L.; Keller, M.G.; Souter, I.; Hauser, R.; Chavarro, J.E. Dietary patterns and outcomes of assisted reproduction. *Am. J. Obstet. Gynecol.* **2019**, *220*, 567.e1–567.e18. [[CrossRef](#)]
32. Chavarro, J.E.; Mínguez-Alarcón, L.; Chiu, Y.H.; Gaskins, A.J.; Souter, I.; Williams, P.L.; Calafat, A.M.; Hauser, R. Soy intake modifies the relation between urinary bisphenol a concentrations and pregnancy outcomes among women undergoing assisted reproduction. *J. Clin. Endocrinol. Metab.* **2016**, *101*, 1082–1090. [[CrossRef](#)]
33. Vanegas, J.C.; Afeiche, M.C.; Gaskins, A.J.; Mínguez-Alarcón, L.; Williams, P.L.; Wright, D.L.; Toth, T.L.; Hauser, R.; Chavarro, J.E. Soy food intake and treatment outcomes of women undergoing assisted reproductive technology. *Fertil. Steril.* **2015**, *103*, 749–755.e2. [[CrossRef](#)] [[PubMed](#)]
34. Gaskins, A.J.; Mínguez-Alarcón, L.; Fong, K.C.; Awad, Y.A.; Di, Q.; Chavarro, J.E.; Ford, J.B.; Coull, B.A.; Schwartz, J.; Kloog, I.; et al. Supplemental Folate and the Relationship Between Traffic-Related Air Pollution and Livebirth Among Women Undergoing Assisted Reproduction. *Am. J. Epidemiol.* **2019**, *188*, 1595–1604. [[CrossRef](#)]
35. Mínguez-Alarcón, L.; Gaskins, A.J.; Chiu, Y.-H.; Souter, I.; Williams, P.L.; Calafat, A.M.; Hauser, R.; Chavarro, J.E. Dietary folate intake and modification of the association of urinary bisphenol A concentrations with in vitro fertilization outcomes among women from a fertility clinic. *Reprod. Toxicol.* **2016**, *65*, 104–112. [[CrossRef](#)]
36. Fung, J.L.; Hartman, T.J.; Schleicher, R.L.; Goldman, M.B. Association of vitamin D intake and serum levels with fertility: Results from the Lifestyle and Fertility Study. *Fertil. Steril.* **2017**, *108*, 302–311. [[CrossRef](#)] [[PubMed](#)]
37. Li, M.C.; Nassan, F.L.; Chiu, Y.H.; Mínguez-Alarcón, L.; Williams, P.L.; Souter, I.; Hauser, R.; Chavarro, J.E. Intake of Antioxidants in Relation to Infertility Treatment Outcomes with Assisted Reproductive Technologies. *Epidemiology* **2019**, *30*, 427–434. [[CrossRef](#)] [[PubMed](#)]
38. Gaskins, A.J.; Chiu, Y.H.; Williams, P.L.; Keller, M.G.; Toth, T.L.; Hauser, R.; Chavarro, J.E. Maternal whole grain intake and outcomes of in vitro fertilization. *Fertil. Steril.* **2016**, *105*, 1503–1510.e4. [[CrossRef](#)] [[PubMed](#)]
39. Eskew, A.M.; Wormer, K.C.; Matthews, M.L.; Norton, H.J.; Papadakis, M.A.; Hurst, B.S. The association between fatty acid index and in vitro fertilization outcomes. *J. Assist. Reprod. Genet.* **2017**, *34*, 1627–1632. [[CrossRef](#)]
40. Mumford, S.L.; Chavarro, J.E.; Zhang, C.; Perkins, N.J.; Sjaarda, L.A.; Pollack, A.Z.; Schliep, K.C.; Michels, K.A.; Zarek, S.M.; Plowden, T.C.; et al. Dietary fat intake and reproductive hormone concentrations and ovulation in regularly menstruating women. *Am. J. Clin. Nutr.* **2016**, *103*, 868–877. [[CrossRef](#)] [[PubMed](#)]
41. Wise, L.A.; Wesselink, A.K.; Tucker, K.L.; Saklani, S.; Mikkelsen, E.M.; Cueto, H.; Riis, A.H.; Trolle, E.; Mckinnon, C.J.; Hahn, K.A.; et al. Original Contribution Dietary Fat Intake and Fecundability in 2 Preconception Cohort Studies. *Am. J. Epidemiol.* **2018**, *187*, 60–74. [[CrossRef](#)]
42. Nassan, F.L.; Chiu, Y.-H.; Vanegas, J.C.; Gaskins, A.J.; Williams, P.L.; Ford, J.B.; Attaman, J.; Hauser, R.; Chavarro, J.E. Intake of protein-rich foods in relation to outcomes of infertility treatment with assisted reproductive technologies. *Am. J. Clin. Nutr.* **2018**, *108*, 1104–1112. [[CrossRef](#)]
43. Wise, L.A.; Wesselink, A.K.; Mikkelsen, E.M.; Cueto, H.; Hahn, K.A.; Rothman, K.J.; Tucker, K.L.; Sorensen, H.T.; Hatch, E.E. Dairy intake and fecundability in 2 preconception cohort studies. *Am. J. Clin. Nutr.* **2017**, *105*, 100–110. [[CrossRef](#)] [[PubMed](#)]
44. Souter, I.; Chiu, Y.H.; Batsis, M.; Afeiche, M.C.; Williams, P.L.; Hauser, R.; Chavarro, J.E. The association of protein intake (amount and type) with ovarian antral follicle counts among infertile women: Results from the EARTH prospective study cohort. *BJOG An Int. J. Obstet. Gynaecol.* **2017**, *124*, 1547–1555. [[CrossRef](#)] [[PubMed](#)]

45. Wesselink, A.K.; Wise, L.A.; Rothman, K.J.; Hahn, K.A.; Mikkelsen, E.M.; Mahalingaiah, S.; Hatch, E.E. Caffeine and caffeinated beverage consumption and fecundability in a preconception cohort. *Reprod. Toxicol.* **2016**, *62*, 39–45. [[CrossRef](#)]
46. Grieger, J.A.; Grzeskowiak, L.E.; Bianco-Miotto, T.; Jankovic-Karasoulos, T.; Moran, L.J.; Wilson, R.L.; Leemaqz, S.Y.; Poston, L.; Mccowan, L.; Kenny, L.C.; et al. Pre-pregnancy fast food and fruit intake is associated with time to pregnancy. *Hum. Reprod.* **2018**, *33*, 1063–1070. [[CrossRef](#)] [[PubMed](#)]
47. Agrawal, R.; Burt, E.; Gallagher, A.M.; Butler, L.; Venkatakrishnan, R.; Peitsidis, P. Prospective randomized trial of multiple micronutrients in subfertile women undergoing ovulation induction: A pilot study. *Reprod. Biomed. Online* **2012**, *24*, 54–60. [[CrossRef](#)] [[PubMed](#)]
48. Xu, Y.; Nisenblat, V.; Lu, C.; Li, R.; Qiao, J.; Zhen, X.; Wang, S. Pretreatment with coenzyme Q10 improves ovarian response and embryo quality in low-prognosis young women with decreased ovarian reserve: A randomized controlled trial. *Reprod. Biol. Endocrinol.* **2018**, *16*, 1–11. [[CrossRef](#)]
49. Jensen, A.; Nielsen, M.L.; Guleria, S.; Kjaer, S.K.; Heitmann, B.L.; Kesmodel, U.S. Chances of live birth after exposure to vitamin D–fortified margarine in women with fertility problems: results from a Danish population-based cohort study. *Fertil. Steril.* **2020**, 1–8. [[CrossRef](#)]
50. Lyngsø, J.; Kesmodel, U.S.; Bay, B.; Ingerslev, H.J.; Nybo Andersen, A.M.; Ramlau-Hansen, C.H. Impact of female daily coffee consumption on successful fertility treatment: A Danish cohort study. *Fertil. Steril.* **2019**, *112*, 120–129.e2. [[CrossRef](#)]
51. Jahangirifar, M.; Taebi, M.; Nasr-Esfahani, M.H.; Askari, G.; Fung, J.L.; Hartman, T.J.; Schleicher, R.L.; Goldman, M.B.; Nassan, F.L.; Chiu, Y.Y.; et al. Dietary patterns and the outcomes of assisted reproductive techniques in women with primary infertility: A prospective cohort study. *Int. J. Fertil. Steril.* **2017**, *12*, 316–323. [[CrossRef](#)]
52. Fatemi, F.; Mohammadzadeh, A.; Sadeghi, M.R.; Akhondi, M.M.; Mohammadmoradi, S.; Kamali, K.; Lackpour, N.; Jouhari, S.; Zafadoust, S.; Mokhtar, S.; et al. Role of vitamin E and D3 supplementation in Intra-Cytoplasmic Sperm Injection outcomes of women with polycystic ovarian syndrome: A double blinded randomized placebo-controlled trial. *Clin. Nutr. ESPEN* **2017**, *18*, 23–30. [[CrossRef](#)]
53. Braga, D.P.A.F.; Halpern, G.; Setti, A.S.; Figueira, R.C.S.; Iaconelli, A.; Borges, E. The impact of food intake and social habits on embryo quality and the likelihood of blastocyst formation. *Reprod. Biomed. Online* **2015**, *31*, 30–38. [[CrossRef](#)] [[PubMed](#)]
54. Setti, A.S.; Braga, D.P.d.A.F.; Halpern, G.; Figueira, R.d.C.S.; Iaconelli, A.; Borges, E. Is there an association between artificial sweetener consumption and assisted reproduction outcomes? *Reprod. Biomed. Online* **2018**, *36*, 145–153. [[CrossRef](#)] [[PubMed](#)]
55. Skalnaya, M.G.; Tinkov, A.A.; Lobanova, Y.N.; Chang, J.S.; Skalny, A.V. Serum levels of copper, iron, and manganese in women with pregnancy, miscarriage, and primary infertility. *J. Trace Elem. Med. Biol.* **2019**, *56*, 124–130. [[CrossRef](#)]
56. Ricci, E.; Noli, S.; Cipriani, S.; La Vecchia, I.; Chiaffarino, F.; Ferrari, S.; Mauri, P.A.; Reschini, M.; Fedele, L.; Parazzini, F. Maternal and paternal caffeine intake and art outcomes in couples referring to an Italian fertility clinic: A prospective cohort. *Nutrients* **2018**, *10*, 1116. [[CrossRef](#)] [[PubMed](#)]
57. Ricci, E.; Bravi, F.; Noli, S.; Somigliana, E.; Cipriani, S.; Castiglioni, M.; Chiaffarino, F.; Vignali, M.; Gallotti, B.; Parazzini, F. Mediterranean diet and outcomes of assisted reproduction: an Italian cohort study. *Am. J. Obstet. Gynecol.* **2019**, *221*, 627.e1–627.e14. [[CrossRef](#)]
58. Espino, J.; Macedo, M.; Lozano, G.; Ortiz, Á.; Rodríguez, C.; Rodríguez, A.B.; Bejarano, I. Impact of melatonin supplementation in women with unexplained infertility undergoing fertility treatment. *Antioxidants* **2019**, *8*, 338. [[CrossRef](#)]
59. Gaskins, A.J.; Chiu, Y.H.; Williams, P.L.; Ford, J.B.; Toth, T.L.; Hauser, R.; Chavarro, J.E. Association between serum folate and Vitamin B-12 and outcomes of assisted reproductive technologies. *Am. J. Clin. Nutr.* **2015**, *102*, 943–950. [[CrossRef](#)]
60. Michels, K.A.; Wactawski-Wende, J.; Mills, J.L.; Schliep, K.C.; Gaskins, A.J.; Yeung, E.H.; Kim, K.; Plowden, T.C.; Sjaarda, L.A.; Chaljub, E.N.; et al. Folate, homocysteine and the ovarian cycle among healthy regularly menstruating women. *Hum. Reprod.* **2017**, *32*, 1743–1750. [[CrossRef](#)]
61. Shahdadian, F.; Ghiasvand, R.; Abbasi, B.; Feizi, A.; Saneei, P.; Shahshahan, Z. Association between Major Dietary Patterns and Polycystic Ovary Syndrome: Evidence from a case-control study. *Appl. Physiol. Nutr. Metab.* **2018**, *44*, 52–58. [[CrossRef](#)]

62. Wadolowska, L.; Ulewicz, N.; Sobas, K.; Wuenstel, J.W.; Slowinska, M.A.; Niedzwiedzka, E.; Czlapka-Matyasik, M. Dairy-related dietary patterns, dietary calcium, body weight and composition: A study of obesity in polish mothers and daughters, the MODAF project. *Nutrients* **2018**, *10*, 90. [CrossRef]
63. Davis, C.; Bryan, J.; Hodgson, J.; Murphy, K. Definition of the mediterranean diet: A literature review. *Nutrients* **2015**, *7*, 9139–9153. [CrossRef] [PubMed]
64. Chavarro, J.E.; Rich-Edwards, J.W.; Rosner, B.; Willett, W.C. A prospective study of dairy foods intake and anovulatory infertility. *Hum. Reprod.* **2007**, *22*, 1340–1347. [CrossRef] [PubMed]
65. Al Sarakbi, W.; Salhab, M.; Mokbel, K. Dairy products and breast cancer risk: A review of the literature. *Int. J. Fertil. Womens Med.* **2005**, *50*, 244–249. [PubMed]
66. Sobas, K.; Wadolowska, L.; Slowinska, M.A.; Czlapka-Matyasik, M.; Wuenstel, J.; Niedzwiedzka, E. Like mother, like daughter? Dietary and non-dietary bone fracture risk factors in mothers and their daughters. *Iran. J. Public Health* **2015**, *44*, 939–952.
67. Salas-Huetos, A.; Bullo, M.; Salas-Salvado, J. Dietary patterns, foods and nutrients in male fertility parameters and fecundability: A systematic review of observational studies. *Hum. Reprod. Update* **2017**, *23*, 371–389. [CrossRef]
68. Karamali, M.; Kashanian, M.; Alaeinasab, S.; Asemi, Z. The effect of dietary soy intake on weight loss, glycaemic control, lipid profiles and biomarkers of inflammation and oxidative stress in women with polycystic ovary syndrome: A randomised clinical trial. *J. Hum. Nutr. Diet.* **2018**. [CrossRef] [PubMed]
69. Jefferson, W.N. Adult ovarian function can be affected by high levels of soy. *J. Nutr.* **2010**, *140*, 2322S–2325S. [CrossRef] [PubMed]
70. Patel, S.; Zhou, C.; Rattan, S.; Flaws, J.A. Effects of Endocrine-Disrupting Chemicals on the Ovary. *Biol. Reprod.* **2015**, *93*, 20. [CrossRef]
71. Williams, J.; Mai, C.T.; Mulinare, J.; Isenburg, J.; Flood, T.J.; Ethen, M.; Frohnert, B.; Kirby, R.S. Updated estimates of neural tube defects prevented by mandatory folic Acid fortification—United States, 1995–2011. *MMWR Morb. Mortal. Wkly. Rep.* **2015**, *64*, 1–5.
72. Zhu, Y.; Wu, T.; Ye, L.; Li, G.; Zeng, Y.; Zhang, Y. Prevalent genotypes of methylenetetrahydrofolate reductase (MTHFR) in recurrent miscarriage and recurrent implantation failure. *J. Assist. Reprod. Genet.* **2018**, *35*, 1437–1442. [CrossRef]
73. Serapinas, D.; Boreikaite, E.; Bartkeviciute, A.; Bandzeviciene, R.; Silkunas, M.; Bartkeviciene, D. The importance of folate, vitamins B6 and B12 for the lowering of homocysteine concentrations for patients with recurrent pregnancy loss and MTHFR mutations. *Reprod. Toxicol.* **2017**, *72*, 159–163. [CrossRef]
74. Mumford, S.L.; Garbose, R.A.; Kim, K.; Kissell, K.; Kuhr, D.L.; Omosigho, U.R.; Perkins, N.J.; Galai, N.; Silver, R.M.; Sjaarda, L.A.; et al. Association of preconception serum 25-hydroxyvitamin D concentrations with livebirth and pregnancy loss: A prospective cohort study. *Lancet Diabetes Endocrinol.* **2018**, *6*, 725–732. [CrossRef]
75. Neville, G.; Martyn, F.; Kilbane, M.; O’Riordan, M.; Wingfield, M.; McKenna, M.; McAuliffe, F.M. Vitamin D status and fertility outcomes during winter among couples undergoing in vitro fertilization/intracytoplasmic sperm injection. *Int. J. Gynecol. Obstet.* **2016**, *135*, 172–176. [CrossRef] [PubMed]
76. Abadia, L.; Gaskins, A.J.; Chiu, Y.H.; Williams, P.L.; Keller, M.; Wright, D.L.; Souter, I.; Hauser, R. Serum 25-hydroxyvitamin D concentrations and treatment outcomes of women undergoing assisted reproduction. *Am. J. Clin. Nutr.* **2016**, *104*, 729–735. [CrossRef] [PubMed]
77. Liu, X.; Zhang, W.; Xu, Y.; Chu, Y.; Wang, X.; Li, Q.; Ma, Z.; Liu, Z.; Wan, Y. Effect of vitamin D status on normal fertilization rate following in vitro fertilization. *Reprod. Biol. Endocrinol.* **2019**, *17*, 59. [CrossRef] [PubMed]
78. Chu, J.; Gallos, I.; Tobias, A.; Robinson, L.; Kirkman-Brown, J.; Dhillon-Smith, R.; Harb, H.; Eapen, A.; Rajkhowa, M.; Coomarasamy, A. Vitamin D and assisted reproductive treatment outcome: A prospective cohort study. *Reprod. Health* **2019**, *16*, 1–10. [CrossRef]
79. Wilson, L.R.; Tripkovic, L.; Hart, K.H.; Lanham-New, S.A. Vitamin D deficiency as a public health issue: Using vitamin D2 or vitamin D3 in future fortification strategies. *Proc. Nutr. Soc.* **2017**, *76*, 392–399. [CrossRef]



Article

The Microbiota of Edam Cheeses Determined by Cultivation and High-Throughput Sequencing of the 16S rRNA Amplicon

Beata Nalepa ^{1,*}, Sławomir Ciesielski ² and Marek Aljewicz ³

¹ Department of Industrial and Food Microbiology, Faculty of Food Science, University of Warmia and Mazury in Olsztyn, Pl. Cieszyński 1, 10-726 Olsztyn, Poland

² Department of Environmental Biotechnology, Faculty of Geoengineering, University of Warmia and Mazury in Olsztyn, ul. Stoneczna 45G, 10-719 Olsztyn, Poland; slawomir.ciesielski@uwm.edu.pl

³ Department of Dairy Science and Quality Management, Faculty of Food Science, University of Warmia and Mazury in Olsztyn, ul. Oczapowskiego 7, 10-719 Olsztyn, Poland; marek.aljewicz@uwm.edu.pl

* Correspondence: beata.nalepa@uwm.edu.pl; Tel.: +48-8-9523-4995

Received: 4 May 2020; Accepted: 10 June 2020; Published: 12 June 2020

Abstract: The aim of this study was to evaluate the microbiome of industrially produced ripened Edam cheeses by next-generation sequencing. The samples for analyses were collected in spring and autumn. Spring samples were characterized by significantly higher *Lactococcus* and *Bacillus* counts and lower counts of Enterobacteriaceae, *Enterococcus*, and yeasts than autumn samples. The predominant microorganisms identified by the Illumina high-throughput sequencing technology belonged to four phyla: Firmicutes, Actinobacteria, Proteobacteria and Bacteroidetes. The dominant species were starter culture bacteria. *Lactobacillus rhamnosus*, *Lactobacillus kefir*, *Lactobacillus kefirnofaciens*, *Lactobacillus casei*, *Streptococcus thermophilus*, and *Bifidobacterium* had the highest share of microbial cheese communities. The number of γ -Proteobacteria reads was higher in autumn cheese samples. A high number of reads was also noted in the genus *Clostridium*. The counts of spore-forming bacteria of the genus *Bacillus* were higher in cheeses produced in spring. The study revealed highly similar relationships between the analyzed production periods. The present results contribute to the existing knowledge of cheese microbiota, and they can be used to improve and modify production processes based on the composition of microbial communities, as well as to improve the quality of the final product.

Keywords: microbiota; seasonal variations; high-throughput sequencing; NGS

1. Introduction

The quality of fermented foods is determined mostly by microbial genera and species colonizing food products. The above applies to all processing stages, from the raw material to the final product [1–3]. Microorganisms are ubiquitous in the farm environment (soil, water, feed, natural fertilizers, and premises). They are also present on animal skin, in animal digestive tracts, and in animal secretions (such as milk), and they colonize the surface of fodder plants. Microorganisms are found on the surface of processing lines, devices, machines, conveyor belts, pipelines, packaging, and auxiliary raw materials. They are added to products as starter cultures, and they are present on the hands of dairy plant employees [4,5]. Microorganisms spread from the above sources to raw materials and end products, and they influence the attributes of fermented foods. Therefore, cheese microbiota constitute one of the critical factors during cheese ripening and the formation of the sensory properties of cheese. The formation of sensory attributes is a complex biochemical process where environmental and process conditions, such as the heating temperature of the cheese slurry and the

time and temperature of cheese ripening, affect the composition and metabolic activity of microbiota [6]. Microbial communities colonizing fermented foods are highly complex, and they have not been thoroughly investigated to date [1–3]. Many microbial species cannot be cultured in vitro on standard microbiological media, which prevents their identification. Some microorganisms are weakened or sublethally damaged by processing operations, and they enter the viable but not culturable (VBNC) state [7]. Other microorganisms cannot be identified with the use of culture-dependent methods due to their small population size and the overwhelming effect of predominant species, such as starter culture bacteria. A knowledge of the biodiversity of bacterial communities in fermented foods is highly valuable because every microbial species, including low-abundance species, contribute specific enzymes, metabolites, bacteriocins, and genetic material to the metabiome. A better understanding of the interactions between microorganisms, their metabolites, the effects of process parameters, external factors, and disruptions in the production cycle can expand our knowledge of specific microbial communities. This knowledge can be used to develop new tools for designing the most desirable attributes of fermented foods and to precisely control the production process to achieve the desired effects. Considerable advances have been made in molecular analysis since the late 1980s, and they have led to the development of the PCR technique by Kary Mullis in 1983 [8], which supports analyses of the complex ecosystems of fermented foods. Technological progress introduced molecular biology methods to traditional food microbiology. The last decade witnessed the emergence of new methods such as next-generation sequencing (NGS) and new research fields such as metagenomics and metatranscriptomics [9]. Modern NGS techniques support the high-throughput sequencing of genes, metagenomes, and metatranscriptomes, and they deliver new insights into the diversity and metabolic properties of fermented food microbiota, including the microbiota of ripened cheese [10]. The resulting data add to current knowledge about the interactions between microorganisms, the environment, and other microorganisms, and they support the development of strategies for improving the production process and cheese quality. In recent years, metagenomic and/or metatranscriptomic analyses have been conducted on samples of regional cheeses, including water buffalo mozzarella cheese [11], Belgian Herve cheese [12], Italian Plaisentif, Mozzarella, Grana Padano and Parmigiano Reggiano cheese [13,14], Mexican Cotija cheese [15], and French Tomme d’Orchies Livarot-type cheese [16,17], as well as industrially produced Dutch-type [18] and Swiss-type cheese [19]. The microbiological quality of ripened cheese has been widely researched in the literature [20–22]. However, the formerly applied analytical methods have failed to provide comprehensive information about the microbiome of ripened cheese. Recent advances in molecular biology can be deployed to fill this knowledge gap. Therefore, the aim of this study was to determine the microbiota of Edam cheeses produced industrially in Poland with the use of the Illumina technology.

2. Materials and Methods

2.1. Cheese Sampling

The study was performed on Swiss–Dutch-type (Edam) cheeses manufactured by a dairy plant in north-eastern Poland. Raw milk for cheese production was pasteurized (72.5 °C for 15 s) and standardized (to 3.0% fat content). Calcium chloride, a coloring agent, and rennet (Chymax, Ch. Hansen, Poland) were added, and milk was inoculated with deep-frozen cheese starters (CSK Food Enrichment, Poland). Milk was inoculated with 0.7% (v/v) of the lactic acid bacterial starter (*Lactococcus lactis* subsp. *lactis*, *Leuconostoc mesenteroides* subsp. *cremoris*) and 0.007% (v/v) of the propionic acid bacterial starter (*Propionibacterium freudenreichii* subsp. *shermanii*). After brining, cheeses were wrapped in FCC-type (Fesco Pack, Malbork, Poland) heat shrink oxygen barrier bags and cold-stored under controlled conditions. The cheeses were ripened for 10 days at 12 °C and a relative humidity of 85%. After 10 days, the ripening temperature was increased to 21 °C for 42 days. After 52 days of ripening, cheese samples were randomly collected for analysis. Three random cheese samples were collected each month. The representative cheeses were sampled in compliance with ISO 707:2008 [23]. Before the

experiment, the samples collected over one month (April or October) were grated with a Santos 2 grater (Lyon, France) and combined with the samples collected in the following month (May or November, respectively) of the same season. All cheeses were sampled over a period of 2 years. The resulting averaged sample was used for further analysis. Cheeses produced in April–May were regarded as spring samples, and cheeses produced in October–November were regarded as autumn samples.

2.2. Chemical Composition

Cheese samples were analyzed in triplicate to determine their salt content by the IDF method (IDF 88; ISO 5943:2006) [24], fat content was determined by the Van Gulik method (IDF 222, ISO 3433:2008) [25], and moisture content was determined by oven drying at 102 °C (AOAC 926.08) [26].

2.3. Determination of the Counts of Selected Bacterial Groups by the Culture-Dependent Method

The counts of bacteria of the genera *Lactobacillus*, *Lactococcus*, *Leuconostoc*, *Propionibacterium*, Enterobacteriaceae, *Enterococcus*, *Staphylococcus*, *Clostridium*, and *Bacillus*, as well as yeasts, were determined by the standard plate count method on the appropriate culture media. The applied culture media and incubation conditions are presented in Table 1.

Table 1. Culture media and incubation conditions applied in the study.

Microorganism	Medium	Incubation Conditions
<i>Lactobacillus</i> spp.	MRS agar (Merck)	37 °C, 48 h, anaerobic incubation
<i>Lactococcus</i> spp.	M17 agar (Merck)	30 °C, 48 h
<i>Leuconostoc</i> spp.	Sucrose agar: (sucrose—50 g/L; yeast extract—10 g/L; agar—15 g/L; pH 7.2–7.4)	30 °C, 72 h
<i>Propionibacterium</i> spp.	Lactate agar: (peptone—10 g/L; yeast extract—5 g/L; calcium lactate—10 g/L; agar—15 g/L; pH 7.0–7.2)	30 °C, 72–96 h, anaerobic incubation
Enterobacteriaceae	VRBG (Merck)	37 °C, 24–48 h
<i>Enterococcus</i> spp.	Slanetz–Bartley agar (Merck)	37 °C, 48 h
<i>Staphylococcus</i> spp.	RPF agar (Merck)	37 °C, 48 h
<i>Clostridium</i> spp.	RCM agar (Oxoid)	37 °C, 48 h, anaerobic incubation
<i>Bacillus</i> spp.	Nutrient agar (Merck)	30 °C, 48 h
Yeasts and molds	YGC agar (Merck)	25 °C, 72–96 h

2.4. DNA Isolation

Metagenomic DNA was directly isolated from cheese samples with the use of the Genomic Mini AX FOOD kit (A@A Biotechnology, Gdańsk, Poland) according to the manufacturer's instructions, and it was stored at −80 °C until further analyses.

2.5. Amplicon Sequencing and Bioinformatics Analysis

The microbial communities colonizing the analyzed samples were examined by the sequencing of the V3–V4 region of the 16S rRNA gene. The 16S rRNA gene fragment was amplified with the PCR primers recommended for the Illumina technique. The primers were developed by adding Illumina adapter overhang nucleotide sequences to the PCR primers given by Klindworth et al. [27]. Amplicons were indexed using the Nextera® XT Index Kit (Illumina, Inc. San Diego, CA, United States) according to the manufacturer's instructions. DNA was sequenced in Illumina MiSeq in the 2 × 250 paired-end mode. Demultiplexing and FASTQ file generation were performed using Miseq Reporter v.2.4. (Illumina, Inc. San Diego, CA, United States).

Sequencing results in the form of FASTQ files were uploaded to the MetaGenome Rapid Annotation Subsystems Technology (MG-RAST) server for analysis [28]. Each file underwent quality control (QC), which included quality filtering (removing sequences with ≥ 5 ambiguous base pairs) and length filtering (removing sequences with a length ≥ 2 standard deviations from the mean). The UCLUST algorithm was used to cluster the identified rRNA sequences. A representative sequence of each cluster was used for taxonomic identification based on the Greengenes reference database. Illumina metagenomic datasets are available at MG-RAST under accession numbers 4,730,840.3, 4,730,841.3, 4,730,842.3, and 4,734,160.3. Additionally, sequencing data were deposited in the Sequence Read Archive (SRA) NCBI (<https://www.ncbi.nlm.nih.gov/>) as a Bioproject under the accession code: PRJNA637891.

2.6. Statistical Analysis

The results of chemical composition analysis and bacterial counts were verified for normal distribution and homogeneity of variance. The interactions between production seasons were determined by a one-way ANOVA. The results were statistically analyzed with the Statistica software (Statsoft; 2018, Kraków, Poland) at $p \leq 0.05$. All data (microbiological and physicochemical parameters) are presented as means \pm standard deviation.

3. Results and Discussion

3.1. Chemical Composition

The analyzed cheeses did not significantly differ in water content. The average water, fat, and sodium chloride content of all samples were determined at 42%, 27%, and 1.5%, respectively (Table 2). The production period had no significant effect on the composition of the cheeses. The absence of significant differences between the cheeses could be attributed to adequate standardization of the raw material and the use of more automated production lines.

Table 2. Chemical composition of Edam cheeses *.

Composition [%]	Season	
	Autumn	Spring
water	42.50 \pm 0.87	42.20 \pm 0.77
fat	27.51 \pm 0.38	27.19 \pm 1.26
sodium chloride	1.49 \pm 0.07	1.51 \pm 0.06

* The results are expressed as means \pm standard deviation; $n = 3$. The analyses were conducted after 52 days of cheese ripening.

3.2. Determination of the Counts of Selected Bacterial Groups by the Culture-Dependent Method

The abundance of the selected bacterial groups was determined by the traditional culture-dependent method. The applied culture media are presented in Table 3. The microbiological quality of cheese depends on climatic conditions, cow health, cow nutrition, lactation period, and the type and number of starters. Despite the standardization of raw materials and the automation of cheese production, even the same types of cheese sampled from various vats can differ in microbiological quality.

The addition of a starter culture was responsible for the high counts of *Lactococcus*, *Leuconostoc*, and *Propionibacterium*. The statistical analysis revealed that *Lactococcus* counts were significantly influenced by the production season ($p \leq 0.05$), and the average *Lactococcus* counts in autumn cheeses were determined at log 6.55 cfu/g and were lower than in spring cheeses (log 7.16 cfu/g). Cheeses produced with *Lactococcus* starter cultures were characterized by high *Lactococcus* counts. In turn, high *Lactococcus* counts in mature cheeses were attributed to the availability of suitable carbon and nitrogen energy sources, including bacterial metabolites (low-molecular-weight peptides, free amino acids, citrate, RNA (ribose), and DNA (deoxyribose) produced during starter lactic acid bacteria (SLAB)

lysis. Similar results have been reported by other authors [29–31]. Season had no significant effect on *Leuconostoc* and *Propionibacterium* counts, which were determined at 4.43 and 5.75 cfu/g on average, respectively (Table 3). Interestingly, *Lactobacillus* counts were around 11% ($p > 0.05$) higher in the spring cheese than in the autumn cheese samples. Due to seasonal changes in the microbiological quality of the raw material, some dairies add larger amounts of starter cultures to cheese vats to accelerate ripening and obtain cheeses with desirable sensory attributes. The presence of higher *Lactococcus* and *Propionibacterium* counts in the spring cheeses seems to confirm the above observation. During ripening, starter cultures undergo autolysis, which leads to the release of cell wall elements and nucleic acids. These compounds are used by bacteria, including *Lactobacillus* strains, as a source of carbon or nitrogen. Similarly to *Lactobacillus*, *Enterococcus* strains are also classified as non-starter lactic acid bacteria (NSLAB). The high *Enterococcus* counts in mature cheeses could be explained by the fact that *Enterococcus* spp. are highly resistant to pasteurization temperature and that milk fat exerts protective effects [32]. The counts of *Enterococcus* and Enterobacteriaceae were significantly influenced by season. The average counts of *Enterococcus* and Enterobacteriaceae reached 3.63 and 2.50 cfu/g, respectively, and were higher (log 0.50 and log 0.86 cfu/g, respectively) in cheeses produced in spring. *Enterococcus* counts were similar to those reported by other authors in Swiss-type cheese (2–3 cfu/g) [29], but they were significantly lower than in Spanish cheese (6–8 log cfu/g) [33]. The low Enterobacteriaceae counts could probably be attributed to the fermenting activity of Lactic Acid Bacteria (LAB) and the synthesis of antibacterial compounds (bacteriocins, organic acids, ethanol, and H₂O₂) that reduce microbial counts by increasing the permeability of bacterial cell walls [29,30]. The lower counts of *Enterococcus* and Enterobacteriaceae in autumn cheeses could also indicate that hygiene standards are strictly observed by dairy employees.

Table 3. Counts of selected microbial groups in Edam cheeses determined by the culture-dependent method.

Bacteria	Season	
	Autumn	Spring
<i>Lactococcus</i>	6.55 ± 0.25 ^{b,*}	7.16 ± 0.33 ^a
<i>Leuconostoc</i>	4.60 ± 0.99	4.25 ± 0.86
<i>Propionibacterium</i>	5.64 ± 0.53	5.85 ± 0.12
<i>Lactobacillus</i>	5.97 ± 0.55	6.64 ± 0.51
Enterobacteriaceae	2.50 ± 0.55 ^a	2.00 ± 0.01 ^b
<i>Enterococcus</i>	3.63 ± 0.36 ^a	2.77 ± 0.85 ^b
<i>Staphylococcus</i>	3.00 ± 0.24	2.70 ± 0.79
<i>Clostridium</i>	4.32 ± 0.40	3.87 ± 1.15
<i>Bacillus</i>	3.35 ± 0.66 ^b	4.53 ± 0.47 ^a
Yeasts	2.83 ± 0.26 ^a	2.00 ± 0.01 ^b

* Values are means ± standard deviation for $n = 6$, ^{a,b} Means in rows with different superscript letters are significantly different ($p \leq 0.05$).

Yeast counts were below log 2 cfu/g in spring cheeses, and they were significantly lower in autumn cheeses (log 2.82 cfu/g). The observed yeast counts were below the values given by other authors in Swiss-type cheese (3.48 cfu/g) [29], Gouda-type cheese (3.22–50 cfu/g) [29,31], Chihuahua cheese (5 cfu/g) [34], and Serrano cheese (4–4.5 cfu/g) [30]. Similar results were reported by Sánchez-Gamboa et al. [34]; in their study, yeast counts were 50% higher in cheeses produced in autumn. Different results were reported by de Souza et al., [30]. Higher yeast counts in autumn cheeses probably resulted from the low microbiological quality of brine or cheese contamination during packaging.

Autumn cheeses are made from the milk of pasture-grazed cows, which is why *Clostridium* counts in autumn cheeses should have been lower than in spring cheeses. Despite the above, *Clostridium* counts were approximately 10% ($p > 0.05$) higher in autumn cheeses than in spring cheeses. In a

study by Bermúdez et al. [35], *Clostridium* counts were also approximately 9% higher in autumn than in spring cheeses. In recent years, many milk producers have been increasing the proportions of silage in the diets of lactating cows to maximize milk yields and to allow for greater flexibility in managing cattle diets. Such practices contribute to the accumulation of *Clostridium* spores in the bovine digestive tract. Bacterial spores can be transferred to milk during milking, especially if teats are not properly cleaned [35]. Lower *Clostridium* counts in autumn cheeses probably result from higher levels of bacteriocin synthesis by LAB (mainly: *Lactococcus*, *Propionibacterium*, and *Lactobacillus*) [36].

3.3. Determination of the Microbiota of Edam Cheeses by High-Throughput Sequencing (HTS)

The number of 16S rRNA sequence reads ranged from 332,280 to 436,468 in cheese samples after 52 days of ripening. The predominant microbial groups belonged to four phyla: Firmicutes, Actinobacteria, Proteobacteria, and Bacteroidetes (Figure 1).

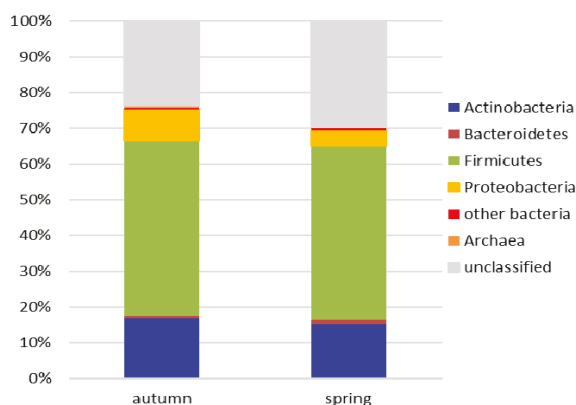


Figure 1. The average relative abundance (%) of the sequences identified at phylum level in samples of Edam cheese.

Eleven predominant genera were identified in the group of 32 genera and taxonomic groups that accounted for at least 0.5% of the bacterial community. They were: *Acetobacter*, *Alcaliphilus*, *Bacillus*, *Bacteroides*, *Bifidobacterium*, *Cellulomonas*, *Clostridium*, *Lactococcus*, *Lactobacillus*, *Leucobacter*, *Propionibacterium*, and one group of γ -Proteobacteria. Similar results were reported in a study of Oscypek, a traditional Polish smoked cheese made of sheep's milk [37]. The authors demonstrated the predominance of the same four phyla and identified nine identical genera and taxonomic groups in 40 operational taxonomic units (OTUs). The proportions of the remaining genera were below 0.5%, and not all genera were identified in all samples. The average bacterial identification levels were similar (75–70%) in the spring and autumn seasons. In autumn and spring samples, 25% and 30% of the sequences could not be identified, respectively. The genera represented by dozens or hundreds of reads, including Archaea and algae (Eukaryota), accounted for a large part of the taxonomic spectrum in cheese samples. A high number of DNA sequences were not classified in the remaining cheese samples (Figure 1). The above could be attributed to the presence of microorganisms that have not yet been classified or microorganisms containing degraded DNA. Fernandes et al. [38] observed that DNA was degraded to very short fragments during corn dough fermentation. The content of bacterial proteases, proteinases, and peptidases increases gradually during cheese ripening and storage. Similarly to bacterial proteases, DNA-degrading enzymes (nucleases) can also be released into the cheese matrix during the autolysis of starter and non-starter lactic acid bacteria [39], or they can be bacteriophage-derived [19].

The highest number of reads was obtained for two out of the three genera of starter bacteria: *Lactococcus* and *Propionibacterium*. In the analyzed group of the SLAB, *Lactococcus* was the predominant

genus in the phylum Firmicutes, and it accounted for 43.78% and 53.35% of the microbial communities in autumn and spring cheese samples, respectively. The second most dominant starter culture belonged to the genus *Propionibacterium*, phylum Actinobacteria. *Propionibacterium* counts were lower, and they were determined at 9.41% and 12.37% in spring and autumn cheese samples, respectively. A comparison of the number of reads for the selected bacterial genera revealed important differences, including in starter bacteria that are added in strictly controlled amounts to every cheese batch. The number of reads for the third genus of starter bacteria, *Leuconostoc*, was very low at a fraction of a percent (Figure 2 and Table S1). The analyzed cheeses were characterized by highly diverse microbiota. Starter bacteria develop in the first stages of the production process and dominate over residual microflora and the microorganisms from secondary infections. During ripening, bacterial starter cells are gradually autolyzed, which promotes the growth of non-starter bacteria that can also influence the attributes of the final product [40]. For this reason, the microbiota of ripened cheese are more diverse than those observed immediately after production or short ripening. Alessandria et al. [41] demonstrated that the microbiota of Grana-like cheese begin to diversify upon brining and undergo significant changes during two months of ripening. In the present study, starter bacteria were predominant in the Edam cheese. *Lactococcus* and *Propionibacterium* from starter cultures accounted for 56–65% of all bacteria, whereas *Leuconostoc* represented only a fraction of percent of the overall microbial community. Similar results were reported by Almeida et al. [42]; in their study, the number of sequence reads for *Leuconostoc* was also low. A predominance of starter bacteria was reported by Ceugniz et al. [16], who found that starter bacteria accounted for 85% of the microbiota in the core samples of Tomme d’Orchies cheese, and by Alessandria et al. [41], who demonstrated that *Lactobacillus* and *Streptococcus* predominated in Grana-like cheese inoculated with natural whey starters (NWS). Duru et al. [19] also found that *Lactococcus*, *Lactobacillus*, and *Propionibacterium* bacteria accounted for 80–82% of the microbiota in industrially produced Swiss cheese. However, in a study by Porcelato et al. [18], starter bacteria (*Lactococcus*, *Leuconostoc*, and *Lactobacillus*) represented more than 99% of the bacterial community in industrially produced Dutch cheese.

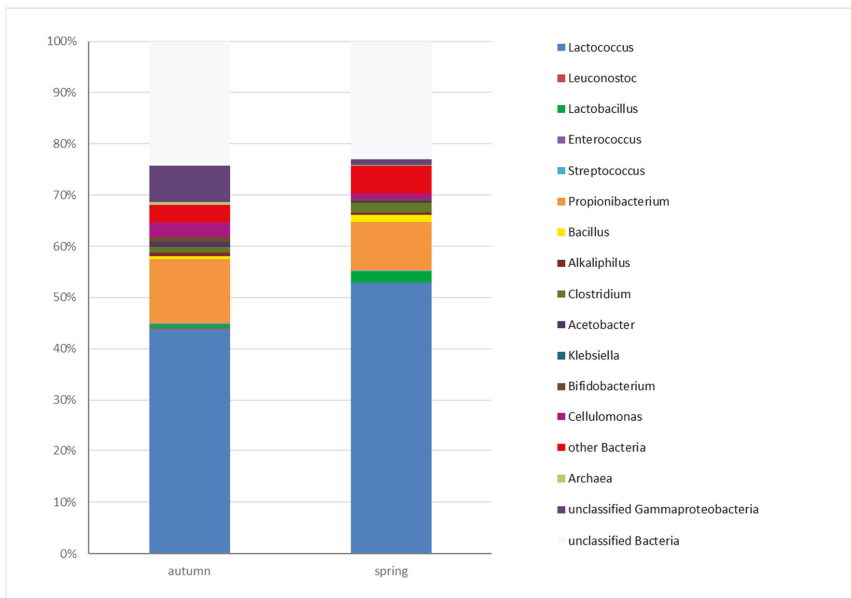


Figure 2. The average relative abundance (%) of the sequences identified at genus level in samples of Edam cheese.

The results of the SLAB and NSLAB analyses performed with the use of both methods (culture-dependent and NGS) revealed a certain regularity. When plate counts (expressed in log cfu/g) were one log unit higher in one bacterial genus than in another, the corresponding number of reads was approximately 10 times higher (Table 3 and Table S1).

Despite the high proportions of starter bacteria in cheese samples, a high number of reads was noted for the NSLAB. In the phylum Actinobacteria, the abundance of *Cellulomonas* in the microbial community was relatively high, and it ranged from 1% to 3% in all cheese samples. The genera *Bifidobacterium* and *Leucobacter* were less abundant, and their proportions were determined at 0.40%/0.94% and 0.18%/0.33%, respectively. The remaining identified genera of the phylum Actinobacteria accounted for up to 0.2% of the investigated microbial communities (Table S1). Spring cheese samples differed considerably from the remaining samples in the frequency of *Lactobacillus*, which was higher in spring samples (approximately 1.5%) (Table S1). In the genus *Lactobacillus*, the highest number of reads was obtained for *Lactobacillus rhamnosus*, *Lactobacillus kefir*, *Lactobacillus kefiranofaciens*, and *Lactobacillus casei* (data not shown). The relative frequency of *Bifidobacterium* and *Streptococcus* was 0.6% and 0.3% higher, respectively, only in individual samples relative to the remaining cheese samples (0.08%) (data not shown). Similar results were reported in other studies of industrially produced cheeses. Porcelato et al. [18] detected *Lactobacillus* and *Streptococcus* in Dutch-type cheese, and Duru et al. [19] identified *Enterococcus* and *Streptococcus* in Swiss-type cheese.

The phylum Firmicutes also includes bacteria that cause technological defects in cheeses. In the group of contaminating bacteria, the highest number of reads was obtained for spore-forming bacteria of the genus *Clostridium*. The relative proportions of *Clostridium* were 0.97% higher in spring samples than in autumn samples. The genus *Clostridium* was represented mainly by three species: *Clostridium butyricum*, *Clostridium longisporum*, and *Clostridium tyrobutyricum*. In spring samples with the highest number of reads for the genus *Clostridium*, the predominant species was *C. tyrobutyricum*, whose abundance was around 10-fold higher in comparison with *C. butyricum* and *C. longisporum* in the remaining samples (data not shown). In the current study, next-generation sequencing supported the detection of *C. tyrobutyricum*, which could be responsible for late blowing, a cheese defect resulting from butyric acid fermentation [43,44]. This is a very valuable observation that can be used to introduce the required adjustments during cheese production, ripening, and storage. Spore-forming bacteria of the genus *Bacillus* also had a relatively high share of microbial communities, particularly in spring samples where the average frequency of *Bacillus* was 0.81% higher than in autumn samples. The proportions of spore-forming bacteria of the genus *Bacillus* were higher in spring cheeses than in autumn cheeses. The observed variations can be probably attributed to dietary factors because cows graze naturally on grass in summer and autumn. Henderson et al. [45] demonstrated that the abundance of bacterial genera in the bovine rumen changed with the cows' diet. The presence of bacteria in milk can also differ because raw milk microbiota are much more diverse and contain more environmental bacteria and microorganisms from the bovine digestive tract in summer and autumn. In winter and spring, cows are fed with hay and silage, which increases the counts of spore-forming bacteria of the genus *Bacillus* in the environment, milk, and, consequently, cheese. The autumn samples were characterized by the greatest differences in the frequency of *Enterococcus* spp. (0.06%), and they differed ($p > 0.05$) from spring samples (Table S1). The analyzed cheeses also contained trace amounts of DNA of the microorganisms colonizing the natural environment and cows. The remaining identified bacterial genera of the phylum Firmicutes accounted for up to 0.2% of the analyzed microbial communities. On rare occasions, selected genera, including *Veillonella*, *Laceyella*, *Streptococcus*, *Eubacterium*, and *Ruminococcus*, were more abundant (Table S1). Bacteria of the phylum Proteobacteria accounted for 3.26% (spring samples) and 8.69% (autumn samples) of microbial communities. They were mostly represented by members of the class γ -Proteobacteria whose DNA sequences could not be identified to the genus level. The proportion of γ -Proteobacteria ranged from 1.11% in spring samples to 7.11% in autumn samples (Figure 2 and Table S1). Among the identified genera, the predominant class was α -Proteobacteria of the genus *Acetobacter*, which accounted for 0.39–1.01% of microbial communities in

spring and autumn samples, respectively. The class γ -Proteobacteria of the genus *Acinetobacter* was also abundantly represented in spring samples at 1.56% (Table S1). The phylum Bacteroidetes accounted for 0.52–0.84% of microbial communities in the analyzed cheese samples, and it was represented mostly by the genus *Bacteroides*, whose abundance ranged from 0.15% in spring samples to 0.30% in autumn cheese samples. Other genera were sporadically noted, including *Prevotella* and *Chryseobacterium* (Table S1). Cheeses were also colonized by bacteria of the genera *Acinetobacter*, *Chryseobacterium*, and *Alkaliphylus* which are ubiquitous in soil and water, as well as *Cellulomonas*, *Eubacterium*, *Rothia*, and *Ruminococcus*, which are found in the bovine digestive tract [11,13,41]. Interestingly, the unexpected bacterial genera *Alloscardovia*, *Prevotella* and *Veillonella* from animal respiratory and digestive systems [45,46]—as well as *Laceyella*, which are found in bottom sediments, soil, and patients with farmer’s lung disease [47]—were also identified at relatively high concentrations in individual samples. The DNA of *Erysipelothrix rhusiopathiae*, a bacterium responsible for swine erysipelas disease [48], was detected in a single sample in our study. The proportion of this bacterium in the sample was surprisingly high at 0.22%, which can probably be attributed to the accidental contamination of raw milk by veterinarians or farm personnel. Bokulich and Mills [49] also identified various bacterial and fungal genera that were not added as starter cultures. The presence of the DNA of unexpected bacterial genera and species provides detailed information about the quality of raw milk, and it can be used to prevent contamination of milk and the final product.

In the present study, the variations in bacterial genera colonizing the evaluated samples were very high, despite the fact that all samples were obtained from the same dairy plant, and the raw milk was produced in the same Polish region. Alessandria et al. [41] also found differences in the composition of microbial populations colonizing cheeses from the same dairy plant. They observed considerable microbial diversity of cheeses produced in spring at weekly intervals. The above could imply that minor fluctuations in the production process significantly influence the composition of cheese microbiota. Differences in microbiological quality can also result from various stages of cheese ripening, variations in the microbial composition of raw milk, environmental factors, other disruptive factors, and minor deviations from production procedures. In this study, certain seasonal changes in cheese microbiota were also noted, though only in communities of contaminating microorganisms.

4. Conclusions

High levels of milk production in dairies and the combination of raw materials from different milk producers (different regions of the country) contribute to the high microbial biodiversity of cheese and the absence of significant differences in the OTU reads across production seasons. This study demonstrated that despite the application of different testing techniques, the relationships between the analyzed production periods were highly similar. Both next-generation sequencing and culture-dependent approaches are sources of bias, but they provide complementary information about the microbial ecology of cheese. The evaluated Edam cheeses were characterized by a predominance of starter bacteria and the presence of non-starter lactic acid bacteria from the microflora of the dairy plant and the cattle environment. Trace amounts of bacteria that are pathogenic for cattle were also identified. High-throughput sequencing also supported the identification of low-abundance bacteria, as well as bacteria that had not been previously detected in ripened cheeses. Advanced analytical tools developed by “omics” sciences can provide new insights into the metagenomes of fermented foods, including ripened cheeses. Metagenomic profiling has created unprecedented opportunities for analyzing cheese ecology. The identification of the genes and genomes of microbial communities in ripened cheeses supports the detection of the most desirable strains, the description of their development and transfer, and the identification of microbial contaminants and pathogens.

Supplementary Materials: The following are available online at <http://www.mdpi.com/2076-3417/10/12/4063/s1>, Table S1: Percentages of the most abundant taxonomic groups in Edam cheese samples after 52 days of ripening.

Author Contributions: B.N. developed the research concept and administered the research project. B.N., S.C., and M.A. procured the materials, developed the methodology, analyzed and curated the data, performed formal

analyses, and wrote the manuscript. B.N. and M.A. acquired research funds, visualized data, and reviewed and edited the manuscript. All authors have read and agreed to the published version of the manuscript.

Funding: The project was financially supported by the Minister of Science and Higher Education under the program entitled “Regional Initiative of Excellence” for the years 2019–2022, Project No. 010/RID/2018/19, amount of funding PLN 12,000,000 and by University of Warmia and Mazury in Olsztyn (statutory research, Projects No. 17.610.015-300 and 17.610.003-110).

Conflicts of Interest: The authors declare no conflict of interest.

References

1. Ogier, J.-C.; Lafarge, V.; Girard, V.; Rault, A.; Maladen, V.; Gruss, A.; Leveau, J.-Y.; Delacroix-Buchet, A. Molecular fingerprinting of dairy microbial ecosystems by use of temporal temperature and denaturing gradient gel electrophoresis. *Appl. Environ. Microbiol.* **2004**, *70*, 5628–5643. [[CrossRef](#)] [[PubMed](#)]
2. Randazzo, C.L.; Vaughan, E.E.; Caggia, C. Artisanal and experimental Pecorino Siciliano cheese: Microbial dynamics during manufacture assessed by culturing and PCR-DGGE analyses. *Int. J. Food Microbiol.* **2006**, *109*, 1–8. [[CrossRef](#)] [[PubMed](#)]
3. Ricciardi, A.; Guidone, A.; Ianniello, R.G.; Cioffi, S.; Aponte, M.; Pavlidis, D.; Tsakalidou, E.; Zotta, T.; Parente, E. A survey of non-starter lactic acid bacteria in traditional cheeses: Culture dependent identification and survival to simulated gastrointestinal transit. *Int. Dairy J.* **2015**, *43*, 42–50. [[CrossRef](#)]
4. Beresford, T.P.; Fitzsimons, N.A.; Brennan, N.L.; Cogan, T.M. Recent advances in cheese microbiology. *Int. Dairy J.* **2001**, *11*, 259–274. [[CrossRef](#)]
5. Czerwińska, E.; Piotrowski, W. Potential sources of milk contamination influencing its quality for consumption. *Rocz. Ochrona Środow.* **2011**, *13*, 635–652. (in Polish).
6. Lawlor, J.; Delahunty, C.M.; Wilkinson, M.G.; Sheehan, J. Swiss-type and Swiss–cheddar hybrid-type cheeses: Effects of manufacture on sensory character and relationships between the sensory attributes and volatile compounds and gross compositional constituents. *Int. J. Dairy Technol.* **2003**, *56*, 39–51. [[CrossRef](#)]
7. Joux, F.; Lebaron, P. Use of fluorescent probes to assess physiological functions of bacteria at single-cell level. *Microbes Infect.* **2000**, *2*, 1523–1535. [[CrossRef](#)]
8. Dove, A. PCR: Thirty-five years and counting. *Science* **2018**, *360*, 670–672. [[CrossRef](#)]
9. Cocolin, L.; Mataragas, M.; Bourdichon, F.; Doulgeraki, A.; Pilet, M.-F.; Jagadeesan, B.; Rantsiou, K.; Phister, T. Next generation microbiological risk assessment meta-omics: The next need for integration. *Int. J. Food Microbiol.* **2018**, *287*, 3–9. [[CrossRef](#)]
10. Kergourlay, G.; Taminiau, B.; Daube, G.; Champomier Verges, M.C. Metagenomic insights into the dynamics of microbial communities in food. *Int. J. Food Microbiol.* **2015**, *213*, 31–39. [[CrossRef](#)]
11. Ercolini, D.; De Filippis, F.; La Stora, A.; Iacono, M. “Remake” by high-throughput sequencing of the microbiota involved in the production of water buffalo mozzarella cheese. *Appl. Environ. Microbiol.* **2012**, *78*, 8142–8145. [[CrossRef](#)] [[PubMed](#)]
12. Delcenserie, V.; Taminiau, B.; Delhalle, L.; Nezer, C.; Doyen, P.; Crevecoeur, S.; Roussey, D.; Korsak, N.; Daube, G. Microbiota characterization of a Belgian protected designation of origin cheese, Herve cheese, using metagenomic analysis. *J. Dairy Sci.* **2014**, *97*, 6046–6056. [[CrossRef](#)] [[PubMed](#)]
13. Dalmaso, A.; de los Dolores Soto del Rio, M.; Civera, T.; Pattono, D.; Cardazzo, B.; Bottero, M.T. Characterization of microbiota in Plaisentif cheese by high-throughput sequencing. *LWT-Food Sci. Technol.* **2016**, *69*, 490–496. [[CrossRef](#)]
14. De Filippis, F.; Genovese, A.; Ferranti, P.; Gilbert, J.A.; Ercolini, D. Metatranscriptomics reveals temperature-driven functional changes in microbiome impacting cheese maturation rate. *Sci. Rep.* **2016**, *6*, 21871. [[CrossRef](#)]
15. Escobar-Zepeda, A.; Sanchez-Flores, A.; Quirasco Baruch, M. Metagenomic analysis of a Mexican ripened cheese reveals a unique complex microbiota. *Food Microbiol.* **2016**, *57*, 116–127. [[CrossRef](#)]
16. Ceugniz, A.; Taminiau, B.; Coucheny, F.; Jacques, P.; Delcenserie, V.; Daube, G.; Drider, D. Use of a metagenetic approach to monitor the bacterial microbiota of “Tomme d’Orchies” cheese during the ripening process. *Int. J. Food Microbiol.* **2017**, *247*, 65–69. [[CrossRef](#)]

17. Dugat-Bony, E.; Straub, C.; Teissandier, A.; Onesime, D.; Loux, V.; Monnet, C.; Irlinger, F.; Landaud, S.; Leclercq-Perlat, M.N.; Bento, P.; et al. Overview of a surface-ripened cheese community functioning by meta-omics analyses. *PLoS ONE* **2015**, *10*, e0124360. [[CrossRef](#)]
18. Porcellato, D.; Skeie, S.B. Bacterial dynamics and functional analysis of microbial metagenomes during ripening of Dutch-type cheese. *Int. Dairy J.* **2018**, *61*, 182–188. [[CrossRef](#)]
19. Duru, I.C.; Laine, P.; Andreevskaya, M.; Paulin, L.; Kananen, S.; Tynkkynen, S.; Auvinen, P.; Smolander, O.-P. Metagenomic and metatranscriptomic analysis of the microbial community in Swiss-type Maasdam cheese during ripening. *Int. J. Food Microbiol.* **2018**, *281*, 10–22. [[CrossRef](#)]
20. Albenzio, M.; Corbo, M.R.; Rehman, S.U.; Fox, P.F.; De Angelis, M.; Corsetti, A.; Sevi, A.; Gobetti, M. Microbiological and biochemical characteristics of Canestrato Pugliese cheese made from raw milk, pasteurized milk or by heating the curd in hot whey. *Int. J. Food Microbiol.* **2001**, *67*, 35–48. [[CrossRef](#)]
21. Dahl, S.; Tavaría, F.K.; Malcata, F.X. Relationships between flavour and microbiological profiles in Serra da Estrela cheese throughout ripening. *Int. Dairy J.* **2000**, *10*, 255–262. [[CrossRef](#)]
22. Marini, M.; Maifreni, M.; Rondinini, G. Microbiological characterization of artisanal Montasio cheese: Analysis of its indigenous lactic acid bacteria. *FEMS Microbiol. Lett.* **2003**, *229*, 133–140. [[CrossRef](#)]
23. ISO 707:2008 (IDF 50:2008). *Milk and Milk Products—Guidance on Sampling*; International Standard Organization: London, UK, 2008.
24. ISO 3433:2008 (IDF 222: 2008). *Cheese-Determination of Fat Content-Van Gulik Method*; International Standard Organization: London, UK, 2008.
25. ISO 5943:2006 (IDF 88:2006). *Cheese and Processed Cheese Products-Determination of Chloride Content-Potentiometric Titration Method*; International Standard Organization: London, UK, 2006.
26. AOAC International 2005. *Official Methods of Analysis*, 18th ed.; AOAC International: Gaithersburg, MD, USA, 2005.
27. Klindworth, A.; Pruesse, E.; Schweer, T.; Schweer, T.; Peplies, J.; Quast, C.; Horn, M.; Glockner, F.O. Evaluation of general 16S ribosomal RNA gene PCR primers for classical and next-generation sequencing-based diversity studies. *Nucleic Acids Res.* **2013**, *41*, e1. [[CrossRef](#)] [[PubMed](#)]
28. Meyer, F.; Paarmann, D.; D’Souza, M.; Olson, R.; Glass, E.M.; Kubal, M.; Paczian, T.; Rodriguez, A.; Stevens, R.; Wilke, A.; et al. The metagenomics RAST server—a public resource for the automatic phylogenetic and functional analysis of metagenomes. *BMC Bioinformatics* **2008**, *9*, 386–394. [[CrossRef](#)] [[PubMed](#)]
29. Aljewicz, M.; Cichosz, G. Influence of probiotic (*Lactobacillus acidophilus* NCFM, *L. paracasei* LPC37, and *L. rhamnosus* HN001) strains on starter cultures and secondary microbiota in Swiss-and Dutch-type cheeses. *J. Food Process. Preserv.* **2017**, *41*, e13253. [[CrossRef](#)]
30. de Souza, C.F.V.; Dalla Rosa, T.; Ayub, M.A.Z. Changes in the microbiological and physicochemical characteristics of Serrano cheese during manufacture and ripening. *Braz. J. Microbiol.* **2003**, *34*, 260–266. [[CrossRef](#)]
31. Park, W.; Yoo, J.; Oh, S.; Ham, J.S.; Jeong, S.G.; Kim, Y. Microbiological characteristics of Gouda cheese manufactured with pasteurized and raw milk during ripening using next generation sequencing. *Food Sci. Animal Resource* **2019**, *39*, 585–600. [[CrossRef](#)]
32. Van Hoorde, K.; Heyndrickx, M.; Vandamme, P.; Huys, G. Influence of pasteurization, brining conditions and production environment on the microbiota of artisan Gouda-type cheeses. *Food Microbiol.* **2010**, *27*, 425–433. [[CrossRef](#)]
33. Martín-Platero, A.M.; Maqueda, M.; Valdivia, E.; Purswani, J.; Martínez-Bueno, M. Polyphasic study of microbial communities of two Spanish farmhouse goats’ milk cheeses from Sierra de Aracena. *Food Microbiology* **2009**, *6*, 294–304. [[CrossRef](#)]
34. Sánchez-Gamboa, C.; Hicks-Pérez, L.; Gutiérrez-Méndez, N.; Heredia, N.; García, S.; Nevárez-Moorillón, G. Microbiological changes during ripening of Chihuahua cheese manufactured with raw milk and its seasonal variations. *Foods* **2018**, *7*, 153. [[CrossRef](#)]
35. Bermúdez, J.; González, M.J.; Olivera, J.A.; Burgueño, J.A.; Juliano, P.; Fox, E.M.; Reginensi, S.M. Seasonal occurrence and molecular diversity of clostridia species spores along cheesemaking streams of 5 commercial dairy plants. *J. Dairy Sci.* **2016**, *99*, 3358–3366. [[CrossRef](#)] [[PubMed](#)]
36. Matijasic, B.B.; Rajsp, M.K.; Perko, B.; Rogelj, I. Inhibition of *Clostridium tyrobutyricum* in cheese by *Lactobacillus gasseri*. *Int. Dairy J.* **2007**, *17*, 157–166. [[CrossRef](#)]

37. Alegria, A.; Szczesny, P.; Mayo, B.; Bardowski, J.; Kowalczyk, M. Biodiversity in Oscypek, a traditional Polish cheese, determined by culture-dependent and -independent approaches. *Appl. Environ. Microbiol.* **2012**, *78*, 1890–1898. [[CrossRef](#)] [[PubMed](#)]
38. Fernandes, T.J.R.; Oliveira, M.B.P.P.; Mafra, I. Tracing transgenic maize as affected by breadmaking process and raw material for the production of a traditional maize bread, broa. *Food Chem.* **2013**, *138*, 687–692. [[CrossRef](#)] [[PubMed](#)]
39. Cichosz, G.; Szpendowski, J.; Cichosz, A.J.; Kornacki, M. Paracasein degradation in gouda cheeses produced with *Lactobacillus* culture. *ŻYWNOSĆ. Nauka. Technologia. Jakość* **2006**, *1*, 58–65, (in Polish, abstract in English).
40. Czarán, T.; Rattray, F.P.; Møller, C.O.A.; Christensen, B.B. Modelling the influence of metabolite diffusion on non-starter lactic acid bacteria growth in ripening Cheddar cheese. *Int. Dairy J.* **2018**, *80*, 35–45. [[CrossRef](#)]
41. Alessandria, V.; Ferrocino, I.; De Filippis, F.; Fontana, M.; Rantsiou, K.; Ercolini, D.; Cocolin, L. Microbiota of an Italian Grana-like cheese during manufacture and ripening, unraveled by 16S rRNA-based approaches. *Appl. Environ. Microbiol.* **2016**, *82*, 3988–3995. [[CrossRef](#)]
42. Almeida, M.; Hébert, A.; Abraham, A.-L.; Rasmussen, S.; Monnet, C.; Pons, N.; Delbès, C.; Loux, V.; Batto, J.-M.; Leonard, P.; et al. Construction of a dairy microbial genome catalog opens new perspectives for the metagenomic analysis of dairy fermented products. *BMC Genomics* **2014**, *15*, 1101–1117. [[CrossRef](#)]
43. Klijn, N.; Nieuwenhof, F.F.J.; Hoolwerf, J.D.; van der Waals, C.B.; Weerkamp, A.H. Identification of *Clostridium tyrobutyricum* as the causative agent of late blowing in cheese by species-specific PCR amplification. *Appl. Environ. Microbiol.* **1995**, *61*, 2919–2924. [[CrossRef](#)]
44. Bassi, D.; Puglisi, E.; Coconcelli, P.S. Understanding the bacterial communities of hard cheese with blowing defect. *Food Microbiol.* **2015**, *52*, 106–118. [[CrossRef](#)]
45. Henderson, G.; Cox, F.; Ganesh, S.; Jonker, A.; Young, W.; Global Rumen Census Collaborators; Janssen, P.H. Rumen microbial community composition varies with diet and host, but a core microbiome is found across a wide geographical range. *Sci. Rep.* **2015**, *5*, 14567. [[CrossRef](#)] [[PubMed](#)]
46. Jami, E.; Mizrahi, I. Similarity of the ruminal bacteria across individual lactating cows. *Anaerobes* **2012**, *18*, 338–343. [[CrossRef](#)] [[PubMed](#)]
47. Goodfellow, M.; Jones, A.L. Laceyella. *Bergey's Man. Syst. Arch. Bact.* **2015**. [[CrossRef](#)]
48. Brooke, C.J.; Riley, T.V. *Erysipelothrix rhusiopathiae*: Bacteriology, epidemiology and clinical manifestations of an occupational pathogen. *J. Medical Microbiol.* **1999**, *48*, 789–799. [[CrossRef](#)]
49. Bokulich, N.A.; Mills, D.A. Facility-specific “house” microbiome drives microbial landscapes of artisan cheesemaking plants. *Appl. Environ. Microbiol.* **2013**, *79*, 5214–5223. [[CrossRef](#)] [[PubMed](#)]



© 2020 by the authors. Licensee MDPI, Basel, Switzerland. This article is an open access article distributed under the terms and conditions of the Creative Commons Attribution (CC BY) license (<http://creativecommons.org/licenses/by/4.0/>).

Review

Metabolic Syndrome-Preventive Peptides Derived from Milk Proteins and Their Presence in Cheeses: A Review

Anna Iwaniak * and Damir Mogut *

Faculty of Food Science, University of Warmia and Mazury in Olsztyn, Pl. Cieszyński 1, 10-726 Olsztyn-Kortowo, Poland

* Correspondence: ami@uwm.edu.pl (A.I.); damir.mogut@uwm.edu.pl (D.M.)

Received: 11 March 2020; Accepted: 14 April 2020; Published: 17 April 2020

Abstract: The metabolic syndrome (MetS) is defined as the occurrence of diet-related diseases such as abdominal obesity, atherogenic dyslipidemia, hyperglycemia (insulin resistance) and hypertension. Milk-derived peptides are well-known agents acting against high blood pressure, blood glucose level, and lipoprotein disproportion. The aim of this review are metabolic syndrome-preventive peptides derived from milk proteins which were identified in cheeses. Special attention was paid to the sequences acting as angiotensin converting enzyme (ACE), dipeptidyl peptidase IV (DDP4), and α -glucosidase inhibitors, as well as antioxidative, hypocholesterolemic, antiobesity, and anti-inflammatory agents. Some results of meta-analyses concerning the consumption of cheese and the risk of MetS diseases were also presented.

Keywords: biopeptides; BIOPEP-UWM database; cheese; metabolic syndrome; milk proteins

1. Introduction

The metabolic syndrome (MetS) is defined as a clustering of four major cardiovascular risk factors, namely: abdominal obesity, atherogenic dyslipidemia, hyperglycemia (insulin resistance), and hypertension (Figure 1) [1]. Moreover, the pathogenesis of MetS involves both genetic and acquired factors contributing to the inflammation [2]. MetS also represents a significant risk factor for the development of cardiovascular disease (CVD), type 2 diabetes mellitus (T2D), and all-cause mortality [1]. Moore et al. [3] analyzed data derived from the National Health and Nutrition Examination Survey (NHANES). Based on the analysis including the period from 1988 to 2012, MetS was defined as at least three conditions from these listed further that have to occur in a patient: elevated waist circumference, elevated level of triglycerides, reduced high-density lipoprotein cholesterol level, high blood pressure, and elevated fasting blood glucose level. According to the above-mentioned definition of MetS, in 2012 there were more than 66 million adults in the US with recognized MetS symptoms. They were observed in every sociodemographic group [3].

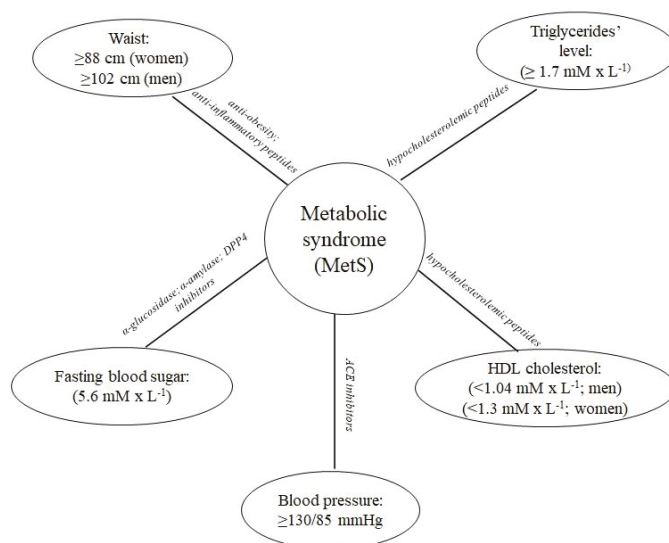


Figure 1. Metabolic syndrome criteria and related preventive agents according to Huang [4].

The following enzymes are involved in MetS: dipeptidyl peptidase IV (EC 3.4.14.5; DPP4), α -glucosidase (EC 3.2.1.20), α -amylase (EC 3.2.1.1), and angiotensin-converting enzyme (EC 3.4.15.1; ACE). The first three affect the postprandial blood glucose level, whereas ACE is the key enzyme involved in the regulation of the blood pressure. Thus, peptides being the inhibitors of the above-mentioned enzymes may be considered anti-MetS agents [5]. Additionally, peptides also reduce cholesterol level, antioxidative stress [6], act as anti-obesity [7], and anti-inflammatory agents [8].

Milk is the first functional food for every mammalian species. The contents of its nutrients, such as proteins (and their proportions), fat, sugar, vitamins, and minerals, vary between species as well as breeds. Moreover, milk composition is affected by feeding methods, age of an animal, and many other [9]. Milk and dairy products were also studied as anti-metabolic syndrome foods [10].

A cohort study made in 2018 on 136,384 individuals from 21 countries on five continents demonstrated that dairy product consumption (especially of milk and yogurt) can be associated with a lower risk, of not only CVD, but also mortality. According to this study, even one serving of milk or yogurt significantly lowered the risks of the above-mentioned events. Additionally, the higher consumption of dairy products can be associated with significantly lower risk of stroke [10]. According to another study, every 200 mL increase of daily milk consumption reduced the risk of CVD by 6%. Based on the data from 2015 it was shown that three main milk constituents were responsible for the MetS-preventive activity, namely calcium, fat, and proteins [11]. One of the MetS-preventive potentials of milk and dairy products resulting from the presence of proteins might be related to the action of biologically active peptides [5]. It also reflects vast information found in. e.g., Scopus database [www.scopus.com]. Providing the following words as the input query “ALL (metabolic AND syndrome AND milk AND peptides)” revealed 7459 hits (accessed in September 2019).

The first mentions about cheese manufacturing appeared around 5500 BC. Early adult humans were unable to digest lactose. Thus, making cheese was a good way to consume health beneficial nutrients derived from milk, without getting ill [11]. The casein, main milk protein, during cheese maturation is hydrolyzed into a variety of peptides. Their composition varies and depends on the activity of endogenous proteases and peptidases of milk, rennet, starter culture, and microbial flora [12]. Bovine casein has been shown to possess a variety of bioactivities, including MetS-preventive ones. In silico analyses and reviews conducted on bovine casein confirmed the casein-derived peptides to

exhibit these activities [13,14]. Hence, considering the increasing role of biopeptides in the prevention of MetS, the aim of this paper was to describe MetS-preventive peptides derived mainly from bovine milk proteins which were also identified in the ripened cheeses. The main attention was paid to the peptides exerting antidiabetic, antihypertensive, antioxidative, cholesterol-reducing, antiobesity, and anti-inflammatory effects.

2. Antidiabetic Agents

One of the body enzymes involved in the regulation of the glucose level is DPP4 [15]. This enzyme is involved in the incretin effect after meal consumption. Incretins, like glucagon-like peptide 1 (GLP-1) and glucose-dependent insulinotropic polypeptide (GIP), are hormones that decrease blood glucose levels by stimulating insulin secretion and inhibiting glucagon release. GIP serves several additional functions including promotion of growth and survival of the pancreatic beta-cell and stimulation of adipogenesis [15]. This effect is hindered by DPP4, therefore inhibition of DPP4 prolongs the incretin effect and lowers the postprandial blood glucose level (Figure 2) [16].

Uenishi et al. [17] identified DPP4 inhibitory peptides in water-soluble Gouda cheese extracts. Peptides derived from β -casein (LPQNIPPL) and α_{S1-7} , α_{S2-7} , β -caseins (LPQ) evoked the highest DPP4-inhibiting effect in vitro. Their IC₅₀ values were 46.0 and 56.7 μ M, respectively. The bioactivity of the LPQNIPPL sequence was also tested on rats (Female Sprague Dawley, 8-week-old). The administration of this peptide at 300 mg \times kg⁻¹ body weight reduced significantly the postprandial glucose level in those rats [16]. Other peptides with DPP4 inhibitory bioactivity that were identified in Gouda cheese water-soluble-extracts (WSE) were characterized with the following sequences: VPITPTL (110 μ M), VPITPT (130 μ M), FPGPIPN (260 μ M), YPFPGPIPN (670 μ M), PGPIHNS (1000 μ M), IPPLTQTPV (1300 μ M), PQNIPPL (1500 μ M), and VPPFIQPE (2500 μ M). Their activity expressed in IC₅₀ values was provided in brackets [17].

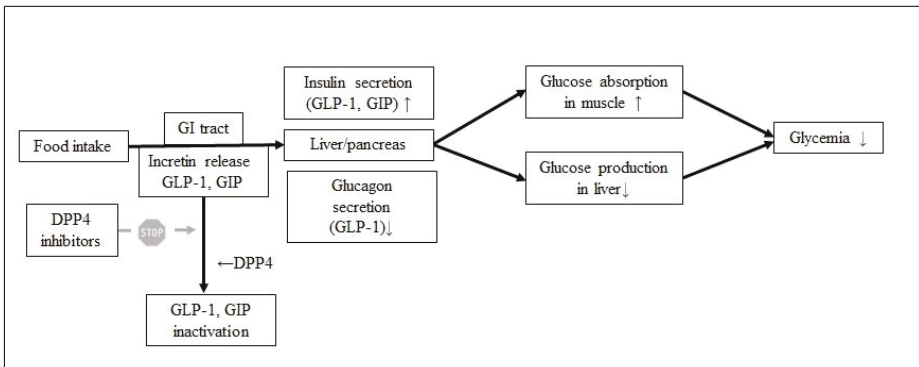


Figure 2. The involvement of the dipeptidyl peptidase IV inhibitors in prolonging the incretin effect according to Mkele [16].

Antidiabetic properties of peptides may also result from their ability to inhibit α -glucosidase (EC 3.2.1.20). α -Glucosidase is an enzyme located in the brush border of enterocytes of the jejunum in the small intestine and is a key enzyme in carbohydrate breakdown. It cleaves carbohydrate to easy absorbable glucose. Thus, one of the T2D preventive strategies is to decrease the postprandial hyperglycemia by delaying glucose absorption through the inhibition of α -glucosidase (Figure 3). α -Glucosidase inhibitors also play a crucial role in the secretion of GLP-1 in healthy and diabetic patients, due to the prolonged incretin effect [18].

α -Amylase is another enzyme involved in the regulation of the blood sugar level [5]. This enzyme is responsible for the initial hydrolysis of the α -D-(1-4) glycosidic bonds of polysaccharides like glycogen

and starch to oligosaccharides. Then, oligosaccharides are further hydrolyzed into monosaccharides by α -glucosidase (see above), which are next transferred into bloodstream [5].

Some milk proteins were reported as the sources of α -glucosidase inhibitors. Whey proteins: α -lactalbumin, β -lactoglobulin, serum albumin, and lactoferrin hydrolysates obtained by peptic digestion were confirmed to exert such an inhibiting effect. β -Lactoglobulin and whey protein isolate hydrolysates were found to inhibit α -glucosidase (IC_{50} value of 3.5 and 4.5 $mg \times mL^{-1}$, respectively) [18]. Dipeptide, like arginine-proline (RP), derived from whey proteins and being the component of commercial Pep2Dia[®] product, affected the inhibition of α -glucosidase with an IC_{50} value of 0.0025 $mg \times mL^{-1}$ [19]. To the best of our knowledge, there is no research papers about α -amylase inhibitors identified milk proteins and dairy products. Only one article concerned cheese as a source of α -glucosidase inhibitors. According to Grom et al. [20], Prato cheese inhibited α -glucosidase activity in vitro by 52.6%. Although, it was concluded that the consumption of probiotic Prato cheese can contribute to the reduction of postprandial glycemia in healthy individuals, but no peptide was identified [20].

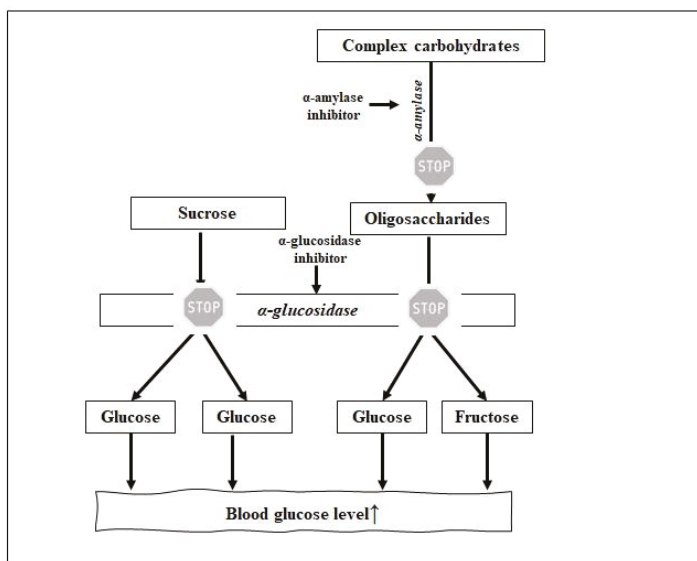


Figure 3. The delay of carbohydrate breakdown by α -glucosidase and α -amylase inhibitors according to Iwaniak et al. [5] and Patil et al. [18].

It was evidenced on mice that peptides from cheese effectively decreased glucose level. Some epidemiological surveys showed a slightly higher risk of T2D development with increasing cheese consumption, but most of the meta-analyses concluded that increasing cheese consumption was correlated with a significant decreasing in T2D development risk [21]. Another epidemiological and cohort studies showed that dairy products can be beneficial in type 2 diabetes prevention. The latest research carried out on 34,224 men in the Health Professionals Follow-Up Study (1986–2012), 76,531 women in the Nurses' Health Study (1986–2012), and 81,597 women in the Nurses' Health Study II (1991–2013) suggested that the decrease of total dairy intake by > 1.0 serving per day over a period of 4 years was associated with an 11% increase of T2D development risk [22]. However, there were some opposite remarks to these above. For example, it was stated that increasing cheese consumption by > 0.5 serving per day, caused a 9% increase of T2D development risk, when compared to the maintained, stable cheese intake [22]. In turn, these findings were not consistent with other studies. For example, the meta-analysis made by Gao et al. [23], concerning seven studies with a total of

178,429 subjects and 14,810 cases, led to opposite conclusions. They found an inverse linear correlation between the consumption of cheese and the risk of T2D development. The consumption of 30 g per day cheese decreased the relative risk (RR) of T2D development (RR 0.80 ± 0.12). The obtained results suggested that a modest increase in cheese consumption might prevent from T2D but further research is needed [23]. Another eight cohort studies concerning the meta-analysis of dairy food consumption and its effect on the T2D risk revealed that the consumption of 50 g cheese per day decreased the risk of T2D development (RR 0.92 ± 0.07) and a non-linear negative correlation was observed between cheese consumption and T2D risk [24]. The cohort study conducted on 2809 participants for 12 years showed a negative dose-response relation between cheese consumption and risk of T2D development. Out of the 1867 participants with no T2D symptoms, 902 were diagnosed as prediabetic. Consumption of ≥ 4 servings of cheese per week lowered the risk of T2D incident by 70%. Less than one cheese serving per week was associated with a 63% reduction of T2D incidents. None of the abovementioned meta-analyses, however, considered what type of cheese caused the risk-reducing effect [25].

3. Peptides with Antihypertensive Activity

The regulation of blood pressure that takes place in the organism involves several modes of ACE action. They include renin-angiotensin, kinin-nitric-oxide, and neutral endopeptidase systems. The first one (RAS; renin-angiotensin system), also called renin-angiotensin-aldosterone system (RAAS), is considered as the major in blood pressure regulation. Briefly, renin (EC 3.4.22.15) activates angiotensinogen and releases angiotensin I. Then, ACE (Figure 4) transforms angiotensin I into angiotensin II (known as potent vasoconstrictor) and induces the release of aldosterone. Moreover, the increase of the blood pressure caused by angiotensin II causes some dysfunctions like damages of body organs leading to e.g., heart and kidney failure. Thus, the action of ACE receptor blockers or ACE-inhibiting peptides contributes to the blood pressure reduction [26].

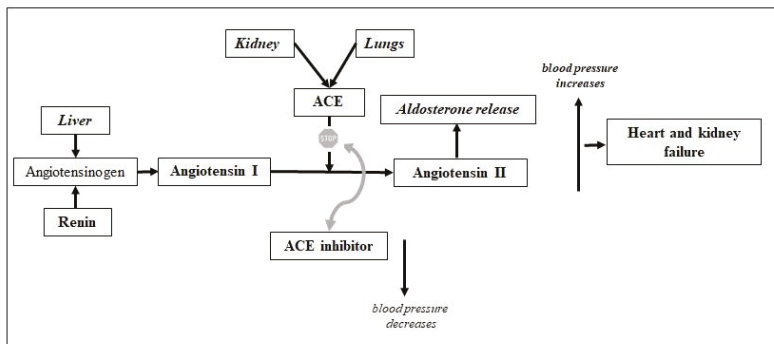


Figure 4. Brief description of the mechanism of action of ACE and its inhibitors according to Iwaniak et al. [26].

Milk proteins have been reported as the reservoir of ACE inhibitors for many years [27]. The most known sequences are VPP and IPP identified in β - and κ -casein, respectively. Due to their antihypertensive potential tested in animals and humans, they became the components of commercial milk drink nutraceuticals such as Calpis, Evolus, and Valio [28]. VPP and IPP sequences were also identified in 36 cheeses of Swiss origin (Table 1). Depending on the type of Swiss cheese, the content of these two sequences varied. For VPP, it ranged from 0 to 224 mg per kg of cheese, whereas for IPP from 0 to 95.4 mg. The highest content of both peptides, VPP and IPP, was identified in the hard cheese “Hobelkäse from the Bernese Oberland” (224.1 and 95.4 mg \times kg⁻¹, respectively). That cheese sample had the highest ACE inhibitory activity of all analyzed cheeses, with an IC₅₀ value of 2.6 mg \times mL⁻¹ [29]. Different concentrations of these two peptides in cheeses were probably related

to milk pretreatment, cultures, scalding conditions, and ripening time. Thus, it is recommended to develop a reproducible cheese-making process to produce higher concentrations of these peptides that could be used for clinical trials [30].

The potential of some cheeses containing the high concentrations of VPP and IPP to reduce blood pressure was tested in spontaneously hypertensive rats (SHR). Blood pressure was monitored after 6 h since oral administration. It was observed that the decrease of systolic blood pressure (SBP) differed depending on the cheese variety. The level of the SBP reduction (mmHg) in SHR was as follows: -24.7 and -17.2 (Gouda, aged 8 and 24 months, respectively), -17.2 (Gouda, aged 24 months), -20.7 (Edam), -20.3 (Blue), -20.0 (Havarti), and -13.0 (Emmental) [31].

Table 1. Quantification of VPP and IPP in cheeses of Swiss origin with their corresponding ACE inhibitory activity expressed with IC_{50} values. Adapted with permission from [29], Copyright Elsevier, 2007.

Cheese	VPP	IPP	IC_{50}
	($mg \times kg^{-1}$)	($mg \times kg^{-1}$)	($mg \text{ cheese} \times mL^{-1}$)
Hard cheeses			
Emmental:			
cave-aged, aged 12 months	100.1	23.5	7.1 ± 0.2
reserve, aged 8 months	68.6	13.2	9.9 ± 0.2
organic, aged 4 months	153.7	35.8	7.5 ± 1.8
classic, aged 4 months	42.6	4.6	10.5 ± 0.6
Gouda old	97.7	90.1	2.0 ± 0.3
Gruyere AOC:			
vieux, aged 12 months	13.7	7.9	29.4 ± 16.8
salé, aged 10 months	68.7	20.4	14.2 ± 0.9
mi-salé, aged 8 months	22.7	14.9	18.7 ± 6.1
doux, aged 5 months	53.0	9.3	14.9 ± 0.7
Hobelkäse from the Bernese Oberland	*224.1	95.4	2.6 ± 0.2
Parmino	2.0	0.8	28.6 ± 4.2
Sbrinz	28.0	9.4	16.4 ± 5.5
Semi-hard cheeses			
Appenzeller:			
aged 7–10 months (1/4 fat)	94.4	64.9	4.2 ± 1.6
extra, aged 6–7 months	29.3	14.5	16.8 ± 1.1
surchoix, aged 4 months	26.7	17.8	8.0 ± 1.0
aged 3 months (1/4 fat)	56.0	10.5	7.1 ± 1.9
classic, aged 3 months	22.0	8.5	17.6 ± 7.6
Edam	1.0	0.1	13.3 ± 0.4
Küsnachter	25.7	18.0	19.6 ± 2.4
Mountain cheese Graubünden:			
$\frac{1}{4}$ fat	32.0	22.7	4.8 ± 0.0
$\frac{1}{2}$ fat	10.4	7.1	8.9 ± 4.1
full fat	25.1	4.3	9.2 ± 1.4

Table 1. Cont.

Cheese	VPP	IPP	IC ₅₀
	(mg × kg ⁻¹)	(mg × kg ⁻¹)	(mg cheese × mL ⁻¹)
Raclette:			
from raw milk	12.6	2.6	8.8 ± 0.0
from pasteurized milk	1.0	0.1	9.0 ± 0.3
St. Paulin	5.2	1.0	23.5 ± 6.3
Tête de Moine	98.0	15.5	7.1 ± 1.9
Tilsit:			
from raw milk	120.2	30.0	4.4 ± 0.2
from pasteurized milk	1.2	0.1	18.0 ± 6.3
Vacherin fribourgeois	62.1	46.7	5.0 ± 0.3
Wangener Geissmutschli (goat cheese)	33.2	0.0	7.9 ± 0.5
Winzerkäse	97.7	27.1	9.9 ± 1.8
Soft cheeses			
Brie	0.4	0.3	25.9 ± 3.0
Camembert	0.2	0.2	Very weak
Mozarella:			
from buffalo milk	0.1	0.0	-
from cow milk	0.0	0.0	-
Tomme vaudoise	0.0	0.0	14.9 ± 3.7
Vacherin Mont d'Or	0.2	0.1	21.4 ± 9.6

***Bold** - the highest concentration of peptide in the analyzed category (hard, semi-hard, and soft cheese).

According to the scientific reports, sequential motif located between 60 and 70 residue of β -casein is considered as strategic zone due to its ACE-inhibiting, immunostimulating, and opioid potential [32]. The example of peptide derived from β -casein showing dual bioactivity is β -casomorphin-7 (YPFPGPI; fragment 60–66) acting as opioid and ACE inhibitory agent [26]. De Noni and Cattaneo [33] identified this peptide in different dairy products including commercial cheeses like e.g., Brie, Cheddar, Gouda, Fontina, and Gorgonzola (see Table 2).

Table 2. The Concentration of YPFPGPI in commercial cheeses before and after in vitro simulated gastro-intestinal digestion. Adapted with permission from [33], Copyright Elsevier, 2010.

Cheese	Concentration of YPFPGPI (mg × kg ⁻¹)	
	Before Simulated Digestion	After Simulated Digestion
Brie	0.15	2.07 ± 0.09
Caprino	0	1.51 ± 0.09
Cheddar	0.11	15.22 ± 0.13
Fontina	0.04	10.43 ± 0.12
Gorgonzola	0.01	5.41 ± 0.08
Gouda	0.10	21.77 ± 0.12
Grana Padano (aged 25 months)	0	11.06 ± 0.08
Grana Padano (aged 17 months)	0	12.55 ± 0.09
Grana Padano (aged 10 months)	0	8.79 ± 0.04
Taleggio	0	7.15 ± 0.07

Some ACE inhibitors which matched the sequences of caseins were identified in Spanish cheeses. Those peptides which sequences fulfilled the structural requirements for being a potent ACE inhibitors were synthesized [34]. Their structural characteristics included the presence amino acids like lysine, arginine or residues possessing hydrophobic side chains as well as C-terminal proline [35]. Finally, it was reported that eight peptides (out of 11) inhibited ACE. Among them DKIHHP peptide was found as the most potent ($IC_{50} = 113.1 \mu M$) but the addition C-terminal phenylalanine (DKIHHPF) caused the dramatic reduction of its ACE-inhibiting potential ($IC_{50} = 2419.4 \mu M$) [36]. The ACE-inhibiting activity of synthesized peptide DKIHHP (source Manchego cheese; β -casein) was also measured using different protecting groups, namely *tert*-butyloxycarbonyl (Boc) and fluorenyl-methyloxycarbonyl (Fmoc). The IC_{50} values for DKIHHP were 113.18 and 577.92 μM , respectively. It was concluded that the differences above were attributed to the presence of less active conformers in the structure of the peptide [37]. The other sequences of ACE inhibitors identified in some Spanish cheeses are given in Table 3.

Table 3. ACE inhibitors identified in Spanish cheeses. Adapted by permission from Springer, European Food Research and Technology [36], 2006.

Cheese	Peptide	IC_{50} (μM)	Precursor	Reference
Manchego, Roncal, Idiazábal, Cabrales, goat	DKIHHP	113.1	β -casein	[36]
	DKIHHPF	2419.4		
Goat	VRGP	120.9	various fragments	[36]
	PPF	144.4		
Manchego	FP	1215.7	α_{s1} -casein	[30]
	PP	2284.7		
	KKYNNVPQL	77.2		
	VRYL	24.1		
Manchego, Roncal, Idiazabal, Goat	QP	598.1	various fragments	[36]
Roncal	PKHP	709.1	α_{s1} -casein	

Sequences of caseins were also the sources of other ACE-inhibiting peptides that were identified in cheeses: RPKHPIKHQ (source: α_{s1} -casein; Cheddar and Gouda; $IC_{50} = n.d.$ and 13.4 μM , respectively), RPKHPIKHQGLPQ (source: α_{s1} -casein; Gouda; $IC_{50} = n.d.$), YPFPGPIP (source: β -casein; Gouda; $IC_{50} = 14.8 \mu M$), MPFPKYPVQPF (source: β -casein; Gouda; $IC_{50} = n.d.$), RPKHPIK, RPKHPI, FVAPFPEVFGK (source: α_{s1} -casein, Cheddar; $IC_{50} = n.d.$), YQEPVLGPVRGPFPIIV (source: β -casein; Cheddar; $IC_{50} = n.d.$), RPKHPIKHQGLPQEV, RPKHPIKHQGLPQEVLNEN, LLR, EVLNENLLRF (source: α_{s1} -casein, Fresco; $IC_{50} = n.d.$), FVAPFPEVFGK, YQEPVLGPVRGPF, YQEPVLGPVRGPFPI, YQEPVLGPVRGPFPIIV (source: β -casein; Fresco; $IC_{50} = n.d.$) [30]. Tonouchi et al. [38] isolated two peptides (LQP and MAP) from Danish skimmed milk cheese. LQP was originally known as ACE inhibitor identified in α -zein hydrolyzed with thermolysin. MAP sequence was identified in β -casein and exhibited ACE inhibition ($IC_{50} = 0.8 \mu M$) and antihypertensive effect in SHR. Significant hypotensive effect of MAP tripeptide was observed at 8 h since oral administration (-17.0 mm Hg ; dose $3 \text{ mg} \times \text{kg}^{-1}$ body weight) [38].

The potential of cheeses as diet components that may affect the reduction of blood pressure is also in the focus of interest of the scientists aiming at meta-analyses [39]. Nilsen et al. [39] carried out a cross-sectional study to analyze the impact of the consumption of Gamalost cheese (a traditional Norwegian cheese) on the reduction of the risk of hypertension development. Based on data obtained from the questionnaires of 168 participants, the average intake of Gamalost servings per week was 2 and the average value of systolic and diastolic blood pressures was 128 and 78 mmHg, respectively. The increase of Gamalost servings reduced the systolic blood pressure by 0.72 mmHg. Moreover, it

was concluded that blood pressure reduction related to Gamalost consumption was associated with the presence of ACE inhibitory peptides [39]. Crippa et al. [40] investigated the antihypertensive effect resulting from the consumption of Grana Padano cheese and observed that supplementation of Grana Padano cheese at a dose 30 g per day significantly lowered the systolic and diastolic blood pressure in mild-hypertensive subjects (−3.5 and −2.4 mm Hg, respectively) [40].

One of the meta-analyses concerned studies evaluating the association of CVD, coronary heart disease (CHD), and stroke with high vs. low cheese consumption. This analysis revealed that high cheese consumption lowered the relative risk for: total CVD (RR 0.90; 7; 8076), CHD (RR 0.86; 8; 7631), and stroke (RR 0.90; 7; 10,449). Respective numbers in the brackets represent: relative risk, number of studies, and number of documented events provided. Finally, the results indicated a nonlinear relationship between cheese consumption and decreasing risks of CVD, CHD, and stroke. Consumption of approximately 40 g of cheese per day ensured the best results in reducing the risks of dysfunctions related to hypertension [41].

To conclude, epidemiological studies suggested that the antihypertensive potential of cheeses can be linked to the presence of biopeptides. According to above-mentioned analyses, the optimal daily cheese dose to reduce the risk of hypertensive dysfunctions was 30–40 g. These results suggest that cheese-as part of a diet-can prevent from the hypertension-related diseases.

4. Antioxidative Peptides

Free radicals are involved in many signaling processes, i.e., as defending the body from infections. Thus, the accumulation of free radicals in the organism can lead to unwanted cell damage. Oxidized cells can then initiate several body dysfunctions like e.g., rapid ageing, atherosclerosis, arthritis, diabetes, and cancer (Figure 5). It is the so-called oxidative stress defined as the process of formation of highly reactive molecules (that is, reactive oxygen species-ROS). In order to act against the destructive activity of ROS, it is important to look for diet-derived compounds acting as antioxidants [42].

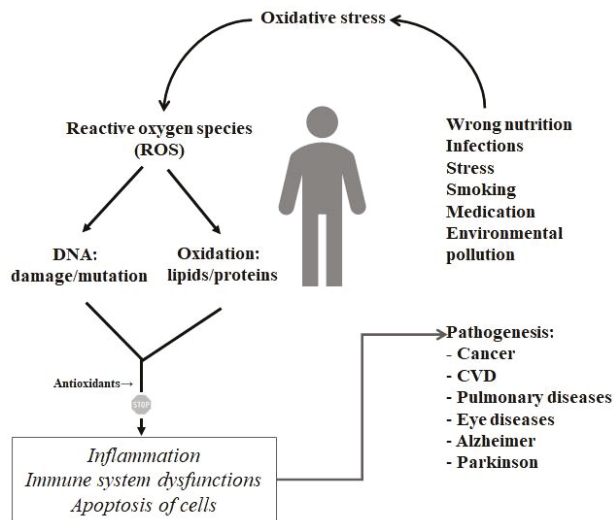


Figure 5. The preventive activity of antioxidants on the formation of diseases according to Sarmadi and Ismail [42].

Gupta et al. [43] produced Cheddar cheese using different *Lactobacillus casei* cultures and screened for antioxidant activity. Two antioxidative peptides matching the fragments of bovine β -casein (VKEAMAPK) and α_{S1} -casein (HIQKEDVPSEK) were identified in Cheddar. Both peptides exhibited

2,2-diphenyl-1-picryl-hydrazyl (DPPH) radical scavenging activity comparable to the commercial antioxidants such as butylated hydroxyanisole (BHA), *tert*-butyl hydroquinone (t-BHQ) or ferulic acid [44]. The results indicated that the antioxidant activity of the water-soluble cheese extracts (WSE) was dependent on the ripening period of cheese. The highest bioactivity was observed after 4 months of ripening. After that, the activity started to decrease, up until the 7th month of ripening and remained similar after 9 months [44]. Another research group evaluated the inhibition of DPPH radicals by the WSE of Australian Cheddar cheeses. They found a moderate antioxidant activity of the fractions containing peptides with a molecular weight > 10 kDa, although peptide identification was not carried out [45]. A study conducted to analyze the antioxidative potential of Mexican Cotija cheese revealed that the maximal antioxidant activity of this cheese was achieved after 24 weeks of ripening. Although no specific peptides were identified, it was concluded that the antioxidative potential of cheese was related to a significantly high content of bioactive sequences [46].

Timón et al. [47] produced hard cow cheese and analyzed the antioxidative potential of its WSE. After the fractionation of WSE, it was discovered that some of the extracts exhibited DPPH-radical scavenging and metal chelating bioactivity. Moreover, two peptides, namely EIVPN and DKIHPP which were known from their ACE-inhibiting function, were identified in WSE of the hard cheese. Another sequence i.e., VAPFPQ identified in cheese-derived extract was discovered as a new metal chelating peptide. To conclude, it was postulated that antioxidative potential of cheese water-soluble extracts may be the result of the presence of the above-mentioned peptides. However, the bioactivity of these sequences should be confirmed on synthetic peptides [47].

Some peptides with the antioxidative potential were identified in WSE of the Burgos-type cheese. It was shown that 22 fractions derived from Burgos-type cheese extracts exhibited radical scavenging activity (oxygen radical absorbance capacity with fluorescein (ORAC-FL) assay). Liquid chromatography and tandem mass spectrometry (LC-MS/MS) identification revealed the presence of the aromatic amino acids like tyrosine, phenylalanine or tryptophan in some fractions of cheeses extracts. These amino acids itself possess the antioxidative potential [48]. It was also reported that some of the Burgos-type cheese-originating peptide fractions contained the sequences, namely: SDIPNPIGSENSEKTTMPLW (source: α_{s1} -casein), YQQPVLGPVRGPFPIIV (source: β -casein), and LLYQQPVLGPVRGPFPIIV (source: β -casein) [49]. According to Timón et al. [49], peptides matching the sequences of β -casein have already been known as antioxidative agents. The sequence SDIPNPIGSENSEKTTMPLW is probably found as the new peptidic antioxidant, however further tests to measure this activity need to be performed [49].

5. Hypocholesterolemic Peptides

Plasma lipoproteins are composed of the following elements: cholesterol, triglycerides, phospholipids, and apoproteins. Their varying composition affects the density, size, and electrophoretic mobility of each lipoprotein particle which enables for the classification of lipoprotein disorders [50]. According to Cox et al. [50], cholesterol is an essential precursor of some substances as adrenal and gonadal steroid hormones and bile acids. Moreover, it is an element of the animal cell membranes. Triglycerides are the major component of dietary fat as well as animal fat depots. Abnormal concentrations of cholesterol and triglycerides in blood indicate some dysfunctions in synthesis, degradation, and transport of lipoproteins and their increase levels lead to the different variants of hypercholesterolemia and hypertriglyceridemia [50]. In turn, phospholipids are the constituents of the natural membranes. They are polar lipids which are e.g., the components of the milk fat globule membrane involved in the circulation of the lipid droplets secreted by the mammary gland cells [51].

It was reported that some peptides/protein-derived hydrolysates exhibited activity against metabolic lipids' dysfunctions and their effect was tested in cellular systems and animal models [52]. To the best of our knowledge, no peptides acting as hypolipidemic were identified in cheeses. When thinking about milk, most of the studies concerning their "anticholesterolemic effect" conducted so far, have concerned the whey proteins. The ingestion of whey protein was observed to be correlated with

a significant reduction in total cholesterol levels in rats fed cholesterol-free and cholesterol-enriched diets [53]. The cholesterol reducing activity of β -lactoglobulin was due to the presence of two major biopeptides, namely lactostatin (IIAEK) and β -lactotensin (HIRL) [54]. According to the literature, consumption of 300 mg IIAEK \times kg⁻¹ body weight per day reduced LDL level as well as increased HDL cholesterol level, and fecal steroid excretion. The lactostatin activity was linked to the degradation of cholesterol into bile acids in hepatic cells [55,56]. The HIRL sequence was shown to be involved in the reduction of total (22.7%), and LDL plus VLDL (32.0%) cholesterol levels in mice after 2 days of administration at the dose of 30 mg \times kg⁻¹ body weight [57]. The activity of both peptides was tested on mice fed a cholesterol-enriched diet. Despite the optimistic results, it should be noted that the exact mechanisms of the hypocholesterolemic activity of peptides are still unclear. It is speculated that it might be linked to the amino acid composition, but further research is needed in this respect [54].

6. Antiobesity and Anti-Inflammatory Peptides

The studies concerning the effectiveness of different types of diets and proportions of macronutrients on the weight loss is in the focus of the interest of the many scientists [58]. Some studies have shown that the high-protein content diet is the most effective when thinking about the reduction of body weight. It results from the fact that consumption of the protein contributes to the increased satiety and the reduction of the energy intake in addition to a greater dietary thermogenesis [59].

Although proteins accelerate caloric metabolism, some of them are more efficient on weight loss than others. It was observed that soybean-originating proteins more efficiently enhance weight loss than bovine milk proteins [60]. One of the explanations of this phenomenon results from the fact that peptides produced from proteins during gastrointestinal digestion initiate satiety signals from the gut and hence suppress food intake. Thus, scientists try to explain reliably the mechanisms of a protein-rich diet on the body's health [5]. Some of them include e.g., the impact of dietary protein on cholecystokinin (CKK) release, the activation of GLP-1 receptor to suppress appetite, and/or modulating the adipose genes affecting metabolic and vascular functions [60].

It was reported that opioid peptides may also contribute to the weight loss due to the reduction of food intake [61]. For example, casomorphins interact with gastric opioid receptors and slow down the motility of the gastrointestinal tract, which inhibits food intake [60]. The example of the opioid peptide identified both in bovine casein and several types of cheeses is β -casomorphin-7 (YPPFGPI) which was described above (see Section 2). It was indicated that dose of 179 mg \times kg⁻¹ body weight of modified β -casomorphins effectively impaired gastric emptying in pup rats. It was probably related to direct interaction of β -casomorphins with opioid receptors in the gut [62].

Some studies confirmed the causal direction of the relationship between adiposity and inflammation (the greater adiposity, the higher C-reactive protein level) [63]. Citing the words by Zielińska et al. [64], inflammation is defined as a “complex biological process, occurring through a variety of mechanisms and leading to changes in local blood flow and the release of several molecular mediators”. Uncontrolled inflammation may lead to chronic dysfunctions such as rheumatoid arthritis, atherosclerosis, and it is linked to cancer [65]. It was reported that VPP and IPP milk-derived ACE-inhibiting tripeptides exhibited anti-inflammatory activity. First reduced leukocyte-endothelial cell interaction *in vitro* and this effect was related to that of inhibition of MAPK (mitogen-activated protein kinase) signaling pathway. The anti-inflammatory effect of both peptides was also tested in a model of intestinal enterocolitis. It was found that VPP and IPP were protective against atherosclerosis in mice with defect of endogenous apoprotein E (ApoE). These peptides suppressed the mRNA for inflammatory cytokines, oxidized low density lipoprotein receptor, and transcription regulators [65]. These two peptides were also identified in the different types of cheeses (see Section 2).

To the best of our knowledge, there is no more specific anti-inflammatory peptides that could be identified in cheeses. However, it was found that water-soluble extracts of Cheddar cheese possessed such an activity which was determined based on nitric oxide (NO) production in lipopolysaccharide-stimulated macrophage (RAW-264.7) cells [66].

7. Multi-Activity of Peptides in MetS Prevention: A Screening Using BIOPEP-UWM Database

Loads of publication data concern the analysis of the proteins as the sources of biopeptides exhibiting only one biological effect while the information about dual or multifunctional properties of peptides is rather poor [5]. Such statement may also refer to the MetS-preventive peptides. To the best of our knowledge, there is no a “universal” peptide sequence that would show all bioactivities described in this paper. Thus, databases of biological information like BIOPEP-UWM, available at: <http://www.uwm.edu.pl/biochemia>, may be a suitable option to acquire the knowledge about peptides exhibiting more than one biological function [67]. BIOPEP-UWM is a curated database providing comprehensive information on 3899 bioactive peptide sequences (accessed: March 2020).

We applied BIOPEP-UWM database to retrieve the profiles of potential biological activities of the four major casein fractions (see Table A1). Profile of the potential biological activity of the protein is defined as the type and the location of bioactive fragment in a protein chain [67]. Briefly, such analysis enables to answer the question: what bioactive fragments match the protein sequence? Then, each peptide sequence was pasted again to BIOPEP-UWM database of bioactive peptide sequences using the search option “sequence” and ticking “exact” [67]. Such searching was helpful to show what additional activities are exhibited by this peptide (the pasted one). This approach led us find that 66 peptides had dual i.e., ACE and DPP4 inhibitory function, and 17 were acting as ACE inhibitory and antioxidant agents. Some peptides exerted a triple bioactivity, i.e., eight dipeptides inhibited ACE and DPP4 as well as exerted an antioxidant activity. The example of the sequence with triple inhibitory bioactivity is YP peptide present in α_{S1-7} , β -, and κ -casein sequence. It has proven ACE, α -glucosidase and DPP4 inhibitory function. The brief summary of peptides encrypted in the sequences of caseins and exerting e.g., more than one biological effect is shown in Table 4. For checking what particular sequences were found as dual or multiactive, see Table A1.

Table 4. The summary of casein-derived peptides showing more than one biological activity (based on BIOPEP-UWM database screening; <http://www.uwm.edu.pl/biochemia>; accessed on March 2020).

Dual and Triple Activity of Casein-Derived Peptides	Number of Peptides Encrypted in the All Casein Sequences
ACE and DPP4 inhibitor	66
ACE inhibitor and antioxidative	17
DPP4 and α -glucosidase inhibitor	1
DPP4 inhibitor and opioid	1
ACE inhibitor and opioid	5
DPP4 inhibitor and antioxidative	5
ACE, DPP4 inhibitor, and antioxidative	8
ACE, DPP4, and α -glucosidase inhibitor	1
Total	104
Peptides Showing one Bioactivity	
ACE inhibitor	171
α -glucosidase inhibitor	0
antioxidative	52
DPP4 inhibitor	127
opioid agonist	3
opioid antagonist	2
opioid	4
Total	359
Total Number of Bioactive Sequences	463

Although, our bioinformatic approach is useful for searching multifunctions of peptides, it has some limitations. The important one is based on the idea of the positive selection assuming that sequence of interest matches the peptide sequences present in databases. Thus, it may not include peptides that are “new” and they are, at the time of screening, not displayed in the database. Thus, some authors postulate for the regular update of the databases with newly-reported bioactive peptides [68]. Nevertheless, such databases, if curated and reliable, may contribute to acquiring of some information about the peptides which multi-activity can be described as “MetS-preventive”.

8. Conclusions

Some milk-derived peptides were identified in different types of cheeses. These biopeptides exhibited bioactivities playing an important role in the prevention from the dysfunctions related to metabolic syndrome. It needs to be noted that majority of studies concerned the identification of peptides in cheeses and did not included studies on animal and humans. Several epidemiological and cohort studies confirmed the positive effect of cheese consumption on the reduction of the risk of MetS diseases. A majority of studies concerning milk-derived peptides and their identification in cheeses focus on the determination of only one biological effect. Despite its limitations, bioinformatic-assisted approach can be helpful in the screening of multifunctional effect of peptides being the promising agents in the prevention of MetS.

Author Contributions: D.M. wrote Sections 3–7, and was involved in draft preparation and editing; A.I. was responsible for conceptualization, wrote Section 1, Section 2, Section 8, and reviewed the article. All authors have read and agreed to the published version of the manuscript.

Funding: Project financially supported by Minister of Science and Higher Education in the range of the program entitled “Regional Initiative of Excellence” for the years 2019–2022, Project No. 010/RID / 2018 / 19, amount of funding 12,000,000 PLN as well as the funds of the University of Warmia and Mazury in Olsztyn (Project No. 17.610.014-110).

Acknowledgments: The authors wish to thank Małgorzata Darewicz for her valuable scientific suggestions when preparing this manuscript.

Conflicts of Interest: The authors declare no conflict of interest.

Abbreviations

ACE	Angiotensin-converting enzyme (EC 3.4.15.1)
ApoE	ndogenous apoprotein E
BHA	butylated hydroxyanisole
BIOPEP-UWM	database of bioactive peptide sequences [68]
Boc	tert-butyloxycarbonyl
CHD	coronary heart disease
CVD	cardiovascular disease
DPP4	dipeptidyl peptidase IV (EC 3.4.14.5)
DPPH	2,2-diphenyl-1-picryl-hydrazyl)
Fmoc	fluorenylmethyloxycarbonyl
GIP	glucose-dependent insulintropic polypeptide
GLP-1	glucagon-like peptide 1
IP3	inositol 1,4,5-triphosphate
LC-MS/MS	Liquid Chromatography and Tandem Mass Spectrometry
LDL cholesterol	low density lipoprotein cholesterol
MAPK	mitogen-activated protein kinase
MetS	metabolic syndrome
NHANES	Health and Nutrition Examination Survey
NO	nitric oxide
NTR2	neurotensin receptor 2

ORAC-FL	Oxygen Radical Absorbance Capacity with Fluorescein
RAAS	renin-angiotensin-aldosterone system
RAS	renin-angiotensin system
ROS	reactive oxygen species
RR	relative risk
SBP	systolic blood pressure
SHR	spontaneously hypertensive rats
T2D	type 2 diabetes mellitus
t-BHQ	tert-butyl hydroquinone
VLDL cholesterol	very low density lipoprotein cholesterol
WSE	water-soluble cheese extracts

Appendix A

Table A1. Biopeptides (MetS-preventive sequences) Present in the Sequences of Bovine Caseins - Data Acquired from the BIOPEP-UWM Database (accessed on March 2020).

BIOPEP-UWM ID	Activity	Sequence	Protein	Location
7590/8637	1*	AA	κ -casein	(86–87)
8758	12	AE	α_{S1} -casein	(77–78), (131–132)
			α_{S2} -casein	(77–78)
7583/8759	1	AF	β -casein	(189–190)
8193	9	AI	α_{S2} -casein	(42–43)
			κ -casein	(128–129)
8559	12	AL	α_{S1} -casein	(13–14)
			α_{S2} -casein	(13–14), (96–97), (190–191)
			κ -casein	(13–14), (70–71)
3177/7584	1	AP	α_{S1} -casein	(41–42), (191–192)
			β -casein	(103–104)
7742	9	AR	α_{S1} -casein	(15–16)
			κ -casein	(117–118)
8762	12	AS	κ -casein	(147–148)
8763	12	AT	α_{S2} -casein	(80–81)
			κ -casein	(165–166)
			α_{S1} -casein	(11–12)
8764/8951	1	AV	α_{S2} -casein	(11–12), (131–132)
			β -casein	(177–178)
			κ -casein	(87–88), (159–160), (189–190)
			α_{S1} -casein	(178–179)
7543/8460/8695	7	AW	α_{S1} -casein	(178–179)
3563/7866/8765	7	AY	α_{S1} -casein	(158–159), (173–174)
7606	9	DA	α_{S1} -casein	(172–173), (190–191)
9075	9	DM	α_{S2} -casein	(155–156)
			β -casein	(184–185)
8768	12	DQ	α_{S1} -casein	(66–67)
			α_{S2} -casein	(125–126)

Table A1. Cont.

BIOPEP-UWM ID	Activity	Sequence	Protein	Location
7623	9	EA	α_{S1} -casein	(76-77)
			β -casein	(100-101)
			κ -casein	(158-159)
7622/8770	1	EG	α_{S1} -casein	(140-141)
8771	12	EH	α_{S2} -casein	(20-21)
			α_{S1} -casein	(85-86), (125-126)
			α_{S2} -casein	(99-100)
			β -casein	(11-12)
7826/8772	1	EI	κ -casein	(139-140), (179-180)
			α_{S1} -casein	(50-51), (207-208)
			α_{S2} -casein	(38-39), (172-173)
			β -casein	(31-32)
7840/8558	1	EK	κ -casein	(33-34)
			α_{S1} -casein	(54-55), (156-157), (163-164)
			β -casein	(2-3), (5-6), (44-45)
			α_{S1} -casein	(148-149)
8529	12	EP	β -casein	(117-118), (195-196)
			κ -casein	(150-151)
			α_{S1} -casein	(62-63), (78-79)
8773	12	ES	α_{S2} -casein	(27-28), (75-76), (157-158)
			β -casein	(14-15), (21-22)
			κ -casein	(161-162), (175-176)
			α_{S2} -casein	(33-34)
8774	12	ET	α_{S1} -casein	(29-30), (45-46)
			α_{S2} -casein	(57-58), (78-79), (83-84), (160-161)
7828/8775	1	EV	β -casein	(91-92)
			κ -casein	(172-173)
			α_{S2} -casein	(66-67)
7752/8777	1	EY	α_{S2} -casein	(189-190)
3176	12	FA	β -casein	(52-53)
			α_{S2} -casein	(54-55)
9342	11	FC	α_{S2} -casein	(54-55)
7605	9	FG	α_{S1} -casein	(47-48)
			α_{S2} -casein	(178-179)
			β -casein	(87-88), (190-191)
8555	12	FL	κ -casein	(6-7), (18-19), (76-77)
			α_{S1} -casein	(43-44)
			α_{S2} -casein	(107-108)
3502/8506	1	FP	β -casein	(62-63), (111-112), (157-158), (205-206)
			β -casein	(33-34)
8779/9076	1	FQ	β -casein	(33-34)
7592/8780	1	FR	α_{S1} -casein	(165-166)

Table A1. Cont.

BIOPEP-UWM ID	Activity	Sequence	Protein	Location
3556	9	FY	α_{S1} -casein	(160–161), (168–169)
			α_{S2} -casein	(103–104)
7598/8524	1	GA	α_{S1} -casein	(177–178)
			κ -casein	(20–21)
7615/8781	1	GE	β -casein	(10–11)
			κ -casein	(149–150)
7596/8785	1	GI	α_{S1} -casein	(141–142)
7611	9	GK	α_{S1} -casein	(48–49)
7599/8561	1	GL	α_{S1} -casein	(25–26)
			κ -casein	(60–61)
3169/7512	1	GP	α_{S2} -casein	(117–118)
			β -casein	(64–65), (199–200), (203–204)
7607	9	GS	α_{S1} -casein	(60–61), (202–203)
			α_{S2} -casein	(70–71)
7612	9	GT	α_{S1} -casein	(185–186)
7608/8786	1	GV	α_{S1} -casein	(152–153)
			β -casein	(94–95)
3532/8788	1	GY	α_{S1} -casein	(108–109)
3184	12	HA	α_{S1} -casein	(143–144)
8793	12	HI	α_{S1} -casein	(95–96)
7844	9	HK	β -casein	(106–107)
			β -casein	(134–135)
3317/7602/8557	7	HL	κ -casein	(123–124)
			α_{S1} -casein	(19–20)
7842/8520	1	HP	κ -casein	(119–120), (121–122)
			β -casein	(50–51)
8795	12	HS	α_{S1} -casein	(136–137)
8797	12	HV	α_{S2} -casein	(21–22)
3494/8799	1	HY	α_{S2} -casein	(92–93)
7562/8525	1	IA	κ -casein	(43–44), (146–147)
			β -casein	(30–31)
7827	9	IE	κ -casein	(174–175)
			α_{S2} -casein	(5–6)
7595	9	IG	α_{S1} -casein	(59–60), (151–152), (201–202)
			α_{S2} -casein	(69–70)
8800	12	IH	α_{S1} -casein	(142–143)
			β -casein	(49–50)
8801	12	II	α_{S2} -casein	(29–30)
			β -casein	(207–208)
8802/9079	1	IL	α_{S1} -casein	(5–6)
			κ -casein	(11–12), (94–95)

Table A1. Cont.

BIOPEP-UWM ID	Activity	Sequence	Protein	Location
8804	12	IN	α_{S2} -casein	(43–44), (100–101)
			β -casein	(26–27)
			κ -casein	(72–73), (143–144), (180–181)
7581/8501	1	IP	α_{S1} -casein	(197–198)
			α_{S2} -casein	(216–217)
			β -casein	(66–67), (74–75)
8805	12	IQ	κ -casein	(47–48), (129–130), (140–141)
			α_{S1} -casein	(96–97)
			α_{S2} -casein	(209–210)
3258/8215/8806	7	IR	β -casein	(187–188)
			κ -casein	(49–50)
			κ -casein	(30–31)
3174/7743	1	KA	α_{S2} -casein	(95–96), (203–204)
			β -casein	(176–177)
8134	11	KD	α_{S1} -casein	(57–58)
			κ -casein	(34–35)
7841/8808	1	KE	α_{S1} -casein	(49–50), (98–99), (139–140), (147–148)
			α_{S2} -casein	(47–48), (56–57)
			β -casein	(99–100), (107–108)
7692/8809	1	KF	α_{S2} -casein	(2–3), (106–107), (188–189)
			β -casein	(32–33)
8811	12	KH	α_{S1} -casein	(18–19), (22–23), (94–95)
			α_{S2} -casein	(91–92)
			β -casein	(105–106)
8812	12	KI	α_{S2} -casein	(85–86), (181–182)
			β -casein	(29–30), (48–49)
			κ -casein	(42–43)
8813	12	KK	α_{S1} -casein	(117–118)
			α_{S2} -casein	(151–152), (164–165), (180–81)
			β -casein	(28–29)
7693	9	KL	κ -casein	(132–133)
			α_{S1} -casein	(2–3)
			α_{S2} -casein	(167–168)
7810/8218/8519	7	KP	α_{S2} -casein	(206–207)
			κ -casein	(67–68), (84–85)
7586/8814	1	KR	α_{S2} -casein	(128–129)
8815	12	KS	κ -casein	(3–4), (107–108)
			α_{S1} -casein	(208–209)
8816	12	KT	α_{S2} -casein	(152–153), (165–166), (196–197), (212–213)
			κ -casein	(137–138)

Table A1. Cont.

BIOPEP-UWM ID	Activity	Sequence	Protein	Location
8817	12	KV	α_{S1} -casein	(51–52), (120–121)
			α_{S2} -casein	(214–215)
			β -casein	(97–98), (169–170)
7691/8819	1	KY	α_{S1} -casein	(118–119)
			β -casein	(113–114)
			κ -casein	(45–46)
3175/7585	1	LA	α_{S1} -casein	(14–15), (157–158)
			α_{S2} -casein	(10–11), (14–15)
			κ -casein	(12–13)
3551	9	LF	α_{S1} -casein	(164–165)
7619	9	LG	α_{S1} -casein	(107–108), (184–185)
			β -casein	(198–199)
			κ -casein	(19–20)
3305/8820	6	LH	α_{S1} -casein	(135–136)
			β -casein	(133–134)
8821	12	LI	α_{S1} -casein	(4–5)
			κ -casein	(71–72)
8217	11	LK	α_{S1} -casein	(116–117)
			α_{S2} -casein	(179–180), (195–196)
3182	12	LL	α_{S1} -casein	(3–4), (35–36), (113–114)
			α_{S2} -casein	(9–10)
			β -casein	(139–140), (191–192)
7832/8823	1	LN	α_{S1} -casein	(31–32)
			α_{S2} -casein	(97–98), (121–122), (138–139), (176–177)
			β -casein	(6–7)
			κ -casein	(61–62)
3180	12	LP	α_{S1} -casein	(26–27)
			α_{S2} -casein	(191–192)
			β -casein	(70–71), (135–136), (137–138), (151–152), (171–172)
7831	9	LQ	κ -casein	(16–17), (77–78)
			α_{S2} -casein	(111–112)
			β -casein	(45–46), (88–89), (140–141)
9213	9	LR	κ -casein	(95–96)
			α_{S1} -casein	(36–37), (114–115)
8824	12	LT	α_{S1} -casein	(6–7)
			α_{S2} -casein	(168–169)
			β -casein	(77–78), (125–126), (127–128)
			κ -casein	(14–15)

Table A1. Cont.

BIOPEP-UWM ID	Activity	Sequence	Protein	Location
8825	12	LV	α_{S1} -casein	(9–10)
			β -casein	(58–59)
			κ -casein	(7–8)
3389/8462/8688	7	LW	α_{S1} -casein	(213–214)
3381/7872	2	LY	α_{S2} -casein	(114–115)
			β -casein	(192–193)
3173	12	MA	α_{S2} -casein	(41–42)
			β -casein	(102–103)
			κ -casein	(116–117), (127–128)
7839/8826	1	ME	α_{S1} -casein	(69–70), (75–76)
			α_{S2} -casein	(19–20), (156–157)
3385/8827	1	MF	β -casein	(156–157)
7609/8828	1	MG	β -casein	(93–94)
8829	12	MH	β -casein	(144–145)
8830	12	MI	α_{S1} -casein	(150–151)
			α_{S1} -casein	(1–2), (138–139)
			α_{S2} -casein	(1–2), (205–206)
8831	12	MK	κ -casein	(2–3)
			α_{S1} -casein	(1–2)
			α_{S2} -casein	(1–2)
8833/9085/9086	7	MM	κ -casein	(1–2)
3171	12	MP	α_{S1} -casein	(211–212)
			β -casein	(109–110), (185–186)
8839	12	NA	α_{S2} -casein	(61–62), (130–131)
8841	12	NE	α_{S1} -casein	(32–33), (53–54)
			α_{S2} -casein	(63–64), (98–99)
7683/8842	1	NF	α_{S2} -casein	(177–178)
7698	9	NK	β -casein	(27–28)
			α_{S1} -casein	(34–35)
			α_{S2} -casein	(49–50)
8845	12	NL	β -casein	(132–133)
			α_{S2} -casein	(40–41)
8846	12	NM	α_{S2} -casein	(40–41)
8847	12	NN	κ -casein	(73–74)
8530	12	NP	α_{S1} -casein	(199–200)
			α_{S2} -casein	(44–45), (122–123)
8848	12	NQ	α_{S1} -casein	(154–155)
			α_{S2} -casein	(101–102)
			κ -casein	(25–26), (74–75), (134–135)
8849	12	NR	α_{S2} -casein	(139–140), (174–175)
8850	12	NT	α_{S2} -casein	(17–18)
			κ -casein	(102–103), (144–145), (181–182)

Table A1. Cont.

BIOPEP-UWM ID	Activity	Sequence	Protein	Location
8851	12	NV	β -casein	(7–8)
7682/8853	1	NY	κ -casein	(62–63)
3179	12	PA	κ -casein	(85–86), (91–92), (105–106)
			α_{S1} -casein	(42–43)
8854	12	PF	β -casein	(51–52), (61–62), (86–87), (110–111), (118–119), (204–205)
			κ -casein	(17–18)
7625/8855	1	PG	β -casein	(9–10), (63–64)
7843/8856	1	PH	β -casein	(147–148)
			κ -casein	(120–121), (122–123)
			α_{S1} -casein	(20–21), (200–201)
8857	12	PI	α_{S2} -casein	(118–119), (133–134)
			β -casein	(65–66), (186–187), (206–207)
			κ -casein	(29–30), (48–49)
			α_{S1} -casein	(17–18)
8858	12	PK	α_{S2} -casein	(211–212)
			β -casein	(104–105), (112–113)
			κ -casein	(131–132)
7513/8638	1	PL	α_{S1} -casein	(183–184), (212–213)
			β -casein	(76–77), (136–137), (138–139), (150–151)
8859	12	PM	α_{S1} -casein	(149–150)
8860	12	PN	α_{S1} -casein	(88–89), (128–129), (198–199)
			β -casein	(67–68)
3170/7836	1	PP	β -casein	(75–76), (85–86), (152–153), (158–159)
			κ -casein	(130–131), (177–178)
			α_{S1} -casein	(27–28), (122–123)
7837/8861	1	PQ	α_{S2} -casein	(108–109), (192–193)
			β -casein	(71–72), (159–160), (174–175), (181–182)
8862	12	PS	α_{S1} -casein	(102–103), (175–176), (192–193)
			α_{S2} -casein	(45–46)
			κ -casein	(57–58)
			α_{S2} -casein	(136–137)
7833/8863	1	PT	β -casein	(153–154)
			κ -casein	(113–114), (141–142), (151–152), (155–156)
8864	12	PV	β -casein	(81–82), (115–116), (172–173), (196–197), (200–201)
			κ -casein	(68–69)

Table A1. Cont.

BIOPEP-UWM ID	Activity	Sequence	Protein	Location
8190/8865	6	PW	α_{S2} -casein	(123–124), (207–208)
8866	12	PY	α_{S2} -casein	(217–218)
			β -casein	(179–180)
			κ -casein	(78–79), (80–81)
8867	12	QA	α_{S1} -casein	(67–68)
			β -casein	(188–189)
			κ -casein	(110–111)
8868	12	QD	β -casein	(46–47)
			κ -casein	(135–136)
			α_{S1} -casein	(28–29), (155–156)
8869	12	QE	α_{S2} -casein	(32–33), (37–38)
			β -casein	(194–195)
			κ -casein	(22–23), (26–27)
			α_{S1} -casein	(167–168)
8870	12	QF	α_{S2} -casein	(102–103)
			κ -casein	(75–76)
			α_{S1} -casein	(24–25)
7617/8871	1	QG	α_{S2} -casein	(116–117)
8872	12	QH	α_{S2} -casein	(200–201)
8873	12	QI	κ -casein	(93–94)
			α_{S1} -casein	(93–94), (97–98), (146–147)
			α_{S2} -casein	(94–95), (105–106), (187–188), (202–203)
7680	9	QK	β -casein	(175–176)
			κ -casein	(66–67)
			α_{S1} -casein	(112–113), (123–124), (170–171)
8874	12	QL	α_{S2} -casein	(142–143)
			β -casein	(72–73)
8875	12	QN	κ -casein	(24–25)
			α_{S2} -casein	(210–211)
			β -casein	(89–90), (146–147), (149–150)
8532	12	QP	κ -casein	(28–29), (112–113)
			α_{S1} -casein	(145–146)
			β -casein	(38–39), (39–40)
8876	12	QQ	κ -casein	(65–66)
			β -casein	(34–35), (56–57), (123–124), (141–142), (160–161), (167–168)
			α_{S2} -casein	(126–127)
8877	12	QS	β -casein	(34–35), (56–57), (123–124), (141–142), (160–161), (167–168)
8878	12	QT	β -casein	(40–41), (54–55), (79–80)
8879	12	QV	α_{S2} -casein	(126–127)
			κ -casein	(98–99), (184–185)

Table A1. Cont.

BIOPEP-UWM ID	Activity	Sequence	Protein	Location
8880	12	QW	κ -casein	(96–97)
8881	12	QY	α_{S1} -casein	(187–188)
			α_{S2} -casein	(109–110), (112–113), (193–194)
			κ -casein	(50–51)
3489	9	RF	α_{S1} -casein	(37–38)
			κ -casein	(37–38)
8882/9173	1	RG	β -casein	(202–203)
8883	12	RH	κ -casein	(118–119)
8884	12	RI	β -casein	(25–26)
3257/8886	1	RL	α_{S1} -casein	(115–116), (134–135)
			α_{S2} -casein	(175–176)
8888	12	RN	α_{S2} -casein	(60–61), (129–130)
7582/8518	1	RP	α_{S1} -casein	(16–17)
			α_{S1} -casein	(105–106)
3380	9	RY	α_{S2} -casein	(185–186), (220–221)
			κ -casein	(55–56)
			α_{S1} -casein	(193–194)
7685/8891	1	SF	κ -casein	(4–5), (125–126)
			α_{S1} -casein	(176–177)
7618	9	SG	κ -casein	(148–149)
			α_{S1} -casein	(79–80)
8893	12	SI	α_{S2} -casein	(28–29), (68–69)
			β -casein	(22–23)
			α_{S1} -casein	(56–57)
8894	12	SK	α_{S2} -casein	(46–47), (150–151)
			β -casein	(96–97), (168–169)
			β -casein	(15–16), (57–58), (69–70), (124–125), (164–165)
8560	12	SL	β -casein	(15–16), (57–58), (69–70), (124–125), (164–165)
8505	12	SP	κ -casein	(90–91), (170–171), (176–177)
			α_{S1} -casein	(63–64)
9184	9	ST	α_{S2} -casein	(52–53), (144–145), (158–159)
			κ -casein	(153–154), (162–163), (187–188)
			α_{S1} -casein	(90–91)
8895	12	SV	β -casein	(161–162)
			β -casein	(142–143)
8896	12	SW	β -casein	(142–143)
7684/8897	1	SY	κ -casein	(58–59)
8531	12	TA	κ -casein	(188–189)
8898	12	TD	α_{S1} -casein	(189–190)
			β -casein	(128–129)

Table A1. Cont.

BIOPEP-UWM ID	Activity	Sequence	Protein	Location
7830/8899	1	TE	α_{S1} -casein	(64–65)
			α_{S2} -casein	(81–82), (159–160), (169–170)
			β -casein	(41–42), (120–121)
			κ -casein	(138–139), (157–158)
8185/8900	1	TF	α_{S2} -casein	(53–54)
8903	12	TI	κ -casein	(10–11), (142–143), (145–146)
8904	12	TK	α_{S2} -casein	(163–164), (166–167), (213–214)
8905	12	TL	α_{S2} -casein	(137–138)
			β -casein	(126–127)
			κ -casein	(15–16), (166–167)
8906	12	TM	α_{S1} -casein	(210–211)
			α_{S2} -casein	(18–19)
			κ -casein	(115–116)
8503/9073	1	TP	α_{S2} -casein	(135–136)
			β -casein	(80–81)
			κ -casein	(154–155)
7834/8908	1	TQ	α_{S1} -casein	(186–187)
			β -casein	(55–56), (78–79)
8909	12	TR	β -casein	(24–25)
8910	12	TS	α_{S2} -casein	(145–146)
			κ -casein	(152–153), (186–187)
8911	12	TT	α_{S1} -casein	(209–210)
			κ -casein	(114–115), (156–157)
8912	12	TV	α_{S2} -casein	(87–88), (153–154), (197–198)
			β -casein	(154–155)
			κ -casein	(103–104), (163–164), (182–183)
8219/8914	6	TY	α_{S2} -casein	(34–35)
3172	12	VA	α_{S1} -casein	(10–11), (12–13), (40–41)
			α_{S2} -casein	(12–13), (79–80)
			κ -casein	(69–70), (164–165)
8915	12	VD	α_{S2} -casein	(88–89), (154–155)
7829/8916	1	VE	α_{S1} -casein	(91–92)
			β -casein	(13–14), (116–117), (130–131)
			κ -casein	(160–161)
3384/8917	1	VF	α_{S1} -casein	(46–47)
			α_{S2} -casein	(161–162)
8920	12	VI	α_{S2} -casein	(215–216)
			κ -casein	(173–174)
7558/8921	1	VK	α_{S2} -casein	(84–85), (127–128)
			β -casein	(98–99)

Table A1. Cont.

BIOPEP-UWM ID	Activity	Sequence	Protein	Location
8922	12	VL	α_{S1} -casein	(30–31)
			α_{S2} -casein	(120–121)
			β -casein	(162–163), (170–171), (197–198)
			κ -casein	(52–53), (99–100)
8923	12	VM	β -casein	(92–93), (155–156)
8924	12	VN	α_{S1} -casein	(52–53), (153–154)
3181/7587	1	VP	α_{S1} -casein	(87–88), (101–102), (121–122), (127–128), (182–183)
			α_{S2} -casein	(132–133)
			β -casein	(8–9), (84–85), (173–174), (178–179)
			κ -casein	(104–105)
8925	12	VQ	κ -casein	(183–184)
7628/8594	1	VR	α_{S2} -casein	(59–60), (219–220)
			β -casein	(201–202)
			κ -casein	(88–89)
8926	12	VS	α_{S2} -casein	(22–23)
			β -casein	(95–96)
8927	12	VT	κ -casein	(9–10), (185–186)
3183	12	VV	α_{S2} -casein	(58–59)
			β -casein	(82–83), (83–84)
			κ -casein	(8–9)
3492/8224/8929	7	VY	α_{S2} -casein	(198–199)
			β -casein	(59–60)
8930	12	WD	α_{S2} -casein	(124–125)
8679	12	WI	α_{S2} -casein	(208–209)
8682/9090	1	WM	β -casein	(143–144)
8678	12	WQ	κ -casein	(97–98)
7898/8683	6	WY	α_{S1} -casein	(179–180)
7589/8932	1	YA	κ -casein	(82–83)
8935	12	YF	α_{S1} -casein	(159–160)
3553/8936	1	YG	κ -casein	(59–60)
8938	12	YI	κ -casein	(46–47)
7697/8939	1	YK	α_{S1} -casein	(119–120)
			α_{S2} -casein	(35–36)
			α_{S1} -casein	(106–107), (109–110)
8940	12	YL	α_{S2} -casein	(110–111), (113–114), (194–195), (221–222)
			α_{S1} -casein	(161–162), (174–175)
3666/8521/9548	8	YP	β -casein	(60–61), (114–115), (180–181)
			κ -casein	(56–57), (79–80)

Table A1. Cont.

BIOPEP-UWM ID	Activity	Sequence	Protein	Location
8943	12	YQ	α_{S1} -casein	(169–170)
			α_{S2} -casein	(93–94), (104–105), (115–116), (186–187), (199–200)
			β -casein	(193–194)
			κ -casein	(64–65)
8945	12	YS	α_{S2} -casein	(67–68)
8696	12	YT	α_{S1} -casein	(188–189)
8946/9077	1	YV	α_{S1} -casein	(181–182)
			α_{S2} -casein	(218–219)
			κ -casein	(51–52)
8948	12	YY	α_{S1} -casein	(180–181)
			κ -casein	(63–64), (81–82)
9042	9	AFL	β -casein	(189–191)
3597	9	AIP	κ -casein	(128–130)
9029	9	ALP	α_{S2} -casein	(190–192)
3370	9	AVP	α_{S2} -casein	(131–133)
			β -casein	(177–179)
9359	11	CLV	α_{S1} -casein	(8–10)
7823	9	FAL	α_{S2} -casein	(189–191)
7560	9	FFL	κ -casein	(5–7)
3377	9	FGK	α_{S1} -casein	(47–49)
7554	9	GEP	κ -casein	(149–151)
7509	9	GLP	α_{S1} -casein	(25–27)
7545/9116	1	GPV	β -casein	(199–201)
3311	11	HPH	κ -casein	(119–121), (121–123)
9027	9	HQG	α_{S1} -casein	(23–25)
7626	9	IAK	κ -casein	(43–45)
3167	12	IPI	κ -casein	(47–49)
3522	9	IPP	β -casein	(74–76)
			κ -casein	(129–131)
7803	9	IPY	α_{S2} -casein	(216–218)
8184/8693	1	IQP	α_{S2} -casein	(209–211)
8149/8180	2	IQY	κ -casein	(49–51)
9365	11	KKY	α_{S1} -casein	(117–119)
8133	11	KVI	α_{S2} -casein	(214–216)
3558	9	LAY	α_{S1} -casein	(157–159)
9031	9	LEE	β -casein	(3–5)
9206	9	LFR	α_{S1} -casein	(164–166)
7508	9	LGP	β -casein	(198–200)
7995	11	LHL	β -casein	(133–135)

Table A1. Cont.

BIOPEP-UWM ID	Activity	Sequence	Protein	Location
8000	11	LHS	α_{S1} -casein	(135–137)
8484	11	LLR	α_{S1} -casein	(35–37), (113–115)
8509	9	LNF	α_{S2} -casein	(176–178)
3544	9	LNP	α_{S2} -casein	(121–123)
9026	9	LNY	κ -casein	(61–63)
9040	9	LPF	κ -casein	(16–18)
8616	12	LPL	β -casein	(135–137), (137–139)
3391	9	LPP	β -casein	(151–153)
9339	12	LPQ	α_{S1} -casein	(26–28)
			α_{S2} -casein	(191–193)
			β -casein	(70–72)
3542/8689	1	LQP	β -casein	(88–90)
9163	11	LTC	α_{S1} -casein	(6–8)
8402	9	LVY	β -casein	(58–60)
9241	9	MAP	β -casein	(102–104)
8958	9	MKP	α_{S2} -casein	(205–207)
9363	11	NEN	α_{S1} -casein	(32–34)
7965	11	NYV	κ -casein	(62–64)
8139	11	PEL	α_{S1} -casein	(162–164)
8029	11	PHL	κ -casein	(122–124)
8032	11	PHQ	β -casein	(147–149)
3094/7510	5	PLG	α_{S1} -casein	(183–185)
2664	9	PLP	β -casein	(136–138), (150–152)
3531	9	PLW	α_{S1} -casein	(212–214)
7645	9	PPK	κ -casein	(130–132)
8652	12	PPL	β -casein	(75–77)
3373	9	PQR	β -casein	(181–183)
7559	9	PSY	κ -casein	(57–59)
8040	11	PWD	α_{S2} -casein	(123–125)
8044	11	PWI	α_{S2} -casein	(207–209)
3372	9	PYP	β -casein	(179–181)
			κ -casein	(78–80)
3307	11	PYY	κ -casein	(80–82)
9146	9	QGP	α_{S2} -casein	(116–118)
9543	9	RYL	α_{S1} -casein	(105–107)
			α_{S2} -casein	(220–222)
8382/8474	2	RYQ	α_{S2} -casein	(185–187)
7498	9	TVV	α_{S2} -casein	(197–199)
3521	9	VAP	α_{S1} -casein	(40–42)
7635	9	VAV	α_{S1} -casein	(10–12)

Table A1. Cont.

BIOPEP-UWM ID	Activity	Sequence	Protein	Location
2653	9	VLP	β -casein	(170–172)
8347	12	VPL	α_{S1} -casein	(182–184)
3524	9	VPP	β -casein	(84–86)
9046	9	VQV	κ -casein	(183–185)
8384	9	VRV	α_{S2} -casein	(219–221)
3505	9	VYP	β -casein	(59–61)
7962	11	WYY	α_{S1} -casein	(179–181)
7963	11	YFY	α_{S1} -casein	(159–161)
3973	9	YGL	κ -casein	(59–61)
7959	11	YLY	α_{S2} -casein	(113–115)
2870	15	YPF	β -casein	(60–62)
8617/9550	3	YPY	κ -casein	(79–81)
8487	11	YQL	α_{S1} -casein	(169–171)
8150	11	YVL	κ -casein	(51–53)
7634	9	YVP	α_{S1} -casein	(181–183)
7939	11	YYA	κ -casein	(81–83)
7948	11	YYQ	κ -casein	(63–65)
7942	11	YYV	α_{S1} -casein	(180–182)
8369	9	AFLI	β -casein	(189–192)
7668	9	AIPP	κ -casein	(128–131)
8380/8472	2	AYPS	α_{S1} -casein	(173–176)
8591	12	FLQP	β -casein	(87–90)
7499	9	FVAP	α_{S1} -casein	(39–42)
8489	11	FYQL	α_{S1} -casein	(168–171)
8371/8467	2	GTQY	α_{S1} -casein	(185–188)
3306	11	HPHL	κ -casein	(121–124)
7661	9	LFRQ	α_{S1} -casein	(164–167)
2668	9	LHLP	β -casein	(133–136)
2665	9	LPLP	β -casein	(135–138)
3397	9	LQSW	β -casein	(140–143)
9236	9	LRFF	α_{S1} -casein	(36–39)
3331	9	LVYP	β -casein	(58–61)
3374	9	PFPE	α_{S1} -casein	(42–45)
7896	11	PYPQ	β -casein	(179–182)
8357	9	RYLG	α_{S1} -casein	(105–108)
8378/8470	2	RYPV	κ -casein	(55–58)
8221	11	TSTA	κ -casein	(186–189)
8483	11	TVYQ	α_{S2} -casein	(197–200)
8593	12	VLGP	β -casein	(197–200)
8309	9	VRSP	κ -casein	(88–91)

Table A1. Cont.

BIOPEP-UWM ID	Activity	Sequence	Protein	Location
7801	9	VRYL	α_{S2} -casein	(219–222)
8308	9	VVPP	β -casein	(83–86)
8592	12	WIQP	α_{S2} -casein	(208–211)
8381/8473	2	YAKP	κ -casein	(82–85)
8485	11	YGLN	κ -casein	(59–62)
9420/9421	2	YLGY	α_{S1} -casein	(106–109)
8482	11	YLKT	α_{S2} -casein	(194–197)
8140	11	YPEL	α_{S1} -casein	(161–164)
2868	15	YFPF	β -casein	(60–63)
3218/8615	4	YPYY	κ -casein	(79–82)
7878	11	YQEP	β -casein	(193–196)
8477	11	YQLD	α_{S1} -casein	(169–172)
3399/7660	9	AMKPW	α_{S2} -casein	(204–208)
9229	9	ARHPH	κ -casein	(117–121)
3371	9	AVPYP	β -casein	(177–181)
3519	9	AYFYP	α_{S1} -casein	(158–162)
3497	9	FFVAP	α_{S1} -casein	(38–42)
8368	9	FPIIV	β -casein	(205–209)
9378	9	FPPQS	β -casein	(157–161)
8141	11	FYPEL	α_{S1} -casein	(160–164)
9375	9	GLPQE	α_{S1} -casein	(25–29)
8478	11	GYLEQ	α_{S1} -casein	(108–112)
2666	9	HLPLP	β -casein	(134–138)
8613	12	IPIQY	κ -casein	(47–51)
7627	9	KDERF	κ -casein	(34–38)
9552	9	KFPQY	α_{S2} -casein	(106–110)
8618	12	LPLPL	β -casein	(135–139)
7631/8614	1	LPYPY	κ -casein	(77–81)
2671	9	NLHLP	β -casein	(132–136)
8157	9	PGPIP	β -casein	(63–67)
9242	9	PLPLL	β -casein	(136–140)
9243	9	PPEIN	κ -casein	(177–181)
8373/8469	2	RHPHP	κ -casein	(118–122)
9244	9	RINKK	β -casein	(25–29)
8481	11	RLKKY	α_{S1} -casein	(115–119)
8358	9	RYLGY	α_{S1} -casein	(105–109)
8375	9	RYQKF	α_{S2} -casein	(185–189)
9246	9	SLPQN	β -casein	(69–73)

Table A1. Cont.

BIOPEP-UWM ID	Activity	Sequence	Protein	Location
3332	9	SLVYP	β -casein	(57–61)
8379/8471	2	SRYPS	κ -casein	(54–58)
7485	9	TKVIP	α_{S2} -casein	(213–217)
8278/9556	6	VPYPQ	β -casein	(178–182)
8370/8466	2	YAKPA	κ -casein	(82–86)
8480	11	YPELF	α_{S1} -casein	(161–165)
3263	13	YPFPG	β -casein	(60–64)
8486	11	YQKFP	α_{S2} -casein	(104–108)
8372/8468	2	ARHPHP	κ -casein	(117–122)
3501	9	AYFYPE	α_{S1} -casein	(158–163)
7493	9	DKIHPP	β -casein	(47–52)
7629	9	EKDERF	κ -casein	(33–38)
3511	9	EMPPFK	β -casein	(108–113)
7480	9	FALPQY	α_{S2} -casein	(189–194)
7487	9	KVLPVP	β -casein	(169–174)
3513	9	LAYFYP	α_{S1} -casein	(157–162)
2667	9	LHLPLP	β -casein	(133–138)
8179	9	LKKISQ	α_{S2} -casein	(179–184)
9238	9	LVYPPF	β -casein	(58–63)
8152/8178	2	PYVRYL	α_{S2} -casein	(217–222)
3426	9	QSLVYP	β -casein	(56–61)
8479	11	RDMPIQ	β -casein	(183–188)
3128	14	RYLGYL	α_{S1} -casein	(105–110)
3217	14	SRYPSY	κ -casein	(54–59)
3127/3530	5	TTMPLW	α_{S1} -casein	(209–214)
9248	9	VLSRYP	κ -casein	(52–57)
8658	12	VPITPT	α_{S2} -casein	(132–137)
7481	9	VTSTAV	κ -casein	(185–190)
9251	9	VVVPPF	β -casein	(82–87)
3504	9	VYPPFG	β -casein	(59–64)
7887/8376	2	YFYPEL	α_{S1} -casein	(159–164)
7630	9	YPIQY	κ -casein	(46–51)
3500	9	YKVPQL	α_{S1} -casein	(119–124)
3265	15	YLGYLE	α_{S1} -casein	(106–111)
9252	12	YPVEPF	β -casein	(114–119)
7662/9253	9	YQEPVL	β -casein	(193–198)
8383	9	YYQQKP	κ -casein	(63–68)
3480/7875	2	AVPYPQR	β -casein	(177–183)
8359	9	AYFYPEL	α_{S1} -casein	(158–164)
7496	9	FPEVFGK	α_{S1} -casein	(43–49)

Table A1. Cont.

BIOPEP-UWM ID	Activity	Sequence	Protein	Location
8659	12	FPGPIP	β -casein	(62–68)
7659	9	FPQYLQY	α_{S2} -casein	(107–113)
8181	9	FSDKIAK	κ -casein	(39–45)
8159	9	GPFPIIV	β -casein	(203–209)
8285	11	IPIQYVL	κ -casein	(47–53)
9373	9	KEDVPSE	α_{S1} -casein	(98–104)
9234	9	KKYKVPQ	α_{S1} -casein	(117–123)
3498	9	KVLPVPQ	β -casein	(169–175)
7565	9	LHLPLPL	β -casein	(133–139)
8657	12	LPQNIPP	β -casein	(70–76)
8155	9	LTLTDVE	β -casein	(125–131)
2669	9	NLHLPLP	β -casein	(132–138)
9058	12	PQNIPPL	β -casein	(71–77)
3473	13	RYLGYLE	α_{S1} -casein	(105–111)
8476	11	TIASGEP	κ -casein	(145–151)
3333	9	TQSLVYP	β -casein	(55–61)
7877	11	VLPVPQK	β -casein	(170–176)
8475	11	VLSRYPS	κ -casein	(52–58)
9249	12	VPITPTL	α_{S2} -casein	(132–138)
9250	9	VPSERYL	α_{S1} -casein	(101–107)
3262/7665	5	YPPFGPI	β -casein	(60–66)
3214	15	YPSYGLN	κ -casein	(56–62)
9254	9	YQKFPQY	α_{S2} -casein	(104–110)
8377	9	AYFYPELF	α_{S1} -casein	(158–165)
3512	9	DAYPSGAW	α_{S1} -casein	(172–179)
9539	9	EKVNELSK	α_{S1} -casein	(50–57)
2672	9	ENLHLPLP	β -casein	(131–138)
7658/8151	2	FALPQYLK	α_{S2} -casein	(189–196)
7876	11	KVLPVPQK	β -casein	(169–176)
9235	12	LPQNIPPL	β -casein	(70–77)
3398	9	MKPWIQPK	α_{S2} -casein	(205–212)
7802	9	NMAINPSK	α_{S2} -casein	(40–47)
9168/9273	9	PFPEVFGK	α_{S1} -casein	(42–49)
3334	9	QTQSLVYP	β -casein	(54–61)
8160	9	RGPFPIIV	β -casein	(202–209)
7796	11	VKEAMAPK	β -casein	(98–105)
7492	9	VYPPFGPI	β -casein	(59–66)
2869/7501	5	YPPFGPIP	β -casein	(60–67)
7879	11	YQEPVLGP	β -casein	(193–200)
7804	9	ALNEINQFY	α_{S2} -casein	(96–104)

Table A1. Cont.

BIOPEP-UWM ID	Activity	Sequence	Protein	Location
3395/7497	9	AMKPWIQPK	α_{S2} -casein	(204–212)
3335	9	AQTQSLVYP	β -casein	(53–61)
8660	12	IPPLTQTPV	β -casein	(74–82)
9380	9	LGPVVRGPF	β -casein	(198–206)
7494	9	LNVPGEIVE	β -casein	(6–14)
8396	9	QSWMHQPHQ	β -casein	(141–149)
7483	9	RPKHPIKHQ	α_{S1} -casein	(16–24)
9376	9	VEQKHIQKE	α_{S1} -casein	(91–99)
7566	9	VRGPFPIIV	β -casein	(201–209)
7486	9	YFPFGPIPN	β -casein	(60–68)
8156	9	YQQRDMPIQ	β -casein	(180–188)
8397	9	YYAKPAAVR	κ -casein	(81–89)
3336	9	FAQTQSLVYP	β -casein	(52–61)
8169/8286	2	GPVVRGPFPII	β -casein	(199–208)
9231	12	INNQLFPYPY	κ -casein	(72–81)
7495	9	NIPPLTQTPV	β -casein	(73–82)
3216/3495	5	YIPIQYVLSR	κ -casein	(46–55)
7805	9	ALNEINQFYQK	α_{S2} -casein	(96–106)
7797	11	ARHPPHLSFM	κ -casein	(117–127)
9237	9	LTQTPVVVPPF	β -casein	(77–87)
3503	9	TPVVVPPFLQP	β -casein	(80–90)
3251	13	YFPFGPIPNSL	β -casein	(60–70)
9377	9	EIVPNSAEERLH	α_{S1} -casein	(125–136)
7800	9	FFVAPFPEVFGK	α_{S1} -casein	(38–49)
3337	9	HPFAQTQSLVYP	β -casein	(50–61)
3338	9	IHPFAQTQSLVYP	β -casein	(49–61)
9379	9	QEPVLRGVRGPF	β -casein	(194–206)
3339	9	KIHPFAQTQSLVYP	β -casein	(48–61)
9240	9	LVYFPFGPIPNSLPQN	β -casein	(58–73)
7564	9	LVYFPFGPIPNSLPQNIPP	β -casein	(58–76)

*1-ACE and DPP4 inhibitor; 2-ACE inhibitory and antioxidative activity; 3-DPP4 and α -glucosidase inhibitor; 4-DPP4 inhibitory and opioid activity; 5- ACE inhibitory and opioid activity; 6- DPP4 inhibitory and antioxidative activity; 7- ACE, DPP4 inhibitory, and antioxidative activity; 8- ACE, DPP4, and α -glucosidase inhibitor; 9-ACE inhibitor; 10- α -glucosidase inhibitor; 11- antioxidative activity; 12- DPP4 inhibitor; 13-opioid agonist activity; 14 -opioid antagonist activity; 15-opioid activity.

References

1. Karadag, A.S.; Ozlu, E.; Lavery, M.J. Cutaneous manifestations of diabetes mellitus and the metabolic syndrome. *Clin. Dermatol.* **2018**, *36*, 89–93. [[CrossRef](#)]
2. Rochlani, Y.; Pothineni, N.V.; Kovelamudi, S.; Mehta, J.L. Metabolic syndrome: Pathophysiology, management, and modulation by natural compounds. *Ther. Adv. Cardiovasc. Dis.* **2017**, *11*, 215–225. [[CrossRef](#)] [[PubMed](#)]
3. Moore, J.X.; Chaudhary, N.; Akinyemiju, T. Metabolic syndrome prevalence by race/ethnicity and sex in the united states, national health and nutrition examination survey, 1988–2012. *Prev. Chronic Dis.* **2017**, *14*, 1–16. [[CrossRef](#)]
4. Huang, P.L. A comprehensive definition for metabolic syndrome. *Dis. Model. Mech.* **2009**, *2*, 231–237. [[CrossRef](#)]

5. Iwaniak, A.; Darewicz, M.; Minkiewicz, P. Peptides Derived from Foods as Supportive Diet Components in the Prevention of Metabolic Syndrome. *Compr. Rev. Food Sci. Food Saf.* **2018**, *17*, 63–81. [[CrossRef](#)]
6. González-Ortega, O.; López-Limón, A.R.; Morales-Domínguez, J.F.; Soria-Guerra, R.E. Production and purification of recombinant hypocholesterolemic peptides. *Biotechnol. Lett.* **2015**, *37*, 41–54. [[CrossRef](#)] [[PubMed](#)]
7. Singh, B.P.; Vij, S.; Hati, S. Functional significance of bioactive peptides derived from soybean. *Peptides* **2014**, *54*, 171–179. [[CrossRef](#)]
8. Yuan, L.; Shu, W.; Shen, Y.; Jin, W.; Gao, R. Inflammation and food-derived anti-inflammatory peptides. *Biomed. Res. Sci.* **2019**, *1*, 1001.
9. Xu, Q.; Yan, X.; Zhang, Y.; Wu, J. Current understanding of transport and bioavailability of bioactive peptides derived from dairy proteins: A review. *Int. J. Food Sci. Technol.* **2019**, *54*, 1930–1941. [[CrossRef](#)]
10. Dehghan, M.; Mente, A.; Rangarajan, S.; Sheridan, P.; Mohan, V.; Iqbal, R.; Gupta, R.; Lear, S.; Wentzel-Viljoen, E.; Avezum, A.; et al. Association of dairy intake with cardiovascular disease and mortality in 21 countries from five continents (PURE): A prospective cohort study. *Lancet* **2018**, *392*, 2288–2297. [[CrossRef](#)]
11. Abedini, M.; Falahi, E.; Roosta, S. Dairy product consumption and the metabolic syndrome. *Diabetes Metab. Syndr. Clin. Res. Rev.* **2015**, *9*, 34–37. [[CrossRef](#)] [[PubMed](#)]
12. López-Expósito, I.; Amigo, L.; Recio, I. A mini-review on health and nutritional aspects of cheese with a focus on bioactive peptides. *Dairy Sci. Technol.* **2012**, *92*, 419–438. [[CrossRef](#)]
13. Darewicz, M.; Dziuba, B.; Minkiewicz, P.; Dziuba, J. The Preventive Potential of Milk and Colostrum Proteins and Protein Fragments. *Food Rev. Int.* **2011**, *27*, 357–388. [[CrossRef](#)]
14. Skwarek, A.; Darewicz, M.; Borawska-Dziadkiewicz, J. Ripened cheese as a source of bioactive peptides. *Biotechnol. Food Sci.* **2018**, *82*, 49–60.
15. McIntosh, C.H.S.; Widenmaier, S.; Kim, S. Chapter 15 Glucose-Dependent Insulinotropic Polypeptide (Gastric Inhibitory Polypeptide; GIP). *Vitam. Horm.* **2009**, *80*, 409–471. [[CrossRef](#)]
16. Mkele, G. Dipeptidyl peptidase-4 inhibitors: Their role in the management of type 2 diabetes. *S. Afr. Fam. Pr.* **2013**, *55*, 508–510. [[CrossRef](#)]
17. Uenishi, H.; Kabuki, T.; Seto, Y.; Serizawa, A.; Nakajima, H. Isolation and identification of casein-derived dipeptidyl-peptidase 4 (DPP-4)-inhibitory peptide LPQNIPPL from gouda-type cheese and its effect on plasma glucose in rats. *Int. Dairy J.* **2012**, *22*, 24–30. [[CrossRef](#)]
18. Patil, P.; Mandal, S.; Tomar, S.K.; Anand, S. Food protein-derived bioactive peptides in management of type 2 diabetes. *Eur. J. Nutr.* **2015**, *54*, 863–880. [[CrossRef](#)]
19. Sartorius, T.; Weidner, A.; Dharsono, T.; Boulter, A.; Wilhelm, M.; Schön, C. Postprandial Effects of a Proprietary Milk Protein Hydrolysate Containing Bioactive Peptides in Prediabetic Subjects. *Nutrients* **2019**, *11*, 1700. [[CrossRef](#)]
20. Grom, L.C.; Rocha, R.S.; Balthazar, C.F.; Guimarães, J.T.; Coutinho, N.M.; Barros, C.P.; Pimentel, T.C.; Venâncio, E.L.; Collopy Junior, I.; Maciel, P.M.C.; et al. Postprandial glycemia in healthy subjects: Which probiotic dairy food is more adequate? *J. Dairy Sci.* **2020**, *103*, 1110–1119. [[CrossRef](#)]
21. Hutchison, A.T.; Piscitelli, D.; Horowitz, M.; Jones, K.L.; Clifton, P.M.; Standfield, S.; Hausken, T.; Feinle-Bisset, C.; Luscombe-Marsh, N.D. Acute load-dependent effects of oral whey protein on gastric emptying, gut hormone release, glycemia, appetite, and energy intake in healthy men. *Am. J. Clin. Nutr.* **2015**, *102*, 1574–1584. [[CrossRef](#)] [[PubMed](#)]
22. Drouin-Chartier, J.-P.; Li, Y.; Ardisson Korat, A.V.; Ding, M.; Lamarche, B.; Manson, J.E.; Rimm, E.B.; Willett, W.C.; Hu, F.B. Changes in dairy product consumption and risk of type 2 diabetes: Results from 3 large prospective cohorts of US men and women. *Am. J. Clin. Nutr.* **2019**, *110*, 1201–1212. [[CrossRef](#)] [[PubMed](#)]
23. Gao, D.; Ning, N.; Wang, C.; Wang, Y.; Li, Q.; Meng, Z.; Liu, Y.; Li, Q. Dairy Products Consumption and Risk of Type 2 Diabetes: Systematic Review and Dose-Response Meta-Analysis. *PLoS ONE* **2013**, *8*, e73965. [[CrossRef](#)]
24. Aune, D.; Norat, T.; Romundstad, P.; Vatten, L.J. Dairy products and the risk of type 2 diabetes: A systematic review and dose-response meta-analysis of cohort studies. *Am. J. Clin. Nutr.* **2013**, *98*, 1066–1083. [[CrossRef](#)] [[PubMed](#)]

25. Hruby, A.; Ma, J.; Rogers, G.; Meigs, J.B.; Jacques, P.F. Associations of Dairy Intake with Incident Prediabetes or Diabetes in Middle-Aged Adults Vary by Both Dairy Type and Glycemic Status. *J. Nutr.* **2017**, *147*, 1764–1775. [[CrossRef](#)] [[PubMed](#)]
26. Iwaniak, A.; Minkiewicz, P.; Darewicz, M. Food-Originating ACE Inhibitors, Including Antihypertensive Peptides, as Preventive Food Components in Blood Pressure Reduction. *Compr. Rev. Food Sci. Food Saf.* **2014**, *13*, 114–134. [[CrossRef](#)]
27. Hryniewicz, M.; Iwaniak, A.; Bucholska, J.; Minkiewicz, P.; Darewicz, M. Structure-activity prediction of ACE inhibitory/bitter dipeptides - a chemometric approach based on stepwise regression. *Molecules* **2019**, *24*, 950. [[CrossRef](#)] [[PubMed](#)]
28. Beltrán-Barrientos, L.M.; Hernández-Mendoza, A.; Torres-Llanaez, M.J.; González-Córdova, A.F.; Vallejo-Córdoba, B. Invited review: Fermented milk as antihypertensive functional food. *J. Dairy Sci.* **2016**, *99*, 499–4110. [[CrossRef](#)]
29. Bütikofer, U.; Meyer, J.; Sieber, R.; Wechsler, D. Quantification of the angiotensin-converting enzyme-inhibiting tripeptides Val-Pro-Pro and Ile-Pro-Pro in hard, semi-hard and soft cheeses. *Int. Dairy J.* **2007**, *17*, 968–975. [[CrossRef](#)]
30. Pihlanto, A. Lactic fermentation and bioactive peptides. In *Lactic Acid Bacteria. R & D for Food, Health and Livestock Purposes*; Kongo, J.M., Ed.; IntechOpen: London, UK, 2013; pp. 309–332. [[CrossRef](#)]
31. Sieber, R.; Bütikofer, U.; Egger, C.; Portmann, R.; Walther, B.; Wechsler, D. ACE inhibitory activity and ACE-inhibiting peptides. *Dairy Sci. Technol.* **2010**, *90*, 47–73. [[CrossRef](#)]
32. Haque, E.; Chand, R. Antihypertensive and Antimicrobial Bioactive Peptides from Milk Proteins. *Eur. Food Res. Technol.* **2008**, *227*, 7–15. [[CrossRef](#)]
33. De Noni, I.; Cattaneo, S. Occurrence of β -casomorphins 5 and 7 in commercial dairy products and in their digests following in vitro simulated gastro-intestinal digestion. *Food Chem.* **2010**, *119*, 560–566. [[CrossRef](#)]
34. Gómez-Ruiz, J.Á.; Ramos, M.; Recio, I. Angiotensin-converting enzyme-inhibitory peptides in Manchego cheeses manufactured with different starter cultures. *Int. Dairy J.* **2002**, *12*, 697–706. [[CrossRef](#)]
35. Pripp, A.H.; Isaksson, T.; Stepaniak, L.; Sørhaug, T. Quantitative structure-activity relationship modelling of ACE-inhibitory peptides derived from milk proteins. *Eur. Food Res. Technol.* **2004**, *219*, 579–583. [[CrossRef](#)]
36. Gómez-Ruiz, J.Á.; Taborda, G.; Amigo, L.; Recio, I.; Ramos, M. Identification of ACE-inhibitory peptides in different Spanish cheeses by tandem mass spectrometry. *Eur. Food Res. Technol.* **2006**, *223*, 595–601. [[CrossRef](#)]
37. Gómez-Ruiz, J.A.; Recio, I.; Belloque, J. ACE-Inhibitory Activity and Structural Properties of Peptide Asp-Lys-Ile-His-Pro [β -CN f(47–51)]. Study of the Peptide Forms Synthesized by Different Methods. *J. Agric. Food Chem.* **2004**, *52*, 6315–6319. [[CrossRef](#)]
38. Tonouchi, H.; Suzuki, M.; Uchida, M.; Oda, M. Antihypertensive effect of an angiotensin converting enzyme inhibitory peptide from enzyme modified cheese. *J. Dairy Sci.* **2008**, *75*, 284–290. [[CrossRef](#)]
39. Nilsen, R.; Pripp, A.H.; Høstmark, A.T.; Haug, A.; Skeie, S. Short communication: Is consumption of a cheese rich in angiotensin-converting enzyme-inhibiting peptides, such as the Norwegian cheese Gamalost, associated with reduced blood pressure? *J. Dairy Sci.* **2014**, *97*, 2662–2668. [[CrossRef](#)]
40. Crippa, G.; Zabzuni, D.; Bravi, E.; Piva, G.; De Noni, I.; Bighi, E.; Rossi, F. Randomized, double blind placebo-controlled pilot study of the antihypertensive effects of Grana Padano D.O.P. cheese consumption in mild—Moderate hypertensive subjects. *Eur. Rev. Med. Pharmacol. Sci.* **2018**, *22*, 7573–7581. [[CrossRef](#)] [[PubMed](#)]
41. Chen, G.-C.; Wang, Y.; Tong, X.; Szeto, I.M.Y.; Smit, G.; Li, Z.-N.; Qin, L.-Q. Cheese consumption and risk of cardiovascular disease: A meta-analysis of prospective studies. *Eur. J. Nutr.* **2017**, *56*, 2565–2575. [[CrossRef](#)]
42. Sarmadi, B.H.; Ismail, A. Antioxidative peptides from food proteins: A review. *Peptides* **2010**, *31*, 1949–1956. [[CrossRef](#)]
43. Gupta, A.; Mann, B.; Kumar, R.; Sangwan, R.B. Antioxidant activity of Cheddar cheeses at different stages of ripening. *Int. J. Dairy Technol.* **2009**, *62*, 339–347. [[CrossRef](#)]
44. Gupta, A.K.; Mann, B.; Kumar, R.; Sangwan, R. Identification of antioxidant peptides in cheddar cheese made with adjunct culture *Lactobacillus casei* ssp. *casei* 300. *Milchwissenschaft* **2010**, *65*, 396–399.
45. Pritchard, S.R.; Phillips, M.; Kailasapathy, K. Identification of bioactive peptides in commercial Australian organic cheddar cheeses. *Aust. J. Dairy Technol.* **2010**, *65*, 170–173. [[CrossRef](#)]

46. Hernández-Galán, L.; Cardador-Martínez, A.; López-del-Castillo, M.; Picque, D.; Spinnler, H.E.; Martín del Campo, S.T. Antioxidant and angiotensin-converting enzyme inhibitory activity in fresh goat cheese prepared without starter culture: A preliminary study. *CyTA J. Food* **2016**, *15*, 1–9. [[CrossRef](#)]
47. Timón, M.L.; Andrés, A.; Otte, J.; Petró, M.J. Antioxidant peptides (<3 kDa) identified on hard cow milk cheese with rennet from different origin. *Food Res. Int.* **2019**, *120*, 643–649. [[CrossRef](#)]
48. Udenigwe, C.C.; Aluko, R.E. Chemometric analysis of the amino acid requirements of antioxidant food protein hydrolysates. *Int. J. Mol. Sci.* **2011**, *12*, 3148–3161. [[CrossRef](#)]
49. Timón, M.L.; Parra, V.; Otte, J.; Broncano, J.M.; Petró, M.J. Identification of radical scavenging peptides (<3 kDa) from Burgos-type cheese. *LWT-Food Sci. Technol.* **2014**, *57*, 359–365. [[CrossRef](#)]
50. Cox, R.A.; García-Palmieri, M.R. Cholesterol, Triglycerides, and Associated Lipoproteins. In *Clinical Methods: The History, Physical, and Laboratory Examinations*, 3rd ed.; Walker, H.K., Hall, W.D., Hurst, J.W., Eds.; Butterworths: Boston, MA, USA, 1990; Chapter 31; pp. 153–160.
51. Contarini, G.; Povo, M. Phospholipids in milk fat: Composition, biological and technological significance, and analytical strategies. *Int. J. Mol. Sci.* **2013**, *14*, 2808–2831. [[CrossRef](#)]
52. Udenigwe, C.C.; Rouvinen-Watt, K. The Role of Food Peptides in Lipid Metabolism during Dyslipidemia and Associated Health Conditions. *Int. J. Mol. Sci.* **2015**, *16*, 9303–9313. [[CrossRef](#)]
53. Hsieh, C.-C.; Hernández-Ledesma, B.; Fernández-Tomé, S.; Weinborn, V.; Barile, D.; de Moura Bell, J.M.L.N. Milk Proteins, Peptides, and Oligosaccharides: Effects against the 21st Century Disorders. *Biomed Res. Int.* **2015**, *2015*, 146840. [[CrossRef](#)]
54. Nagaoka, S. Structure-function properties of hypolipidemic peptides. *J. Food Biochem.* **2019**, *43*, e12539. [[CrossRef](#)]
55. Wakasa, Y.; Tamakoshi, C.; Ohno, T.; Hirose, S.; Goto, T.; Nagaoka, S.; Takaiwa, F. The Hypocholesterolemic Activity of Transgenic Rice Seed Accumulating Lactostatin, a Bioactive Peptide Derived from Bovine Milk β -Lactoglobulin. *J. Agric. Food Chem.* **2011**, *59*, 3845–3850. [[CrossRef](#)] [[PubMed](#)]
56. Cabanos, C.; Ekoy, A.; Amari, Y.; Kato, N.; Kuroda, M.; Nagaoka, S.; Takaiwa, F.; Utsumi, S.; Maruyama, N. High-level production of lactostatin, a hypocholesterolemic peptide, in transgenic rice using soybean A1aB1b as carrier. *Transgenic Res.* **2013**, *22*, 621–629. [[CrossRef](#)] [[PubMed](#)]
57. Yamauchi, R.; Ohinata, K.; Yoshikawa, M. β -Lactotensin and neurotensin rapidly reduce serum cholesterol via NT2 receptor. *Peptides* **2003**, *24*, 1955–1961. [[CrossRef](#)]
58. Keller, U. Dietary Proteins in Obesity and in Diabetes. *Int. J. Vitam. Nutr. Res.* **2011**, *81*, 125–133. [[CrossRef](#)] [[PubMed](#)]
59. Campos-Nonato, I.; Hernandez, L.; Barquera, S. Effect of a High-Protein Diet versus Standard-Protein Diet on Weight Loss and Biomarkers of Metabolic Syndrome: A Randomized Clinical Trial. *Obes Facts.* **2017**, *10*, 238–251. [[CrossRef](#)] [[PubMed](#)]
60. Erdmann, K.; Cheung, B.W.; Schröder, H. The possible role of food-derived peptides in reducing the risk of cardiovascular disease. *J. Nutr. Biochem.* **2008**, *19*, 643–654. [[CrossRef](#)] [[PubMed](#)]
61. Bhat, Z.F.; Kumar, S.; Bhat, H.F. Bioactive peptides of animal origin: A review. *J. Food Sci. Technol.* **2015**, *52*, 5377–5392. [[CrossRef](#)] [[PubMed](#)]
62. Kondrashina, A.; Brodtkorb, A.; Giblin, L. Dairy-derived peptides in satiety. *J. Funct. Foods* **2020**, *66*, 103801. [[CrossRef](#)]
63. Monteiro, R.; Azevedo, I. Chronic inflammation in obesity and the metabolic syndrome. *Mediat. Inflamm.* **2010**, *2010*, 289645. [[CrossRef](#)]
64. Zielińska, E.; Baraniak, B.; Karaś, M. Antioxidant and Anti-Inflammatory Activities of Hydrolysates and Peptide Fractions Obtained by Enzymatic Hydrolysis of Selected Heat-Treated Edible Insects. *Nutrients* **2017**, *9*, 970. [[CrossRef](#)]
65. Marcone, S.; Belton, O.; FitzGerald, D.J. Milk-derived bioactive peptides and their health-promoting effects: A potential role in atherosclerosis. *Br. J. Clin. Pharmacol.* **2017**, *83*, 152–162. [[CrossRef](#)] [[PubMed](#)]
66. Rafiq, S.; Huma, N.; Rakariyatham, K.; Hussain, I.; Gulzar, N.; Hayat, I. Anti-inflammatory and anticancer activities of water-soluble peptide extracts of buffalo and cow milk Cheddar cheeses. *Int. J. Dairy Technol.* **2017**, *71*, 432–438. [[CrossRef](#)]

67. Minkiewicz, P.; Iwaniak, A.; Darewicz, M. BIOPEP-UWM Database of Bioactive Peptides: Current Opportunities. *Int. J. Mol. Sci.* **2019**, *20*, 5978. [[CrossRef](#)] [[PubMed](#)]
68. Iwaniak, A.; Darewicz, M.; Mogut, D.; Minkiewicz, P. Elucidation of the role of *in silico* methodologies in approaches to studying bioactive peptides derived from foods. *J. Funct. Foods* **2019**, *61*, 103486. [[CrossRef](#)]



© 2020 by the authors. Licensee MDPI, Basel, Switzerland. This article is an open access article distributed under the terms and conditions of the Creative Commons Attribution (CC BY) license (<http://creativecommons.org/licenses/by/4.0/>).

Article

Soybean (*Glycine max*) Protein Hydrolysates as Sources of Peptide Bitter-Tasting Indicators: An Analysis Based on Hybrid and Fragmentomic Approaches

Anna Iwaniak ^{*,†}, Monika Hryniewicz [†], Piotr Minkiewicz, Justyna Bucholska and Małgorzata Darewicz ^{*}

Faculty of Food Science, University of Warmia and Mazury in Olsztyn, Chair of Food Biochemistry, Pl. Cieszyński 1, 10-719 Olsztyn-Kortowo, Poland; monika.protasiewicz@uwm.edu.pl (M.H.); minkiew@uwm.edu.pl (P.M.); justyna.bucholska@uwm.edu.pl (J.B.)

* Correspondence: ami@uwm.edu.pl (A.I.); darewicz@uwm.edu.pl (M.D.); Tel.: +48-89-523-3722 (A.I.)

† These authors equally contributed to this work.

Received: 2 March 2020; Accepted: 3 April 2020; Published: 6 April 2020

Abstract: The aim of this study was to analyze soybean proteins as sources of peptides likely to be bitter using fragmentomic and hybrid approaches involving *in silico* and *in vitro* studies. The bitterness of peptides (called parent peptides) was theoretically estimated based on the presence of bitter-tasting motifs, particularly those defined as bitter-tasting indicators. They were selected based on previously published multilinear stepwise regression results. Bioinformatic-assisted analyses covered the hydrolysis of five major soybean-originating protein sequences using bromelain, ficin, papain, and proteinase K. Verification of the results in experimental conditions included soy protein concentrate (SPC) hydrolysis, RP-HPLC (for monitoring the proteolysis), and identification of peptides using RP-HPLC-MS/MS. Discrepancies between *in silico* and *in vitro* results were observed when identifying parent peptide SPC hydrolysate samples. However, both analyses revealed that conglycinins were the most abundant sources of parent peptides likely to taste bitter. The compatibility percentage of the *in silico* and *in vitro* results was 3%. Nine parent peptides with the following sequences were identified in SPC hydrolysates: LSVISPK, DVLVIPLG, LIVILNG, NPFLFG, ISSTIV, PQMIIV, PFPSIL, DDFFL, and **FFEITPEK** (indicators are in bold). The fragmentomic idea of research might provide a supportive method for predicting the bitterness of hydrolysates. However, this statement needs to be confirmed experimentally.

Keywords: bioinformatics; BIOPEP-UWM database; bitter-tasting peptides; hydrolysates; soybean proteins

1. Introduction

Soybean has been known as a food for thousands of years [1] and recently has become increasingly popular among consumers for ecological, ethical, and health-beneficial concerns [2]. Its health-beneficial properties are due to the presence of biologically active components like isoflavones, saponins, protease inhibitors, and peptides. Briefly, their activity is related to their preventive potential against cardiovascular disease, diabetes, menopausal symptoms, osteoporosis, prostate, and breast cancers. According to the literature, peptides derived from soybean proteins are responsible for a variety of activities that regulate body functions, e.g., reduction of blood pressure, cholesterol, and carbohydrate levels, as well as exhibit anti-inflammatory, antioxidative, and anticancer effects. The first three “reducing” functions of peptides are related to the inhibition of the following enzymes: ACE (angiotensin converting enzyme, EC 3.4.15.1),

DPP IV (dipeptidyl peptidase IV; EC 3.4.14.5), and HMGR (3-hydroxy-3-methylglutaryl-coenzyme A reductase; EC 1.1.1.34), respectively [1].

Quite often, the biological function of a peptide is associated with bitter taste; thus, both peptides and protein hydrolysates may not be acceptable by consumers due to the undesired taste profile [3]. Due to the fact that peptides are derived from food proteins, they are considered as “natural”. Thus, their sensory acceptance poses a challenge for food scientists and technologists who aim at producing functional foods [3], especially when some of the bioactive peptides negatively affect the taste of a protein hydrolysate [4].

Currently, three approaches are used to study peptides from foods [5]. The first one is called a classical approach, and briefly, it is an experimental protocol consisting of the main methodological steps like hydrolysis of protein, identification of peptides, and determination of the bioactivity of the hydrolysate(s), as well as the peptide(s). The other two approaches benefit from the progress in the development and application of bioinformatics and chemometrics in the food science. This results from the increasing popularity of databases of biomolecules as sources of information about, e.g., peptides, as well as programs serving for peptide analyses. Thus, the method for studying peptides involving the application of bioinformatic and/or cheminformatic predictions is called an *in silico* approach, whereas the combination of the classical and *in silico* protocols is defined as a hybrid approach [5].

Some *in silico* studies were undertaken to analyze the impact of the amino acid composition of peptides on their bitterness. For example, the bitterness of peptides was found to result from the presence of residues with bulky and branched side chains, like Leu, Ile, Tyr, Phe, and Val. According to the literature, the first three of these amino acids were found to be extremely bitter with an unpleasant flavor and odor [6].

The fact that some regularities can be observed between the presence of the specific amino acid(s) and the function of a whole peptide sequence has prompted some scientists to find the foundations for introducing the fragmentomic idea of research. According to this idea, shorter motifs (fragments) with a known property encrypted in a molecule of interest may affect its function [7]. According to Liu et al. [8], motifs are generally understood as reproducible patterns in a protein or peptide sequence that are ascribed to a specific biological function (in this case, taste). This applies also to peptides identified in a food protein hydrolysate. For example, a sequence identified (i.e., precursor/parent peptide) that contains peptide motifs with confirmed bitterness (i.e., bitter-tasting motifs) may suggest the bitter-tasting potential of a parent sequence. Such an idea of research was applied by Iwaniak et al. [9] for the hybrid analysis of bovine milk protein hydrolysates as sources of bitter-tasting motifs, especially those with an “indicator” status.

To sum up, soybean protein hydrolysates are known sources of bioactive peptides. According to the literature, soybean hydrolysates taste bitter, which may be due to the presence of peptide sequences [10]. Taking into account these two facts, the aim of this study was to apply the hybrid protocol for an analysis of soybean protein hydrolysates as sources of peptides likely to be bitter due to the presence of bitter-tasting motifs, particularly those defined as bitter-tasting indicators. According to the definition introduced by Iwaniak et al. [9], bitter-tasting indicators should be literally understood as “shorter motifs with known bitterness, which found in the sequences of peptides, may potentially determine their taste”.

2. Materials and Methods

2.1. Soybean Protein Sequences and Computer Simulation of Their Hydrolysis

Five sequences of soybean (*Glycine max*) proteins, namely: 7S globulin (403 aa, P13917), glycinin (492 aa, P04347), β -chain of β -conglycinin, (414 aa, P25974), α -chain of β -conglycinin (543 aa, P13916), and profilin (130 aa, O65809), were acquired from the UniProt database [11] (accessed December 2018). The number of amino acids in a protein chain, as well as the accession number of proteins in UniProt are provided in brackets.

The BIOPEP-UWM database [12] tool called “Enzyme(s) action” was applied for computer simulation of hydrolysis. Each soybean protein sequence was theoretically hydrolyzed by bromelain, ficin, papain, and proteinase K, respectively. The following steps were required to hydrolyze protein when opening the BIOPEP-UWM tool: Sensory peptides and amino acids → Analysis → Enzyme(s) action → For your sequence → Paste the protein sequence (e.g., 7S globulin) → Select the enzyme (e.g., bromelain) → View the report with the results. Motifs that were theoretically released from a protein, excluding single amino acids, were copied, and each of them was searched for the presence of bitter-tasting peptides, according to the following protocol: BIOPEP-UWM sensory peptides and amino acids → Analysis → Profiles of proteins potential sensory activity → For your sequence → Paste the released peptide (e.g., VFDG) → Report. Bitter-tasting indicators (see below) were searched manually after making the above-mentioned analysis. Moreover, the potentially released peptide was searched for showing an additional bioactivity (if any) using an analogical procedure, by selecting “Bioactive peptides” instead of the “Sensory peptides and amino acids” tab after opening the BIOPEP-UWM database.

2.2. Bitter-Tasting Peptide Indicators

Peptides possessing a status of bitter-tasting indicators were selected from the BIOPEP-UWM database collection of 102 bitter di- and tri-peptides (51 sequences of di- and tri-peptides each) that were analyzed using multivariate linear stepwise regression (MLR) [13]. Based on the MLR results, those peptides whose experimental measures of bitterness were approximative to the theoretical ones were defined as bitter-tasting peptidic indicators. They were as follows: PK(0.17;0.08), AD(0.17;0.10), VD(0.08;0.10), VE(0.17;0.15), EI(0.25;0.18), YG(0.33;0.27), VL(0.17;0.21), VI(0.17;0.21), LG(0.05;0.16), GV(0.22;0.25), GP(0.17;0.25), RG(0.13;0.21), IG(0.22;0.19), LE(0.33;0.32), KP(0.33;0.33), VF(0.33;0.37), VY(0.33;0.37), LL(0.4;0.37), FI(0.67;0.56), IF(0.67;0.56), FL(0.67;0.60), FF(0.83;0.72), PGR(0.04;0.26), GGP(0.11;0.12), GGV(0.03;0.10), GLG(0.1;0.17), PPG(0.11;0.03), LGL(0.20;0.07), FGG(0.22;0.02), VVV(0.22;0.05), GGL(0.1;0.12), GVV(0.22;0.17), PGP(0.11;0.25), KPK(0.33;0.37), YGG(0.43;0.52), PGI(0.43;0.48), PPP(0.50;0.66), GLL(0.67;0.69), LLL(0.83;0.64), GGF(0.67;0.76), GGY(0.67;0.74), PIP(0.70;0.82), GYY(2.50; 2.32). Finally, 21 dipeptides and 21 tripeptides achieved the status of a bitter taste indicator. Their experimental and theoretical bitterness are provided in the brackets, respectively. The experimental bitterness of a peptide was expressed as Rcaf. value, meaning the threshold concentration for 1 mM caffeine solution as a standard (the higher the Rcaf. value, the bitterer the peptide is) [14].

2.3. Materials and Reagents

Soy protein concentrate (SPC) called Isomil®(containing 68 % protein, according to the product specification) was produced by Libra Poland Ltd. (Warsaw, Poland). Enzymes: bromelain (EC 3.4.22.32; 5–15 units/mg protein; Cat. No. B5144), ficin (EC 3.4.22.3, ≥1 unit/mg protein; Cat. No. F4125), papain (EC 3.4.22.2, 10 units/mg protein; Cat. No. P4762), and proteinase K from *Tritirachium album* (EC 3.4.21.64, ≥30 units/mg protein; Cat. No. P2308), and trifluoroacetic acid (TFA), acetonitrile (ACN), 2,2-bis(hydroxymethyl)-2,2',2''-nitrilotriethanol (Bis-Tris), 2-mercaptoethanol, and urea were purchased from Sigma-Aldrich Sp. z o.o. (Poznań, Poland). All chemicals were of analytical grade. Water used to formulate solutions and buffers was prepared using a Milli-Q PLUS system (Millipore Corp., New York, NY, USA).

2.4. Hydrolysis of SPC

SPC hydrolysis was carried out according to the protocol provided by Peña-Ramos and Xiong [15] with slight modifications. Firstly, five separate water solutions of SPC containing 3% protein (w/v) each were prepared. All of them had the non-adjusted pH of 7.0±0.1. SPC solutions were continuously and gently stirred, as well as pre-heated for 5 min using a Heidolph Unimax Modular Incubator 1010 (Heidolph Instruments GmbH & CO. KG, Schwabach, Germany). The preincubation temperatures were

typical of the activity of enzymes used, according to their specifications provided by the manufacturer, and were as follows: bromelain and ficin (50 °C), papain (65 °C), and proteinase K (37 °C). Finally, 3 hour hydrolysis of four SPC samples was conducted under continuous stirring and the enzyme-to-substrate ratio (protein) of 1:100 (w/w) [15,16]. The pH values of SPC solutions were optimal for enzyme activity as provided by the manufacturer, i.e.: 7.0 for bromelain, papain, and proteinase K; and 6.5 for ficin. In the case of the last sample, its pH was adjusted using 0.1 M HCl. Afterwards, all hydrolysates were heated at 90 °C for 15 min to inactivate the enzymes and then freeze-dried. Finally, four SPC hydrolysates were produced, namely B-SPC, F-SPC, P-SPC, and PK-SPC, the abbreviations referring to bromelain-, ficin-, papain-, and proteinase-K-SPC hydrolysates, respectively, according to the convention used in the previous paper [9]. The fifth sample, 0-SPC, was a reference sample being the non-hydrolyzed SPC solution. All hydrolysates were prepared in duplicate.

2.5. RP-HPLC for Monitoring the Process of SPC Hydrolysis and RP-HPLC-MS/MS for the Identification of SPC-Originating Peptides

RP-HPLC (reversed-phase high performance liquid chromatography) was applied to observe the progress in the hydrolysis of SPC using the above-mentioned enzymes. The preparation of SPC/SPC hydrolysate samples taken for RP-HPLC and RP-HPLC-MS/MS (reversed-phase high performance liquid chromatography online with tandem mass spectrometry), as well as the parameters of devices for chromatography were exactly the same as in the protocol by Iwaniak et al. [9].

Firstly, two milligrams of freeze-dried SPC/SPC hydrolysate sample were dissolved in 300 μ L of a buffer containing 0.1 M Bis-Tris and 4 M urea. Then, two microliters of 2-mercaptoethanol were added, and the mixture was vortexed and finally incubated at room temperature (1 hour). Then, six-hundred-eighty microliters of 6 M urea solution in a mixture of ACN and H₂O (v/v; 100: 900; pH 2.2 was adjusted by the addition of TFA) were added to the sample and stirred. Finally, the samples were centrifuged (10 min; 10,000 \times g) [9].

The RP-HPLC analysis was carried out on Shimadzu[®] devices comprised of two LC-20AD pumps, an SIL-20AC HT autosampler, a CBM-20A controller, a CTO-10AS VP thermostat, an SPD-M20A photodiode detector, a DGU-20A5 degasser, and an FRC-10A fraction collector. The Jupiter Proteo Phenomenex[®] column (Torrance, CA, USA; 250 \times 2 mm; particle diameter: 4 μ m; pore diameter: 90 \AA) was applied for RP-HPLC analysis of the samples. According to the protocol by Iwaniak et al. [9], Solvent A was 0.01 % TFA water solution (v/v), whereas Solvent B was 0.01 % (v/v) TFA dissolved in acetonitrile (ACN). The gradient of Solvent B increased from 0 to 40 % during 60 min. The column was washed with Solvent B (40–100 %, 60–65 min; 100%, 65–70 min, 100 - 0 %, 70–71 min; 0 %, 71–80 min). Data registration was between the 0th and 80th minute of the RP-HPLC analysis. The injection volume was 30 μ L; the flow rate was 0.2 mL \times min⁻¹; and the column temperature was 30 °C. All chromatograms were acquired at 220 nm [9]. Finally, the chromatographic profiles of the samples taken before the 60th min of the RP-HPLC analysis were the subject of discussion.

Similarly, the exact procedure as that described by Iwaniak et al. [9] was applied for the identification of peptides released from SPC hydrolysates using RP-HPLC-MS/MS. Briefly, the identification of peptides was carried out using the VARIAN[®] 500-MS (Agilent Technologies, Santa Clara, CA, USA) ion trap mass spectrometer with an electrospray ion source and an RP-HPLC assembly comprised of two 212-LC pumps, a ProStar 410 autosampler, a Degassit degasser (MetaChem Technologies[®], Torrance, CA, USA), and a nitrogen generator (Parker Domnick Hunter Scientific[®], Gateshead, U.K.). Data were registered between 5 and 60 min. The other parameters for mass spectrometry included: needle and shield voltages: 5000 and 600 V, respectively; spraying and drying gas (nitrogen) pressure: 55 and 30 psi, respectively; drying gas temperature: 390 °C; flow rate of damping gas (helium): 0.8 mL \times min⁻¹; positive polarity with current ionization: 600 V; capillary voltage: 100 V; retardation factor loading: 100 %; isolation window: 3.0; excitation storage level m/z = 100–2000 Da; flow rate: 0.2 mL \times min⁻¹; injection volume: 15 μ L; frequency of data recording: 0.05–0.07 Hz single scan averaged from five microscans. The gradient and column type including its

parameters were identical to those presented above [9]. Peptides were identified by comparison of experimental mass-to-charge ratios, and the ratios were calculated using the Fragment Ion Calculator program (<http://db.systemsbio.net:8080/proteomicsToolkit/FragIonServlet.html>) as described in our previous article [9]. All analyses were performed in duplicate.

We introduced an additional parameter to compare the susceptibility of proteins to particular proteolytic enzymes:

$$C = (S_{\text{shorter}} - S_{0\text{shorter}}) / S_{\text{longer}} \quad (1)$$

where:

S_{shorter} : relative area of peaks between 14.00 and 39.99 min in the chromatogram of the hydrolysate;

$S_{0\text{shorter}}$: relative area of peaks between 14.00 and 39.99 min in the chromatogram of the non-hydrolyzed sample;

S_{longer} : relative area of peaks between 40.00 and 60.00 min in the chromatogram of the hydrolysate.

Retention time prediction is a helpful strategy supporting peptide identification by mass spectrometry [17]. To facilitate peptide identification, their theoretical retention times ($t_{R\text{ predicted}}$) were calculated and then compared with the experimental ($t_{R\text{ experimental}}$) ones. The $t_{R\text{ predicted}}$ was predicted using Sequence Specific Retention Calculator (SSRCalc) (<http://hs2.proteome.ca/SSRCalc/SSRCalc.html>; accessed: December 2019) [18] according to the mathematical formula introduced by Darewicz et al. [19]:

$$t_{R\text{ predicted}} = 0.0002 \times (t_{R\text{ SSRCalc}})^3 - 0.0085 \times (t_{R\text{ SSRCalc}})^2 + 1.0415 \times (t_{R\text{ SSRCalc}}) + 8.6434 \quad (2)$$

where:

$t_{R\text{ SSRCalc}}$: retention time (min) calculated with Sequence Specific Retention Calculator (SSRCalc).

The specific parameters implemented in the software to obtain $t_{R\text{ SSRCalc}}$, like the retention time of the substance not adsorbed on the column (parameter "a"), the parameter dependent on the acetonitrile gradient (parameter "b"), pore diameter, column, and TFA concentration, were as described by Iwaniak et al. [9].

3. Results

3.1. In Silico Analysis

Many data concerning molecules can be found in databases [5]. The BIOPEP-UWM database of sensory peptides and amino acids [20] was used to analyze the in silico fragments released from soybean proteins. These peptides were searched for the presence of shorter bitter-tasting fragments, including indicators. The results are shown in Tables 1 and A1 (in the Appendix A). They include only released fragments that (a) contained bitter-tasting motifs and (b) consisted of four amino acid residues at a minimum. Shorter fragments were not discussed. They were di- and tri-peptides that could already match the sequences with a known taste sensation (i.e., bitterness).

Table 1. Number of parent peptides including these containing bitter-tasting indicators found in soybean protein sequences.

Parent Peptides Released from Profilin Due to the Simulated Action of:			
B ¹	F	P	PK
Number of parent peptides/number of parent peptides containing bitter-tasting indicators			
9/7	5/2	7/5	4/1
Total number of parent peptides/total number of parent peptides containing bitter-tasting indicators = 25/15			
Parent peptides released from globulin 7S due to the simulated action of:			
B	F	P	PK

Table 1. Cont.

Number of parent peptides/number of parent peptides containing bitter-tasting indicators			
24/16	10/5	20/16	14/4
Total number of parent peptides/total number of parent peptides containing bitter-tasting indicators = 68/41			
Parent peptides released from glycinin due to the simulated action of:			
B	F	P	PK
Number of parent peptides/number of parent peptides containing bitter-tasting indicators			
28/17	12/4	18/11	17/8
Total number of parent peptides/total number of parent peptides containing bitter-tasting indicators = 75/38			
Parent peptides released from β-conglycinin (β-chain) due to the simulated action of:			
B	F	P	PK
Number of parent peptides/number of parent peptides containing bitter-tasting indicators			
30/18	9/4	26/17	13/4
Total number of parent peptides/total number of parent peptides containing bitter-tasting indicators = 78/43			
Parent peptides released from β-conglycinin (α-chain) due to the simulated action of:			
B	F	P	PK
Number of parent peptides/number of parent peptides containing bitter-tasting indicators			
32/23	16/8	27/17	17/5
Total number of parent peptides/total number of parent peptides containing bitter-tasting indicators = 92/53			

¹ B, bromelain; F, ficin; P, papain; PK, proteinase K. The complete list of peptide sequences is presented in the Appendix A (Table A1).

Regardless of the substrate and enzyme applied, all released fragments were the potential sources of motifs matching the sequences collected in the BIOPEP-UWM database and known in the literature as bitter-tasting. Thus, it was the premise to define them as parent peptides. Taking into consideration all enzymes applied in the study, the highest number of parent peptides was potentially released from β -conglycinin (α -chain), while profilin was the protein revealing the smallest number of peptides produced. Generally, the best in silico enzymatic potential aiming to produce parent peptides from all soybean protein sequences was represented by bromelain and papain. Other enzymes, i.e., ficin and proteinase K, produced less parent peptides than the above enzymes. However, in most of the cases, proteinase K was predicted to be slightly better than ficin considering the number of peptides potentially released from soybean proteins. The most abundant potential sources of parent peptides containing one bitter-tasting indicator at minimum were: profilin (7 sequences, enzyme used: bromelain), 7S globulin (16 sequences each, enzymes used: bromelain and papain), glycinin (17 sequences, enzyme used: bromelain), β -conglycinin (β -chain) (18 and 17, enzymes used: bromelain and papain, respectively), and β -conglycinin (α -chain) (23 sequences, enzyme used: bromelain). The highest total number of parent peptides with encrypted bitter-tasting indicators, regardless of the enzyme used, was determined in the β - and α -chain of β -conglycinin (43 and 53 out of 78 and 93 generally released, respectively). Considering the enzymes that produced such parent peptides (i.e., with encrypted indicators), their ranking was as follows: bromelain > papain > ficin > proteinase K. The criterion in this ranking was the total number of parent peptides (i.e., the higher the number, the better place in the rank) containing one indicator of bitter taste at a minimum.

Dipeptides rather than tripeptides with or without the status of a bitter-tasting indicator were the great majority of motifs found in the parent peptides. Both two and three amino acid fragments were observed in the following peptides: ERPG-RP, RPG (source: profilin hydrolyzed with ficin); RQLEENLVVFDLA-VF, LE, LV, DL, EEN (source: 7S globulin hydrolyzed with proteinase K); SRPG-RP, RPG (source: 7S globulin hydrolyzed both with bromelain and ficin); EENL-EEN (source: 7S

globulin hydrolyzed with proteinase K); VEENICTMK-**VE**, EEN (source: glycinin hydrolyzed with bromelain); ESEGGL-EGG, GL, **GGL**, EG-EGGSV-GR, EGG-EG; EGGL-EGG, EG, **GGL**, GL (source: glycinin hydrolyzed with proteinase K); LLLPH-**LL**, **LL**, **LLL**, PFPSILG-FP, PF, PFP, **LG**, IL (source: β -chain of β -conglycinin hydrolyzed with papain), EENL-EEN (source: β -chain of β -conglycinin hydrolyzed with proteinase K); EIPRPRPRQHPEREPQQPG-RP, RP, RP, PR, PR, PR, **EI**; EEDEDEQPRPIPFPRPQPRQEEHEQREEQEWPRK-RP, RP, PR, PR, PR, PR, FP, PF, PFP, **PIP**; SEEEDEDEDEEQDERQFPFPRPPHQK-PP, RP, PR, FP, FP, PFP, PF, PFP (source: α -chain of β -conglycinin hydrolyzed with both bromelain and ficin); LLLPHFNSK-**LL**, **LL**, **LLL**; PVVVNA-**VVV**, VV, VV (source: α -chain of β -conglycinin hydrolyzed with bromelain); PIPFPR-PR, FP, PF, PFP, **PIP** (source: α -chain of β -conglycinin with papain); QFPFPR-PR, FP, FP, PFP, PF, PFP, PNTLLLPNH-**LL**, **LL**, **LLL**, LLLPH-**LL**, **LL**, **LLL**, and PVVVNA-**VVV**, VV, VV (source: α -chain of β -conglycinin hydrolyzed with proteinase K). Motifs in bold were the fragments with the status of being an indicator.

Some of the parent peptides in silico released from proteins contained such bitter-tasting motifs possessing or not possessing the status of indicators that fully or almost fully overlapped their whole sequences. They were for example encrypted in: VIRG-**VI**, **RG** (profilin, enzyme used: bromelain); EITLG-**LG**, **EI** (7S globulin, enzyme used: bromelain); DVLVIPLG-**VL**, **VI**, **LG**, LV (glycinin, enzymes used: bromelain and papain); VVLY/VV, **VL** (glycinin, enzyme used: bromelain); VVFK-**VF**, VV (glycinin, enzyme used: papain); EGGL-EGG, EG (glycinin, enzyme used: proteinase K); DIFL-**FL**, **IF** (α - and β -chain of β -conglycinin, enzyme used: ficin); FVDA-FV, **VD**, DA (α - and β -chain of β -conglycinin, enzyme used: papain); VLFG-**VL**, FG, LF, VIVE-**VI**, **VE**, IV; PFPSILG-FP, PF, PFP, **LG**, IL (β -chain of β -conglycinin, enzyme used: papain); and NILE-**LE**, IL (α -chain of β -conglycinin, enzyme used: papain).

3.2. Monitoring the Process of SPC Hydrolysis

Taking into account the ranking of enzymes suitable for soybean protein hydrolysis, as well as the number of peptide bitter-tasting indicators produced, the next step was to produce soybean hydrolysates to compare in silico and in vitro results. Five samples representing 0-SPC, B-SPC, F-SPC, P-SPC, and PK-SPC were subjected to RP-HPLC separation to observe the progress in SPC hydrolysis (see Figure 1 and Table 2). Three major time segments could be distinguished in all chromatograms, namely: 0.00–13.99, 14.00–39.99, and 40.00–60.00 min. The first time segment contained the highest peak eluting for about 10 min (not shown in Figure 1). It was an injection peak that could contain non-retained substances like the buffers used for protein/hydrolysate solutions and low molecular weight compounds present in protein concentrates [9].

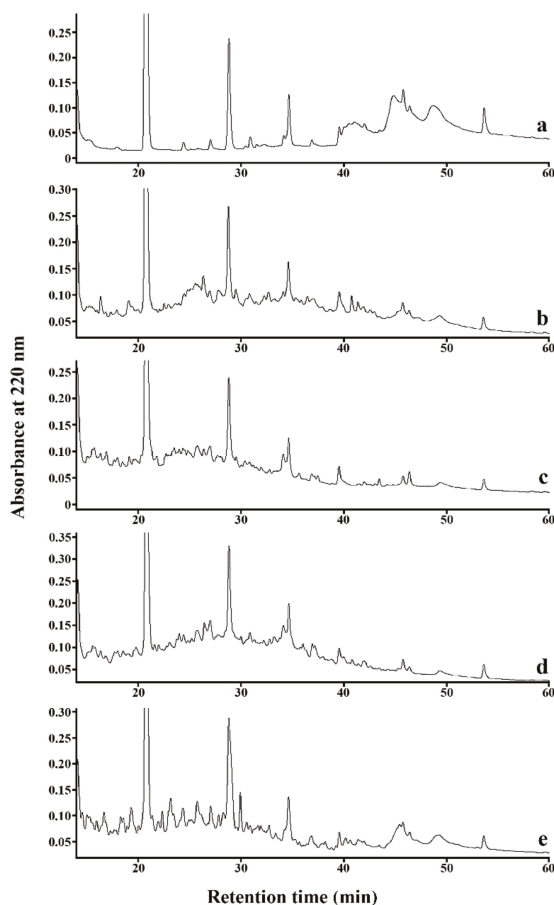


Figure 1. RP-HPLC (Reversed-Phase High Performance Liquid Chromatography) chromatograms of 0-soy protein concentrate (SPC) (a), B-SPC (b), F-SPC (c), P-SPC (d), and PK-SPC (e). Retention time range displayed in the Figure is between 14th and 60th minute. Chromatograms were acquired at $\lambda = 220$ nm as recommended by Visser et al. [21]. Abbreviations: 0-SPC-soy protein concentrate, B-SPC, F-SPC, P-SPC and PK-SPC: bromelain-, ficin-, papain-, and proteinase K-soybean protein hydrolysate, respectively.

Three major time segments could be distinguished in all chromatograms, namely: 0.00–13.99, 14.00–39.99, and 40.00–60.00 min. The first time segment contained the highest peak eluting for about 10 min (not shown in Figure 1). It was an injection peak that could contain non-retained substances like the buffers used for protein/hydrolysate solutions and low molecular weight compounds present in protein concentrates [9]. In our previous experiment [9], the shape and area of an injection peak were approximately the same in all chromatograms. Therefore, peaks that could be observed within in 0.00 and 13.99 min were not considered for further interpretation. Peaks eluting between 40.00 and 60.00 min corresponded to high molecular weight compounds, like, e.g., proteins [9,22]. On the other hand, the chromatogram of the unhydrolyzed SPC sample contained much material with a short retention time (Table 2) as compared with the unhydrolyzed milk protein concentrate analyzed in our previous experiment [9].

Table 2. Results of soybean protein hydrolysis as revealed by RP-HPLC (Reversed-Phase High Performance Liquid Chromatography).

Time Interval (min)	Relative Area of Chromatographic Peaks (%) ¹				
	0-SPC ²	B-SPC	F-SPC	P-SPC	PK-SPC
14.00–39.99	50.1	83.3	96.7	93.6	85.2
40.00–60.00	49.9	16.7	3.3	6.4	14.8
C ³	0.0	4.0	14.2	6.8	2.4

¹ The area of all peaks between 14 and 60 min is 100% (See Figure 1); ² 0-SPC, B-SPC, F-SPC, P-SPC, PK-SPC: non-hydrolyzed soy protein concentrate, soy protein concentrate hydrolyzed by bromelain, ficin, papain, or proteinase K, respectively (see the Materials and Methods); ³ Calculated according to Equation (1).

The area of peaks within the range of 14.00–39.99 min and 40.00–60.00 min was almost equal in this experiment (see Table 2), whereas for milk protein concentrate, the ratio of total peak area within a shorter t_R range to a longer t_R range was only ca. 0.05 [9]. Taking the above into account, we introduced the parameter C (Equation (1)) to compare results obtained during experiments performed with soybean proteins (this experiment) and milk proteins [9].

All chromatograms differed when looking at the time interval between 14.00 and 39.99 min. It was also reflected in the differences between the percentages of total peak areas observed in these time segments (Table 2). The order of the C parameter value was as follows: ficin > papain > proteinase K > bromelain, which suggested that ficin was the most efficient among the proteolytic enzymes used for hydrolysis of the soybean protein concentrate. The order of susceptibility of milk protein concentrate (MPC) [9] was reported to be as follows: proteinase K (C = 19.6) > ficin (C = 18.4) > papain (C = 7.8) > bromelain (C = 1.6). Ficin seemed to be sufficient for hydrolysis of both MPC and SPC. Proteinase K hydrolyzed MPC more extensively than SPC. There was a relatively high amount of unhydrolyzed proteins after the hydrolysis of both protein preparations by bromelain.

3.3. Identification of Peptides Likely to Be Bitter Derived from SPC Hydrolysates

The results of identification of parent peptides in SPC hydrolysate samples are present in Table 3. The highest number of such peptides was identified in ficin and bromelain hydrolysates of SPC (five and four, respectively). Peptides derived from F-SPC matched the sequences originally encrypted in: 7S globulin (1 peptide), glycinin (1 peptide), and β -chain of β -conglycinin (3 peptides). In turn, in the case of B-SPC, parent peptides were matched glycinin and the β -chain of β -conglycinin (two peptides each). One parent peptide was reported in papain SPC hydrolysate (source: α -chain of β -conglycinin), whereas no peptides were found in proteinase K soybean protein hydrolysate. To summarize, the most effective enzymes producing in vitro the highest number of parent peptides were ficin > bromelain > papain. One parent sequence, i.e., LIVILNG, was identified in both B-SPC and P-SPC and matched both chains of β -conglycinin analyzed. All parent peptides identified in SPC hydrolysates contained motifs both with and without the status of a bitter-tasting indicator. Taking into consideration 339 parent peptides as the total sum of the sequences predicted as identified after in silico hydrolysis of soybean proteins and 10 parent peptides in vitro identified in SPC hydrolysates, the compatibility of the in silico and in vitro results of peptide identification was ca. 2.95%.

Table 3. Parent peptides identified in SPC hydrolysates using LC-MS/MS (Reversed-Phase High Performance Liquid Chromatography online with tandem Mass Spectrometry).

Protein Source	Parent Peptide	m/z (Da)	t _R predicted (min)	t _R experimental (min)	Motif ¹
B-SPC ²					
glycinin	LSVISPK	743.466	25.430	22.580	PK, VI
	DVLVIPLG	825.509	43.140	39.540	VL, VI, LG, LV ³
β-conglycinin (β-chain)	LIVILNG	741.487	38.280	39.390	VI, IV, LI, IL
	NPFLFG	694.356	41.170	39.860	FG, FL, LF, PF
F-SPC					
7S globulin glycinin	ISSTIV	619.367	25.520	24.770	IV
	PQMIIV	700.407	34.500	40.620	II, IV
β-conglycinin (β-chain)	PFPSIL	673.392	27.530	27.050	FP, PF, PFP, IL
	DDFFL	656.293	41.170	34.782	FF, FL
	FFEITPEK	1010.520	35.950	36.200	FF, EI
P-SPC					
β-conglycinin (α-chain)	LIVILNG	741.487	38.280	39.390	VI, IV, LI, IL

¹ Bitter-tasting indicators are given in bold; ² B-SPC, F-SPC, and P-SPC: bromelain-, ficin-, and papain-soybean protein hydrolysate, respectively (see the Materials and Methods); ³ peptides with no indicator status are given in normal font.

Parent peptides were considered as identified in SPC hydrolysate if (a) the fragment ions were observed in the particular retention time (t_R) and (b) t_R predicted and t_R experimental differed within the range of ±10% [19,22]. Peptide identification was understood as detection of a group of fragment (daughter) ions eluted in the same retention time [19,22,23]. Some of them could be formed via the non-sequential charge-directed pathway, leading to their formation by loss of water or the ammonia neutral molecule [24].

An example of a parent peptide that was identified in SPC hydrolysate fulfilling the above-mentioned criteria was the FFEITPEK sequence (Figure 2) containing two bitter-tasting indicators: FF and EL. The FFEITPEK was identified in an F-SPC sample and matched the β-chain of β-conglycinin. The m/z of the precursor (M+H)⁺ ion was 1010.500 Da. An intensive peak was observed in t_R experimental = 36.200 min (t_R predicted = 35.950 min). Moreover, the detection of this peptide in an F-SPC sample was confirmed by the presence of eight fragment ions that eluted within the above-mentioned time. They were as follows: X₄⁺, C₄⁺, B₈⁺, B₇⁺, B₆⁺, A₈⁺, Z₇⁺, and Y₅⁺, and their intensity was expressed from several hundred (Y₅⁺ ion) to thousands of counts (kCounts; all other fragment ions).

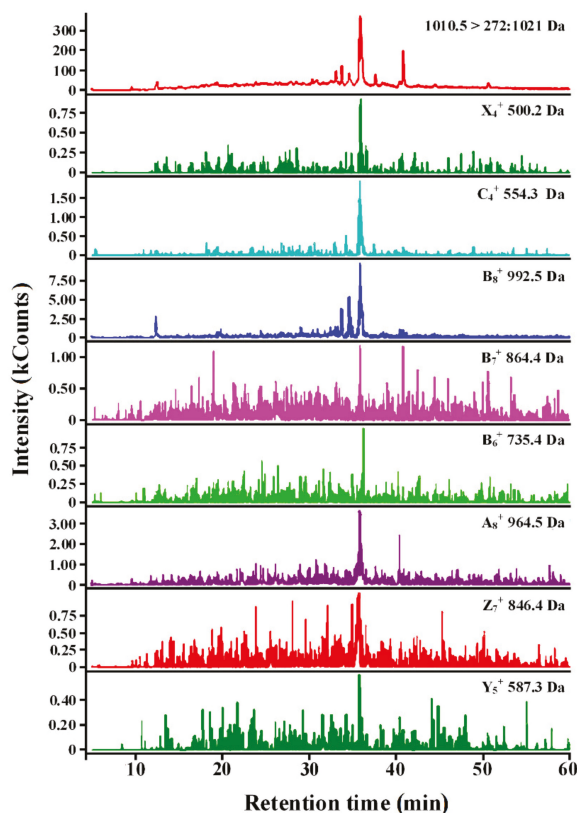


Figure 2. LC-MS/MS (Reversed-Phase High Performance Liquid Chromatography online with tandem Mass Spectrometry) chromatograms of total ion current (upper chromatogram: 1010.5 > 272:1021 Da) and daughter ions of the FFEITPEK peptide matching the β -conglycinin (β -chain) fragment, identified among products of the soybean protein concentrate hydrolyzed by ficin. Nomenclature of daughter ions according to Roepstorff and Fohlman [25].

One peptide, i.e., DDFFL, with two encrypted indicators: FF and FL, was identified in F-SPC. It matched the β -chain of β -conglycinin. The most intensive peak eluted for about 35 min (see Figure 3); however, the theoretical retention time calculated for this peptide was 41.170 min. The difference between $t_{R \text{ predicted}}$ and $t_{R \text{ experimental}}$ exceeded the threshold value of 10% for defining the peptide as identified [21]. The m/z of the $(M+H)^+$ precursor ion of the DDFFL peptide was 656.300 Da, and nine intensive peaks were observed in 35 min. They were the following fragment ions: X_2^+ , C_4^+ , B_4^+ , B_3^+ , B_2^+ , A_3^+ , A_5^+ , Z_2^+ , and Z_4^+ . All of them occurred in thousands of counts. Thus, the DDFFL peptide was considered as identified in the F-SPC sample. Some differences between predicted and experimental RT (retention time) were observed during the microLC-ToF-MS (i.e., micro liquid chromatography time-of-flight mass spectrometry) identification of bioactive peptides derived from yoghurt. According to Kunda et al. [26], such an unequivocal identification based on retention time differences is called Type 1 identity conflict.

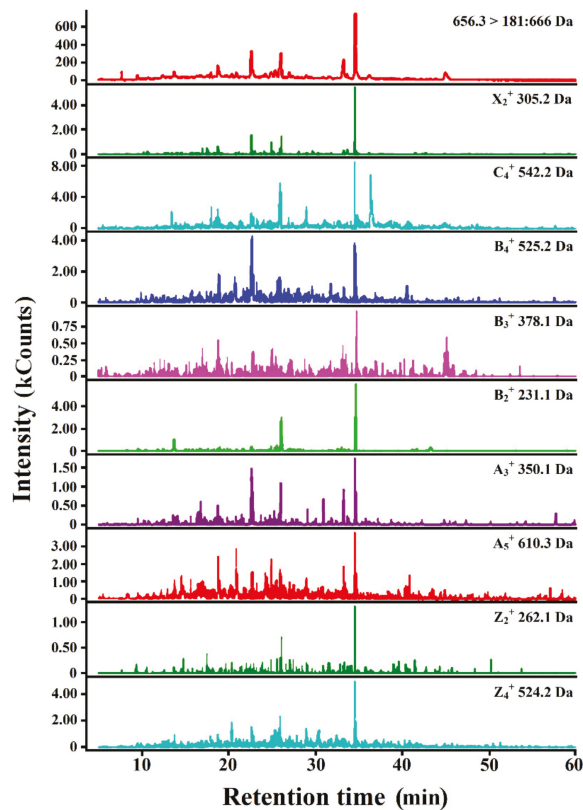


Figure 3. LC-MS/MS chromatograms of total ion current (upper chromatogram—656.3 > 181: 666 Da) and daughter ions of the DDFFL peptide matching the β -conglycinin (β -chain) fragment identified among products of hydrolysis of soybean protein concentrate by ficin. Nomenclature of daughter ions according to Roepstorff and Fohlman [25].

It is well documented in the literature that some biopeptides impart bitter taste, which is a limitation when thinking about their implementation in foods supporting the prophylaxis of diet-related diseases [27]. This especially concerns ACE-inhibiting peptides [28]. Some of the bitter-tasting motifs encrypted in all parent peptides identified in SPC hydrolysates showed an additional biological effect as judged by BIOPEP-UWM database screening (see Table 4). A more comprehensive list of the bioactivities of bitter peptides may be found in the Supplement to our previous review [29]. It was evidenced that the application of different proteases or the fermentation process of soybean proteins leads to obtaining the unique peptide profiles exhibiting, e.g., antihypertensive [30,31], hypocholesterolemic [32], antioxidative [33], and antidiabetic [1] effects. The majority of bitter fragments occurring in parent peptides that were identified in all SPC hydrolysates were associated with ACE-, DPP-IV-, and DPP-III-inhibiting or glucose uptake-stimulating activity. The first activity plays an important role in the reduction of blood pressure [34], while DPP-IV inhibitors are responsible for the antidiabetic effect [35], and the latter ones are involved in prolonging the action of endogenously released or exogenously applied enkephalins (i.e., a promising agent in chronic pain management) [36].

Table 4. Additional bioactivity of bitter motifs found in parent peptides identified in SPC (soybean protein concentrate) hydrolysate samples.

Parent Peptide	Motif ¹	Bioactivities
LSVISPK	PK ; VI, SV, SP	DPP IV inhibitor
DVLVIPLG	VL ; VI; LV; IP; PL LG ; PL; IP; PLG PLG VL ; LV	DPP IV inhibitor ACE inhibitor Opioid Stimulating glucose uptake
LIVILNG	VI ; LI; IL; LN; NG IL; LN; NG IV; IL; LI	DPP IV inhibitor ACE inhibitor Stimulating glucose uptake
NPFLFG	FL ; PF; NP FL ; PF FG ; LF	DPP IV inhibitor DPP III inhibitor ACE inhibitor
ISSTIV	IV ST TI	Stimulating glucose uptake ACE inhibitor DPP IV inhibitor
PQMIIV	II; MI; PQ IV; II PQ	DPP IV inhibitor Stimulating glucose uptake ACE inhibitor
PFPSIL	FP; PFP; IL FP; PF; IL; PS; SI IL PF	ACE inhibitor DPP IV inhibitor Stimulating glucose uptake DPP III inhibitor
DDFFL	FL FFL; DF	DPP IV inhibitor; DPP III inhibitor ACE inhibitor
FFEITPEK	EI ; TP; EK PE	DPP IV inhibitor; ACE inhibitor DPP III inhibitor

¹ Bitter-tasting indicators are given in bold, and peptides with no indicator status are given in normal font. Abbreviations: ACE, Angiotensin-converting enzyme (EC 3.4.15.1); DPP III, dipeptidyl peptidase III (EC 3.4.14.4); DPP IV, dipeptidyl peptidase IV (EC 3.4.14.5).

4. Discussion

The study above was divided into two steps: bioinformatic and experimental analyses. According to Tu et al. [37], bioinformatic analyses help in better understanding biological data and hence their application in food and nutrition increases. Moreover, the fact of the presence of some unique fragments within the primary structures of peptides underlies their different biofunctions. Bioinformatic studies enable minimizing the number of experiments involved to determine the impact of the structure of a peptide on its biological function [37]. Moreover, in silico experiments are relatively easy and less costly to carry out, and they do not require reagent and sample preparation [38]. Combining the bioinformatics with an experimental verification of the results is, in turn, a kind of methodology called an integrated (i.e., hybrid) approach. This term was introduced by Udenigwe [38], and ever since, many studies on bioactive peptides, including the present one, have implemented procedures to solve a problem using databases of biological information and then involving laboratory analyses [5].

To the best of our knowledge, the hybrid and fragmentomic approaches have not been applied so far to analyze the potential of soybean proteins as the reservoir of bitter-tasting motifs. Moreover, our protocol of research was partially based on positive selection [39], i.e., finding in the protein the sequential motifs with already known biological function (i.e., provided in a database). Fu et al. [39] employed this strategy to evaluate the potential of patatin (*Solanum tuberosum*; potato protein) as a source of biopeptides. The biological dataset (peptide sequences) was acquired from the BIOPEP-UWM database. The novel aspect of our research was the use of the positive selection to define bitter-tasting motifs (especially peptide indicators) in parent sequences potentially released from soybean. According

to Agyei et al. [40], the prediction of the bitter taste of foods may support the development of the procedures for masking this taste. Although such a strategy of research has some limitations, it may help discover new peptides [40]. This is a universal approach that may be applicable to in silico assessment of any protein as the reservoir of peptides with any biological function. Although the term “fragmentomics” is not widely used in publications, it represents one of the common contemporary strategies of research on bioactive peptides. Recent applications of fragmentomics concerning the bioactivity of peptides derived from various food sources have been described by Sutopo et al. [41], Alcaide-Hidalgo et al. [42], and Kinariwala et al. [43].

As was said above, the substrate for bioinformatic analyses was the sequences of five soybean proteins, which were subjected to the theoretical hydrolysis using four enzymes: bromelain, ficin, papain, and proteinase K. According to the literature, soybean is widely used in human nutrition and animal feeding due to the high biological value of its proteins. Moreover, it is the least expensive source of protein, which may be helpful in solving feeding and agronomical problems [44]. However, hydrolysis of proteins, also these from soybean, contributes to the production of peptides that taste bitter and are not accepted by Western consumers, even if they offer a health-beneficial value [45,46]. Our initial bioinformatic predictions also confirmed the potential of soybean proteins as the richest sources of bitter-tasting sequences when comparing them to the other sequences of proteins derived from grains, oil, and leguminous plants (21 sequences in total; data not shown). This comparison was made based on one of the criteria serving to evaluate proteins as sources of peptides with a particular bioactivity (i.e., bitterness in this case) defined as the frequency of the occurrence of bitter peptides in a protein chain, a parameter called “A” available in the BIOPEP-UWM database (data not shown). According to the scientific reports, the higher the A, the better the potential of a protein to release peptides with a specified biofunction [47]. A similar trend was successfully followed by Kęska and Stadnik [48], who analyzed 16 sequences of porcine proteins as sources of tastant peptides. The potency of myofibrillar and sarcoplasmic proteins was estimated based on the values of a parameter called “abundance of taste-active peptides/amino acids in a protein sequence” (A_R), being mathematically a twin version of the A value provided in the BIOPEP-UWM database. A_R calculations enabled a theoretical indication about which of the porcine proteins may have the strongest impact on the sensory properties of meat products [48].

Most of the endopeptidases that are applied to produce soybean protein hydrolysates are derived from microorganisms and/or plants. Among them, bromelain, papain, and ficin are stated as the enzymes with large scale availability when comparing them to the proteases originating from animal sources [49]. Although, the analysis of the scientific reports did not show any data about the possible application of the fourth enzyme, i.e., proteinase K, aiming to produce peptides from soybean proteins, this enzyme was included on the in silico part of the study. This decision resulted from the comparison of the effectiveness of almost all enzymes available in BIOPEP-UWM (expressed as the number of peptides released) to produce potentially bioactive peptides, especially tastant peptides (data not shown). The comparison excluded pepsin, trypsin, and chymotrypsin as digestive tract enzymes. They naturally digest proteins when ingested [46].

The results of the enzymatic release of a fragment containing bitter-tasting motifs with and without the status of an indicator are presented in Table 1. This way of data analysis fits the research trend of fragmentomics relying on ascribing the “unknown” biological function of a molecule to the known function of motifs occurring in it and is based on positive selection (see above) [7,39]. In our study, the molecule with no predicted function was a compound called the parent peptide, whereas the motif deciding its possible function was the bitter-tasting peptide. Thus, to be consistent with the fragmentomic idea, data analysis was limited to the released peptides composed of at least four amino acids. Data about the bitterness of such peptides were implemented from the BIOPEP-UWM database of sensory peptides and amino acids [20]. Based on the MLR stepwise regression analysis, some of these peptides were selected as bitter-tasting peptidic indicators, i.e., peptides with approximate predicted and experimental R_{caf} values [13]. MLR is one of the chemometric techniques that enables analyzing

the relationship between the structure (i.e., sequence) of a peptide and its biological activity, which is called QSAR (i.e., quantitative structure-activity relationship) [50]. According to Chanput et al. [51], the QSAR methodology is one of the important methods for the analysis of the functionality of peptides. The results of MLR showed that the bitter taste of a peptide is attributable to the presence of some specific residues, like Leu, Ile, Val, Phe, and Tyr [13]. This observation was consistent with the statements of other authors studying bitter peptides using QSAR techniques [52].

Ample *in silico* studies have been undertaken to evaluate proteins as sources of peptides with various bioactivities using the BIOPEP-UWM database [12]. The analysis of data concerning theoretical release of peptides can be considered from several perspectives, namely: how the length of motifs affects their match to the parent peptides; how the length of the parent peptide contributes to the presence of a bioactive motif in it; and finally, how the length of protein affects the number of parent peptides to be produced. As could be seen, parent peptides that were theoretically released from soybean proteins were the sources of bitter motifs with and/or without the status of an indicator. The great majority of such motifs were dipeptides. According to Iwaniak and Dziuba [53], the match of the motif to the query sequence depends on its chain length (i.e., the shorter, the better). The potential of parent peptides as sources of peptides with a specified function can be quantitatively evaluated using the A parameter (see above). So far, the discriminant A had been successfully applied to compare proteins according to the rule: the higher the A value, the better source of biopeptides the protein of interest is [47]. As regards the parent sequences, no regularities were observed between their chain length and the increasing tendency in the occurrence of bitter-tasting motifs. An example in this case is the DIFL/FL, IF peptide (from β -conglycinin β -chain hydrolyzed with ficin). Its A value was 0.500. The ETSFHSEFEEIN peptide was derived from the same source as DIFL and contained two bitter-tasting motifs: EI, EF. Hence, its A value was 0.166. In the case of parent peptides, also their particular amino acid composition is crucial to predict their biological function including the likelihood of them to taste bitter. To exemplify it, these two criteria were fulfilled for parent peptide FSHNILETSFHSEFEEINRVLFG/FG, LF, VL, LE, IL, EI, EF theoretically released from β -conglycinin β -chain hydrolyzed with bromelain. The A value for this peptide was 0.304. Finally, those protein sequences that had the longest amino acid chains represented the best potential to produce several tens of peptides. This rule also suggested the higher probability of peptide release in laboratory conditions [54]. In the case of the *in silico* results obtained, the highest number of parent peptides likely to be bitter due to the presence of bitter-tasting motifs was produced from α - and β -chains of soybean β -conglycinins. According to literature reports, glycinin and β -conglycinin represent about 65–85 % of the total soybean proteins, and they are known as good reservoirs of bioactive peptides [46].

All *in silico* results encouraged us to continue studies using laboratory analyses, starting from the hydrolysis of SPC. Hydrolysis was conducted for 3% (w/v) water solutions of SPC. According to Arboleda et al. [55], commercial soybean preparations available in the form of powder (as used in our study) are highly soluble in water if the protein solution does not exceed 20 %. The enzyme-to-substrate ratio for all four samples to be hydrolyzed was 1:100 (protein; w/w). Such proportions of enzymes and substrate were applied by Peña-Ramos and Xiong [15] for the hydrolysis of soy protein isolate using crude enzymes, like papain, pepsin, and chymotrypsin, as well as commercial proteases to measure the antioxidant activity of hydrolysates.

RP-HPLC comparison of the percentages of the peak areas of all SPC hydrolysate samples allowed monitoring the process of their hydrolysis. The analysis of RP-HPLC chromatograms was successfully applied to observe the progress of hydrolysis of carp, herring, and milk proteins [9,22]. The changes in peak areas observed in different time intervals enabled concluding that SPC hydrolysis took place and allowed identifying parent peptides in the SPC hydrolysate samples using RP-HPLC-MS/MS.

Discrepancies were observed between the number of parent peptides that were identified *in silico* and *in vitro*, which is a common fact in the literature [56]. One of the possible reasons behind differences between the *in silico* and *in vitro* results was the fact that the sequences produced using the *in silico* method had to match those already present in the database [9]. The results of this work showed

the successful identification of nine parent peptides in total (see Table 3) in all SPC hydrolysates, whereas the *in silico* simulation of hydrolysis of soybean sequences allowed obtaining 339 parent peptides. Bucholska and Minkiewicz [22] defined the likely reasons that may affect the unsuccessful identification of peptides in a hydrolysate sample. They included no detectable amount of peptide in the sample (e.g., if some peptide bonds likely to be cleaved are actually resistant to hydrolysis) and no detectable fragmentation in an ion trap mass spectrometer. Additionally, peptides identified in SPC hydrolysates are defined as proteotypic peptides, and their identification is dependent on the mass spectrometer used. Finally, there is no method that would serve for the identification of all possible peptides in a protein hydrolysate [22]. The last reason for the discrepancy might be the fact that *in silico* predictions assume that all peptide bonds are hydrolyzed in a protein chain.

Ficin was the most effective enzyme for producing peptides *in vitro*, whereas bromelain in the theoretical production of parent peptides likely to be bitter. Enzyme rankings were as follows: bromelain > papain > ficin > proteinase K (in *in silico* results) and ficin > bromelain > papain (in *in vitro* results). There was no correlation between the results of RP-HPLC (C parameter from Table 2) and the number of identified peptides with bitterness indicators. Despite the differences between these rankings, the richest source of parent peptides produced by the applied enzymes turned out to be conglycinins. No parent peptides that were identified in all SPH matched the sequences known as bitter themselves. Moreover, none of these peptides were found as bioactive themselves (see Table 4). Iwaniak et al. [9] identified some parent peptides likely to be bitter in milk protein hydrolysates. For example, the PFPIIV peptide matched the bitter-tasting sequence in the BIOPEP-UWM sensory peptide database (peptide ID in the database: 195). PFPIIV was known as bitter itself, contained PFP, PE, IV, **FP**, **II** bitter motifs, and was identified in bromelain, ficin, and papain hydrolysates of milk protein concentrate. Moreover, two milk protein-derived peptides: TTMLPW (source: papain hydrolysate) and VLPVPQK (source: bromelain hydrolysate), served additional biofunctions. Based on information found in the BIOPEP-UWM bioactive peptide database, the first sequence exhibited opioid, immunomodulating, and ACE inhibitory effects (peptide IDs in the database: 3127, 8172, and 3520, respectively). The second one was reported as an antioxidative agent (peptide ID: 7877) [9]. As was said above, bitterness associated with bioactive peptides may be found as an unwanted property when thinking about the production of food that is health-beneficial and sensorially-attractive [57]. Hence, our concept relying on the fragmentomic idea of research was useful to: (1) find out if the parent peptides were bitter/bioactive themselves or (2) motifs like, e.g., peptidic bitterness indicators that are encrypted in a sequence exhibiting other activities, may “suggest” the bioactivity/taste of the parent sequence. This concept shows also the potential of enzymes to produce motifs supposed to be bioactive/bitter. The enzymes’ potential to produce unwanted peptides may initially be also an indicative criterion of their “negative” selection (i.e., rejection) when considering the production of non- or less bitter hydrolysates. However, according to Fu et al. [39], it needs to be noted that although the theoretical predictions concerning the potential of proteins as sources of peptides and enzymes involved in their production can support further research, such predictions are never 100% consistent with experimental results. This is also true concerning our concept.

The discrepancies between *in silico* and *in vitro* results may be associated with the specificity of bioinformatic and experimental analyses. Bioinformatic issues are related to the tools used for predictions, especially databases of biological information. Many data on biological peptides are published every year. Our quick search in Scopus (accessed: January 2020) showed 188 records reflecting the number of articles that were published in 2018 (about 15.7 per month) and contained the following exact words as queries “bioactive peptides AND food proteins”. The same query words were used to the search for the articles published in 2019. This simple search showed 241 papers published in 2019 (i.e., 20.08 per month). Both searches were limited to articles, and they excluded conference abstracts. Thus, it may appear that there are some biological activities represented by both parent peptides and their bitter-tasting motifs that were published after this paper was released, and thus, they were not included when we ran these studies. A similar search for the latest publications

concerning sensory peptides showed no new sequences with confirmed bitterness that could be downloaded to the BIOPEP-UWM database and used for further analyses. Thus, our results concerning the presence of bitter-tasting motifs in parent sequences seemed to be relatively steady. Nevertheless, it is recommended to carry out the regular update of databases [38], as well as to use curated databases, like, e.g., BIOPEP-UWM [12].

Experimental issues that possibly affect the differences between *in silico* and *in vitro* results may be related to the hydrolysis of protein. Theoretical hydrolysis via bioinformatic tools, including BIOPEP-UWM, is based on the specificity of an enzyme, and hypothetically, all peptide bonds are accessible to enzymatic cleavage [58]. The cleavage of peptide bonds is one of the descriptors characterizing the nature of the enzyme [59]. However, the effectiveness of enzymatic hydrolysis depends also on the temperature, the pH, the enzyme-to-substrate ratio [46], and the types of the molecules affecting the inhibition of the enzyme [60], which are difficult parameters to be included as the “elements” of programs serving for theoretical proteolysis. Moreover, such predictive hydrolysis is relatively simple, especially when the protein is not chemically modified. For example, glycosylated amino acids present in a protein may block the breakdown of a peptide bond in experimental conditions [61]. Additionally, the computer simulation of hydrolysis does not consider the complexity of the protein structure that might hinder its interactions with proteolytic enzyme [58]. Rawlings [62] added to this list some other factors likely to affect the results of proteolysis carried out in experimental conditions, i.e.: location of the enzyme and substrate in different extra- and intra-cellular regions and the involvement of inhibitors. They are not considered by programs for theoretical hydrolysis. In turn, Ashaolu [46] highlighted that proteolysis of soybean carried out in experimental conditions enabled the reduction of waste, establishing the mild conditions of reaction, avoiding unwanted reactions; however, the obstacle is the cost of enzymes, as well as the recovery and/or removal of bitter taste [46].

Despite the discrepancies between the *in silico* and *in vitro* results of the hydrolysis of proteins aiming to produce biopeptides, scientists use the hybrid approach more often [63]. Iwaniak et al. [9] applied this protocol to hydrolyze milk protein concentrate using exact enzymes as in the study above. They showed that the results of experimental and theoretical analyses differed. Twenty-eight peptides with the potential to affect the bitter taste of hydrolysates were produced in laboratory conditions, which was consistent by ca. 12 % with computer simulations (226 parent peptides identified *in silico*). Darewicz et al. [19] used the *in silico/in vitro/ex vivo* analyses to study the potential of salmon (*Salmo salar*) proteins as the source of ACE inhibitory peptides. To verify the *in silico* results in laboratory conditions, protein hydrolysis was carried out *in vitro* (with commercial enzymes) and *ex vivo* (using digestive juices from volunteers). It was confirmed that some ACE inhibitors were identified in both hydrolysates; however, some of them were observed either in the *ex vivo* or in the *in vitro* salmon protein hydrolysate [19].

To recapitulate, the comparison of *in silico* and *in vitro* results also differed in our experiment concerning soybean proteins as the material. Nevertheless, they still can be supportive when predicting the bitter-tasting properties of parent peptides based on the fragmentomic approach. Citing the words of Li et al. [64], “the BIOPEP-UWM database is a useful data source that supports the analysis of connections between peptide molecular structures and their sensory properties, and additionally enables users to build a potential sensory profile of peptides”. The BIOPEP-UWM database was applied to predict the umami taste of peptides derived from clam *M. meretrix Linnaeus* [64]. Garcia-Vaquero et al. [45] applied the hybrid approach to assess the bitter taste properties of novel peptide ACE inhibitors derived from *U. lactuca* (green algae). To this end, green algae proteins were *in vitro* (enzyme used: papain) and *in silico* (tool used: PeptideCutter) hydrolyzed. The bitterness of peptides that were identified in the hydrolysates of *U. lactuca* was predicted based on the calculation of the Q-value introduced by Ney [65]. The Q-value is empirically associated with the hydrophobicity of each amino acid in a peptide sequence. Such a correlation is defined as the Q-rule, according to which the peptide likely to be bitter should have Q over 1400 cal/mole [66]. Based on the Q-rule, it was found that the following green algae-originating sequences: SAGVLPWK (GV, VL), GAAPTPSPPPATKPSTPPKPPT (PK,

KP, PPP), IECCLLFALV (**LL**), PVGCLPK (**PK**), DAVEIWRVK (**VE, EI**), DEVIPGAL (**VI**), **PKPPALCN (PK, KP)**, and PPNPPNPPN, were characterized with Q-values ranging from 1440 to 1743.33 cal/mol, which suggested they could taste bitter [45]. Defining these sequences as “parent peptides” and implementing the fragmentomic idea, we found that seven out of eight such peptides contained motifs (in bold) described as bitter-tasting indicators (provided in brackets). Working the opposite way, we calculated Q-values (cal/mole) for all parent peptides that were experimentally identified in SPC hydrolysates. They were as follows: 1611.43 (**LSVISPK**), 1793.75 (**DVLVIPLG**), 1780.00 (**LIVILNG**), 1721.66 (**NPFLFG**), 1358.33 (**ISSTIV**), 1908.33 (**PQMIIIV**), 2220.00 (**PFPSIL**), 1760.00 (**DDFFL**), and 1741.25 (**FFEITPEK**). Only one peptide (**ISSTIV**) had the Q-value below 1400 cal/mole. Based on the Q-value, the other peptides identified in SPC hydrolysates containing bitter-tasting motifs with and without the status of an indicator could be classified as bitter. However, some studies on the bitterness of peptides indicated that some of them with the Q-value lower than 1400 cal/mole also tasted bitter. An example of such a peptide is the **EVLN** sequence (Q-value = 1162.5 cal/mole) identified in cheddar cheese and matching α_{s1} -casein as a protein precursor [67]. Moreover, taking into account our point of view, this peptide contains the **VL** bitter-tasting motif, which may be crucial in defining the taste of the whole sequence. Another aspect related to parent peptides likely to be bitter is their size [68]. According to the literature, peptide fractions of soybean protein hydrolysates with molecular weight ranging from 1.9 to 3.3 kDa were characterized by the highest bitterness, whereas the bitterness of other fractions with lower or higher molecular weight than indicated above was milder [68]. Our parent peptides differed in the molecular weight. Thus, the strategy for the elimination of the unwanted taste of a hydrolysate should also be based on the knowledge concerning the amino acid composition of peptides [49]. This point of view fits the fragmentomic idea of the research presented in this article.

The example of positive selection [39] (see above) can be also applicable to enzymes used for the hydrolysis of protein to release peptides. Briefly, the enzyme that is *in silico* the most effective at producing bioactive peptides may be selected for the hydrolysis of proteins in experimental conditions. This allows identifying the most effective enzymes releasing peptides likely to be bitter (i.e., possessing an unwanted property) from soybean proteins. When thinking about bitterness, such a strategy of research may be the starting point for negative selection, which is the elimination of such enzymes to avoid the production of peptides with the undesired taste. However, the elimination of the enzyme might be problematic if it produces many bitter sequences exhibiting an additional, health-beneficial effect. In such a case, some further procedures should be considered to reduce the bitterness of bioactive hydrolysates. An example of such a procedure is the treatment with exopeptidases [69]. Cheung et al. [69] hydrolyzed whey protein isolates with different commercial endopeptidases and obtained a bitter-tasting ACE-inhibitory hydrolysate. To reduce its bitterness, the hydrolysis was extended with exopeptidases treatment. The taste of this hydrolysate was then more acceptable because of the removal of terminal residues as a result of exopeptidase action [69].

To summarize, our idea of research showed that the potential property of peptides released from proteins might be predicted based on the presence of sequential motifs with already known function (so-called positive selection). This helps understanding some relationships between the structure of a molecule and its activity (e.g., bitter taste). It needs to be noted that although it is possible to prognose the potential of released peptides to taste bitter, such a statement should be confirmed in laboratory conditions [70].

Our methodology might be an effective and universal way to analyze the biological functions of peptides found in protein hydrolysates. Although each of the methodologies contributing to the discovery of bioactive peptides has some limitations and specific character, the strategies involving the wide range of *in silico* approaches combined with conventional studies can play an important role in the generation and discovery of new peptides [71]. Thus, the employment of several methods for the theoretical prediction of the bitterness of a molecule is inscribed into this trend and is highly recommended.

5. Conclusions

Results concerning the production of peptides likely to be bitter derived from soybean proteins showed the discrepancies between *in silico* and *in vitro* results. These discrepancies concerned the number of parent peptides released when applying theoretical and experimental hydrolysis, as well as the ranking of enzymes effective in the production of peptides possessing di- and tri-peptide motifs defined as indicators. The compatibility percentage of *in silico* and *in vitro* results was less than 3%. However, all parent peptides that were identified in SPC hydrolysates contained motifs having or not the status of bitter-tasting indicators. Their Q-values suggested they could taste bitter. Thus, it could be concluded that the fragmentomic idea of research analyzing the composition of a parent sequence might be a supportive tool for the prediction of the taste of foods. Moreover, it broadens the knowledge about the structural nature of peptides as bioactive/tastant molecules. However, it is postulated that such statements concerning the peptides likely to be bitter should be evaluated experimentally.

Author Contributions: Conceptualization, A.I.; methodology, A.I., M.H., and P.M.; investigation, A.I., M.H., J.B., P.M., and M.D.; resources, M.D. and P.M.; writing, A.I. and M.H.; writing, review and editing, A.I. and M.D.; funding acquisition, M.D. All authors have read and agreed to the published version of the manuscript.

Funding: Project financially supported by the Minister of Science and Higher Education in the range of the program entitled “Regional Initiative of Excellence” for the years 2019-2022, Project No. 010/RID/2018/19, amount of funding 12,000,000 PLN, as well as the funds of the University of Warmia and Mazury in Olsztyn (Project No. 17.610.014-110).

Conflicts of Interest: The authors declare no conflict of interest.

Abbreviations

0-SPC	Soybean protein concentrate before hydrolysis
A	Depending on the context: one-letter symbol alanine (amino acid) or A-type fragment (daughter) ion according to Roepstorff and Fohlman [25]
ACE	Angiotensin-converting enzyme (EC 3.4.15.1)
ACN	Acetonitrile
B	Depending on the context: bromelain (EC 3.4.22.32) or B-type fragment (daughter) ion according to Roepstorff and Fohlman [25]
BIOPEP-UWM	Depending on the context: database of bioactive peptide sequences [12] or database of sensory peptides and amino acids [20]
Bis-Tris	2,2-bis(hydroxymethyl)-2,2',2''-nitrilotriethanol
B-SPC	Soybean protein concentrate hydrolyzed by bromelain
C	Depending on the context: parameter to compare susceptibility of proteins to proteolytic enzymes on the basis of chromatograms (calculated using Equation (1)) or C-type fragment (daughter) ion according to Roepstorff and Fohlman [25]
DPP III	Dipeptidyl peptidase III (EC 3.4.14.4)
DPP IV	Dipeptidyl peptidase IV (EC 3.4.14.5)
F	Depending on the context: ficin (EC 3.4.22.3) or one-letter symbol of amino acid phenylalanine in peptide sequences
F-SPC	Soybean protein concentrate hydrolyzed by ficin
HMGCR	3-hydroxy-3-methylglutaryl-coenzyme A reductase (HMG-CoA reductase) (EC 1.1.1.34)
HPLC	High performance liquid chromatography
MLR	Multivariate linear stepwise regression
MPC	Milk protein concentrate
P	Depending on the context: papain (EC 3.4.22.2) or one-letter symbol of amino acid proline in peptide sequences
P-SPC	Soybean protein concentrate hydrolyzed by papain
PK	Depending on the context: proteinase K (EC 3.4.21.64) or dipeptide prolyl-lysine annotated using one-letter code

PK-SPC	Soybean protein concentrate hydrolyzed by proteinase K
Q-value	Average free energy for the transfer of the amino acid chains from ethanol to water [65]
RP-HPLC	Reversed-phase high performance liquid chromatography
RP-HPLC-MS/MS	Reversed-phase high performance liquid chromatography online with tandem mass spectrometry
S	Depending on the context: symbol of relative area of peaks in defined data interval (in Equation (1)) or one-letter symbol of amino acid serine in peptide sequences
SPC	Soybean protein concentrate
SSRCalc	Sequence-Specific Retention Calculator
TFA	Trifluoroacetic acid
t _r	Retention time (e.g., in Equation (2))
UWM	University of Warmia and Mazury in Olsztyn
Y	Depending on the context: one-letter symbol of amino acid tyrosine in peptide sequences or Y-type fragment (daughter) ion according to Roepstorff and Fohlman [25]

Appendix A

Table A1. Parent peptides released in silico from soybean proteins containing bitter-tasting peptides with and without the indicator status (bold and normal font, respectively).

Parent peptides released from proflin due to the simulated action of:			
B ¹	F	P	PK
VDDHLLCDIEG/VD, LL, EG	CDIEG/EG	VDDH/VD	EGNH/EG
IIG/II, IG	IIG/II, IG	LLCDIE/LL	QGEP/GE
QSTDFPQFK/FP	QSTDFPQFK/FP	QSTDFPQFK/FP	RGKKG/PG, GP
PEEITA/EI	PEEITA/EI	MVIQG/VI	DQGY/GY
MVIQG/VI	ERPG/RP, RPG	LIIG/II, IG , LI	
VIRG/VI, RG		QCNMVE/VE	
LIIG/II, IG		LIDQG/LI	
QCNMVERPG/RP, RPG, VE			
LIDQG/LI			
Parent peptides released from globulin 7S due to the simulated action of:			
B	F	P	PK
PINLVLPVQNDG/VL, LV	PFCHSTQCSRA/PF	PINLVLPVQNDG/VL, LV	QNDGSTGL/GL
RTPLMQVPVLVDLNG/VL, VD, LV, DL	SRPG/RP, RPG	TPLMQVPVLVDLNG/VL, VD, LV, DL	AASRP/RP
PFCHSTQCSRA/PF	PQFL/FL	DVLA/VL	GCHKNTCGL/GL
SRPG/RP, RPG	PSFL/FL	STQQLG/LG	TQQTGL/GL
EDVLA/VL	SHFG/FG	STQQLG/LG	GEDV/GE
STQQLG/LG	IIFG/FG, IF , II	PLVTVPQFLFSCA/FL, LE, LV	QKGL/GL
PLVTVPQFLFSCA/FL, LE, LV	QDIFHDL/IF, DL	LV	RNTQGV/GV
PSFLVQK/FL, LV	ISSTIV/IV	PSFLVQK/FL, LV	GDAP/DA
LPRNTQG/PR	MQPRA/PR	IIFG/FG, IF , II	QGEY/GE, EY
SHFG/FG	EITL/EI	QFQNQDIFH/IF	SGEDL/GE, DL
IIFG/FG, IF , II		SVFPLNK/FP, VF	RAEI/EI
PNNMRQFNQDIFHDLA/IF, DL		ISSTIV/IV	EENL/EEN
NVRVNSIRINQHSVFPLNK/FP, VF		MVLVQSVY/VY, VL	HSHGV/GV
ISSTIV/IV		FTQVFA/VF	KCADL/AD, DL
TMISTSTPHMVLQSVY/VY, VL		QQLPK/PK	
FTQVFA/VF		PSVDLVMDK/VD, LV, DL	
QQLPK/PK		DLMVQA/DL	
PSVDLVMDK/VD, LV, DL		VTCLG/LG	
EDLMVQA/DL		MQPR/PR	
VTCLG/LG		ITLG/LG	
MQPRA/PR		NLVVFDLA/VF, LV, DL	
EITL/LG, EI		DLFNFA/LE, DL	
RQLEENLVVFDLA/VF, LE, LV, DL, EEN			
DLFNFA/LE, DL			

Table A1. Cont.

LEPDHRVESEG/VE, LE, EG	ESEG/EG	PQMIIVVQG/IV, II, VV	TSSKF/KF
LIETWNSQHPPELQCA/LI, EL	SQHPEL/EL	DVLVPLG/VL, VI, LG, LV	ESEGL/EGG, GL, GGL, EG
PQMIIVVQG/IV, II, VV	PQMII/II, IV	PVVA/VV	QCAGV/GV
PQQQSSRRG/RR, RG	PQQQSSRRG/RR, RG	ISPLDTSNFNN	QQQSSRRGSRSSQQQL/RR, RG
IRHFNEG/EG	QHRQQEEEG/EG	QLDQNP/PR, LD	NEGDV/EG
DVLVPLG/VL, VI, LG, LV	ISPK/PK	SVLSG/VL	QQQQQKSHGG
DEPVVA/VV	WQEQEDEDEDEEY/EY	QIVTVE/VE, IV	RKQGQHRQQEEE
ISPLDTSNFNNQLDQNP/PR, VF, LD	PPRRPSHG/RR, PP, RP, PR	LSVISPK/PK, VI	GGSV/GR, EGG, EG
QHRQQEEEG/EG	PR	DQPR/PR	EGGL/EGG, EG, GGL, GL
SVLSG/VL	HEDEDEDEEEDQP	PPQR/PP	QEQEDEDEDEEY/EY
HFLA/FL	RPDHPQRPSR	VVLY/VV, VL	GRTP/GR
QIVTVEG/VE, IV, EG	PEQQEPRG/PP, RG, RP, RP, PR, PR	VVNCQG/VV	RGRCCQTRNGV/RG, RG, GR, GV
LSVISPK/PK, VI	RP, RP, PR, PR	VFDG/VF	SRADF/AD
WQEQEDEDEDEEY/EY	RPSRA/RP	QLLVVPQNP/LL, LV, VV	KAGRI/GR
PPRRPSHG/RR, PP, RP, PR	RQFG/FG	VVFK/VF, VV	TRGKGRV/RG, GR
HEDEDEDEEED	TMTRG/RG	DVFR/VF	DGEL/GE, EL
QPRPDHPQRPSRPEQQ		VIPSE/VI	RRQL/RR, RG
EPRG/PP, RG, RP, RP, PR, PR, PR		VLSNSY/VL	AEQGGEQGL/GE, GL
VEENICTMK/VE, EEN		PLVNP/LV	QGNSSGP/GP
RPSRA/RP			
LRQFG/FG			
VVLY/VV, VL			
NSVTMTRG/RG			
RVRVNCQG/VV			
VFDG/VF			
ELRRG/RR, RG, EL			
QLLVVPQNP/LL, LV, VV			
VVFK/VV, VF			
DVFRVIPSEVLSNSY/VF, VI, VI			
PLVNP/LV			
Parent peptides released from β-conglycinin (β-chain) due to the simulated action of:			
B	F	P	PK
VREENNPFY/PF	QRFN/RF	NNPFY/PF	QSKP/KP
FRSSNSFQTLFENQNVIR	DDFFL/FF, FL	SSNSFQTLFE/LF	HHADAF/AD, AD, DA
LLQRFNK/RF, LE, LL	ETSFHSEFEIN/EI, EF	LLQR/LL	SGRAI/GR
RSPQLENLRDY/LE	EEEEQRQQEG/EG	SPQLE/LE	GDAQRI/DA
RIVQFQSK/IV	SRRA/RR	IVQFQSK/IV	HSEF/EF
PNTILLPHHA/LL, IL	TISSEDPFN/PF	PNTILLPH/LL, IL	GEEEEQRQQEGV/GV, GE, EG
DFLFLVLSG/FV, FL, LE, VL, LL	FFEITPEK/FF, EI	DFLFLVLSG/FV, FL, LE, VL, LL	SRRAKSSSRKTI/RR
ILTLVNNDDRDSY/LV, IL	DIFL/FL, IF	ILTLVNNDDR/LV, IL	NEGAL/EG
LVNPHDHQNLK/LV	PPPSIL/FP, PE, PFP, IL	LVNPH/LV	NEGANI/DA, EG
DDFFLSTQA/FF, FL		DDFFLSTQA/FF, FL	RAEL/EL
FSHNILETSFHSEFEINRVLFG/FG,		NILE/LE, IL	AGEKDNV/GE
LE, VL, LE, IL, EI, EF		VLFG/VL, FG, LF	DAQP/DA
EEEEQRQQEG/EG		VIVE/VI, VE, IV	QQKEGSKGRKGP/GR, GP, EG
VIVELSK/VI, VE, IV, EL		PFNLR/PF	
EQIRQLSRRA/RR		SNNFG/FG	
TISSEDPFNLRSRNPIY/PF		DLDFLSSVDINE/FL, IF, VD, LD, DL	
SNNFG/FG		LLLPH/LL, LL, LLL	
FFEITPEK/FF, EI		IVILVINE/VI, VI, IV, LV, IL	
NPQLRDLDFLSSVDINEG/FL, IF,		DDVFVIPA/FV, VE, VI	
VD, LD, DL, EG		PFVVNA/FV, PE, VV	
LLLPHFNSK/LL, LL, LLL		TSNLNFLA/FL	
IVILVINEG/VI, VI, IV, LV, IL, EG		NFLA/FL	
NIELVG/LV, EL, VG		DNVVR/VV	
QEEEPLEVQRY/LE		QDVE/VE	
ELSEDDVFVIPA/FV, VF, VI, EL		FVDA/FV, VD, DA	
PFVVNA/FV, PE, VV		PPPSILG/FP, PE, PFP, LG, IL	
TSNLNFLA/FL			
ENNQRNFLA/FL			
DNVVRQIERQVQELA/EL, VV			
QDVERLLK/VE, LL			
FVDA/FV, VD, DA			
PPPSILG/FP, PE, PFP, LG, IL			
LY			

Table A1. Cont.

Parent peptides released from β -conglycinin (α -chain) due to the simulated action of:			
B	F	P	PK
EECEEG/EG	EECEEG/EG	PIPFPR/PR, FP, PF, PFP, PIP	EKEECEGEI/GE, EG, EI
EIPRPRPRQHPEREPQPG/RP, RP, RP, PR, PR, EI	EIPRPRPRQHPER	PQPR/PR	GEKEEDEDEQP/GE
EEDEDEQPRPIPFPRPQ	EPQQPG/RP, RP, RP, PR, PR, EI	QFPFPR/PR, FP, FP, PFP, PE, PFP	RKEEKRGKGSSEED
PRQEEHEQREEQEWPRK/RP, RP, PR, PR, PR, FP, PF, PFP, PIP	EEDEDEQPRPIPFPR	NPFLFG/FG, FL, LF, PF	EDEDEQDERQF/RG, GE
SEEEDEDEEEQDE	PQPRQEEHEQR	TLFK/LF	HQKEERNEEEDDEE
RQFPFPRPHQK/PP, RP, PR, FP, FP, PFP, PF, PFP	EEQEWPRK/RP, RP, PR, PR, PR, PR, FP, PF, PFP, PIP	VLQR/VL	QQRESESESEL/EL
EERNEEEDDEEQRE	DERQFPFPRPHQK/PP, RP, PR, FP, FP, PFP, PF, PFP	PNTLLLPNH/LL, LL, LLL	RRHKNKNP/RR
SESESESELRRHK/RR, EL	SEEEDEDEEEQ	LIVLNG/VI, IV, LI, IL	GSNRF/RF
NPFLFG/FG, FL, LF, PF	EESESESEL/EL	ILSLVNNDDR/LV, IL	NSKP/KP
SNRFETLFK/RF, LF	PPF	VVNPDNNE/VV	NHADADY/AD, AD, DA
RIRVLQRFNQRSPLQNLRDY/RF, VL	EEDEDEEQQR	LITLA/LI	QSGDAL/DA
RILEFNISK/LE, IL, EF	RRHK/RR	SFFLSSTE/FF, FL	DTKF/KF
PNTLLLPNHA/LL, LL, LLL	RFETL/RF	NILE/LE, IL	SREEGQQGEQRL/GE, EG
LIVLNG/VI, IV, LI, IL	QRFN/RF	VLFSR/LE, VL	SSDEKP/KP
ILSLVNNDDRDSY/LV, IL	RFESFFL/FF, RF, FL	SVIVE/VI, VE, IV	NEGAL/EG
VVNPDNNENLRLITLA/LI, VV	FEIN/EI	PFNLR/PF	NEGDANI/DA, EG
RFESFLSSTEA/FF, RF, FL	FSREEG/EG	DLDFLSIVDMNE/FL, IF, IV, VD, LD, DL	RAEL/EL
FSRNILEA/LE, IL	EISK/EI	LLLPH/LL, LL, LLL	DAQP/DA
FEIN/KI	FFEITPEK/FF, EI	IVILVINE/VI, VI, IV, LV, IL	KKKEEGNKGRKGP/GR, GP, EG
VLFSREEG/LE, VL, EG	DIFL/FL, IF	QPLE/LE	
EQRLQESVIVEISK/VI, VE, IV, EI	SEQDIFV/FV, IF	QDIFVIPA/FV, IF, VI	
PFNLRSDPIY/PF	SSIL/IL	PVVVNA/VVV, VV, VV	
FFEITPEK/FF, EI		TSNLNFFA/FF	
NPQLRDLDFLSIVDMNEG/FL, IF, IV, VD, LD, DL, EG		NFLA/FL	
LLLPHFNISK/LL, LL, LLL		SQDNVISQIPVQVE/VI	
IVILVINEG/VI, VI, IV, LV, IL, EG		FVDA/FV, VD, DA	
NIELVG/LV, EL, VG		PLSSILR/IL	
EQQQEQQQEQPLEVRK/LE			
ELSEQDIFVIPA/FV, IF, VI, EL			
PVVVNA/VVV, VV, VV			
TSNLNFFA/FF			
ENNQRNFLA/FL			
SQDNVISQIPVQVELA/VI, EL			
FVDA/FV, VD, DA			
PLSSILRA/IL			

¹ B, bromelain; F, ficin; P, papain; PK, proteinase K.

References

- Chatterjee, C.; Gleddie, S.; Xiao, C.W. Soybean bioactive peptides and their functional properties. *Nutrients* **2018**, *10*, 1211. [[CrossRef](#)] [[PubMed](#)]
- Rizzo, G.; Baroni, L. Soy, soy foods and their role in vegetarian diets. *Nutrients* **2018**, *10*, 43. [[CrossRef](#)] [[PubMed](#)]
- Chakrabarti, S.; Guha, S.; Majumder, K. Food-derived bioactive peptides in human health: Challenges and opportunities. *Nutrients* **2018**, *10*, 1738. [[CrossRef](#)] [[PubMed](#)]
- Ding, Y.; Li, X.; Kan, J. Isolation and identification of flavor peptides from douchi (traditional Chinese soybean food). *Int. J. Food Prop.* **2017**, *20*, 1982–1994. [[CrossRef](#)]
- Iwaniak, A.; Darewicz, M.; Mogut, D.; Minkiewicz, P. Elucidation of the role of in silico methodologies in approaches to studying bioactive peptides derived from foods. *J. Funct. Foods* **2019**, *61*, 103486. [[CrossRef](#)]
- Lyndqvist, M. Flavour Improvement of Water Solutions Comprising Bitter Amino Acids. Master's Thesis, Swedish University of Agricultural Sciences, Department of Food Science, Uppsala, Sweden, 2010; Publication No. 277.
- Zamyatnin, A.A. Fragmentomics of natural peptide structures. *Biochemistry (Moscow)* **2009**, *74*, 1575–1585. [[CrossRef](#)]
- Liu, Z.P.; Wu, L.Y.; Wang, Y.; Zhang, X.S.; Chen, L. Bridging protein local structures and protein functions. *Amino Acids* **2008**, *35*, 627–650. [[CrossRef](#)]

9. Iwaniak, A.; Minkiewicz, P.; Hryniewicz, M.; Bucholska, J.; Darewicz, M. Hybrid approach in the analysis of bovine milk protein hydrolysates as a source of peptides containing di- and tripeptide bitterness indicators. *Pol. J. Food Nutr. Sci.* **2020**, *70*, 139–150. [[CrossRef](#)]
10. Ashaolu, T.J. Application of soy protein hydrolysates in the emerging functional foods: A review. *Int. J. Food Sci. Technol.* **2019**, *55*, 421–428. [[CrossRef](#)]
11. The UniProt Consortium. UniProt: A worldwide hub of protein knowledge. *Nucl. Acids Res.* **2019**, *47*, D506–D515. [[CrossRef](#)]
12. Minkiewicz, P.; Iwaniak, A.; Darewicz, M. BIOPEP-UWM database of bioactive peptides: Current opportunities. *Int. J. Mol. Sci.* **2019**, *20*, 5978. [[CrossRef](#)] [[PubMed](#)]
13. Iwaniak, A.; Hryniewicz, M.; Bucholska, J.; Minkiewicz, P.; Darewicz, M. Understanding the nature of bitter-taste di- and tripeptides derived from food proteins based on chemometric analysis. *J. Food Biochem.* **2019**, *43*, e12500. [[CrossRef](#)] [[PubMed](#)]
14. Otagiri, K.; Miyake, I.; Ishibashi, N.; Fukui, H.; Kanehisa, H.; Okai, H. Studies of bitter peptides from casein hydrolyzate. II. Syntheses of bitter peptide fragments and analogs of BPIa (Arg-Gly-Pro-Pro-Phe-Ile-Val) from casein hydrolysate. *Bull. Chem. Soc. Jpn.* **1983**, *56*, 1116–1119. [[CrossRef](#)]
15. Peña-Ramos, E.A.; Xiong, Y.L. Antioxidant activity of soy protein hydrolysates in a liposomal system. *J. Food Sci.* **2002**, *67*, 2952–2956. [[CrossRef](#)]
16. Lee, J. Soy Protein Hydrolysate: Solubility, Thermal Stability, Bioactivity, and Sensory Acceptability in a Tea Beverage. Master's Thesis, University of Minnesota, Minneapolis, MN, USA, 2011; pp. 1–137.
17. Moruz, L.; Käll, L. Peptide retention time prediction. *Mass Spectrom. Rev.* **2017**, *36*, 615–623. [[CrossRef](#)] [[PubMed](#)]
18. Spicer, V.; Yamchuk, A.; Cortens, J.; Sousa, S.; Ens, W.; Standing, K.G.; Wilkins, J.A.; Krokhin, O.V. Sequence-specific retention calculator. A family of peptide retention time prediction algorithms in reversed-phase HPLC: Applicability to various chromatographic conditions and columns. *Anal. Chem.* **2007**, *79*, 8762–8768. [[CrossRef](#)]
19. Darewicz, M.; Borawska, J.; Vegarud, G.E.; Minkiewicz, P.; Iwaniak, A. Angiotensin I-converting enzyme (ACE) inhibitory activity and ACE inhibitory peptides of salmon (*Salmo salar*) protein hydrolysates obtained by human and porcine gastrointestinal enzymes. *Int. J. Mol. Sci.* **2014**, *15*, 14077–14101. [[CrossRef](#)]
20. Iwaniak, A.; Minkiewicz, P.; Darewicz, M.; Sieniawski, K.; Starowicz, P. BIOPEP database of sensory peptides and amino acids. *Food Res. Int.* **2016**, *85*, 155–161. [[CrossRef](#)]
21. Visser, S.; Slangen, C.J.; Rollema, H.S. Phenotyping of bovine milk proteins by reversed-phase high-performance liquid chromatography. *J. Chromatogr. A* **1991**, *548*, 361–370. [[CrossRef](#)]
22. Bucholska, J.; Minkiewicz, P. The use of peptide markers of carp and herring allergens as an example of detection of sequenced and non-sequenced proteins. *Food Technol. Biotechnol.* **2016**, *54*, 266–274. [[CrossRef](#)]
23. Monaci, L.; Losito, I.; Palmisano, F.; Visconti, A. Reliable detection of milk allergens in food using a high-resolution, stand-alone mass spectrometer. *J. AOAC Int.* **2011**, *94*, 1034–1042. [[CrossRef](#)] [[PubMed](#)]
24. Paizs, B.; Suhai, S. Fragmentation pathways of protonated peptides. *Mass Spectrom. Rev.* **2005**, *24*, 508–548. [[CrossRef](#)] [[PubMed](#)]
25. Roepstorff, P.; Fohlman, J. Proposal for a common nomenclature for sequence ions in mass spectra of peptides. *Biomed. Mass Spectrom.* **1984**, *11*, 601. [[CrossRef](#)] [[PubMed](#)]
26. Kunda, P.B.; Benavente, F.; Catalá-Clariana, S.; Giménez, E.; Barbosa, J.; Sanz-Nebot, V. Identification of bioactive peptides in a functional yogurt by liquid chromatography time-of-flight mass spectrometry assisted by retention time prediction. *J. Chromatogr. A* **2012**, *1229*, 121–128. [[CrossRef](#)]
27. Murray, N.M.; O'Riordan, D.; Jacquier, J.-C.; O'Sullivan, M.; Holton, A.; Wyne, K.; Robinson, R.C.; Barile, D.; Nielsen, S.D.; Dallas, D.C. Peptidomic screening of bitter and nonbitter casein hydrolysate fractions for insulinogenic peptides. *J. Dairy Sci.* **2018**, *101*, 2826–2837. [[CrossRef](#)]
28. Fan, J.; Saito, M.; Tatsumi, E.; Li, L. Preparation of angiotensin I-converting enzyme inhibiting peptides from soybean protein by enzymatic hydrolysis. *Food Sci. Technol. Res.* **2003**, *9*, 254–256. [[CrossRef](#)]
29. Iwaniak, A.; Minkiewicz, P.; Darewicz, M.; Hryniewicz, M. Food protein-originating peptides as tastants—Physiological, technological, sensory, and bioinformatic approaches. *Food Res. Int.* **2016**, *89*, 27–38. [[CrossRef](#)]

30. Matsui, T.; Zhu, X.L.; Shiraishi, K.; Ueki, T.; Noda, Y.; Matsumoto, K. Antihypertensive effect of salt-free soy sauce, a new fermented seasoning, in spontaneously hypertensive rats. *J. Food Sci.* **2010**, *75*, H129–H134. [[CrossRef](#)]
31. Wang, W.; Dia, V.P.; Vasconez, M.; de Mejia, E.G.; Nelson, R.L. Analysis of soybean protein-derived peptides and the effect of cultivar, environmental conditions, and processing on lunasin concentration in soybean and soy products. *J. AOAC Int.* **2008**, *91*, 936–994. [[CrossRef](#)]
32. Zhong, F.; Liu, J.; Ma, J.; Shoemaker, C.F. Preparation of hypocholesterol peptides from soy protein and their hypocholesterolemic effect in mice. *Food Res. Int.* **2007**, *40*, 661–667. [[CrossRef](#)]
33. De Mejia, E.G.; de Lumen, B.O. Soybean bioactive peptides: A new horizon in preventing chronic diseases. *Sex. Reprod. Menop.* **2006**, *4*, 91–95. [[CrossRef](#)]
34. Iwaniak, A.; Minkiewicz, P.; Darewicz, M. Food-originating ACE inhibitors, including antihypertensive peptides, as preventive food components in blood pressure reduction. *Comp. Rev. Food Sci. Food Saf.* **2014**, *13*, 114–134. [[CrossRef](#)]
35. Liu, R.; Cheng, J.; Wu, H. Discovery of food-derived dipeptidyl peptidase IV inhibitory peptides: A review. *Int. J. Mol. Sci.* **2019**, *20*, 463. [[CrossRef](#)] [[PubMed](#)]
36. Khaket, T.P.; Redhu, D.; Dhanda, S.; Singh, J. *In Silico* evaluation of potential DPP-III inhibitor precursors from dietary proteins. *Int. J. Food Prop.* **2015**, *18*, 499–507. [[CrossRef](#)]
37. Tu, M.; Cheng, S.; Lu, W.; Du, M. Advancement and prospects of bioinformatics analysis for studying bioactive peptides from food-derived protein: Sequence, structure, and functions. *TrAC Trends Analyt. Chem.* **2018**, *105*, 7–17. [[CrossRef](#)]
38. Udenigwe, C.C. Bioinformatic approaches, prospects and challenges of food bioactive peptide research. *Trends Food Sci. Technol.* **2014**, *36*, 137–143. [[CrossRef](#)]
39. Fu, Y.; Wu, W.; Zhu, M.; Xiao, Z. *In silico* assessment of the potential of patatin as a precursor of bioactive peptides. *J. Food Biochem.* **2016**, *40*, 366–370. [[CrossRef](#)]
40. Agyei, D.; Bambarandage, E.; Udenigwe, C. The role of bioinformatics in the discovery of bioactive peptides. In *Encyclopedia of Food Chemistry*, 2nd ed.; Melton, L., Shahidi, F., Varelis, P., Eds.; Elsevier Inc.: Cambridge, MA, USA, 2018; Volume 2, pp. 337–344. [[CrossRef](#)]
41. Sutopo, C.C.Y.; Sutrisno, A.; Wang, L.-F.; Hsu, J.-L. Identification of a potent angiotensin-I converting enzyme inhibitory peptide from black cumin seed hydrolysate using orthogonal bioassay-guided fractionations coupled with *in silico* screening. *Process Biochem.* **2020**, in press. [[CrossRef](#)]
42. Alcaide-Hidalgo, J.M.; Romero, M.; Duarte, J.; López-Huertas, E. Antihypertensive effects of virgin olive oil (unfiltered) low molecular weight peptides with ACE inhibitory activity in spontaneously hypertensive rats. *Nutrients* **2020**, *12*, 271. [[CrossRef](#)]
43. Kinariwala, D.; Panchal, G.; Sakure, A.; Hati, S. Exploring the potentiality of Lactobacillus cultures on the production of milk-derived bioactive peptides with antidiabetic activity. *Int. J. Pept. Res. Ther.* **2020**. [[CrossRef](#)]
44. Orts, A.; Revilla, E.; Rodriguez-Morgado, B.; Castaño, A.; Tejada, M.; Parrado, J.; Garcá-Quintanilla, A. Protease technology for obtaining a soy pulp extract enriched in bioactive compounds: Isoflavones and peptides. *Heliyon* **2018**, *5*, e01958. [[CrossRef](#)] [[PubMed](#)]
45. Garcia-Vaquero, M.; Mora, L.; Hayes, M. *In vitro* and *in silico* approaches to generating and identifying angiotensin-converting enzyme I inhibitory peptides from green macroalga ulva lactuca. *Mar. Drugs* **2019**, *17*, 204. [[CrossRef](#)] [[PubMed](#)]
46. Ashaolu, T.J. Health applications of soy protein hydrolysates. *Int. J. Pept. Res. Ther.* **2020**. [[CrossRef](#)]
47. Darewicz, M.; Borawska-Dziadkiewicz, J.; Pliszka, M. Carp proteins as a source of bioactive peptides—An *in silico* approach. *Czech J. Food Sci.* **2016**, *34*, 111–117. [[CrossRef](#)]
48. Keška, P.; Stadnik, J. Taste-active peptides and amino acids of pork meat as components of dry-cured meat products: An *in-silico* study. *J. Sens. Stud.* **2017**, *32*, e12301. [[CrossRef](#)]
49. Sun, X.D. Enzymatic hydrolysis of soy proteins and the hydrolysates utilisation. *Int. J. Food Sci. Technol.* **2011**, *46*, 2447–2459. [[CrossRef](#)]
50. Hryniewicz, M.; Iwaniak, A.; Bucholska, J.; Minkiewicz, P.; Darewicz, M. Structure-activity prediction of ACE inhibitory/bitter dipeptides—A chemometric approach based on stepwise regression. *Molecules* **2019**, *24*, 950. [[CrossRef](#)]

51. Chanput, W.; Nakai, S.; Theerakulkait, C. Introduction of a new computer softwares for classification and prediction purposes of bioactive peptides: Case study in antioxidative peptides. *Int. J. Food Prop.* **2010**, *13*, 947–959. [CrossRef]
52. Wu, J.; Aluko, R.E. Quantitative structure-activity relationship study of bitter di- and tri-peptides including relationship with angiotensin I-converting enzyme inhibitory activity. *J. Pept. Sci.* **2007**, *13*, 63–69. [CrossRef]
53. Iwaniak, A.; Dziuba, J. BIOPEP-PBIL tool in the analysis of the structure of biologically active motifs derived from food proteins. *Food Technol. Biotechnol.* **2011**, *49*, 118–127.
54. Iwaniak, A.; Dziuba, J. Animal and plant origin proteins as the precursors of peptides with ACE inhibitory activity. Proteins evaluation by means of in silico methods. *Food Technol. Biotechnol.* **2009**, *47*, 441–449.
55. Arboleda, J.C.; Rojas, O.J.; Lucia, L.A. Acid-generated soy protein hydrolysates and their interfacial behavior on model surfaces. *Biomacromolecules* **2014**, *15*, 4336–4342. [CrossRef] [PubMed]
56. Mallick, P.; Schirle, M.; Chen, S.S.; Flory, M.R.; Martin, D.; Ranish, J.; Raught, B.; Schmitt, R.; Werner, T.; Kustr, B.; et al. Computational prediction of proteotypic peptides for quantitative proteomics. *Nat. Biotechnol.* **2007**, *25*, 125–131. [CrossRef] [PubMed]
57. Iwaniak, A.; Hryniewicz, M.; Bucholska, J.; Darewicz, M.; Minkiewicz, P. Structural characteristics of food protein-originating di- and tripeptides using principal component analysis. *Eur. Food Res. Technol.* **2018**, *244*, 1751–1758. [CrossRef]
58. Panjaitan, F.C.A.; Gomez, H.L.R.; Chang, Y.-W. In silico analysis of bioactive peptides released from giant grouper (*Epinephelus lanceolatus*) roe proteins identified by proteomics approach. *Molecules* **2018**, *23*, 2910. [CrossRef]
59. Vermeirssen, V.; van der Bent, A.; Van Camp, J.; van Amerongen, A.; Verstraete, W. A quantitative in silico analysis calculates angiotensin I converting enzyme (ACE) inhibitory activity in pea and whey protein digests. *Biochimie* **2004**, *86*, 231–239. [CrossRef]
60. Pokora, M.; Zambrowicz, A.; Zabłocka, A.; Dąbrowska, A.; Szoltyś, M.; Babij, K.; Eckert, E.; Trziszka, T.; Chrzanowska, J. The use of serine protease from *Yarrowia lipolytica* yeasts in the production of biopeptides from denatured egg white proteins. *Acta Biochim. Pol.* **2017**, *64*, 245–253. [CrossRef]
61. Khaldi, N. Bioinformatic approaches for identifying new therapeutic bioactive peptides in food. *Funct. Food Health Dis.* **2012**, *2*, 325–338. [CrossRef]
62. Rawlings, N.D. A large and accurate collection of peptidase cleavages in the MEROPS database. *Database (Oxford)* **2009**, *2009*, bap015. [CrossRef]
63. Worsztynowicz, P.; Białas, W.; Grajek, W. Integrated approach for obtaining bioactive peptides from whey proteins hydrolysed using a new proteolytic lactic acid bacteria. *Food Chem.* **2020**, *312*, 126035. [CrossRef]
64. Li, X.; Xie, X.; Wang, J.; Xu, Y.; Yi, S.; Zhu, W. Identification, taste characteristics and molecular docking study of novel umami peptides derived from the aqueous extract of the clam *Meretrix meretrix* Linnaeus. *Food Chem.* **2020**, *312*, 126053. [CrossRef] [PubMed]
65. Ney, K. Voraussage der Bitterkeit von Peptiden aus deren Aminosäurezu-sammensetzung. Prediction of bitterness of peptides from their amino acid composition. *Z. Lebensm. Unters. Forsch.* **1971**, *147*, 64–68. [CrossRef]
66. Maehashi, K.; Huang, L. Bitter peptides and bitter taste receptors. *Cell. Mol. Life Sci.* **2009**, *66*, 1661–1671. [CrossRef] [PubMed]
67. Lemieux, L.; Simard, R.E. Bitter flavour in dairy products. II. A review of bitter peptides from caseins: Their formation, isolation and identification, structure masking and inhibition. *Lait* **1992**, *72*, 335–382. [CrossRef]
68. Wang, W.; Gonzalez de Mejia, E. A new frontier in soy bioactive peptides that may prevent age-related chronic diseases. *Compr. Rev. Food Sci. Food Saf.* **2005**, *4*, 63–78. [CrossRef]
69. Cheung, L.K.Y.; Aluko, R.E.; Cliff, M.A.; Li-Chan, E.C.Y. Effects of exopeptidase treatment on antihypertensive activity and taste attributes of enzymatic whey protein hydrolysates. *J. Funct. Foods* **2015**, *13*, 262–275. [CrossRef]
70. Gallego, M.; Mora, L.; Toldrá, F. The relevance of dipeptides and tripeptides in the bioactivity of dry-cured ham. *Food Prod. Process. Nutr.* **2019**, *1*, 2. [CrossRef]
71. FitzGerald, R.J.; Cermeño, M.; Khalesi, M.; Kleekayai, T.; Amigo-Benavent, M. Application of in silico approaches for the generation of milk protein-derived bioactive peptides. *J. Funct. Foods* **2020**, *64*, 103636. [CrossRef]



Article

Agricultural Entrepreneurship in the European Union: Contributions for a Sustainable Development

Vítor João Pereira Domingues Martinho ^{1,2}

¹ Agricultural School (ESAV) and CI&DETS, Polytechnic Institute of Viseu (IPV), 3504-510 Viseu, Portugal; vdmartinho@esav.ipv.pt

² Centre for Transdisciplinary Development Studies (CETRAD), University of Trás-os-Montes and Alto Douro (UTAD), 5000-801 Vila Real, Portugal

Received: 24 February 2020; Accepted: 17 March 2020; Published: 19 March 2020

Abstract: Entrepreneurship is sometimes seen as a glimmer of hope which may bring about some contribution towards improving economic dynamics and performance, specifically in the creation of employment by young people, in general, with further educational training, greater flexibility and who are better prepared for working with new technologies. However, entrepreneurship in the agricultural sector is, in certain circumstances, viewed as being something incompatible or, at least, difficult to implement. More scientific studies in these fields could provide interesting contributions on the road to highlighting new ideas inside the farming sector. In this framework, the objective of this study is to explore the entrepreneurship dimensions within the European Union agriculture towards a more sustainable sector. In fact, without an economic dimension in farm management, its sustainability in the medium and long run may be compromised, increasing the abandonment of farming, namely in more disadvantaged regions. For this, the literature which is available on the platform Web of Science relating to the following three topics was initially analysed: entrepreneurship, agriculture, and the European Union. This literature was clustered through the VOSviewer software, an interesting tool for performing bibliometric analysis. Secondly, statistical information related to European Union agricultural entrepreneurship considering empirical approaches was also explored. The analysis carried out shows that the realities across European Union countries are, in fact, different, where the instruments from the common agricultural policies, for example, may play a crucial role in promoting more farming entrepreneurship in a more sustainable way.

Keywords: VOSviewer software; bibliometric analysis; statistical analysis; agricultural innovation

1. Introduction

Bringing about new ideas is a fundamental approach in every sector. This is particularly important in agriculture, considering its specificities and lower capacity to sometimes create innovation, and in less favoured contexts of the European Union, such as in rural areas, frequently suffering from a lack in dynamics. In some European Union countries, such as Portugal, many things have already been done in this manner, namely with European financial funds, but there is still much to do. This is primarily due to the fact that for many years, the European agricultural policies within the framework of the Common Agricultural Policy (CAP) are or were socially unjust (favouring larger farms) and economically inefficient (conditioning farmers to opt for the most subsidised productions) in some member-states. On the other hand, the European agricultural strategies could be more directed towards promoting agricultural entrepreneurship and leadership. This is a typical problem which stems from having common policy instruments for a set of countries and regions with great differences amongst them. In any case, these frameworks have limited the potential for the development of farms which are located in certain regions [1].

The consequences of this are the vast differences in the levels of development across farms from different European countries and sometimes across farms from diverse regions within the same member-state. Another question, in addition or in parallel to the economic performance, refers to the discussion about the social and environmental contributions of the farms, namely in less affluent regions, where the agricultural sector, specifically family farming, provides a decisive contribution towards balanced development. However, it would be interesting if the model of this family farming inside the European Union were to be rethought, as some of this agriculture is practiced by older farmers or by farmers who, with their current levels of income, will probably decide in the near future to abandon this sector and the regions in which they live [1].

In this way, it is fundamental to bring about new approaches and sometimes to look at things from a different perspective in order to renew/refresh the agricultural sector, specifically in regions with a greater risk of abandonment. Innovation and entrepreneurship should play an important part here, not only in the agro-food sector, but namely in the production sector (agrarian sectors). It is specifically important to attract younger generations as well as the most qualified professionals.

Considering this context, this study aims to highlight the main insights available in the scientific literature related with agricultural entrepreneurship in the European Union. To deeper explore these insights, the literature review was complemented with bibliometric analysis. Data and empirical analyses were also performed to better explore the actual realities in these domains. These approaches made it possible to find a set of proposals to improve the sustainability of farms in the European Union regions.

Further Explanation of the Research Approach

This subsection aims to clarify the following aspects: What is the main contribution of the paper? How does the existing literature miss the role of entrepreneurship? Does the EU sufficiently support this problem in its policies? How exactly is entrepreneurship defined and measured?

This research intends to bring more insights for the understanding of agricultural entrepreneurship, specifically, for the context of the European Union. There are interesting contributions about these topics, as highlighted in the literature review, but there is still enormous potential to be explored, because agricultural entrepreneurship is a topic that does not attract as much attention from the several stakeholders as in some other sectors. In fact, it is important to further explore the scientific literature available on the Web of Science platform. It is also important to analyse the statistical information available for some fields considered by the literature as relevant to agricultural entrepreneurship, such as, for example, those related to women and young people. In turn, it is relevant to show how these variables influence agricultural performance in the European Union, namely, for instance, to eventually propose policy adjustments.

Following these motivations, the bibliometric analysis was considered, namely, to highlight the main insights of the scientific literature and to support the organization of the literature review. The information obtained with the bibliometric analysis and literature review was considered to identify the main variables related to these domains to be explored through data analysis and econometric approaches.

The concept of agricultural entrepreneurship was considered in all its dimensions. In fact, agricultural entrepreneurship is important for more competitive farms, to strengthen their position in the market, but also for more familiar farms, to improve their socioeconomic and environmental contributions. In practice, entrepreneurship presupposes innovation and new ideas for any stage, from production to final consumption.

2. Material and Methods

The study proposed here aimed to identify the main gaps in the scientific literature related to these topics under analysis and to identify the main factors that influence agricultural entrepreneurship within the European Union. With these objectives, the intention was namely to provide further

insight into the design or redesigning of new strategic plans that will promote entrepreneurship in the agricultural sector whilst taking advantage of the available resources, specifically from agroforestry land. In this way, the scientific literature relative to the subjects analysed was explored through bibliometric analysis and literature survey, so as to highlight how entrepreneurship may be further developed inside the agricultural framework. The bibliometric analysis is an interesting approach, specifically, to support the organization of this research. Subsequently, statistical information was examined through descriptive (data analysis) and empirical (regressions based on the Cobb–Douglas model) analyses, namely in order to stress the impacts from entrepreneurship variables on social and economic dimensions. The Cobb–Douglas model (production function) allows us to analyse relationships between several production factors and the output and has its relevance within this study. This approach was followed so as to interconnect the literature survey about agricultural entrepreneurship in the European Union with the empirical reality verified in the several member-states mirrored by variables related with these topics and available in the main statistical databases (namely Eurostat). It was considered important to present these interrelationships and the selection of the chosen variables already took into account the insights from the literature analysis (where, for example, the role of women and younger people in farm management was stressed, as well as, for instance, the sustainability of farms).

3. Bibliometric Analysis of the Literature Available on the Web of Science

In this section, the literature was first analysed through the VOSviewer software (Nees Jan van Eck and Ludo Waltman, Leiden, The Netherlands) [2], considering the scientific studies available on the platform Web of Science [3] and through the University of Burgos (Spain), where we stayed for a week on an Erasmus+ mission. On this scientific platform, 89 studies were found (including 76 articles, 20 meetings and 3 books) in a search performed at the end of May 2018 that included the topics: entrepreneurship; agriculture; European Union. After this initial analysis, in a subsequent sub-section, scientific studies through a literature review will be further explored. It is worth stressing that this kind of analysis for the agricultural sector follows studies such as, for example, that developed by Martinho [4], where the bibliometric analysis is an interesting tool with relevant outcomes.

3.1. Literature Analysis through the VOSviewer

Considering a minimum number of occurrences in all documents of a term of 5, the VOSviewer software selected the 70 terms presented in Table 1 with the respective number of occurrences and relevance score. This minimum number was chosen as after several simulations this was the value which possessed a greater relevance for the main terms. The relevance score indicates the terms which were more demonstrative of the topics analysed [2]. It is worth stressing that despite the importance of the agricultural policies for the questions related to farming entrepreneurship, as stressed before, it seems that the literature gave them little relevance, as shown in the bibliometric analysis performed through the VOSviewer software (in Table 1 the term “policy” appears with a low relevance of 0.51). These aspects related to agricultural policy will be explored at the end of this study, considering the findings obtained from the bibliometric and statistical analyses.

To improve the interpretation of the map, the following terms of relevance below 1.00 were excluded, with the exception of terms related to countries (Spain and Greece) and the European Union. The selection of terms such as rural development and sustainability was maintained. The map with all the terms is presented in Figure 1, where it is possible to identify 4 groups.

The terms considered by the software for each group are presented in Table 2. By analysing Tables 1 and 2 and Figure 1, it is possible to observe that in group 1 the terms for the European Union are those with a greater number of occurrences (11) and women is the term with the most relevance (1.51). For group 2, the term combination presents a higher occurrence and the term mean has greater relevance. In group 3, the term the Netherlands has greater occurrence and the term multifunctional

agriculture shows higher relevance. Finally, for group 4, the terms sustainability and difference are those with greater occurrence and relevance, respectively.

On the other hand, it is important to stress the proximity (relatedness) of terms such as: European Union, rural development and, for example, Greece in group 1; combination, place, attitude, industry and, for example, Spain for group 2; the Netherlands, transition, multifunctional agriculture and, for example, management for group 3.

Table 1. Number of occurrences and respective relevance of each term.

Term	Occurrences	Relevance
multifunctional	5	5.31
agricultural		
mean	5	3.23
transition	6	2.50
attitude	6	2.40
view	6	2.09
possibility	7	1.63
woman	7	1.51
management	8	1.48
difference	7	1.37
crisis	7	1.32
Netherlands	15	1.32
case	7	1.28
significance	6	1.20
industry	8	1.20
case study	9	1.19
combination	9	1.17
world	5	1.15
sample	10	1.15
improvement	8	1.12
cost	5	1.12
place	9	1.10
basis	7	1.09
economic performance	5	1.07
initiative	9	1.05
addition	6	0.99
success	11	0.99
experience	9	0.97
adoption	6	0.96
literature	10	0.94
ability	5	0.93
effect	10	0.92
recent year	5	0.92
situation	11	0.89
response	6	0.89
framework	14	0.88
issue	8	0.85
challenge	9	0.83
diversification	9	0.82
author	7	0.80
year	7	0.79
extent	7	0.77
Spain	8	0.77
outcome	8	0.74
relationship	12	0.72
value	12	0.72
agricultural sector	13	0.67
term	9	0.66
risk	9	0.66
Greece	8	0.60
company	8	0.60
order	9	0.60
country	8	0.58
demand	12	0.57
service	13	0.57
performance	9	0.56
element	6	0.52
policy	13	0.51
society	8	0.50
person	8	0.50
impact	11	0.49
product	11	0.49
way	9	0.48
article	12	0.47
rural area	18	0.47
end	5	0.46
European Union	11	0.44
rural development	10	0.44
sustainability	14	0.43
quality	14	0.30
information	10	0.27

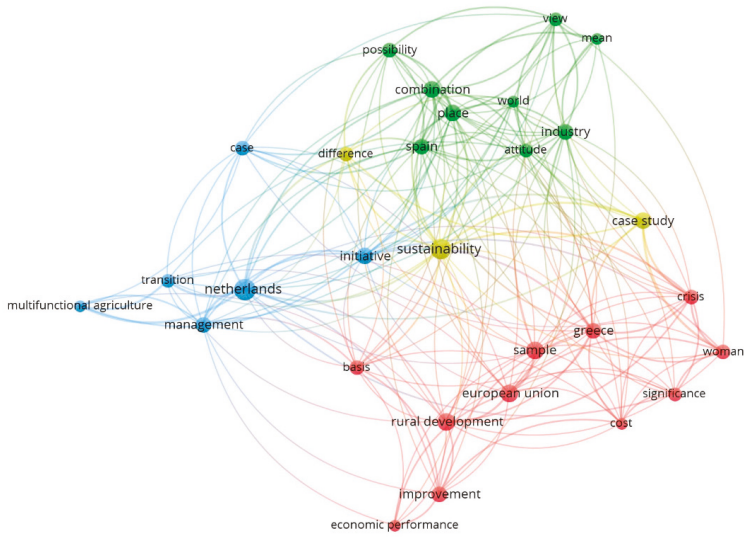


Figure 1. Map containing all the terms.

Table 2. Terms included in each group.

Groups	Terms
Group 1 (11 terms)	basis cost crisis economic performance European Union Greece improvement rural development sample significance woman
Group 2 (9 terms)	attitude combination industry mean place possibility Spain view world
Group 3 (6 terms)	case initiative management multifunctional agriculture Netherlands transition
Group 4 (3 terms)	case study difference sustainability

3.2. Literature Review

In this subsection for the literature analysis, several scientific documents related to agricultural entrepreneurship were grouped considering the terms previously identified for the four clusters presented in the previous subsection, namely in Table 2.

3.2.1. The European Union and Agricultural Entrepreneurship

The agricultural context in the European Union is, indeed, complex, considering the diversity of realities between countries and regions; however, these frameworks are sometimes considered as benchmarks for other countries [5] because there are relevant examples. In turn, some contexts of agricultural development in Europe were also influenced in some parts of history by other global realities, specifically the American one [6] in globalized trade. These scenarios have their implications in the dynamics of entrepreneurship in the agricultural sector, characterized by their specific particularities within several economic activities [7]. Specifically regarding entrepreneurship amongst women, it is necessary to highlight its importance as a specific field with many potentialities, namely in female empowerment and in the promotion of local resources, activities and endogenous productions [8–10].

In a new paradigm of rural development in the European Union, the various forms of European support for the creation of small businesses provide interesting contributions towards entrepreneurship in rural regions [11]; however, some barriers, namely administrative ones, continue to complicate the process [12]. The perception of the numerous stakeholders concerning entrepreneurship can also condition its implementation [13]. Due to the European Union's support, specifically for multifunctional agriculture and market globalization, there has been a rise in entrepreneurial attitudes amongst European farmers [14], or this has at least had an influence on farm organization and farmers' perspectives [15]. In addition, investments in research and education (specifically educational training) from the several agricultural stakeholders have helped to promote innovation and entrepreneurship in the farming sector and this increases the performance in agriculture [16–19].

3.2.2. Some Concepts Associated with Farming Entrepreneurship

The attitude and perspectives of the several stakeholders (sometimes the entrepreneurship is seen as something distant, for others and that can disturb the status quo) are determinant for effective farming entrepreneurship and benchmarking may play an interesting role here [20], because it allows farmers to see other realities where entrepreneurial practices are implemented with success. In any case, the economic impact of innovation and entrepreneurship initiatives is not yet totally clear in some sectors and regions [21]. Nevertheless, professional skills and technological/entrepreneurial/developmental competences are fundamental for the promotion for entrepreneurship and innovation [22,23], namely in rural areas where job availability is limited [24]. Self-confidence and good planning for businesses and investments are crucial for success in entrepreneurship [25]. Social capital (social networks, participation in agricultural institutions and access to information) also has its importance [26]. Information, communication and technology (ICT) may be a useful way to promote and increase farming and rural entrepreneurship [27]; however, there is still some work to be done in these fields, namely to overcome several constraints that complicate their utilization by farmers and other agricultural stakeholders [28]. The same happens with other new technologies, such as with nanotechnology [29,30].

The local cultural and historical contexts condition the decisions of farmers and this has an influence on the way the several activities are developed [31]. On the other hand, a social perspective of farmers and constructive personal characteristics can positively influence agricultural entrepreneurship [32]. In any case, the organization of employment and working conditions has its influence on the business and entrepreneurship dynamic [33]. Gender is another factor with an influence on entrepreneurship characteristics and motivation [34–36], as well as the age of the farmers in question [37]. The social

construct concerning the relationships between the rural and urban areas [38], sometimes influences the dynamics developed within the several frameworks.

In the context of crisis, agricultural entrepreneurship is, in general, an alternative way to reduce unemployment through self-employment [39,40].

3.2.3. Multifunctional Farming and Agricultural Entrepreneurship

There are several activities complementary to agricultural production that can be developed in rural areas [41], some even from within the farms, such as agro-tourism [42], organic farming [43,44] and direct marketing [45], where, for example, multifunctional agriculture may be an option, from a perspective of farmers, producers and entrepreneurs [46]. Nonetheless, the multifunctional agricultural and innovative activities in farms are not free from criticism in some European contexts [47]. Aquaculture in some specific contexts may bring contributions to this multifunctionality; however, some constraints should be carefully analysed and solved [48]. In this multifunctional role of farms, bioenergy production may be a good example, in favourable contexts [49–51], as well as heating entrepreneurship in rural Finland [52]. Another question is the multiple businesses of the farm owners [53,54] that may promote the adoption of innovative and entrepreneurial options. In turn, the agricultural sector is fundamental for industrial performance [55], namely for the industries closely related to agriculture.

Agricultural entrepreneurship is often related to the diversification of activities in farms, where networking is crucial to promote changes within businesses [56–58] and to promote exchanges in experience [59]. However, this networking between the several agricultural and rural stakeholders is not always symmetric and does not provide benefits for everyone [60]. Trust, engagement and reciprocity amongst the several agents are important for success [61] and for creating environmental entrepreneurship [62], as well as the concerns for ethics [63].

In any case, the multifunctional land organization needs interdisciplinary approaches involving the several stakeholders [64] with the same objectives [65]. However, sometimes the transition from family farming to entrepreneurial management is associated with more stress for farmers, where agricultural policies are one of the causes of stress [66–68].

3.2.4. Agricultural Sustainability and Entrepreneurship

The relationships between farming sustainability and agricultural entrepreneurship sometimes depend on the form in which the sector is organized [69]. The sustainability of farms is a concern in several countries, namely in those with more environmental problems [70]. A balanced and sustainable relationship between farms and their surrounding context is the main goal for several agricultural stakeholders [71]. Entrepreneurship may bring about interesting contributions to a balanced relationship among the economic, social and environmental dimensions [72,73]. For entrepreneurial and sustainable farms, institutions play a crucial role, namely the cooperatives [74] and the universities for technological transfer [75], as well as the rural policies [76,77]. Social entrepreneurship in rural regions [78] and social farming [79–81] are interesting perspectives for farming and rural sustainability. The solution of social and environmental problems are the main goals for several farmers [82], or, at least, they should be [83], namely those who practice agriculture in disadvantaged regions and receive subsidies to stay there. Another example of agricultural contributions towards sustainability is urban agriculture, as a form of food production, occupation for unemployed persons and for the creation of skills in a process of lifelong learning [84], where there are economic, social and environmental concerns [85].

The farmers who remain in the less affluent regions and smaller farms, some with low profitability, have determinant importance for regional sustainability [86]. The current world contexts call for virtuous circles in sustainable landscape management [87] and for new forms of dealing with these new realities [88], where agroforestry has its place [89]. Innovation in farms brings about important insights for sustainability and animal welfare [90,91]. The aversion to change and to implementing new approaches is one important barrier against improving overall sustainability [92,93].

4. Data Analysis for Agricultural Entrepreneurship in the European Union

This section is aimed at complementing the analysis carried out before for the bibliometric approach. The data available in the Eurostat [94] will be analysed considering data which are more related with agricultural entrepreneurship in European Union regions (NUTS 2) and for 2016 (one observation by region), namely (Figure 2): the number of farms; the utilized agricultural area (hectare); the standard output (euro); the directly employed labour (annual working unit); and the number of farms whose household consumes more than 50% of the final production. These variables are important to understand the current and potential context around European agricultural entrepreneurship. On the other hand, these variables are important to perform the regressions with the Cobb–Douglas model (where the output is regressed, namely, in function of the labour and capital inputs). The standard output was considered as a dependent variable and the utilized agricultural area and the number of farms (as proxies for the capital) and labour were used as independent variables. Having said that, the database used does not present data for Italian regions in all variables considered and for some regions relative to the number of farms whose household consumes more than 50% of the final production.

Considering the relevance outlined by the literature towards the influence of aspects related to gender and age in agricultural entrepreneurship, the number of farms managed by males and females and by different age groups will also be analysed (Figure 3). In fact, as referred to before, gender is an important factor with an influence upon entrepreneurship characteristics and motivation [34–36], as well as the age of farmers [37].

To better understand the distribution of the values from the different variables across the European Union regions, shapefiles were considered obtained from the Eurostat [95] and worked upon with the QGIS [96] and with the GeoDa [97]. Several maps were created considering the GeoDa percentile methodologies. In these maps, the dark blue is for the percentile with lower values and the dark red is for the percentile with higher values. To improve the presentation of the figures, the overseas regions (Guadeloupe, Guyane, La Réunion, Mayotte and Martinique) were removed from the maps.

Figure 2 shows that the regions of Sud-Vest Oltenia, Sud-Muntenia and Nord-Est (all from Romania) are those with greater numbers of farms. It is also worth stressing that regions from Portugal, Spain and others from the nearby countries of Romania (Greece, Croatia, Hungary, Poland and Lithuania) have relatively high values for the number of farms. This context reflects, in some cases, the small size of the farms. It is on these smaller farms that innovation and entrepreneurship may play a relevant role.

On the other hand, the regions with a greater utilized agricultural area are located in Spain (Andalucía, Castilla-la Mancha and Castilla y León). Other regions, for example, from Spain, Portugal, France, Ireland, the United Kingdom and Romania have a relatively high agricultural area. In some of these regions, the large number of hectares is a consequence of the high number of farms, although with a low average area.

Relatively to the standard output, Andalucía (Spain), Bretagne and Pays de la Loire (France) are the regions with better performance. However, when we look at the productivity of area (standard output by hectare), the higher values go to the Dutch regions. The Dutch farming sector is always a specific context, considering its land particularities that allow other kinds of agricultural organization. Concerning labour productivity, the higher values appear in regions from the United Kingdom and Denmark. This structure emphasizes farm performance in northern European regions.

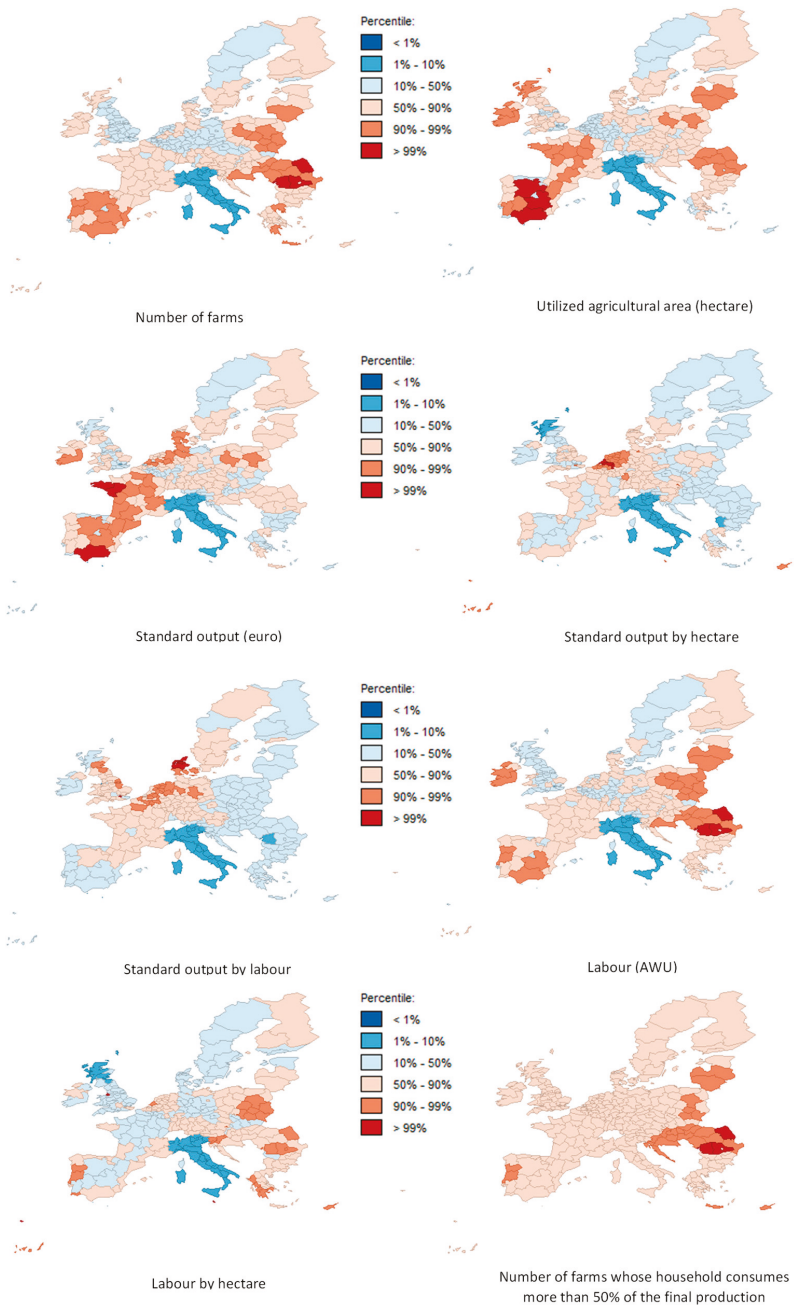


Figure 2. Some further variables associated with agricultural entrepreneurship in the EU.

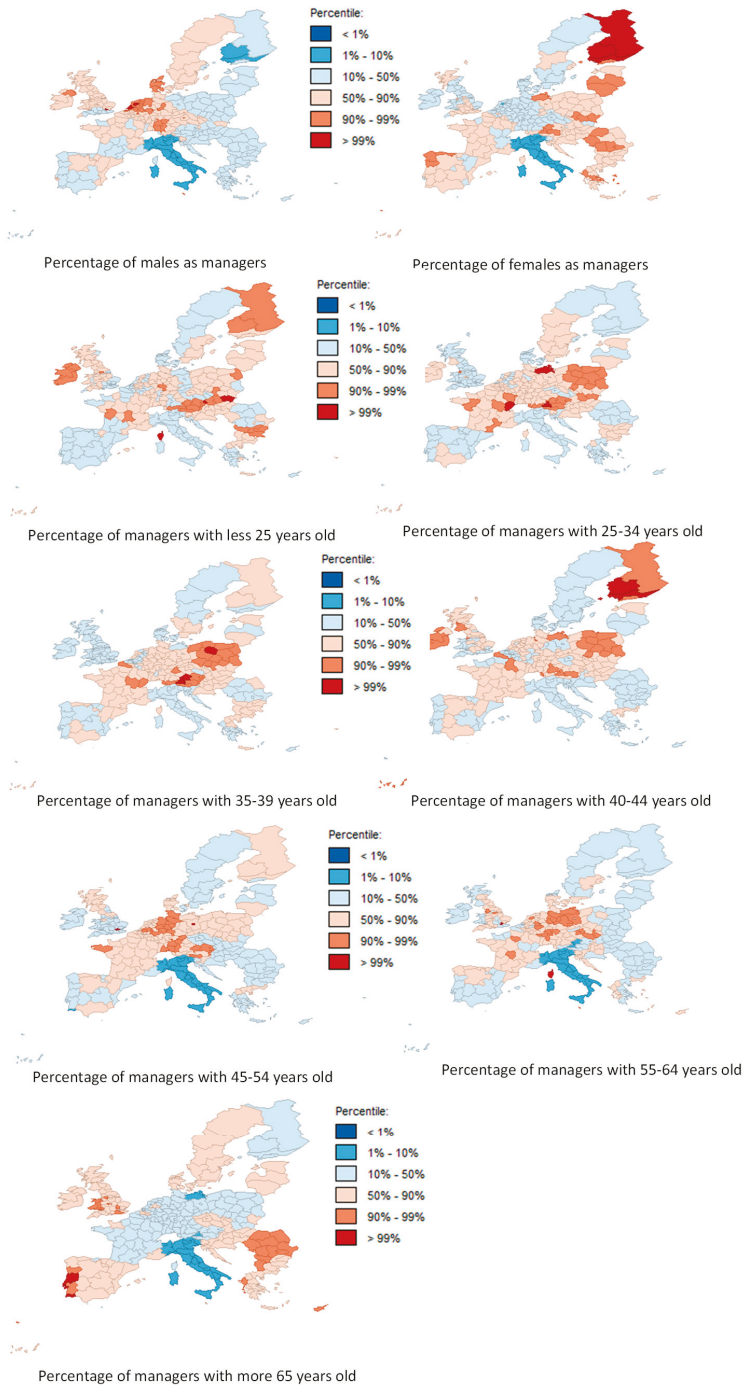


Figure 3. Number of farms disaggregated by gender and age of the managers.

The values for the labour force employed directly by the agricultural sector have a similar distribution as those verified and described by the number of farms, showing that a high number of farms, in some circumstances, is synonymous with small size and little mechanization. The Romanian regions with a higher number of farms and agricultural workers are, also, the same as those with a greater number of farms whose household consumes more than 50% of the final production. Malta, Madeira (Portugal) and Merseyside (the United Kingdom) seem to be the regions with a higher amount of labour per hectare. Other regions from Portugal (Norte, Centro and Algarve) present, also, relatively high values for labour by area. These high labour values per hectare are good from a social point of view, but they, also, show that there is work to be done to make the social and economic dimensions more compatible. In fact, some of these farms are located in mountainous or disadvantaged areas, managed from the perspective of the family, but, even here, measures can be taken for more adjusted management, claiming for agricultural innovation and entrepreneurship. In any case, the social and environmental contributions of these farms are unquestionable and clearly justify the financial support available in the European Union for these contexts. However, these subsidies could be more linked to more innovative and entrepreneurial management, maintaining the social and environmental role of this agriculture. Without this innovative approach for farms located in disadvantaged regions, the consequence, in the medium and long term, will be abandonment.

Regions from the countries of the southern European Union (Portugal, Spain, France and Greece) and from the countries of central and Eastern Europe seem to be those with more area, number of farms, labour and, in some cases, standard output. However, when the area and labour productivities are analysed, the greater performance is verified in regions from the northern countries (the Netherlands and Denmark).

Disaggregating the number of farms by gender and age of the managers, Figure 3 shows that Dutch farms are mostly managed by men and the Finnish agricultural units are managed by women. Women also play a relevant role in farm management in some regions of Germany, Poland, Austria, Romania, Latvia, Lithuania and in the north of Portugal and Spain. Considering the importance of women for more entrepreneurial management, their role should be rethought in the European Union, including from a policy perspective.

Younger managers (less than 25 years old) appear in farms of regions from Slovakia, as well as from France, Austria, Bulgaria, Poland, Finland and Ireland. Germany, Austria and France are the countries with regions where there are more managers aged 25–34 years old. It is also worth stressing that regions from Poland have a relevant number of farms managed by people between the ages of 25 and 34 years old. Regions from Austria and Poland are those with more farms managed by farmers in the 35–39 age group. The farms with managers between 40 and 44 years old appear more in Finnish regions and with 45–64 years old in regions from the central European countries (around France, Germany and the United Kingdom, for example). The greater number of farms with the oldest managers (more than 65 years old) appears in the Portuguese regions, as well as in regions from Romania, Bulgaria, Greece and the United Kingdom. Also, taking into account the role of young people in the agricultural sector, the several CAP instruments should be redesigned to be more effective in bringing youngsters to the farms, namely, in countries where this context is more problematic.

5. Results for Cross-Section Regressions

Considering the data available in the Eurostat database (all variables in logarithms), the standard output (euros) was regressed, through cross-section regression for 2016 and across the European Union regions (NUTS 2), in function of the labour directly employed (AWU), the utilized agricultural area (hectare) and number of farms (Equation 1), taking into account the Cobb and Douglas [98] model as a base. The utilized agricultural area and the number of farms were considered as proxies for the capital.

The number of farms has the advantage of being considered by the database disaggregated by genders and ages, two important questions referred to by the literature.

$$so_j = \alpha_0 + \alpha_1 labour_j + \alpha_2 uaa_j + \alpha_3 nf_j + \varepsilon \quad (1)$$

where so is the logarithm of standard output, $labour$ is the logarithm of labour directly employed, uaa is the logarithm of utilized agricultural area, nf is the logarithm of number of farms and j the European Union regions.

5.1. Stressing the Cobb–Douglas Model Adequacy for Agriculture

It is important to highlight that the variables selection took into account the original Cobb–Douglas model, the literature review carried out before and to avoid problems of multicollinearity. The Cobb–Douglas model, with proper adjustments, was considered in analyses for the agricultural sector by several authors, namely for efficiency surveys with data envelopment analysis [99] or through stochastic frontier [100].

Specifically for agriculture in the European Union and with the most diverse approaches (including efficiency analysis), several studies considered the Cobb–Douglas model from the theory of production and taking into account different databases with micro- or macroeconomic statistical information. For example, Aggelopoulos et al. [101] explored data related to production factors and output from 80 Greek pig farms through the Cobb–Douglas developments. These authors highlighted the relevance of the results obtained with the Cobb–Douglas production function and the adequacy of this approach for the agricultural sector. The relevance of the model in terms of economic and agronomic dimensions was also stressed by Gornott and Wechsung [102]. Bille et al. [103] considered microeconomic data from the Italian Farm Accountancy Data Network and used variables such as area and labour as inputs. Galdeano-Gomez et al. [104] used financial data from 56 Spanish farming-marketing cooperatives to analyse the externalities from sustainability on agricultural productivity, considering as a base the Cobb–Douglas model. Martinho [1] considered the Cobb–Douglas developments to analyse the common agricultural policy impacts on the dynamics of the Portuguese agricultural sector. Utnik-Banas et al. [105] analysed the technical efficiency from some Polish broiler production farms, taking into account as a base the Cobb–Douglas model and considering as inputs, for example, several costs, labour and fixed capital. In fact, in these models, namely when regression approaches are considered, it is important to limit the number of variables to avoid statistical problems, specifically multicollinearity. Typically, inputs which are taken into account are those such as labour and capital (or proxies for it) and other variables for extended versions.

5.2. Regressions and Results Analysis

Several regressions were made through the cross-sectional methodologies, considering the Stata [106] procedures, some with the number of farms disaggregated by gender and age groups for management. The results are presented in Table 3. The labour and the utilized agricultural area are control variables from the Cobb–Douglas model and the variables related to the number of farms disaggregated by gender and age groups for the management are decision variables, considering the previous literature analysis and to capture the age and gender effects on the agricultural output.

Table 3 reveals that this is, indeed, explained positively by the number of agricultural workers and the area, whilst negatively by number of farms, showing that, in general, the regions with more farms have smaller scale economies and less output. To analyse the eventual problems of multicollinearity among the independent variables, the results were compared, for example, for models 1 and 2, which seems to suggest an absence of this statistical infraction. On the other hand, considering the Breusch–Pagan test for heteroscedasticity and the Ramsey RESET test, the more statistically consistent models are those with the number of farms disaggregated by age groups, specifically for younger managers.

Table 3. Cross-section results based on the production function model (standard output logarithm as dependent variable).

Variables	Model1	Model2 (Corrected)	Model3 (Corrected)	Model4 (Corrected)	Model5	Model6	Model7	Model8	Model9 (Corrected)	Model10 (Corrected)	Model10 (Corrected)	Model11 (Corrected)
Constant	13.660* (40.300)	10.040* (28.570)	10.222* (27.150)	8.305* (24.260)	9.632* (17.590)	9.929* (19.410)	9.936* (17.130)	9.996* (21.620)	10.062* (24.540)	9.673* (24.220)	8.315* (19.750)	9.850* (28.580)
Logarithm of labour	0.702* (20.020)	0.708* (19.880)	0.785* (19.770)	0.776* (18.530)	0.540* (17.590)	0.476* (19.410)	0.689* (17.130)	0.550* (21.620)	0.404* (24.540)	0.690* (24.220)	0.691* (19.750)	0.580* (28.580)
Logarithm of utilized agricultural area	0.601* (13.160)	0.601* (12.560)	0.611* (12.720)	0.554* (14.000)	0.563* (11.140)	0.593* (12.750)	0.600* (11.920)	0.588* (12.800)	0.614* (12.610)	0.612* (12.990)	0.524* (11.800)	0.576* (13.160)
Logarithm of number of farms	-0.439* (-6.250)	-0.026* (-8.530)	-0.244* (-3.470)	-0.421* (-11.590)	-0.371* (-8.180)	-0.270* (-4.500)	-0.481* (-6.620)	-0.341* (-5.110)	-0.001* (-6.350)	-0.362* (-4.760)	-0.002* (-8.400)	-0.001* (-9.440)
Logarithm of farms managed by men												
Logarithm of farms managed by women												
Logarithm of farms managed by persons aged less than 25 years old												
Logarithm of farms managed by persons aged between 25 and 34 years old												
Logarithm of farms managed by persons aged between 35 and 39 years old												
Logarithm of farms managed by persons aged between 40 and 44 years old												
Logarithm of farms managed by persons aged between 45 and 54 years old												
Logarithm of farms managed by persons aged between 55 and 64 years old												
Logarithm of farms managed by persons aged over 65 years old												
Breusch-Pagan test for heteroscedasticity	0.270 [0.604]	6.720* [0.009]	10.040* [0.001]	2.870 [0.090]	7.330* [0.006]	2.280 [0.131]	0.060 [0.805]	1.260 [0.261]	7.320* [0.006]	11.190* [0.000]	1.180 [0.276]	12.620* [0.000]
Ramsey RESET test using powers of the fitted values	18.460* [0.000]	4.920* [0.002]	5.690* [0.000]	1.870 [0.135]	0.630 [0.532]	1.100 [0.411]	2.070 [0.105]	1.090 [0.353]	6.930* [0.000]	1.110 [0.344]	0.160 [0.925]	4.060* [0.007]
VIF (Variance Inflation Factor)	1.000	8.420	6.920	7.520	4.950	5.070	6.440	6.230	7.530	8.750	5.460	4.400
Number of observations	250	250	250	249	249	243	212	245	249	250	250	249

Note: *, statistically significant at 5% or less. Model 2 (Corrected), this model was corrected by changing the number of farms squared. Model 3 (Corrected), this model was corrected by changing the number of farms managed by men squared. Model 4 (Corrected), this model was corrected by changing the number of farms managed by women to the number of farms managed by men squared. Model 9 (Corrected), this model was corrected by changing the number of farms managed by persons aged between 45 and 54 years old cubed. Model 10 (Corrected), this model was corrected by changing the number of farms managed by persons aged between 55 and 64 years old cubed. Model 11 (Corrected), this model was corrected by changing the number of farms managed by persons aged over 65 to the number of farms managed by persons aged over 65 cubed.

In any case, the Variance Inflation Factor (test for multicollinearity) was run and, in fact, the results suggest the absence of collinearity (all the results are below 10). On the other hand, to solve the problems related with heteroscedasticity and with omitted variables, several alternatives have been tried, namely through the translog model; however, in the simulations performed, the results are not statistically significant. In this way, it was opted to transform, in the models with problems for the Breusch–Pagan and Ramsey RESET tests, the variable related to the number of farms. In the beginning, for each model with heteroscedasticity and with the omitted variable problems, the variables from the translog model were simulated and some of the best statistical results were those where the respective number of farms variable was squared. However, this transformation was not enough for the models with statistical problems and related to farms managed by older farmers. In these cases, the respective number of farms variable was cubed. With these transformations, it was possible to confirm the impact from the several variables in the standard output and to compare results between models.

Model 6, for farms with managers from 25 to 34 years of age, this seems to be where (amongst the younger generations) the number of farms influences the standard output less negatively (-0.270). These findings suggest that the problems related to the number of farms (and probably related with the scale economies of the farms and their performance) may be better solved when the farmers are younger people, with an age ranging from 25 to 34 years. For balanced rural development and for farm sustainability, where the questions related to the economic dimension may not be the only determinant aspect in farm management, it will be important to attract younger, more qualified, innovative people and with more entrepreneurial capacities. In fact, innovation and entrepreneurial skills allow for a deeper exploitation of the multifunctionality of farms, promoting both social and environmental dimensions, with interesting returns for the farmer, as referred to before in the literature review.

In turn, farms which are managed by women influence the agricultural output more negatively than those managed by men. This shows that there still remains a long way to go across the whole of the European Union agricultural sector towards improving the role of women in farms, namely promoting more empowerment in resolving historical and sociological contexts.

Finally, amongst the older farmers (more than 45 years old), the farms managed by people between 55 and 64 were those with more negative impacts on the agricultural performance. The experience accumulated by the older farmers is important for agricultural dynamics; however, sometimes age is an impediment for innovation and entrepreneurship.

6. Discussions

This study was designed and planned with the aim of analysing entrepreneurship in the European Union agricultural sector, exploring the literature available on the Web of Science platform and related to the three topics: entrepreneurship, agriculture, and the European Union. This literature was further explored with bibliometric approaches through the VOSviewer software. These topics were also explored statistically, considering empirical methodologies.

The literature review shows that some terms such as gender, age, multifunctional agriculture, sustainability and rural development, for example, are important expressions when they are analysed as topics related with agricultural entrepreneurship in the European Union. These are relevant insights because the role of women and young people may, indeed, make a difference on European Union farms. These aspects may, in certain circumstances, be obvious findings, but have not been yet fully addressed by the several stakeholders, namely policymakers. In fact, women have an increasing role in society and, consequently, in farm management. Younger people have more training and inclination to use new technologies, namely those related to information and communications technology. If we want to do things differently and with greater return, then multifunctional agriculture and innovation are interesting approaches. In all these contexts, we cannot forget sustainability and a balanced development, where we unite economics, the environment and social aspects. On the other hand, countries such as The Netherlands are, also, important terms in this kind of analysis. In these frameworks related to agricultural entrepreneurship, the environments across the European

Union countries are really quite diverse, where the common agricultural policy may have a more effective influence in reducing asymmetries. Indeed, the bibliometric analysis, namely the information presented in Table 1, reveals that the questions related to agricultural policies are frequently referred to in the literature relative to agricultural entrepreneurship in the European Union (the term “policy” has an occurrence of 13, a number which resides amongst the higher values), but with a relatively low relevance (0.51). Considering these findings, it will be important that the several stakeholders, namely policymakers, design policy instruments which have a greater impact on agricultural entrepreneurship in the different European member-states, so as to increase the relevance of the interrelationships between agricultural policies and entrepreneurship.

The data analysis shows that European Union countries from the southern and eastern regions have a greater number of farms, more utilized agricultural area and more labour, and, in consequence, in some contexts, have smaller farms and with fewer technological resources. These contexts require more adjusted strategies that promote more entrepreneurial management, because the social and environmental dimensions of these farms are important, but should be balanced with the economic dimension. However, it is those farms from the north which have higher labour and area productivities. Maybe, in some cases, these farms could be considered benchmarks for the remaining European sector. In turn, regions from Finland, for example, have more women and younger people as managers. The regions from Portugal are those where the managers are older (more than 65 years old). Indeed, these questions should be addressed in the design of agricultural policies, namely in further promoting the importance of women and younger people in farm management and improving farming productivities in certain member-states. Low productivities may be an obstacle for creating more added value and consequently to bring about more qualified, innovative and entrepreneurial people.

The results obtained with the cross-section regressions, considering a model based on a Cobb–Douglas production function, reveal that the standard output is positively influenced by the agricultural workers and the area, whilst it is negatively influenced by the number of farms. Again, these considerations may be considered obvious, but they continue to deserve special attention from policymakers, because of the productivity weaknesses. In turn, improvements are needed in the output of small farms. Entrepreneurial approaches may here bring relevant contributions. In addition, the results confirm the importance of the age groups on the farms’ performance. Another question to be taken into account by the policymakers is to clearly distinguish between agricultural economic entrepreneurship, agricultural social entrepreneurship and agricultural environmental entrepreneurship. It will be important, also, to define the sectors and regions where each one of these agricultural entrepreneurships is more likely. In fact, the literature shows that relative to agricultural entrepreneurship, economic aspects are determinant, but so too are sustainability and multifunctionality dimensions for integrated rural development. Empowerment for female farmers and bringing together farmers’ experience and innovation will be another big challenge.

7. Conclusions

As a final remark, it is worth stressing that entrepreneurship dynamics in the agricultural sector are influenced by its particularities and often follow a pattern different to those verified in other economic sectors, such as industry. For example, a great number of firms in industry are often seen as a sign of good dynamics, whereas in the agricultural sector a high number of farms negatively influence the regional standard output (because a greater number of farms is, frequently, synonymous with lower scale economies and lower dynamics).

Thinking about the agricultural and rural policies, this study has brought to light some interesting contributions to the discussion about these topics, namely when highlighting the importance of more effective strategies that promote the several dimensions of agricultural entrepreneurship (economic, social and environmental) within the European Union. This is, in fact, a gap in the CAP instruments that could be redesigned to deeper address these dimensions. In the present version of the CAP strategies, the environmental dimensions, for instance, are clearly addressed, but innovation and

entrepreneurship could be more specific. For example, something like the “Greening” instrument of the first pillar could be created for farming entrepreneurship. There are already incentives to attract young farmers (in the first and second pillars of the CAP), but they could be redesigned to be more effective, namely, to maintain these farmers for longer periods in the sector. Another aspect in which the agricultural policies could be rethought is regarding the role of the women in the sector and their empowerment.

On the other hand, the importance of younger generations and women for agricultural entrepreneurship has also been stressed. However, it will be important to compare these results, in future studies, with those that may be obtained with other topics and other variables. For example, analysing the relationships between agricultural entrepreneurship and the activities of R&D or further analysing the interrelationship between agricultural entrepreneurship and agricultural, agro-environmental, and rural policies in the European Union, may provide interesting future contributions. Agricultural entrepreneurship has great potential to be explored. The consideration of other variables, some without information in the main statistical databases, but which may be obtained through the implementation, for example, of surveys in representative farms, will allow for a deeper examination of the technical orientation and business model for farms. Considering analysis by European Union country and other approaches in order to build the variables (ordinal variables, for example) could be another interesting suggestion for future research.

In any case, to address these and other approaches in future studies related with agricultural entrepreneurship, for example, some recent reviews such as those performed by Fitz-Koch et al. [107], Wuepper and Lybbert [108] and Dias et al. [109] are suggested. Other studies, such as the following, may also bring about further interesting insights: Morris et al. [110] and Dias and Franco [111].

Funding: This work is financed by national funds through FCT - Fundação para a Ciência e Tecnologia, I.P., under the project UID/Multi/04016/2019. Furthermore we would like to thank the Instituto Politécnico de Viseu and CI&DETS for their support. This work is supported by national funds, through the FCT – Portuguese Foundation for Science and Technology under the project UID/SOC/04011/2019.

Acknowledgments: I would like to thank the Erasmus+ Programme of the European Union, the Polytechnic Institute of Viseu, Portugal, and the University of Burgos, Spain.

Conflicts of Interest: The authors declare no conflict of interest. The funders had no role in the design of the study; in the collection, analyses, or interpretation of data; in the writing of the manuscript, or in the decision to publish the results.

References

1. Martinho, V.J.P.D. Output Impacts of the Single Payment Scheme in Portugal: A Regression with Spatial Effects. *Outlook Agric.* **2015**, *44*, 109–118. [CrossRef]
2. VOSviewer—Visualizing Scientific Landscapes. Available online: <http://www.vosviewer.com/> (accessed on 7 June 2018).
3. Web of Science [v.5.29]. Available online: https://apps.whoofknowledge.com/UA_GeneralSearch_input.do?product=UA&search_mode=GeneralSearch&SID=E5zQKcA9bhGgk28itCg&preferencesSaved= (accessed on 23 May 2018).
4. Martinho, V.J.P.D. Interrelationships between renewable energy and agricultural economics: An overview. *Energy Strategy Rev.* **2018**, *22*, 396–409. [CrossRef]
5. Akhmetshina, L. European experience in development of agricultural entrepreneurship. *Upravlencheskie Nauki* **2014**, *1*, 59–64.
6. Clar, E. A World of Entrepreneurs: The Establishment of International Agribusiness During the Spanish Pork and Poultry Boom, 1950–2000. *Agric. Hist.* **2010**, *84*, 176–194. [CrossRef] [PubMed]
7. Aleknevičienė, V.; Martirosianienė, L. Agriculture Funding Measures in Lithuania: Demand and Opportunities. In *Economic Science for Rural Development: Rural Business and Finance: 1. Rural Business Economics and Administration, 2. Finance and Taxes*; Zvirbulė-Berzina, A., Ed.; Nordic Association of Agricultural Scientists: Uppsala, Sweden, 2012; pp. 145–151. ISBN 978-9934-8304-1-9.

8. Anthopoulou, T. Food knowhow and entrepreneurial dynamics of rural women. Case study in the Peloponnese (Greece). *Cah. Agric.* **2008**, *17*, 577–581.
9. Anthopoulou, T. Rural women in local agrofood production: Between entrepreneurial initiatives and family strategies. A case study in Greece. *J. Rural Stud.* **2010**, *26*, 394–403. [[CrossRef](#)]
10. Zirham, M.; Palomba, R. Female agriculture in the short food supply chain: A new path towards the sustainability empowerment. In *Florence Sustainability of Well-Being International Forum 2015: Food for Sustainability and Not Just Food*; Menghini, S., Pfoestl, E., Marinelli, A., Eds.; Elsevier: Amsterdam, The Netherlands, 2016; Volume 8, pp. 372–377. ISBN 9781510836105.
11. Babuchowska, K.; Marks-Bielska, R. The Growth of Rural Entrepreneurship in the Context of the Implementation of the Rural Development Programme in 2007–2013. In *Proceedings of the Rural Development 2013, Akademija, Lithuania, 28–29 November 2013*; Atkociuniene, V., Ed.; Aleksandras Stulginskis University: Akademija, Lithuania, 2013; Volume 6, pp. 493–498.
12. Dan, M.-C.; Popescu, C. Entrepreneurship in the rural areas of Romania. The impact of the 2007-2013 EU funding programmes. *Proc. Int. Conf. Bus. Excell.* **2017**, *11*, 1129–1136. [[CrossRef](#)]
13. Zvirgzdina, R.; Auzina, A. Factors Impeding the Start of Entrepreneurship in Rural Areas. In *Economic Science for Rural Development: Rural and Regional Development*; Jakusonoka, I., Ed.; Latvia University of Agriculture: Jelgava, Latvia, 2008; pp. 289–295. ISBN 978-9984-39-498-5.
14. Morgan, S.L.; Marsden, T.; Miele, M.; Morley, A. Agricultural multifunctionality and farmers' entrepreneurial skills: A study of Tuscan and Welsh farmers. *J. Rural Stud.* **2010**, *26*, 116–129. [[CrossRef](#)]
15. Vehkamäki, S.; Ylätalo, M.; Aro, E. Resource Use and Entrepreneurship on Dairy Farms in South Ostrobothnia (Finland). In *Economic Science for Rural Development: Primary and Secondary Production, Consumption*; Jakusonoko, I., Ed.; Latvia University of Agriculture: Jelgava, Latvia, 2008; pp. 203–209, ISBN 978-9984-9997-0-8.
16. Smit, A.B. Changing external conditions require high levels of entrepreneurship in agriculture. In *Proceedings of the XV International Symposium on Horticultural Economics and Management*, Berlin, Germany, 29 August–3 September 2004; Bokelmann, W., Ed.; International Society for Horticultural Science: Leuven, Belgium, 2004; pp. 167–173, ISBN 90-6605-056-X.
17. Seuneke, P.; Lans, T.; Wiskerke, J.S.C. Moving beyond entrepreneurial skills: Key factors driving entrepreneurial learning in multifunctional agriculture. *J. Rural Stud.* **2013**, *32*, 208–219. [[CrossRef](#)]
18. Seben Zatkova, T. The new VET Professionals—Entrepreneurship Trainers for VET. In *Proceedings of the IX International Conference on Applied Business Research (ICABR 2014)*, Talca, Chile, 6–10 October 2014; pp. 977–988, ISBN 978-80-7509-223-6.
19. Coca, O.; Stefan, G.; Mironiuc, M. Empirical evidences regarding the relationship between innovation and performance in the agriculture of European Union. *Sci. Pap. Ser. Manag. Econ. Eng. Agric. Rural Dev.* **2017**, *17*, 99–110.
20. Al-Hasan, S.; Thomas, B.; Haines, M. Strategic implications of benchmarking for agricultural cooperatives and farmer-controlled enterprises in Wales. *Outlook Agric.* **2002**, *31*, 267–274. [[CrossRef](#)]
21. Alarcon, S.; Sanchez, M. Business strategies, profitability and efficiency of production. *Span. J. Agric. Res.* **2013**, *11*, 19–31. [[CrossRef](#)]
22. Iliopoulos, C.; Theodorakopoulou, I.; Lazaridis, P. Innovation implementation strategies for consumer driven fruit supply chains. *Br. Food J.* **2012**, *114*, 798–815. [[CrossRef](#)]
23. Lans, T.; van Galen, M.A.; Verstegen, J.A.A.M.; Biemans, H.J.A.; Mulder, M. Searching for entrepreneurs among small business ownermanagers in agriculture. *NJAS Wagening. J. Life Sci.* **2014**, *68*, 41–51. [[CrossRef](#)]
24. Brezuleanu, C.O.; Brezuleanu, S.; Iatco, C. Development of labour market and entrepreneurial spirit in rural areas. *Environ. Eng. Manag. J.* **2013**, *12*, 693–698.
25. Makinen, H. Farmers' managerial thinking and management process effectiveness as factors of financial success on Finnish dairy farms. *Agric. Food Sci.* **2013**, *22*, 452–465. [[CrossRef](#)]
26. Pospesch, P.; Spesna, D. What is the importance of social capital in Czech agriculture? An analysis of selected components. *Agric. Econ. Zemedelska Ekon.* **2011**, *57*, 279–287. [[CrossRef](#)]
27. Teodoro, A.; Dinis, I.; Simoes, O.; Gomes, G. Success factors for small rural tourism units: An exploratory study in the Portuguese region of Serra da Estrela. *Eur. J. Tour. Res.* **2017**, *17*, 136–148.

28. Briz, J.; Cristina Fernandez, M.; de Felipe, I.; Briz, T. E-commerce and ICT adoption in the Spanish agri-food sector: Looking for key factors performance in e-food markets. In *Food Supply Networks: Trust and E-Business*; Canavari, M., Fritz, M., Schiefer, G., Eds.; CAB International: Wallingford, UK, 2016; ISBN 978-1-84593-638-9.
29. Stevenson, P.; Williams, G. Current European agribusiness opinion on biotech market and technology issues. *Agro Food Ind.* **2002**, *13*, 39–42.
30. Moskvins, G.; Spakovica, E.; Moskvins, A.; Shakhtarina, A.; Beldavs, V. Development of nanotechnology in agriculture for small northern European country. In Proceedings of the 11th International Scientific Conference on Engineering for Rural Development, Jelgava, Latvia, 24–25 May 2012; Malinovska, L., Osadcuks, V., Eds.; Latvia University of Agriculture: Jelgava, Latvia, 2012; Volume 11, pp. 157–163.
31. Dana, L.P. A historical study of the traditional livestock merchants of Alsace. *Br. Food J.* **2006**, *108*, 586–598. [\[CrossRef\]](#)
32. De Lauwere, C.C. The role of agricultural entrepreneurship in Dutch agriculture of today. *Agric. Econ.* **2005**, *33*, 229–238. [\[CrossRef\]](#)
33. Navajas-Romero, V.; Carmen Lopez-Martin, M.; Ariza-Montes, A. Dependent self-employed workers in Europe. *CIRIEC Espana Rev. Econ. Publica Soc. Cooperativa* **2017**, *89*, 167–198.
34. Dieguez-Castrillon, M.I.; Gueimonde-Canto, A.; Sinde-Cantorna, A.; Blanco-Cerradelo, L. Turismo rural, emprendedorismo e género: Um estudo de caso na comunidade autónoma da Galiza. *Rev. Econ. Sociol. Rural* **2012**, *50*, 371–381. [\[CrossRef\]](#)
35. Fhlatharta, A.M.N.; Farrell, M. Unravelling the strands of “patriarchy” in rural innovation: A study of female innovators and their contribution to rural Connemara. *J. Rural Stud.* **2017**, *54*, 15–27. [\[CrossRef\]](#)
36. Jackova, S.; Kapsdorferova, Z.; Kadlecikova, M. Challenges and opportunities for rural Slovak women in agribusiness. In Proceedings of the Agrarian Perspectives XXVI Competitiveness of European Agriculture and Food Sectors, Prague, Czech Republic, 13–15 September 2017; Tomsik, K., Ed.; Czech University of Life Sciences Prague, Faculty of Economics and Management: Prague, Czech Republic, 2017; pp. 123–130, ISBN 978-80-213-2787-0.
37. Rivaroli, S.; Bertazzoli, A.; Ghelfi, R.; Laghi, A. Multifunctional farming in Emilia-Romagna region: An analysis through agricultural census data. *New Medit.* **2016**, *15*, 37–44.
38. Smith, R.; McElwee, G. Confronting Social Constructions of Rural Criminality: A Case Story on “Illegal Pluriactivity” in the Farming Community. *Sociol. Ruralis* **2013**, *53*, 112–134. [\[CrossRef\]](#)
39. Liontakis, A.; Tzouramani, I. Economic Sustainability of Organic Aloe Vera Farming in Greece under Risk and Uncertainty. *Sustainability* **2016**, *8*, 338. [\[CrossRef\]](#)
40. Hausmann, R.; Nedelkoska, L. Welcome home in a crisis: Effects of return migration on the non-migrants’ wages and employment. *Eur. Econ. Rev.* **2018**, *101*, 101–132. [\[CrossRef\]](#)
41. Eimermann, M. Two sides of the same coin: Dutch rural tourism entrepreneurs and countryside capital in Sweden. *Rural Soc.* **2016**, *25*, 55–73. [\[CrossRef\]](#)
42. Kordel, S. Selling ruralities: How tourist entrepreneurs commodify traditional and alternative ways of conceiving the countryside. *Rural Soc.* **2016**, *25*, 204–221. [\[CrossRef\]](#)
43. Lynggaard, K. Conflicts Over Meaning and Policy Entrepreneurship within the CAP (1986–1992). In *The Common Agricultural Policy and Organic Farming: An Institutional Perspective on Continuity and Change*; Centre for Agriculture and Bioscience International: Wallingford, UK, 2006; ISBN 978-1-84593-114-8.
44. Lynggaard, K. The Formation of a Policy Field: Organic Farming Within the CAP (1993–2005). In *The Common Agricultural Policy and Organic Farming: An Institutional Perspective on Continuity and Change*; Centre for Agriculture and Bioscience International: Wallingford, UK, 2006; ISBN 978-1-84593-114-8.
45. Steiner, L.; Hoffmann, V. Multifunctional agriculture through creative diversification—A taxonomic study in the middle and south of Germany. *Berichte Uber Landwirtschaft* **2012**, *90*, 235–257.
46. Vesala, H.T.; Vesala, K.M. Entrepreneurs and producers: Identities of Finnish farmers in 2001 and 2006. *J. Rural Stud.* **2010**, *26*, 21–30. [\[CrossRef\]](#)
47. Desein, J.; Bock, B.B.; de Krom, M.P.M.M. Investigating the limits of multifunctional agriculture as the dominant frame for Green Care in agriculture in Flanders and the Netherlands. *J. Rural Stud.* **2013**, *32*, 50–59. [\[CrossRef\]](#)
48. Bostock, J.; Lane, A.; Hough, C.; Yamamoto, K. An assessment of the economic contribution of EU aquaculture production and the influence of policies for its sustainable development. *Aquac. Int.* **2016**, *24*, 699–733. [\[CrossRef\]](#)

49. Voytenko, Y.; Peck, P. Organisational frameworks for straw-based energy systems in Sweden and Denmark. *Biomass Bioenergy* **2012**, *38*, 34–48. [[CrossRef](#)]
50. Voytenko, Y.; Peck, P. Organization of straw-to-energy systems in Ukraine and Scandinavia. *Biofuels Bioprod. Biorefin.* **2011**, *5*, 654–669. [[CrossRef](#)]
51. Cantale, C.; Petrazzuolo, F.; Correnti, A.; Farneti, A.; Felici, F.; Latini, A.; Galeffi, P. Triticale for Bioenergy Production. In *Florence Sustainability of Well-Being International Forum 2015: Food for Sustainability and Not Just Food*; Agriculture and Agricultural Science Procedia; Menghini, S., Pfoestl, E., Marinelli, A., Eds.; Elsevier: Amsterdam, The Netherlands, 2016; Volume 8, pp. 609–616.
52. Huttunen, S. Wood energy production, sustainable farming livelihood and multifunctionality in Finland. *J. Rural Stud.* **2012**, *28*, 549–558. [[CrossRef](#)]
53. Carter, S. Multiple business ownership in the farm sector: Assessing the enterprise and employment contributions of farmers in Cambridgeshire. *J. Rural Stud.* **1999**, *15*, 417–429. [[CrossRef](#)]
54. Hansson, H.; Ferguson, R.; Olofsson, C.; Rantamaki-Lahtinen, L. Farmers' motives for diversifying their farm business—The influence of family. *J. Rural Stud.* **2013**, *32*, 240–250. [[CrossRef](#)]
55. Ermolenko, O.D. Small and Medium Entrepreneurship in Agriculture: International Experience and Perspectives in Russia. *Ekonomika Skokhozyaistvoennykh Pererabatyvayushchikh Predpriyatii* **2016**, *12*, 54–58.
56. Clark, J. Entrepreneurship and diversification on English farms: Identifying business enterprise characteristics and change processes. *Entrep. Reg. Dev.* **2009**, *21*, 213–236. [[CrossRef](#)]
57. Hermans, F.; Stuiver, M.; Beers, P.J.; Kok, K. The distribution of roles and functions for upscaling and outscaling innovations in agricultural innovation systems. *Agric. Syst.* **2013**, *115*, 117–128. [[CrossRef](#)]
58. Vinholis, M.D.M.B.; Souza Filho, H.M.D.; Carrer, M.J.; Chaddad, F.R. Determinants of recognition of TRACES certification as valuable opportunity at the farm level in São Paulo, Brazil. *Production* **2016**, *26*, 78–90. [[CrossRef](#)]
59. Dell'Olio, M.; Hassink, J.; Vaandrager, L. The development of social farming in Italy: A qualitative inquiry across four regions. *J. Rural Stud.* **2017**, *56*, 65–75. [[CrossRef](#)]
60. Lambrecht, E.; Kuhne, B.; Gellynck, X. Asymmetric relationships in networked agricultural innovation processes. *Br. Food J.* **2015**, *117*, 1810–1825. [[CrossRef](#)]
61. Larsson, M. Environmental Entrepreneurship in Organic Agriculture in Jarna, Sweden. *J. Sustain. Agric.* **2012**, *36*, 153–179. [[CrossRef](#)]
62. Marsden, T.; Smith, E. Ecological entrepreneurship: Sustainable development in local communities through quality food production and local branding. *Geoforum* **2005**, *36*, 440–451. [[CrossRef](#)]
63. Pompe, V. Moral Entrepreneurship: Resource Based Ethics. *J. Agric. Environ. Ethics* **2013**, *26*, 313–332. [[CrossRef](#)]
64. Johansen, P.H.; Ejrnaes, R.; Kronvang, B.; Olsen, J.V.; Praestholm, S.; Schou, J.S. Pursuing collective impact: A novel indicator-based approach to assessment of shared measurements when planning for multifunctional land consolidation. *Land Use Policy* **2018**, *73*, 102–114. [[CrossRef](#)]
65. Macedo, M. Port Wine Landscape: Railroads, Phylloxera, and Agricultural Science. *Agric. Hist.* **2011**, *85*, 157–173. [[CrossRef](#)]
66. Kallioniemi, M.K.; Simola, A.; Kaseva, J.; Kymalainen, H.-R. Stress and Burnout Among Finnish Dairy Farmers. *J. Agromed.* **2016**, *21*, 259–268. [[CrossRef](#)]
67. Kallioniemi, M.K.; Simola, A.J.K.; Kymaelaainen, H.-R.; Vesala, H.T.; Louhelainen, J.K. Stress among Finnish farm entrepreneurs. *Ann. Agric. Environ. Med.* **2008**, *15*, 243–249. [[PubMed](#)]
68. Kallioniemi, M.K.; Simola, A.J.K.; Kymalainen, H.-R.; Vesala, H.T.; Louhelainen, J.K. Mental symptoms among Finnish farm entrepreneurs. *Ann. Agric. Environ. Med.* **2009**, *16*, 159–168. [[PubMed](#)]
69. Adamisin, P.; Kotulic, R.; Kravcakova Vozarova, I. Legal form of agricultural entities as a factor in ensuring the sustainability of the economic performance of agriculture. *Agric. Econ. Zemedelska Ekon.* **2017**, *63*, 80–92.
70. Blom-Zandstra, M.; van Keulen, H. Innovative concepts towards sustainability in organic horticulture: Testing a participatory technology design. *Int. J. Agric. Sustain.* **2008**, *6*, 195–207. [[CrossRef](#)]
71. Methorst, R.; Roep, D.; Verstegen, J.; Wiskerke, J.S.C. Three-Fold Embedding: Farm Development in Relation to Its Socio-Material Context. *Sustainability* **2017**, *9*, 1677. [[CrossRef](#)]

72. De Wolf, P.L.; Schoorlemmer, H.B.; Smit, A.B.; de Lauwere, C.C. Analysis and development of entrepreneurship in agriculture. In Proceedings of the XV International Symposium on Horticultural Economics and Management, Berlin, Germany, 29 August–3 September 2004; Bokelmann, W., Ed.; International Society for Horticultural Science: Leuven, Belgium, 2004; pp. 199–208, ISBN 90-6605-056-X.
73. Golebiewska, B. Significance of Connections with the Environment of Agricultural Farms in Poland for their Production and Economic Situation. In *Economic Science for Rural Development: Production and Taxes*; Mazure, G., Ed.; Latvia University of Agriculture: Jelgava, Latvia, 2011; pp. 40–49. ISBN 978-9984-9997-5-3.
74. Pitoska, E.; Gatziooufa, P. Business efficiency of the agricultural cooperatives: The case of the saffron producers' cooperative of Kozani. In Proceedings of the 3rd Annual Euromed Conference of the Euromed Academy of Business: Business Developments across Countries and Cultures, Nicosia, Cyprus, 4–5 November 2010; Vrontis, D., Weber, Y., Kaufmann, H.R., Tarba, S., Eds.; University of Nicosia: Nicosia, Cyprus, 2010; pp. 849–860, ISBN 978-9963-634-83-5.
75. Vac, C.S.; Fitiu, A. Building Sustainable Development through Technology Transfer in a Romanian University. *Sustainability* **2017**, *9*, 2042. [[CrossRef](#)]
76. Gonzalez, J.J.; Benito, C.G. Profession and identity. The case of family farming in Spain. *Sociol. Ruralis* **2001**, *41*, 343–357. [[CrossRef](#)]
77. Egea, P.; Perez, L. Sustainability and multifunctionality of protected designations of origin of olive oil in Spain. *Land Use Policy* **2016**, *58*, 264–275. [[CrossRef](#)]
78. Greblikaite, J.; Rakstys, R.; Caruso, D. Social entrepreneurship in rural development of Lithuania. *Manag. Theory Stud. Rural Bus. Infrastruct. Dev.* **2017**, *39*, 157–165. [[CrossRef](#)]
79. Hassink, J.; Grin, J.; Hulsink, W. Enriching the multi-level perspective by better understanding agency and challenges associated with interactions across system boundaries. The case of care farming in the Netherlands: Multifunctional agriculture meets health care. *J. Rural Stud.* **2018**, *57*, 186–196. [[CrossRef](#)]
80. Hassink, J.; Grin, J.; Hulsink, W. Multifunctional Agriculture Meets Health Care: Applying the Multi-Level Transition Sciences Perspective to Care Farming in the Netherlands. *Sociol. Ruralis* **2013**, *53*, 223–245. [[CrossRef](#)]
81. Guirado, C.; Valldeperas, N.; Tulla, A.F.; Sendra, L.; Badia, A.; Evard, C.; Cebollada, A.; Espluga, J.; Pallares, L.; Vera, A. Social farming in Catalonia: Rural local development, employment opportunities and empowerment for people at risk of social exclusion. *J. Rural Stud.* **2017**, *56*, 180–197. [[CrossRef](#)]
82. Migliore, G.; Schifani, G.; Romeo, P.; Hashem, S.; Cembalo, L. Are Farmers in Alternative Food Networks Social Entrepreneurs? Evidence from a Behavioral Approach. *J. Agric. Environ. Ethics* **2015**, *28*, 885–902. [[CrossRef](#)]
83. Zvirgzdina, R.; Pelse, M. Development Possibilities of Farms in Latvia. In *Economic Science for Rural Development: Rural Business and Finance: 1. Rural Business Economics and Administration, 2. Finance and Taxes*; Zvirbule Berzina, A., Ed.; Nordic Association of Agricultural Scientists: Uppsala, Sweden, 2012; pp. 133–138, ISBN 978-9934-8304-1-9.
84. Magrefi, F.; Orsini, F.; Bazzocchi, G.; Gianquinto, G. Learning through gardening: The Hortis experience. In Proceedings of the 6th International Conference on Education and New Learning Technologies EDULEARN14, Barcelona, Spain, 7–9 July 2014; Chova, L.G., Martinez, A.L., Torres, I.C., Eds.; IATED: Valencia, Spain, 2014; pp. 5366–5374, ISBN 978-84-617-0557-3.
85. Specht, K.; Weith, T.; Swoboda, K.; Siebert, R. Socially acceptable urban agriculture businesses. *Agron. Sustain. Dev.* **2016**, *36*, 17. [[CrossRef](#)]
86. Moroney, A.; O'Reilly, S.; O'Shaughnessy, M. Taking the leap and sustaining the journey: Diversification on the Irish family farm. *J. Agric. Food Syst. Commun. Dev.* **2016**, *6*, 103–123. [[CrossRef](#)]
87. Selman, P.; Knight, M. On the nature of virtuous change in cultural landscapes: Exploring sustainability through qualitative models. *Landsc. Res.* **2006**, *31*, 295–307. [[CrossRef](#)]
88. Van der Schilden, M.; Verhaar, C.H.A. A concept of modern entrepreneurship in Dutch horticulture. In Proceedings of the XIV International Symposium on Horticultural Economics, Guernsey, UK, 12–15 September 2000; Ogier, J.P., Ed.; ISHS Commission Economics and Management: Leuven, Belgium, 2000; pp. 439–446, ISBN 90-6605-982-6.
89. Vrahnakis, M.; Nasiakou, S.; Kazoglou, Y.; Blanas, G. A conceptual business model for an agroforestry consulting company. *Agrofor. Syst.* **2016**, *90*, 219–236. [[CrossRef](#)]

90. Spoelstra, S.F.; Koerkamp, P.W.G.G.; Bos, A.P.; Elzen, B.; Leenstra, F.R. Innovation for sustainable egg production: Realigning production with societal demands in The Netherlands. *Worlds Poult. Sci. J.* **2013**, *69*, 279–297. [CrossRef]
91. Zeverte-Rivza, S.; Paula, L. Innovations in the equine sector in Latvia. In *Economic Science for Rural Development: Marketing and Sustainable Consumption—Rural Development and Entrepreneurship—Home Economics*; Mazure, G., Ed.; Latvia University of Agriculture: Jelgava, Latvia, 2014; pp. 246–254, ISBN 978-9934-8466-2-5.
92. Tsekouropoulos, G.; Andreopoulou, Z.; Samathrakis, V.; Grava, F. Sustainable development through agriculture entrepreneurship opportunities: Introducing internet consulting for market places. *J. Environ. Protec. Ecol.* **2012**, *13*, 2240–2248.
93. Stal, H.I. Inertia and change related to sustainability—An institutional approach. *J. Clean. Prod.* **2015**, *99*, 354–365. [CrossRef]
94. Eurostat Home. Available online: <http://ec.europa.eu/eurostat> (accessed on 19 June 2018).
95. Eurostat NUTS. Available online: <http://ec.europa.eu/eurostat/web/gisco/geodata/reference-data/administrative-units-statistical-units/nuts> (accessed on 19 June 2018).
96. QGIS. Welcome to the QGIS Project! Available online: <https://qgis.org/en/site/> (accessed on 19 June 2018).
97. GeoDa: An Introduction to Spatial Data Analysis. Spatial@UChicago. The University of Chicago. Available online: <https://spatial.uchicago.edu/geoda> (accessed on 19 June 2018).
98. Cobb, C.W.; Douglas, P.H. A Theory of Production. *Am. Econ. Rev.* **1928**, *18*, 139–165.
99. Martinho, V.J.P.D. Efficiency, total factor productivity and returns to scale in a sustainable perspective: An analysis in the European Union at farm and regional level. *Land Use Pol.* **2017**, *68*, 232–245. [CrossRef]
100. Huy, H.T.; Nguyen, T.T. Cropland rental market and farm technical efficiency in rural Vietnam. *Land Use Policy* **2019**, *81*, 408–423. [CrossRef]
101. Aggelopoulos, S.; Pavlouti, A.; Karipidis, P.; Dotas, V.; Mitsopoulos, I. Suggestions for reformation and financing programs in pig holdings based on the type of nutrition. *J. Food Agric. Environ.* **2007**, *5*, 355–358.
102. Gornott, C.; Wechsung, F. Statistical regression models for assessing climate impacts on crop yields: A validation study for winter wheat and silage maize in Germany. *Agric. For. Meteorol.* **2016**, *217*, 89–100. [CrossRef]
103. Bille, A.G.; Salvioni, C.; Benedetti, R. Modelling spatial regimes in farms technologies. *J. Prod. Anal.* **2018**, *49*, 173–185. [CrossRef]
104. Galdeano-Gomez, E.; Cespedes-Lorente, J.; Martinez-del-Rio, J. Environmental performance and spillover effects on productivity: Evidence from horticultural firms. *J. Environ. Manag.* **2008**, *88*, 1552–1561. [CrossRef]
105. Utnik-Banas, K.; Zmija, J.; Krawczyk, J.; Poltowicz, K. Changes in technical efficiency of the broiler production in Poland, 1994–2013. *Br. Poult. Sci.* **2018**, *59*, 245–249. [CrossRef]
106. Stata Data Analysis and Statistical Software. Available online: <https://www.stata.com/> (accessed on 19 June 2018).
107. Fitz-Koch, S.; Nordqvist, M.; Carter, S.; Hunter, E. Entrepreneurship in the Agricultural Sector: A Literature Review and Future Research Opportunities. *Entrep. Theory Pract.* **2018**, *42*, 129–166. [CrossRef]
108. Wuepper, D.; Lybbert, T.J. Perceived Self-Efficacy, Poverty, and Economic Development. *Ann. Rev. Resour. Econ.* **2017**, *9*, 383–404. [CrossRef]
109. Dias, C.S.L.; Rodrigues, R.G.; Ferreira, J.J. What’s new in the research on agricultural entrepreneurship? *J. Rural Stud.* **2019**, *65*, 99–115. [CrossRef]
110. Morris, W.; Henley, A.; Dowell, D. Farm diversification, entrepreneurship and technology adoption: Analysis of upland farmers in Wales. *J. Rural Stud.* **2017**, *53*, 132–143. [CrossRef]
111. Dias, C.; Franco, M. Cooperation in tradition or tradition in cooperation? Networks of agricultural entrepreneurs. *Land Use Policy* **2018**, *71*, 36–48. [CrossRef]



© 2020 by the author. Licensee MDPI, Basel, Switzerland. This article is an open access article distributed under the terms and conditions of the Creative Commons Attribution (CC BY) license (<http://creativecommons.org/licenses/by/4.0/>).

Article

Evaluation of Non-Conventional Biological and Molecular Parameters as Potential Indicators of Quality and Functionality of Urban Biosolids Used as Organic Amendments of Agricultural Soils

Miriam del Rocío Medina-Herrera ¹, María de la Luz Xochilt Negrete-Rodríguez ^{1,2}, José Luis Álvarez-Trejo ³, Midory Samaniego-Hernández ², Leopoldo González-Cruz ¹, Aurea Bernardino-Nicanor ¹ and Eloy Conde-Barajas ^{1,2,*}

¹ Department of Biochemical Engineering of Tecnológico Nacional de México/IT de Celaya, Celaya 38010, Guanajuato, Mexico; ibqmmolina@gmail.com (M.d.R.M.-H.); xochilt.negrete@itcelaya.edu.mx (M.d.L.L.X.N.-R.); leopoldo.gonzalez@itcelaya.edu.mx (L.G.-C.); aurea.bernardino@itcelaya.edu.mx (A.B.-N.)

² Department of Environmental Engineering, Tecnológico Nacional de México/IT de Celaya, Celaya 38010, Guanajuato, Mexico; midory.samaniego@itcelaya.edu.mx

³ Management of Administrative and Operation of the Wastewater Treatment Plant (WWTP) of Celaya, Ecosistema de Celaya S.A. de C.V., Celaya 38037, Guanajuato, Mexico; jalvarez@ticsa.com.mx

* Correspondence: eloy.conde@itcelaya.edu.mx; Tel.: +52-46-1611-7575

Received: 18 November 2019; Accepted: 7 January 2020; Published: 10 January 2020

Abstract: Biosolids are waste from wastewater treatment and have a high content of organic matter and nutrients. In this study, not conventional physicochemical and biological properties of biosolids produced during different seasons of the year were evaluated. These properties are not considered in environmental regulations; however, they are of agronomic interest as indicators of quality and functionality in soils. Also, molecular analysis by Fourier-transform infrared (FTIR) was conducted, enzymatic analysis using the APIZYM[®] system was performed and two indices of functional and microbial diversity were established. The results showed that the biosolids had a high content of total organic carbon, total nitrogen, P, and K. FTIR analyses showed that chemical composition of biosolids was similar during all year. The C and N of microbial biomass demonstrated presence of active microorganisms, as well as a uniformity in its richness and abundance of species that could present a positive synergy with soil microorganisms. The enzymatic activities showed that the biosolids contained an enzymatic machinery available to promote the mineralisation of the organic matter of biosolids and could even transcend into the soil. Finally, biological properties can be used as indicators of quality and functionality of biosolids before being used as an organic amendment, especially in agricultural soils.

Keywords: biosolids; quality index; microbial biomass; enzymatic activity; micro and macronutrients; organic amendment

1. Introduction

Waste sludge is a waste product that originated in the wastewater treatment process. Wastewater treatment consists of a series of physical, chemical, and biological processes that have the purpose of eliminating the contaminants present in the water [1,2]. The wastewater treatment process usually has three stages (primary, secondary, and tertiary). The first stage aims to remove large solids (garbage), sand and suspended solids from the affluent, through a system of sieves or screens, sandblasting and sedimentation [1,3]. The sludge generated at this stage named primary sludge is hazardous waste

and is sent to confinement [2]. The second stage of wastewater treatment aims to eliminate dissolved organic matter present in wastewater [1–3]. This stage is carried out mainly through processes of a biological nature that have in common the use of microorganisms to remove biodegradable organic matter [4]. The third stage of wastewater treatment aims to remove the residual organic load and those persistent pollutants not removed in previous treatments, e.g., N and P [3,5]. The sludge generated in the secondary and tertiary stages of wastewater treatment is combined and sent to stabilisation processes [5]. These sludges are known as residual sludges and are characterized by a high content of easily degradable organic matter and nutrients, which can be used as soil improvers and even fertilizers for crops. However, due to the nature of their origin, they also contain germs, viruses, and pathogenic parasites that must be eliminated prior to use [3,5]. Therefore, the sludge is subjected to stabilisation processes to eliminate contaminants.

The sludge stabilisation processes can be biological, chemical, and thermal. Biological methods include aerobic and anaerobic digestion and composting [6,7]. The most commonly used chemical method is lime stabilisation [8–10]. The thermal stabilisation processes used are pyrolysis, burns or complete incineration [7,9]. Due to efficiency and costs, the most common process is biological stabilisation, which can be performed under anaerobic (fermentation) and aerobic (oxidative stabilisation) conditions [9,11]. Aerobic digestion, which is of interest in this study, involves the use of the process of decomposition of organic matter contained in sludge through microbial activity under aerobic conditions [4,9]. The organic matter in the sludge is a substrate for the three-phase microbial metabolic chain [9]. In the first phase, easily degradable organic matter is oxidized by interaction of enzymes produced by microorganisms that live in the activated sludge, resulting in rapid multiplication of microorganisms [4]. Microorganisms use organic matter to increase their biomass and synthesis of enzymes this occurs until easily degradable organic matter is depleted [2,9]. In the second phase, after the depletion of organic matter, the cellular material is oxidized, and the microorganisms obtain energy from the self-oxidation of these cellular substances [3,9]. In the third phase, further intracellular oxidation is continued. Phases two and three are called aerobic stability [2,3,9]. The stabilized residual sludges are called biosolids and can be used as soil improvers and fertilizers as long as they comply with the established regulations [1,3,9].

The generation of biosolids during urban effluent treatment has increased in Mexico, as there has been an increase in the number of urban wastewater treatment plants (UWWTPs). By 2016, the National Water Commission (CONAGUA) registered 2536 wastewater treatment plants in operation [10]. This represented an increase in the flow of treated wastewater of 25,946.58 L/s. As a result, the amount of biosolids generated throughout the country increased at the same rate. Therefore, there is a need to develop strategies for the management, use, and final disposal of biosolids with a minimum impact on society and the environment. Both nationally and internationally, it has been necessary to recycle and reduce the amount of biosolids sent to landfills, avoiding saturation [11]. In the same context, incineration and application to sanitary landfills and incineration and application to soils have been the main forms of final disposal of biosolids [12]. However, the disposal of biosolids in landfills or by incineration are technologies in which these biosolids rich in organic matter (OM) and nutrients are not used for crops or plants [13]. In addition, most incineration technologies release hazardous chemicals such as dioxins, furans, NO_x, SO₂, and hydrocarbons into the atmosphere [14]. The application of biosolids to soils provides a source of nutrients available to plants because biosolids have been reported to contain valuable amounts of stable organic matter, providing long-term benefits for soil structure and fertility [15]. However, biosolids also need to be evaluated from different points of view—for example, in the aspect of their characterisation over time from their generation source (UWWTP). The variability of the C and N content, as well as of the micro and macro nutrients in the biosolids before their application to the soils, should be evaluated. Also, the safety of biosolids and the cumulative effects of various physicochemical and biological parameters over time need to be considered in the assessment.

In the same context, biosolids contain pathogens, parasites, heavy metals, and xenobiotic organic compounds that can cause health and environmental damage [16–20]. There are regulatory standards

at the national [21] and international level [22,23] for the application of biosolids to both agricultural and forest soils (Table 1), which include the control of parasites (Helminth), pathogens (total coliforms and *Salmonella* sp.), and heavy metals (As, Cd, Cu, Cr, Hg, Ni, Pb, and Zn), principally. However, there are no regulatory standards regarding the speed of application of biosolids to agricultural soils. In the same context, there are also not many studies evaluating the variability over time of their properties or of biological and molecular parameters only in biosolids. These properties and parameters have been evaluated to monitor the effects of the application of biosolids to soils over time but have not been evaluated to be used as indicators of quality and functionality of a substrate per se (e.g., biosolids) as an improved in agricultural soils. These evaluations include the following: analysis of functional groups by FTIR, microbial biomass C and N (MBC and MBN), biochemical relationships (C_{mic}/N_{mic}), metabolic coefficients or microbial activity (qCO_2 , $qFDA$), enzymatic activities that relate the cycles of C, N and P, such as lipases, esterases and proteases (FDA); dehydrogenases (DHS), the proportion of DHS and FDA, urease activity (URS) and the production of respiration (CO_2). Also included are enzyme activity monitoring systems that allow the establishment of “fingerprints” or activity enzyme “profiles” such as the API ZYM[®] system. As well, the establishment of indices of functional diversity and microbial activity, such as the Shannon index (H') and synthetic enzymatic index (SEI) is also important for their potential contribution as indicators of quality and agronomic functionality of biosolids before and after being applied as soil improvers [24–40]. Only U.S.A. regulation stipulates that the agronomic speed of application cannot be exceeded [41]; to protect the quality of groundwater or surface water, nitrogen must be regulated through an agronomic rate approach, which requires an estimate of the need for N from the crop and the availability of N in biosolids [41,42].

In context, there is unfortunately no reliable parameter as an adequate indicator of the stability and maturity of biosolids used as organic amendments in soils. However, some biochemical parameters, such as microbial biomass and enzymatic activities, are useful indicators of ecosystem quality and functionality [26,28]. Microbial biomass represents the living part of an ecosystem and is responsible for the transformation of organic matter, therefore the importance of assessing its status in biosolids [24]. The microorganisms have a set of enzymes both intracellular (e.g., dehydrogenases) and extracellular (hydrolytic enzymes such as glucosidase, esterases, proteases, etc.) responsible for the breakdown of organic matter, nitrogen transformations and can provide information on the biological status of biosolids. Hydrolytic activity of extracellular enzymes has received attention for several reasons: (1) these activities play a key role in the hydrolysis and mineralisation of organic wastes; (2) the characterisation of enzyme activities can provide insight into the biochemical factors controlling nutrient mineralisation; and (3) patterns of enzyme activities can be useful in identifying microbial populations [43]. Several enzyme assays are available to determine the hydrolytic activity in different environmental matrices. One of these enzymatic assays is the API ZYM[®] system which has been used in environmental matrices with complex biochemical processes e.g., soils, compost, activated sludge and sediments [34–39,44]. This system provides rapid and semi-quantitative information on the hydrolytic activity of 19 enzymes associated with the biodegradation of lipids, proteins, carbohydrates, and nucleic acids [34,36,39]. Therefore, the importance of monitoring a wide range of enzymes involved in various biochemical processes such as those occurring in biosolids is emphasized. It is also proposed to monitor these enzymes to establish the possible effects before adding them to the soil in order to establish a better management of these biosolids as organic amendments in agricultural soils. Derived from the above, the following hypothesis was proposed: biosolids, regardless of the time they are generated in a stabilized wastewater treatment process, possess physicochemical and/or biological properties or characteristics of agronomic interest that can be used for their application as soil improvers. Finally, the present study evaluated, over time, the conventional physicochemical parameters of agricultural interest, as well as the biological and molecular parameters of agronomic interest, but not those contemplated in the regulations, of urban biosolids from a UWWTP. It also aimed to establish technical-scientific arguments in the use of these non-standardised biological and molecular parameters as indicators of quality and functionality of the biosolids used as soil improvers.

The biological and molecular results obtained could be considered as indicators of functionality when establishing application rates in agricultural soils. The results obtained also aim to contribute to the correct management, recovery and use of this type of waste generated in a WWTP, regardless of the time of year in which they are generated.

Table 1. Regulatory standards for the application of biosolids in soils established in national and international standards.

Parameter	Value *	MPL of Contaminants in Biosolids		
		Mexico	EE. UU.	E.U.
Fecal coliforms (MPN g ⁻¹)	210,000	<2,000,000	<2,000,000	N.R.
<i>Salmonella sp.</i> (MPN g ⁻¹)	<3	<300	<4	N.R.
Helminth Eggs (eggs g ⁻¹)	<1	<35	<1	N.R.
As (mg kg ⁻¹)	1.81	75	41	N.R.
Cd (mg kg ⁻¹)	7.41	85	39	20–40
Cu (mg kg ⁻¹)	107.28	4300	1500	1000–1750
Cr (mg kg ⁻¹)	28.46	3000	N.R.	N.R.
Hg (mg kg ⁻¹)	1.03	840	17	16–25
Ni (mg kg ⁻¹)	30.19	57	420	300–400
Pb (mg kg ⁻¹)	38.19	420	300	750–1200
Zn (mg kg ⁻¹)	707.95	7500	2800	2500–4000

* The results are reported on a dry basis and are the average of the data obtained in the half-yearly analyses carried out by UWWTP of Celaya from 2014 to December 2018. MPL = Maximum permissible limit; EE. UU. = United States; E.U. = European Union; N.R. = Not regulated. MPL data were obtained for Mexico from NOM-004-SEMARNAT-2002, for the United States from EPA Standard 40CFR- 503 and for the European Union from 86/278/EEC [21–23].

2. Materials and Methods

2.1. Production, Sampling and Status of Biosolids

The biosolids were sampled monthly during 2018 at a UWWTP in Guanajuato, Mexico, located at geographic coordinates 100°51'64'' W and 20°30'78'' N (Figure 1). The biosolids were produced by biological treatments and aerobic digestion processes. After the aerobic digestion process, the produced solids were dehydrated by means of pressed band filtration systems. The biosolids were taken six times over a four-hour period on the conveyor belt at the outlet of the filter press. Approximately 30 kg in total of the sample on a wet basis (85%) were collected during each sampling performed [21]. The samples were taken at random in triplicate from day 7 to day 23 of each month, for 1 year, with a total of 36 samples. The samples were taken to the laboratory, dried in the air, sieved through a 2 mm diameter mesh and stored at 4 °C for further analysis. The analysis of their physicochemical and biological properties did not exceed the storage time of 1 week [45,46].

As an antecedent, the biosolids produced in this study have been evaluated from August 2014 to December 2018 (three times a year randomly), complying with the physicochemical standards established in current national and international regulations [21–23,41] for their correct final disposal. These standards only include the content of pathogens, parasites, and heavy metals in biosolids produced in a UWWTP. The biosolids have been below the permissible limits both nationally and internationally for their use (Table 1). Therefore, biosolids before this study were applied to agricultural soils but without characterisations under other parameters that are potentially applicable as biological and molecular indicators of agronomic interest or fertility for soils.

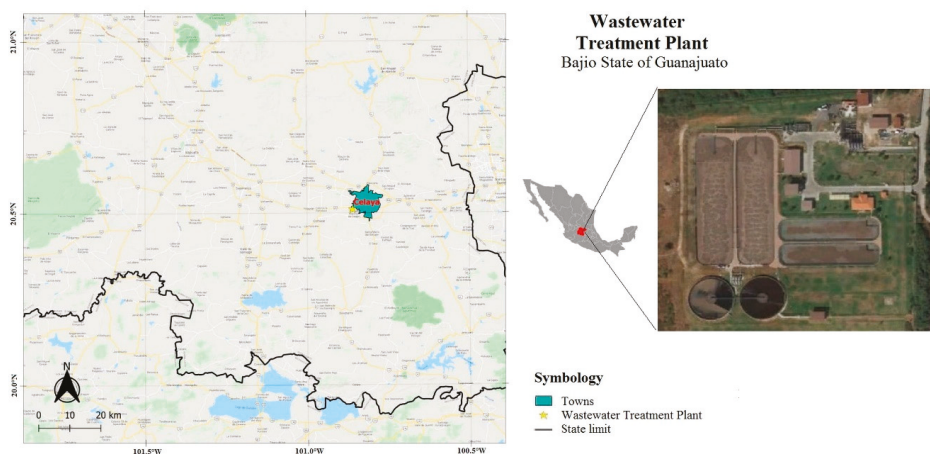


Figure 1. Location map of the urban wastewater treatment plant of the municipality of Celaya, Guanajuato, Mexico with geographical coordinates 100°51'64'' W and 20°30'78'' N.

2.2. Physicochemical Characterisation of Biosolids and Obtaining FTIR Spectra

The characterisation of the biosolids was carried out every month, for 1 year. The pH and electrical conductivity (EC) were measured in a mixture of biosolids and deionised water, at a ratio of 1:2.5 and 1:5 (m:v), respectively [45,47,48]. Total organic carbon (TOC) was determined by oxidation with potassium dichromate according to the Walkley and Black method [49], modified by downscaling and colorimetric determination [50]. Total nitrogen (TN) was analysed by micro-Kjeldhal system [51]. With the TOC and TN values, the C/N ratios were obtained. Macro and micronutrients (P, K, Fe, B, Mn, Zn, and Cu) were determined by microwave digestion with the EPA3051A/2007 method [52]. Briefly, the digested samples were cooled to room temperature, filtered (Watman paper 41), and measured at 50 mL with distilled water [53]. The content of each element was determined by inductively coupled plasma atomic emission spectrometry (ICP-AES), which was calibrated with a target and 5 standards [54].

For molecular analyses using Fourier transform infrared spectra (FTIR), samples of approximately 2 g of ground and sieved biosolids (<0.5 mm) were placed in an oven at 105 °C for 24 h. A subsample of 5 mg (dry basis) was mixed with 500 mg of KBr, crushed and homogenised in an agate mortar to form a fine powder. A translucent KBr tablet was formed from a press. The FTIR absorbance spectra of the biosolids were determined by scanning the tablets at a wave number range of 4000 to 400 cm^{-1} with a resolution of 8 using a FTIR Spectrometer. The main functional groups detected in biosolids were identified by comparison with Johnston and Aochi [29] and Martínez et al. [33].

2.3. Biological Characterisation and Enzymatic Profile of Biosolids

For the characterisation of biological parameters not considered in the standards of regulation the C and N of the microbial biomass (MBC and MBN) was determined by the fumigation method extraction at 25 °C [55]. With the values of MBC and MBN, the $C_{\text{mic}}/N_{\text{mic}}$ ratio was calculated.

The enzyme activity of dehydrogenase (DHS) was determined according to Von Mersi and Schinner [28]. The microbial and enzymatic activity of families of lipases, esters and proteases were evaluated by hydrolysis of fluorescein diacetate (FDA) using the method established by Green et al. [32]. The DHS/FDA ratio was calculated with the values obtained for the DSH and FDA enzymatic activities, respectively [56]. The enzymatic activity of urease (URS) was determined according to Kandeler and Gerber [25].

Basal respiration was determined by C-CO₂ produced after 20 days of incubation at 25 °C, as reported by Anderson [57]. The metabolic coefficient (qCO₂) was estimated by the quotient of

microbial basal respiration (C-CO₂) and MBC [27]. Specific hydrolytic activity (qFDA) was calculated by dividing the FDA activity value and MBC content as established by Perucci et al. [30].

To evaluate the enzymatic profiles in the biosolids studied during 1 year, the API ZYM[®] system was used, consisting of sterile galleries with 20 domes for control and 19 hydrolytic enzymes, including 3 phosphatases (alkaline phosphatase, acid phosphatase, Naphthol-AS-BI-phosphohydrolase), 3 esterases (lipase, esterase-lipase, esterase), 3 aminopeptidases (leucine arylamidase, valine arylamidase, cystine arylamidase), 2 proteases (trypsin and α -chemotrypsin) and 8 glycosyl hydrolases (α -galactosidase, β -galactosidase, β -glucuronidase, α -glucosidase, β -glucosidase, N-acetyl- β -glucosaminidase, α -mannosidase, α -fucosidase). The activity of these hydrolytic enzymes in biosolids was determined according to the manufacturer's instructions (BioMérieux), by means of aqueous extracts, in triplicate [58]. The aqueous extracts were prepared from a mixture of biosolid:distilled water (1:3, m/v), stirred for 20 min at 25 °C and centrifuged at 2000 rpm for 10 min as established by Tiquia et al. [34]. The supernatant was filtered and used for enzymatic analysis. In each dome, 65 μ L of the supernatant was distributed, the chamber was covered and incubated at 37 °C for 4 h [58]. After incubation, 30 μ L of each ZYM A and ZYM B reagent were added to each dome and allowed to stand for 5 min to reveal the colour change in the substrates. After this time, the enzyme activity intensity reading was taken by assigning numerical values from 0 to 5 to each reaction according to the manufacturer's reading table and reported in the literature [34,36,37]. Colour intensity readings for enzymatic reactions were performed by 4 independent observers [38]. With the results obtained, an extracellular enzyme profile diagram was designed as established by Patel et al. [39]. The diagram is obtained by classifying the enzymes in the 5 families (phosphatase, esterase/lipase, amino peptidase, protease and glucosyl hydrolases) and their intensity was placed according to the following scale: (1) high activity for enzymes with intensity number obtained according to the manufacturer reading; (2) moderate activity for enzymes with intensity numbers between 2 and 3; (3) low activity for enzymes with intensity number 1; and (4) activity not detected for enzymes with intensity number 0. Subsequently, all the enzymes that showed activity ≥ 1 , ≥ 2 , ≥ 4 and =0 are added. Thus, the state of the hydrolytic activities of the enzymes were evaluated by API ZYM[®].

In addition, the Shannon index was determined to assess the status of the microbial community in biosolids based on their distribution and diversity using Equation (1) [59].

$$H' = - \sum p_i \ln p_i \quad (1)$$

where p_i is the relationship of the activity of an enzyme to total enzyme activity. On the other hand, biochemical functional diversity or total enzyme activity was expressed by a synthetic enzyme index (SEI) that was calculated as reported by Dumontet et al. [31]. The SEI was evaluated as the sum of the colour intensity developed later in the enzymatic reactions translated into terms of amount of hydrolysed substrate, where 0 is 0 nmol of hydrolysed substrate, 1 is 5, 2 is 10, 3 is 20, 4 is 30 and 5 is ≥ 40 nmol hydrolysed substrate, respectively [35].

2.4. Statistical Analysis

Statistical analysis of the results obtained in physicochemical and biological characterisation was performed using the statistical analysis software, Minitab v. 18 [60]. The statistical significance of the differences between the parameter means was carried out by means of an ANOVA followed by a Tukey test ($p \leq 0.05$). To calculate the general correlation between physicochemical and biological parameters, the Pearson product-moment correlation was used [39].

3. Results and Discussion

As an introduction to the results obtained, it is important to emphasize that sustainable management of biosolids requires that special attention be paid to the rate and type of biosolids most

appropriate for the level of soil fertility required, in order to minimize the risk of eutrophication and maximize the benefits for soil ecosystem services [61–63].

3.1. Physicochemical Characterisation of Biosolids

The physicochemical characteristics of the biosolids at different times of the year are presented in Table 2. The pH values obtained ranged between 6.10 and 6.41, so they were considered slightly acidic. These pH values were not significantly different ($F = 0.237$, $p = 0.869$) from each other. The tendency to present a slight acidity may be due to the presence of organic acids derived from the degradation of organic matter present in wastewater. In other studies, in which biosolids have been generated from urban wastewater treatment and used for organic amendments, pH values have been reported in a range of 5.5 to 6.5 [13,63], similar to those obtained in this study. Torres et al. [64] established that the slightly acidic pH of organic amendments (e.g., biosolids) can be attributed to mineralisation processes of organic matter due to the presence of labile organic compounds available for microbial metabolism. These compounds may be aliphatic organic acids, amino acids and their polymeric derivatives (e.g., proteins and polypeptides), polysaccharides, lipids and other low molecular weight organic compounds. Thus, the slightly acidic pH of the evaluated biosolids may be related to the chemical composition of the organic matter present in the biosolids and their mineralisation. The EC in biosolids evaluated at different times of the year showed significant differences ($F = 8.43$, $p = 0.007$) (Table 2). Values between 1.60 and 5.71 dS m^{-1} were observed, which implied an important salt content, characteristic of biosolids from urban wastewater treatment [65,66]. The highest value was presented in spring (5.71 dS m^{-1}) and the lowest in autumn (1.60 dS m^{-1}). However, the EC values obtained were within the range of those reported in the literature (0.90 to 12.5 dS m^{-1}) for biosolids generated during urban wastewater treatment of aerobic and anaerobic processes [67–69]. Studies on the application of biosolids and their effect on soil physicochemical properties have reported an increase in EC values, including as a function of the application rates used [19,70–72]. On the other hand, Lloret et al. [72] evaluated the effect of the application of biosolids coming from aerobic and anaerobic treatments on the chemical and biological properties of the soil. The evaluated soil presented an EC value of 0.48 dS m^{-1} . After the application of the aerobic and anaerobic biosolids, the EC in the soil increased to 2.0 and 2.8 dS m^{-1} , respectively, and these values were maintained for the 2 months that the experiment lasted. With this information, the EC and its variation in biosolids generated in urban wastewater treatment plants, both in aerobic and anaerobic processes, should be monitored over time [21,61], as well as before and after being applied to agricultural soils, to prevent possible salt accumulations causing salinity or salinity-sodicity problems in soils [73].

Under the same context, the benefit of applying biosolids as organic amendments to agricultural soils lies in the presence of labile organic matter, which can constitute an energy reserve in the soil [74]. Therefore, for a better use of biosolids, it is important to know the total organic carbon content (TOC) and its variation over time before its application to agricultural soils. TOC varied in the biosolids sampled at different times of the year in an interval of 36.90 to 57.94% (Table 2). The highest TOC value was in summer (57.94%) and the lowest was in winter (36.90%). The TOC values obtained at different times of the year were significantly different ($F = 55.655$, $p = 0.000$) from each other. With respect to TOC values in biosolids and sewage sludge reported in the literature, these are lower than those obtained in the present study. Rowell et al. [75], for the purpose of soil application, evaluated different biosolids from different UWWTP as a result of both aerobic and anaerobic wastewater treatment and digestion processes. The values obtained were lower than those obtained in this study ranging in a TOC range from 31.80 to 35.10%. In similar studies of different types of biosolids from aerobic digestion processes and activated sludge or anaerobic digestion systems, the average TOC values reported were below those obtained in this study [11,68]. Thus, the biosolids analysed in this study, despite their variability in TOC content, probably due to the biochemical composition of wastewater, wastewater treatments and sludge stabilisation processes, presented a high C content. It is then argued that the biosolids in this study can be used as potential sources of labile or affordable sources of C, for application in agricultural

soils or with fertility problems. However, due to their variability, the need to monitor the TOC content of biosolids produced in the WWTPs over time, especially before and after their application to agricultural soils, is highlighted. The above is needed for a better design or application plan (dosage) and does not only consider the total amount of biosolids (Ton Ha^{-1}), as is currently practiced at the local or regional level. In addition, due to the variability of TOC presented in the evaluated biosolids, it is important to establish short- and long-term studies on its effects on C mineralisation rates (CO_2 emissions), incorporation into microbial biomass (MBC), enzymatic activities, and global C balances (inputs and outputs) when applied to soils. Biosolids have been characterised as an organic residue rich in nitrogen [19]. The TN content of the biosolids analysed at different times of the year ranged between 6.35% and 6.78%, with no significant differences ($F = 0.200, p = 0.893$) between them. From the values obtained, it was considered that the evaluated TN is a stable parameter regardless of the time of year in which it is analysed. In function to the non-variability in the N content observed in the evaluated biosolids, this parameter could then be used as an indicator or criterion of quality and functionality during the design of agronomic doses or application rates to agricultural soils or soils with N deficiencies. However, the values obtained were high (1.54 to 4.07%) compared to those reported in other studies where biosolids have been characterised for organic amendments to agricultural soils [11,18,75]. In the same context, the effect of applying biosolids to soils makes the N content increase and is also available to crops longer, especially when the organic N content is mineralised (nitrification) to inorganic forms, mainly N-NH_4^+ and N-NO_3^- [68,76,77]. Thus, a physicochemical indicator of functionality or quality of biosolids to consider, which is linked to biological processes of N mineralisation, can be, not only the N content in soil and N requirements in crops, but also the N content in biosolids, especially during the design of soil application dosages [19,78].

The content of C and N in biosolids are 2 parameters of interest during the application of organic amendment to soils. Although the C and N content in the analysed biosolids was high compared to the values reported in the literature, the C/N ratio was within the previously reported values [18,68]. The C/N ratio of biosolids ranged from 5.64 to 8.64 for different times of the year and were statistically different ($F = 10.243, p = 0.004$). The highest C/N ratio was presented in summer (8.64) and the lowest in spring (5.64). These results are within the range of 4.4 to 22.0 obtained for the C/N ratio of biosolids analysed in other studies [13,45,66]. Hseu and Huang [79], evaluated the mineralisation of N in 2 biosolids, 1 anaerobic and 1 aerobic, with a C/N ratio of 6.7 and 4.7, respectively, establishing that the C/N ratio is an important factor to evaluate in the mineralisation processes of biosolids in agricultural soils. Flores-Marguez et al. [67] conducted a study of biosolids mineralisation in agricultural soils and established that the C/N ratio was inversely related to the mineralisation rate of C and N. These results coincide with Brady and Weil [80] "organic amendments with low C/N ratio decompose more rapidly, once incorporated into the soil, than those with a high C/N ratio (>25). Matos et al. [11], established that low rates of C mineralisation in soils are potentially related to high C/N ratios (>30) and organic matter stability. Therefore, biosolids with an average C/N of 6.94 can conserve the C/N of the soil-biosolids system, without affecting C mineralisation rates by avoiding organic matter losses in the soil. One of the advantages of using biosolids as organic amendments is that they contain nutrients other than N, such as P and K, as well as micronutrients [81]. The content of P and K in the analysed biosolids was from 1.48 to 2.65% and from 0.59 to 1.09%, respectively. The content of P and K was significantly different ($F = 51.778, p = 0.000$ and $F = 28.732, p = 0.001$, respectively) between the seasons of the year. In spring, the highest P and K contents were presented, at 2.65 and 1.09%, respectively. The lowest value for P was 1.48% and corresponds to summer, while for K it was 0.59% in autumn. The results obtained from P and K in the evaluated biosolids were higher than those obtained by Paramashivam et al. [13], who reported P and K values for aerobic biosolids of 0.14 and 0.46%, respectively. Lü et al. [81] established that for different biosolids (aerobic, anaerobic and digested), the N, P and K content ranged from 2 to 8%, 1.5 to 3%, and 0.1 to 0.6%, respectively. The N and P content of the biosolids evaluated in this study were within the reported range; however, K was above that reported in other studies [81–83]. In addition, it is important to establish the amount of nutrients provided by biosolids as they are added

to the soil, because although biosolids are a source of nutrients (N, P and K), they often do not replace the use of commercial fertilisers, since their content of N, P and K may be less than that required for crops. Zhang et al. [84] conducted a long-term field experiment (4 years) with 3 doses of biosolids applied to the soil and found that it was necessary to add chemical fertilisers of P and K to cover the growth needs of the crops. However, the P released (organic P to inorganic P) from the biosolids increased in the soil depending on the application rate of the biosolids.

Table 2. Physicochemical characteristics and nutrient content in biosolids collected and evaluated in the urban wastewater treatment plant (UWWTP) at different season of year.

Parameters	Biosolids Analysed for Each Season of the Year			
	Spring	Summer	Autumn	Winter
pH	6.10 ± 0.17 a	6.20 ± 0.40 a	6.17 ± 0.17 a	6.41 ± 0.83 a
EC (dS m ⁻¹)	5.71 ± 1.93 a	3.38 ± 1.25 a, b	1.60 ± 0.01 b	1.65 ± 0.18 b
TOC (%)	37.25 ± 4.37 c	57.94 ± 1.25 a	50.25 ± 0.96 b	36.90 ± 1.17 c
TN (%)	6.67 ± 0.98 a	6.78 ± 0.82 a	6.59 ± 0.47 a	6.35 ± 0.42 a
C/N	5.64 ± 0.78 b	8.64 ± 1.18 a	7.65 ± 0.56 a, b	5.83 ± 1.38 b
P (%)	2.65 ± 0.17 a	1.48 ± 0.14 b	1.76 ± 0.03 b	2.28 ± 0.13 a
K (%)	1.09 ± 0.12 a	0.69 ± 0.07 b, c	0.59 ± 0.03 c	0.86 ± 0.04 b
Fe (g kg ⁻¹) †	16.10 ± 0.40 c	39.28 ± 1.77 a	20.43 ± 0.59 b	17.34 ± 1.91 c
B (mg kg ⁻¹) †	143.33 ± 12.01 b	145.00 ± 8.00 b	172.62 ± 2.13 a	122.41 ± 8.41 b
Mn (mg kg ⁻¹) †	130.00 ± 8.00 c	215.62 ± 7.39 a	166.30 ± 4.59 b	126.85 ± 7.56 c
Zn (mg kg ⁻¹) †	778.67 ± 13.50 b	635.65 ± 10.55 c	602.76 ± 2.34 d	813.51 ± 10.58 b
Cu (mg kg ⁻¹) †	133.64 ± 12.01 a	112.39 ± 5.56 b	95.22 ± 2.84 b	132.42 ± 5.64 a

EC = Electrical conductivity, TOC = Total organic carbon and C/N = carbon-nitrogen ratio. The values are the mean ± standard deviation (3 replicates). Rows with different letters are significantly different according to Tukey's analysis with $p \leq 0.05$. † The units correspond to biosolids on a dry basis.

Similarly, studies have reported that the content of K in biosolids (0.1 to 0.6%) is generally very small [82–85]. The low K content in biosolids significantly increases the nutrient imbalance in terms of the N:P:K ratio, so the most common practice is to add K fertilisers independently of biosolids when necessary [85]. However, the biosolids analysed in this work presented a content of 0.59 to 1.09% K, being above the commonly reported value for biosolids; however, they cannot be considered high without analysing the K content in the soil and the K requirements depending on the type of crop. Therefore, the importance of knowing the content of these macronutrients in biosolids is reiterated, in order to avoid adverse environmental effects or low crop yields.

The micronutrients present in the biosolids studied were Fe (16.10 to 39.28 g kg⁻¹ dry biosolids), B (122.41 to 172.62 mg kg⁻¹ dry biosolids), Mn (126.85 to 215.62 mg kg⁻¹ dry biosolids), Zn (602.76 to 813.51 mg kg⁻¹ dry biosolids), and Cu (95.22 to 132.42 mg kg⁻¹ dry biosolids). These results are similar to some previous studies of different biosolids that have reported the presence of micronutrients [86–88]. From the above, the results established in the literature is confirmed in the sense that biosolids not only contribute organic matter to soils, but also macro and micronutrients that can be used by crops. However, the results obtained from all micronutrients in the evaluated biosolids were significantly different (Fe, $F = 314.456$, $p = 0.000$; B, $F = 22.683$, $p = 0.002$; Mn, $F = 144.483$, $p = 0.000$; Zn, $F = 405.291$, $p = 0.000$; Cu, $F = 21.570$, $p = 0.003$) at different seasons of the year. Confirming the importance of analysing the amount of each of these micronutrients present in biosolids and their evolution over time at the site that has been generated (e.g., UWWTP), as well as after being incorporated depending on the dose of application to the soil. In addition, the quantity of each of these elements required in the soil, as well as in the crops, must also be considered, taking into account the needs of each species to be cultivated in order to maintain a balance of micronutrients suitable both for the soil and for the plants.

3.2. Characteristics of the FTIR Spectrum of Biosolids

Fourier Transform Infrared Spectrometry (FTIR) was used to identify functional groups present in biosolids. The FTIR spectra for biosolids evaluated at different times of the year were very similar to that shown in Figure 2. The bands observed between 3400 and 3500 cm^{-1} were attributed to O–H stretching of hydroxyl groups in carboxylic groups, phenols, polysaccharides, and saturated aliphatic species [89,90]. In addition, aliphatic methylene groups between 2850 and 2930 cm^{-1} were detected in all biosolids samples, mainly related to fats and lipids [33,91,92]. Bands found between 1650 and 1750 cm^{-1} , due to C=O stretching vibrations, indicated the presence of ketones, aldehydes, and carboxylic acid derivatives in biosolids [81,93]. On the other hand, the 1650 cm^{-1} band was attributed to C–N stretching vibrations in the primary amides of proteins [33,90,91]. The presence of primary amides in the evaluated biosolids is confirmed by the presence of bands between 1630 and 1640 cm^{-1} , which corresponds to bending vibrations of N–H [92,94]. In addition, the absorption bands found that between 1540 and 1560 cm^{-1} were attributed to secondary amide bonds of protein origin that probably came from human cells present in biosolids [91,95]. Reflection spectral of bands observed that between 1430 and 1450 cm^{-1} indicated the presence of aliphatic chains, possibly hemicellulose and lignin, due to stretching and bending vibrations C–H in CH_2/CH_3 [90,93]. Likewise, the bands found that between 1440 and 1450 cm^{-1} have been attributed to aromatic compounds due to stretching vibrations C=C, mainly related to aromatic components of humic acids [81,96]. In addition, a characteristic band at 1434 cm^{-1} has been reported for aldehydes and ketones due to composting vibrations C=O, as a result of the presence of humic and fulvic acids in the stabilisation process of biosolids organic matter because of UWWTP secondary digestion treatments [92]. The bands found that between 1380 and 1400 cm^{-1} were attributed to symmetrical COO stretching and CH_3 bending vibrations, related to proteins and lipids [93,95]. Likewise, bands observed between 1230 and 1250 cm^{-1} were associated with tertiary amines due to C–N stretching and N–H bending vibrations [90], as well as antisymmetric PO_2 stretching vibrations related to compounds with phosphodiester bonds, such as phospholipids and nucleic acids: RNA (ribonucleic acid) and DNA (deoxyribonucleic acid) [94]. Finally, absorbance bands between 875 and 1050 cm^{-1} corresponded to C–O and C–C stretching vibrations caused by polysaccharides and aromatic compounds [81,92]. Overall, the band-reflection spectra obtained by FTIR from the evaluated biosolids were like the results reported in the literature on biosolids and sewage sludge [90–93]. In fact, these molecular analyses showed a similar chemical composition in all the biosolids analysed in the different seasons of the year, presenting mostly the same absorbance bands. Therefore, it was possible to mention that the evaluated biosolids presented the same functional groups indicating that the chemical compounds present in the different seasons of the year were very similar and of low variability.

With respect to the changes in the “absorbance intensity” of the bands identified in the FTIR reflection spectra, these changes were not significant (see Figure 3; A, $F = 1.427$, $p = 0.304$; B, $F = 0.999$, $p = 0.441$; C, $F = 2.846$, $p = 0.106$; D, $F = 5.023$, $p = 0.030$; E, $F = 2.217$, $p = 0.122$; F, $F = 0.013$, $p = 0.998$; G, $F = 0.859$, $p = 0.500$; H, $F = 1.589$, $p = 0.267$; I, $F = 0.751$, $p = 0.552$) between seasons of the year. It was then determined that the “functional groups” identified for each of the analysed bands were similar in all biosolids samples, regardless of the time of year. This may be due to the fact that the wastewater treated throughout the year has the same origin and the UWWTP wastewater treatment process has been stable, without significant modifications at least during the study period of the biosolids generated. It could also be inferred that during the evaluation period, the handling of sewage sludge and its stabilisation process to be transformed into biosolids was stable.

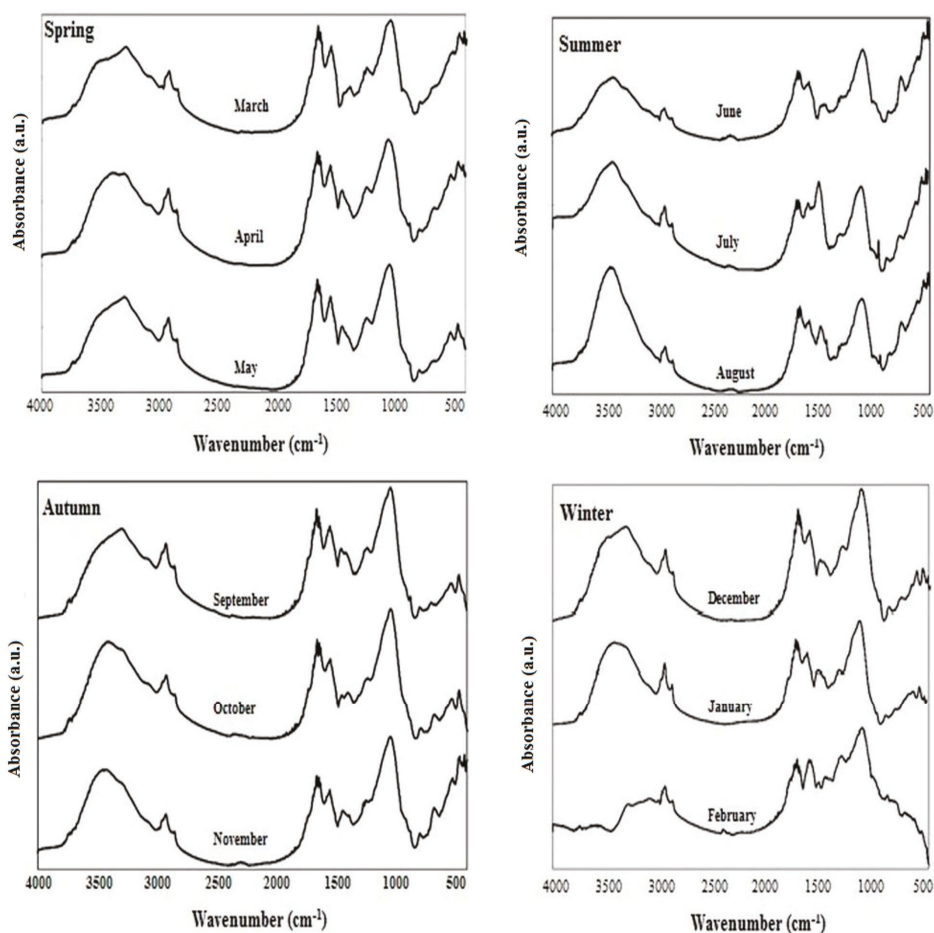


Figure 2. FTIR spectra of biosolids collected and evaluated in the UWWTP during different season of the year.

With the information obtained from the analysis of the absorption bands of the main functional groups evaluated in biosolids of the different seasons of the year, the presence of easily biodegradable molecules was established: carboxylic acids, proteins, lipids and aliphatic hydrocarbons, as well as recalcitrant or hardly biodegradable molecules (e.g., hemicellulose, cellulose and lignin). Therefore, establishing a “biostability indicator” related to the biodegradability of these biosolids is difficult without evaluating biological aspects related to the mineralisation processes of biosolids, such as microbial and enzymatic activity, and their relationship with the chemical composition of biosolids. Lü et al. [81], mentioned that microbial activity is directly associated with the content of bioavailable organic matter, and therefore, this parameter is relevant to being widely included during the evaluation of the “biostability” of organic residues such as biosolids. Thus, microbial activity reflected in enzyme activity may be directly related to the presence of some compounds in biosolids, e.g., lipases with lipids, proteases and aminopeptidases with peptides and proteins, phosphatases with phospholipids and nucleic acids, hydrolases glycosylated with aliphatic compounds, polysaccharides, etc. For this reason, it is important to evaluate biological characteristics not included in the sanitary regulations applicable to biosolids before and after their application to soils, especially to soils with agricultural activity.

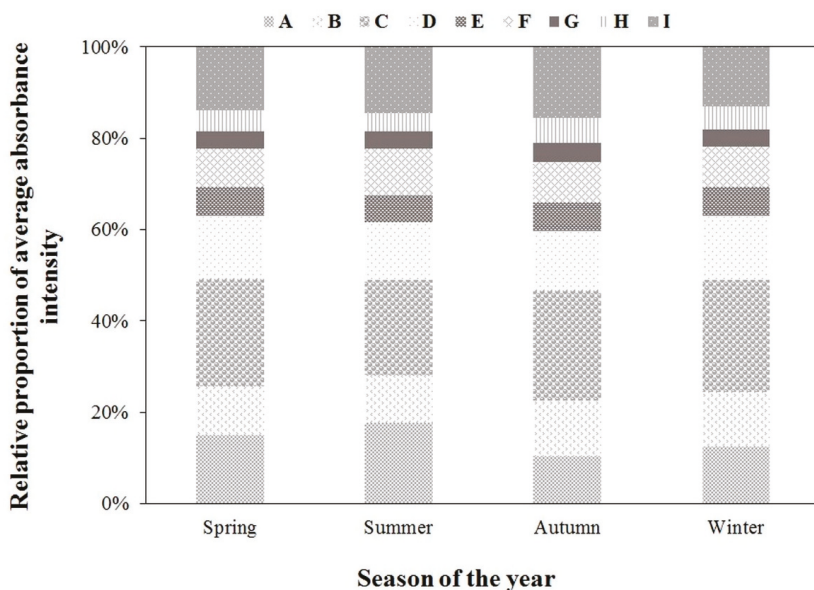


Figure 3. Distribution of absorbance intensity for each set of peaks found in the FTIR analysis of biosolids samples for each season of the year. Each box in the bars represents the absorbance peaks ordered according to wavelength: (A) 3400–3500 cm^{-1} , (B) 2850–2930 cm^{-1} , (C) 1650–1750 cm^{-1} , (D) 1630–1650 cm^{-1} , (E) 1540–1550 cm^{-1} , (F) 1430–1450 cm^{-1} , (G) 1380–1400 cm^{-1} , (H) 1230–1250 cm^{-1} and (I) 875–1050 cm^{-1} .

3.3. Biological Characterisation of Biosolids

Biostability is a key feature in biosolids to evaluate their use as organic amendment in soils. In the last decade, studies in soils with various organic amendments have focused on using biological properties for their sensitivity to change, as indicators of the dynamics of organic matter transformation, nutrient cycling, stress and regeneration processes [66,97–99]. Therefore, it was important to evaluate biological parameters for 1 year to establish indicators of quality and functionality of biosolids that have been added to soils, and thus be able to elucidate the positive or negative effects of adding these biosolids to soils before their application.

The biological parameters evaluated in the biosolids obtained in the UWWTP can be found in Table 3. Microbial biomass (MB), defined as the living microbial component of an ecosystem [26], is the primary terrestrial ecosystem agent responsible for decomposition of organic matter, nutrient cycling and energy flow [100,101]. In addition, the MB is considered an important ecological parameter in environmental ecosystems, because it represents the amount of energy stored by microorganisms [102,103]. Through the establishment of MB in biosolids and by carefully interpreting their values, it is possible to evaluate and monitor the functionality and quality of biosolids as an organic amendment, and thus predict their effects on soil microbial activity and their relationship with productivity, fertility and resistance to degradation forces. In this case, the MB in biosolids was determined by 3 parameters: C for microbial biomass (MBC), N for microbial biomass (MBN) and the relationship between C and microbial N ($C_{\text{mic}}/N_{\text{mic}}$). These biological parameters were selected because they have been widely used in previous studies of agricultural soils with application of biosolids as organic amendment because they are considered as sensitive and rapid indicators of restoration or ecological stress of the soil or environmental system investigated [63,104,105]. The MBC and MBN are the most labile C and N stores in soils [106,107], so their values are likely to be altered quickly in the event of any disturbance in the ecosystem. In addition, MBC and MBN are general

indices of microbial activity in soils [102,107]. Different soil management practices such as the addition of biosolids greatly affect the MBC and MBN in the soil [108]. For this reason, in order to understand the effect on soils of the application of biosolids, it is necessary to know the values of MBC and MBN in the biosolids before they are added to the soil. The results obtained from MBC in biosolids for different times of the year ranged between 587.22 and 1251.95 mg C_{mic} kg⁻¹ dry biosolids. These results were significantly different ($F = 26.318$, $p = 0.000$) between seasons of the year (Table 3). In winter the lowest MBC content was presented (587.22 mg C_{mic} kg⁻¹ dry biosolid) and the highest content was in summer (1251.95 mg C_{mic} kg⁻¹ dry biosolid). The previous MBC values represented a range of 0.16 to 0.26% of the TOC present in biosolids for the different seasons of the year. However, these values are considerably lower than those established for soils where MBC corresponded to 1 to 3% of TOC [94,96]. The values obtained for MBC in biosolids at different times of the year were higher than those obtained in other agricultural soil studies with addition of biosolids where MBC values ranged from 20.1 to 820 mg C kg⁻¹ dry soil [107,109]. Debosz et al. [109] observed that the application of biosolids to the soil presented a significant increase in MBC from the first 7 days to 60 days of application, and then a decrease to stabilize, so they considered the effect to be temporary. In addition, Fernandes et al. [108] found that MBC presented important variations at different application doses of biosolids to the soil, being directly proportional the increase of MBC with the application dose. However, none of these studies evaluated the MBC content of biosolids before they were added; therefore, with the results obtained in this study and as stipulated in the literature, it can be established that biosolids provide active microorganisms and affordable organic matter that could have a “positive synergy” with active soil microorganisms. This was stated in this study since in previous studies of application of biosolids to soils a biostimulation of soil MBC has been observed when using biosolids as an organic amendment.

Table 3. Biological characteristics in biosolids collected and evaluated in the UWWTP at different season of the year.

Parameters	Biosolids Analysed for Each Season of the Year			
	Spring	Summer	Autumn	Winter
MBC (mg C _{mic} kg ⁻¹) †	966.6 ± 46.4 b	1251.9 ± 134 a	1149 ± 115 a,b	587.2 ± 76.7 c
MBN (mg N _{mic} kg ⁻¹) †	84.25 ± 10.6 b	109.3 ± 1.4 b	304.7 ± 32.9 a	119.0 ± 20.1 b
C _{mic} /N _{mic}	11.66 ± 2.09 a	11.46 ± 1.32 a	3.82 ± 0.77 b	5.07 ± 1.32 b
DSH (mg INF * kg ⁻¹ h ⁻¹) †	2631.8 ± 147 a	2209.5 ± 119 a	2426.1 ± 230 a	2277.6 ± 225 a
FDA (mg F ** kg ⁻¹ h ⁻¹) †	342.7 ± 40.0 b	279.7 ± 30.0 b	437.96 ± 44.2 a	368.6 ± 24 a, b
DSH/FDA (mg INF mg ⁻¹ F *)	7.78 ± 1.35 a	7.99 ± 1.26 a	5.55 ± 0.22 a	6.21 ± 0.84 a
URS (mg N-NH ₄ ⁺ kg ⁻¹ h ⁻¹) †	186.0 ± 17.1 a	194.5 ± 23.0 a	109.8 ± 7.7 b	186.5 ± 13.7 a
qCO ₂ (mg C-CO ₂ g ⁻¹ C _{mic} d ⁻¹)	157.95 ± 7.40 b	124.31 ± 13.5 b	115.42 ± 11.6 b	270.19 ± 32.9 a
qFDA (mg F ** g ⁻¹ C _{mic} h ⁻¹)	356.27 ± 56.7 b	223.27 ± 4.84 b	381.57 ± 26.9 b	636.39 ± 106 a

The results are the mean ± standard deviation (3 replicates). Rows with different letters are significantly different according to Tukey’s analysis with $p \leq 0.05$. † The units correspond to biosolids on a dry basis.

* INF = Iodonitrotetrazolium formazan (1-(4-Iodophenyl)-5-(4-nitrophenyl)-3 phenyl formazan). ** F = Fluorescein.

In the same context, the results obtained for MBN in the evaluated biosolids ranged between 84.25 and 304.70 mg N_{mic} kg⁻¹ dry biosolids, exhibiting very significant differences ($F = 240.960$, $p = 0.000$) between autumn biosolids compared to the biosolids of the rest of the year (Table 3). A content of MBN was observed that corresponded to a range of 0.13 to 0.46% of the NT present in biosolids for different times of the year. MBN in soils constitutes more than 5% of NT [107]. The MBN of biosolids was found to be below that reported in soils. The results reported in the literature for MBN of soil with added biosolids have ranged from 3.1 to 101 mg N_{mic} kg⁻¹ dry soil [107–109]. However, based on previous studies [108,109], as with MBC, an increase in MBN would be expected with the addition of biosolids to soils. Masunga et al. [110] established that MBN in agricultural ecosystems controls the availability and loss of inorganic N from the soil, especially in systems with high N inputs such as agriculture. Therefore, adding an organic amendment, such as biosolids, with active microbial biomass (MBC and

MBN) can affect natural soil processes, such as the mineralisation of C and N as a consequence of a change in microbial structure [65,111]. For this reason, it is important to evaluate both MBC and MBN in soils and biosolids as organic amendments [65,105].

With respect to the C_{mic}/N_{mic} relationship, this has sometimes been used to describe the structure and state of the microbial community [106]. On the other hand, the C_{mic}/N_{mic} ratio of microbial isolates, extracted from soils or obtained from culture collections and cultivated under optimal conditions, varies from 7 to 12 in fungi and from 3 to 6 in bacteria [24]. The results obtained in this study of C_{mic}/N_{mic} varied from 3.82 to 11.66 (Table 3) and presented significant differences ($F = 23.377, p = 0.000$) between the seasons of the year. During spring and summer, C_{mic}/N_{mic} values were >11 , with no significant differences ($F = 0.019, p = 0.898$) between these 2 seasons of the year. However, in autumn and winter, the C_{mic}/N_{mic} ratio was <5 , and there were also no significant differences ($F = 1.992, p = 0.231$) between them. With these results, it was deduced that in spring and summer there was a greater predominance of fungi in the microbiota of biosolids, while in autumn and winter there was a greater predominance of bacteria. The predominance of microbial flora in biosolids can also be attributed to climatic conditions, as in spring and summer 2018 the local ambient temperature ranged from 11.93 to 30.97 °C and 13.83 to 27.76 °C, respectively, in autumn and winter 2018 it ranged from 11.70 to 25.83 °C and 6.27 to 24.27 °C, respectively [112]. Thus, fungal growth is promoted in a temperature range of 20 to 40 °C [113], while for bacteria the range is 4 to 60 °C [114]. With this information, it is possible to explain the predominance of fungi in spring and summer and bacteria in autumn and winter.

With respect to the enzymatic activity of dehydrogenase (DSH), this enzyme is an indicator of microbial activity in biological systems such as biosolids, reflecting primary metabolism and cellular respiration because it only occurs in viable cells [115,116]. In the biosolids evaluated at different times of the year, values of 2209.51 to 2426.10 mg INF kg⁻¹ dry biosolids h⁻¹ were found. The DSH of the biosolids did not present significant differences ($F = 3.009, p = 0.095$) at the different times of the year. With this it can be considered that, independently of the time of the year in which the biosolids were produced, their microbiota presented a similar cellular respiratory activity and primary metabolism. On the other hand, the DSH activity of the biosolids analysed was higher than that reported in the literature in soils with different management histories [117–119]. Pascual et al. [120] studied the activity of DSH as a biomarker of degradation and remediation processes in abandoned natural and agricultural soils. They observed that natural soils had higher DSH activity (61.2 mg INF kg⁻¹ dry soil h⁻¹) compared to soils without agricultural activity for different periods. The decrease in DSH activity, which they reported over time, was attributed to the progressive erosion of soils without agricultural activity because of low levels of organic matter. Other studies applying biosolids to agricultural soils as an organic amendment have shown that DSH activity in soils increases with the addition of biosolids, which has been attributed to a high content of labile organic matter present in biosolids [121–123]. However, biosolids have not been considered to present a high DSH activity as evaluated in this study (DSH activity > 2000 mg INF kg⁻¹ biosolids h⁻¹). Therefore, the addition of these biosolids to soils would be expected to increase DSH activity, not only because of their high organic matter content, but also because of the contribution of an active microbiota with available enzymatic machinery adapted to the organic matter present in the biosolids. Finally, to obtain information as observed from the evaluated enzymatic activity (DSH), before the addition of biosolids to agricultural soils, this information could be used to predict, with more ecological and biological arguments, the positive or negative effects of microbial interactions in agricultural soils with added biosolids.

On the other hand, with respect to the secondary metabolism of microorganisms, which is related to reserve energy consumption [56], microbial activity was determined by hydrolysis of fluorescein diacetate (FDA) in biosolids. Fluorescein diacetate is hydrolysed by proteases, lipases, and esterases, which are enzymes involved in the microbial breakdown of organic matter [32,124]. At different times of the year, biosolids presented an FDA activity between 279.71 and 437.96 mg Fluorescein kg⁻¹ dry biosolids h⁻¹ (Table 3). Significant differences ($F = 10.270, p = 0.004$) from FDA between different

seasons of the year were observed. In summer, it presented the lowest FDA activity (279.71 mg Fluorescein kg⁻¹ dry biosolids h⁻¹), and in autumn, the highest activity (437.96 mg Fluorescein kg⁻¹ dry biosolids h⁻¹). These values obtained at different times of the year could be due to the availability of energy reserve compounds in the biosolids, mainly lipids, esters and proteins as observed in the spectra of the FTIR analyses (Figures 1 and 2, Table 3). The observed increase in FDA activity was also related to a high content of labile organic matter in the evaluated biosolids, i.e., easily mineralizable organic compounds available as substrates for microbial metabolism [105,125]. However, the values obtained for biosolids evaluated independently of the season of year were higher than those reported in the literature in soils and soils with added biosolids [66,126,127]. Gajda et al. [124] evaluated the changes in FDA activity of 2 types of soil, 1 silty and the other sandy, without addition of organic amendments and with the same types of tillage, finding that FDA activity ranged from 50.50 to 126.70 mg fluorescein kg⁻¹ dry soil h⁻¹ and from 40.20 to 77.20 mg fluorescein kg⁻¹ dry soil h⁻¹, respectively. These results were lower than those obtained in this study for biosolids of all seasons of the year; even in summer the value obtained was 2.2 times higher than the highest value obtained in the silty soil evaluated in that study. On the other hand, Carlson et al. [127], evaluated the effect on FDA activity by adding organic amendments to an agricultural soil with 5 treatments: (1) control; (2) 137 mg urban vegetative compost ha⁻¹; (3) 202 mg biosolids ha⁻¹; (4) 404 mg biosolids ha⁻¹ and (5) designed mixture (202 mg biosolids ha⁻¹, 10.3 mg biochar ha⁻¹, and 5.7 µg Fe₂O₃ oxide ha⁻¹), obtaining values of 38, 90, 75, 50, and 70 mg fluorescein kg⁻¹ dry soil ha⁻¹, respectively. Thus, Carlson et al. [127], established that the organic amendments they used significantly increased FDA activity in soil, especially with biosolids, and suggested that organic amendments may contain extracellular hydrolytic enzymes or microorganisms that have these enzymes. With the results obtained in this study, the FDA's activity in biosolids could be demonstrated as suggested by Carlson et al. [127], and then it would be expected that by adding the biosolids evaluated in the present study to an agricultural soil, they would provide labile organic matter and enzymatic machinery already prepared for their degradation. In summary, an increase in FDA activity is expected by adding the evaluated biosolids to soils, as similarly reported in previous studies [66,125,127].

Barragán-Sánchez et al. [56], established a biosolids stability index expressed as DHS/FDA, providing information about the predominance between the primary metabolism (breathing processes, etc.) and the secondary metabolism (consumption of energy reserves) in the microorganisms present. If the DHS/FDA quotient is small, it can be mentioned that the secondary phase of metabolism referring to endogenous processes predominates in the system and vice versa. The results obtained in the biosolids analysed for this DHS/FDA index ranged from 5.55 to 7.99 mg INF mg⁻¹ Fluorescein, and there were no significant differences ($F = 3.96$, $p = 0.069$) between the seasons of the year (Table 3). The results obtained from DHS/FDA were lower than those obtained by Barragán-Sánchez et al. [56], who obtained values of 58 to 10 µmol O₂ µmol⁻¹ FDA hydrolysed (equivalent to 164.49 to 28.37 mg INF mg⁻¹ Fluorescein) during the monitoring of an aerobic process of stabilisation of residual sludge. With this it could be established that the secondary metabolism was the dominant one in the evaluated biosolids. The biosolids evaluated were a stabilised solid residue that is in a more markedly endogenous phase. Thus, when adding biosolids to agricultural soils, total enzyme activity in the soil would be expected to increase because the biosolids are in the endogenous phase, i.e., the microorganisms present are adapted and consume energy reserves for the production of hydrolytic enzymes that transform current organic matter into energy for the maintenance process [43,128]. This behaviour may also be related to the quality of organic matter present in biosolids [92,93], which according to the FTIR spectra observed (Figures 1 and 2), was stable and with little variability during the different seasons of the year. Therefore, the type and quantity of substrates available in biosolids has a significant influence on the development and predominance of the endogenous phase of the microorganisms present. In the same way, it can be established that the evaluated biosolids possess, besides labile organic matter, extracellular enzymes ready for the process of mineralisation of organic matter.

In reference to the evaluation of extracellular enzymatic activities, the activity of urease (URS) in biosolids in different seasons of the year was evaluated. URS is an enzyme that catalyses the hydrolysis of urea into carbon dioxide and ammonia by acting on the C–N bonds of different peptides [129]. Therefore, the activity of the URS is of great importance in the biotransformation processes of nitrogenous organic compounds [99]. The values reached for the activity of URS in the biosolids analysed at different times of the year ranged from 109.82 to 194.55 mg N-NH₄⁺ kg⁻¹ dry biosolids h⁻¹ (Table 3). The activity of the URS in the biosolids evaluated for the autumn presented significant differences ($F = 17.771$, $p = 0.001$) with respect to the rest of the year and was also the lowest value obtained (109.82 mg N-NH₄⁺ kg⁻¹ dry biosolids h⁻¹). This could indicate that in autumn there could have been fewer nitrogenous organic compounds than in the rest of the year, so less urease enzyme activity was required. Previous research has focused on evaluating the effect of URS activity in agricultural soils with added biosolids but has not considered evaluating URS activity in biosolids per se for a better understanding of the mineralisation processes of nitrogen compounds after the addition of biosolids to soils. In investigations on the application of biosolids in agricultural soils, an increase in the activity of URS has been observed; however, the values obtained have oscillated from 20 to 100 mg of N-NH₄⁺ kg⁻¹ dry soil h⁻¹ [108,122,127,129]. However, the results of the URS activity obtained in these studies were lower than those obtained in this paper. This enzymatic activity then becomes an indicator of the presence and potential contribution of nitrogenous sources of biosolids when applied to soils. On the other hand, with the results obtained, the importance of evaluating the activity of the URS in agricultural soils when biosolids are applied as organic amendment in short (maximum 180 days of incubation in laboratory experiments) and long (>1 year in field experiments) treatments was also established. Kızılkaya and Bayraklı [129] evaluated the effect of the addition of biosolids on URS activity at different doses of biosolids (0, 100, 200, and 300 ton ha⁻¹) in agricultural soil in a short-term laboratory-scale incubation experiment (90 days incubation). In these experiments it was observed that the activity of the URS increased rapidly until reaching a maximum activity in 15 days after the application of the biosolids; then, the activity of the URS decreased significantly until reaching values below the initial values (day 0) at 90 days of incubation. However, other long-term studies (1 and 4 years, respectively) conducted by Roig et al. [122] and Carlson et al. [127] agreed that URS activity was not affected by the addition of biosolids to agricultural soils. Thus, the increase in URS activity in soils with short-term application of biosolids could be a consequence of the stimulation of endemic soil microorganisms by the addition of N present in biosolids, increasing their metabolic capacity, and therefore, the production and activity of the urease enzyme. However, this increase in URS activity in agricultural soils with the addition of biosolids in the short-term applications could also be attributed to the fact that biosolids provide both labile organic matter and microorganisms with active enzymatic machinery ready for N transformation. Hence, the importance of evaluating URS activity in biosolids before application to soil becomes clear, especially since biosolids have been presented as an organic amendment with an important content of nitrogen compounds, such as amides, peptides and proteins, as observed in studies and analysis of FTIR spectra (Figures 2 and 3). Determining this enzymatic activity over time and in biosolids can be a usable indicator of quality and functionality to ensure the biotransformation of nitrogen-rich organic matter in soils prior to application.

Other biological parameters related to soil quality and functionality that have been used in assessing the effect of organic amendments such as biosolids on agricultural soils are the metabolic quotient (qCO₂) and specific hydrolytic activity (qFDA) [47,66,130]. The qCO₂ expresses the amount of CO₂ produced per unit of biomass and time. This indicator has been used as an indicator of the physiological status of microorganisms in biosolids [66,131]. The qCO₂ has also been used to detect alterations or stress of MB in the soil or in organic amendments due to disturbances or environmental changes [63,66,72]. The qCO₂ obtained in the biosolids analysed in this study for each time of year were 157.95, 124.31, 115.42, and 270.19 mg C-CO₂ g⁻¹ dry biosolids d⁻¹ for spring, summer, autumn and winter, respectively. Winter qCO₂ was significantly different ($F = 41.951$, $p = 0.000$) from the rest of the year. Therefore, it can be attributed that during the winter the biosolids presented an alteration

that allowed them to increase their respiration rate (Table 3). This increase could be possibly due to a lower MB content or climatic conditions, as already mentioned. The lower MB content or climatic conditions can propitiate a structural change of the microbial community [113]. Although there are no reported data in the literature on qCO_2 for biosolids per se, Sciubba et al. [66] established that qCO_2 in soils amended with biosolids presented a greater impact as the application rate of biosolids to the soil increased, thus confirming that qCO_2 can emphasise the effects of biosolids on soil properties. Tian et al. [131] in a field study on the application of biosolids to agricultural soils in the long term (>20 years) found that qCO_2 was lower in soil with application of biosolids than control soil without biosolids, thus concluding that there was an improvement in the microbial metabolism of C as a result of stress relief in soil microorganisms, due also to an increase in C sequestration in soils with biosolids. Thus, they expanded the concept of qCO_2 to assess microbial stress relief and restoration of microbial physiology in agricultural soils with biosolids amendment. Lloret et al. [72] evaluated the application of 2 types of biosolids: aerobic thermophilic (AT) and anaerobic mesophilic (AM) to an agricultural soil to establish if there are differences of these biosolids according to the stabilisation processes with which they were obtained and found that qCO_2 was higher in the soil with biosolids AM both with respect to the control soil (without amendment), as well as in the soil with biosolids AT. They concluded that AT biosolids produced minor changes in soil microbiota and improved soil microbial activity. Therefore, it is important to monitor these parameters in biosolids before their application to agricultural soils, to expect or not possible alterations to the soil microbiota and therefore to establish an adequate management of biosolids.

The qFDA is an index established by Perucci et al. [30] and was based on the measurement of the global hydrolytic capacity of a specific microbial biomass. The qFDA expresses the ratio of hydrolysed fluorescein diacetate (FDA) per C unit of microbial biomass [126,132]. This index has been used mainly for the evaluation of soil disturbance and stress due to the presence of xenobiotics [126]. The interest in using qFDA in the analysed biosolids was based on establishing if this parameter can be a useful tool, on the global hydrolytic activity and as a function of the C stored in the BM of the biosolids, which is very similar to how they have been used in soils [132,133]. The qFDA results obtained in the biosolids analysed for each season of the year were 356.27, 223.27, 381.57, and 636.39 mg Fluorescein $g^{-1} C_{mic} h^{-1}$ for spring, summer, autumn and winter, respectively (Table 2). The winter, qFDA was significantly different ($F = 23.371, p = 0.000$) from the rest of the year. This behaviour was like that obtained for qCO_2 , presenting the highest values. Yakushev et al. [130] conducted studies on the effect on the physiological state of the microbial community in compost and vermicompost, revealing higher qCO_2 and qFDA, indicating that organic matter is less accessible to microorganisms and that there is a greater consumption of energy for oxidation of substrates. Sánchez-Monedero et al. [126] evaluated the effect on qFDA dynamics during the application of biosolids compost to agricultural soils in an incubation experiment at 60 days. These researchers observed that qFDA was characterised by stable values during incubation time, i.e., qFDA dynamics were not affected by incubation time and addition of biosolids. Thus, it can be deduced that in winter the biosolids under study presented a more complex chemical composition, probably due to the presence of recalcitrant compounds, with respect to the other seasons of the year, presumably making the organic matter of the biosolids less accessible in winter. So, it can be established that the qFDA parameter in biosolids could be a useful quality and functional indicator, giving valuable information on the accessibility of organic matter in biosolids before its application to soils.

Biological parameters evaluated in biosolids, such as MBC and MBN content, as well as, the C_{mic}/N_{mic} ratio, demonstrated that biosolids have a significant content of active microorganisms, which could be produce a “positive synergistic” effect on the activity of soil microorganisms. In addition, in the biosolids evaluated over time, it has been possible to elucidate a high metabolic activity (DSH, FDA, and URS activity), presumably due to the content of substrates such as polysaccharides, proteins, fats and lipids that are easily assimilated by the microorganisms present. In addition, the DSH/FDA ratio established a predominance for secondary metabolism due to the presence of energy reserve compounds

already mentioned. Due to the active enzymatic machinery, this will facilitate the mineralisation of the organic matter of the biosolids, reducing the energetic barrier for the decomposition of the foreign complex organic matter for the microorganisms of the soil. The qCO₂ and qFDA allowed for the evaluation of the physiological state of the microorganisms of the evaluated biosolids, giving information through time about their capacity to assimilate the organic matter present in the biosolids, which will depend on the labile or complex chemical composition it has. Thus, having information on the biological/biochemical/molecular status of biosolids before their application to soils will allow predicting possible positive as well as negative effects on them, and thus will allow making better decisions on the management and disposal of these biosolids as an amendment or soil improvers, especially agricultural ones.

3.4. Extracellular Enzyme Profiles per API ZYM[®] Kit for Biosolids

The mineralisation of organic matter is mainly mediated by microorganisms, which possess the adequate enzymatic machinery to obtain the energy necessary to carry out their metabolic processes [39,134]. The enzymes involved in the degradation of organic matter can be divided into hydrolytic enzymes that are responsible for the acquisition of C, N and P to support primary and oxidative metabolism, oxidative enzymes that degrade recalcitrant compounds such as lignin during the acquisition of nutrients [135,136]. These groups of enzymes may respond differently to the addition of organic amendments such as biosolids. Torri et al. [62] stated that the addition of biosolids to soils can improve and maintain biological activity in soils over the long term. However, little information is available on the enzymatic activity of biosolids due to the lack of methodologies or analytical methods that provide information quickly and inexpensively. In recent decades, the API ZYM[®] system has been used and validated to evaluate enzymatic profiles of soils, compost, activated sludge and sediments [34,36–39,44,134,137,138]. However, the API ZYM[®] system has not been used directly and over time in biosolids samples as a system for the rapid determination of 19 extracellular hydrolytic enzymatic reactions related to the C, N and P cycles. The objective of using the API ZYM[®] system to evaluate biosolids at different season of the year was to quickly obtain information on the extracellular enzyme profile of biosolids. With the information obtained, it could be used as a background on the possible positive or negative effects on soil functional diversity when biosolids are used as an organic amendment. The extracellular enzyme profile of the biosolids analysed for each season of year is shown in Figure 4. The enzyme activity was classified into 5 families: (1) phosphatases (catalyses the removal of phosphate groups from substrates as nucleic acids), (2) esterases-lipases (hydrolyse ester bonds mainly in fats and oils), (3) aminopeptidases (hydrolyse peptide bonds in peptides), (4) proteases (hydrolyse peptide bonds in proteins) and (5) glycosyl hydrolases (catalyses the hydrolysis of glycosidic bonds in carbohydrates). The enzymatic activities presented differences and similarities for each season of the year.

In spring, a mainly moderate enzymatic activity was obtained (Figure 4). Within the 19 enzymes determined in biosolids in March and April, only 1 enzyme showed no activity, and it belonged to the family of glycosyl hydrolases. In biosolids produced in May, there were no activities of 3 enzymes, 2 glycosyl hydrolases and 1 protease. Low enzymatic activity in 4, 7 and 5 enzymes were detected in biosolids for March, April, and May, respectively. These enzymes belonged to the families esterases-lipases, aminopeptidases, proteases and glycosyl hydrolases (Figure 4). The enzyme activity of the biosolids was moderate for March, April, and May in 10, 6 and 8 enzymes, respectively, and were distributed within the 5 families. In March, April and May biosolids, high enzyme activity was presented for 4, 5 and 3 enzymes, respectively, mainly from the phosphatase family.

In summer, the enzyme profile of biosolids showed a predominantly high enzyme activity for all enzyme families. Undetected enzyme activity was obtained for 1 glycosyl hydrolase enzyme in June and July biosolids, while in August there were 2 enzymes, 1 glycosyl hydrolase and the other aminopeptidase. In June, low biosolids biological activity was obtained for 3 enzymes of the glycosyl hydrolases and aminopeptidases families. Moderate summer enzyme activity was presented in 9, 6

and 3 enzymes for June, July and August biosolids, respectively (Figure 4). The esterases-lipases and aminopeptidases families were the main ones that presented moderate enzymatic activity. The high enzyme activity for June, July and August biosolids was exhibited in 6, 12 and 4 enzymes, respectively. The families of phosphatases, proteases and glycosyl hydrolases had an important activity in summer.

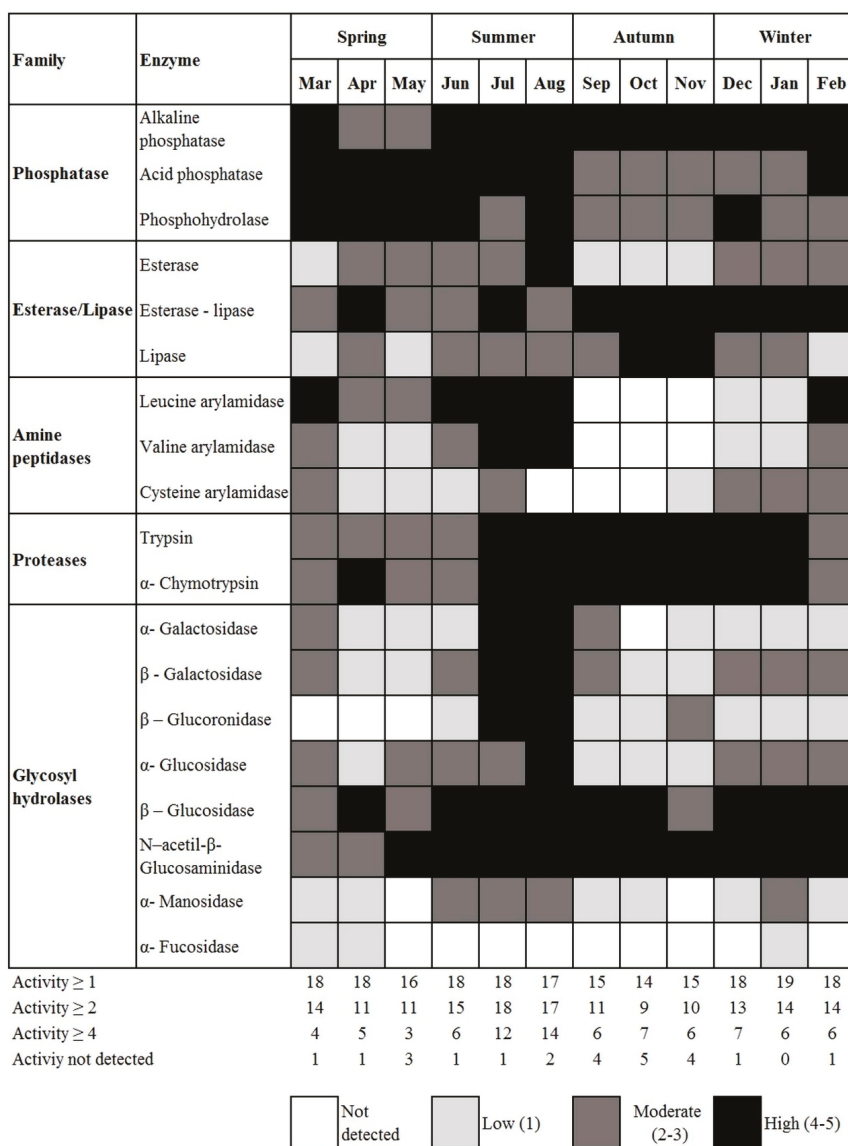


Figure 4. Profile of 19 extracellular enzymes determined by the API ZYM® system in the biosolids analysed during one year of UWWTP operation. The shading in the table represents the relative abundance of enzymes. The values are as follows: White, not detected; light grey, low intensity reactions (value = 1); dark grey, moderate intensity reactions (value = 2 and 3); black, high intensity reactions (value = 4 and 5). The number of enzymes showing reactions ≥ 1 , ≥ 2 and ≥ 4 , as well as the total number of enzymes showing no activity for each month are indicated below each column.

In autumn, the enzyme activity of biosolids was moderate to high; however, this was the season of the year with the highest number of enzymes with undetected activity. In September and November there was undetected enzyme activity in 4 enzymes, and in October there was undetected enzyme activity in 6 enzymes. The aminopeptidase family showed no enzyme activity in any of the biosolids samples analysed for the fall. There was low enzyme activity in September and October in the biosolids observed in this phenomenon in 4 enzymes. In November this low activity was only present in 5 enzymes. Most of the low activity enzymes were glycosylhydrolase. With moderate enzyme activity, 5, 2 and 4 enzymes were obtained for the September, October and November biosolids, respectively (Figure 4). The predominant moderate enzymatic activity in the biosolids in the autumn season corresponded to phosphatases, being that this time of the year was the one that had less enzymatic activity for this family of enzymes in the analysed biosolids. Finally, for the biosolids analysed in autumn in the months of September and November, the number of enzymes with high activity was 6 and 7 for the biosolids of October, mainly from the families of proteases and hydrolases of glycosil.

In winter, the enzymatic activity of the biosolids analysed in a different season of the year was moderate to high. In the biosolids of December and February, the enzyme α -Fucosidase showed no activity. Low enzyme activity was detected for 5 enzymes in December and January and 4 enzymes for February, mainly from the aminopeptidase family. Thus, moderate enzyme activity for December biosolids was obtained in 6 enzymes, and for January and February biosolids, 8 enzymes were distributed in the 5 families (Figure 4). Finally, 7 enzymes presented high activity for December and 6 enzymes for January and February, with the proteases and glycosyl hydrolases families standing out.

The extracellular enzyme profile (Figure 4) showed that 9 enzymes were similar in “intensity” during different season of the year (acid phosphatase, phosphohydrolase, alkaline phosphatase, esterase lipase, trypsin, α -chemotrypsin, β -glucosidase, *N*-acetyl- β -glucosaminidase, α -fucosidase). On the other hand, 10 enzymes showed differences in intensity during different season of the year (esterase, lipase, leucine arylamidase, valine arylamidase, cysteine arylamidase, α -galactosidase, β -galactosidase, β -glucuronidase, α -glucosidase and α -manosidase). These results demonstrated that biosolids are not only a source of organic matter, but also have an important contribution of hydrolytic enzymes, confirming the importance of evaluating the biological parameters in biosolids prior to their addition to soils. However, the enzymatic machinery of the biosolids varied in the intensity of their activity in more than 50% of the 19 enzymes. Nevertheless, in average for all seasons of the year, 13 enzymes present an activity with a moderate to high intensity, which can positively influence the mineralisation processes of organic matter, mainly in hydrolysis process considered as the limiting stage of the transformation process of organic matter [139]. Extracellular soil enzymes are synthesised and secreted by soil microorganisms and are the proximate agents of organic matter formation and decomposition [140]. The activities of soil enzymes can provide useful information on the mechanisms of microbial sensitivity to the addition of C, N and P. From the above, the importance of establishing that enzymatic activities exist in biosolids before their application to matrices that are also complex in their enzymatic machinery, such as soils, is further emphasised. Thus, it is possible to elucidate even more that enzymatic activities are predominant and which ones cease or which changes exist after the application of these biosolids and how to correlate them with the processes of mineralisation, assimilation and maintenance of sources of C, N and P in soils.

Also, depending on the results of this study, the importance of knowing beforehand and its evolution over time of enzymes and their activities in biosolids to further elucidate the possible synergies or ecological relationships of microorganisms of biosolids and their enzymes with microorganisms and their hydrolytic enzymes in the soil that support the primary and oxidative metabolism for the acquisition of sources of C, N and P was established. The study also established the importance of knowing beforehand the evolution of enzymes and their activities in biosolids to further elucidate the possible synergies or ecological relationships of microorganisms of biosolids and their enzymes with the microorganisms and their hydrolytic enzymes in the soil that support the primary and oxidative metabolism for the acquisition of sources of C, N and P. An example of possible and complex

enzymatic relationships of the addition of organic amendments to soil can be established with the one reported by Wang et al. [140], who reported that the increase of N inputs increased the activity of *N*-acetyl- β -glucosaminidase but decreased the activity of β -glucosidase in 3 sizes of soil aggregates.

The profile of the 5 families of extracellular enzymes in biosolids, evaluated in the different seasons of the year, was compared based on their contribution percentages of their analysed activities (Figure 5). The microbial communities of the analysed biosolids reflected a variation in their availability to synthesise hydrolytic extracellular enzymes in different seasons of the year. In general, the family of enzymes, phosphatase, esterase/lipase and glycosyl hydrolase, which are related to the P and C cycles, were more actively synthesised in biosolids regardless of the season and they were not statistically different ($F = 1.921, p = 0.20$; $F = 1.569, p = 0.272$; $F = 1.325, p = 0.332$, respectively). However, in the 2 families of enzymes related to the N cycle, amine peptidases and proteases, the behaviour was different. In the amino peptidases no significant difference was found ($F = 2.078, p = 0.182$) at any time of the year. However, significant differences were found in the proteases evaluated in biosolids at different times of the year ($F = 5.547, p = 0.023$). Thus, the biosolids have an active hydrolytic enzymatic machinery during different seasons of the year, but their synthesis is not constant at all times and can be attributed to the chemical composition and the variable content of microbial biomass in the biosolids (see Table 3).

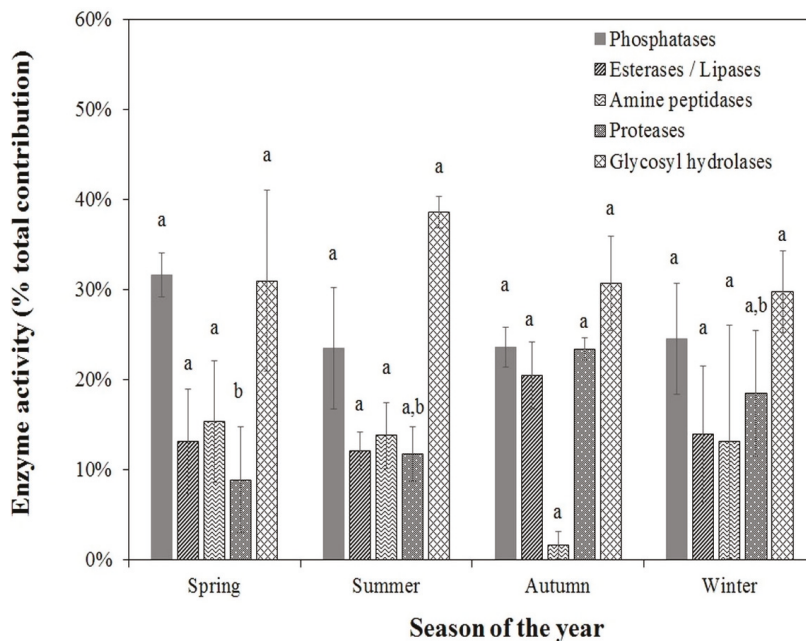


Figure 5. Contribution of extracellular enzyme activity separated into families for biosolids obtained at different times of the year. The bar represents the standard deviation of 3 replicates. Different letters on each column represent significant difference for that family of enzymes between seasons of the year.

Some mathematical indices have been used to describe the “richness and distribution” of species of organisms in a community, including the Shannon Diversity Index (H') and the Synthetic Enzyme Index (SEI). The Shannon Diversity Index reflects the heterogeneity of a community based on 2 factors: the number of species (richness) and their relative abundance [59,141]. Shannon diversity index values were generally between 1.5 and 4.0, where values close to 1.5 indicate low diversity, and values close to 4.0 indicate high diversity [142]. In addition, the Shannon Diversity Index has been used to

describe the status of the microbial community and its response to stress caused by disturbances in the environmental matrix [39]. Thus, stressed microbial communities with low diversity are less adapted to cope with environmental changes and stress than biologically adapted communities with a higher degree of diversity [109,143]. Shannon diversity index calculations obtained in this study for different seasons of the year ranged from 2.46 to 2.78 (Table 4). In addition, the results obtained did not present significant differences ($F = 0.989$, $p = 0.445$) between seasons of the year. With this, it can be deduced that the microbial diversity present in biosolids was similar always of the year and that their diversity was catalogued as average. These results meant that biosolids, regardless of the season of year in which they were obtained, were homogeneous in terms of both the number of microbial species and their relative abundance. Therefore, they can be considered with a biologically adapted microbial community capable of tolerating environmental changes and stress. Thus, biosolids being used as an organic amendment in soils can be expected to have a positive effect on the processes of adaptation and changes in the microbial structure of soils. Finally, the Shannon index could contribute to providing valuable information on the degree of biological stability (bioindicator) of a biosolid, applicable to agricultural soils as an organic amendment. This bioindicator would be based on the determination of microbial diversity as a function of changes in its enzymatic activities, especially when there is a lack of information on the composition of the structure and its microbial functioning in biosolids.

Table 4. Indices of microbial and functional diversity of biosolids collected and evaluated in the UWWTP at different season of the year.

Parameters	Biosolids Analysed for Each Season of the Year			
	Spring	Summer	Autumn	Winter
H'	2.61 ± 0.08 a	2.78 ± 0.17 a	2.46 ± 0.12 a	2.60 ± 0.10 a
* SEI	293.3 ± 63.3 b	488.3 ± 115.6 a	311.7 ± 36.9 a, b	331.7 ± 40.7 a, b

The results are the mean ± standard deviation (3 replicates). Rows with different letters are significantly different according to Tukey's analysis with $p \leq 0.05$. * (nmol hydrolysed substrate).

The synthetic enzymatic index (SEI) is an index that represents the sum of all enzymatic activities in the evaluated environmental matrix [33,143], as well as the metabolic activity or biochemical functioning of the evaluated substrate or, in this case, the biosolids [31,143]. The SEI then becomes a “biochemical fingerprint” [33]. The maximum and minimum SEI values were 760 nmol hydrolysed substrate (high functional diversity) and 0 nmol hydrolysed substrate (low functional diversity); this is because it was obtained through the sum of the 19 hydrolytic enzymes obtained in the APIZYM system for each biosolid. The SEI in biosolids ranged from 293.33 to 488.30 nmol hydrolysed substrate at different season of the year and were significantly different ($F = 4.721$, $p = 0.033$). The lowest SEI value (293.33 nmol hydrolysed substrate) was obtained in spring, and the highest (488.30 nmol hydrolysed substrate) was obtained in summer. In autumn and winter, the values of SEI were 311.72 and 331.79 nmol hydrolysed substrate and were not different from each other ($F = 0.398$, $p = 0.562$) compared to those from the other seasons of the year. Thus, it can be established that the functional diversity of biosolids is within a medium activity. The SEI can also relate microbial enzymatic activities to the degradation processes of organic matter—that is, the greater the enzymatic activity, the greater the degradation of organic matter and vice versa [31]. Thus, it was established that biosolids in spring had less potential for organic matter degradation than those obtained in summer. Therefore, this parameter is important for biosolids to be used as an organic amendment, since having a high SEI could have a greater impact on processes related to the degradation and mineralisation of organic matter added to the soil and the recycling of its nutrients.

3.5. Relationship between Biological and Physicochemical Parameters and Nutrient Content

Analysis of the establishment of possible relationships of biological parameters linked to nutrients and physicochemical parameters were established. This was done in order to see dependencies or

influences of the biological parameters on those. A product-moment correlation of Pearson was made (Table 5). Significant correlations occurred for MBC, MBN, C_{mic}/N_{mic} , DSH activity, FDA activity, URS activity, qCO_2 , $qFDA$, H' and SEI. MBC correlated positively with TOC, C/N, Fe, B and Mn and negatively with P, Zn, Cu, qCO_2 and $qFDA$. MNB had positive correlations with B and FDA and negative correlations with K, Zn, Cu, C_{mic}/N_{mic} and H' . The C_{mic}/N_{mic} relationship correlated positively with EC, URS and H' and negatively with FDA and $qFDA$. The DSH activity only presented negative correlation with SEI. The FDA activity presented negative correlations with Fe, URS and H' . URS activity correlated positively with K, Cu and H' and negatively with B and N-MB. The qCO_2 showed positive correlations with Zn, Cu, and $qFDA$ and negative correlations with TOC, B and Mn. $qFDA$ correlated positively with TOC and Zn and negatively with C/N, Fe and Mn. With respect to H' index, there was a positive correlation with Fe and SEI. SEI correlated positively with TOC, Fe and Mn.

Table 5. Pearson’s product moment correlation coefficient between biological and physicochemical parameters in the biosolids collected and evaluated in the UWWTP at different season of the year.

Parameters	Correlation Coefficient (r ²)	Parameters	Correlation Coefficient (r ²)
MBC		FDA Activity	
TOC	0.798 **	Fe	-0.585 *
C/N	0.643 *	URS	-0.643 *
P	-0.585 *	H'	-0.832 ***
Fe	0.646 *		
B	0.693 *	URS Activity	
Mn	0.748 **	K	0.578 *
Zn	-0.823 ***	B	-0.702 **
Cu	-0.631 *	Cu	0.637 *
qCO_2	-0.957 ***	H'	0.714 **
$qFDA$	-0.899 ***		
		qCO_2	
MBN		COT	-0.692 *
K	-0.707 **	B	-0.798 **
B	0.753 **	Mn	-0.624 *
Zn	-0.660 *	Zn	0.810 ***
Cu	-0.791 **	Cu	0.650 *
C_{mic}/N_{mic}	-0.729 **	$qFDA$	0.892 ***
FDA activity	0.723 **		
URS activity	-0.900 ***	$qFDA$	
H'	-0.701 **	TOC	0.712 **
		C/N	-0.580 *
C_{mic}/N_{mic}		Fe	-0.655 *
EC	0.794 **	Mn	-0.711 **
FDA activity	-0.744 **	Zn	0.641 *
URS	0.618 *		
$qFDA$	-0.647 *	H'	
H'	0.721 **	Fe	0.69 *
		SEI	0.832 ***
DSH Activity			
SEI	-0.627 *	SEI	
		TOC	0.613 *
		Fe	0.803 **
		Mn	0.639 *

Only significant correlations are shown. The data include all biosolids samples collected in different seasons. *, ** and *** indicate *p* values less than 0.05, 0.01 and 0.001, respectively (n = 36).

Regarding the establishment of correlations between physicochemical and biological parameters (Table 5), it was observed that MBC, MBN, C_{mic}/N_{mic} , qCO_2 , $qFDA$ and URS activity could be used to predict the behaviour of some physicochemical properties such as TOC or of agronomic interest in biosolids samples. For example, a high MBC content would correspond to a high TOC content in

biosolids ($r = 0.798, p \leq 0.01$), and a high MBN content would imply significant FDA microbial activity ($r = 0.723, p \leq 0.01$) in biosolids. Thus, these parameters could also be used as quality and functionality indicators of biosolids for use as organic amendment and predict the possible positive or negative effects of their addition to agricultural soils. Among the effects that could be highlighted could be the availability or loss of inorganic N in the soil, affecting the mineralisation processes of C and N as a consequence of the addition of a substrate with active microbial biomass in terms of MBC and MBN, as well as qCO_2 and $qFDA$, as has been described in the literature by Scciuba et al. [105] and Molina-Herrera and Romanyà [111]. Another important effect to consider is a temporary increase of MBC in agricultural soils with the addition of biosolids as established by Debosz [109].

4. Conclusions

Biosolids proved to be a rich source of organic matter, as well as of macro- and micronutrients. The pH was slightly acidic, which could be favourable for agricultural soils with alkalinity problems. However, the electric conductivity was established as a parameter to be considered when establishing the application doses of biosolids to agricultural soils, especially those soils that present salinity or sodicity problems. In reference to the chemical-molecular composition of biosolids determined by FTIR analysis, it was concluded that biosolids can provide molecules, functional groups or chemically similar compounds, independent of the time in which these biosolids are generated, minimising the problem of their variability, which is a problem presented if they are used as an organic amendment to soils in the short- and long-term. With respect to biological properties, it was established that biosolids present an active microbial biomass that when applied in agricultural soils can present positive synergies with microorganisms present in soils and positively impact the mineralisation processes of C and N sources over time. This was supported by the presence of various enzymatic activities in the biosolids evaluated over time. On the other hand, with respect to microbial diversity in the biosolids evaluated, it was concluded that this was stable or similar throughout the year, reflected in the Shannon index obtained. This stability denoted a “uniformity” that translates, in the ecological context, into a richness and relative abundance of microbial species present in biosolids and desired in complex ecosystems such as soils. Moreover, the biosolids presented a mean functional enzymatic diversity determined by SEI, concluding that microbial biomass and its enzymatic activities were active with high potential to influence processes related to the mineralisation of organic matter and the recycling of nutrients when the biosolids were applied to soils. Finally, in reference to the established correlations of physicochemical parameters with biological parameters measured over time, it is concluded that microbial biomass carbon, microbial biomass nitrogen, urease activity, metabolic coefficient, specific hydrolytic activity, C_{mic}/N_{mic} ratio and synthetic enzymatic index are parameters that could be used as indicators of biological quality and functionality of biosolids before being used as organic amendments or fertilisers, especially for soils with agricultural activity.

Author Contributions: All authors contributed to the intellectual input and provided assistance in the study. Conceptualization, M.d.R.M.-H. and E.C.-B.; methodology, E.C.-B., M.d.R.M.-H., M.d.I.L.X.N.-R. and J.L.Á.-T.; software, M.d.R.M.-H.; validation, E.C.-B., L.G.-C., A.B.-N., and J.L.Á.-T.; formal analysis, E.C.-B. and M.d.R.M.-H.; investigation, M.d.R.M.-H. and M.S.H.; resources, M.d.I.L.X.N.-R. and M.S.-H.; data curation, M.d.R.M.-H. and M.d.I.L.X.N.-R.; writing—original draft preparation, M.d.R.M.-H.; writing—review and editing, E.C.-B. and M.d.R.M.-H.; visualization, M.d.R.M.-H.; supervision, E.C.-B.; project administration, E.C.-B.; funding acquisition, E.C.-B. All authors have read and agreed to the published version of the manuscript.

Funding: This research was funded by Consejo Nacional de Ciencia y Tecnología (CONACYT)-Secretaría de Educación Pública (SEP) and Tecnológico Nacional de México/IT de Celaya, Gto., Mexico. SEP-CONACYT Project, grant numbers CB-2014-01 No. 236674 and No. 212522. Tecnológico Nacional de México/IT de Celaya Project, grant number 5569.19-P. The APC was funded by SEP-CONACYT Project, No. 236674.

Acknowledgments: To Municipal Drinking Water and Sewerage Board of the Municipality of Celaya, Guanajuato (JUMAPA). Special acknowledgements to the master's in engineering Patricia Adriana Estrada Orozco, manager of the sanitation area of JUMAPA, and to environmental engineering master José Luis Álvarez Trejo, manager of administrative and operation of the wastewater treatment plant (WWTP) of Celaya, Gto., for the administrative-technical management facilities in obtaining the urban biosolids used for the present investigation.

Conflicts of Interest: The authors declare no conflict of interest.

References

1. De Melo, J.J.; Camara, A.S. Models for the optimization of regional wastewater treatment systems. *Eur. J. Oper. Res.* **1994**, *73*, 1–16. [CrossRef]
2. Wang, Q.; Wei, W.; Gong, Y.; Yu, Q.; Li, Q.; Sun, J.; Yuan, Z. Technologies for reducing sludge production in wastewater treatment plants: State of the art. *Sci. Total Environ.* **2017**, *587*, 510–521. [CrossRef]
3. Rodríguez, N.H.; Granados, R.J.; Blanco-Varela, M.T.; Cortina, J.L.; Martínez-Ramírez, S.; Marsal, M.; Guillem, M.; Puig, J.; Fos, C.; Larrotcha, E.; et al. Evaluation of a lime-mediated sewage sludge stabilisation process. Product characterisation and technological validation for its use in the cement industry. *Waste Manag.* **2012**, *32*, 550–560. [CrossRef] [PubMed]
4. Wei, Y.; Van Houten, R.T.; Borger, A.R.; Eikelboom, D.H.; Fan, Y. Minimization of excess sludge production for biological wastewater treatment. *Water Res.* **2003**, *37*, 4453–4467. [CrossRef]
5. Reungoat, J.; Escher, B.I.; Macova, M.; Argaud, F.X.; Gernjak, W.; Keller, J. Ozonation and biological activated carbon filtration of wastewater treatment plant effluents. *Water Res.* **2012**, *46*, 863–872. [CrossRef]
6. Pronk, M.; De Kreuk, M.K.; De Bruin, B.; Kamminga, P.; Kleerebezem, R.V.; Van Loosdrecht, M.C.M. Full scale performance of the aerobic granular sludge process for sewage treatment. *Water Res.* **2015**, *84*, 207–217. [CrossRef]
7. Fyttili, D.; Zabaniotou, A. Utilization of sewage sludge in EU application of old and new methods—A review. *Renew. Sustain. Energy Rev.* **2008**, *12*, 116–140. [CrossRef]
8. Samaras, P.; Papadimitriou, C.A.; Haritou, I.; Zouboulis, A.I. Investigation of sewage sludge stabilization potential by the addition of fly ash and lime. *J. Hazard. Mater.* **2008**, *154*, 1052–1059. [CrossRef]
9. Kazimierczak, M. Sewage sludge stabilization indicators in aerobic digestion—a review. *Annals of Warsaw University of Life Sciences-SGGW. Land Reclam.* **2012**, *44*, 101–109. [CrossRef]
10. Conagua. *Inventario Nacional de Plantas Municipales de Potabilización y de Tratamiento de Aguas Residuales en Operación*; Comisión Nacional del Agua/Secretaría de Medio Ambiente y Recursos Naturales: Ciudad de México, México, 2016; 308p, Available online: <https://agua.org.mx/biblioteca/inventario-plantas-potabilizadoras-municipales-2016/> (accessed on 14 November 2019).
11. Matos, A.T.; Diniz, I.C.; Matos, M.P.; Borges, A.C.; Pereira, A.A. Degradation rate of anaerobically digested sewage sludge in soil. *J. Water Sanit. Hyg. Dev.* **2018**, *8*, 17–26. [CrossRef]
12. Zhang, Q.; Hu, J.; Lee, D.J.; Chang, Y.; Lee, Y.J. Sludge treatment: Current research trends. *Bioresour. Technol.* **2017**, *243*, 1159–1172. [CrossRef] [PubMed]
13. Paramashivam, D.; Dickinson, N.M.; Clough, T.J.; Horswell, J.; Robinson, B.H. Potential environmental benefits from blending biosolids with other organic amendments before application to land. *J. Environ. Qual.* **2017**, *46*, 481–489. [CrossRef] [PubMed]
14. Wang, H.; Brown, S.L.; Magesan, G.N.; Slade, A.H.; Quintern, M.; Clinton, P.W.; Payn, T.W. Technological options for the management of biosolids. *Environ. Sci. Pollut. Res.* **2008**, *15*, 308–317. [CrossRef] [PubMed]
15. Nicholson, F.; Bhogal, A.; Taylor, M.; McGrath, S.; Withers, P. Long-term Effects of Biosolids on Soil Quality and Fertility. *Soil Sci.* **2018**, *183*, 89–98. [CrossRef]
16. Obrador, A.; Rico, M.I.; Mingot, J.I.; Alvarez, J.M. Metal mobility and potential bioavailability in organic matter-rich soil-sludge mixtures: Effect of soil type and contact time. *Sci. Total Environ.* **1997**, *206*, 117–126. [CrossRef]
17. Alvarez, E.A.; Mochon, M.C.; Sánchez, J.J.; Rodríguez, M.T. Heavy metal extractable forms in sludge from wastewater treatment plants. *Chemosphere* **2002**, *47*, 765–775. [CrossRef]
18. Usman, K.; Khan, S.; Ghulam, S.; Khan, M.U.; Khan, N.; Khan, M.A.; Khalil, S.K. Sewage sludge: An important biological resource for sustainable agriculture and its environmental implications. *Am. J. Plant Sci.* **2012**, *3*, 1708. [CrossRef]
19. Sharma, B.; Sarkar, A.; Singh, P.; Singh, R.P. Agricultural utilization of biosolids: A review on potential effects on soil and plant grown. *Waste Manag.* **2017**, *64*, 117–132. [CrossRef]
20. Pepper, I.L.; Brooks, J.P.; Gerba, C.P. Land Application of Organic Residuals: Municipal Biosolids and Animal Manures. In *Environmental and Pollution Science*, 3rd ed.; Brusseau, M.L., Pepper, I.L., Gerba, C.P., Eds.; Academic Press, Elsevier: London, UK, 2019; Part III; pp. 419–434. [CrossRef]

21. Secretaría del Medio Ambiente y Recursos Naturales (Semarnat). Norma Oficial Mexicana NOM-004-SEMARNAT-2002. Protección Ambiental. Lodos y Biosólidos. Especificaciones y Límites Máximos Permisibles de Contaminantes Para su Aprovechamiento y Disposición Final. 2002. *Diario Oficial de la Federación, México*. 15 August 2003. Available online: <http://biblioteca.semarnat.gob.mx/janium/Documentos/Ciga/libros2009/DO2251.pdf> (accessed on 8 January 2020).
22. Environmental Protection Agency (EPA). *Federal Register. Title 40—Protection of Environment: Part 503—Standards for the Use or Disposal of Sewage Sludge*; Environmental Protection Agency: Washington, DC, USA, 2002.
23. European Economic Community (EEC). Directiva 86/278/CEE de 12 de junio de 1986, relativa a la protección del medio ambiente y, en particular, de los suelos, en la utilización de lodos de depuradora en agricultura (86/278/CEE). *Diario Oficial de las Comunidades Europeas*. 1986. Available online: <https://eur-lex.europa.eu/legal-content/ES/TXT/PDF/?uri=CELEX:31986L0278&from=ES> (accessed on 8 January 2020).
24. Anderson, J.P.E.; Domsch, K.H. Quantities of plant nutrients in the microbial biomass of selected soils. *Soil Sci.* **1980**, *130*, 211–216. [[CrossRef](#)]
25. Kandeler, E.; Gerber, H. Short-term assay of soil urease activity using colorimetric determination of ammonium. *Biol. Fertil. Soils* **1988**, *6*, 68–72. [[CrossRef](#)]
26. Sparling, G.P.; West, A.W. Modifications to the fumigation extraction technique to permit simultaneous extraction and estimation of soil microbial C and N. *Commun Soil Sci Plant Anal.* **1988**, *19*, 327–344. [[CrossRef](#)]
27. Anderson, T.H.; Domsch, K.H. Application of eco-physiological quotients (qCO₂ and qD) on microbial biomasses from soils of different cropping histories. *Soil Biol. Biochem.* **1990**, *22*, 251–255. [[CrossRef](#)]
28. Von Mersi, W.; Schinner, F. An improved and accurate method for determining the dehydrogenase activity of soils with iodinitrotetrazolium chloride. *Biol. Fertil. Soils* **1991**, *11*, 216–220. [[CrossRef](#)]
29. Johnston, C.T.; Aochi, Y. Fourier transform infrared and raman spectroscopy. In *Methods of Soil Analysis*; Bartels, J.M., Bigham, J.M., Eds.; Soil Science Society of America, American Society of Agronomy: Madison, WI, USA, 1996; pp. 269–321. [[CrossRef](#)]
30. Perucci, P.; Dumontet, S.; Bufo, S.A.; Mazzatura, A.; Casucci, C. Effects of organic amendment and herbicide treatment on soil microbial biomass. *Biol. Fertil. Soils* **2000**, *32*, 17–23. [[CrossRef](#)]
31. Dumontet, S.; Mazzatura, A.; Casucci, C.; Perucci, P. Effectiveness of microbial indexes in discriminating interactive effects of tillage and crop rotations in a Vertic Ustorthens. *Biol. Fertil. Soils* **2001**, *34*, 411–416. [[CrossRef](#)]
32. Green, V.S.; Stott, D.E.; Diack, M. Assay for fluorescein diacetate hydrolytic activity: Optimization for soil samples. *Soil Biol. Biochem.* **2006**, *38*, 693–701. [[CrossRef](#)]
33. Martínez, E.J.; Fierro, J.; Sánchez, M.E.; Gómez, X. Anaerobic co-digestion of FOG and sewage sludge: Study of the process by Fourier transform infrared spectroscopy. *Int. Biodeterior. Biodegrad.* **2012**, *75*, 1–6. [[CrossRef](#)]
34. Tiquia, S.M. Evolution of extracellular enzyme activities during manure composting. *J. Appl. Microbiol.* **2002**, *92*, 764–775. [[CrossRef](#)]
35. Baldrian, P.; Voříšková, J.; Dobiášová, P.; Merhautová, V.; Lisá, L.; Valášková, V. Production of extracellular enzymes and degradation of biopolymers by saprotrophic microfungi from the upper layers of forest soil. *Plant Soil* **2011**, *338*, 111–125. [[CrossRef](#)]
36. Boluda, R.; Roca-Pérez, L.; Iranzo, M.; Gil, C.; Mormeneo, S. Determination of enzymatic activities using a miniaturized system as a rapid method to assess soil quality. *Eur. J. Soil Sci.* **2014**, *65*, 286–294. [[CrossRef](#)]
37. Shemekite, F.; Gómez-Brandón, M.; Franke-Whittle, I.H.; Praehauser, B.; Insam, H.; Assefa, F. Coffee husk composting: An investigation of the process using molecular and non-molecular tools. *Waste Manag.* **2014**, *34*, 642–652. [[CrossRef](#)]
38. Martínez, D.; Molina, M.J.; Sanchez, J.; Moscatelli, M.C.; Marinari, S. API ZYM assay to evaluate enzyme fingerprinting and microbial functional diversity in relation to soil processes. *Biol. Fertil. Soils* **2016**, *52*, 77–89. [[CrossRef](#)]
39. Patel, D.; Gismondi, R.; Alsaffar, A.; Tiquia-Arashiro, S.M. Applicability of API ZYM to capture seasonal and spatial variabilities in lake and river sediments. *Environ. Technol.* **2019**, *40*, 3227–3239. [[CrossRef](#)] [[PubMed](#)]
40. Wolińska, A.; Fraç, M.; Oszust, K.; Szafranek-Nakonieczna, A.; Zielenkiewicz, U.L.; Stepniewska, Z. Microbial biodiversity of meadows under different modes of land use: Catabolic and genetic fingerprinting. *World J. Microbiol. Biotechnol.* **2017**, *33*, 154. [[CrossRef](#)]

41. Environmental Protection Agency (EPA). *A Guide to the Biosolids Risk Assessments for the EPA Part 503 Rule*; Tech. Rep. EPA/832-B-93-005; Office of Wastewater Management: Washington, DC, USA, 1995.
42. Lu, Q.; He, Z.L.; Stoffella, P.J. Land application of biosolids in the USA: A review. *Appl. Environ. Soil Sci.* **2012**, *2012*, 201462. [[CrossRef](#)]
43. Coello-Oviedo, M.C.; Barragán-Sánchez, J.B.; Quiroga-Alonso, J.Q. Enzymatic estimation of biosolids stability in aerobic digestion systems. *Enzyme Microb. Technol.* **2005**, *36*, 191–197. [[CrossRef](#)]
44. Boczar, B.A.; Begley, W.M.; Larson, R.J. Characterization of enzyme activity in activated sludge using rapid analyses for specific hydrolases. *Water Environ. Res.* **1992**, *64*, 792–797. [[CrossRef](#)]
45. Ho, C.P.; Yuan, S.T.; Jien, S.H.; Hseu, Z.Y. Elucidating the process of co-composting of biosolids and spent activated clay. *Bioresour. Technol.* **2010**, *101*, 8280–8286. [[CrossRef](#)]
46. Tian, G.; Franzluebbers, A.J.; Granato, T.C.; Cox, A.E.; O’connor, C. Stability of soil organic matter under long-term biosolids application. *Appl. Soil Ecol.* **2013**, *64*, 223–227. [[CrossRef](#)]
47. Thomas, G.W. Soil pH and Soil Acidity. In *Methods of Soil Analysis Part 3—Chemical Methods*; Sparks, D.L., Page, A.L., Helmke, P.A., Loeppert, R.H., Eds.; Soil Science Society of America: Madison, WI, USA, 1996; pp. 475–490. [[CrossRef](#)]
48. Hendrickx, J.M.H.; Das, B.; Corwin, D.L.; Wraith, J.M.; Kachanoski, R.G. Relationship between soil water solute concentration and apparent soil electrical conductivity. In *Methods of Soil Analysis: Part 4. Physical Methods*; Dane, J.H., Topp, G.C., Eds.; Soil Science Society of America: Madison, WI, USA, 2002; pp. 1275–1282. [[CrossRef](#)]
49. Walkley, A.; Black, C.A. An examination of different methods for determining soil organic matter and a proposed modification of the chromic acid titration method. *Soil Sci.* **1934**, *37*, 29–38. [[CrossRef](#)]
50. Alef, K.; Nannipieri, P. *Methods in Applied Soil Microbiology and Biochemistry*; Academic Press: London, UK, 1995; pp. 60–61. [[CrossRef](#)]
51. Bremner, J.M. Nitrogen—Total. In *Methods of Soil Analysis Part 3—Chemical Methods*; Sparks, D.L., Page, A.L., Helmke, P.A., Loeppert, R.H., Eds.; Soil Science Society of America: Madison, WI, USA, 1996; pp. 1085–1121. [[CrossRef](#)]
52. US-EPA Method 3051A. *Microwave Assisted Acid Digestion of Sediment, Sludges, Soils, and Oils*; United States Environmental Protection Agency: Washington, DC, USA, 2007. Available online: <https://www.epa.gov/sites/production/files/2015-12/documents/3051a.pdf> (accessed on 14 November 2019).
53. Link, D.D.; Walter, P.J.; Kingston, H.M. Development and validation of the new EPA microwave-assisted leach method 3051A. *Environ. Sci. Technol.* **1998**, *32*, 3628–3632. [[CrossRef](#)]
54. Bettinelli, M.; Baroni, U. A microwave oven digestion method for the determination of metals in sewage sludges by ICP-AES and GFAAS. *Int. J. Environ. Anal. Chem.* **1991**, *43*, 33–40. [[CrossRef](#)]
55. Sparling, G.P.; Williams, B.L. Microbial biomass in organic soils: Estimation of biomass C, and effect of glucose or cellulose amendments on the amounts of N and P released by fumigation. *Soil Biol. Biochem.* **1986**, *18*, 507–513. [[CrossRef](#)]
56. Barragán-Sánchez, J.; Quiroga-Alonso, J.M.; Coello-Oviedo, M.D. Use of microbial activity parameters for determination of a biosolid stability index. *Bioresour. Technol.* **2006**, *97*, 562–568. [[CrossRef](#)]
57. Anderson, J.P. Soil respiration. In *Methods of Soil Analysis Part 2—Chemical and Microbiological Properties*; Page, L., Ed.; Soil Science Society of America: Madison, WI, USA, 1982; pp. 831–871. [[CrossRef](#)]
58. API ZYM 25200. *Sistema de investigación de actividades enzimáticas*; 07883F-es-2014/01; bioMérieux SA: Marcy-l’Étoile, France, 2014; p. 5.
59. Kennedy, A.C.; Smith, K.L. Soil microbial diversity and the sustainability of agricultural soils. *Plant Soil* **1995**, *170*, 75–86. [[CrossRef](#)]
60. Minitab, Inc. *Minitab Version 18*; Minitab, Inc.: State College, PA, USA, 2018.
61. Withers, P.J.A.; Flynn, N.J.; Warren, G.P.; Taylor, M.; Chambers, B.J. Sustainable management of biosolid phosphorus: A field study. *Soil Use Manag.* **2016**, *32*, 54–63. [[CrossRef](#)]
62. Torri, S.I.; Correa, R.S.; Renella, G. Biosolid application to agricultural land—A contribution to global phosphorus recycle: A review. *Pedosphere* **2017**, *27*, 1–16. [[CrossRef](#)]
63. Sánchez-Monedero, M.A.; Mondini, C.; De Nobili, M.; Leita, L.; Roig, A. Land application of biosolids. Soil response to different stabilization degree of the treated organic matter. *Waste Manag.* **2004**, *24*, 325–332. [[CrossRef](#)]

64. Torres, D.; Mendoza, B.; Meru Marco, L.; Gómez, C. Riesgos de salinización y sodificación por el uso de abonos orgánicos en la depresión de Quibor-Venezuela. *Multiciencias* **2016**, *16*, 133–142. Available online: <https://www.redalyc.org/articulo.oa?id=90452745003> (accessed on 15 July 2019).
65. Cytryn, E.; Kautsky, L.; Ofek, M.; Mandelbaum, R.T.; Minz, D. Short-term structure and functional changes in bacterial community composition following amendment with biosolids compost. *Appl. Soil Ecol.* **2011**, *48*, 160–167. [CrossRef]
66. Sciubba, L.; Cavani, L.; Negroni, A.; Zanolli, G.; Fava, F.; Ciavatta, C.; Marzadori, C. Changes in the functional properties of a sandy loam soil amended with biosolids at different application rates. *Geoderma* **2014**, *221*, 40–49. [CrossRef]
67. Flores-Margez, J.P.; Corral-Díaz, B.; Sapien-Mediano, G. Mineralización de nitrógeno de biosólidos estabilizados con cal en suelos agrícolas. *Terra Latinoam.* **2007**, *25*, 409–417. Available online: <http://portal.amelica.org/ameli/jatsRepo/57315558009> (accessed on 8 January 2020).
68. Potisek-Talavera, M.D.C.; Figueroa-Viramontes, U.; González-Cervantes, G.; Jasso-Ibarra, R.; Orona-Castillo, I. Aplicación de biosólidos al suelo y su efecto sobre contenido de materia orgánica y nutrientes. *Terra Latinoam.* **2010**, *28*, 327–333. Available online: <http://www.scielo.org.mx/pdf/tl/v28n4/v28n4a4.pdf> (accessed on 8 January 2020).
69. González-Flores, E.; Ramos-Barragán, J.E.; Tornero-Campante, M.A.; Murillo-Murillo, M. Evaluación de dosis de biosólidos urbanos en maíz bajo condiciones de invernadero. *Rev. Mex. Cienc. Agríc.* **2017**, *8*, 119–132. Available online: <http://www.scielo.org.mx/pdf/remexca/v8n1/2007-0934-remexca-8-01-119-en.pdf> (accessed on 20 December 2019).
70. Singh, R.P.; Agrawal, M. Effect of different sewage sludge applications on growth and yield of *Vigna radiata* L. field crop: Metal uptake by plant. *Ecol. Eng.* **2010**, *36*, 969–972. [CrossRef]
71. Xue, D.; Huang, X. The impact of sewage sludge compost on tree peony growth and soil microbiological, and biochemical properties. *Chemosphere* **2013**, *93*, 583–589. [CrossRef]
72. Lloret, E.; Pascual, J.A.; Brodie, E.L.; Bouskill, N.J.; Insam, H.; Juárez, M.F.D.; Goberna, M. Sewage sludge addition modifies soil microbial communities and plant performance depending on the sludge stabilization process. *Appl. Soil Ecol.* **2016**, *101*, 37–46. [CrossRef]
73. United States Salinity Laboratory Staff (USSLS). *Diagnosis and Improvement of Saline and Alkali Soils*; United States Department of Agriculture and Government Printing Office: Washington, DC, USA, 1954. Available online: https://www.ars.usda.gov/ARSUserFiles/20360500/hb60_pdf/hb60complete.pdf (accessed on 14 November 2019).
74. Pérez-Sanz, A.; Lucena, J.J.; Graham, M.C. Characterization of Fe–humic complexes in an Fe-enriched biosolid by-product of water treatment. *Chemosphere* **2006**, *65*, 2045–2053. [CrossRef]
75. Rowell, D.M.; Prescott, C.E.; Preston, C.M. Decomposition and nitrogen mineralization from biosolids and other organic materials. *J. Environ. Qual.* **2001**, *30*, 1401–1410. [CrossRef]
76. Gilmour, J.T.; Cogger, C.G.; Jacobs, L.W.; Evanylo, G.K.; Sullivan, D.M. Decomposition and plant-available nitrogen in biosolids. *J. Environ. Qual.* **2003**, *32*, 1498–1507. [CrossRef]
77. Rigby, H.; Clarke, B.O.; Pritchard, D.L.; Meehan, B.; Beshah, F.; Smith, S.R.; Porter, N.A. A critical review of nitrogen mineralization in biosolids-amended soil, the associated fertilizer value for crop production and potential for emissions to the environment. *Sci. Total Environ.* **2016**, *541*, 1310–1338. [CrossRef] [PubMed]
78. Jin, V.L.; Johnson, M.V.V.; Haney, R.L.; Arnold, J.G. Potential carbon and nitrogen mineralization in soils from a perennial forage production system amended with class B biosolids. *Agric. Ecosyst. Environ.* **2011**, *141*, 461–465. [CrossRef]
79. Hseu, Z.Y.; Huang, C.C. Nitrogen mineralization potentials in three tropical soils treated with biosolids. *Chemosphere* **2005**, *59*, 447–454. [CrossRef] [PubMed]
80. Brady, N.C.; Weil, R.R. *The Nature and Properties of Soils*, 14th ed.; Prentice Hall: Upper Saddle River, NJ, USA, 2008; pp. 100–109.
81. Lü, F.; Shao, L.M.; Zhang, H.; Fu, W.D.; Feng, S.J.; Zhan, L.T.; Chen, Y.M.; He, P.J. Application of advanced techniques for the assessment of bio-stability of biowaste-derived residues: A minireview. *Bioresour. Technol.* **2018**, *248*, 122–133. [CrossRef] [PubMed]

82. Sullivan, D.M.; Cogger, C.G.; Bary, A.I. *Fertilising with Biosolids*; A Pacific North West Extension Publication, Oregon State University: Corvallis, OR, USA; Washington State University: Pullman, WA, USA; University of Idaho: Moscow, ID, USA, 2015; Available online: https://catalog.extension.oregonstate.edu/sites/catalog/files/project/pdf/pnw508_0.pdf (accessed on 17 December 2019).
83. Sigua, G.C. Recycling biosolids and lake-dredged materials to pasture-based animal agriculture: Alternative nutrient sources for forage productivity and sustainability. A review. *Agron. Sustain. Dev.* **2009**, *29*, 143–160. [CrossRef]
84. Zhang, M.; Heaney, D.; Henriquez, B.; Solberg, E.; Bittner, E. A four-year study on influence of biosolids/MSW cocompost application in less productive soils in Alberta: Nutrient dynamics. *Compost Sci. Util.* **2006**, *14*, 68–80. [CrossRef]
85. Kokkora, M.I.; Antille, D.L.; Tyrrel, S.F. Considerations for recycling of compost and biosolids in agricultural soil. In *Soil Engineering*; Dedousis, A.P., Bartzanas, T., Eds.; Springer: Berlin/Heidelberg, Germany, 2010; Volume 20, pp. 195–215. [CrossRef]
86. Bedoya-Urrego, K.; Acevedo-Ruiz, J.M.; Peláez-Jaramillo, C.A.; Agudelo-López, S.D.P. Caracterización de biosólidos generados en la planta de tratamiento de agua residual San Fernando, Itagüí (Antioquia, Colombia). *Rev. Salud Pública* **2013**, *15*, 778–790. Available online: https://www.scielo.org/scielo.php?script=sci_arttext&pid=S0124-00642013000500013 (accessed on 20 April 2019).
87. Dede, G.; Özdemir, S.; Dede, Ö.H.; Altundağ, H.; Dündar, M.Ş.; Kızıloğlu, F.T. Effects of biosolid application on soil properties and kiwi fruit nutrient composition on high-pH soil. *Int. J. Environ. Sci. Technol.* **2017**, *14*, 1451–1458. [CrossRef]
88. Burducea, M.; Zheljzkov, V.D.; Lobiuc, A.; Pintilie, C.A.; Virgolici, M.; Silion, M.; Asandulesa, M.; Burducea, I.; Zamfirache, M.M. Biosolids application improves mineral composition and phenolic profile of basil cultivated on eroded soil. *Sci. Hortic.* **2019**, *249*, 407–418. [CrossRef]
89. Wang, K.; Li, W.; Gong, X.; Li, Y.; Wu, C.; Ren, N. Spectral study of dissolved organic matter in biosolid during the composting process using inorganic bulking agent: UV-vis, GPC, FTIR and EEM. *Int. Biodeterior. Biodegrad.* **2013**, *85*, 617–623. [CrossRef]
90. Zhou, Y.; Selvam, A.; Wong, J.W. Evaluation of humic substances during co-composting of food waste, sawdust and Chinese medicinal herbal residues. *Bioresour. Technol.* **2014**, *168*, 229–234. [CrossRef]
91. Zhang, J.; Lü, F.; Shao, L.; He, P. The use of biochar-amended composting to improve the humification and degradation of sewage sludge. *Bioresour. Technol.* **2014**, *168*, 252–258. [CrossRef] [PubMed]
92. Soobhany, N.; Gunasee, S.; Rago, Y.P.; Joyram, H.; Raghoo, P.; Mohee, R.; Garg, V.K. Spectroscopic, thermogravimetric and structural characterization analyses for comparing Municipal Solid Waste composts and vermicomposts stability and maturity. *Bioresour. Technol.* **2017**, *236*, 11–19. [CrossRef]
93. El Fels, L.; Zamama, M.; El Asli, A.; Hafidi, M. Assessment of biotransformation of organic matter during co-composting of sewage sludge-lignocellulosic waste by chemical, FTIR analyses, and phytotoxicity tests. *Int. Biodeterior. Biodegrad.* **2014**, *87*, 128–137. [CrossRef]
94. Tandy, S.; Healey, J.R.; Nason, M.A.; Williamson, J.C.; Jones, D.L.; Thain, S.C. FT-IR as an alternative method for measuring chemical properties during composting. *Bioresour. Technol.* **2010**, *101*, 5431–5436. [CrossRef] [PubMed]
95. Aksoy, C.; Severcan, F. Role of vibrational spectroscopy in stem cell research. *J. Spectrosc.* **2012**, *27*, 167–184. [CrossRef]
96. Droussi, Z.; D’orazio, V.; Provenzano, M.R.; Hafidi, M.; Ouattmane, A. Study of the biodegradation and transformation of olive-mill residues during composting using FTIR spectroscopy and differential scanning calorimetry. *J. Hazard. Mater.* **2009**, *164*, 1281–1285. [CrossRef] [PubMed]
97. Bastida, F.; Zsolnay, A.; Hernández, T.; García, C. Past, present and future of soil quality indices: A biological perspective. *Geoderma* **2008**, *147*, 159–171. [CrossRef]
98. Paz-Ferreiro, J.; Fu, S. Biological indices for soil quality evaluation: Perspectives and limitations. *Land Degrad. Dev.* **2016**, *27*, 14–25. [CrossRef]
99. Joniec, J. Enzymatic activity as an indicator of regeneration processes in degraded soil reclaimed with various types of waste. *Int. J. Environ. Sci. Technol.* **2018**, *15*, 2241–2252. [CrossRef]
100. Wardle, D.A. A comparative assessment of factors which influence microbial biomass carbon and nitrogen levels in soil. *Biol. Rev.* **1992**, *67*, 321–358. [CrossRef]

101. Rinklebe, J.; Langer, U. Relationship between soil microbial biomass determined by SIR and PLFA analysis in floodplain soils. *J. Soil Sediments* **2010**, *10*, 4–8. [CrossRef]
102. Anderson, T.H.; Domsch, K.H. Soil microbial biomass: The eco-physiological approach. *Soil Biol. Biochem.* **2010**, *42*, 2039–2043. [CrossRef]
103. Rittmann, B.E.; McCarty, P.L. *Environmental Biotechnology: Principles and Applications*; McGraw-Hill Series in Water Resources and Environmental Engineering; McGraw-Hill: Boston, MA, USA, 2001.
104. Nayak, B.S.; Levine, A.D.; Cardoso, A.; Harwood, V.J. Microbial population dynamics in laboratory-scale solid waste bioreactors in the presence or absence of biosolids. *J. Appl. Microbiol.* **2009**, *107*, 1330–1339. [CrossRef]
105. Sciubba, L.; Cavani, L.; Marzadori, C.; Ciavatta, C. Effect of biosolids from municipal sewage sludge composted with rice husk on soil functionality. *Biol. Fertil. Soils* **2013**, *49*, 597–608. [CrossRef]
106. Moore, J.M.; Klose, S.; Tabatabai, M.A. Soil microbial biomass carbon and nitrogen as affected by cropping systems. *Biol. Fertil. Soils* **2000**, *31*, 200–210. [CrossRef]
107. Li, F.M.; Song, Q.H.; Jjemba, P.K.; Shi, Y.C. Dynamics of soil microbial biomass C and soil fertility in cropland mulched with plastic film in a semiarid agro-ecosystem. *Soil Biol. Biochem.* **2004**, *36*, 1893–1902. [CrossRef]
108. Fernandes, S.A.P.; Bettiol, W.; Cerri, C.C. Effect of sewage sludge on microbial biomass, basal respiration, metabolic quotient and soil enzymatic activity. *Appl. Soil Ecol.* **2005**, *30*, 65–77. [CrossRef]
109. Debosz, K.; Petersen, S.O.; Kure, L.K.; Ambus, P. Evaluating effects of sewage sludge and household compost on soil physical, chemical and microbiological properties. *Appl. Soil Ecol.* **2002**, *19*, 237–248. [CrossRef]
110. Masunga, R.H.; Uzokwe, V.N.; Mlay, P.D.; Odeh, I.; Singh, A.; Buchan, D.; De Neve, S. Nitrogen mineralization dynamics of different valuable organic amendments commonly used in agriculture. *Appl. Soil Ecol.* **2016**, *101*, 185–193. [CrossRef]
111. Molina-Herrera, S.; Romanyà, J. Synergistic and antagonistic interactions among organic amendments of contrasted stability, nutrient availability and soil organic matter in the regulation of C mineralisation. *Eur. J. Soil Biol.* **2015**, *70*, 118–125. [CrossRef]
112. Servicio Meteorológico Nacional (SMN). *Resúmenes Mensuales de Temperaturas y Lluvia*; Servicio Meteorológico Nacional: Ciudad de México, México, 2019. Available online: <https://smn.conagua.gob.mx> (accessed on 18 August 2019).
113. Sautour, M.; Dantigny, P.; Divies, C.; Bensoussan, M. A temperature-type model for describing the relationship between fungal growth and water activity. *Int. J. Food Microbiol.* **2001**, *67*, 63–69. [CrossRef]
114. Ratkowsky, D.A.; Lowry, R.K.; McMeekin, T.A.; Stokes, A.N.; Chandler, R.E. Model for bacterial culture growth rate throughout the entire biokinetic temperature range. *J. Bacteriol.* **1983**, *154*, 1222–1226. [CrossRef] [PubMed]
115. Nannipieri, P.; Trasar-Cepeda, C.; Dick, R.P. Soil enzyme activity: A brief history and biochemistry as a basis for appropriate interpretations and meta-analysis. *Biol. Fertil. Soils* **2018**, *54*, 11–19. [CrossRef]
116. Wolińska, A.; Bennicelli, R.P. Dehydrogenase activity response to soil reoxidation process described as varied conditions of water potential, air porosity and oxygen availability. *Pol. J. Environ. Stud.* **2010**, *19*, 651–657.
117. Quilchano, C.; Marañón, T. Dehydrogenase activity in Mediterranean forest soils. *Biol. Fertil. Soils* **2002**, *35*, 102–107. [CrossRef]
118. Kumar, S.; Chaudhuri, S.; Maiti, S.K. Soil dehydrogenase enzyme activity in natural and mine soil—A review. *Middle East J. Sci. Res.* **2013**, *13*, 898–906. [CrossRef]
119. Wolińska, A.; Rekosz-Burlaga, H.; Goryluk-Salmonowicz, A.; Błaszczuk, M.; Stepniwska, Z. Bacterial Abundance and Dehydrogenase Activity in Selected Agricultural Soils from Lublin Region. *Pol. J. Environ. Stud.* **2015**, *24*, 2677–2682. [CrossRef]
120. Pascual, J.A.; Garcia, C.; Hernandez, T.; Moreno, J.L.; Ros, M. Soil microbial activity as a biomarker of degradation and remediation processes. *Soil Biol. Biochem.* **2000**, *32*, 1877–1883. [CrossRef]
121. Paz-Ferreiro, J.; Gascó, G.; Gutiérrez, B.; Méndez, A. Soil biochemical activities and the geometric mean of enzyme activities after application of sewage sludge and sewage sludge biochar to soil. *Biol. Fertil. Soils* **2012**, *48*, 511–517. [CrossRef]
122. Roig, N.; Sierra, J.; Martí, E.; Nadal, M.; Schuhmacher, M.; Domingo, J.L. Long-term amendment of Spanish soils with sewage sludge: Effects on soil functioning. *Agric. Ecosyst. Environ.* **2012**, *158*, 41–48. [CrossRef]

123. Wijesekara, H.; Bolan, N.S.; Thangavel, R.; Seshadri, B.; Surapaneni, A.; Saint, C.; Hetherington, C.; Matthews, P.; Vithanage, M. The impact of biosolids application on organic carbon and carbon dioxide fluxes in soil. *Chemosphere* **2017**, *189*, 565–573. [CrossRef] [PubMed]
124. Gajda, A.M.; Przewłoka, B.; Gawryjolek, K. Changes in soil quality associated with tillage system applied. *Int. Agrophys.* **2013**, *27*, 133–141. [CrossRef]
125. Muscolo, A.; Settineri, G.; Attinà, E. Early warning indicators of changes in soil ecosystem functioning. *Ecol. Ind.* **2015**, *48*, 542–549. [CrossRef]
126. Sánchez-Monedero, M.A.; Mondini, C.; Cayuela, M.L.; Roig, A.; Contin, M.; De Nobile, M. Fluorescein diacetate hydrolysis, respiration and microbial biomass in freshly amended soils. *Biol. Fertil. Soils* **2008**, *44*, 885–890. [CrossRef]
127. Carlson, J.; Saxena, J.; Basta, N.; Hundal, L.; Busalacchi, D.; Dick, R.P. Application of organic amendments to restore degraded soil: Effects on soil microbial properties. *Environ. Monit. Assess.* **2015**, *187*, 109. [CrossRef] [PubMed]
128. Diacono, M.; Montemurro, F. Long-term effects of organic amendments on soil fertility. In *Sustainable Agriculture*; Lichtfouse, E., Hamelin, M., Navarrete, M., Debaeke, P., Eds.; Springer: Dordrecht, The Netherlands, 2011; Volume 2, pp. 761–786. [CrossRef]
129. Kızılkaya, R.; Bayraklı, B. Effects of N-enriched sewage sludge on soil enzyme activities. *Appl. Soil Ecol.* **2005**, *30*, 192–202. [CrossRef]
130. Yakushev, A.V.; Blagodatsky, S.A.; Byzov, B.A. The effect of earthworms on the physiological state of the microbial community at vermicomposting. *Microbiology* **2009**, *78*, 510–519. [CrossRef]
131. Tian, G.; Chiu, C.Y.; Franzluebbers, A.J.; Oladeji, O.O.; Granato, T.C.; Cox, A.E. Biosolids amendment dramatically increases sequestration of crop residue-carbon in agricultural soils in western Illinois. *Appl. Soil Ecol.* **2015**, *85*, 86–93. [CrossRef]
132. Sofo, A.; Scopa, A.; Dumontet, S.; Mazzatura, A.; Pasquale, V. Toxic effects of four sulphonylureas herbicides on soil microbial biomass. *J. Environ. Sci. Health Part B* **2012**, *47*, 653–659. [CrossRef]
133. Seal, A.; Datta, A.; Saha, S.; Chatterjee, A.K.; Barik, A.K.; Bhattacharyya, S.; Levin, Y.; Nain, A.S.; Asthana, A.; Bera, R. Soil Microbial Rejuvenation through Soil Resource Recycling as a part of Sustainable Management Programme: A Case Study from Lakhipara Tea Estate, Dooars, West Bengal, India. *J. Agric. Sci. Technol.* **2016**, *5*, 18–34. Available online: <http://orgprints.org/31300/1/1248-4636-1-PB%20%28Lakhipara%20Compost%29.pdf> (accessed on 20 December 2019).
134. Tian, L.; Dell, E.; Shi, W. Chemical composition of dissolved organic matter in agroecosystems: Correlations with soil enzyme activity and carbon and nitrogen mineralization. *Appl. Soil Ecol.* **2010**, *46*, 426–435. [CrossRef]
135. Tiemann, L.K.; Billings, S.A. Indirect effects of nitrogen amendments on organic substrate quality increase enzymatic activity driving decomposition in a mesic grassland. *Ecosystems* **2011**, *14*, 234–247. [CrossRef]
136. Zhao, S.; Li, K.; Zhou, W.; Qiu, S.; Huang, S.; He, P. Changes in soil microbial community, enzyme activities and organic matter fractions under long-term straw return in north-central China. *Agric. Ecosyst. Environ.* **2016**, *216*, 82–88. [CrossRef]
137. Bending, G.D.; Turner, M.K.; Jones, J.E. Interactions between crop residue and soil organic matter quality and the functional diversity of soil microbial communities. *Soil Biol. Biochem.* **2002**, *34*, 1073–1082. [CrossRef]
138. Kemmitt, S.J.; Lanyon, C.V.; Waite, I.S.; Wen, Q.; Addiscott, T.M.; Bird, N.R.; O'Donnell, A.G.; Brookes, P.C. Mineralization of native soil organic matter is not regulated by the size, activity or composition of the soil microbial biomass—A new perspective. *Soil Biol. Biochem.* **2008**, *40*, 61–73. [CrossRef]
139. Burns, R.G.; DeForest, J.L.; Marxsen, J.; Sinsabaugh, R.L.; Stromberger, M.E.; Wallenstein, M.D.; Weintraub, M.; Zoppini, A. Soil enzymes in a changing environment: Current knowledge and future directions. *Soil Biol. Biochem.* **2013**, *58*, 216–234. [CrossRef]
140. Wang, X.; Song, D.; Liang, G.; Zhang, Q.; Ai, C.; Zhou, W. Maize biochar addition rate influences soil enzyme activity and microbial community composition in a fluvo-aquic soil. *Appl. Soil Ecol.* **2015**, *96*, 265–272. [CrossRef]
141. Yeshitela, K. Effects of Anthropogenic Disturbance on the Diversity of Follicolous Lichens in Tropical Rainforests of East Africa: Godere (Ethiopia), Budongo (Uganda) and Kakamega (Kenya). Ph.D. Thesis, Universität Koblenz-Landau, Mainz, Germany, 2008; pp. 13–14.

142. Wang, C.; Liu, D.; Bai, E. Decreasing soil microbial diversity is associated with decreasing microbial biomass under nitrogen addition. *Soil Biol. Biochem.* **2018**, *120*, 126–133. [[CrossRef](#)]
143. Stone, M.M.; DeForest, J.L.; Plante, A.F. Changes in extracellular enzyme activity and microbial community structure with soil depth at the Luquillo Critical Zone Observatory. *Soil Biol. Biochem.* **2014**, *75*, 237–247. [[CrossRef](#)]



© 2020 by the authors. Licensee MDPI, Basel, Switzerland. This article is an open access article distributed under the terms and conditions of the Creative Commons Attribution (CC BY) license (<http://creativecommons.org/licenses/by/4.0/>).

Article

Amaranth Meal and Environmental *Carnobacterium maltaromaticum* Probiotic Bacteria as Novel Stabilizers of the Microbiological Quality of Compound Fish Feeds for Aquaculture

Iwona Gołaś^{1,*}, Jacek Potorski¹, Małgorzata Woźniak², Piotr Niewiadomski³,
Ma Guadalupe Aguilera-Arreola⁴, Araceli Contreras-Rodríguez⁵ and Anna Gotkowska-Płachta¹

¹ Department of Water Protection Engineering and Environmental Microbiology, University of Warmia and Mazury in Olsztyn, Prawocheńskiego 1, 10-720 Olsztyn, Poland; jacek.potorski@uwm.edu.pl (J.P.); aniagp@uwm.edu.pl (A.G.-P.)

² Department of Tourism, Recreation and Ecology, University of Warmia and Mazury in Olsztyn, Oczapowskiego 5, 10-957 Olsztyn, Poland; mawoz@uwm.edu.pl

³ Department of Ichthyology and Aquaculture, University of Warmia and Mazury in Olsztyn Oczapowskiego 5, 10-957 Olsztyn, Poland; piotr.niewiadomski@uwm.edu.pl

⁴ Medical Bacteriology Laboratory, Department of Microbiology, Instituto Politécnico Nacional, Escuela Nacional de Ciencias Biológicas, Mexico City, Mexico, Prolongación de Carpio y Plan de Ayala s/n, Col. Santo Tomás, Del. Miguel Hidalgo, Mexico City D.F. CP. 11340, Mexico; lupita_aguilera@hotmail.com

⁵ General Microbiology Laboratory, Department of Microbiology, Instituto Politécnico Nacional, Escuela Nacional de Ciencias Biológicas, Mexico City, Mexico. Prolongación de Carpio y Plan de Ayala s/n, Col. Santo Tomás, Del. Miguel Hidalgo, Mexico City D.F. CP. 11340, Mexico; aracelicontreras21@gmail.com

* Correspondence: iwonag@uwm.edu.pl; Tel.: +48-89-523-4557

Received: 24 June 2020; Accepted: 23 July 2020; Published: 25 July 2020

Abstract: Fish feed should be characterized by microbiological stability to guarantee the optimal health of farmed fish. The aim of this study was to determine the efficacy of amaranth meal (*Amaranthus cruentus*) and a highly active environmental strain of probiotic bacteria, *Carnobacterium maltaromaticum*, as novel supplements that stabilize the quantitative and qualitative composition of microbiota in compound fish feeds for aquaculture, regardless of storage temperature. The total viable counts of mesophilic bacteria at 28 °C (TVC 28 °C), hemolytic mesophilic bacteria (Hem 37 °C), *Staphylococcus* sp. bacteria, aerobic spore-forming bacteria (ASFB), sulfite-reducing anaerobic spore-forming *Clostridium* sp. bacteria, yeasts, and molds were analyzed in control feed (CF), in feed supplemented with amaranth meal (AF), and in feed supplemented with amaranth meal and *C. maltaromaticum* (ACF), stored at a temperature of 4 °C and 20 °C for 98 days. *Amaranthus cruentus* and *C. maltaromaticum* significantly reduced bacterial counts in fish feeds, regardless of the temperature and duration of storage. The antibacterial and antifungal effects of the tested additives were statistically significant ($p \leq 0.05$). The studied novel supplements contribute to the microbiological safety of compound fish feeds. The tested additives could be recognized as the key ingredients of organic, environmentally friendly fish feeds, which guarantee the high quality of fish intended for human consumption.

Keywords: aquaculture; compound feed; antimicrobial stabilizers; *Amaranthus cruentus*; *Carnobacterium maltaromaticum*

1. Introduction

Feed is one of the main factors that influence fish welfare and the microbiological status of water in aquaculture and freshwater ecology [1]. The nutritional value and microbiological quality of feed

determine fish weight gains, and the sanitary and epidemiological safety of aquatic organisms and the aquatic environment [2–6].

Synbiotics containing probiotics and prebiotics enhance the health benefits of feed. They promote the growth and metabolic activity of beneficial microorganisms in the host's gastrointestinal tract without compromising endogenous gut microbiota [7–9]. Probiotics are natural microbiome bacteria that deliver multidirectional beneficial effects for living organisms (humans and animals) at the local and systemic level [2,10]. The role of probiotic feed microbiota in the maintenance of gut homeostasis is increasingly recognized as a critical success factor in fish breeding [6,11–13].

The group of probiotic bacteria includes members of the genus *Carnobacterium* [14–17]. *Carnobacterium maltaromaticum*, which colonizes natural aquatic habitats, is one of the most metabolically active probiotic bacteria in the digestive tract of animals. This bacterial species easily adapts to changes in habitat conditions such as temperature, salinity, and pH, and it delivers health benefits for the host organism [14,18–20]. *Carnobacterium maltaromaticum* effectively inhibits the development of pathogenic bacteria and is regarded as a potent immune stimulator in fish [14,21–23].

The growth and activity of probiotic bacteria are influenced by environmental conditions that can be optimized with the use of prebiotics [24,25]. Prebiotics are non-digestible food ingredients that beneficially affect the host by selectively stimulating the growth and/or activity of bacteria colonizing the gastrointestinal tract [7].

Animal and plant meals are one of the main ingredients of fish feeds [26]. However, plant meals contain anti-nutritional factors, and their applicability in compound fish feeds is limited [27]. One of exceptions is amaranth meal, characterized by a low content of anti-nutritional factors, mainly saponins and phytic acid [28].

Amaranth meal contains lignins and various compounds with antioxidant, antibacterial, antiviral, and fungistatic properties [29–31]. Amaranth seeds are also abundant in other health-promoting substances, such as squalene and fiber [32,33]. In a study by Niewiadomski et al. [34], feed supplemented with 20% of amaranth meal promoted the growth of rainbow trout (*Oncorhynchus mykiss*) and improved the digestibility of dietary nutrients. A microbiological analysis in a pilot study conducted by Potorski and Niewiadomski [35] revealed that amaranth supplementation can prevent excessive growth and proliferation of *Staphylococcus* sp. bacteria, *Clostridium* sp. anaerobic spore-forming bacteria, yeasts, and molds in compound fish feeds. A similar beneficial influence of amaranth meal on selected probiotic strains was also observed by Vieira et al. [36] who demonstrated that amaranth meal stimulated the fermentation ability of ten probiotic strains (*Lactobacillus* spp. and *Bifidobacterium* spp.)

The microbiological composition of fish feeds significantly influences fish health and weight gains. This parameter is particularly important if feeds contain harmful microorganisms that compromise fish health, disrupt digestive metabolism, and compromise the reproduction and survival of farmed fish [4]. Feeds should be characterized by microbiological stability and high quality to guarantee the optimal health status and physiological condition of farmed fish. Nevertheless, not all undesirable microorganisms are eliminated during fish feed production. According to the literature [4,37], the standard extrusion process does not guarantee complete elimination of various microorganisms from fish feeds. Furthermore, the metabolic activity of heterotrophic bacteria that survive in ready-made feeds involves the oxidative degradation of lipids and proteins. As a result, the nutritional value of feeds can be modified by natural feed microbiota or by contamination with exogenous microorganisms. Inadequate storage temperature and prolonged storage can also promote the development and metabolic activity of various groups, genera, and species of heterotrophic microorganisms [38].

Our previous experiment [39], which investigated the effect of *C. maltaromaticum* on heterotrophic microbiota, revealed that probiotic bacteria were the main factor responsible for a decrease in the counts of all analyzed bacterial groups in commercial fish feed. The results of studies conducted by other authors [40–42] demonstrated that amaranth meal increased the survival and growth rates of probiotic bacteria and improved the microbial stability of foods. The combined use of environmental probiotic bacteria and amaranth meal as stabilizers of the microbiological quality of fish feeds remains

insufficiently researched. These facts have prompted the authors to evaluate the effectiveness of a highly active environmental isolate of *C. maltaromaticum* and amaranth meal in stabilizing the microbiological quality of fish feed. The aim of this study was to determine the efficacy of amaranth meal (*Amaranthus cruentus*) and a highly active environmental strain of probiotic bacteria, *C. maltaromaticum*, as novel supplements that stabilize the quantitative and qualitative composition of microbiota in compound fish feeds for aquaculture, regardless of storage temperature.

2. Materials and Methods

2.1. Isolation and Identification of *C. Maltaromaticum* Probiotic Bacteria

A probiotic strain of *C. maltaromaticum* was isolated from water samples collected from the benthic zone of Lake Legińskie (at a depth of 34 m) located in north-eastern Poland (N = 53°58'51" N and E = 21°8'4"). The strain had been isolated during a previous study conducted by the Department of Environmental Microbiology of the University of Warmia and Mazury in Olsztyn.

The isolate was identified to species level by matrix-assisted laser desorption/ionization time-of-flight mass spectrometry (MALDI-TOF VITEK® MS) at the Department of Microbiology, Escuela Nacional de Ciencias Biológicas, Instituto Politécnico Nacional, in Mexico City, Mexico. The identification was additionally verified by 16S rDNA (recombinant DNA) sequencing with the BigDye Terminator v3.1 kit in the ABI 3730xl genetic analyzer (Applied Biosystems, Foster City, USA). In addition, 16S rDNA genes were sequenced by PCR with the use of 27F (5'-AGAGTTTGATCATTGGCTCAG-3') and 1492R (5'-GGTACC-TTGTTACGACTT-3') primers according to the method described by Gillan et al. [43]. The BLAST program available on the website of the National Center of Biotechnology Information [44] was used to identify DNA sequences. The results of 16S rDNA sequencing are presented in Table S1 (Supplementary Materials).

After the identification process, *C. maltaromaticum* was considered as a probiotic strain based on the hemolysis assay, and its acid and bile tolerance properties, according to the guidelines developed by a joint FAO/WHO working group [45]. The hemolytic activity of *C. maltaromaticum* was determined on tryptone soya agar (TSA; Oxoid, Basingstoke, UK) with 5% addition of defibrinated sheep blood incubated at 37 °C for 48 h [46]. The bile salt tolerance test of the studied strain was performed in MRS broth culture medium (Sigma - Aldrich, Germany) containing 0.5%, 1.0%, or 2.0% bile salts (Oxoid LP0055) according to the procedure proposed by Succi et al. [47]. The *C. maltaromaticum* isolate was tested for acid tolerance based on its growth on medium with varying pH (1.5, 2.5, 3.5, and 4.5), as described by Vijayarajarama et al. [48].

2.2. Determination of the Metabolic Activity of Probiotic Bacteria Based on the Utilization of Different Carbon Sources

The applicability of the environmental *C. maltaromaticum* isolate for further analysis was determined by analyzing the bacteria's metabolism based on its utilization of various carbon sources. The biochemical activity of the *C. maltaromaticum* probiotic isolate and its potential to compete for nutrients with feed microbiota were estimated using the OmniLog®System (Biolog, USA). A 96-well plate containing various carbon compounds was inoculated with the evaluated bacterial strain. The plate was incubated, and biochemical parameters were read in a microstation reader. The strain's utilization of different carbon compounds as sources of energy was determined based on the intensity of color reactions.

2.3. Compound Feed

The experiment was performed on three types of extruded compound feeds: Control feed (CF) without the addition of amaranth meal, experimental feed containing 20% of amaranth meal (AF), and experimental feed containing 20% of amaranth meal and *C. maltaromaticum* probiotic bacteria (ACF). The composition of each feed is presented in Table 1. All feeds were formulated based on

the recommendations of Hart et al. [49] and NRC [50]. The feeds were extruded with a co-rotating twin screw extruder (Metalchem, Poland) equipped with a Ø 4.5 mm pellet stencil. The following extrusion processing parameters were applied: Screw speed—105–125 rpm, cutter speed—50 rpm, head temperature—120 °C, barrel temperature of 130–150 °C in 30 s, die diameter—2.0 mm. Compound feeds were enhanced with a mixture of fish oil and soybean oil (5% each). The tested strain of *C. maltaromaticum* was added to the oil mixture. Next, the probiotic oil suspension was added to two experimental feed samples. The oil mixture was pumped into the feed at 0.9 Mpa for 5 min with the use of a vacuum pump. The feed contained 40.0% crude protein, 15.0% crude fat, 3.0% crude ash, 37.0 nitrogen-free extract (NFE), and 5% water.

Table 1. Feeds composition (g·100 g⁻¹ dry diet).

Ingredients	Feed Type		
	CF ¹	AF ²	ACF ³
Soybean meal	32.00	27.00	27.00
Wheat flour	25.00	10.00	10.00
Amaranth meal	0.00	20.00	20.00
Fishmeal	15.00	15.00	15.00
Hydrolyzed feather meal	15.00	15.00	15.00
Codliver oil	5.00	5.00	5.00
Soybean oil	5.00	5.00	5.00
Vitamin premix ⁴	1.00	1.00	1.00
Mineral premix ⁵	2.00	1.00	1.00
<i>C. maltaromaticum</i> (CFU·g ⁻¹)	0.00	0.00	1.5 × 10 ⁹

¹—control feed (CF); ²—feed containing 20% amaranth (AF); ³—feed containing 20% of amaranth and *Carnobacterium maltaromaticum* (ACF); ⁴—Composition of the vitamin premix (IU·1 kg⁻¹ dry diet): Vitamin A—70,000 IU; vitamin D—200,000 IU; vitamin E—17,500 IU; vitamin K—867 IU; vitamin C—28,500 IU; vitamin B1—1067 IU; vitamin B2—2000 IU; vitamin B5—5334 IU; vitamin B6—1334 IU; vitamin B12—400 IU; biotin—200 IU; niacin—12,000 IU; folic acid—800 IU; inositol—20,000 IU; choline chloride—120,000 IU; betaine—75,000 IU; ⁵—Composition of the mineral premix (g·1 kg⁻¹ dry diet): FeSO₄·H₂O—4334 g; KI—0.734 g; CuSO₄·5H₂O—0.267 g; MnO—0.734 g; ZnSO₄·H₂O—1250 g; ZnO—0.750 g; Na₂SeO₄—0.034 g; CFU—colony forming unit.

2.4. Experimental Design

The prepared feeds (CF, AF, and ACF) were used in an experiment that lasted for 98 days. The control feed (CF) was divided into two equal parts, and the feed containing 20% amaranth meal (AF) was divided into four equal parts under sterile conditions. Every CF and AF sample was placed in a separate, sterile, and tightly closed vessel made of dark glass. Two samples (CF 4 °C, AF 4 °C) were chill-stored at a temperature of 4 °C, and two samples (CF 20 °C, AF 20 °C) were stored at a temperature of 20 °C throughout the experiment. Cultures of the environmental *C. maltaromaticum* strain were added to the remaining two samples (AF) at 1.5 × 10⁹ CFU·g⁻¹ (Table 1). One of the samples containing probiotic bacteria (ACF 4 °C) was chill-stored at 4 °C, and the other sample (ACF 20 °C) was stored at 20 °C for 98 days.

2.5. Microbiological Analyses

All feed samples (CF, AF, and ACF) stored at 4 °C and 20 °C were subjected to microbiological analyses after 7, 14, 21, 28, 35, 42, 49, 56, 63, 70, 77, 84, 91, and 98 days of the experiment. The following parameters were determined: Total counts of *C. maltaromaticum* bacteria on tryptone soya agar (TSA; Oxoid, Basingstoke, UK) with the addition of 3% yeast extract and 1.5% (*w/v*) NaCl [14], total counts of mesophilic bacteria on tryptone soya agar (TSA; Oxoid, Basingstoke, UK) incubated at 28 °C for 48 h (TVC 28 °C), total counts of hemolytic mesophilic bacteria on tryptone soya agar (TSA; Oxoid, Basingstoke, UK) with 5% addition of defibrinated sheep blood incubated at 37 °C for 48 h (hemolytic mesophilic bacteria (Hem) 37 °C), total counts of aerobic spore-forming bacteria (ASFB) on an agar/broth medium (Biocorp, Warsaw, Poland) with glucose incubated at 28 °C for 72 h, counts of *Staphylococcus* sp. bacteria on the Chapman medium (Merck KgaA, Darmstadt, Germany) incubated at 37 °C for 48 h,

counts of sulfite-reducing anaerobic spore-forming *Clostridium* sp. bacteria on the Wilson-Blair medium (Merck KgaA, Darmstadt, Germany) incubated at 37 °C for 18 h, and total yeast and mold counts on the Rose-Bengal-Chloramphenicol Agar (RGBC; Merck KgaA, Darmstadt, Germany) incubated at 28 °C for 5 days.

All analyses were performed according to Polish Standard [51]. The potential pathogenicity of Hem 37 °C, *Staphylococcus* sp., and *Clostridium* sp. bacteria was determined based on their hemolytic activity on tryptone soya agar (TSA; Oxoid, Basingstoke, UK) with 5% addition of defibrinated sheep blood incubated at 37 °C for 48 h. Hemolysis was confirmed when a transparent zone was formed around the inoculated colonies [46]. Mean microbial counts were calculated based on the values determined in three replicates of the same sample of compound fish feed. Finally, the counts of all analyzed microorganisms were expressed in CFU·1 g⁻¹ of compound feed.

2.6. Statistical Analysis

The mean values, standard deviations, standard errors, and confidence interval (CI = 95%, N = 3) of microbial counts in feeds (CF, AF, ACF) stored at a temperature 4 °C and 20 °C were calculated. The relationships between *C. maltaromaticum* bacterial counts and microbial (TVC 28 °C, Hem 37 °C, ASFB, *Staphylococcus* sp., *Clostridium* sp., yeasts, and molds) counts were determined by Spearman's non-parametric rank correlation test ($p \leq 0.05$). The significance of differences in microbial counts between the analyzed types of fish feed (CF, AF, ACF) stored at different temperatures (4 and 20 °C) and for different periods of time (7, 14, 21, 28, 35, 42, 49, 56, 63, 70, 77, 84, 91, and 98 days) was determined by one-way analysis of variance (ANOVA). Leven's test was used to assess the homogeneity of variance. The verified hypothesis was rejected when Leven's test produced statistically significant results. The Kruskal–Wallis test, a non-parametric version of the classical one-way ANOVA, was then applied. Statistical analyses were performed in the Statistica 13.3 software package (TIBCO Software Inc., Palo Alto, USA) [52].

3. Results

3.1. Probiotic Properties of *Carnobacterium Maltaromaticum*

The studied *C. maltaromaticum* isolate was not capable of causing hemolysis, which suggested that the strain was not pathogenic.

The strain tolerated the tested pH values. After 3 h acid exposure, the isolate's survival rate was higher at pH 2.5 (76.1%) than at pH 1.5 (65%), and it reached 82.3% at pH 3.5 and 87.8% at pH 4.5. The bile salt tolerance test revealed a small difference in the survival rates of *C. maltaromaticum*. The highest isolate viability (85.2%) was observed at a 2% concentration of bile salts, whereas the lowest viability (79.5%) was noted at a 0.5% concentration of bile salts; 83.2% of *C. maltaromaticum* bacteria survived at a 1.0% concentration of bile salts (data not shown).

The *C. maltaromaticum* isolate tested in our study could be classified as a probiotic strain based on the results of the above analyses and according to the guidelines developed by a joint FAO/WHO working group [45].

3.2. Metabolic Activity of *C. maltaromaticum* Probiotic Bacteria

The results of the analyses examining the utilization of various carbon sources by the environmental *C. maltaromaticum* isolate are presented in Figure 1. The analyses performed in the Omnilog Gen III system (Biolog, Hayward, CA, USA) revealed that the evaluated strain actively metabolized 70 carbon sources. The studied *C. maltaromaticum* strain was capable of growth at pH 5 and 6, and in the presence of 1%, 4%, and 8% NaCl. The tested isolate did not metabolize the following substrates: L-alanine, L-arginine, L-aspartic acid, L-glutamic acid, histidine, D-gluconic acid, and mucic acid. The analyzed strain did not metabolize vancomycin, tetrazolium blue chloride, L-pyrroglutamic acid, α -ketoglutaric acid, α -ketobutyric acid, and acetoacetic acid. These results confirmed the very high biochemical

activity of the studied environmental probiotic isolate, and suggested its potential to compete for nutrients with feed microbiota.

Negative control	Positive control	D-Maltose	D-Trehalose	D-Cellobiose	Gentobiose
Sucrose	D-Turanose	Stachyose	Dextrin	pH 6	pH5
D-Raffinose	α -D-Lactose	D-Melibiose	1% NaCl	4% NaCl	8% NaCl
N-Acetyl- β -D-Mannosamine	N-Acetyl-D-Galactosamine	N-Acetyl Neuraminic acid	Methyl-D-Glucoside	D-Salicin	N-Acetyl-D-Glucosamine
α -D-Glucose	D-Mannose	D-Fructose	D-Galactose	3-Methyl Glucose	D-Fucose
L-Fucose	L-Rhamnose	Inosine	Sodium Lactate	Fusidic acid	D-Serine
D-Sorbitol	D-Mannitol	Arabitol	myo-Inositol	Glycerol	D-Glucose-6PO ₄
D-Fructose-6PO ₄	D-Aspartic acid	D-Serine	Troleandomycin	Rifamycin SV	Minocycline
Gelatin	Glycyl-L-Proline	L-Alanine	L-Arginine	L-Aspartic acid	L-Glutamic acid
Histidine	D-Glucuronic acid	L-Serine	Lincomycin	Guanidine HCl	Niaproof
Pectin	Nalidixic acid	L-Galactonic acid	D-Gluconic acid	Methyl Pyruvate	Glucuronamide
Mucic acid	Quinic acid	D- Saccharic acid	Vancomycin	Tween 40	Tetrazolium Blue
p-Hydroxy-Phenylacetic acid	L-Pyroglutamic acid	D-Lactic Acid Methyl Ester	L-Lactic acid	Lithium Chloride	α -Ketoglutaric acid
D-Malic acid	L-Malic acid	Bromosuccinic acid	D-Galacturonic acid	Citric acid	Potassium Tellurite
Tetrazolium Violet	γ -Aminobutyric acid	α -Hydroxybutyric acid	β -Hydroxy-D,L-Butyric acid	α -Ketobutyric acid	Acetoacetic acid
Propionic acid	Acetic acid	Formic acid	Aztreonam	Sodium Butyrate	Sodium Bromate



 - positive reaction |
  - negative reaction

Figure 1. The results of a metabolic activity test analyzing the chemical sensitivity of an environmental *Carnobacterium maltaromaticum* probiotic isolate and its ability to utilize different carbon sources (GEN III MicroPlate™). Purple color—metabolic activity of the *C. maltaromaticum* isolate, white color—no metabolic activity of the *C. maltaromaticum* isolate.

3.3. The Quantitative and Qualitative Composition of Bacterial Microbiota in Compound Fish Feeds

The mean (of three replicates) counts of mesophilic bacteria (TVC 28 °C), hemolytic mesophilic bacteria (Hem 37 °C), *Staphylococcus* sp., *Clostridium* sp., aerobic spore-forming bacteria (ASFB), yeasts and molds in CF, AF, and ACF, and *C. maltaromaticum* bacteria stored at a temperature of 4 °C and 20 °C during the 98-day experiment are presented in Figure 2. The mean values, standard deviations, standard errors, and confidence interval of three replicates of microbial counts are shown in Table S2 (Supplementary Materials). In CF, microbial counts differed by several orders of magnitude, depending on the analyzed microbial group and the temperature and time of feed storage. In CF 4 °C samples, TVC 28 °C and *Clostridium* sp. counts increased several-fold after 14 and 28 days of storage, respectively, relative to initial values. The counts of other microbial groups (Hem 37 °C, *Staphylococcus* sp., yeasts,

and molds) in CF 4 °C samples continued to decrease in successive weeks of the experiment. The noted decrease ranged from 10¹ to 10⁵ CFU across the analyzed microbial groups, subject to storage time (Figure 2A).

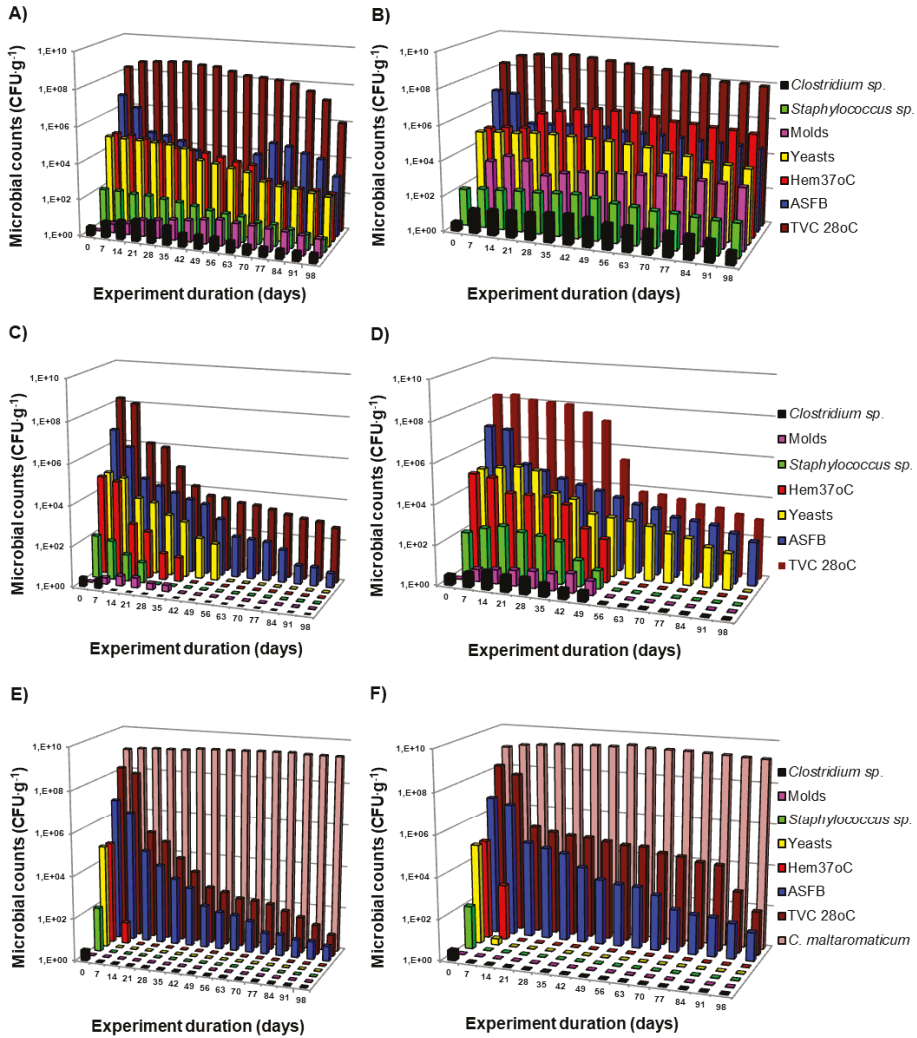


Figure 2. The mean (of three replicates) total viable counts (CFU.g⁻¹) of mesophilic bacteria (TVC 28 °C), hemolytic mesophilic bacteria (Hem 37 °C), *Staphylococcus sp.*, *Clostridium sp.*, aerobic spore-forming bacteria (ASFB), yeasts, and molds in: (A) Control feed (CF 4 °C) stored at a temperature of 4 °C, (B) control feed (CF 20 °C) stored at a temperature of 20 °C, (C) feed supplemented with 20% amaranth

meal (AF 4 °C) stored at a temperature of 4 °C, (D) feed supplemented with 20% amaranth meal (AF 20 °C) stored at a temperature of 20 °C, (E) feed supplemented with 20% amaranth meal and *Carnobacterium maltaromaticum* bacteria (ACF 4 °C) stored at a temperature of 4 °C, and (F) feed supplemented with 20% amaranth meal and *Carnobacterium maltaromaticum* bacteria (ACF 20 °C) stored at a temperature of 20 °C during a 98 day experiment. The mean values, standard deviations, standard errors, and confidence interval of three replicates of microbial counts are shown in Table S2 (Supplementary Materials).

The counts of nearly all microorganisms (excluding ASBF) increased by around 100% in CF 20 °C samples after 14, 28, and 42 days. In CF 20 °C samples, TVC 28 °C and yeast counts peaked on day 28 at 92×10^7 and 12×10^4 CFU·g⁻¹, respectively. The highest counts of potentially pathogenic bacteria (Hem 37 °C, *Staphylococcus* sp., *Clostridium* sp.) were noted after 42 days of feed storage. The maximum counts of Hem 37 °C, *Staphylococcus* sp., *Clostridium* sp., and molds were determined at 2.8×10^6 , 3.0×10^2 , 45, and 2.5×10^3 CFU·g⁻¹, respectively. A minor decrease in microbial counts was noted in successive weeks of the experiment. However, on day 98, the counts of all evaluated microorganisms in CF 20 °C samples were several-fold to several hundred-fold higher than those in CF 4 °C samples (Figure 2B).

In feed samples supplemented with 20% amaranth meal stored at a temperature of 4 °C (AF 4 °C), the counts of all analyzed microbial groups decreased by several orders of magnitude after 14 days of the experiment. On day 28, Hem 37 °C (20 CFU·g⁻¹) was the only potentially pathogenic microorganism in the studied samples. Toward the end of the experiment, AF 4 °C samples were colonized only by TVC 28 °C (500 CFU·g⁻¹) and ASFB (5 CFU·g⁻¹) (Figure 2C).

In AF 20 °C samples, the decrease in the counts of potentially pathogenic Hem 37 °C bacteria was considerably lower than that in AF 4 °C samples. On day 28, Hem 37 °C counts in AF 20 °C samples were determined at 1.0×10^4 CFU·g⁻¹, and they were 500-fold higher than those in AF 4 °C samples on the same day. The counts of TVC 28 °C, ASBF, and yeasts were also several-fold to several dozen-fold higher in AF 20 °C samples than in AF 4 °C samples on the same days (Figure 2D). Hem 37 °C, *Staphylococcus* sp., and *Clostridium* sp. survived for longer periods of time in AF 20 °C than in AF 4 °C. Hem 37 °C, *Staphylococcus* sp., and *Clostridium* sp. were eliminated from AF 20 °C samples only after 56 days, and from AF 4 °C—already after 14 or 28 days of the experiment (Figure 2C,D).

Feed samples supplemented with 20% amaranth meal and a highly active environmental strain of *C. maltaromaticum* probiotic bacteria (ACF 4 °C, ACF 20 °C) were characterized by the lowest counts (Figure 2E,F) and the lowest survival rate of all analyzed microbial groups, regardless of storage temperature (Table S3). Potentially pathogenic *Staphylococcus* sp., *Clostridium* sp., and Hem 37 °C bacteria were not detected in ACF 4 °C and ACF 20 °C samples already after 7 days. In the first two weeks of the experiment, TVC 28 °C counts decreased around 1000 fold, ASFB counts decreased more than 100-fold, and yeast counts decreased several fold in ACF 4 °C and ACF 20 °C samples relative to the initial values. On day 98, ACF 4 °C samples were colonized only by TVC 28 °C and ASBF at 10 and 5 CFU·g⁻¹, respectively (Figure 2E). TVC 28 °C and ASFB counts were higher in ACF 20 °C at 120 and 20 CFU·g⁻¹, respectively (Figure 2F). Additionally, Spearman's test revealed significant ($p \leq 0.05$) negative correlations between *C. maltaromaticum* counts and almost all microbial populations (except for *Clostridium* sp. and molds) in ACF, regardless of storage temperature (Table 2).

The differences in the quantitative and qualitative composition of bacterial and fungal microbiota in the analyzed types of fish feeds (CF, AF, and ACF) stored at different temperatures (4 °C and 20 °C) and for different periods of time were confirmed by the statistical analysis (Table 3). The Kruskal–Wallis test revealed significant ($p \leq 0.05$) differences in the counts of all analyzed microorganisms between the evaluated feeds (CF, AF, and ACF) and in ASFB and yeast counts in feed samples stored for different periods of time. Significant ($p \leq 0.05$) differences were also observed in *Staphylococcus* sp., *Clostridium* sp., and mold counts in feed samples stored at different temperatures, and in TVC 28 °C, Hem 37 °C, *Staphylococcus* sp., and *Clostridium* sp. counts in feed samples stored for different periods of time.

Table 2. The values of correlation coefficients between microbial counts in feed supplemented with 20% amaranth meal and *C. maltaromaticum* probiotic bacteria (ACF) stored at 4 and 20 °C. The correlations between microbial counts in ACF 4 °C (N = 14) and ACF 20 °C (N = 14) samples were analyzed with Spearman’s test.

	Microorganisms									
	<i>C. maltaromaticum</i>		TVC 28 °C ¹		Hem 37 °C ²		<i>Staphylococcus</i> sp.		Yeasts	
	4 °C	20 °C	4 °C	20 °C	4 °C	20 °C	4 °C	20 °C	4 °C	20 °C
TVC 28 °C ¹	−0.904 *	−0.535 *								
Hem 37 °C ²	−0.763 *	−0.713 *	0.723 *	0.763 *						
<i>Staphylococcus</i> sp.	−0.677 *	−0.580 *	0.511	0.577	0.715 *	0.755 *				
Yeasts	−0.763 *	−0.578 *	0.763 *	0.975 *	0.997	0.782 *	0.755 *	0.591		
ASFB ³	−0.894 *	−0.535 *	0.957	0.999	0.723 *	0.763 *	0.577	0.577	0.763 *	0.975 *

¹—mesophilic bacteria (TVC 28 °C); ²—hemolytic mesophilic bacteria (Hem 37 °C); ³—aerobic spore-forming bacteria (ASFB); *—statistically significant correlations in Spearman’s test ($p \leq 0.05$).

Table 3. The quantitative composition of microorganisms in control feed (CF), feed supplemented with 20% amaranth meal (AF), and feed supplemented with 20% amaranth meal and *Carnobacterium maltaromaticum* bacteria (ACF) stored at different temperatures (4 and 20 °C) for 7, 14, 21, 28, 35, 42, 49, 56, 63, 70, 77, 84, 91, and 98 days, validated in the Kruskal–Wallis test (N = 84).

Microorganisms	Differences (p) between		
	Feed Type	Storage Temperature	Storage Time
TVC 28 °C ¹	0.0000 *	0.2194	0.0242 *
Hem 37 °C ²	0.0000 *	0.3058	0.0476 *
<i>Staphylococcus</i> sp.	0.0000 *	0.0456 *	0.0493 *
Yeasts	0.0050 *	0.0550	0.0011 *
ASFB ³	0.0005 *	0.2785	0.0005 *
<i>Clostridium</i> sp.	0.0001 *	0.0238 *	0.0483 *
Molds	0.0003 *	0.0048 *	0.9979

¹—mesophilic bacteria (TVC 28 °C); ²—hemolytic mesophilic bacteria (Hem 37 °C); ³—aerobic spore-forming bacteria (ASFB); *—statistically significant differences; one-way ANOVA, $p \leq 0.05$.

4. Discussion

The analyses of the quantitative and qualitative composition of microbiota in fish feed samples revealed significant differences ($p \leq 0.05$) across the examined types of feed (CF, AF, ACF), feed storage temperatures, and feed storage times. Control feed (CF) was characterized by the highest counts, highest survival rates, and longest survival times of all analyzed microbial groups, which indicates that feed ingredients promote the growth of both specific feed microorganisms and potentially pathogenic microorganisms [37,53,54]. Similar results were reported by Petreska [4] and Gołaś et al. [55] who analyzed the counts of heterotrophic mesophilic bacteria and selected potentially pathogenic bacteria, yeasts, and molds in commercial feeds administered to intensively reared *Silurus glanis* L.

In our study, the counts of all specific feed microbiota and potentially pathogenic microorganisms (Hem 37 °C, *Staphylococcus* sp., *Clostridium* sp.) in feed supplemented with 20% amaranth meal (AF 4 °C, AF 20 °C) decreased by 1 to 4 orders of magnitude relative to those determined in CF 4 °C and CF 20 °C. The survival times of potentially pathogenic bacteria (Hem 37 °C, *Staphylococcus* sp., *Clostridium* sp.) were also significantly shorter in AF 4 °C and AF 20 °C than in CF 4 °C and CF 20 °C. The obtained results and the presence of significant differences ($p \leq 0.05$) in the counts of all analyzed microbial groups between CF and AF samples indicate that feed supplementation with 20% amaranth meal inhibits the growth of bacterial and fungal microbiota regardless of storage temperature or duration (Table 3). The antibacterial and antifungal properties of amaranth meal are also confirmed by the decrease in the counts of the remaining microbial groups (TVC 28 °C, ASFB, yeasts, molds) in

AF 4 °C and AF 20 °C samples in successive weeks of the experiment. The above could be attributed to the fact that amaranth meal contains lignins whose antioxidant, antibacterial, antiviral, and fungistatic properties contribute to the maintaining of the adequate microbiological quality of feed [31,56–59]. The addition of amaranth meal stabilizes natural microbiota in animal feeds, enhances the nutritional value of feeds, and improves performance.

Research studies have confirmed the beneficial influence of amaranth-supplemented feeds on the health status and body weight gains of rats [60], intensively farmed pigs [61,62], chickens [63], calves, lambs, sheep, and ruminants [56]. Studies investigating the effect of amaranth-supplemented feeds on fish in different farming systems also demonstrated that amaranth meal stimulated the immune system of fish [64], their growth performance, and the enzymatic activity of their gut microbiota [5,65]. The results of the present study indicate that amaranth meal can be effectively used to improve the quality and microbiological safety of fish feeds.

The counts of all studied microorganisms (TVC 28 °C, Hem 37 °C, ASFB, *Staphylococcus* sp., *Clostridium* sp., yeasts, and molds) were lowest in ACF 4° and ACF 20° relative to AF and CF stored at the corresponding temperatures. The counts, percentage viability, and survival times of the evaluated microbial groups were considerably lower in ACF 4° and ACF 20° than in AF 4° and AF 20° (Figure 2C–F; Table S3), which indicates that amaranth meal and *C. maltaromaticum* probiotic bacteria exert antibacterial and antifungal effects on natural microbiota and potentially pathogenic microorganisms in compound feed. The synergistic effects of the tested feed additives could be attributed to the symbiotic relationship between amaranth meal and the evaluated probiotic bacteria, and their ability to inhibit the growth and development of various microbial groups and genera. An in vitro study [57,66] revealed that amaranth is a source of bioactive compounds that suppress the proliferation of many microorganisms, including *Staphylococcus aureus*, *Bacillus*, *Escherichia coli*, *Salmonella typhi*, *Pseudomonas aeruginosa*, *Proteus mirabilis*, *Klebsiella pneumoniae*, and *Candida albicans*. Amaranth meal also promotes the development of many species of probiotic bacteria, such as *Lactobacillus plantarum*, *L. paralimentarius*, *L. helveticus*, *L. sakei*, *Pediococcus pentosaceus*, *L. paralimentarius*, *Enterococcus mundtii*, *E. hermanniensis*, *E. durans*, *Enterococcus* sp., and *Leuconostoc mesenteroides*, whose metabolic activity enhances the nutritional value and health benefits of food products [67–69]. An in vitro study conducted by Gullón et al. [70] demonstrated that amaranth was characterized by a high prebiotic potential and promoted the growth of probiotic microflora isolated from the human digestive tract. By inhibiting the growth and development of naturally occurring microorganisms and pathogenic microbiota in foodstuffs and feedstuffs [5,66] probiotic bacteria and amaranth contribute to improving fish welfare and performance in various aquaculture systems [71–73].

The lowest counts of all evaluated microbial groups and genera and the shortest microbial survival times were noted in ACF samples regardless of storage temperature and storage time, which indicates that amaranth meal and *C. maltaromaticum* probiotic bacteria exert synergistic effects on the quantitative and qualitative composition of feed microbiota. Feed supplementation with 20% amaranth meal and *C. maltaromaticum* (ACF) bacteria completely inhibited the growth of most analyzed microorganisms (excluding ASFB and TVC 28 °C) in feeds stored at 4 °C and 20 °C for 7 days. The results of our in vitro study were validated statistically, which suggests that the novel tested additives contribute to the microbiological stability of fish feeds regardless of storage conditions and storage time.

5. Conclusions

The results of the present study, which investigated the supplementation of compound fish feeds with innovative additives, amaranth meal, and a highly active environmental strain of probiotic bacteria, *C. maltaromaticum*, indicate that the tested additives exert synergistic effects and contribute to the microbiological stability of fish feeds regardless of the temperature and time of storage. The evaluated components decreased the counts, percentage viability, and survival times of various groups and genera of microorganisms that occur naturally in feeds, which suggests that they can minimize feed losses resulting from the growth and metabolic activity of autochthonous

and allochthonous microbiota in feeds that are stored for excessive periods of time and/or at inadequate temperature. Excessive microbial growth lowers the nutritional value of feed, and decreases nutrient digestibility and assimilability, which may negatively affect fish performance in aquaculture. The addition of 20% amaranth meal and a highly active environmental strain of probiotic bacteria, *C. maltaromaticum*, to fish feed inhibited the growth of potentially pathogenic microbiota (Hem 37°, *Staphylococcus* sp., and *Clostridium* sp.) in vitro, which is important for the growth rate and welfare of fish. Due to their novel synergistic health-promoting properties, amaranth meal and environmental *C. maltaromaticum* bacteria could be recognized as the key ingredients of organic, environmentally friendly fish feeds, which guarantee the high quality of fish intended for human consumption.

Supplementary Materials: The following are available online at <http://www.mdpi.com/2076-3417/10/15/5114/s1>, Table S1: The identification of an environmental strain of *Carnobacterium maltaromaticum* bacteria based on 16S rDNA sequence analysis. Table S2: The mean values (X), confidence interval (CI) (CI = 95%, N = 3), standard deviations (SD), and standard errors (SE) of microbial counts in control feed (CF), in feed supplemented with 20% amaranth meal (AF), and in feed supplemented with 20% amaranth meal and *Carnobacterium maltaromaticum* bacteria (ACF) stored at 4 and 20 °C during 98 days of the experiment. Table S3: Survival rates of microorganisms (%) in control feed (CF), feed supplemented with 20% amaranth meal (AF), and feed supplemented with 20% amaranth meal and *Carnobacterium maltaromaticum* bacteria (ACF) stored at 4 and 20 °C during 98 days of the experiment.

Author Contributions: Conceptualization, I.G. and M.W.; methodology, I.G., J.P., M.W., P.N., M.G.A.-A. and A.C.-R.; software, I.G.; validation, I.G., J.P., M.W. and P.N.; formal analysis, J.P. and P.N.; investigation, I.G., J.P., M.W. and P.N.; resources, I.G., M.W., M.G.A.-A. and A.C.-R.; data curation, I.G. and J.P.; writing—original draft preparation, I.G. and M.W.; writing—review and editing, M.W. and A.G.-P.; visualization, A.G.-P.; supervision, I.G. All authors have read and agreed to the published version of the manuscript.

Funding: This research received no external funding.

Acknowledgments: This study was supported by research grants No. 18.610-004-300 and No. 18.610.001-300 from the Ministry of Science and Higher Education (Poland). The project was financially co-supported by the Minister of Science and Higher Education under the program entitled “Regional Initiative of Excellence” for the years 2019–2022, Project No. 010/RID/2018/19, amount of funding PLN 12,000,000. The authors would like to thank Z. Filipkowska and E. Korzeniewska, Professors at the University of Warmia and Mazury in Olsztyn for the culturing and sequencing of 16S rDNA of the tested *C. maltaromaticum* strain, and K. Glińska-Lewczuk (University of Warmia and Mazury in Olsztyn) for help in the statistical processing of data.

Conflicts of Interest: The authors declare that they have no conflict of interest. The funders had no role in the design of the study; in the collection, analyses, or interpretation of data; in the writing of the manuscript, or in the decision to publish the results.

References

- Golaś, I.; Szmyt, M.; Potorski, J.; Łopata, M.; Gotkowska-Płachta, A.; Glińska-Lewczuk, K. Distribution of *Pseudomonas fluorescens* and *Aeromonas hydrophila* bacteria in a recirculating aquaculture system during farming of uropean grayling (*Thymallus thymallus* L.) broodstock. *Water* **2019**, *11*, 376. [CrossRef]
- Banu, M.R.; Akter, S.; Islam, M.R.; Mondol, M.N.; Hossain, M.A. Probiotic yeast enhanced growth performance and disease resistance in freshwater catfish gulsa tengra, *Mystus cavasius*. *Aquac. Res.* **2020**, *16*. [CrossRef]
- Lauzon, H.L.; Dimitroglou, A.; Merrifield, D.L.; Ringo, E.; Davies, S.J. Probiotics and Prebiotics: Concepts, Definitions and History. In *Aquaculture Nutrition: Gut Health, Probiotics and Prebiotics*; Merrifield, D.L., Ringo, E., Eds.; Wiley Blackwell: Chichester, UK, 2014; pp. 169–184.
- Petreska, M.; Ziberoski, J.; Zekiri, M. Fish feed microbiological status. *JHED* **2013**, *4*, 16–19.
- Ramesh, S.; Chelladurai, G.; Haniffa, M.A. Isolation of enzyme producing bacteria from gut of *Channa striatus* fed on different herbs and probiotics diet. *Int. J. Pharm. Pharm. Sci.* **2013**, *5*, 195–198.
- Robertson, P.A.W.; O’Dowd, C.; Burrells, C.; Williams, P.; Austin, B. Use of *Carnobacterium* sp. as a probiotic for Atlantic salmon (*Salmo salar* L.) and rainbow trout (*Oncorhynchus mykiss*, Walbaum). *Aquaculture* **2000**, *185*, 235–243. [CrossRef]
- Gibson, G.R.; Roberfroid, M.B. Dietary modulation of the human colonic microbiota: Introducing the concept of prebiotics. *J. Nutr.* **1995**, *125*, 1401–1412. [CrossRef]

8. Andersson, H.; Asp, N.-G.; Bruce, Å.; Roos, S.; Wadström, T.; Wold, A.E. Health effects of probiotics and prebiotics. A literature review on human studies. *Scand. J. Food Nutr.* **2001**, *45*, 58–75. [[CrossRef](#)]
9. Celi, P.; Verlhac, V.; Pérez, C.E.; Schmeisser, J.; Klünter, A.-M. Biomarkers of gastrointestinal functionality in animal nutrition and health. *Anim. Feed Sci. Technol.* **2019**, *250*, 9–31. [[CrossRef](#)]
10. Alvarez-Olmos, M.I.; Oberhelman, R.A. Probiotic agents and infectious diseases: A modern perspective on a traditional therapy. *Clin. Infect. Dis.* **2001**, *32*, 1567–1576. [[CrossRef](#)]
11. Kim, D.H.; Austin, B. Cytokine expression in leucocytes and gut cells of rainbow trout, *Oncorhynchus mykiss* Walbaum, induced by probiotics. *Vet. Immunol. Immunopathol.* **2006**, *114*, 297–304. [[CrossRef](#)]
12. Merrifield, D.L.; Burnard, D.; Bradley, G.; Davies, S.J.; Baker, R.T.M. Microbial community diversity associated with the intestinal mucosa of farmed rainbow trout (*Oncorhynchus mykiss*). *Aquac. Res.* **2009**, *40*, 1064–1072. [[CrossRef](#)]
13. Wache, Y.; Auffray, F.; Gatesoupe, F.J.; Zambonino, J.; Gayet, V.; Labbe, L.; Quentelc, C. Cross effects of the strain of dietary *Saccharomyces cerevisiae* and rearing conditions on the onset of intestinal microbiota and digestive enzymes in rainbow trout, *Oncorhynchus mykiss*, fry. *Aquaculture* **2006**, *258*, 470–478. [[CrossRef](#)]
14. Kim, D.H.; Austin, B. Characterization of probiotic carnobacteria isolated from rainbow trout (*Oncorhynchus mykiss*) intestine. *Lett. Appl. Microbiol.* **2008**, *47*, 141–147. [[CrossRef](#)] [[PubMed](#)]
15. Servin, A.L.; Coconnier, M.H. Adhesion of probiotic strains to the intestinal mucosa and interaction with pathogens. *Best Pract. Res. Clin. Gastroenterol.* **2003**, *17*, 741–754. [[CrossRef](#)]
16. Timmerman, H.M.; Koning, C.J.M.; Mulder, L.; Rombouts, F.M.; Beynen, A.C. Monostrain, multistrain and multispecies probiotics. A comparison of functionality and efficacy. *Int. J. Food Microbiol.* **2004**, *96*, 219–233. [[CrossRef](#)]
17. Verschuere, L.; Rombaut, G.; Sorgeloos, P.; Verstraete, W. Probiotic bacteria as biological control agents in aquaculture. *Microbiol. Mol. Biol. Rev.* **2000**, *64*, 655–671. [[CrossRef](#)]
18. Alfaro, B.; Hernández, I.; Le Marc, Y.; Pin, C. Modelling the effect of the temperature and carbon dioxide on the growth of spoilage bacteria in packed fish products. *Food Control* **2013**, *29*, 429–437. [[CrossRef](#)]
19. Kim, D.; Kang, K.; Hae Kyung, C.; Jisoon, I.; Kwisung, P. Carnobacterium isolated from caviar of sturgeon (*Acipenser ruthenus*) farmed in Korea. *J. Bacteriol. Virol.* **2015**, *45*, 151–154. [[CrossRef](#)]
20. Leroi, F. Occurrence and role of lactic acid bacteria in seafood products. *Food Microbiol.* **2010**, *27*, 698–709. [[CrossRef](#)]
21. Haniffa, M.A.; Ramakrishnan, C.M.; Sheela, P.J. Effect of probiotics on survival and growth of *Heteropneustes fossilis*. *Int. J. Pharma Res. Health Sci.* **2015**, *3*, 784–793.
22. Ringø, E. The ability of carnobacteria isolated from fish intestine to inhibit growth of fish pathogenic bacteria: A screening study. *Aquac. Res.* **2008**, *39*, 171–180. [[CrossRef](#)]
23. Ringø, E.; Schillinger, U.; Holzapfel, W. Antibacterial abilities of lactic acid bacteria isolated from aquatic animals and the use of lactic acid bacteria in aquaculture. In *Microbial Ecology in Growing Animals*; Holzapfel, W., Naughton, P., Eds.; Elsevier: Edinburgh, UK; London, UK; New York, NY, USA; Oxford, UK; Philadelphia, PA, USA; St Louis, MO, USA; Sydney, Australia; Toronto, ON, Canada, 2005; pp. 418–453.
24. Gatesoupe, F.J. Probiotics and prebiotics for fish culture, at the parting of the ways. *Aqua Feeds Formul. Beyond* **2005**, *2*, 3–5.
25. Tripathi, M.K.; Giri, S.K. Probiotic functional foods: Survival of probiotics during processing and storage. *Food Funct.* **2014**, *9*, 225–241. [[CrossRef](#)]
26. Damusaru, J.H.; Moniruzzaman, M.; Parka, Y.; Seong, M.; Jung, J.-Y.; Kim, D.-J.; Bai, S.C. Evaluation of fish meal analogue as partial fish meal replacement in the diet of growing Japanese eel *Anguilla japonica*. *Anim. Feed Sci. Technol.* **2019**, *247*, 41–52. [[CrossRef](#)]
27. Krogdahl, Å.; Penn, M.; Thorsen, J.; Refstie, S.; Bakke, A.M. Important antinutrients in plant feedstuffs for aquaculture: An update on recent findings regarding responses in salmonids. *Aquac. Res.* **2010**, *41*, 333–344. [[CrossRef](#)]
28. Escudero, N.L.; de Arellano, M.L.; Luco, J.M.; Giménez, M.S.; Mucciarelli, S.I. Comparison of the chemical composition and nutritional value of *Amaranthus cruentus* flour and its protein concentrate. *Plant Food Hum. Nutr.* **2004**, *59*, 15–21. [[CrossRef](#)] [[PubMed](#)]

29. Januszewska-Jóźwiak, K.; Synowiecki, J. Characteristics and suitability of amaranth components in food biotechnology. *Biotechnologia* **2008**, *3*, 89–102. (In Polish)
30. Ratusz, K.; Wirkowska, M. Characterization of seeds and lipids of amaranthus. *Oilseed Crops* **2006**, *26*, 243–250. (In Polish)
31. Smeds, A.I.; Eklund, P.C.; Sjöholm, R.E.; Willfor, S.M.; Nishibe, S.; Deyama, T.; Holmbom, B.R. Quantification of a broad spectrum of lignans in cereals, oilseeds, and nuts. *J. Agric. Food Chem.* **2007**, *55*, 1337–1346. [CrossRef]
32. Gamel, T.H.; Linssen, J.P.; Mesallam, A.S.; Damir, A.A.; Shekib, L.A. Seed treatments affect functional and antinutritional properties of amaranth flours. *J. Sci. Food Agric.* **2006**, *86*, 1095–1102. [CrossRef]
33. Venskutonis, P.R.; Kraujalis, P. Nutritional components of amaranth seed and vegetables: A Review on composition, properties, and uses. *Compr. Rev. Food Sci. Food Saf.* **2013**, *12*, 381–412. [CrossRef]
34. Niewiadomski, P.; Gomulka, P.; Poczyczyński, P.; Woźniak, M.; Szmyt, M. Dietary effect of supplementation with amaranth meal on growth performance and apparent digestibility of rainbow trout *Oncorhynchus mykiss*. *Pol. J. Nat. Sci.* **2016**, *31*, 459–469.
35. Potorski, J.; Niewiadomski, P. The effect of amaranth meal on the quantitative and qualitative composition of microbiota in compound feeds stored at different temperatures. In Proceedings of the Poster Session Presentation at the 9th Polish Hydromicrobiological Conference—Hydromicro 2017, Microorganisms—Achievements and Challenges, Conference Proceedings, Olsztyn, Poland, 17–19 September 2017; p. 52.
36. Vieira, A.D.S.; Bedani, R.; Albuquerque, M.A.C.; Biscola, V.; Saad, S.M.I. The impact of fruit and soybean by-products and amaranth on the growth of probiotic and starter microorganisms. *Food Res. Int.* **2017**, *97*, 356–363. [CrossRef] [PubMed]
37. Ubiebi, C.O. Isolation and identification of bacterial isolates from poultry and fish feeds sold in Abraka, Delta State, Nigeria. *J. Ind. Technol.* **2017**, *2*, 14–20.
38. Zmysłowska, I.; Lewandowska, D. The effect of storage temperature on microbiological quality of fish feeds. *Pol. J. Environ. Stud.* **2000**, *9*, 223–226.
39. Potorski, J.A.; Golaś, I. The effect of *Carnbacterium maltaromaticum* probiotic bacteria on commercial fish feed heterothropic microbiota. *Fisheries Communiques* **2018**, *4*, 1–5. (In Polish)
40. Kocková, M.; Valík, L. Suitability of cereal porridges as substrate for probiotic strain *Lactobacillus rhamnosus* GG. *Potravin. Slovak J. Food Sci.* **2013**, *7*, 22–27. [CrossRef]
41. Liptáková, D.; Matejčková, Z.; Valík, L. Lactic acid bacteria and fermentation of cereals and pseudocereals. In *Fermentation Processes*; Jozala, A.F., Ed.; Intech Publisher: London, UK; Rijeka, Croatia, 2017; pp. 223–254. [CrossRef]
42. Matejčková, Z.; Liptáková, D.; Valík, L. Fermentation of milk- and water-based amaranth mashes. *Acta Chim. Slov.* **2015**, *8*, 140–145. [CrossRef]
43. Gillan, D.C.; Speksnijder, A.; Zwart, G.; De Ridder, C. Genetic diversity of the biofilm covering *Montacuta ferruginosa* (Mollusca, Bivalvia) as evaluated by denaturing gradient gel electrophoresis analysis and cloning of PCR-amplified gene fragments coding for 16S rRN. *Appl. Environ. Microbiol.* **1998**, *64*, 3464–3472. [CrossRef]
44. NCBI. National Center for Biotechnology Information, U.S. National Library of Medicine. Available online: <http://blast.ncbi.nlm.nih.gov/Blast.cgi> (accessed on 10 April 2017).
45. Guidelines for the Evaluation of Probiotics in Food. Food and Agriculture Organization of the United Nations, World Health Organization. In Proceedings of the Report of a Joint FAO/WHO Working Group on Drafting Guidelines for the Evaluation of Probiotics in Food, London, ON, Canada, 30 April–1 May 2002.
46. Chang, C.I.; Liu, W.Y.; Shyu, C.Z. Use of prawn blood agar hemolysis to screen for bacteria pathogenic to cultured tiger prawns *Penaeus monodon*. *Dis. Aquat. Organ.* **2000**, *43*, 153–157. [CrossRef]
47. Succi, M.; Tremonte, P.; Reale, A.; Sorrentino, E.; Grazia, L.; Pacifico, S.; Coppola, R. Bile salt and acid tolerance of *Lactobacillus rhamnosus* strains isolated from Parmigiano Reggiano cheese. *FEMS Microbiol. Lett.* **2005**, *244*, 129–137. [CrossRef] [PubMed]

48. Vijayaram, S.; Robinson, J.P.; Kannan, S. Synthesis of antibacterial and anticancer substances by *Bacillus* sp. PRV3 and *Bacillus* sp. PRV23, an intestinal probiotics of Indian fresh water fish. *Int. J. Pharm. Sci. Rev. Res.* **2017**, *43*, 208–219.
49. Hart, S.D.; Brown, B.J.; Gould, M.L.; Robar, M.L.; Witt, E.M.; Brown, P.B. Predicting the optimal dietary amino acid profile for growth of juvenile yellow perch with whole body amino acid concentrations. *Aquac. Nutr.* **2010**, *16*, 248–253. [CrossRef]
50. NRC. Nutrient Requirements of Fish and Shrimp. National Research Council (US). In *Committee on the Nutrient Requirements of Fish and Shrimp*; The National Academy Press: Washington, DC, USA, 2011.
51. Polish Standard PN-R-64791:1994. Animal Feeds. Microbiological Requirements and Analyses. Available online: <http://www.statsoft.com/Products/STATISTICA/Product-Index> (accessed on 6 January 2019).
52. Crump, J.A.; Griffin, P.M.; Angulo, F.J. Bacterial contamination of animal feed and its relationship to human foodborne illness. *Clin. Infect. Dis.* **2002**, *35*, 859–865. [CrossRef]
53. Zmysłowska, I.; Kolman, R.; Krause, J. Bacteriological evaluation of water, feed and sturgeon (*Acipenser baeri* Brandt) fry quality during intensive rearing in cooling water. *Arch. Pol. Fish.* **2003**, *1*, 91–98.
54. Golaś, I.; Zmysłowska, I.; Harnisz, M.; Teodorowicz, M. The microbiological state of fish feed, water and *Silurus glanis* L. skin of fry during intensive rearing. *Bull. Sea Fish. Inst.* **2004**, *1*, 3–14.
55. Alegbejo, J.O. Nutritional value and utilization of amaranthus (*Amaranthus* sp.)—A review. *BAJOPAS* **2013**, *6*, 136–143. [CrossRef]
56. Amare, G.A.; Unakal, C.G. Effect of aqueous and ethanol extracts of *Ocimum lamifolium* and *Amaranthus dubius* against bacteria isolated from clinical specimen. *IJPIR* **2013**, *3*, 10–14.
57. Peter, K.; Gandhi, P. Rediscovering the therapeutic potential of *Amaranthus* species: A review. *EJBAS* **2017**, *4*, 196–205. [CrossRef]
58. Smeds, A.I.; Willfor, S.M.; Pietarinen, S.P.; Peltonen-Sainio, P.; Reunanen, M.H.T. Occurrence of “mammalian” lignans in plant and water sources. *Planta* **2007**, *226*, 632–646. [CrossRef]
59. Kamela, S.L.A.; Mouokeu, R.S.; Rawson, A.; Maffo Tazoho, G.; Moh, L.G.; Etienne, P.T.; Jules-Roger, K. Influence of processing methods on proximate composition and dieting of two *Amaranthus* species from West Cameroon. *J. Food Sci.* **2016**, *1*–8. [CrossRef]
60. Olufemi, B.E.; Assiak, I.E.; Ayoade, G.O.; Onigemo, M.A. Studies on the effect of *Amaranthus spinosus* leaf extract on the hematology of growing pigs. *Afr. J. Biomed. Res.* **2003**, *6*, 149–150. [CrossRef]
61. Zraly, Z.; Pisarikova, B.; Hudcova, H.; Trckova, M.; Herzig, I. Effect of feeding amaranth on growth efficiency and health of market pigs. *Acta Vet. Brno* **2004**, *73*, 437–444. [CrossRef]
62. Ravindran, V.; Hood, R.L.; Gill, R.J.; Kneale, C.R.; Bryden, W.L. Nutritional evaluation of grain amaranth (*Amaranthus hypochondriacus*) in broiler diets. *Anim. Feed Sci. Technol.* **1996**, *63*, 323–331. [CrossRef]
63. Vaseeharan, B.; Thaya, R. Medicinal plant derivatives as immunostimulants: An alternative to chemotherapeutics and antibiotics in aquaculture. *Aquac. Int.* **2014**, *22*, 1079–1091. [CrossRef]
64. Virk, P.; Saxena, P.K. Potential of *Amaranthus* seeds in supplementary feed and its impact on growth in some carps. *Bioresour. Technol.* **2003**, *86*, 25–27. [CrossRef]
65. Maiyo, Z.C.; Ngure, R.M.; Matasyoh, J.C.; Chepkorir, R. Phytochemical constituents and antimicrobial activity of leaf extracts of three *Amaranthus* plant species. *Afr. J. Biotechnol.* **2010**, *9*, 3178–3182.
66. Carrizo, S.L.; Montes de Oca, C.E.; Hébert, M.E.; Saavedra, L.; Vignolo, G.; LeBlanc, J.G.; Rollán, G.C. Lactic acid bacteria from urope grain amaranth: A Source of vitamins and functional value enzymes. *J. Mol. Microbiol. Biotechnol.* **2017**, *27*, 289–298. [CrossRef]
67. Jekle, M.; Houben, A.; Mitzscherling, M.; Becker, T. Effects of selected lactic acid bacteria on the characteristics of amaranth sourdough. *J. Sci. Food Agric.* **2010**, *90*, 2326–2332. [CrossRef]
68. Sterr, Y.; Weiss, A.; Schmidt, H. Evaluation of lactic acid bacteria for sourdough fermentation of amaranth. *Int. J. Food Microbiol.* **2009**, *136*, 75–82. [CrossRef]
69. Gullón, B.; Gullón, P.; Tavaría, F.K.; Yáñez, R. Assessment of the prebiotic effect of quinoa and amaranth in the human intestinal ecosystem. *Food Funct.* **2016**, *14*, 3782–3788. [CrossRef] [PubMed]
70. Allameh, S.K.; Noaman, V.; Nahavandi, R. Effects of probiotic bacteria on fish performance. *Adv. Tech. Clin. Microbiol.* **2017**, *1*, 11.
71. Lara-Flores, M.; Olvera-Novoa, M.A.; Guzmán-Méndez, B.E.; López- Madrid, W. Use of the bacteria *Streptococcus faecium* and *Lactobacillus acidophilus*, and the yeast *Saccharomyces cerevisiae* as growth promoters in Nile tilapia (*Oreochromis niloticus*). *Aquaculture* **2003**, *216*, 193–201. [CrossRef]

72. Mohapatra, S.; Chakraborty, T.; Prusty, A.K.; Das, P.; Paniprasad, K.; Mohanta, K.N. Use of different microbial probiotics in the diet of rohu, *Labeo rohita* fingerling: Effects on growth, nutrient digestibility and retention, digestive enzyme activities and intestinal microflora. *Aquac. Nutr.* **2012**, *18*, 1–11. [[CrossRef](#)]
73. Ringø, E.; Løvmo, L.; Kristiansen, M.; Bakken, Y.; Salinas, I.R.; Myklebust, R.; Olsen, R.E.; Mayhew, T.M. Lactic acid bacteria vs. pathogens in the gastrointestinal tract of fish. *Aquac. Res.* **2010**, *41*, 451–467. [[CrossRef](#)]



© 2020 by the authors. Licensee MDPI, Basel, Switzerland. This article is an open access article distributed under the terms and conditions of the Creative Commons Attribution (CC BY) license (<http://creativecommons.org/licenses/by/4.0/>).

Effects of Colored Light on Growth and Nutritional Composition of Tilapia, and Biofloc as a Food Source

Daniela Lopez-Betancur ¹, Ivan Moreno ², Carlos Guerrero-Mendez ¹,
Domingo Gómez-Meléndez ¹, Manuel de J. Macías P. ³ and Carlos Olvera-Olvera ^{1,*}

¹ Unidad Académica de Ingeniería Eléctrica, Universidad Autónoma de Zacatecas, Campus Siglo XXI, Zacatecas C.P. 98160, Mexico; danielalopez106@uaz.edu.mx (D.L.-B.); guerrero_mendez@uaz.edu.mx (C.G.-M.); domag5@hotmail.com (D.G.-M.)

² Unidad Académica de Ciencia y Tecnología de la Luz y la Materia, Universidad Autónoma de Zacatecas, Campus Siglo XXI, Zacatecas C.P. 98160, Mexico; imorenoh@uaz.edu.mx

³ Unidad Académica de Ciencias Química, Universidad Autónoma de Zacatecas, Campus Siglo XXI, Zacatecas C.P. 98160, Mexico; mmacias@uaz.edu.mx

* Correspondence: colvera@uaz.edu.mx; Tel.: +52-492-107-0307

Received: 28 November 2019; Accepted: 30 December 2019; Published: 3 January 2020

Abstract: Light stimulation and biofloc technology can be combined to improve the efficiency and sustainability of tilapia production. A 73-day pilot experiment was conducted to investigate the effect of colored light on growth rates and nutritional composition of the Nile tilapia fingerlings (*Oreochromis niloticus*) in biofloc systems. The effect of colored light on the nutritional composition of bioflocs as a food source for fish was measured. Three groups were illuminated in addition to natural sunlight with colored light using RGB light emitting diodes (LEDs) with peak wavelengths (λ) of 627.27 nm for red (R), 513.33 nm for green (G), and 451.67 nm for blue (B) light. LED light intensity was constant (0.832 mW/cm²), and had an 18-h photoperiod of light per day throughout the study. The control group was illuminated only with natural sunlight (natural). Tilapia had an average initial weight of 0.242 g. There was a significant effect of colored light on tilapia growth and composition. The R group showed the best growth rate, highest survival, and highest lipid content. The B group showed homogeneous growth with the lowest growth rate and lipid content, but the highest protein level. On the other hand, the biofloc composition was influenced by the green light in the highest content of lipids, protein, and nitrogen-free extract.

Keywords: food science; light; color; LEDs; sustainable aquaculture; fish production; preliminary results

1. Introduction

Aquaculture is one of the fastest-growing food production areas and it is one of the most important sources of food, nutrition, income, and livelihood for hundreds of millions of people worldwide [1]. By 2030, the production of freshwater species such as carp, catfish, and tilapia is expected to represent about 60% of total aquaculture production [2,3]. However, fish farming requires the use of land, freshwater, and environmental resources, which are increasingly scarce and expensive worldwide. By 2030, the world could have a global water deficit of 40% in the usual commercial scenario, and by 2050, the demand for water is expected to increase by 55% in all sectors of production [4]. Therefore, an increase in aquaculture production must be carefully planned, minimizing the environmental impact and optimizing the use of natural resources.

Today, sustainable aquaculture systems produce more fish without affecting the environment, such as using biofloc technology (BFT). In systems with BFT, there are limited exchanges of water and, thus, there is an accumulation of organic matter and nutrients that promote the development of

a microbial community called a bioflocs [5]. Bioflocs are conglomerates of phytoplankton, bacteria, zooplankton, microbial grazers, and particulate organic matter, which are mainly heterotrophic bacteria. When this conglomerate is mixed with an added external carbon source, the growth of heterotrophic bacteria is stimulated and the absorption of nitrogen occurs through the production of microbial proteins, which serve as a food source for fish that is available 24 h per day [6–9]. Biofloc systems are mainly used to cultivate tilapia (*Oreochromis* sp.) and white shrimp (*Litopenaeus vannamei*) because both species can eat biofloc and live in environments with high levels of turbidity [10]. The biofloc community can also be used to improve water quality by adding carbon sources to the pond [11,12].

The development of new technologies and scientific studies in aquaculture is essential to improve intensive fish production. A promising improvement in aquaculture comes from light emitting diode (LED) lighting. It has been shown that lighting in aquaculture can influence embryonic development, releasing reproductive hormones that increase fish growth [13,14]. However, fish are visual feeders that need a minimum light intensity to eat and, thus, grow and develop [15]. In addition to the influence on embryonic development, the intensity and spectrum light in certain photoperiods (intensity, duration, and periodicity) can be used to alter and control the growth of fish [16–20]. Photoperiods also influence the release of reproductive hormones, which play an important role in fish reproduction and growth [13]. In addition, under short wavelengths such as blue light, melatonin (which is the hormone that is responsible for sleep) decreases in the bass fish, and the lower the melatonin, the longer the fish are awake, and the more they feed [21]. However, banana shrimp (*Penaeus merguensis*) have a faster growth related to the intensity of the lighting, and the higher the light intensity, the less the shrimp feed, but they grow faster, possibly because of better efficiency of food assimilation [22]. For shrimp with BFT, it was observed that when low light intensity was used, shrimp production decreased by 48%, and the density of microalgae, zooplankton, and rotifers also decreased by 60%, 60%, and 90%, respectively [23].

Tilapias are generally diurnal feeders that feed at different time periods during the day [24]. Using fluorescent tube lamps with a photoperiod of 18L:6D and illuminance of 2500 lux, it is possible to produce more Nile tilapia seeds (percentage of spawning synchrony and percentage of the sac and swim-up fry stages) compared to a shorter photoperiod with less illumination (2500 lux/15 h, 2500 lux/12 h, 500 lux/18 h, 500 lux/15 h, and 500 lux/12 h) [14]. The promising new LED light technology, which has not been widely explored in aquaculture, especially in BFT systems, can be a useful light source tool if the light parameters (intensity, color, and periodicity) are analyzed and applied to obtain benefits in the production of Nile tilapia in BFT. The rapid development of LED technology in recent years has exceeded the characteristics of incandescent lamps in luminous efficiency, low heat emission, robustness, environment resistance, non-toxicity, durability, and adjustable light intensity and wavelength, which allows precise control of the light spectrum [25,26]. The aim of this study was to investigate the effect of using colored LED light on tilapia growth, the nutritional composition of the Nile tilapia fingerlings, and the composition of the bioflocs that are used as a food source for fish.

2. Materials and Methods

2.1. Ethics Statement

All work with animals in this research was done in accordance with the “Guidelines for the Use of Fishes in Research” published by the American Society of Ichthyologists and Herpetologists (<https://www.asih.org/sites/default/files/2018-05/asf-guidelines-use-of-fishes-in-research-2013.pdf>) and complied with the Mexican law on experimental animals according to the protocols: NOM-062-ZOO-1999 and NOM-033-SAG/ZOO-2014.

The experimental design and the fish-use protocol were approved within the project “LED lighting to improve the production of tilapia in biofloc systems” by the ethics committee for animal research at the “Autonomous University of Zacatecas” (authorization number: ACS/UAZ/036/2018).

The light intensities used in all the experiments did not exceed values that were observed in natural waters. This study did not include endangered or protected species. All fish were acclimatized for greenhouse conditions for 2 weeks, with the lamps off (the fish only received natural light), before the start of the experiment. The duration of our experiment was 73 days and 489 Nile tilapia fingerlings (*Oreochromis niloticus*) were used. During the planning stage of the experiment, water quality parameters (temperature, dissolved oxygen, and pH) were monitored twice a day to confirm optimal living conditions for tilapia. The average water quality parameters for fishponds were: 28.50 °C for temperature, 6.68 mg/L for dissolved oxygen, 7.9 for pH, 0.08 mg/L for ammonia, and 0.83 mg/L for total ammonia nitrogen. The average ammonia and total ammonia nitrogen values were monitored every 8 days. The fishponds were supplied with a 300 W thermostat heater (Grupo acuario LOMAS, Ciudad de Mexico, CDMX, Mexico) to avoid temperature variations. Aeration was provided by a Sino-Aqua blower (1/2 Hp of power, and 9" membrane diffuser discs). Additionally, 10% of the tank water was exchanged each week. During the progress of this experiment, 105 fish died from natural causes such as acclimatization, and no specific pathologies were observed to determine if the fish should be euthanized. At the end of the experiment 384 fish were sacrificed. We carefully used standardized procedures for fish euthanasia. Since Nile tilapia do not tolerate cold water, they were sacrificed by rapid chilling (hypothermic shock) by keeping the tilapia in ice water at 2 °C for 10 min after the opercular movement stopped. The fish were stored in a freezer until chemical analysis of their nutritional composition (approximately 72 h).

2.2. Laboratory Facilities and Fish Stocking

A 73-day experiment was performed in a greenhouse in the prototypes laboratory at the Autonomous University of Zacatecas, Mexico. Before the experiment started, 489 Nile tilapia (*O. niloticus*) fingerlings were purchased from a commercial hatchery (AQUAMOL S.C. DE R.L., Jamay, Jal., Mexico), and moved to the greenhouse, where they underwent a period of acclimatization. The Nile tilapia fingerlings had an initial average weight of 0.242 ± 0.01 g. They were randomly distributed, with a same density of 0.2 kg/m^3 (approximately 123 fish per tank, and exactly 30 g of biomass per tank), in circular tanks (150-L capacity, 39 cm high \times 70 cm in diameter) under natural light. This is a pilot study because in this experimentation there were no replicated tanks ($n = 1$). All results presented are preliminary results, but significant because each tank contained a large number of fish.

2.3. Experimental Design and Setup

The experiment was designed to study the effect of colored light under real light conditions. The experiment could also be transferred to real production because real conditions were present in the experiments, such as all four treatments received natural light, which is consistent with aquaculture farms.

This investigation implemented a special change, in addition to receiving natural light, three treatments were illuminated with red, green, and blue LED lamps for 18 h per day. The illumination was provided by RGB (red, green, and blue monochromatic light) LED lamps with peak wavelengths (λ) of $\lambda = 627.27$ nm for the red light treatment (R), $\lambda = 513.33$ nm for the green light treatment (G), and $\lambda = 451.67$ nm for the blue light treatment (B). LED lamps were positioned 25 cm above the water surface, with the purpose that the lamp opening angle (110°) should focus completely on the water surface of the entire tank diameter. LED light intensity of all the lamps was constant at 0.832 mW/cm^2 , and the natural light provided by the sunlight inside the greenhouse had a maximum of irradiance of 0.95 mW/cm^2 at 14:00 h. The fourth treatment, which we called "Natural" light treatment, only received natural light, and served as a control treatment. The lighting conditions for the four treatments are shown in Figure 1.

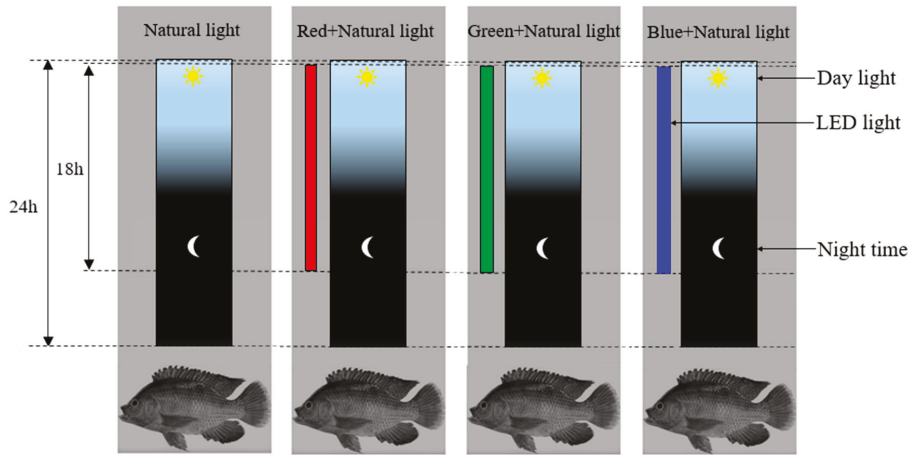


Figure 1. Light periods received by each tank during this research. All treatments received natural light, but three of the treatments were also illuminated with red, green, and blue colored light, which was provided by an LED lamp, with a photoperiod of 18 h per day.

2.4. Characterization of LED Lamps

The LED lamps used in this experiment were optically characterized using a spectrophotometer (USB2000, Ocean Optics, Largo, FL, USA) and a NIST calibrated radiometer (ILT-1400, International Light Technologies Inc., Peabody, MA, USA). Wavelength (λ) and spectral width ($\Delta\lambda$) parameters were measured using the spectrophotometer device. The irradiance or radiant power density on the water surface of each tank was measured using the radiometer. The measured LED lamp parameters are presented in Table 1, where the average irradiance was 0.832 mW/cm². Figure 2 also shows the spectral power distribution of light emitted by each colored LED lamp.

Table 1. Optical properties of light colors in light emitting diode (LED) lamps: red (R), green (G), and blue (B).

Parameters	LED Lamps		
	R	G	B
λ (nm)	627.27	513.33	451.67
$\Delta\lambda$ (nm)	16.92	32.80	23.75
Irradiance (mW/cm ²)	0.87	0.83	0.80

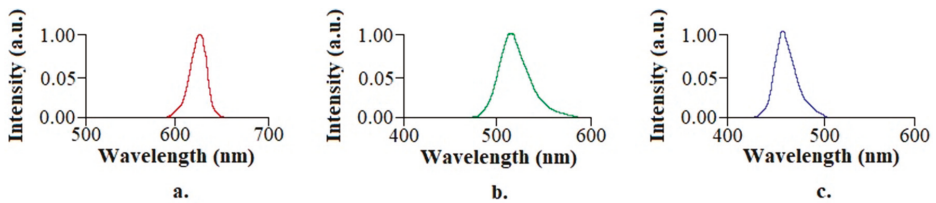


Figure 2. The spectral power distribution of the RGB LED lamps used in the study: (a) R LED lamp; (b) G LED lamp; and (c) B LED lamp.

2.5. Nile Tilapia Fingerlings and the Biofloc System

All treatment groups began the study with tap water, which was previously aerated for 1 week to allow water dechlorination. No water exchange was made, and the formation of the biofloc started from zero when the tilapia arrived. Each tank was fixed at 29 °C using a 300 W thermostat heater to avoid high temperature variations, and to provide a comfortable temperature for the fish. Pure cane sugar was added to each tank as a carbon source, which was calculated using the method described by De Schryver et al. [27]. The use of a carbon-to-nitrogen (C/N) ratio of 20:1 in the tanks ensures the water quality during the biofloc formation because we guarantee a low level of total ammonia nitrogen (TAN) in the water [28,29]. The fish were fed by hand twice a day using the commercial diet I during the first month, and then using the commercial diet II, according to the requirements of the growth stage. The nutritional composition of the commercial diet I, commercial diet II, and cane sugar used are listed in Table 2. The daily amount of food was adjusted every week (the feeding rate started with 10% of the fish's weight per day and it decreased to 5% per day) according to the growth of the fish, fish survival, and the biofloc that was expected in each tank. The fish feed composition was provided by the manufacturer and was also corroborated based on a bromatology test to guarantee the consumption and quality of the feed. During the experimental period, the tanks were checked by hand every day, and any dead fish were removed and recorded.

Table 2. Feed composition for tilapia and cane sugar used as a carbon source.

	Feed					
	Commercial Diet I (Manufacturer)	Commercial Diet I (Laboratory)	Commercial Diet II (Manufacturer)	Commercial Diet II (Laboratory)	Cane Sugar (Manufacturer)	Cane Sugar (Laboratory)
Moisture (%)	12.00	7.90	12.00	8.10	0.00	1.80
Crude protein (%)	53.00	43.00	32.00	40.90	0.00	0.30
Lipids (%)	15.00	12.30	6.00	12.80	0.00	0.00
Crude fiber (%)	2.50	1.70	6.00	2.20	0.00	3.30
Ash (%)	12.00	7.80	15.00	10.00	0.00	0.10
Nitrogen-free extract (%)	5.50	27.30	29.00	26.00	100.00	94.50

2.6. Water Quality Parameters

Temperature, dissolved oxygen (measured by the YSI model 550A dissolved oxygen meter device (Yellow Springs Instrument Co., Yellow Springs, OH, USA)), and pH (measured by the Hanna model HI 98127 device (Hanna Instruments, Woonsocket, RI, USA)) were measured twice a day in each tank at 10:00 and 20:00 h. Ammonia–nitrogen ($NH_3 - N$), which is one form of ammonia in TAN that is toxic for fish, was regulated by adding cane sugar. $NH_3 - N$ levels were measured once per week in the tanks using the ammonia checker device (Hanna model HI715 (Hanna Instruments, Woonsocket, RI, USA)). In addition, the TAN value was calculated using a modified mathematical expression described by Boyd and Tucker [30], which is written as follows:

$$TAN = (NH_3 - N) \times \{1 + \text{antilog} [0.09018 + (2729.92 / (273.15 + T))] - pH\}, \quad (1)$$

where TAN is the total ammonia nitrogen, ($NH_3 - N$) is the ammonia–nitrogen, T is the water temperature (°C), and pH is the water pH.

2.7. Growth Rates

Throughout the experiment, biometric measurements were made every week in a group of randomly selected of 15 fish in each tank. At the end of the experiment, all the fish were weighed and measured, and the growth rates were reported as the mean \pm standard deviation. According to the final number of fish in each treatment, there were 127 fish that underwent R treatment, 79 fish that underwent G treatment, 94 fish that underwent B treatment, and 84 fish that underwent the Natural treatment. The mean \pm standard deviation is presented for the fish weight and length. Additional

measurements to evaluate fish growth were used, as follows: initial weight (g/fish), final weight (g/fish), final body length (cm/fish), survival (%), specific growth rate (SGR), daily weight gain (DWG), and feed conversion rate (FCR). The mathematical expressions of the evaluation metrics were extracted from published studies [31,32]. These evaluation metrics are written as follows:

$$\text{Initial weight (g)} = (\text{initial biomass (g)})/(\text{initial number of fish}), \quad (2)$$

$$\text{Final weight (g)} = (\text{final biomass (g)})/(\text{final number of fish}), \quad (3)$$

$$\text{Final body length (cm)} = \frac{\sum_{i=0}^{\text{Final number of fish}} \text{fish body length (i)}}{\text{final number of fish}}, \quad (4)$$

$$\text{Survival (\%)} = (\text{final number of fish})/(\text{initial number of fish}) \times 100\%, \quad (5)$$

$$\text{SGR (\%/day)} = \frac{\ln(\text{final weight (g)}) - \ln(\text{initial weight (g)})}{\text{number of days}} \times 100\%, \quad (6)$$

$$\text{DWG (g/day)} = (\text{final weight (g)} - \text{initial weight (g)})/(\text{number of days}), \quad (7)$$

$$\text{FCR} = (\text{total feed intake (g)})/(\text{total wet weight gain (g)}), \quad (8)$$

where the initial biomass is the weight of all the fish in each tank at the beginning of the experiment, and the final biomass is the weight of all the fish at the end of the experiment. The total feed intake is the amount of food supplied to the fish, and the total wet weight gain is the difference between the final weight and the initial weight of the entire biomass.

2.8. Nutritional Composition of the Fish Body and Bioflocs

Composition of the fish body is valuable information about the nutritional contribution that the fish meat will have for a consumer. A biofloc nutritional composition study also provided information on whether the diet of the fish could be completed correctly using the biofloc. At the end of the experiment, all the fish were caught for a biomass analysis. The water in the tanks was sieved using a 200-mesh screen to maintain the greatest amount of biofloc. The composition of the fish body and the bioflocs were determined by the composition of lipids, moisture, crude protein, crude fiber, ash, and nitrogen-free extract, according to standard methods [33,34]. The values were determined using Soxhlet extraction apparatus while the other parameters were determined with bromatology using gravimetric techniques. The nutritional composition analysis was performed by the Chemical Laboratory of Special Studies at the Autonomous University of Zacatecas.

2.9. Statistical Analysis

All the measured data and the metrics that were calculated in this research were analyzed to achieve a performance evaluation and a broad comparison between the four light treatments. Since the parameters obtained from the tanks are mean values, a one-way analysis of variance (ANOVA), which compares the “variation” of a group of mean values, was used.

Water quality parameters cannot be analyzed using ANOVA because there are no replicate tanks ($n = 1$). However, growth rates can be analyzed because each tank had many final fish as follows: $n = 127$ for R treatment, $n = 79$ for G treatment, $n = 94$ for B treatment, and $n = 84$ for Natural treatment. Thus, the growth rates were analyzed using the one-way ANOVA, followed by Tukey’s test, with a significance level of 5%. Before performing the one-way ANOVA evaluation, the hypothesis of equality (homogeneity) of variances was verified using the Levene’s test. Data analysis of the biofloc and fish nutritional composition was performed using the mean values of three sample replicates.

3. Results

3.1. Water Quality Parameters

The average values of the water parameters remained approximately equal between all groups during the experimental period. Thus, a constant temperature was maintained, with a variation of less than 1 °C, the pH value showed a difference below 1.25%, the variation of ammonia–nitrogen (NH_3-N) was less than 0.03 mg/L, and the difference in dissolved oxygen and TAN were less than 0.07 and 0.17 mg/L, respectively. The mean values of water quality parameters were calculated, and they are shown in Table 3.

Table 3. Water quality parameters.

Parameters	Treatments			
	R	G	B	Natural
Temperature (°C)	28.03 ± 1.03	28.38 ± 0.96	28.94 ± 1.22	28.65 ± 0.93
Dissolved Oxygen (mg/L)	6.65 ± 0.58	6.67 ± 0.43	6.71 ± 0.47	6.72 ± 0.47
pH	7.91 ± 0.17	7.91 ± 0.16	7.92 ± 0.16	8.01 ± 0.20
NH_3-N (mg/L)	0.07 ± 0.01	0.07 ± 0.01	0.08 ± 0.01	0.10 ± 0.01
TAN (mg/L)	0.79 ± 0.18	0.76 ± 0.21	0.86 ± 0.14	0.93 ± 0.22

Data are presented as the mean ± standard deviation.

3.2. Growth Rates

Mean weight, mean body length, survival, specific growth rate, and feed conversion ratio were used as metrics to evaluate the effect of colored light. According to the measured data, the R group showed the highest final weight among the fish, and it also had the lowest initial weight. Therefore, the R group had the highest performance, with the best growth rates and DWG (see Table 4). In addition, the data obtained show that the R and G groups presented the best gains in weight and length. However, the G group had the worst survival. The feed conversion ratio was better in the R and Natural groups compared with the other groups. The SGR value was significantly higher in the groups R and G compared with the other groups. The quantitative distribution of the final weight of the fish for each group is shown in Figure 3.

Table 4. Growth rates of Nile tilapia.

Parameters	Treatments			
	R	G	B	Natural
Initial biomass (g)	30	30	30	30
Initial weight (g/fish)	0.2	0.2	0.3	0.3
Initial number of fish	133	132	111	113
Final Biomass (g)	2193	1330	1461	1362
Total biomass gained (g)	2163	1300	1431	1332
Final number of fish	127	79	94	84
Final individual weight (g/fish)	17.3 ± 3.3 ^a	16.8 ± 3.1 ^a	15.5 ± 2.8 ^b	16.2 ± 3.0 ^{ab}
Final individual body length (cm/fish)	8.2 ± 1.0 ^a	8.0 ± 0.9 ^a	7.7 ± 0.9 ^b	7.9 ± 0.8 ^{ab}
Survival (%)	95.5	59.9	84.7	74.3
SGR (%/day)	6.0	5.9	5.6	5.7
DWG (g/day)	0.2	0.2	0.2	0.2
FCR	0.8	1.3	1.2	1.0

SGR = specific growth rate; DWR = daily weight gain; FCR = feed conversion rate. Data are presented as the mean ± standard deviation. Values in the same row with different superscript letters indicate significant differences based on the one-way ANOVA and Tukey's test ($p < 0.05$).

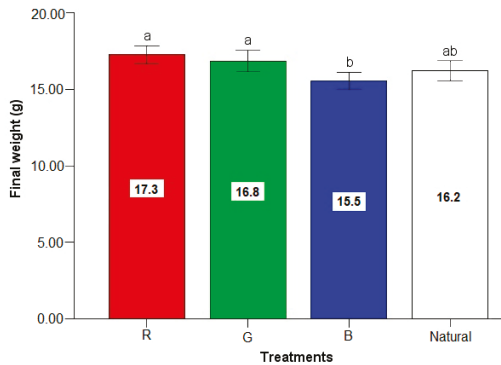


Figure 3. The mean final weight of the fish in each treatment. Each bar represents the mean with the standard deviation. Different letters (such as a, b, and ab) represent significant differences ($p < 0.05$).

3.3. Nutritional Composition of the Fish Body and Bioflocs

The mean values for nutritional composition of the fish and the nutritional composition of the bioflocs as a food source for fish are presented in Figures 4 and 5, respectively. The moisture value was higher in the body of the fish of group B. In addition, the body of the fish in groups B and Natural presented a higher concentration of crude protein compared to the other treatments. The mineral content (ash) in the fish in groups R, G, and Natural was less than that measured in the fish in group B. Lipids in the body composition of the fish were most influenced by the use of colored lights. Fish in group R showed a higher lipid content and nitrogen-free extract.

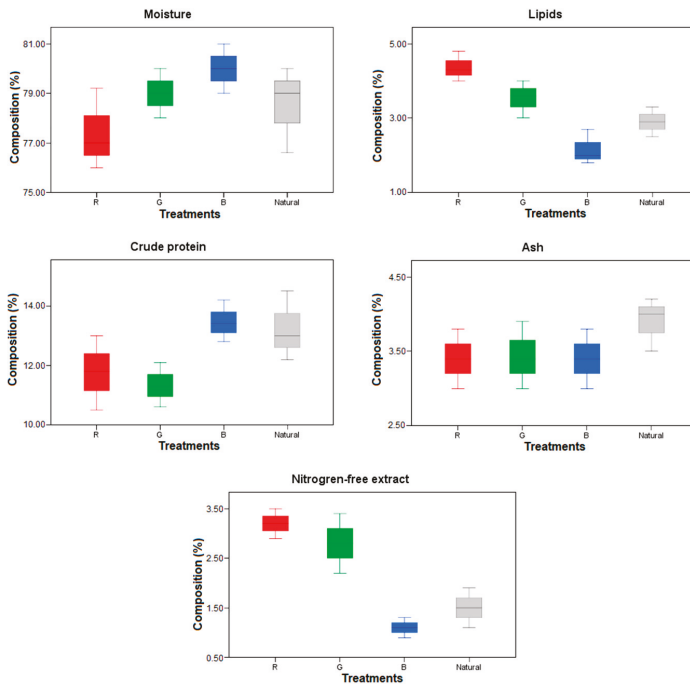


Figure 4. Box-and-whisker plots showing the nutritional composition of the fish (%).

Measurements of the mean nutritional composition of the bioflocs in the G and Natural groups showed a higher concentration of crude protein compared to the other treatments. The ash composition in the bioflocs from the R and G groups was lower than the content measured in the bioflocs from the B and Natural groups. In addition, the mean nutritional composition of the biofloc in group G showed a higher content of lipids and nitrogen-free extract.

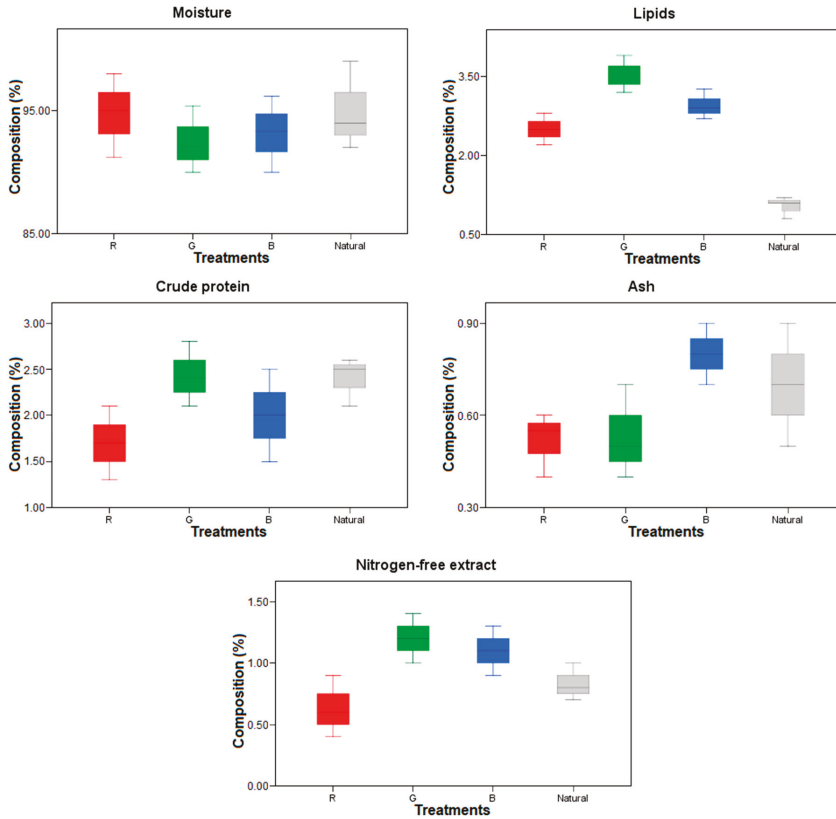


Figure 5. Box-and-whisker plots showing the nutritional composition of the biofloc (%).

4. Discussion

To investigate the effect of colored light in the Nile tilapia fingerlings, the parameters that were not related to the light color were kept constant, but there were slight experimental variations in these parameters that are expected not to significantly change this condition of the research. The mean water temperature was maintained at less than 1 °C of variation, and all the tank water temperatures were in accordance with the optimum range for the growth of the Nile tilapia fingerlings (26–30 °C), as indicated in [35]. The mean water temperature in the four treatments was 28.50 °C, which is very close to the ideal temperature of 28 °C, as reported in [36]. The dissolved oxygen value did not have a very significant variation between all the groups and it was above the level that was acceptable for Nile tilapia (4–5 mg/L), in accordance with [37]. The pH fluctuated between 7 and 8 during the experimental stage, which is the most appropriate range in tilapia aquaculture to obtain the optimum growth and survival rate, as recommended by [38]. The pH value was not different between the R, G, and B groups, which could be because of a greater total amount of bacterial activity that is influenced by the use of artificial light compared to the Natural group. Using a C/N ratio of 20, the TAN concentration has a

similar behavior value to pH and it was maintained at levels that are suitable for Nile tilapia, according to [39]. The $NH_3 - N$ values did not exceed the levels that were considered lethal for Nile tilapia during the experiment, and this value remained below the recommended limit of 0.1 mg/L [40].

Light color was the only intentionally different parameter among all treatments. Therefore, each treatment was only influenced by a certain color or wavelength of the light. There are not many studies reported of the influence of colored light on the growth of Nile tilapia and fish of different species in general [18], and as far as we know, this is the first study on the fingerling stage of development of tilapia. Even more, all previous studies on light effect use other experimental conditions, which include significant differences in: The lack of biofloc, the type or duration of photoperiod, the temperature, the light intensity, peak wavelengths, light spectrum shapes, etc.

In this research, we studied the effect of colored light in Nile tilapia fingerlings and bioflocs, the R light treatment was the aquaculture system that showed superior performance in many aspects. All the groups received the amount of food according to the biomass that was present in each tank.

It is possible to ensure that the R treatment presented the best growth performance because it obtained the best values of total biomass gained, SGR, and DWG. Additionally, there was a great demand for feed intake; when food was provided it was consumed immediately, which was confirmed because the R treatment had the best FCR of 0.8. This is consistent with [41], where feeding conduct was analyzed, but in juvenile Nile tilapia under other experimental conditions, showing (in terms of time (seconds), and chemical cues) that feeding motivation was higher in their red light environment. As well, a similar behavior was found in adult rainbow trout [42], where the growth of fish was increased at red illumination under other experimental conditions, showing low cortisol levels in their blood (less stressful environments).

Nevertheless, the G light environment showed the second-best weight gain, but also had the lowest survival. It is possible to rule out that the low survival was caused by a peak of ammonia and TAN, because during the period in which these fish deaths occurred, measurements of ammonia and TAN were in the optimal range for the life of tilapia. A similar low survival phenomenon using green light was also observed and reported in [43], but in small fish groups (four fish per tank) of adult tilapia under fluorescent lights and other experimental conditions. One possible reason to this phenomenon could be that an aggressive behavior of the fish was observed in a green light environment. Other related study determined (by blood test) the basal plasma cortisol levels (stress response) in adult Nile tilapia, and it was found that cortisol levels increased with green light [44]. This could be a cause of fish mortality because the green light may create stressful environment and increase cortisol levels. A high level of cortisol also affects the nutritional composition of tilapia, causing high moisture levels and low protein levels [45], which agree with our results. The low level of protein can be attributed to an intensive use of muscle protein to get higher energy than that obtained from food, which could be caused by the stress due to green light [46]. Green light may be an important factor of mortality, but research with replicate tanks should be carried out to see all possible mortality factors.

Aly et al. [45] reported that hybrid red tilapia in saline water had a lower growth performance under blue light and other experimental conditions. These results were attributed to a reduced vision of the fish under green light, which reduced feeding (also see [47]). In addition, they reported that hybrid red tilapia that were illuminated under red light had the best growth performance [45]. These observations are in agreement with our results, where the Nile tilapia fingerlings in freshwater under blue light had the lowest growth performance, and those under red light had the best growth performance. In addition, in [43], yellow light was shown to have the best growth performance, which also agrees with our results, because the yellow light has a long wavelength that is close to the wavelength of the red light.

In our research, the effect of colored light on the nutritional composition of Nile tilapia fingerlings, and on the biofloc composition as a food source for tilapia was also measured, and this has not been reported before. The effect of light on body composition of tilapia showed that the R group had the highest lipid content and also the lowest moisture level (this indicates that moisture and lipid content

are inversely related, which is in accordance with [48]). However, under blue light, the fish had the highest percentage of protein and moisture and the lowest level of lipids, while under green light, the fish maintained a low content of lipids and proteins. Under natural light, the fish obtained a high crude protein content and the highest content of ash.

The effect of light color on bioflocs showed that the G group had the highest lipid content. In addition, the bioflocs in the G and Natural groups had the highest protein level. For the ash content, B and Natural groups had the highest percentage. In addition, although the biofloc of B group had a high level of lipids, the fish nutritional composition under B light had a low level of lipids. This opposite relationship could be explained by the stress reduction under blue light [44], and also a stress reduction under the lipid-rich diet [49]. Such a possible stress reduction, would reduce the formation of lipid deposits in fish, indicating that such good health condition of tilapia under B light could be because the lack of stress.

The results discussed above may have an important application in tilapia aquaculture with biofloc systems because they improve our understanding of the significant effect that light color has on the growth of fish and their nutritional composition of both the fish body and the bioflocs.

5. Conclusions

We investigated the influence of RGB colored light on the growth and nutritional composition in tilapia in biofloc systems. We also measured the light effect on the biofloc nutritional composition. The results showed that the peak wavelength or color of light had a significant effect on growth performance and nutritional composition of Nile tilapia, which can be used to improve the sustainability and efficiency of tilapia production based on the needs of the consumer. Fish under blue light had the lowest growth performance, but blue light significantly improved the protein levels, had a low lipid level, and obtained the most homogeneous growth among the treatments. The effect of the red light on fish growth was significant. Tilapia under red light showed the best weight gain, body length, and survival rate, and also showed the highest lipid content. The fish also had a lower ash content under colored light compared to natural light. In addition, colored light influenced the lipid, protein, and ash content in bioflocs.

These results provide support for further studies in aquaculture to improve efficient, sustainable, and intensive fish production. For example, our results suggest that growth rates, feed utilization efficiency, survival, and nutritional body composition may be controlled using colored light, which can significantly modify the nutritional quality provided by Nile tilapia and bioflocs. In addition, future research may include the effect of different intensity levels, photoperiods, and light spectra. For example a broad light spectrum with a designed special shape [50], resulting from the combination of LEDs of different colors and intensities, to obtain the best effects of each light wavelength and maximize the nutritional quality of tilapia and bioflocs. This can be adjusted based on the needs of the consumer and, in the future, the scarcity of food resources.

Author Contributions: Conceptualization, D.L.-B., C.O.-O. and I.M.; Methodology, D.L.-B. and C.G.-M.; Validation, C.O.-O. and I.M.; Formal analysis, D.L.-B., and C.G.-M.; Investigation, D.L.-B. and C.G.-M.; Resources, C.O.-O., D.G.-M. and M.d.J.M.P.; Data curation, D.L.-B. and M.d.J.M.P.; Writing—original draft preparation, D.L.-B.; Writing—review and editing, I.M., and D.L.-B.; Visualization, C.G.-M. and D.G.-M.; Supervision, C.O.-O. and I.M.; Project administration, I.M., C.O.-O. and M.d.J.M.P. All authors have read and agreed to the published version of the manuscript.

Funding: This research received no external funding.

Acknowledgments: This research was supported by CONACYT (Mexican Council for Science and Technology) through financing scholarship granted to Daniela Lopez-Betancur.

Conflicts of Interest: The authors declare no conflict of interest.

References

1. Belton, B.; Bush, S.R.; Little, D.C. Not just for the wealthy: Rethinking farmed fish consumption in the Global South. *Glob. Food Secur.* **2017**, *16*, 85–92. [[CrossRef](#)]
2. FAO. Contributing to food security and nutrition for all. In *The State of World Fisheries and Aquaculture, 2016*; FAO: Rome, Italy, 2016; p. 172.
3. Pauly, D.; Zeller, D. Comments on FAOs state of world fisheries and aquaculture (SOFIA 2016). *Mar. Policy* **2017**, *77*, 176–181. [[CrossRef](#)]
4. WWAP. *The United Nations World Water Development Report 2015: Water for a Sustainable World*; UNESCO: Paris, France, 2015.
5. Arias-Moscoso, J.L.; Espinoza-Barrón, L.G.; Miranda-Baeza, A.; Rivas-Vega, M.E.; Nieves-Soto, M. Effect of commercial probiotics addition in a biofloc shrimp farm during the nursery phase in zero water exchange. *Aquac. Rep.* **2018**, *11*, 47–52. [[CrossRef](#)]
6. Avnimelech, Y. Feeding with microbial flocs by tilapia in minimal discharge bio-flocs technology ponds. *Aquaculture* **2007**, *264*, 140–147. [[CrossRef](#)]
7. Avnimelech, Y.; Verdegem, M.; Kurup, M.; Keshavanath, P. Sustainable land-based aquaculture: Rational utilization of water, land and feed resources. *Mediterr. Aquac. J.* **2008**, *1*, 45–55. [[CrossRef](#)]
8. Azim, M.E.; Little, D.C. The biofloc technology (BFT) in indoor tanks: Water quality, biofloc composition, and growth and welfare of Nile tilapia (*Oreochromis niloticus*). *Aquaculture* **2008**, *283*, 29–35. [[CrossRef](#)]
9. Emerenciano, M.; Ballester, E.L.; Cavalli, R.O.; Wasielesky, W. Biofloc technology application as a food source in a limited water exchange nursery system for pink shrimp *Farfantepenaeus brasiliensis* (Latreille, 1817). *Aquac. Res.* **2012**, *43*, 447–457. [[CrossRef](#)]
10. Green, B.W.; Rawles, S.D.; Webster, C.D.; McEntire, M.E. Effect of Stocking Rate on Growing Juvenile Sunshine Bass, Morone chrysops x M. saxatilis, in an Outdoor Biofloc Production System. *J. World Aquac. Soc.* **2018**, *49*, 827–836. [[CrossRef](#)]
11. Avnimelech, Y. Biofloc technology. In *A Practical Guide Book*; The World Aquaculture Society: Baton Rouge, LA, USA, 2009; p. 182.
12. Crab, R.; Defoirdt, T.; Bossier, P.; Verstraete, W. Biofloc technology in aquaculture: Beneficial effects and future challenges. *Aquaculture* **2012**, *356*, 351–356. [[CrossRef](#)]
13. Boeuf, G.; Le Bail, P.Y. Does light have an influence on fish growth? *Aquaculture* **1999**, *177*, 129–152. [[CrossRef](#)]
14. Ridha, M.; Cruz, E. Effect of light intensity and photoperiod on Nile tilapia *Oreochromis niloticus* L. seed production. *Aquac. Res.* **2000**, *31*, 609–617. [[CrossRef](#)]
15. Moyle, P.B.; Cech, J.J. *Fishes: An Introduction to Ichthyology*; Pearson Prentice Hall: Upper Saddle River, NJ, USA, 2004.
16. Heydarnejad, M.S.; Parto, M.; Pilevarian, A.A. Influence of light colours on growth and stress response of rainbow trout (*Oncorhynchus mykiss*) under laboratory conditions. *J. Anim. Physiol. Anim. Nutr.* **2013**, *97*, 67–71. [[CrossRef](#)] [[PubMed](#)]
17. Karakatsouli, N.; Papoutsoglou, E.S.; Sotiropoulos, N.; Mourtikas, D.; Stigen-Martinsen, T.; Papoutsoglou, S.E. Effects of light spectrum, rearing density and light intensity on growth performance of scaled and mirror common carp *Cyprinus carpio* reared under recirculating system conditions. *Aquac. Eng.* **2010**, *42*, 121–127. [[CrossRef](#)]
18. Ruchin, A.B. Environmental colour impact on the life of lower aquatic vertebrates: Development, growth, physiological and biochemical processes. *Rev. Aquac.* **2018**, 1–18. [[CrossRef](#)]
19. Ruchin, A.B. Influence of Colored Light on Growth rate of Juveniles of Fish. *Fish Physiol. Biochem.* **2004**, *30*, 175–178. [[CrossRef](#)]
20. Karakatsouli, N.; Papoutsoglou, S.E.; Pizzonia, G.; Tsatsos, G.; Tsopelakos, A.; Chadio, S.; Kalogiannis, D.; Dalla, C.; Polissidis, A.; Papadopolou-Daifoti, Z. Effects of light spectrum on growth and physiological status of gilthead seabream *Sparus aurata* and rainbow trout *Oncorhynchus mykiss* reared under recirculating system conditions. *Aquac. Eng.* **2007**, *36*, 302–309. [[CrossRef](#)]
21. Bayarri, M.; Madrid, J.; Sánchez-Vázquez, F. Influence of light intensity, spectrum and orientation on sea bass plasma and ocular melatonin. *J. Opineal Res.* **2002**, *32*, 34–40. [[CrossRef](#)]

22. Hoang, T.; Barchiesi, M.; Lee, S.Y.; Keenan, C.P.; Marsden, G.E. Influences of light intensity and photoperiod on moulting and growth of *Penaeus merguensis* cultured under laboratory conditions. *Aquaculture* **2003**, *216*, 343–354. [[CrossRef](#)]
23. Neal, R.S.; Coyle, S.D.; Tidwell, J.H.; Boudreau, B.M. Evaluation of stocking density and light level on the growth and survival of the Pacific white shrimp, *Litopenaeus vannamei*, reared in zero-exchange systems. *J. World Aquac. Soc.* **2010**, *41*, 533–544. [[CrossRef](#)]
24. Njiru, M.; Okeyo-Owuor, J.; Muchiri, M.; Cowx, I. Shifts in the food of Nile tilapia, *Oreochromis niloticus* (L.) in Lake Victoria, Kenya. *Afr. J. Ecol.* **2004**, *42*, 163–170. [[CrossRef](#)]
25. Moreno, I.; Contreras, U. Color distribution from multicolor LED arrays. *Opt. Express* **2007**, *15*, 3607–3618. [[CrossRef](#)] [[PubMed](#)]
26. Moreno, I.; Sun, C.C. Modeling the radiation pattern of LEDs. *Opt. Express* **2008**, *16*, 1808–1819. [[CrossRef](#)] [[PubMed](#)]
27. De Schryver, P.; Crab, R.; Defoirdt, T.; Boon, N.; Verstraete, W. The basics of bio-flocs technology: The added value for aquaculture. *Aquaculture* **2008**, *277*, 125–137. [[CrossRef](#)]
28. Crab, R.; Kochva, M.; Verstraete, W.; Avnimelech, Y. Bio-flocs technology application in over-wintering of tilapia. *Aquac. Eng.* **2009**, *40*, 105–112. [[CrossRef](#)]
29. Poli, M.A.; Legarda, E.C.; de Lorenzo, M.A.; Martins, M.A.; do Nascimento Vieira, F. Pacific white shrimp and Nile tilapia integrated in a biofloc system under different fish-stocking densities. *Aquaculture* **2019**, *498*, 83–89. [[CrossRef](#)]
30. Boyd, C.E.; Tucker, C.S. *Pond Aquaculture Water Quality Management*; Springer Science and Business Media: Medford, MA, USA, 2012; ISBN 978-1-4615-5407-3.
31. Mansour, A.T.; Esteban, M.Á. Effects of carbon sources and plant protein levels in a biofloc system on growth performance, and the immune and antioxidant status of Nile tilapia (*Oreochromis niloticus*). *Fish Shellfish. Immunol.* **2017**, *64*, 202–209. [[CrossRef](#)]
32. Nhi, N.H.Y.; Da, C.T.; Lundh, T.; Lan, T.T.; Kiessling, A. Comparative evaluation of Brewer’s yeast as a replacement for fishmeal in diets for tilapia (*Oreochromis niloticus*), reared in clear water or biofloc environments. *Aquaculture* **2018**, *495*, 654–660. [[CrossRef](#)]
33. AOAC. *Official Methods of Analysis of AOAC International*, 18th ed.; AOAC International: Gaithersburg, MD, USA, 2005.
34. *NMX Water Analysis-Measurement of Extractables Fats and Oils in Natural Waters, Wastewaters and Treated Wastewaters*; Diario Oficial de la Federacion de la Secretaria de Economia del Gobierno de Mexico: Ciudad de Mexico, CDMX, Mexico, 2013.
35. Azaza, M.; Dhraief, M.; Kraiem, M. Effects of water temperature on growth and sex ratio of juvenile Nile tilapia *Oreochromis niloticus* (Linnaeus) reared in geothermal waters in southern Tunisia. *J. Therm. Biol.* **2008**, *33*, 98–105. [[CrossRef](#)]
36. El-Sayed, A.F.M.; Kawanna, M. Optimum water temperature boosts the growth performance of Nile tilapia (*Oreochromis niloticus*) fry reared in a recycling system. *Aquac. Res.* **2008**, *39*, 670–672. [[CrossRef](#)]
37. Evans, J.J.; Shoemaker, C.A.; Klesius, P.H. Effects of sublethal dissolved oxygen stress on blood glucose and susceptibility to *Streptococcus agalactiae* in Nile tilapia *Oreochromis niloticus*. *J. Aquat. Anim. Health* **2003**, *15*, 202–208. [[CrossRef](#)]
38. El-Sherif, M.S.; El-Feky, A.M.I. Performance of Nile tilapia (*Oreochromis niloticus*) fingerlings. I. Effect of pH. *Int. J. Agric. Biol.* **2009**, *11*, 297–300.
39. Zeitoun, M.M.; EL-Azrak, K.E.D.M.; Zaki, M.A.; Nemat-Allah, B.R.; Mehana, E.S.E. Effects of ammonia toxicity on growth performance, cortisol, glucose and hematological response of Nile Tilapia (*Oreochromis niloticus*). *Aech. J. Anim. Sci.* **2016**, *1*, 21–28. [[CrossRef](#)]
40. El-Shafai, S.A.; El-Gohary, F.A.; Nasr, F.A.; van der Steen, N.P.; Gijzen, H.J. Chronic ammonia toxicity to duckweed-fed tilapia (*Oreochromis niloticus*). *Aquaculture* **2004**, *232*, 117–127. [[CrossRef](#)]
41. Volpato, G.L.; Bovi, T.S.; de Freitas, R.H.; da Silva, D.F.; Delicio, H.C.; Giaquinto, P.C.; Barreto, R.E. Red light stimulates feeding motivation in fish but does not improve growth. *PLoS ONE* **2013**, *8*, e59134. [[CrossRef](#)]
42. Karakatsouli, N.; Papoutsoglou, S.E.; Panopoulos, G.; Papoutsoglou, E.S.; Chadio, S.; Kalogiannis, D. Effects of light spectrum on growth and stress response of rainbow trout *Oncorhynchus mykiss* reared under recirculating system conditions. *Aquac. Eng.* **2008**, *38*, 36–42. [[CrossRef](#)]

43. Luchiari, A.; Freire, F. Effects of environmental colour on growth of Nile tilapia, *Oreochromis niloticus* (Linnaeus, 1758), maintained individually or in groups. *J. Appl. Ichthyol.* **2009**, *25*, 162–167. [[CrossRef](#)]
44. Volpato, G.L.; Barreto, R. Environmental blue light prevents stress in the fish Nile tilapia. *Braz. J. Med. Biol. Res.* **2001**, *34*, 1041–1045. [[CrossRef](#)]
45. Aly, H.; Abdel-Rahim, M.; Lotfy, A.; Abdelaty, B. Impact of Different Colors of Artificial Light on Pigmentation and Growth Performance of Hybrid Red Tilapia (*Oreochromis mosambicus* x *O. hornorum*) Reared in Saline Well Water. *J. Mar. Sci. Res. Dev.* **2017**, *7*, 229. [[CrossRef](#)]
46. Sabri, D.M.; Elnwishy, N.; Nwonwu, F. Effect of environmental color on the behavioral and physiological response of Nile tilapia, *Oreochromis niloticus*. *Glob. J. Front. Res.* **2012**, *12*, 11–20.
47. Douglas, R.H.; Hawryshyn, C.W. Behavioural studies of fish vision: An analysis of visual capabilities. In *The Visual System of Fish*; Douglas, R., Djamgoz, M., Eds.; Springer: Dordrecht, The Netherlands, 1990; pp. 373–418. ISBN 978-94-009-0411-8.
48. Younis, E.S.M.; Al-Quffail, A.S.; Al-Asgah, N.A.; Abdel-Warith, A.W.A.; Al-Hafedh, Y.S. Effect of dietary fish meal replacement by red algae, *Gracilaria arcuata*, on growth performance and body composition of Nile tilapia *Oreochromis niloticus*. *Saudi J. Biol. Sci.* **2018**, *25*, 198–203. [[CrossRef](#)]
49. He, A.Y.; Ning, L.J.; Chen, L.Q.; Chen, Y.L.; Xing, Q.; Li, J.M.; Qiao, F.; Li, D.L.; Zhang, M.L.; Du, Z.Y. Systemic adaptation of lipid metabolism in response to low- and high-fat diet in Nile tilapia (*Oreochromis niloticus*). *Physiol. Rep.* **2015**, *3*, e12485. [[CrossRef](#)] [[PubMed](#)]
50. Moreno, I.; Ramos-Romero, I.R. Light spectrum for maximum luminous efficacy of radiation and high color quality. In *Current Developments in Lens Design and Optical Engineering XIX*; International Society for Optics and Photonics: Bellingham, WA, USA, 2018; Volume 10745.



© 2020 by the authors. Licensee MDPI, Basel, Switzerland. This article is an open access article distributed under the terms and conditions of the Creative Commons Attribution (CC BY) license (<http://creativecommons.org/licenses/by/4.0/>).

Article

Study on Water Saving Potential and Net Profit of *Zea mays* L.: The Role of Surface Mulching with Micro-Spray Irrigation

Zhaoquan He ^{1,2,*}, Xue Shang ¹ and Tonghui Zhang ^{2,3}¹ School of Life Sciences, Yan'an University, Yan'an 716000, China; scher1@163.com² Naiman Desertification Research Station, Northwest Institute of Eco-Environment and Resources, Chinese Academy of Sciences, Lanzhou 730000, China; zhangth@lzb.ac.cn³ Northwest Institute of Eco-Environment and Resources, Chinese Academy of Sciences, Lanzhou 730000, China

* Correspondence: hzq@yau.edu.cn; Tel.: +86-150-9540-3883

Received: 27 November 2019; Accepted: 3 January 2020; Published: 5 January 2020

Abstract: Water shortage threatens agricultural sustainability in Horqin Sandy Land, northeast China. To explore the effects of various surface mulching patterns with micro-spray irrigation on the yield, water consumption (ET_c), and water-saving potential of maize (*Zea mays* L.), we used three treatments: straw mulching (JG), organic fertilizer mulching (NF), and no mulching (WG; control). In each treatment, plants were supplied with 500 mm of total water (irrigation plus precipitation) during the entire growing season and were irrigated with the amount of total water supply minus precipitation. Yield and water use efficiency (WUE) showed a significant negative correlation with water saving potential per unit yield (P_y) and water saving potential per unit area (S_p), which were also consistent with their relationships in the function model. Meanwhile, a remarkably positive correlation occurred between yield, WUE, and net economic profit, respectively. The JG treatment, which was mainly affected by light and temperature production potential (Y_c), grain yield, and ET_c , showed the lowest P_y ($0.16 \text{ m}^3 \text{ kg}^{-1}$) and S_p ($2572.31 \text{ m}^3 \text{ hm}^{-2}$), and the maximum increase in yield, WUE, and net economic profit, extending to $16,178.40 \text{ kg hm}^{-2}$, 3.25 kg m^{-3} , $17,610.09 \text{ yuan hm}^{-2}$, respectively, which were significantly higher than those in NF and WG, ($p < 0.05$). Thus, straw mulching with micro-spray irrigation was the best treatment for maximizing yield and WUE. Organic manure mulching and no mulching need further investigation, as these showed high P_y and S_p , which were together responsible for lower WUE.

Keywords: water resources; surface mulching; water saving potential; micro-spray irrigation; economic profit

1. Introduction

Maize (*Zea mays* L.) is the second most important grain crop in China. Inner Mongolia is one of the major maize production regions of China that supports the livelihood of farmers in the region [1]. Maize requires a substantial amount of water during the growth phase but 80% of Inner Mongolia is arid and semi-arid, and water shortage in these areas continues to worsen with global climate change [2]. In addition, increase in the cultivable area is remarkably slow; therefore, the crop production area is unlikely to expand in the region so increasing yield per unit area is the only solution to continually support maize-production dependent households [3]. The improvement of maize yield per unit area primarily depends on the extension and reform of agricultural water saving planting technologies [4]. On the one hand, surface mulching is commonly used because of its notable positive impact on water conservation and yield. There are reports that mulching conserves

soil moisture by reducing evaporation and saving 12–84% of the irrigation water [5]. Common surface mulching methods include plastic mulching, straw mulching, organic manure mulching, and biochar mulching [6–8]. Effective use of crop straw and animal manure is conducive to the intensive management of agricultural resources, which is of practical significance for improving crop cropping systems, developing sustainable biodiversity of agro-ecosystems, and implementing national poverty reduction policies [9]. In addition, crop straw mulching and fully rotten organic manure mulching can improve the topsoil physics and chemistry nature of soil remarkably, without causing environmental pollution [10]. On the other hand, efficient irrigation contributes to increases in yields of crops and in income for the local farmers, providing evidence of the significance of irrigation in the past and for future poverty alleviation in China [11]. Therefore, combining mulching with advance irrigation method (drip/micro irrigation) increase more significantly crop productivity and water use efficiency (WUE), reduce water consumption (ET_c) in a region where water shortage is the major factor limiting agricultural sustainability [12–14].

The potential and configuration of climate resources (light, heat, and water) affect their utilization and ultimately limit the sustainable development of agricultural production [15]. Therefore, investigation of the characteristics of crop climate production potential is essential. The production potential of light and temperature is the main focus of studies in China. Water saving potential refers to the amount of irrigation water that can be saved per unit scale of crops, involving four scales, that is, crop, field, irrigation area, and regional/basin, respectively, and is a major factor affecting agricultural structure [16,17]. The definition of agricultural water saving potential is mainly based on water efficient methods, various water saving techniques, and management [16,18]. Previously, many approaches have been adopted to measure water saving potential, including efficient irrigation technology and method, irrigation scheduling improvement [19]. For example, some studies used the water balance method and remote sensing technology to calculate water consumption for obtaining the theoretical water saving potential [20,21], while many studies utilized crop models, such as DASSAT and WOFOST [22], to simulate the water consumption of crops and water saving ability, generating favorable results. Additionally, economic profit evaluation of agricultural technology has been largely explored in maize, confirming that the water saving irrigation method is significantly better than traditional irrigation technology [23], and no-till and permanently fixed ridge is better than conventional tillage [24].

Although responses of yield and water consumption of maize to surface mulching have been explored extensively, as mentioned above, research on the water saving potential per unit yield (P_y) and water saving potential per unit area (S_p) of maize (two angles of water-saving potential calculation, that is, crop scale and area scale, respectively) with surface mulching and micro-spray irrigation technology, and on the primary factors affecting the water saving potential of maize, is lacking. In this study, we used the meteorological observation data of the Naiman desertification station to achieve the following two main objectives: (1) to adjust the crop planting structure and farmland irrigation system through the improvement of the efficiency of irrigated agriculture by determining the surface mulching patterns with the greatest water-saving ability; and (2) to establish the optimal crop planting pattern with high net economic benefits and prominent water saving ability to provide theoretical support for the evaluation measures of economic benefits of water-saving planting patterns of farmland crops, thus expanding the appropriate ecological planting scale in this region.

2. Materials and Methods

2.1. Experimental Site

The experiment was carried out at the Naiman Desertification Research Station of the Chinese Academy of Sciences (42°58' N, 120°43' E; 360 m a.s.l.) in April–September 2017, located in the eastern part of Inner Mongolia Autonomous Region, China (Figure 1). Naiman, located in the southwest of Horqin Sandy Land [25], has a semiarid continental monsoon climate. The experimental site,

with sandy soil texture sensitive to wind erosion, has a mean annual precipitation of approximately 360 mm (265 mm in this growing season), an annual mean evaporation of around 1950 mm, and an annual mean temperature of 6.40 °C, of which the minimum monthly average temperature of −13.50 °C occurred in January and the maximum of 23.80 °C in July. In the soil depth of 0–60 cm, soil organic carbon content, pH (1:2.5 water), and electrical conductivity (1:5 water) at 0–30 cm depth before planting are 2.48 g kg⁻¹, 9.23, 62.73 μS cm⁻¹, respectively. Field capacity was 12.77%, wilting point was 5.40%, water saturation was 30.24%, saturated hydraulic conductivity was 0.93 mm min⁻¹, as well as bulk density being 1.55 g cm⁻³.

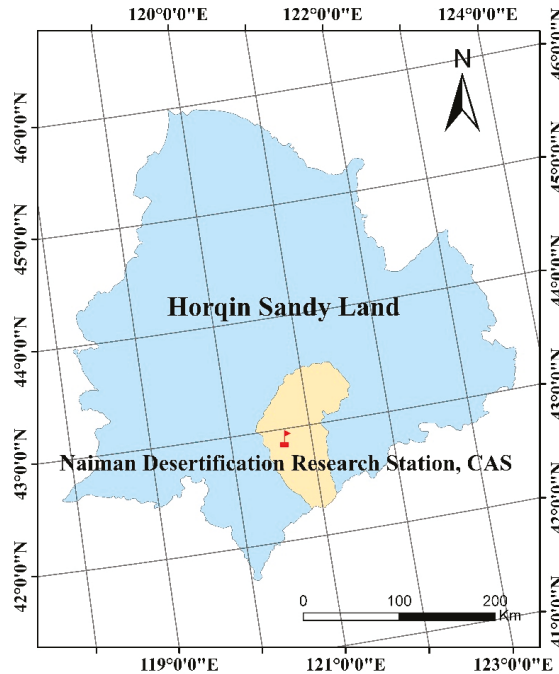


Figure 1. Location of Naiman desertification research station in China. Notes: the blue region represents Horqin Sandy Land; the yellow region represents the Naiman banner; the red flag represents Naiman desertification research station, CAS.

2.2. Test Design

The trial was laid out in a completely randomized plot design. A total of 51 plots (2 m × 2 m), representing 3 treatments and 17 replicates, were created. The *Zea mays* L. cv. Jingke 958 variety was chosen as the tested cultivar for all the treatments and was planted by a tube-shaped seeder on 27 April at a depth of 5 cm. The hole of the seeds was 2.5 cm in the direction of the row and was 3.0 cm in the direction of the column, which was reserved for the space of maize growth. The planting density of maize was 60,000 plants hm⁻². Each plot contained 4 rows, with 6 maize plants per row, that is, 4 rows of 6 columns, at a plant-to-plant spacing of 20 cm and row-to-row spacing of 36 cm (Figure 2). The spacing of 0.5 m between each plot was provided for maintaining independence among treatments, and a buffer channel of 1 m width was provided in the neighborhood of experimental fields to avoid edge effects. The experimental field was oriented west to east. The field was rectangular in shape, with 9 m in the north-south direction and 44 m in the east-west direction. Three treatments were established: straw mulching (JG), organic manure mulching (NF) and no mulching (WG; control).

In the JG treatment, when the maize seedlings reached a height of 20 cm, crushed maize straw was evenly applied to 100% of the soil surface with 4000 kg hm^{-2} (1.6 kg per plot). In the NF treatment, cattle and poultry manure were the sources of organic manure. They were collected from the cattle and poultry farms located in Naiman banner and were uniformly mixed with soil 15 days before applying, making it fully rotten, preventing environmental pollution. Because organic manure that is not fully rotten contains various bacteria, this would cause a high incidence of crop diseases and insect pests, and affect the ecological environment when applied directly to farmland. Physical and chemical properties of the organic manure were, 145.77 g kg^{-1} of soil organic carbon, 260.49 g kg^{-1} of soil organic matter, 10.25 g kg^{-1} of total nitrogen, 8.64 g kg^{-1} of total phosphorous, and 11.57 g kg^{-1} of total potassium. When the maize seedlings reached a height of 20 cm, organic manure was evenly distributed on 100% of the soil surface with $30,000 \text{ kg hm}^{-2}$ (12 kg per plot). In the WG (control) treatment, no surface mulching was used during the entire growth period of the maize.

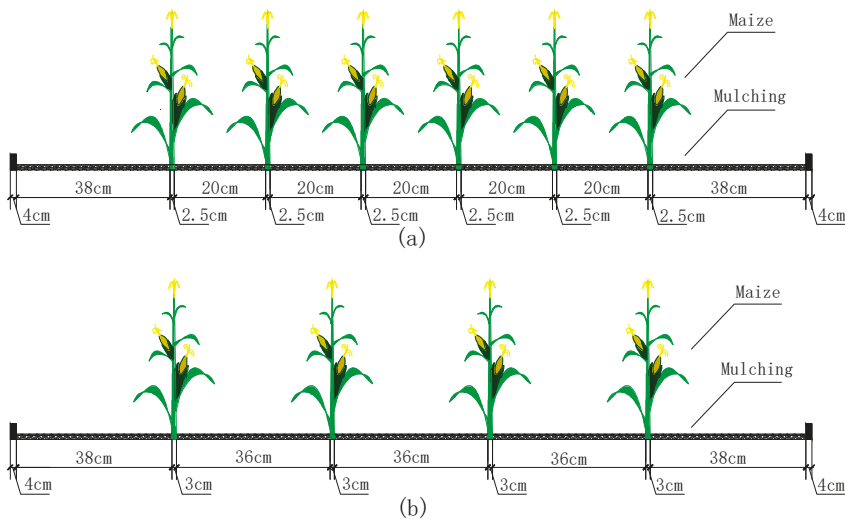


Figure 2. Sketch of experimental site. (a) represents the front view; (b) represents the lateral view.

2.3. Irrigation Scheme

In each treatment, zonal micro-spray irrigation was used. Maize plants were supplied with 500 mm of water, including irrigation and precipitation, during the entire growth season. The irrigation amount was the total water supply minus precipitation. The maize growth season was divided into five stages: seeding, jointing, heading, filling, and ripening. According to the water requirements of maize at each growth stage, 15%, 35%, 22%, and 28% of the total water supply was applied to the seedling-jointing, jointing-heading, heading-filling, and filling-ripening stage, respectively [26]. The irrigation level was the same across all treatments. In each growth phase, if the precipitation exceeded the upper limit of the designed water supply, the water increment needed to be subtracted from the next irrigation, ensuring the same total water supply for all treatments throughout the entire growing season. Maize was irrigated on days with no or low wind ($<1.5 \text{ m s}^{-1}$) to achieve uniform irrigation. Irrigation regimes are summarized in Table 1. Spray lines (42 m) were installed in the middle of the plot along the east-west direction, with a nozzle spacing of 50 cm and discharge rate of 1 L h^{-1} . Irrigation groundwater was measured continuously using flowmeters.

Table 1. The irrigation regimes across the growing season (mm, April–September 2017).

Growth Stage	Precipitation	Irrigation Only	Straw Mulching (JG)	Organic Manure Mulching (NF)	No Mulching (WG)
Seeding-Jointing stage	26 April–28 April			Covers all three treatments: 0.00	
		28 April–1 May	38.97	38.76	39.13
	2 May–22 May	23 May–25 May	5.94	6.02	5.98
	23 May–8 June			Covers all three treatments: 0.60	
Jointing-Heading stage	Total Irrigation from Seeding to Jointing Stage		74.81	74.72	75.01
	Irrigation Deviation	9 June–13 June	–0.19	–0.28	+0.01
		14 June–24 June	87.06	86.95	87.10
		25 June–27 June	38.24	38.09	38.12
Heading-Filling stage	Total Irrigation from Jointing to Heading Stage		185.50	185.24	185.42
	Irrigation Deviation	16 July–20 July	+10.50	+10.24	+10.24
		20 July–28 July	62.88	62.90	62.84
		Total Irrigation from Heading to Filling Stage	98.95	98.60	98.54
Filling-Ripening stage	Irrigation Deviation	29 July–4 August	–11.42	–11.40	–11.46
		5 August–7 August	4.38	4.44	4.40
		5 August–8 September		Covers all three treatments: 34.80	
	Total Irrigation from Filling to Ripening Stage		139.68	139.74	139.70
Total Water Supply (Irrigation Plus Precipitation) in Whole Growing Season (No Decimals)			–0.32	–0.26	–0.30
			500.00	500.00	500.00
Total Precipitation in Whole Growing Season				Covers all three treatments: 261.60	
Total Irrigation Only in Whole Growing Season (No Decimals)			239.00	239.00	239.00

Note: N represents no irrigation; + represents irrigation increment and needs to be subtracted from the next irrigation; – represents irrigation loss, and needs to be added at the next irrigation. Date between precipitation and irrigation is continuous because the precipitation during the days of irrigation is automatically counted as the amount of precipitation in the interval between that irrigation and the next irrigation.

2.4. Field Management

The field was tilled approximately 1 week before sowing. At the time of tilling, a basal dose of fertilizer was evenly and equably distributed in the topsoil at a rate of 375 kg ha^{−1} (1.35 kg per plot) of diammonium phosphate (N-P₂O₅-K₂O, 18-46-0) based on the N and P requirements; the fertilizer was applied in spade slits to avoid loss over the soil surface and sprinkled near the maize roots to ensure full absorption by the crops. No pesticides and insecticides were used during the whole growth period of maize to prevent the test results from being affected.

2.5. Climate Data

Slight fluctuations in temperature occurred among the different growth stages. The mean temperature was 24.60 °C (Figure 3). Relative humidity was significantly higher in July and August, reaching a maximum of 100%, compared with other months (Figure 3). It was found that, from the calculation of the food and agriculture organization (FAO) Penman–Monteith Equation (2), reference crop evapotranspiration (ET₀) and precipitation were 501 and 261 mm, respectively (Figure 4). The average ET₀ was 3.61 mm d^{−1}, with remarkable seasonal variation; ET₀ increased from April to July and then declined significantly after August, along with the decrease in solar radiation intensity and temperature. In August, lower ET₀ was positively related to lower temperature and higher relative humidity.

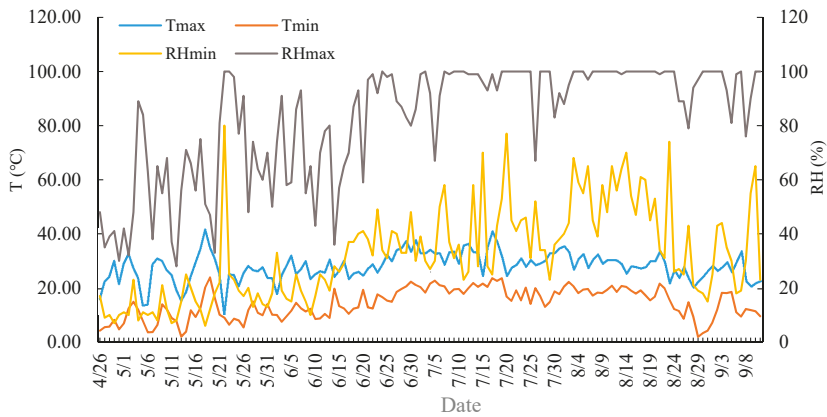


Figure 3. Variation of the temperature and relative humidity of the experimental site during the growth period of maize. Note: T_{max} represents the maximum of temperature; T_{min} represents the minimum of temperature; RH_{max} represents the maximum of relative humidity; RH_{min} represents the minimum of relative humidity.

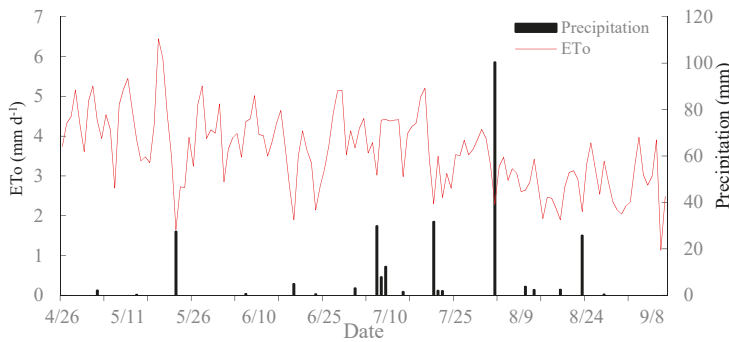


Figure 4. Variation of the reference crop evapotranspiration and precipitation during the growth period of maize. Note: ET_o represents reference crop evapotranspiration, mm. ET_o was calculated by means of the FAO Penman–Monteith Equation (2) for the entire growth season of maize.

2.6. Measurement of Indicators

Soil water content of 0–20 cm, 20–40 cm, 40–60 cm, 60–80 cm, and 80–100 cm in each growth stage was determined by the gravimetric method.

Soil temperature in the soil layer of 0–20 cm was measured by a thermometer during each growth period of maize.

Maize of each plot was harvested at the ripening stage, and 6 ears that were growing well were selected randomly in each plot. Drying the grain to constant weight at 85 °C, weighing by an electric balance for grain yield, the grain yields were then converted to a standard grain water content of 15.50% wet basis [27].

ET_c was calculated daily during the growing season by the soil water balance Equation (1) [28]:

$$ET_c = I + P + C_r - D_w - R_f \pm \Delta s \dots \tag{1}$$

where ET_c was the total amount of actual evapotranspiration for the entire season (mm), I was the amount of irrigation water applied (mm), P was the precipitation (mm), C_r was the capillary rise (mm), D_w was the amount of drainage water (mm), R_f was the amount of runoff (mm), and Δs was the

change in the soil moisture content (mm). The soil moisture content measurement was used by the conventional oven-dry method in soil layers (0–20 cm, 20–40 cm, 40–60 cm, 60–80 cm, and 80–100 cm). No runoff was observed during the trials. Capillary rise was considered as negligible due to the deep water table level. Drainage water included precipitation under the effective rooting depth, according to the soil water content measurements in the soil layer at the effective rooting depth, was determined.

ET_0 was calculated per day during the growing season by using the FAO Penman–Monteith equation. The FAO Penman–Monteith equation is given by (2):

$$ET_0 = \frac{0.408\Delta(R_n - G) + \gamma \frac{900}{T+273} \mu_2 (e_s - e_a)}{\Delta + \gamma(1 + 0.34\mu_2)} \quad (2)$$

where ET_0 was the reference evapotranspiration (mm day^{-1}), R_n was net radiation at the crop surface ($\text{MJ m}^{-2} \text{ day}^{-1}$), G was soil heat flux density ($\text{MJ m}^{-2} \text{ day}^{-1}$), T was mean daily air temperature at 2 m height ($^{\circ}\text{C}$), μ_2 was wind speed at 2 m height (m s^{-1}), e_s was the saturation vapor pressure (kPa), e_a was the actual vapor pressure (kPa), $e_s - e_a$ was the saturation vapor pressure deficit (kPa), γ was the slope of the saturation vapor pressure curve ($\text{kPa } ^{\circ}\text{C}^{-1}$), and Δ was the psychrometric constant ($\text{kPa } ^{\circ}\text{C}^{-1}$). Meteorological parameters needed to calculate ET_0 were derived from a local meteorological station.

Water use efficiency (kg m^{-3}) was calculated as (3) [29]:

$$WUE = Y/ET_c \dots \quad (3)$$

where WUE was the water use efficiency (kg m^{-3}), Y was the grain yield (kg hm^{-2}), ET_c was the total amount of actual evapotranspiration for the entire season (mm).

Net economic profit (yuan hm^{-2}) was calculated as (4):

$$\text{Net profit} = \text{total revenue} - \text{total cost} \quad (4)$$

where, total revenue = grain yields \times average local price. The average local price for maize was $1.70 \text{ yuan kg}^{-1}$. The total cost included the cost of seed, fertilizers, sows, micro-spray irrigation belts, water pipes, maize straw, and organic fertilizers during the trial.

Light and temperature production potential (kg hm^{-2}) was calculated by the photosynthetic production potential multiplied by the revised function of temperature effect, and the expression is given by (5):

$$Y_c = Y_p \cdot f(T) \dots \quad (5)$$

Y_c was the light and temperature production potential, kg hm^{-2} ;

Y_p was the photosynthetic production potential, kg hm^{-2} ;

$f(T)$ was the revised function of the temperature effect.

Water saving potential per unit yield ($\text{m}^3 \text{ kg}^{-1}$) was calculated as (6):

$$P_y = \frac{1}{WUE_a} - \frac{1}{WUE_t} \dots \quad (6)$$

P_y was water saving potential per unit yield, $\text{m}^3 \text{ kg}^{-1}$;

WUE_a was actual crop water productivity, kg m^{-3} ;

WUE_t was the theoretical crop water productivity, kg m^{-3} .

Water saving potential per unit area ($\text{m}^3 \text{ hm}^{-2}$), was calculated as (7):

$$S_p = P_p \times W \dots \quad (7)$$

S_p was the water saving potential per unit area, $\text{m}^3 \text{ hm}^{-2}$;

P_p was the proportion of crop water saving potential, %;

W was the irrigation quota, $\text{m}^3 \text{ hm}^{-2}$.

2.7. Data Collations and Statistical Methods

Effects of various surface mulching patterns on soil water content, soil temperature, yield, water consumption, water saving potential, and net profit of maize were plotted using Origin 8.0. Variance, correlation and stepwise regression analyses were performed using SPSS 20.0, while significant differences were detected using the least significant difference (LSD) test. The cost and net profit of various surface mulching patterns were compared using the quota comparison method. Tables were created in Excel 2010.

3. Results

3.1. Changes in the Soil Temperature and the Soil Water Content

Under micro-spray irrigation, variation in soil temperature and soil water content during the entire growth period of maize was not affected by the different surface mulching patterns. Soil temperature increased from the seedling stage to the heading stage, which remained relatively stable until the filling stage, and then declined. In each treatment, the soil water content was significantly higher at heading and maturity than at other growth stages (Figure 5).

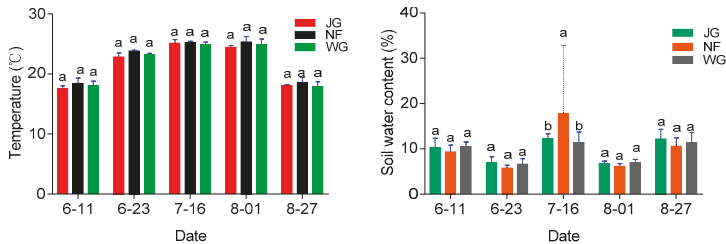


Figure 5. Soil temperature (soil layer of 0–20 cm) and soil water content (soil layer of 0–100 cm) of maize at different growth stages. Note: JG represents straw mulching; NF represents organic fertilizer mulching; WG represents no mulching; data represents mean ± standard error (*n* = 17). Bars labeled with different letters (lowercase) differed significantly among the treatments (*p* < 0.05).

The temperature of the 0–20 cm soil layer was the highest from the seedling stage to the heading stage, and the rate of increase of soil temperature reached 42.99%, 36.71%, and 37.55% in the JG, NF, and WG treatments, respectively (Figure 5). Then, the soil temperature decreased from the heading to the ripening stage by 28.29%, 26.51%, and 28.24% in the JG, NF, and WG treatments, respectively. Overall, during the entire growth period of maize, the mean soil temperature (0–20 cm layer) in different treatments was in the order: NF > WG > JG.

Soil water content at each growth stage was lower in JG and WG treatments than in the NF treatment (Figure 5); thus, the soil water content was directly related to the variation in soil temperature in different mulching treatments. However, there was no significant difference between JG, and WG, respectively, for the mean soil water content. In all three treatments, the soil water content was the highest at the heading stage, which was directly responsible for the higher irrigation proportion (35% of the total water supply). Compared with the seedling stage, the heading stage showed an increase in soil water content of 18.70%, 91.05%, and 8.33% in the JG, NF, and WG treatments, respectively.

3.2. Water Saving Potential (Per Unit Yield and Per Unit Area)

Values of P_y and S_p of maize in the JG treatment were significantly lower than those in the NF and WG treatments. Compared with the JG treatment, values of P_y and S_p were significantly higher by 31.73% and 34.51%, respectively, in the NF treatment and by 20.21% and 20.08%, respectively in the WG treatment (*p* < 0.05); however, no significant differences were detected in P_y and S_p between the

NF and WG treatments. Thus, under micro-spray irrigation, P_y and S_p of maize in various treatments were in the order: NF and WG > JG (Figure 6).

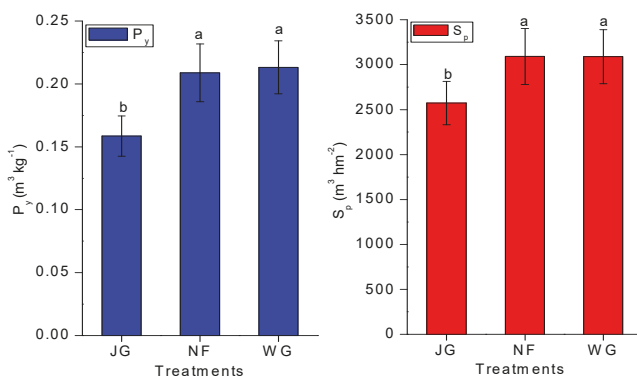


Figure 6. Water saving potential per unit yield and per unit area of maize under various surface mulching patterns. Note: JG represents straw mulching; NF represents organic fertilizer mulching; WG represents no mulching; P_y represents water saving potential per unit yield, $m^3 kg^{-1}$; S_p represents water saving potential per unit area, $m^3 hm^{-2}$. Bars labeled with different letters (lowercase) differed significantly among the treatments ($p < 0.05$).

The P regression model affecting the water-saving potential per unit yield and per unit area was 0.00, R^2 was up to 0.92, 1.00, respectively, with high fitting degree (Table 2). This elucidated that under various surface mulching patterns, the index that affected P_y was yield ($R^2 = 0.92$), and indexes that affected S_p were light and temperature production potential (Y_c), yield and water consumption (ET_c).

Table 2. Stepwise regression coefficient of indexes affecting water saving potential of maize.

Indicator	Model	Regression Coefficient	t	P	R^2
P_y	(Constant)	0.696	13.358	0.000	0.920
	Y	-3.320×10^{-5}	-9.648	0.000	
S_p	(Constant)	299.478	102.482	0.000	0.988
	Y_c	0.057	2029.233	0.000	
	Y	-0.151	-1866.520	0.000	
	ET_c	-0.237	3.857	0.012	

Notes: P_y represents water saving potential per unit yield, $m^3 kg^{-1}$; S_p represents water saving potential per unit area, $m^3 hm^{-2}$; Y_c represents light and temperature production potential of crop, $kg hm^{-2}$; Y represents grain yield, $kg hm^{-2}$; ET_c represents water consumption, mm. t represents significance test values of regression parameters. P represents significant value.

3.3. Light and Temperature Production Potential, Yield and Water Consumption

The JG treatment showed the lowest ET_c and the highest yield and WUE (Figure 7); however, no significant differences were detected in these parameters between the NF and WG treatments. The value of ET_c was essentially the same in JG, NF, and WG treatments. Values of Y_c in the NF and WG treatments were 16.18% and 13.32% higher than those in the JG treatment, respectively ($p < 0.05$). However, maize yield in the JG treatment was 9.53% and 12.10% higher than that in the NF and WG treatments ($p < 0.05$). In the current study, ET_c was approximately 500 mm in the JG, NF, and WG treatments during the entire growth season; no significant differences were detected among them, probably because of the thickness of maize straw in the JG treatment and organic fertilizer in the NF treatment, which requires further investigation. Moreover, this difference was closely related to differences in the region, maize variety, and irrigation approach.

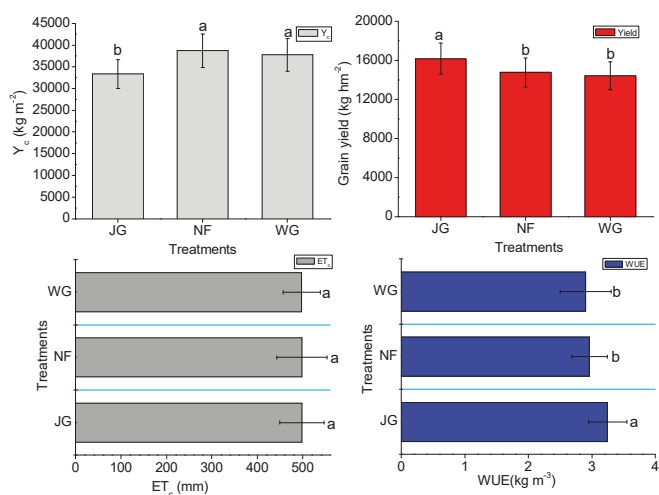


Figure 7. Light and temperature production potential, yield, water use efficiency and water consumption of maize under various mulching patterns. Note: JG represents straw mulching; NF represents organic fertilizer mulching; WG represents no mulching. Y_c represents light and temperature production potential; ET_c represents water consumption of maize; WUE represents water use efficiency. Bars labeled with different letters (lowercase) differed significantly among the treatments ($p < 0.05$).

In the JG, NF, and WG treatments, correlation coefficients between water saving potential (P_y and S_p) of maize and indexes affecting water saving potential were greater than 0.80 (Table 3), indicating a high correlation. Values of P_y and S_p changed significantly with yield ($R > 0.90$).

Table 3. Correlations between indexes affecting water saving potential.

Index	Treatment	Y (kg hm^{-2})	Index	Y_c (kg m^{-2})	Y (kg hm^{-2})	ET_c (mm)
P_y ($\text{m}^3 \text{kg}^{-1}$)	JG	0.951 *	S_p ($\text{m}^3 \text{hm}^{-2}$)	-0.982 **	0.905 *	0.887 *
	NF	-0.999 **		-0.982 **	-0.982 **	-0.997 **
	WG	0.982 **		-0.817 *	0.982 **	1.000 **

Notes: * represents the significant difference at the level of 0.05 (bilateral); ** represents the significant difference at the level of 0.01 (bilateral).

3.4. Economic Profits

Analysis of the economic profits of various treatments showed that the WG treatment with micro-spray irrigation was the least expensive ($9575.33 \text{ yuan hm}^{-2}$; Figure 8) because this treatment had no associated cost of surface mulching material. However, the WG treatment showed no significant difference compared with the JG and NF treatments because of the higher labor cost associated with no mulching in the WG treatment. Net profit was the highest in the JG treatment, which was significantly higher by 18.26% and 17.71% than those in the NF and WG treatments, respectively ($p < 0.05$). The profit:cost ratio was 1.78 in the JG treatment, which was 22.14% and 13.93% higher than that in the NF and WG treatments, respectively. According to the regression fitting analysis, the net profit of maize showed a significantly negative linear correlation with P_y and S_p , with the coefficient of determination (R^2) of 0.898 and 0.989, respectively (Figure 9). The higher the water saving potential, the smaller the net economic profit of maize; this explained why the net economic profit of maize in the JG treatment was higher than that in the NF and WG treatments.

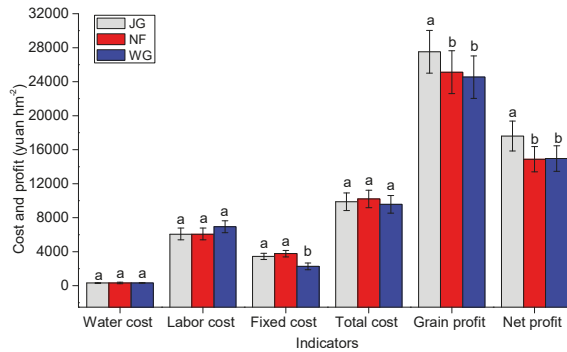


Figure 8. Cost and profit of maize under various mulching planting patterns. Note: JG represents straw mulching; NF represents organic fertilizer mulching; WG represents no mulching. The average local price for maize was 1.70 yuan kg⁻¹. The total cost included the cost of seed, fertilizers, sows, micro-spray irrigation belts, water pipes, maize straw, organic fertilizers during the trial. Labor costs included the layout of the sample plot, weeding, sampling, irrigation, spreading fertilizer, and determination of sample. Bars labeled with different letters (lowercase) differed remarkably among different indexes ($p < 0.05$).

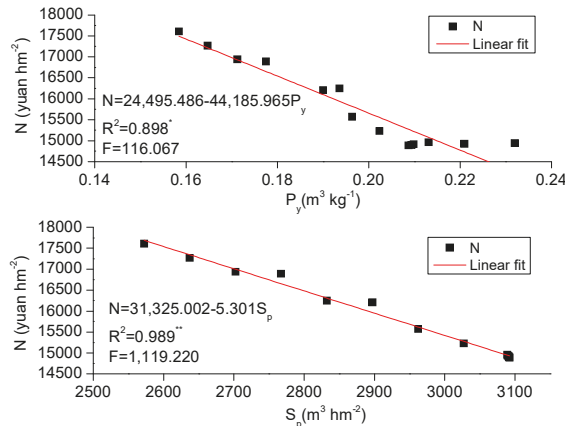


Figure 9. Relationships between water saving potential and net economic profit of maize. Note: N represents net economic profit, yuan hm⁻²; P_y represents water saving potential per yield, m³ kg⁻¹; S_p represents water saving potential per unit area, m³ hm⁻². * represents regression effect was significant; ** represents regression effect was remarkably significant.

4. Discussion

4.1. Water Saving Potential

Currently, climate change is one of the major concerns of the environmental problem facing mankind, and agriculture is highly sensitive to climate change [30]. Temporal and spatial distribution patterns of climate resources, such as water and heat, are directly affected by meteorological factors, including solar radiation, temperature, and precipitation. Fluctuations in temperature and precipitation during the growing season affect crop productivity, ultimately affecting regional agricultural production [31]. Therefore, spatiotemporal distribution characteristics of the crop climate production potential represent the basis of comprehensive food production potential and provide a crucial theoretical basis for agricultural productivity planning and agricultural structural

adjustment [32]. Water saving potential is a vital evaluation index for adjusting agricultural structure. In this study, soil water content at each growth stage was lower in JG and WG treatments than in the NF treatment (Figure 5). However, there was no significant difference between JG, and WG, respectively, for the mean soil water content. This resulted mainly from the type and rate of the irrigation and the mulches. Because the soil moisture strongly depended on the precipitation and irrigation pattern (see irrigation scheme), the precipitation, irrigation pattern, and irrigation amount applying to all three treatments were the same. In addition, Zhao et al. [33] found that, compared with deep tillage with no mulch, mean soil water content of sunflowers was only higher by 5.75%, 2.50%, respectively, in 2011 and 2013, when straw mulch was used at a rate of 12,000 kg hm⁻², which was significantly higher than that of our study (4000 kg hm⁻²). Teame et al. [34] indicated that, by exploring the efficacy of organic mulching, sorghum straw mulching and rice straw mulching with a rate of 10,000 kg hm⁻² increased mean water soil content of sesame by 33.29%, 42.05%, respectively, compared to no mulch. The efficiency of increasing soil water was more significant than that in Zhao et al. [33], which would be due to the difference in the crops and the mulches. Therefore, it was suggested that yield, P_y, and S_p were not affected significantly by the water soil content, based on the results of the stepwise regression analysis (Table 2) and the insignificant difference among the three treatments for water soil content (Figure 5). The water saving potential was mainly affected by Y_c, grain yield and ET_c, and showed a positive correlation with Y_c and negative correlation with grain yield and ET_c. Therefore, both P_y and S_p were the lowest in the JG treatment; however, the WUE and water saving capacity of the JG treatment were significantly higher than that of the NF and WG treatments.

Photosynthetic production potential represents the maximum crop yield achieved only under light conditions. Y_c was the maximum yield of crop subjected to both light and temperature constraints [35]. Regions that experienced a rapid decrease in the climate production potential of maize over the last 30 years show a dramatic increase in Y_c, resulting from a dry climate [32]. Radiation and temperature are the most critical factors affecting Y_c; these factors decreased by -12.70% and -6.10%, respectively, when solar radiation of maize decreased by 10% or temperature increased by 1 °C during the growing season [35]. Under micro-spray irrigation, maize yield was the highest in the JG treatment, in which Y_c was considerably lower than that in the NF and WG treatments, although no significant differences were detected in ET_c among the three treatments. The photosynthetic production potential of the yield has been the main focus of research in northeast China [36]. The decrease in solar radiation is primarily responsible for the decrease in the photosynthetic production potential of maize. Spatial variation characteristics of the photosynthetic production potential of maize were similar to those of the surface solar radiation, both of which showed a decreasing trend from the southwest to the northeast [37]. Licker et al. systematically analyzed global maize yields and concluded that the maize yield would increase by 50%, if 95% of the maize cultivation areas worldwide met the climate potential. However, the difference between climate production potential and actual production was approximately 20% because of improvements in traditional farming patterns, economic costs, and technological measures, and the yield potential of maize was mainly affected by unreasonable farmland management and low technical levels. Therefore, conclusions explored in our study on the water saving potential of maize using different planting patterns and micro-spray irrigation are extremely conducive to the rational planning of the layout of planting areas, effectively improving maize yield and ensuring food security.

4.2. Yield and Water Consumption

Mulching has been adopted in numerous parts of the world as an approach to increase crop productivity [38]. Maize yield in the JG treatment was 9.53% and 12.10% higher than that in the NF and WG treatments ($p < 0.05$), and was significantly higher than that reported by Sharma et al. [39] and similar to that reported by many scholars. Li and colleagues [40] showed that plastic mulching dramatically increases crop yield. Yin et al. [41] found that compared to conventional tillage without straw residue, integrating no tillage with two-year plastic and straw mulching improved grain yields by 13.8%, reduced soil evaporation by 9.0%, and reduced soil evaporation by 9.0%. However,

in another study, straw mulching did not significantly affect yield under limiting soil water content [42]. In addition, ET_c was approximately 500 mm in the JG, NF, and WG treatments during the entire growth season; no significant differences were detected among them, probably because of the thickness of maize straw in the JG treatment and organic fertilizer in the NF treatment, which requires further investigation. Our results of ET_c were in contrast to those of previous studies. For example, Yin et al. [43] reported that plastic film together with straw mulching decreased total evapotranspiration by an average of 4.60% ($p < 0.05$) compared with no mulching; Brar et al. [44] suggested that straw mulching resulted in 19.00% higher yield compared with no mulching, resulting in 36.20 mm higher transpiration and 44.20 mm lower soil evaporation; Sun et al. [45] confirmed that crop water consumption was reduced by 32 mm under straw mulching compared with no mulching, with no significant differences in WUE. Zhou et al. [46] indicated that compared with no mulching, straw mulching increased maize yield by 10.6% and 12.5% under a drip irrigation system in 2016 and 2017, respectively, and achieved 6.1% lower water consumption. The contradiction was mostly responsible for the enhanced maize straw mulching amount in their study, which was significantly higher than that of our study. Moreover, this difference was closely related to differences in the region, maize variety, and irrigation approach.

4.3. Economic Profits

Economic profits include the rate of input application and the rate of consumptive use in irrigation and fertilizer [47]. Net profit was the highest in the JG treatment, which was significantly higher by 18.26% and 17.71% than those in the NF and WG treatments, respectively ($p < 0.05$). Similar net profit has been reported in rice using straw mulching in water saving production systems [48]. In this study, the profit: cost ratio was 1.78 in the JG treatment, which was 22.14% and 13.93% higher than that in the NF and WG treatments, respectively. This was consistent with the results of Sharma et al. [39]; the authors showed that the profit: cost ratio was the highest (0.62) with straw mulching, although this ratio was markedly lower than that obtained in our study. In other studies, drip irrigation resulted in net economic profits of 4359.58–6240.19 yuan hm^{-2} , which were higher than those obtained by furrow irrigation [44]. Small amounts of maize cob biochar would also attain higher net profit through increased yields [49]. Sweet maize and green beans grown in rotation resulted in a greater increase in net profits compared with potato monoculture [50]. Therefore, straw mulching with micro-spray irrigation elevated furthest economic profits of maize, compared to organic manure mulching and no mulching.

5. Conclusions

Under micro-spray irrigation, maize yield and WUE were the highest in the JG treatment with 16,178.40 kg hm^{-2} , 3.25 kg m^{-3} , respectively, in which Y_c was significantly lower than that in the NF and WG treatments. The three treatments showed no significant differences in ET_c . The water saving potential (including P_y and S_p) of maize was positively affected by Y_c and negatively affected by grain yield and WUE. Therefore, values of P_y and S_p were the lowest in the JG treatment, were just 0.16 $m^3 kg^{-1}$ and 2572.31 $m^3 hm^{-2}$, respectively, but no significant differences were found, compared to NF and WG treatments. The net economic profit of maize was negatively correlated with the water saving potential in all treatments, which was primarily responsible for the negative relationship between water saving potential and yield, WUE, respectively. So, the maximum of net economic profit appeared in the JG treatment, was up to 17,610.09 yuan hm^{-2} , and was higher than that in the NF and WG treatments ($p < 0.05$).

The yield, WUE, and water saving capacity of the JG treatment were significantly higher than that of the NF and WG treatments. This suggests that straw mulching with micro-spray irrigation should be applied in local appropriate farmland. Given the lower WUE and higher water saving potential of the NF and WG treatments, it is important to explore these planting patterns further.

Author Contributions: Z.H. designed, performed the experiments, and wrote the original draft; X.S. analyzed the data; T.Z. reviewed and edited the draft. All authors read the final manuscript and approved the submission. All authors have read and agreed to the published version of the manuscript.

Funding: This research was funded by the National Natural Science Foundation of China (Grant No. 41371053, 30972422, 51669034, 51809224), National key research and development project of China (Grant No. 2017YFC0506706, 2017YFC0504704) and Science research launch project of PhD (205040305).

Acknowledgments: We are grateful to all the members of Naiman Desertification Research Station, Chinese Academy of Sciences, for their help in field work. We are also grateful to other anonymous reviewers for their valuable comments on the manuscript.

Conflicts of Interest: The authors declare no competing interests.

Abbreviations

ET _o	REFERENCE CROP EVAPOTRANSPIRATION
ET _c	WATER CONSUMPTION
FAO	FOOD AND AGRICULTURE ORGANIZATION
JG	STRAW MULCHING
NF	ORGANIC MANURE MULCHING
P _y	WATER SAVING POTENTIAL PER UNIT YIELD
S _p	WATER SAVING POTENTIAL PER UNIT AREA
WG	NO MULCHING
WUE	WATER USE EFFICIENCY
Y _c	LIGHT AND TEMPERATURE PRODUCTION POTENTIAL

References

1. He, Q.; Zhou, G. Climate-associated distribution of summer maize in China from 1961 to 2010. *Agri. Ecosyst. Environ.* **2016**, *232*, 326–335. [[CrossRef](#)]
2. Forouzani, M.; Karami, E. Agricultural water poverty index and sustainability. *Agron. Sustain. Dev.* **2011**, *31*, 415–432. [[CrossRef](#)]
3. Foley, J.A.; Ramankutty, N.; Brauman, K.A.; Cassidy, E.S.; Gerber, J.S.; Johnstone, M.; Mueller, N.D.; O'Connell, C.; Ray, D.K.; West, P.C.; et al. Solutions for a cultivated planet. *Nature* **2011**, *478*, 337–342. [[CrossRef](#)] [[PubMed](#)]
4. Chai, Q.; Gan, Y.; Turner, N.C. Water-saving innovations in Chinese agriculture. *Adv. Agron.* **2014**, *126*, 147–197.
5. Kaur, A.; Brar, A.S. Influence of mulching and irrigation scheduling on productivity and water use of turmeric (*Curcuma longa* L.) in north-western India. *Irrigation Sci.* **2016**, *34*, 261–269.
6. Uzoma, K.C.; Inoue, M.; Andry, H.; Fujimaki, H. Effect of cow manure biochar on maize productivity under sandy soil condition. *Soil Use Manag.* **2011**, *27*, 205–212. [[CrossRef](#)]
7. Gan, Y.T.; Siddique, K.H.M.; Turner, N.C. Ridge–furrow mulching systems—an innovative technique for boosting crop productivity in semiarid rain-fed environments—chapter seven. *Adv. Agron.* **2013**, *118*, 429–476.
8. Wang, X.; Jia, Z.; Liang, L. Impacts of manure application on soil environment, rainfall use efficiency and crop biomass under dryland farming. *Sci. Rep.* **2016**, *6*, 20994. [[CrossRef](#)]
9. Hengsdijk, H.; Wang, G.H.; Van den Berg, M.M.; Wang, J.D.; Wolf, J.; Changhe, L.; Roetter, R.P.; Van Keulen, H. Poverty and biodiversity trade-offs in rural development: A case study for Pujiang County, China. *Agric. Syst.* **2007**, *94*, 851–861. [[CrossRef](#)]
10. Li, Z.X.; Dong, S.T.; Hu, C.H.; Wang, K.J.; Zhang, J.W.; Liu, P. Influence of organic manure and inorganic manure interaction on yield of maize and characteristic of topsoil. *J. Maize Sci.* **2004**, *12*, 100–102.
11. Huang, Q.; Rozelle, S.; Lohmar, B.; Huang, J.; Wang, J. Irrigation, agricultural performance and poverty reduction in China. *Food Policy* **2006**, *31*, 30–52. [[CrossRef](#)]
12. Gao, Q.Z.; Du, H.L.; Zu, R.P. The balance between supply and demand of water resources and the water-saving potential for agriculture in the Hexi Corridor. *Chin. Geogr. Sci.* **2002**, *12*, 23–29. [[CrossRef](#)]
13. Guang, X.Z.; Wei, D. The groundwater crisis and sustainable agriculture in northern China. *Water Eng. Manag.* **2002**, *149*, 13–16.

14. Wang, C.; Wang, J.; Xu, D.; Sui, J.; Mo, Y. Water consumption patterns and crop coefficient models for drip-irrigated maize (*Zea mays* L.) with plastic mulching in northeastern China. *Trans. ASABE* **2019**, *62*, 571–584. [[CrossRef](#)]
15. Li, Y.; Yang, X.G.; Dai, S.W.; Wang, W.F. Spatiotemporal change characteristics of agricultural climate resources in middle and lower reaches of Yangtze River. *Chin. J. Appl. Ecol.* **2010**, *21*, 2912–2921.
16. Kang, S.Z.; Yang, J.Z.; Pei, Y.S.; Feng, S.Y.; Huo, Z.L.; Sun, J.S.; Zhang, X.Y.; Wu, J.W.; Wang, J.L.; Tong, L.; et al. *Farmland Water Cycle Process and Agricultural Efficient Water Use Mechanism in Hai River Basin*; Science Press: Beijing, China, 2013; pp. 204–252.
17. Yue, Q.; Zhang, F.; Guo, P. Optimization-Based Agricultural Water-Saving Potential Analysis in Minqin County, Gansu Province China. *Water* **2018**, *10*, 1125. [[CrossRef](#)]
18. Pfeiffer, L.; Lin, C.Y.C. Does efficient irrigation technology lead to reduced groundwater extraction? Empirical evidence. *J. Environ. Econ. Manag.* **2014**, *67*, 189–208. [[CrossRef](#)]
19. Christian-Smith, J.; Cooley, H.; Gleick, P.H. Potential water savings associated with agricultural water efficiency improvements: A case study of California, USA. *Water Policy* **2012**, *14*, 194. [[CrossRef](#)]
20. Liu, L.G.; Cui, Y.L.; Wang, J.P. New calculation method for water saving potential in agriculture based on water balance principle. *Adv. Water Sci.* **2011**, *22*, 696–702.
21. Evett, S.R.; Schwartz, R.C.; Howell, T.A.; Louis Baumhardt, R.; Copeland, K.S. Can weighing lysimeter ET represent surrounding field ET well enough to experiment flux station measurements of daily and sub-daily ET? *Adv. Water Resour.* **2012**, *50*, 79–90. [[CrossRef](#)]
22. Liu, H.L.; Yang, J.Y.; Tan, C.S.; Drury, C.F.; Reynolds, W.D.; Zhang, T.Q.; Bai, Y.L.; Jin, J.; He, P.; Hoogenboom, G. Simulating water content, crop yield and nitrate-N loss under free and controlled tile drainage with subsurface irrigation using the DSSAT model. *Agric. Water Manag.* **2011**, *98*, 1105–1111. [[CrossRef](#)]
23. Rodríguez, M.M.; Sáez Fernández, F.J.; Aragón Correa, J.A. Evaluation of irrigation projects and water resource management: A methodological proposal. *Sustain. Dev.* **2002**, *10*, 13. [[CrossRef](#)]
24. Ram, H.; Dadhwal, V.; Vashist, K.K. Grain yield and water use efficiency of wheat (*Triticum aestivum* L.) in relation to irrigation levels and rice straw mulching in North West India. *Agric. Water Manag.* **2013**, *128*, 92–101. [[CrossRef](#)]
25. Li, Q.S.; Willardson, L.S.; Deng, W.; Li, X.J.; Liu, C.J. Crop water deficit estimation and irrigation scheduling in western Jilin province, Northeast China. *Agric. Water Manag.* **2005**, *71*, 47–60. [[CrossRef](#)]
26. Xiao, J.F.; Liu, Z.D.; Chen, Y.M. Study on the Water requirement and water requirement regulation of maize in China. *J. Maize Sci.* **2008**, *16*, 21–25.
27. Yazar, A.; Gökçel, F.; Sezen, M.S. Maize yield response to partial root zone drying and deficit irrigation strategies applied with drip system. *Plant. Soil Environ.* **2009**, *55*, 494–503. [[CrossRef](#)]
28. Rana, G.; Katerji, N. Measurement and estimation of actual evapotranspiration in the field under Mediterranean climate: A review. *Eur. J. Agron.* **2000**, *13*, 125–153. [[CrossRef](#)]
29. Scott, H.D. Soil physics: Agricultural and environmental applications. *Soil Sci.* **2001**, *166*, 717–718.
30. Griggs, D.J.; Noguera, M. Climate change 2001: The scientific basis. contribution of working group I to the third assessment report of the intergovernmental panel on climate change. *Weather* **2010**, *57*, 267–269. [[CrossRef](#)]
31. Mueller, N.D.; Gerber, J.S.; Johnston, M. Closing yield gaps through nutrient and water management. *Nature* **2012**, *490*, 254–257. [[CrossRef](#)]
32. Sharma, P.; Abrol, V.; Sankar, G.M. Influence of tillage practices and mulching options on productivity, economics and soil physical properties of maize (*Zea mays*)-wheat (*Triticum aestivum*) system. *Indian J. Agr. Sci.* **2011**, *79*, 865–870.
33. Zhao, Y.; Pang, H.; Wang, J.; Huo, L.; Li, Y. Effects of straw mulch and buried straw on soil moisture and salinity in relation to sunflower growth and yield. *Field Crop. Res.* **2014**, *161*, 16–25. [[CrossRef](#)]
34. Teame, G.; Tsegay, A.; Abirha, B. Effect of organic mulching on soil moisture, yield, and yield contributing components of sesame (*Sesamum indicum* L.). *Int. J. Agron.* **2017**, *2017*, 6–12. [[CrossRef](#)]
35. Zhao, H.; Zhu, Y.; Man, L.; Yang, H.W. The correlation of light-temperature indexes and light-temperature potential productivity of spring maize. In Proceedings of the International Conference on Geoinformatics, Wuhan, China, 19–21 June 2016; pp. 1–6.

36. Costa, A.C.T.D.; Oliveira, L.B.D.; Carmo, M.G.F.D. Rust quantification by visual and photosynthetic potential evaluation and its correlations with production in families of pearl millet. *Trop. Plant. Pathol.* **2009**, *34*, 313–321.
37. Gao, Y.N.; YU, G.R.; Yan, H.M.; Zhu, X.J.; Li, S.G.; Wang, Q.F.; Zhang, J.H.; Wang, Y.F.; LI, W.N.; Zhao, L.; et al. A MODIS-based photosynthetic capacity model to estimate gross primary production in Northern China and the tibetan plateau. *Remote Sens. Environ.* **2014**, *148*, 108–118. [[CrossRef](#)]
38. Zhou, W.D.; Zhu, J.H.; Wang, Y.Q.; Li, Y. Change characteristics of Shanghai's agroclimatic resources in the last hundred years. *Resour. Sci.* **2008**, *30*, 642–647.
39. Eduardo, D.O.A.L.; Moreto, V.B.; Glauco, D.S.R. Climatic potential for summer and winter wine production. *J. Sci. Food Agr.* **2018**, *98*, 1280–1290.
40. Li, Q.; Li, H.; Zhang, S. Yield and water use efficiency of dryland potato in response to plastic film mulching on the Loess Plateau. *Acta Agr. Scand. Sect. B Soil Plant Sci.* **2018**, *68*, 175–188. [[CrossRef](#)]
41. Yin, W.; Fan, Z.L.; Hu, F.L.; Yu, A.Z.; Zhao, C.; Chai, Q.; Coulter, J.A. Innovation in alternate mulch with straw and plastic management bolsters yield and water use efficiency in wheat-maize intercropping in arid conditions. *Sci. Rep.* **2019**, *9*, 6364. [[CrossRef](#)]
42. Gao, Y.; Li, Y.; Zhang, J. Effects of mulch, N fertilizer, and plant density on wheat yield, wheat nitrogen uptake, and residual soil nitrate in a dryland area of China. *Nutr. Cycl. Agroecosys.* **2009**, *85*, 109–121. [[CrossRef](#)]
43. Yin, W.; Feng, F.; Zhao, C.; Yu, A.Z.; Hu, F.L.; C, Q. Integrated double mulching practices optimizes soil temperature and improves soil water utilization in arid environments. *Int. J. Biometeorol.* **2016**, *60*, 1423–1437. [[CrossRef](#)]
44. Brar, A.S.; Buttar, G.S.; Thind, H.S.; Singh, K.B. Improvement of Water Productivity, Economics and Energetics of Potato through Straw Mulching and Irrigation Scheduling in Indian Punjab. *Potato Res.* **2019**, *6*, 1–20. [[CrossRef](#)]
45. Sun, H.; Shao, L.; Liu, X.W.; Miao, W.F.; Chen, S.Y.; Zhang, X.Y. Determination of water consumption and the water-saving potential of three mulching methods in a jujube orchard. *Eur. J. Agron.* **2012**, *43*, 87–95. [[CrossRef](#)]
46. Zhou, B.Y.; Ma, D.; Sun, X.F.; Ding, Z.S.; Li, C.F.; Ma, W.; Zhao, M. Straw mulching under a drip irrigation system improves maize grain yield and water use efficiency. *Crop. Sci.* **2019**, *59*, 2806–2819. [[CrossRef](#)]
47. Feinerman, E. Groundwater management: Efficiency and equity considerations. *Agr. Econ. Blackwell.* **1988**, *2*, 1–18. [[CrossRef](#)]
48. Jabran, K.; Hussain, M.; Fahad, S.; Farooq, M.; Bajwa, A.A.; Alharrby, H.; Nasim, W. Economic assessment of various mulches in conventional and water-saving rice production systems. *Environ. Sci. Pollut. R.* **2016**, *23*, 9156. [[CrossRef](#)] [[PubMed](#)]
49. Wang, Z.; Li, Y.K.; Guo, W.Z. Yield, nitrogen use efficiency and economic benefits of biochar additions to Chinese Flowering Cabbage in Northwest China. *Nutr. Cycl. Agroecosys.* **2019**, *113*, 337–348. [[CrossRef](#)]
50. Halloran, J.M.; Griffin, T.S.; Honeycutt, C.W. An economic analysis of potential rotation crops for Maine potato cropping systems. *Am. J. Potato Res.* **2005**, *82*, 155–162. [[CrossRef](#)]



© 2020 by the authors. Licensee MDPI, Basel, Switzerland. This article is an open access article distributed under the terms and conditions of the Creative Commons Attribution (CC BY) license (<http://creativecommons.org/licenses/by/4.0/>).

Article

Effect of Salinity on the Gut Microbiome of Pike Fry (*Esox lucius*)

Tomasz Dulski ^{1,*}, Roman Kujawa ², Martyna Godzieba ¹ and Sławomir Ciesielski ¹

¹ Department of Environmental Biotechnology, University of Warmia and Mazury in Olsztyn, 10-709 Olsztyn, Poland; martyna.godzieba@gmail.com (M.G.); slavcm@uwm.edu.pl (S.C.)

² Department of Ichthyology and Aquaculture, University of Warmia and Mazury in Olsztyn, 10-719 Olsztyn, Poland; reofish@uwm.edu.pl

* Correspondence: tomasz.dulski@uwm.edu.pl; Tel.: +48-89-523-41-64

Received: 15 February 2020; Accepted: 1 April 2020; Published: 5 April 2020

Abstract: The increasing popularity of pike in angling and fish farming has created a need to increase pike production. However, intensive pike farming is subject to limitations due to diseases and pathogens. Sodium chloride (NaCl) could be a good alternative to chemotherapeutics, especially for protecting the fish against pathogens and parasites at early life stages. However, the impact of high salinity on the symbiotic bacteria inhabiting freshwater fish is still unclear. Therefore, our objective was to analyze the gut microbiome to find possible changes caused by salinity. In this study, the influence of 3‰ and 7‰ salinity on pike fry was investigated. High-throughput 16S rRNA gene amplicon sequencing was used to profile the gut microbiome of the fish. It was found that salinity had a statistically significant influence on pike fry mortality. Mortality was highest in the 7‰ salinity group and lowest in the 3‰ group. Microbiological analysis indicated that *Proteobacteria* and *Actinobacteria* predominated in the pike gut microbiome in all examined groups, followed by lower percentages of *Bacteroidetes* and *Firmicutes*. There were no statistically significant differences in the percent abundance of bacterial taxa between the control group and groups with a higher salinity. Our results suggest that salinity influences the gut microbiome structure in pike fry, and that 3‰ salinity may be a good solution for culturing pike at this stage in their development.

Keywords: 16S rRNA; gastrointestinal tract; gut microbiota; sequencing; salinity; *Esox lucius*; microbiome; metagenomics

1. Introduction

The pike (*Esox lucius*) is a large, iteroparous, long-lived, top-predator fish species that occupies a broad range of aquatic environments, such as eutrophic and oligotrophic lakes, rivers, and brackish waters [1]. It is a keystone predator that can exert a top-down influence on fish communities [2]. The pike has become an important species for recreational and commercial fishing because of its size, wide distribution, presence in waters in urban areas, and locally high abundance [3–5]. It is also economically important for inland fisheries [6]. The increasing popularity of pike in angling and fish farming has created a need to increase pike fry production [7]. However, intensive pike farming is subject to limitations due to diseases and pathogens.

Although antimicrobial treatments in aquaculture effectively reduce or prevent mortalities caused by primary pathogens, they may have harmful side-effects that affect the overall health of the fish. Chemotherapeutics like antibiotics, vaccines, and immunostimulants can control and prevent disease outbreaks in fish, but these methods can harm both the fish and consumers, by accumulating in fish tissues [8] and causing immunosuppression of the fish and development of microbial resistance to antibiotics.

In some situations, sodium chloride (NaCl) can be added to tanks to protect fish against pathogens and parasites. NaCl may be a good alternative for controlling fungal outbreaks and external parasites [9]. In a number of studies, NaCl has been found to be an effective prophylactic treatment against important protozoans, helminthes, and fungal pathogens [10–12]. Increased salinity helped to suppress trichodiniasis (one of the major diseases in fish aquaculture worldwide, which causes massive fish mortality) in farmed freshwater tilapia (*Oreochromis niloticus*) [13]. However, changes in salinity can exert stress on fish, and thus affect the growth condition of the animals [14,15]. Furthermore, the salinity influences the osmotic gradients between the environment and the animal, which can impair basic physiological processes and even cause death [16].

Pike appear to be able to tolerate some changes in salinity [17–19]. In the Baltic Sea, this predator is found in both estuaries and coastal areas where salinity is at the average level of 3‰ and 7‰, respectively [20,21]. Therefore, pike might be a good candidate for experiments on the temporary prophylactic addition of NaCl to tanks, especially at the beginning of the juvenile stage, when the morbidity and mortality are highest. However, although there have been some studies on the effect of salinity on freshwater and marine fish [22–24], including pike [17–19], the studies on pike have focused in physiological changes (body weight and length, immune indicators, and cortisol level). It would be interesting to study how the microbiome can change under the influence of salinity levels that freshwater fish can tolerate. So far, information on the effect of salinity on the pike gut microbiota is lacking.

Information on fish gut microbiota is generally useful for understanding the factors that affect fish health, as research has shown that the gut microbiota play a key role in the health and nutrition of the host [25–27]. Fish gut microbiota contribute to digestion and can affect growth, reproduction, overall population dynamics, and the vulnerability of the host fish to disease [28]. Many studies have reported that the structure of the fish gut microbiota is influenced by factors such as the environment, diet, temperature, and pH [29–31]. These factors can affect the microbiome by changing the relative abundance of individual groups of microorganisms. Such changes can have repercussions for physiological, hormonal, or cellular functions, which can result in the development of diseases. To date, only a few studies have investigated the effect of salinity on fish gut microbiota [15,32,33]. However, not only were these studies conducted on other species, but even basic information on the pike gut microbiota is lacking.

It seems that this gap in our knowledge should be filled, because information on fish gut microbiota is generally useful in fish domestication [34]. Identification of the gastrointestinal microbiota contributes to our understanding on the functional interactions between microbes and the host [35]. Furthermore, examining the effects of various factors on the structure of the gut microbiome can help to maintain the fish in a good condition by adjusting those factors. For example, feed can be properly composed and enriched with appropriate probiotics and other supplements, and the length and intensity of prophylactic adjustments to salinity can be optimized.

Therefore, the objective of this study was to study the influence of salinity on the composition of the pike gut microbiome. Furthermore, characterization of the gastrointestinal microbiome of pike (*E. lucius*) using a mass sequencing approach based on genes coding for 16S rRNA was conducted. The differences between the microbiomes of the gastrointestinal tracts of pike from the control tank and tanks with 3‰ and 7‰ salinity levels were investigated. Additionally, we tried to determine if the mortality of juvenile fish in salinity tanks was correlated to changes in the microbiome. Information concerning the influence of salinity on the fish gut microbiome may help to develop our understanding on the functions of the fish gut microbiota, provide insight into growth condition differences, and explain the influence of salinity on host nutrition and/or physiology.

2. Materials and Methods

2.1. Conditions of Fish Rearing

The fish were cultured at the Department of Lake and River Fisheries, University of Warmia and Mazury in Olsztyn, Poland. The experiment was conducted in rectangular glass aquarium tanks with a capacity of 25 dm³. Experimental groups of fish were kept in salinity levels of 3‰ and 7‰, obtained by adding NaCl to tap freshwater in proper amounts. The control group of fish was kept in a freshwater tank. The experiment was conducted by producing two replicates per group of treatment. Each tank had a filter and its own water pump with a separated water cycle. The fish density in the aquarium was 10 fish/dm³. During the experiment, the water temperature was 15 °C. The fish were fed with commercial Artemia Premium Cysts three times per day, with the amount depending on the number of fish in the tank. The experiment lasted for 10 days, which is a typical period of time for pike rearing. During the experiment, the mortality of fish in each tank was counted daily. Each day of the experiment, fish in all tanks were observed. At the end of each day, dead fish were noted and removed from tanks.

An ethics statement is not required for this type of research. No specific permissions were required for the described studies. The studies did not involve endangered or protected species. All experimental procedures were conducted in accordance with Polish law.

2.2. Sampling

At the end of the experiment, pike were randomly chosen from the control group (group TS_0‰) and two studied groups (TS_3‰ and TS_7‰). To obtain the morphological parameters, 20 random fish from each group were weighted and measured. Length and weight measurements were also used to calculate the body condition index (BCI; defined as weight/length³) as an indicator of the overall physiological state [36] and compared among salinity treatments over time. For microbiological analyses, 30 fish were analyzed (10 fish from each salinity group). To sacrifice each fish, MS-222 (150 mg/dm³) was used. To remove excess mucus from the ventral body surface, it was wiped with a paper towel. Then, to sanitize all instruments and surfaces, and the exterior of each fish, they were treated with 70% ethanol, after which, the instruments were flame-sterilized for dissection. For the removal of any remaining ethanol, the ventral body surface was dried with a paper towel. Next, the body cavity was opened and the entire gastrointestinal tract and its contents were aseptically removed from each fish. After this, the guts and their contents were stored at −20 °C until analysis.

2.3. DNA Extraction

For DNA isolation, the entire fish gut and its contents were used. Plastic spatulas were used to homogenize samples. DNA was then extracted using a QIAmp DNA Stool Mini Kit (Qiagen, Hilden, Germany), according to the manufacturer's instructions. To quantify DNA, a Qubit 2.0 Fluorometer (Invitrogen, Carlsbad, CA, USA) was used. For verification of the DNA integrity, 1% agarose gel electrophoresis was performed. Purified DNA was suspended in 60 µL of elution buffer and then stored at −20 °C.

2.4. 16S rRNA Gene Amplicon Library Preparation and Sequencing

To verify the quality and bacterial origin of DNA, PCR was performed with two universal 16S rRNA primers: 8F and 534R [37]. Based on these results, the DNA yield, and quality, 20 samples were chosen (seven from both TS_0‰ and TS_7‰, and six from TS_3‰) and sent to Genomed S.A (Poland) for the mass sequencing of 16S rRNA amplicons. To prepare the 16S rRNA gene amplicons, the Illumina protocol "16S Metagenomic Sequencing Library Preparation" was used. In the PCR reaction, the variable V3 and V4 regions of the 16S rRNA gene were amplified using the following primers: forward (5' CCTACGGGNGGCWGCAG 3') and reverse (5' GACTACHVGGTATCTAATCC 3') [38]. The reaction was performed according to the Illumina protocol. To index the amplicons, a Nextera[®]XTIndex

Kit (Illumina, San Diego, CA, USA) was used according to the producer's instructions. For DNA sequencing, an Illumina MiSeq instrument was used, employing a 2 × 250 paired-end protocol, along with a Miseq reagent kit v3 (Illumina, USA).

2.5. Microbiome Analysis

To process raw paired-end sequences (1,809,106 reads from 20 samples), the QIIME 2 [39] software package (<https://qiime2.org>; version: 2018.8) was employed. Paired ends were merged, reducing the 1,809,106 reads to 1,533,836 reads, and reads that could not be merged were excluded from further analyses. For quality control of the sequences, the Deblur plugin in Qiime 2 [40] was used to associate erroneous sequence reads with the true biological sequence from which they were derived, thus producing high-quality sequence variant data. First, 213,390 reads (13.91% of the data) were removed by applying an initial filtering process quality score ($q = 20$). Second, using Deblur, all reads were trimmed to 285 bp, based on the median quality score. In addition, chimeric sequences were detected and excluded from analyses. 16S rRNA Operational Taxonomic Units (OTUs) were picked from the Illumina reads using a closed-reference OTU picking protocol against the Greengenes database (<https://docs.qiime2.org/2018.8/data-resources>; data files: 13_8) clustered at 99% identity and trimmed to span only the 16S rRNA V4 region flanked by sequencing primers 515F-806R. In the next step, taxonomy assignments were associated with OTUs based on the taxonomy associated with the Greengenes reference sequence defining each OTU. This step discarded most of reads which were not found in the Greengenes database and found only 228,667 reads which were assigned taxonomy. Out of the 228,667 Illumina reads from the V4 region of the bacterial 16S rRNA genes that passed the QIIME quality filters, 90.6% (207,197 reads) matched a reference sequence at a 99% nucleotide sequence identity. Next, OTU counts were binned into genus-level taxonomic groups for plot preparation.

Sequencing data were exported as individual fastq files and have been deposited in the Sequence Read Archive (SRA) NCBI (<https://www.ncbi.nlm.nih.gov/>) under the accession no. SRP226690. Samples can be found under accession numbers from SRX7043689 to SRX7043708.

2.6. Statistical Analysis

Alpha and beta diversity statistics were recorded using the QIIME 2 scripts diversity plugin, which supports metrics for calculating and exploring the community alpha and beta diversity through statistics and visualizations in the context of sample metadata. In the calculation of alpha diversity metrics, normalization was performed using the "rarefaction" QIIME 2 process with standard parameters, setting the `max_rare_depth` (upper limit of rarefaction depths) to the mean sample size. Alpha diversity metrics were calculated using 'observed species', 'Chao1 index' (species richness estimator), 'Shannon's diversity index', and 'Good's coverage'. An alpha-rarefaction plot was created for each metric. The alpha diversity values at the same rarefaction level were calculated.

The normality and homogeneity of variance of all weight, length, and alpha diversity indices obtained from fish gut microbiome analysis were checked by Shapiro–Wilk's and Levene's test. Next, one-way ANOVA followed by Tukey–Kramer's post-hoc test ($p = 0.05$) was used to check the statistical differences between fish of different tanks (STATISTICA v.13.1 (StatSoft, Inc, Tulsa, OK, USA)).

The number of reads across samples was normalized by the sample size and the relative abundance (%) of each taxon was calculated. All taxa found in the gut microbiome were considered for statistical analysis. Statistical analysis of intestinal microbial profiles was performed using the Statistical Analysis of Metagenomics Profiles (STAMP) program (<http://kiwi.cs.dal.ca/Software/STAMP>), retaining unclassified reads [41]. To conduct a reliable statistical analysis, one sample (from TS_0%) was rejected from the analysis due to the low number of reads assigned to taxon levels. All p -values were calculated by ANOVA followed by Tukey–Kramer's post-hoc test and corrected for multiple comparisons using the Benjamini–Hochberg method for a False Discovery Rate (FDR) of 5% [42].

The beta diversity metric is an estimation of the between-sample diversity of the microbial profile and it was calculated by the QIIME 2 "diversity beta-group-significance" script. Both weighted

(abundance matrix) and unweighted (presence/absence matrix) UniFrac distances [43,44] were used. The distance matrices were graphically visualized by three-dimensional principal coordinates analysis (PCoA) representations.

Differences in the beta diversity of bacterial communities were verified using a nonparametric Permutational Multivariate Analysis of Variance (PERMANOVA) test with 999 permutations ($p = 0.05$). A pairwise significance test was also performed by comparing groups from tanks with different salinity levels using the same distance matrix metrics (weighted and unweighted UniFrac distances). These tests were available in QIIME 2.

3. Results

3.1. Fish Culturing

Fish mortality was observed in all tanks during the experiment. The number of dead fish was noted and used to prepare the cumulative mortality of fish plot (Figure 1). The lowest mortality was observed in tanks with 0‰ and 3‰ salinity, representing less than 6% of the cumulative mortality at the end of the experiment. In the TS_7‰ group, mortality increased more intensively and reached 37% at the end of the experiment. At the end of the experiment, the weight and length of fish from each tank ($n = 20$) were measured (Figure 2A). The length and weight were used to calculate the BCI and were presented on a plot (Figure 2B). Statistical analysis showed significant differences in both the length and weight between different salinity groups.

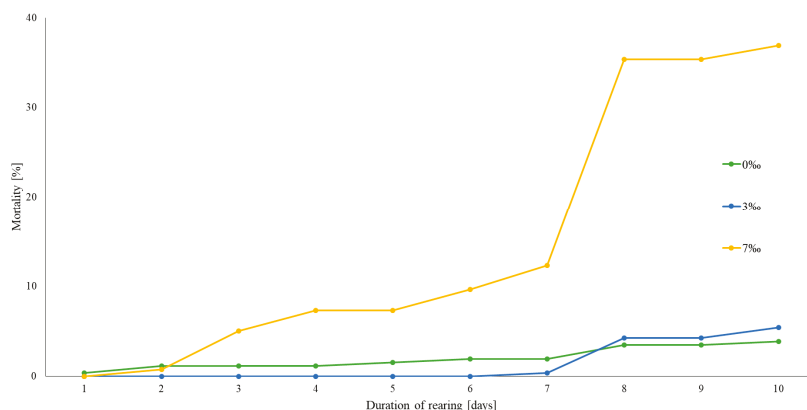


Figure 1. Cumulative mortality of pike fry during 10 days of the experiment. The experiment was conducted in rectangular glass aquarium tanks with a capacity of 25 dm³ ($n = 2$ per each group). Each tank had a filter and its own water pump with a separated water cycle. The density of fish in the aquarium was 10 fish/dm³ and the water temperature was 15 °C. The fish were fed with commercial *Artemia* Premium Cysts three times per day.

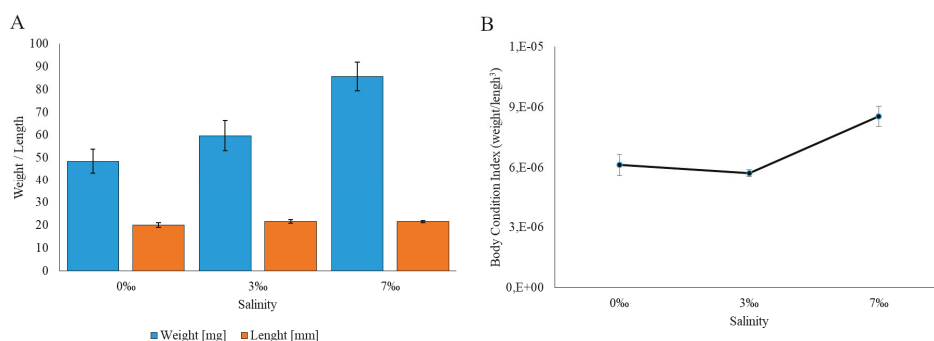


Figure 2. (A) Average weight and length of fish at the end of the experiment (n = 20/group) and (B) the effects of salinity on the pike condition index = weight (g)/fork length (mm)³; the mean ± SEM for each salinity level (n = 20).

3.2. Qiime Analysis of Sequencing Data

The fastq files with data on the gut microbiome of 20 chosen fish obtained from the Illumina MiSeq were analyzed using QIIME 2 software. After filtering for quality, trimming length, and assigned taxonomies, the number of reads taxonomically classified according to the Greengenes database was 207,197 (Table 1). This value corresponded to an average number of 10,360 per sample (range 4260–17,585). A total of 937 OTUs at a 99% nucleotide sequence identity in pike gut content samples were identified. After rarefaction, which normalized the sample to the max rare depth of sequences, the observed species number per sample was between 93 and 235, corresponding to an average number of counts per group between 140 and 196 (Table 1). Good’s coverage values for all groups were ≥0.99, indicating that sequencing coverage was attained and that the OTUs found in the samples were representative of the sampled population (Table 1). All the rarefaction curves tended to plateau (Figure S1). By statistically analyzing the OTU index of the examined groups, it was found that salinity was a factor which affected the species richness. As for the rest of the indices, salinity was not a factor with a significant affect.

Table 1. Mean number of reads per sample assigned to OTUs, and alpha diversity metric values (without one sample with less than 737 reads) of the gut microbial community of pike from different environments.

Group/Tank Salinity	Number of Analyzed Fish	Reads	Observed Species	Shannon	Good’s Coverage	Chao1
TS_0‰	7	9278 ± 5067	172 ± 34	5.1 ± 1.9	0.99 ± 0.0	174.3 ± 34.0
TS_3‰	6	12,111 ± 3021	196 ± 23	5.9 ± 0.6	0.99 ± 0.0	197.3 ± 23.7
TS_7‰	7	11,161 ± 2307	140 ± 39	5 ± 0.9	0.99 ± 0.0	141.9 ± 41.0
Total number of reads taxonomically classified					207,197	
Mean number of reads per sample					10,360	
Total number of OTUs					937	

3.3. Characterization of the Pike Gut Microbiome

The gut microbiome of 20 fish in three groups that were kept at different levels of salinity was examined to characterize its structure and to reveal the differences between groups and individual fish. The microbiome structures of each investigated group of fish at the phylum, class, order, and family level were successfully described. In our study, 15 phyla, 32 classes, 53 orders, and 88 families were classified. The gut microbial community in the groups as a whole and in individual fish are presented at the phylum (Figure 3), class (Figure 4), and order (Figure 5) levels. The figures present taxa with a relative abundance ≥0.5% (up to the class level) and ≥2.5% at the order level. All taxa are shown in Table S1.

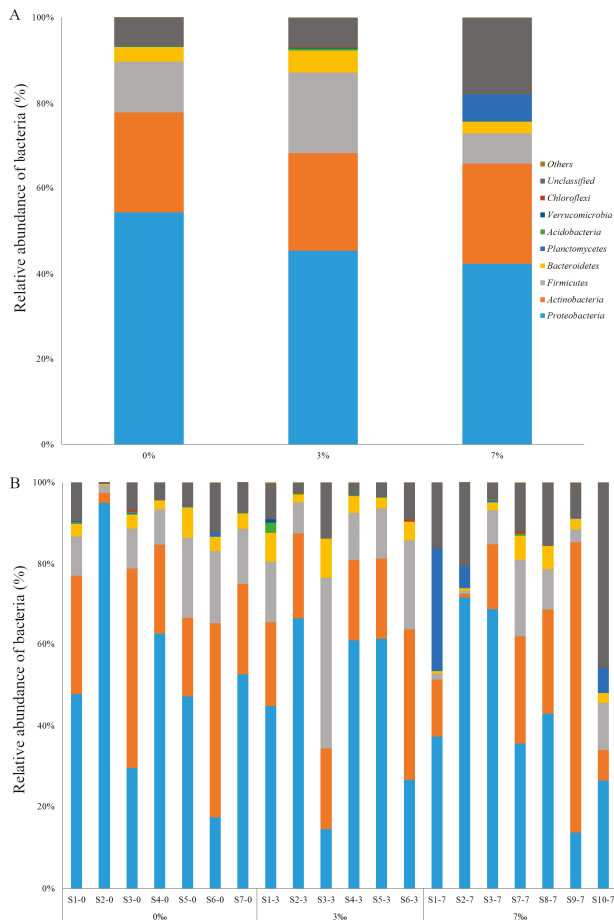


Figure 3. Relative abundance (%) of the most prevalent bacterial phyla in three groups kept at different levels of salinity (A) and in individual pike (B). Figures show all phyla with an abundance >0.5%. Phyla with an abundance ≤0.5% are pooled and labeled as “Others”.

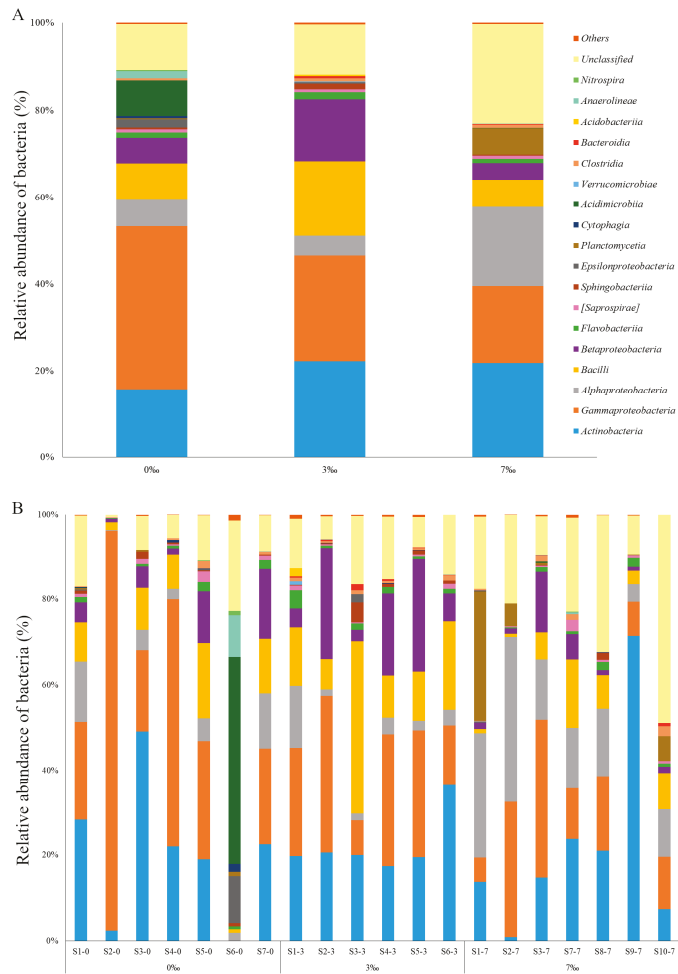


Figure 4. Relative abundance (%) of the most prevalent bacterial classes in three groups kept at different levels of salinity (A) and in individual pike (B). Figures show all classes with an abundance >0.5%. Classes with an abundance ≤0.5% are pooled and labeled as “Others”.

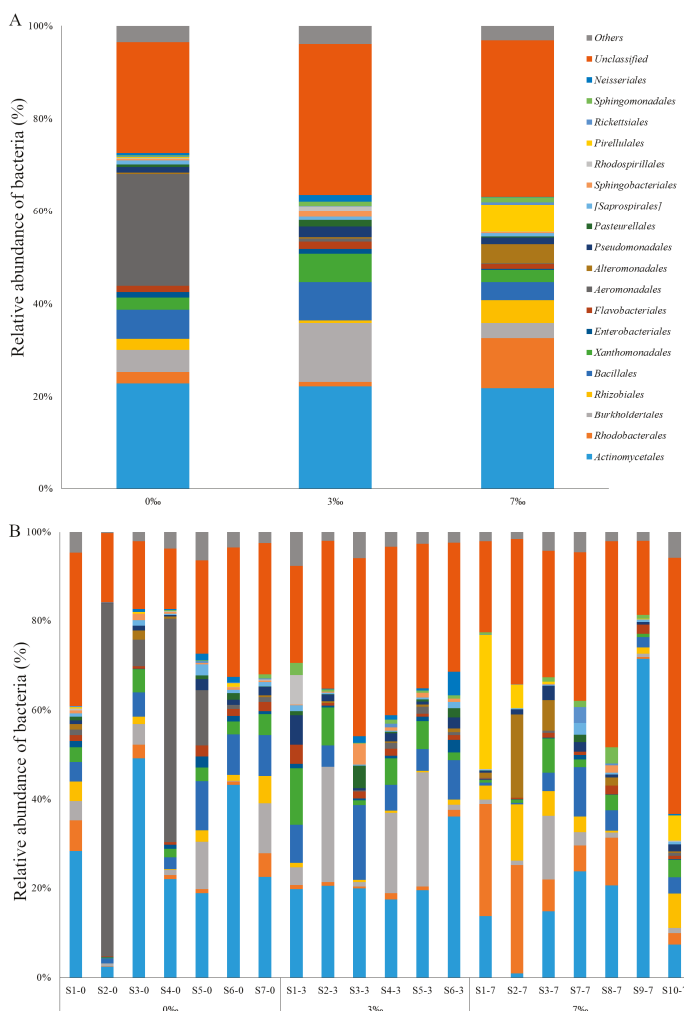


Figure 5. Relative abundance (%) of the most prevalent bacterial orders in three groups kept at different levels of salinity (A) and in individual pike (B). Figures show all orders with an abundance >2.5%. Orders with an abundance ≤2.5% are pooled and labeled as “Others”.

At the phylum level, *Proteobacteria* predominated in each group (mean abundance of 40%–53%), followed by *Actinobacteria*, *Firmicutes*, and *Bacteroidetes* (Figure 3A, Table S1). In individual fish, the composition of the bacterial community was generally similar to that in the groups as a whole, with four exceptions. In fish S3-3, *Firmicutes* predominated (42.7%) (Figure 3B), whereas in fish S3-0, S6-0, and S9-7, *Actinobacteria* predominated (43%–72%). Interestingly, in the 7‰ salinity group, *Planctomycetes* were more abundant in three fish than in the other fish (5.3%–30.2% vs. ≤0.5%)

At the class level, in almost all fish in the investigated groups, the gut microbiome was dominated by members of *Gammaproteobacteria* (17.7%–37.5%) and *Actionobacteria* (15.6%–22.2%) (Figure 4A, Table S1). *Alphaproteobacteria* were third in terms of the percent abundance in all groups. Some of the gut microbiome profiles of individual fish were different from those of other individuals. For example, the gut microbiome of fish S6-0 was dominated by *Acidimicrobiia* (48.64%), whereas in

other fish, its abundance was less or even absent (Figure 4B). The gut microbiome of fish S3-0 was completely dominated by *Gammaproteobacteria* (93.8%), whereas in fish S9-7, the gut was dominated by *Actionobacteria* (71.4%). *Bacili* dominated the gut microbiome of fish S3-3 (40.6%), whereas *Alphaproteobacteria* dominated that of fish S2-7.

At the order level, a higher percent abundance of unclassified bacteria (23.8–33.7%) was observed than at higher taxonomic levels. In all groups, there was a similar predominance of *Actinomycetales* (21.8%–22.8%) (Figure 5A). In TS_7‰, the mean abundance of *Rhodobacterales* was greater (10.84%) than in the rest of the groups (0.97%–2.44%). *Burkholderiales* were present in all groups, but more abundant in TS_3‰ (12.66%) (Figure 5A). The bacterial community composition of the gut of an individual fish tended to be more similar to that of other fish in the same group than to that of fish in other groups. *Rhodobacterales* were present in all fish microbiomes, but in TS_7‰, they were more abundant in five fish (5.8%–25.2%) (Figure 5B). Interestingly, in the 3‰ salinity group, *Aeromonadales* were more abundant in four fish than in the other fish (5.97%–79.4% vs. $\leq 1.57\%$).

One-way ANOVA was calculated and differences were considered significant at $p < 0.05$ after Benjamini–Hochberg FDR correction for multiple comparisons. In addition, the corresponding effect size (ETA-Squared) was calculated. This analysis showed no statistically significant differences between groups in terms of the abundance of each taxa of bacteria. Statistical analyses of all taxa and their relative abundance (%) are reported in Table S1. Although any significant differences in relative abundance (%) of all taxa between groups were not found, it is interesting to note that the abundance of some bacteria was higher for specific salinity concentrations in most of the fish gut microbiome group. At 7‰ salinity, *Planctomycetes*, *Rhodobacterales*, and *Alphaproteobacteria* were more abundant than at other levels of salinity; at 3‰, in contrast, *Betaproteobacteria* and *Burkholderiales* were more abundant; and in the control tanks, *Aeromonadales* were more abundant (Table S1).

Permutation multivariate analysis (PERMANOVA) indicated that, overall, there was a significant divergence between groups only in terms of unweighted UniFrac distance matrices ($p = 0.001$; Pseudo-F = 1.63) (Table 2). The beta-diversity pairwise test on the unweighted UniFrac data showed that the gut microbiomes of fish in 7‰ salinity were significantly different to those of the 3‰ salinity group. Weighted UniFrac did not show a significant overall difference in the abundance of bacteria.

Table 2. Permutation multivariate analysis (PERMANOVA) of weighted and unweighted UniFrac data of intestinal microbiomes of pike living in different environments.

PERMANOVA Analysis	Unweighted UniFrac		Weighted UniFrac	
	<i>p</i> -Value	Pseudo-F	<i>p</i> -Value	Pseudo-F
One-way				
All groups	0.001	1.63	0.052	1.69
PERMANOVA pairwise test:				
0‰ vs. 3‰	0.002		0.241	
0‰ vs. 7‰	0.137		0.146	
3‰ vs. 7‰	0.001		0.031	

QIIME 2 was used to compute microbial beta diversity metrics. Analyses were performed using weighted and unweighted UniFrac distances. Data from UniFrac metrics were used to prepare three-dimensional plots using principal coordinates analysis (PCoA) (Figure 6). PCoA reflected the PERMANOVA results. Weighted UniFrac showed that the 0‰ and 3‰ salinity groups clustered together. Fish from 7‰ salinity were separated from the rest of the samples. PCoA of the unweighted UniFrac distance matrix showed that samples from the 3‰ salinity group clustered together and samples from the other groups were scattered.

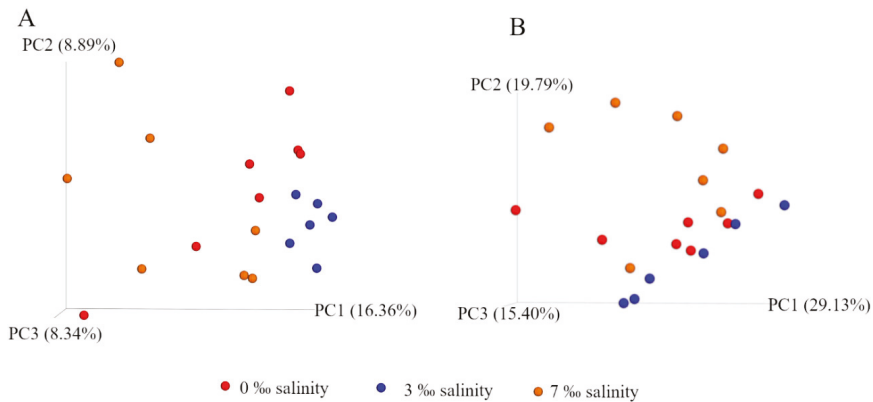


Figure 6. Beta diversity metrics. Principal coordinates analysis (PCoA) of unweighted (A) and weighted (B) Unifrac distances of gut microbial communities associated with different salinity levels. The figures show plots of individual fish according to their microbial profile.

4. Discussion

Recent studies on the effect of salinity on fish have focused on examining how salinity affects the growth, mortality, health condition, and osmotic stress of fish farm [9,13,14,22,45,46] and hatching eggs [47]. This type of research is necessary because it might help to properly choose salt concentrations and times of exposition of fish to keep them healthy during farming. Salt is commonly used as a disinfectant for the prophylactic prevention of disease development in fish farms, and thus might help to keep fish in good health, especially at the beginning of fish fry life. It is a cheaper, and probably healthier, replacement for other chemotherapeutics. However, the effect of salinity on the fish gut microbiome has been poorly investigated. Although there have been studies on the effect of salinity on the gastrointestinal microbiome of a few fish species [15,32,33,48], to the best of our knowledge, there is a lack of studies on the gut microbiome of pike fry (*E. lucius*). Therefore, it was hypothesized that the gut microbiota of pike living in freshwater differ from those of pike living in different salinity concentrations. What is more, a comparison of the morphological parameters and mortality of fish under osmotic stress was conducted. Our results provide information on the gut microbiota of pike and highlight associations between environmental factors (salinity) and gut microbiota. An understanding of these associations provides information that may be useful for addressing problems during the domestication of these valuable freshwater fish.

In our study, the size and weight of pike fry were influenced by long-term salinity tolerance. All examined fish reached a developmental stage where the organs involved in osmoregulation, e.g., the gills, were expected to be fully functional. Although the average length of fish showed little difference between each tank, the mean weight differed to a greater extent (Figure 2A). Generally, along with increasing the salinity, the environment should be cleaner and healthier, which could prevent the excessive development of pathogens, leading to better welfare of animals. However, in our study, the highest growth of fish from the 7‰ group was related to the lowest density of fish caused by the highest mortality. In these conditions, high-salinity fish had better access to food, and thus showed the highest weight values.

Mortality is a common problem in fish fry farms due to diseases mainly caused by pathogens [49]. Salt used in farming freshwater fish which tolerate some salinity is quite effective, cheaper, and much healthier (for fish and consumers). Sometimes, in aquaculture, fish are bathed prophylactically in brine to avoid pathogen development [50]. Our results showed that salinity had a statistically significant effect on cumulative mortality in fish. The greatest mortality was observed in the 7‰ salinity tank, increasing drastically on day 8 of the experiment to about 37% (Figure 1). Here, the length of the fish

was the greatest. It seems that larger pike fry cannot acclimate to these long-term osmotic conditions. This is in good agreement with other studies on pike, where the mortality of larger fish was greater than that of smaller fish [18]. The cumulative mortality of fish from tanks with a 3‰ salinity was surprisingly similar to that of the control group. What is more, the BCI was greater than in the control group. These findings suggest that this level of salinity is well-tolerated by pike, which is consistent with reports of this species in coastal areas all around the Baltic Sea, where salinities vary from 4‰ to 7‰ [18]. The fact that around 97% of fish survived this salinity treatment and had a condition factor similar to that of the controls indicates that the fish in 3‰ salinity did not experience a loss of water due to salinity stress. A loss of water is believed to be one of the reasons why fish have died in salinity treatments [18].

Our study indicated that, in the pike gut microbiome, the phyla *Proteobacteria* and *Actinobacteria* predominate, followed by lower percentages of *Bacteroidetes* and *Firmicutes* (Figure 3), in both control fish and fish in different salinity levels. This observation suggests that these phyla could play important roles in pike gut functioning. Although it is difficult to estimate the contribution of specific bacteria to the function of the whole gut ecosystem, it is reasonable to expect that the overall gut microbiome will be strongly influenced by the predominant microorganisms [28]. The presence of similar bacterial taxa in the gut microbiota of multiple fish species suggests that these bacteria are valuable for the host and could play important roles in digestion, nutrient absorption, and immune responses [51]. These phyla have been found in the intestines of many marine and freshwater fish species [52–56]. However, the proportions of these phyla present in our study were different to those in other studies [33,57,58]. In studies on eight freshwater fish species [55], marine Atlantic cod [59], and Fine flounder [60], *Proteobacteria* has been described as the predominant phylum. On the other hand, *Firmicutes* predominate in the intestinal content of aquacultured Siberian sturgeon [61], grass carp [62], and Atlantic salmon [63]. Our study showed that the mean abundance of *Proteobacteria* of a group might be a predominant phylum (Figure 3A). However, looking at individual fish, the proportions of the percent abundance of main phyla were not similar. Sometimes, *Actinobacteria* predominate over *Proteobacteria*. This observation was noticed in control and salinity tanks, so salinity does not have a significant influence on the gut structure at the phylum level. This may be related to fish development. It appears that the diversity of bacteria increases as fish develop [64]. Ringø and Birkbeck [65], in their review, summarized 24 studies on the microbiome of fish larvae and fry and showed changes during fish development. Furthermore, relatively stable gut microbiota are established within the first 50 days of life for many species [66]. Therefore, gut microbiota of pike might just have been forming during the experiment. Despite these facts, our results suggest that *Proteobacteria*, *Firmicutes*, *Bacteroidetes*, and *Actinobacteria*, which dominate in the fish gut, may play important roles in the gut microbiome of pike at an early life stage.

Various salinity concentrations can lead to osmotic stress in fish. Physiological changes in the host that occur during osmotic stress force its gut microbiome to adapt to the new conditions. Therefore, new species may develop in the gut microbiome. Although significant differences in the abundance of taxa between control and salinity groups (Table S1) were not found, there were small changes in the percent abundance of some groups. In some fish reared in 7‰ salinity, a higher percent abundance of *Planctomycetes* were observed, whereas in the other groups, these bacteria were absent. *Planctomycetes* were found in yellow grouper, which is a marine fish [67]. Another study reported that *Planctomycetes* were found in macroalgae biofilm [68]. This suggests that *Planctomycetes* like salty environments and could multiply under the influence of this stress factor.

In most fish, at all salinity concentrations, *Proteobacteria* usually predominate over other phyla. In contrast to our results, a study on *Oreochromis niloticus* (Nile tilapia) showed that the percent abundance of *Proteobacteria* changed and was higher in fish from a marine environment than in those from a freshwater environment [15]. Furthermore, the study found that *Actinobacteria* and *Bacteroidetes* were more abundant in fish from freshwater than in those from marine water, whereas our study found similar levels of these phyla at all salinity levels. The reason for these results is not yet completely

understood, but the results might depend on many conditions, such as the salinity concentration, fish species, length of exposition, diet, age of the fish, and others. Although significant changes in phyla were not observed, differences in the percent abundance of *Proteobacteria* classes between salinity levels were observed. *Alphaproteobacteria* predominated in 7‰ salinity, whereas in 3‰ and control tanks, *Betaproteobacteria* were more abundant. An effect of salinity on the microbiome structure was also found in black molly (*Poecilia sphenops*), where an increase in salinity induced changes in the dominant bacterial taxa in the microbiomes [32]. In the more saline treatments in their study, unknown *Enterobacteriaceae* (18‰ and 30‰) replaced *Aeromonas* and *Cetobacterium* OTUs that were present in the freshwater treatments (0‰ and 5‰). Although their results differ slightly from our results, they confirm that salinity can influence the gut microbiome. Furthermore, it is interesting to note that *Aeromonadales*, which was more abundant in control fish in our study, was less abundant in fish with salinity treatment. This supports previous findings in other studies [33,34], where microbes differ on broader scales between freshwater and saltwater fish, with the bacteria *Aeromonadales* being enriched in freshwater specimens and anadromous fish collected from freshwater habitats. Those researchers also found that *Vibrio* exhibited a greater prevalence in marine species. Although an increased percent abundance of *Vibrio* in fish with 3‰ and 7‰ salinity was not observed in our study, *Burholderiales* was more abundant in 3‰ salinity, and *Rhodobacterales* was more abundant in 7‰ salinity. However, it is necessary to note that, in the cited studies [33,34], different fish from freshwater or marine water were studied, so it is difficult to evaluate the exact role of salinity in shaping the intestinal microbiota. In contrast, our study focused on one species in different conditions and suggests that the gut microbiota composition is related to salinity.

5. Conclusions

In conclusion, our research provides the first detailed description of the structure of the gut microbiome of juvenile pike (*E. lucius*). The dominant phyla were *Proteobacteria* and *Actinobacteria*, followed by lower percentages of *Bacteroidetes* and *Firmicutes*. These phyla are the main components of the gut microbiome in many other fish species [56,65]. Despite the fact that there were no significant differences in the percent abundance of gut bacteria species, some taxa were more abundant at certain levels of salinity. At 7‰ salinity, *Planctomycetes*, *Rhodobacterales*, and *Alphaproteobacteria* were more abundant than at other levels of salinity; at 3‰, in contrast, *Betaproteobacteria* and *Burholderiales* were more abundant; and in the control tanks, *Aeromonadales* were more abundant. Furthermore, the alpha diversity based on the OTU index showed that salinity affected the number of species. Taken together, these findings indicate that salinity influences the bacterial biodiversity. Our results also suggest that salinity influences the composition of the pike gut microbiome in terms of the percent abundance of bacteria. At 3‰ salinity, mortality was low (similar to that in the control tanks), suggesting that this concentration is tolerated by the pike, beneficial for their development, and protects them from pathogens at an early life stage. Our findings suggest that salinity adjustment can improve fish welfare and aquaculture practices. To test this hypothesis, future interspecific studies should test a wider range of salinity levels and include long-term exposition.

Supplementary Materials: The following are available online at <http://www.mdpi.com/2076-3417/10/7/2506/s1>: Figure S1: Alpha diversity metrics. Rarefaction curves of the gut microbiome structure from pike kept at different levels of salinity. (A) Observed OTU's, (B) species richness (Chao1), and (C) Shannon's diversity index; Table S1: Statistical analysis of the mean relative abundance (%) ± SD of phyla, classes, orders, and families between groups.

Author Contributions: Conceptualization, S.C. and T.D.; methodology, T.D. and S.C.; software, T.D.; validation, T.D.; formal analysis, T.D. and M.G.; investigation, T.D.; resources, R.K.; data curation, T.D.; writing—original draft preparation, T.D.; writing—review and editing, T.D., S.C., R.K., and M.G.; visualization, T.D.; supervision, S.C.; project administration, S.C. and T.D. All authors have read and agreed to the published version of the manuscript.

Funding: The project was financed as part of a grant statutory project (No. 29.610.024-110) of the University of Warmia and Mazury in Olsztyn and financially co-supported by the Minister of Science and Higher Education in the scope of the program entitled "Regional Initiative of Excellence" for the years 2019–2022, Project No. 010/RID/2018/19, amount of funding 12.000.000 PLN.

Conflicts of Interest: The authors declare no conflicts of interest.

References

1. Forsman, A.; Tibblin, P.; Berggren, H.; Nordahl, O.; Koch-Schmidt, P.; Larsson, P. Pike *Esox lucius* as an emerging model organism for studies in ecology and evolutionary biology: A review: *Esox lucius* as a model in ecology and evolution. *J. Fish Biol.* **2015**, *87*, 472–479. [[CrossRef](#)] [[PubMed](#)]
2. Craig, J.F. *Pike: Biology and Exploitation*; Springer: Dordrecht, The Netherlands, 1996; ISBN 978-94-015-8775-4.
3. Pierce, R.B.; Tomcko, C.M.; Schupp, D.H. Exploitation of Northern Pike in Seven Small North-Central Minnesota Lakes. *N. Am. J. Fish. Manag.* **1995**, *15*, 601–609. [[CrossRef](#)]
4. Arlinghaus, R.; Mehner, T. A Management-Orientated Comparative Analysis of Urban and Rural Anglers Living in a Metropolis (Berlin, Germany). *Environ. Manag.* **2004**, *33*, 331–344. [[CrossRef](#)] [[PubMed](#)]
5. Lehtonen, H.; Leskinen, E.; Selén, R.; Reinikainen, M. Potential reasons for the changes in the abundance of pike, *Esox lucius*, in the western Gulf of Finland, 1939–2007: Changes in pike abundance in the gulf of finland. *Fish. Manag. Ecol.* **2009**, *16*, 484–491. [[CrossRef](#)]
6. Balik, Ü.; Cubuk, H.; Özkök, R.; Uysal, R. Reproduction Properties of Pike (*Esox lucius* L., 1758) Population in Lake Karamlık (Afyonkarahisar/Turkey). *Fish. Res. Inst.* **2006**, *30*, 27–34.
7. Muscalu-Nagy, C.; Muscalu-Nagy, R.; Balázs, K. Attempts to increase the growth rhythm of juvenile Northern pike (*Esox lucius*, L.) by adding enzyme based ingredients into dry feed. *Aquac. Aquar. Conserv. Legis.* **2013**, *6*, 99–104.
8. Suguna, P.; Binuramesh, C.; Abirami, P.; Saranya, V.; Poornima, K.; Rajeswari, V.; Shenbagarathai, R. Immunostimulation by poly- β hydroxybutyrate-hydroxyvalerate (PHB-HV) from *Bacillus thuringiensis* in *Oreochromis mossambicus*. *Fish Shellfish Immunol.* **2014**, *36*, 90–97. [[CrossRef](#)]
9. Magondu, E.W.; Rasowo, J.; Oyoo-Okoth, E.; Charo-Karisa, H. Evaluation of sodium chloride (NaCl) for potential prophylactic treatment and its short-term toxicity to African catfish *Clarias gariepinus* (Burchell 1822) yolk-sac and swim-up fry. *Aquaculture* **2011**, *319*, 307–310. [[CrossRef](#)]
10. Noga, E.J. *Fish Disease: Diagnosis and Treatment*, 2nd ed.; Iowa State University Press: Ames, IA, USA, 2000.
11. Schnick, R.A. The Impetus to Register New Therapeutants for Aquaculture. *Progress. Fish Cult.* **1988**, *50*, 190–196. [[CrossRef](#)]
12. Selosse, P.M.; Rowland, S.J. Use of Common Salt to Treat Ichthyophthiriasis in Australian Warmwater Fishes. *Progress. Fish Cult.* **1990**, *52*, 124–127. [[CrossRef](#)]
13. García Magana, L.; Jimenez Vasconcelos, L.; Rodriguez Santiago, A.; Grano Maldonado, M.; Laffon Leal, S. The effectiveness of sodium chloride and formalin in trichodiniasis of farmed freshwater tilapia *Oreochromis niloticus* (Linnaeus, 1758) in southeastern Mexico. *Lat. Am. J. Aquat. Res.* **2019**, *47*, 164–174. [[CrossRef](#)]
14. Lisboa, V.; Barcarolli, I.F.; Sampaio, L.A.; Bianchini, A. Effect of salinity on survival, growth and biochemical parameters in juvenile Lebranch mullet *Mugil liza* (Perciformes: Mugilidae). *Neotrop. Ichthyol.* **2015**, *13*, 447–452. [[CrossRef](#)]
15. Zhang, M.; Sun, Y.; Liu, Y.; Qiao, F.; Chen, L.; Liu, W.-T.; Du, Z.; Li, E. Response of gut microbiota to salinity change in two euryhaline aquatic animals with reverse salinity preference. *Aquaculture* **2016**, *454*, 72–80. [[CrossRef](#)]
16. Edwards, S.L.; Marshall, W.S. Principles and patterns of osmoregulation and euryhalinity in fishes. In *Euryhaline Fishes*, 1st ed.; McCormick, S.D., Farrell, A.P., Brauner, C.J., Eds.; Academic: Oxford, UK, 2013; Volume 32, pp. 1–44.
17. Engström-Öst, J.; Lehtiniemi, M.; Jónasdóttir, S.H.; Viitasalo, M. Growth of pike larvae (*Esox lucius*) under different conditions of food quality and salinity. *Ecol. Freshw. Fish* **2005**, *14*, 385–393. [[CrossRef](#)]
18. Jacobsen, L.; Skov, C.; Koed, A.; Berg, S. Short-term salinity tolerance of northern pike, *Esox lucius*, fry, related to temperature and size. *Fish. Manag. Ecol.* **2007**, *14*, 303–308. [[CrossRef](#)]
19. Sunde, J.; Tamarío, C.; Tibblin, P.; Larsson, P.; Forsman, A. Variation in salinity tolerance between and within anadromous subpopulations of pike (*Esox lucius*). *Sci. Rep.* **2018**, *8*, 1–11. [[CrossRef](#)]
20. Crossman, E.J. Taxonomy and distribution of North American esocids. *Am. Fish. Soc.* **1978**, *11*, 13–26.
21. Mohrholz, V.; Naumann, M.; Nausch, G.; Krüger, S.; Gräwe, U. Fresh oxygen for the Baltic Sea—An exceptional saline inflow after a decade of stagnation. *J. Mar. Syst.* **2015**, *148*, 152–166. [[CrossRef](#)]

22. Abou Anni, I.S.; Bianchini, A.; Barcarolli, I.F.; Varela, A.S.; Robaldo, R.B.; Tesser, M.B.; Sampaio, L.A. Salinity influence on growth, osmoregulation and energy turnover in juvenile pompano *Trachinotus marginatus* Cuvier 1832. *Aquaculture* **2016**, *455*, 63–72. [[CrossRef](#)]
23. Árnason, T.; Magnadóttir, B.; Björnsson, B.; Steinarsson, A.; Björnsson, B.T. Effects of salinity and temperature on growth, plasma ions, cortisol and immune parameters of juvenile Atlantic cod (*Gadus morhua*). *Aquaculture* **2013**, *380*, 70–79. [[CrossRef](#)]
24. Urbina, M.A.; Glover, C.N. Effect of salinity on osmoregulation, metabolism and nitrogen excretion in the amphidromous fish, inanga (*Galaxias maculatus*). *J. Exp. Mar. Biol. Ecol.* **2015**, *473*, 7–15. [[CrossRef](#)]
25. Brugman, S.; Nieuwenhuis, E.E.S. Mucosal control of the intestinal microbial community. *J. Mol. Med.* **2010**, *88*, 881–888. [[CrossRef](#)] [[PubMed](#)]
26. Viney, M.E.; Riley, E.M. From immunology to eco-immunology: More than a new name. In *Eco-Immunology*, 1st ed.; Mala-goli, D., Ottaviani, E., Eds.; Springer: Dordrecht, Holland, 2014; pp. 1–19.
27. Wang, A.R.; Ran, C.; Ringø, E.; Zhou, Z.G. Progress in fish gastrointestinal microbiota research. *Rev. Aquac.* **2018**, *10*, 626–640. [[CrossRef](#)]
28. Ghanbari, M.; Kneifel, W.; Domig, K.J. A new view of the fish gut microbiome: Advances from next-generation sequencing. *Aquaculture* **2015**, *448*, 464–475. [[CrossRef](#)]
29. Eichmüller, J.J.; Hamilton, M.J.; Staley, C.; Sadowsky, M.J.; Sorensen, P.W. Environment shapes the fecal microbiome of invasive carp species. *Microbiome* **2016**, *4*, 44. [[CrossRef](#)] [[PubMed](#)]
30. Hennersdorf, P.; Kleinertz, S.; Theisen, S.; Abdul-Aziz, M.A.; Mrotzek, G.; Palm, H.W.; Saluz, H.P. Microbial Diversity and Parasitic Load in Tropical Fish of Different Environmental Conditions. *PLoS ONE* **2016**, *11*, e0151594. [[CrossRef](#)]
31. Kashinskaya, E.N.; Simonov, E.P.; Kabilov, M.R.; Izvekova, G.I.; Andree, K.B.; Solovyev, M.M. Diet and other environmental factors shape the bacterial communities of fish gut in an eutrophic lake. *J. Appl. Microbiol.* **2018**, *125*, 1626–1641. [[CrossRef](#)]
32. Schmidt, V.T.; Smith, K.F.; Melvin, D.W.; Amaral-Zettler, L.A. Community assembly of a euryhaline fish microbiome during salinity acclimation. *Mol. Ecol.* **2015**, *24*, 2537–2550. [[CrossRef](#)]
33. Sullam, K.E.; Essinger, S.D.; Lozupone, C.A.; O'Connor, M.P.; Rosen, G.L.; Knight, R.; Kilham, S.S.; Russell, J.A. Environmental and ecological factors that shape the gut bacterial communities of fish: A meta-analysis. *Mol. Ecol.* **2012**, *21*, 3363–3378. [[CrossRef](#)]
34. Roeselers, G.; Mittge, E.K.; Stephens, W.Z.; Parichy, D.M.; Cavanaugh, C.M.; Guillemin, K.; Rawls, J.F. Evidence for a core gut microbiota in the zebrafish. *ISME J.* **2011**, *5*, 1595–1608. [[CrossRef](#)]
35. Dulski, T.; Zakeš, Z.; Ciesielski, S. Characterization of the gut microbiota in early life stages of pikeperch *Sander lucioperca*: Gut microbiota of *S. lucioperca*. *J. Fish Biol.* **2018**, *92*, 94–104. [[CrossRef](#)] [[PubMed](#)]
36. Komoroske, L.M.; Jeffries, K.M.; Connon, R.E.; Dexter, J.; Hasenbein, M.; Verhille, C.; Fangué, N.A. Sublethal salinity stress contributes to habitat limitation in an endangered estuarine fish. *Evol. Appl.* **2016**, *9*, 963–981. [[CrossRef](#)] [[PubMed](#)]
37. Nossa, C.W. Design of 16S rRNA gene primers for 454 pyrosequencing of the human foregut microbiome. *World J. Gastroenterol.* **2010**, *16*, 4135. [[CrossRef](#)] [[PubMed](#)]
38. Klindworth, A.; Pruesse, E.; Schweer, T.; Peplies, J.; Quast, C.; Horn, M.; Glöckner, F.O. Evaluation of general 16S ribosomal RNA gene PCR primers for classical and next-generation sequencing-based diversity studies. *Nucleic Acids Res.* **2013**, *41*, e1. [[CrossRef](#)] [[PubMed](#)]
39. Caporaso, J.G.; Kuczynski, J.; Stombaugh, J.; Bittinger, K.; Bushman, F.D.; Costello, E.K.; Fierer, N.; Peña, A.G.; Goodrich, J.K.; Gordon, J.L.; et al. QIIME allows analysis of high-throughput community sequencing data. *Nat. Methods* **2010**, *7*, 335–336. [[CrossRef](#)] [[PubMed](#)]
40. Amir, A.; McDonald, D.; Navas-Molina, J.A.; Kopylova, E.; Morton, J.T.; Zech Xu, Z.; Kightley, E.P.; Thompson, L.R.; Hyde, E.R.; Gonzalez, A.; et al. Deblur Rapidly Resolves Single-Nucleotide Community Sequence Patterns. *MSystems* **2017**, *2*. [[CrossRef](#)] [[PubMed](#)]
41. Parks, D.H.; Beiko, R.G. Identifying biologically relevant differences between metagenomic communities. *Bioinformatics* **2010**, *26*, 715–721. [[CrossRef](#)]
42. Benjamini, Y.; Hochberg, Y. Controlling the false discovery rate: A practical and powerful approach to multiple testing. *J. R. Stat. Soc.* **1995**, *57*, 289–300. [[CrossRef](#)]
43. Lozupone, C.; Knight, R. UniFrac: A New Phylogenetic Method for Comparing Microbial Communities. *Appl. Environ. Microbiol.* **2005**, *71*, 8228–8235. [[CrossRef](#)]

44. Lozupone, C.A.; Hamady, M.; Kelley, S.T.; Knight, R. Quantitative and Qualitative Diversity Measures Lead to Different Insights into Factors That Structure Microbial Communities. *Appl. Environ. Microbiol.* **2007**, *73*, 1576–1585. [[CrossRef](#)]
45. Kang'ombe, J.; Brown, J.A. Effect of Salinity on Growth, Feed Utilization, and Survival of Tilapia rendalli Under Laboratory Conditions. *J. Appl. Aquac.* **2008**, *20*, 256–271. [[CrossRef](#)]
46. Dokuboba, A.; Akinrotimi, O.A.; Dabor, P.O. Effects of Different Physiological Saline Concentrations on the Reproductive Performance of *Clarias gariepinus* (Burchell, 1822). *J. Fish. Sci.* **2018**, *12*, 004–008.
47. Su, B.; Perera, D.A.; Mu, X.; Dunham, R.A. Effect of Sodium Chloride on Hatching Rate on Channel Catfish, *Ictalurus punctatus*, Embryos. *J. Appl. Aquac.* **2013**, *25*, 283–292. [[CrossRef](#)]
48. Dehler, C.E.; Seombes, C.J.; Martin, S.A.M. Seawater transfer alters the intestinal microbiota profiles of Atlantic salmon (*Salmo salar* L.). *Sci. Rep.* **2017**, *7*, 1–11. [[CrossRef](#)]
49. Dewi, R.R. The Efficacy of Sodium Chloride Application in the Control of Fish Lice (*Argulus* sp.) infection on Tilapia (*Oreochromis niloticus*). *Acta Aquat. Aquat. Sci. J.* **2018**, *5*, 4–7. [[CrossRef](#)]
50. Tacchi, L.; Lowrey, L.; Musharrafieh, R.; Crossey, K.; Larragoite, E.T.; Salinas, I. Effects of transportation stress and addition of salt to transport water on the skin mucosal homeostasis of rainbow trout (*Oncorhynchus mykiss*). *Aquaculture* **2015**, *435*, 120–127. [[CrossRef](#)]
51. Romero, J.; Ringø, E.; Merrifield, D.L. The Gut Microbiota of Fish in Aquaculture Nutrition. In *Aquaculture Nutrition: Gut Health, Probiotics and Prebiotics*, 2nd ed.; Merrifield, D., Ringø, E., Eds.; Wiley-Blackwell Publishing: Oxford, UK, 2014; pp. 75–100.
52. Navarrete, P.; Magne, F.; Araneda, C.; Fuentes, P.; Barros, L.; Opazo, R.; Espejo, R.; Romero, J. PCR-TTGE Analysis of 16S rRNA from Rainbow Trout (*Oncorhynchus mykiss*) Gut Microbiota Reveals Host-Specific Communities of Active Bacteria. *PLoS ONE* **2012**, *7*, e31335. [[CrossRef](#)]
53. Li, J.; Ni, J.; Li, J.; Wang, C.; Li, X.; Wu, S.; Zhang, T.; Yu, Y.; Yan, Q. Comparative study on gastrointestinal microbiota of eight fish species with different feeding habits. *J. Appl. Microbiol.* **2014**, *117*, 1750–1760. [[CrossRef](#)]
54. Liu, H.; Guo, X.; Gooneratne, R.; Lai, R.; Zeng, C.; Zhan, F.; Wang, W. The gut microbiome and degradation enzyme activity of wild freshwater fishes influenced by their trophic levels. *Sci. Rep.* **2016**, *6*, 24340. [[CrossRef](#)]
55. Givens, C.; Ransom, B.; Bano, N.; Hollibaugh, J. Comparison of the gut microbiomes of 12 bony fish and 3 shark species. *Mar. Ecol. Prog. Ser.* **2015**, *518*, 209–223. [[CrossRef](#)]
56. Llewellyn, M.S.; Boutin, S.; Hoseinifar, S.H.; Derome, N. Teleost microbiomes: The state of the art in their characterization, manipulation and importance in aquaculture and fisheries. *Front. Microbiol.* **2014**, *5*, 207. [[CrossRef](#)] [[PubMed](#)]
57. Xia, J.H.; Lin, G.; Fu, G.H.; Wan, Z.Y.; Lee, M.; Wang, L.; Liu, X.J.; Yue, G.H. The intestinal microbiome of fish under starvation. *BMC Genom.* **2014**, *15*, 266. [[CrossRef](#)] [[PubMed](#)]
58. Sevellec, M.; Pavey, S.A.; Boutin, S.; Filteau, M.; Derome, N.; Bernatchez, L. Microbiome investigation in the ecological speciation context of lake whitefish (*Coregonus clupeaformis*) using next-generation sequencing. *J. Evol. Biol.* **2014**, *27*, 1029–1046. [[CrossRef](#)] [[PubMed](#)]
59. Star, B.; Haverkamp, T.H.A.; Jentoft, S.; Jakobsen, K.S. Next generation sequencing shows high variation of the intestinal microbial species composition in Atlantic cod caught at a single location. *BMC Microbiol.* **2013**, *13*, 248. [[CrossRef](#)]
60. Ramírez, C.; Romero, J. Fine Flounder (*Paralichthys adspersus*) Microbiome Showed Important Differences between Wild and Reared Specimens. *Front. Microbiol.* **2017**, *8*, 271. [[CrossRef](#)]
61. Geraylou, Z.; Souffreau, C.; Rurangwa, E.; Maes, G.E.; Spanier, K.I.; Courtin, C.M.; Delcour, J.A.; Buyse, J.; Ollevier, F. Prebiotic effects of arabinoxylan oligosaccharides on juvenile Siberian sturgeon (*Acipenser baerii*) with emphasis on the modulation of the gut microbiota using 454 pyrosequencing. *FEMS Microbiol. Ecol.* **2013**, *86*, 357–371. [[CrossRef](#)]
62. Wu, S.; Wang, G.; Angert, E.R.; Wang, W.; Li, W.; Zou, H. Composition, Diversity, and Origin of the Bacterial Community in Grass Carp Intestine. *PLoS ONE* **2012**, *7*, e30440. [[CrossRef](#)]
63. Schmidt, V.; Amaral-Zettler, L.; Davidson, J.; Summerfelt, S.; Good, C. Influence of Fishmeal-Free Diets on Microbial Communities in Atlantic Salmon (*Salmo salar*) Recirculation Aquaculture Systems. *Appl. Environ. Microbiol.* **2016**, *82*, 4470–4481. [[CrossRef](#)]

64. Egerton, S.; Culloty, S.; Whooley, J.; Stanton, C.; Ross, R.P. The Gut Microbiota of Marine Fish. *Front. Microbiol.* **2018**, *9*, 873. [[CrossRef](#)]
65. Ringø, E.; Birkbeck, T.H. Intestinal microflora of fish larvae and fry. *Aquac. Res.* **1999**, *30*, 73–93. [[CrossRef](#)]
66. McIntosh, D.; Ji, B.; Forward, B.S.; Puvanendran, V.; Boyce, D.; Ritchie, R. Culture-independent characterization of the bacterial populations associated with cod (*Gadus morhua* L.) and live feed at an experimental hatchery facility using denaturing gradient gel electrophoresis. *Aquaculture* **2008**, *275*, 42–50. [[CrossRef](#)]
67. Zhou, Z.; Yao, B.; Romero, J.; Waines, P.; Ringø, E.; Emery, M.; Liles, M.; Merrifield, D.L. Methodological approaches used to assess fishgastrointestinal communities. In *Aquaculture Nutrition: Gut Health, Probiotics and Prebiotics*, 2nd ed.; Merrifield, D., Ringø, E., Eds.; Wiley-Blackwell Publishing: Oxford, UK, 2014; pp. 101–127.
68. Lage, O.M.; Bondoso, J. Planctomycetes and macroalgae, a striking association. *Front. Microbiol.* **2014**, *5*, 267. [[CrossRef](#)] [[PubMed](#)]



© 2020 by the authors. Licensee MDPI, Basel, Switzerland. This article is an open access article distributed under the terms and conditions of the Creative Commons Attribution (CC BY) license (<http://creativecommons.org/licenses/by/4.0/>).

MDPI
St. Alban-Anlage 66
4052 Basel
Switzerland
Tel. +41 61 683 77 34
Fax +41 61 302 89 18
www.mdpi.com

Applied Sciences Editorial Office
E-mail: applsci@mdpi.com
www.mdpi.com/journal/applsci



MDPI
St. Alban-Anlage 66
4052 Basel
Switzerland

Tel: +41 61 683 77 34
Fax: +41 61 302 89 18

www.mdpi.com



ISBN 978-3-0365-1125-2